THESIS

Submitted in fulfilment of the requirements for the degree of Doctor of Philosophy at

Sorbonne Université and **Southern Cross University**

Ecole doctorale 129 (SU) and Faculty of Science and Engineering (SCU)

Genomic and eco-evolutionary drivers of adaptive potential to climate warming in Western Pacific reef-building corals

---

Publicly presented and defended on 16 December 2025

Hugo Denis

Under the supervision of

Dr. Véronique BERTEAUX-LECELLIER (Primary supervisor)

Dr. Emily HOWELLS (Primary supervisor)

Dr. Line BAY

Pr. Steven PURCELL

Dr. Gaël LECELLIER

Thesis jury:

M. Abdelfettah SIFFEDINE	DR SU, Paris	President
Ms. Sarah DAVIES	Asst. PR. BU, Boston	External Examiner
M. Pim BONGAERTS	McCosker Chair CAS, San Francisco	External Examiner
Ms. Valérie BURTET	PR UNC, Nouméa	Examiner
M. David COMBOSCH	PR, UOG, Mangilao	Examiner

Declaration

This thesis was conducted under a cotutelle agreement between Sorbonne Université and Southern Cross University.

I certify that the work presented in this thesis is, to the best of my knowledge and belief, original, except as acknowledged in the text, and that the material has not been submitted, either in whole or in part, for a degree at these or any other universities.

I acknowledge that I have read and understood the Universities' rules, requirements, procedures and policy relating to my higher degree research award and to my thesis.

I certify that I have complied with the rules, requirements, procedures and policy of the Universities.

Hugo DENIS



16th December 2025

Abstract

The biodiversity and ecosystem services of coral reefs are threatened by ocean warming and recurrent marine heatwaves, causing widespread bleaching and mortality of reef-building corals. To persist into the future, corals must adapt to rising sea temperatures, and this will largely depend on natural selection acting on heritable variation in heat tolerance. Limited empirical data exist, however, on the variation in heat tolerance traits across spatial scales, their genomic architecture, and interactions with environmental and evolutionary factors. These knowledge gaps cause substantial uncertainty regarding fundamental questions such as where and how quickly adaptation in corals can occur. As a result, it remains challenging to incorporate evolutionary adaptive potential into conservation and restoration strategies.

This thesis addresses these research gaps through the study of the widespread coral *Acropora spathulata* from the Great Barrier Reef, New Caledonia and the Coral Sea. To study the multifactorial components of adaptive potential, whole genome sequencing of >1,100 coral colonies and their dinoflagellate symbionts was combined with environmental data, measurements of individual heat tolerance from acute stress assays and field observations during marine heatwaves.

These data reveal that the acute tolerance of corals aligns with the typical temperatures of their environments. However, heat tolerance varies more widely than previously thought across small spatial scales within reefs, providing the raw material for natural selection. Despite this standing variation, recent marine heatwaves exerted pervasive detrimental effects on the tolerance of corals, and low-latitude populations may be more vulnerable to climate warming as they live closer to their upper thermal limits. These potential limits to adaptation were corroborated by our observations of widespread mortality at several reefs on the Great Barrier Reef during the 2023–2024 marine heatwave.

Population genetic analyses highlighted contrasting spatial patterns of genetic variation between coral hosts and their microalgal symbionts. Local adaptation of symbioses to environmental factors drives the association of *A. spathulata* with five distinct taxa of *Cladocopium*, including across short spatial scales. Conversely, considerable coral larval dispersal, estimated at ~100 km per generation, results in weak genetic structure across vast spatial scales. This high dispersal also contributes to large breeding population sizes that have safeguarded genetic diversity until now. Using demographic inference, I further report the first

evidence of occasional long-distance dispersal and ongoing connectivity between Australian and New Caledonian broadcast-spawning coral populations.

Host genomic associations with thermal environments and heat stress responses demonstrate that despite low overall genetic structure, genetic variants within and nearby specific genes drive polygenic heat adaptation. These signals of adaptation appear mostly non-parallel across reef systems, but point to several key genes repeatedly involved in thermal tolerance. My results also indicate a complex genetic basis of heat tolerance that may partly differ across types of thermal exposure, from acute stress to prolonged heatwaves and long-term climate adaptation. Nevertheless, polygenic scores derived from climate-associated variants substantially improved predictions of individual bleaching and mortality responses during a natural marine heatwave. This finding supports the utility of genetic markers in identifying individuals and populations with elevated heat tolerance.

Overall, my findings reveal that some acroporid corals harbour a wealth of adaptive potential and may be at lower immediate risk of extinction than other coral taxa, but climate action and coordinated conservation networks across Western Pacific countries are necessary to safeguard their future.

Résumé

La biodiversité et les services écosystémiques des récifs coralliens sont menacés par la multiplication des vagues de chaleurs marines, causant des épisodes de blanchissement et de mortalité corallienne massifs. L'adaptation des coraux au réchauffement des océans est indispensable à leur survie, et dépend en grande partie de la sélection naturelle agissant sur la variation héréditaire de leur thermotolérance. Néanmoins, peu de données existent sur la variation de la thermotolérance entre colonies coralliennes à différentes échelles spatiales, ses déterminants génétiques, et interactions avec les facteurs environnementaux et évolutifs. Ces lacunes limitent notre capacité à prédire où, et à quelle vitesse les coraux peuvent s'adapter au réchauffement des océans, ainsi qu'à intégrer ce processus aux stratégies de conservation et de restauration écologique.

Cette thèse étudie les capacités d'adaptation de l'espèce commune *Acropora spathulata* à travers la Grande Barrière de Corail Australienne, les récifs de Nouvelle-Calédonie et les atolls de la Mer de Corail. Dans ce but, le séquençage de génome complet de >1,100 colonies coralliennes et leurs symbiontes dinoflagellés a été combiné avec leurs données environnementales, leurs seuils de tolérance mesurés lors de stress thermique rapides, et des observations de terrain durant des vagues de chaleur.

Ces données révèlent que la tolérance des coraux au stress thermique aigu reflète les températures moyennes de leur environnement. Cette tolérance présente néanmoins de fortes variations au sein des récifs, pouvant favoriser les processus de sélection naturelle. Cependant, les vagues de chaleurs marines récentes diminuent la tolérance à des stress ultérieurs, et les populations de basse latitude pourraient être d'avantage vulnérables car vivant proches de leurs seuils de tolérance actuels. Ces limites potentielles à l'adaptation sont corroborées par des épisodes de mortalité massive observés lors du blanchissement de 2023–2024 sur la Grande Barrière de Corail.

La génétique des populations indique que *A. spathulata* forme des symbioses avec cinq espèces de microalgues différentes, variant sur de courtes distances et contribuant à son adaptation aux conditions locales des récifs. A l'inverse, cette espèce présente des capacités exceptionnelles de dispersion larvaire (~100 km par génération), entraînant une faible structuration génétique à grande échelle et l'interconnexion de vastes populations reproductrices. Ces travaux suggèrent

également que les populations de coraux d'Australie et de Nouvelle-Calédonie maintiennent une connectivité grâce à des dispersions larvaires occasionnelles sur de longues distances.

L'association du génome des coraux avec leur environnement et leurs réponses au stress thermique démontre que des variants génétiques affectant des gènes spécifiques participent à une adaptation polygénique à la chaleur. Les bases génétiques de cette adaptation sont largement spécifiques à chaque système récifal et varient selon la durée et l'intensité des stress thermiques. Toutefois, des signaux évolutifs récurrents suggèrent le rôle central de plusieurs gènes dans l'adaptation à la chaleur. En outre, des scores polygéniques basés sur les variants génétiques associées aux conditions thermiques des récifs permettent de mieux expliquer les différences de survie des colonies lors de vagues de chaleur marines. Ces résultats soutiennent l'utilité des biomarqueurs génétiques pour identifier les individus et populations de coraux susceptibles de mieux résister au réchauffement des océans.

Cette thèse suggère que certaines espèces du genre *Acropora* possèdent des capacités d'adaptation notables, et sont moins vulnérables à court terme que d'autres coraux scléractiniaires. Toutefois, limiter le réchauffement climatique et favoriser les réseaux de conservation concertés entre États du Pacifique demeurent indispensables pour assurer leur survie future.

Acknowledgments

I am deeply grateful to my principal supervisors Dr Véronique Berteaux-Lecellier and Dr Emily J. Howells, and to my co-supervisors Dr Line K. Bay, Prof. Steven W. Purcell and Dr Gaël Lecellier, for their guidance and invaluable support throughout this scientific journey. My profound appreciation goes to Véronique Berteaux-Lecellier and Gaël Lecellier for introducing me to tropical coral reef science and for sparking the passion that led me to pursue further research in this field. I am very thankful to Emily Howells and Line Bay for continuing to nurture this passion on the other side of the Coral Sea, and for supporting me in developing this international collaboration. This PhD experience was also greatly enriched by the continuous supervision and feedback from Steven Purcell. I have been incredibly fortunate to be trained, guided and inspired by such a diverse, empathetic and attentive team. Thank you for helping me grow in every possible aspect of my scientific training.

Je souhaite également exprimer ma profonde gratitude aux différents chercheurs, plongeurs et techniciens qui m'ont accompagné côté Calédonien à l'IRD de Nouméa et à l'Aquarium des Lagons. Je remercie Bertrand Bourgeois, Mahé Dumas, William Roman, Jordi Giraud et Martin Nguyen pour leur aide précieuse sur le terrain. Je suis particulièrement reconnaissant envers Magali Boussion pour son inépuisable enthousiasme et son aide dans de nombreux aspects de ce travail. Je remercie également le Dr. Clarisse Majorel pour sa supervision au labo, et le Dr. Olivier Chateau et Hugues Gossuin pour leur aide dans le design et la construction des systèmes expérimentaux.

I would also like to thank the many institutions and individuals who have provided assistance over these three years in Australia. My special thanks go to Prof. Cynthia Riginos and Assoc. Prof. Cheong Xin Chan for welcoming me into their respective research groups, and introducing me to exciting new areas of research. I sincerely thank the countless research volunteers, students, crew members and staff at the Australian Institute of Marine Science and the University of Queensland for their contributions and help during fieldwork and lab work in Australia. I am especially thankful to Véronique Mocellin and Dr. Samantha Goyen for their guidance at sea and in the lab, as well as Ilha Byrne, Samantha Howitt and Dr. Katharine E. Prata for their hard work in the lab. Thanks also to Dr. Iva Popovic, Dr. Katharine E. Prata and Hisatake Ishida for guiding my analyses and generously sharing their extensive knowledge of genomics. Finally, I feel lucky to have shared this PhD journey and to have collaborated with

Melissa S. Naugle all along. It has been a pleasure having you as colleague and friend throughout this experience.

I greatly appreciate the Traditional Owners of the Great Barrier Reef, and New Caledonia native people for granting permission to enter and conduct research in their sea Country.

Many thanks to the technical team and administrative staff at the Australian Institute of Marine Science, the Coffs Harbour National Marine Science, the UMR ENTROPIE at l'IRD de Nouméa and the University of Queensland for their support, facilities and technical assistance. My special thanks go to Sorbonne Université which awarded a scholarship for this PhD, and to Southern Cross University Graduate School for providing additional funding. One of the most exciting aspects of this journey has been the opportunity to engage with such a wide variety of environments, nationalities, and institutions.

I thank the members of the thesis jury for their time and willingness to examine this work.

Je tiens par ailleurs à vivement remercier toutes les personnes qui ont contribué à rendre cette expérience épanouissante et agréable au quotidien au labo comme en dehors, en particulier Hugo, Baptiste, Noé, Laure, Louis, Antoine, Delphine, Léa, William, Magali, Federica, Maxime, Ines, Paul, Sebastian, Julie, Cinzia, Thibault, Micka, Solène et Doda.

Enfin, et surtout, merci à Marjo pour m'avoir épaulé et motivé durant ces trois années, ainsi qu'à mes parents, ma sœur Manon et mes frères Nohé, Célian et Alix pour leur indéfectible soutien depuis l'autre bout du monde et leurs encouragements à réaliser mes aspirations et mes envies d'aventure.

Funding

I, Hugo Denis, received a scholarship from ED129 at Sorbonne University and funding from Southern Cross University Graduate School.

Work conducted in Australia within this thesis was supported by the Reef Restoration and Adaptation Program funded by the partnership between the Australian Government's Reef Trust and the Great Barrier Reef Foundation.

Work conducted in New Caledonia was supported by the French National Center for Scientific Research (CNRS), the French Institute for Research and Development (IRD) and the Reef Resilient Initiative (Neo Caledonia Biodiversity Agency funding). Sampling in the Chesterfield-Bellona atolls were achieved thanks to the support of the French Navy with the vessel D'Entrecasteaux.

The French Embassy in Australia awarded a Pacific Funds grant, and supported international mobility through the PHC Fasic.

Publications included in this thesis

Denis, H., Bay, L. K., Mocellin, V. J., Naugle, M. S., Lecellier, G., Purcell, S. W., Berteaux-Lecellier, V., & Howells, E. J. (2024a). Thermal tolerance traits of individual corals are widely distributed across the Great Barrier Reef. *Proceedings B*, 291(2030), 20240587.

Denis, H., Prata, K. E., Ishida, H., Popovic, I., Mocellin, V. J. L., Boussion, M., Byrne, I., Purcell, S. W., Bay, L. K., Lecellier, G., Chan, C. X., Riginos, C., Howells, E. J., & Berteaux-Lecellier, V. (2025). Long-distance gene flow and contrasting population structures of reef-building corals and their algal symbionts inform adaptive potential across the Western Pacific. *BioRxiv*. https://doi.org/https://doi.org/10.1101/2025.10.14.682263.

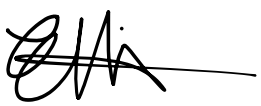
Statement of contribution of others

The Statements of Contribution signed by co-authors can be found in Appendix.

Chapter	Statement of contributions
Chapter 1	H.D. wrote the chapter with feedback from E.J.H., G.L., L.K.B., S.W.P. and V.B.L.
Chapter 2	E.J.H., L.K.B. and V.J.L.M. conceived the research. E.J.H., H.D., L.K.B., M.S.N. and V.J.L.M. performed the fieldwork and experiments. H.D., M.S.N. and V.J.L.M. curated the data. H.D. analysed the data. E.J.H., G.L., L.K.B., S.W.P. and V.B.L. supervised the work. H.D. wrote the manuscript with feedback from all other co-authors.
Chapter 3	G.L., H.D. and V.B.L. conceived the research. H.D. built the experimental system with help from G.L. and V.B.L. G.L., H.D., M.B. and V.B.L. performed the fieldwork. C.M., G.L., H.D., M.B. and V.B.L. performed the experiments, H.D. performed the laboratory analyses. O.S. curated the data. H.D. analysed the data. H.D. wrote the chapter with feedback from E.J.H., G.L., and V.B.L.
Chapter 4	C.R., E.J.H., H.D. and V.B.L. conceived the research. E.H., H.D., L.K.B., and V.M. performed the fieldwork on the GBR. G.L., H.D., M.B. and V.B.L. performed the fieldwork in New Caledonia. DNA extractions were performed by I.B. and K.E.P. for GBR samples, and by H.D. for New Caledonia samples. Whole genome sequence data was curated and analysed by H.D. following a pipeline designed by I.P. Population genetic analyses were performed by H.D. supported by C.R., E.J.H., G.L., I.P., K.E.P. and V.B.L. Demographic analyses were performed by H.D., supported by K.E. P. IbD analyses were performed by K.E.P. Symbiont analyses were performed by H.D. supported by C.X.C. and H.I. H.D. wrote the manuscript with feedback from all co-authors.
Chapter 5	E.J.H., G.L., H.D., L.K.B. and V.B.L. conceived the research. A.S.G., E.J.H., H.D., M.S.N. and V.M. acquired the *in-situ* data. G.L. created the reference genome annotation draft. H.D. analysed the data. H.D. wrote the manuscript with feedback from E.J.H., G.L., S.W.P. and V.B.L.
Chapter 6	H.D. wrote the chapter with feedback from C.R., E.J.H., G.L., S.W.P. and V.B.L.

A.S.G.: Annie S. Guillaume, C.M.: Majorel, C.R.: Cynthia Riginos, C.X.C.: Cheong Xin Chan, E.J.H.: Emily J. Howells, G.L.: Gaël Lecellier, H.D.: Hugo Denis, H.I.: Hisatake Ishida, I.B.: Ilha Byrne, I.P.: Iva Popovic, K.E.P.: Katharine E. Prata, L.K.B.: Line K. Bay, M.B.: Magali Boussion, M.S.N.: Melissa S. Naugle, O.S.: Ombeline Sue, S.W.P.: Steven W. Purcell, V.B.L.: Véronique Berteaux-Lecellier, V.J.L.M.: Veronique J.L. Mocellin

Candidate: 

Principle supervisors:  

Additional publications during candidature

Muller, C., Lett, C., Porri, F., Pattrick, P., Bailey, D., **Denis, H.**, N. Barrier, Warren M. Potts, Kaplan, D. M. (2023). Coastal connectivity of an abundant inshore fish species: model-data comparison along the southern coast of South Africa. *Marine Ecology Progress Series*.

Denis, H., Selmoni, O., Gossuin, H., Jauffrais, T., Butler, C. C., Lecellier, G., & Berteaux-Lecellier, V. (2024). Climate adaptive loci revealed by seascape genomics correlate with phenotypic variation in heat tolerance of the coral *Acropora millepora*. *Scientific Reports*, *14*(1), 22179.

Naugle, M. S., **Denis, H.**, Mocellin, V. J., Laffy, P. W., Popovic, I., Bay, L. K., & Howells, E. J. (2024). Heat tolerance varies considerably within a reef-building coral species on the Great Barrier Reef. *Communications earth & environment*, *5*(1), 525.

Guillaume, A. S., Ferrari, R., Selmoni, O., Mocellin, V. J., **Denis, H.**, Naugle, M., Howells, E., Bay, L. K., & Joost, S. (2025). Harnessing Multiscale Topographic Environmental Variables for Regional Coral Species. *Distribution Models. Ecology and Evolution*, *15*(4), e71292.

Howells, E. J., Abrego, D., Schmidt-Roach, S., Puill-Stephan, E., **Denis, H.**, Harii, S., Bay, L. K., Burt, J. A., Monro, K., & Aranda, M. (2025). Marine heatwaves select for thermal tolerance in a reef-building coral. *Nature Climate Change*. https://doi.org/10.1038/s41558-025-02381-3

Purcell, S. W., Djenidi, L. A. F., **Denis, H.**, Baletaud, F., & Gilbert, A. (2025). Growth and life-history parameters of the high-value sea cucumber, *Holothuria fuscogilva*. *Fisheries Research*, 291, 107539. https://doi.org/10.1016/j.fishres.2025.107539.

Lamb, A. M., Morgans, C. A., McCutchan. G. A., Mocellin, V. J. L., **Denis, H.**, Naugle, M. S., Lemonius, A. J., Edmunds, R. C., Wooster, M. K., Bay, L. K., Howells, E. J., van Oppen, M. J. H. (2025). A selective breeding design based on parental rapid heat stress thresholds did not produce more heat-tolerant coral larvae. *Ecological Solutions and Evidence*, *7*(1), e70178.

Naugle, M. S., **Denis, H.**, Guillaume, A. S., Mocellin, V. J., Nielsen, J. J., Van Orman, B. G., C, A. K., Bay, L. K., & Howells, E. J. (2025). Rapid heat stress assays predict survivors of coral bleaching. [Manuscript submitted for publication].

Table of contents

Declaration ..... **i**

Abstract ..... **ii**

Résumé ..... **iv**

Acknowledgments ..... **vi**

Funding ..... **viii**

Publications included in this thesis ..... **ix**

Statement of contribution of others ..... **x**

Additional publications during candidature ..... **xi**

List of Figures ..... **xvii**

List of Tables ..... **xx**

Glossary ..... **xxi**

Chapter 1. Introduction **1**

1.1) Coral reefs in the face of climate warming 2

1.1.1 Impacts of climate warming and marine heatwaves on coral reefs 2

1.1.2 Mechanisms of coral bleaching 2

Box 1 . The coral holobiont 5

1.1.3 Mass coral bleaching patterns across time and space 6

1.2) Heat tolerance variation in scleractinian corals 7

1.2.1 Ecological and evolutionary implications of variation across biological scales 7

1.2.2 Measuring and monitoring corals' heat tolerance traits 8

1.2.3 Intraspecific variation in coral heat tolerance 10

1.3) Genetic determinants of heat tolerance 13

1.3.1 Insights from other study systems 13

1.3.2 The effect of host genotype 13

1.3.3 The effect of Symbiodiniaceae genetic variation 15

1.4) Identifying genomic markers of heat tolerance 16

1.4.1 Whole genome sequencing 16

1.4.2 Genome wide association studies (GWAS) 17

1.4.3 Gene by environment association studies (GEAs) 19

1.4.4 Discovery power and controlling for confounding effects 20

1.4.5 Combining methods and markers validation 21
1.4.6 Contributions of GWAS and GEAs to heat tolerance genetics 21
1.4.7 Applications to conservation and restoration 22
1.5) Study systems and focal species 23
1.5.1 New Caledonia and the Great Barrier Reef 23
1.5.2 Study sites 24
1.5.3 *Acropora spathulata* 27
1.6) Thesis outline and research questions 29
Chapter 2. Thermal tolerance traits of individual corals are widely distributed across the Great Barrier Reef 32
2.1) Abstract 34
2.2) Introduction 35
2.3) Methods 37
2.3.1 Study sites, experimental design and set-up 37
2.3.2 Phenotypic traits 38
2.3.3 Phenotypic data analysis 39
2.3.4 Heat-tolerance variation analysis 40
2.4) Results 42
2.4.1 Reef-level variation in coral heat tolerance 43
2.4.2 Colony-level variation in coral heat tolerance 44
2.4.3 Response to acute heat stress differs between traits 45
2.4.4 Environmental drivers of acute heat tolerance metrics 46
2.5) Discussion 49
2.5.1 Acute heat-tolerance metrics linked to historical and recent environmental conditions 49
2.5.2 Standing within-reef variation in heat tolerance supports adaptive potential to climate change 50
2.5.3 Coral populations from the southern GBR may live further from their upper thermal limit 51
2.5.4 Divergent effects of acute heat stress on thermal tolerance traits 52
2.6) Conclusion 53
2.7) Acknowledgments 54
Chapter 3. Intraspecific variation in heat tolerance of *Acropora spathulata* in New Caledonia 55

3.1) Methods 57
3.1.1 Study sites, experimental design and set-up 57
3.1.2 Measure of bleaching intensity 58
3.1.3 Phenotypic data analysis 59
3.1.4 Environmental predictors of acute tolerance 59
3.2) Results 59
3.2.1 Reef-level variation in coral heat tolerance 60
3.2.2 Colony-level variation in coral heat tolerance 61
3.2.3 Environmental predictors of acute heat tolerance 62
3.3) Discussion 62
3.3.1 High intraspecific variation in heat tolerance is consistent across reef systems 62
3.3.2 Congruent patterns of heat tolerance distribution across regions 64
3.3.3 Limits of standardised acute heat stress and chlorophyll proxies at Chesterfield-Bellona reefs 65
3.3.4 Impacts of chlorophyll proxies on heat tolerance estimates 66
3.4) Conclusion 67
Chapter 4. Contrasting population structures of reef-building corals and their algal symbionts inform adaptive potential across the Western Pacific 68
4.1) Abstract 70
4.2) Introduction 71
4.3) Methods 74
4.3.1 Study sites and sample collection 74
4.3.2 DNA extraction and sequencing 74
4.3.3 Genomic data pre-variant processing and filtering 75
4.3.4 SNPs calling, clone identification and filtering 76
4.3.5 Host population genomics analyses 76
4.3.6 Population statistics 77
4.3.7 Demographic modeling 78
4.3.8 Isolation by distance analysis and estimating N_e 80
4.3.9 Symbiodiniaceae community analyses 81
4.3.10 Host and symbiont co-clustering analysis 83
4.3.11 Distance based redundancy analysis 83

4.4) Results 85
4.4.1 Genomic data processing and filtering 85
4.4.2 Coral host population structure 85
4.4.3 Population divergence and genetic diversity 86
4.4.4 Dispersal and effective population size 86
4.4.5 Demographic modeling of population divergence and gene flow 87
4.4.6 Symbiodiniaceae genetic diversity based on molecular markers 88
4.4.7 Symbiodiniaceae community divergence based on *k*-mer profiles 89
4.4.8 Drivers of host and symbiont genetic structure 90
4.5) Discussion 93
4.5.1 Regional spatial genetic variation differs among holobiont partners 94
4.5.2 Broadcast spawners maintain long-distance asymmetrical gene flow across the Western Pacific 95
4.5.3 Large breeding population and high dispersal support demographic resilience 96
4.5.4 Habitat-specific symbioses and long-range dispersal affect the evolutionary adaptive potential of *A. spathulata* 98
4.6) Conclusion 99
4.7) Acknowledgements 100
Chapter 5. Genetic basis of coral heat adaptation across thermal exposures from acute stress to climates 101
5.1) Abstract 103
5.2) Introduction 104
5.3) Methods 107
5.3.1 Variant filtering and imputation 107
5.3.2 Genotype by environment association studies 109
5.3.3 Genome-wide association studies (GWAS) 110
5.3.4 Functional analyses 113
5.3.5 Test for repeated signals 115
5.3.6 Genomic prediction of heat stress responses 116
5.4) Results and Discussion 117
5.4.1 Shared evolutionary signals amid predominantly non-parallel local thermal adaptation 118
5.4.2 Functional convergence in acute stress responses despite population-specific polygenic architecture 122

5.4.3 Variability in the genetic basis of heat tolerance across thermal exposures 124
5.4.4 Comparison of genomic signatures from associations with phenotypes and environments 126
5.4.5 Climate-adaptive loci improve predictions of bleaching and mortality during a marine heatwave 127
5.5) Conclusion 130
Chapter 6. General discussion 131
6.1) Can *Acropora spathulata* adapt to climate warming? 137
6.1.1 Evidence for wide distribution of heat tolerance traits 137
6.1.2 Adaptive variation arising from local adaptation of symbioses and coral hosts 138
6.1.3 The effects of large-scale dispersal on adaptive capacity 139
6.1.4 Molecular mechanisms of heat tolerance 140
6.1.5 Impacts of heat tolerance genomic architecture on the likelihood of climate adaptation 141
6.2) Implications for conservation and restoration 143
6.3) Challenges in characterizing the genetic architecture of corals heat adaptation. 144
6.3.1 Measuring ecologically and evolutionary informative phenotypes 144
6.3.2 Future horizons in coral association studies 146
6.3.3 The ongoing challenge of candidate loci validation and genomic prediction 148
6.3.4 The effect of genetic variation within symbiont taxa on coral heat tolerance ... 149
6.4) New Caledonia and Australia as a case study to understand differences in coral reefs tolerance and resilience to marine heatwaves 150
6.5) Conclusion 152
References 153
Appendices 184
Appendix A1. Supplementary data for Chapter 2 184
Appendix A2. Supplementary data for chapter 3 209
Appendix A3. Supplementary data for Chapter 4 213
Appendix A4. Supplementary data for Chapter 5 237
Appendix A5. Statement of co-authorship 266
Appendix A6. Scientific presentations during candidature 270

List of Figures

Main Figures

Figure 1.1. Simplified mechanisms of coral bleaching cascade 4
Figure 1.2. Conceptual representation of the adjustment of thermal optima 8
Figure 1.3. The effect of Symbiodiniaceae genetic variation on coral holobionts heat tolerance and thermal adaptation. 16
Figure 1.4. Map of the 29 reefs where *Acropora spathulata* colonies were sampled across latitudinal and thermal gradients of the GBR and of New Caledonia. 25
Figure 1.5. Detailed map of the 15 reefs where *Acropora spathulata* colonies were sampled on the GBR. 26
Figure 1.6. Detailed map of the 14 reefs where *Acropora spathulata* colonies were sampled in New Caledonia. 27
Figure 1.7. Morphology and distribution of *Acropora spathulata*. 28
Figure 2.1. Variation in *Acropora spathulata* thermal tolerance among 14 reefs on the Great Barrier Reef (GBR) under acute experimental heat stress. 44
Figure 2.2. Spatial distribution of *Acropora spathulata* acute heat tolerance on the Great Barrier Reef 46
Figure 2.3. Environmental drivers of acute heat tolerance of *Acropora spathulata* on the Great Barrier Reef. 48
Figure 3.1. Variation in *Acropora spathulata* thermal tolerance among 8 reefs on the western coast of New Caledonia under acute experimental heat stress. 61
Figure 3.2. Spatial distribution of *Acropora spathulata* acute heat tolerance on the western coast of New Caledonia 62
Figure 3.3. Comparison of variation in *Acropora spathulata* acute heat tolerance between western New Caledonia reefs (NC) and the Great Barrier Reef (GBR). 63
Figure 3.4. Consistent decline in relative acute heat tolerance at lower-latitude reefs in New Caledonia and on the Great Barrier Reef. 65
Figure 4.1. Population genomic structure and connectivity of *Acropora spathulata* 86
Figure 4.2. Generational dispersal and effective population size 87
Figure 4.3. Co-clustering of *Acropora spathulata* coral hosts and associated Symbiodiniaceae 90
Figure 4.4. Variation in the symbiont (Symbiodiniaceae) communities of *Acropora spathulata* across geographic and environmental gradients in the Western Pacific 92
Figure 5.1. Sampling sites, population structure and algal symbioses of the reef-building coral *Acropora spathulata* 106
Figure 5.2. Genotype-by-environment association studies reveal shared evolutionary signals amid predominantly non-parallel local thermal adaptation 121
Figure 5.3. Polygenic architecture of acute heat tolerance in *Acropora spathulata* shows functional convergence across populations 123
Figure 5.4. Variability in the genetic basis of heat tolerance across thermal regimes 125
Figure 5.5. Single nucleotide polymorphisms putatively linked to local thermal adaptation improve predictions of *in-situ* bleaching and mortality 129
Figure 6.1. Adaptive potential of *Acropora spathulata* to climate warming 133
Figure 6.2. Similar accumulated heat stress during the 2023–2024 marine heatwave in the Southern GBR and Southern NC led to drastically different bleaching outcomes 151

Supplementary Figures

Figure A1.1. Location of sample sites and acute heat stress design to quantify variation in the heat tolerance of the reef-building coral *Acropora spathulata* on the Great Barrier Reef. 188
Figure A1.2. Within-site variation in heat tolerance 189
Figure A1.3. Principal component analysis conducted on 24 quantitative environmental predictors of *Acropora spathulata* heat tolerance metrics 189
Figure A1.4. Pigmentation of *A.spathulata* colonies prior to collection 190
Figure A1.5. Pairwise Pearson's correlation coefficients between the 24 quantitative environmental predictors 191
Figure A1.6. Picture of the automated acute heat stress system (Seasim-in-a- box, SSIAB) 192
Figure A1.7. Validation of chlorophyll-a quantification using hyperspectral imaging 193
Figure A1.8. Principle of heat tolerance measurements 194
Figure A1.9. Standardization of colonies depth 195
Figure A1.10. Selection of tuning parameter λ of penalization coefficient for phenotypic traits ridge regression 196
Figure A1.11. Regularization of environmental predictors coefficients 197
Figure A1.12. Details of ridge regression predictors coefficients 198
Figure A1.13. Comparison of temperature records from various sources 199
Figure A1.14. Correlation between temperatures recorded by in-situ loggers and predicted by the eReefs model 200
Figure A1.15. Parameter tuning for conditional inference random forest. 201
Figure A2.1. Picture of the acute heat stress system 209
Figure A2.2. Validation of chlorophyll-a quantification using red channel intensity 209
Figure A2.3. Site-level dose response curves for invert red channel intensity 210
Figure A3.1. Environmental conditions across the Coral Sea 217
Figure A3.2. Summary of bioinformatic analyses workflow 218
Figure A3.3. Assessment of potential batch effects 219
Figure A3.4. Observed and Modeled joint Allelic frequency spectrum 220
Figure A3.5. Bootstrap analysis of *A. spathulata* populations divergence models 221
Figure A3.6. Comparison of ITS2 sequence variants recovered using graftM in hologenome data with conventional amplicon sequencing 222
Figure A3.7. Comparison of samples hierarchical clustering 223
Figure A3.8. Principal component analyses on 27,175 high quality 'hard called' SNPs 224
Figure A3.9. ADMIXTURE cross-validation error 225
Figure A3.10. Ancestral population proportion 225
Figure A3.11. Summary of marker-based and alignment-free approaches used to characterise Symbiodiniaceae 226
Figure A3.12. Summary of BAM files statistics for GBR samples 227
Figure A3.13. Summary of bam files statistics for NC samples 227
Figure A3.14. Distribution of individual missingness and depth 228
Figure A 3.15. Taxa mis-identification within the GBR dataset 229
Figure A3.16. Principal component analysis of the global dataset alongside *A.millepora* samples 229
Figure A3.17. Genetic differentiation between groups using hard-called variants 230
Figure A3.18. Genomic relatedness among individuals 230
Figure A3.19. Principal Component Analysis 231
Figure A3.20. Models considered in demographic modeling analyses 231

Figure A3.21. Pairwise Pearson's correlation coefficients between the 14 quantitative environmental predictors 232
Figure A4.1. Rate of linkage disequilibrium (LD) decay 245
Figure A4.2. Bleaching and Mortality of *Acropora spathulata* during the 2023–2024 marine heatwave 246
Figure A4.3. Controlling for confounding factors in Genome-Wide-Association studies 247
Figure A4.4. Response of *A. spathulata* populations to heat stress during a natural marine heatwave248
Figure A4.5. Average pairwise F_{st} among reefs along the genome 249
Figure A4.6. Candidate genomic markers of local adaptation identified using Genotype by environment association studies 249
Figure A4.7. Little genetic population structure within *Acropora spathulata* populations 251
Figure A4.8. GWAS with *in-situ* traits 252
Figure A4.9. Correlation between heat tolerance traits 253
Figure A4.10. Accuracy of missing genotype imputation 253
Figure A4.11. Correlation of global population structure and environmental condition 254
Figure A4.12. Candidate genomic markers of local adaptation at the regional level 255
Figure A4.13. Sensitivity analysis of GWAS results to model choice 256
Figure A4.14. Predictive accuracy of heat tolerance traits using polygenic risk scores 257
Figure A4.15. Polygenicity, genotypic redundancy and large effective population sizes limit the accuracy of coral bleaching and mortality genomic predictions 258
Figure A4.16. Predictive accuracy of symbionts genetic variation 259
Figure A4.17. Comparison of the predictive accuracy of Genomic estimated breeding values 259

List of Tables

Main Tables

Table 1.1. Comparison of thermal thresholds derived from acute heat stress assays across species of the *Acropora* genus. 10
Table 1.2. Overview of main underlying genetic and non-genetic drivers of intraspecific heat tolerance variation in reef-building corals. 12
Table 4.1. Demographic modeling of *Acropora spathulata* populations divergence 88
Table 4.2. The influence of geography and environmental conditions on host neutral genetic structure of *Acropora spathulata* 93
Table 6.1. Summary of the major findings of this thesis 134

Supplementary Tables

Table A1.1. Summary of sampling conditions and effort 202
Table A1.2. Experimental conditions of acute heat stress assays. 202
Table A1.3. Linear mixed effect models for phenotypic measurements (F_v/F_m and NDVI). 204
Table A1.4. Summary of within and among reef variation in thermal thresholds 205
Table A1.5. Summary of correlations between Fv/Fm and NDVI thermal thresholds (ED50) and performance retention 205
Table A1.6. Environmental variables retrieved for phenotype by environment analysis. 206
Table A1.7. Metrics retained for phenotype x environment analyses 208
Table A2.1. Comparison of experimental conditions, phenotypic data acquisition and analysis between Australia and New Caledonia 211
Table A2.2. Summary of sampling effort and sites conditions in New Caledonia. 211
Table A3.1. Summary of sampling effort across coral reef sites in the Western Pacific 233
Table A3.2. Pre-variant filtering steps summary 234
Table A3.3. Post-variant filtering steps summary 234
Table A3.4. SNPs and genotypes filtering parameters used to conduct the main analyses 235
Table A3.5. Environmental predictors considered for Symbiodiniaceae community distance-based redundancy analysis 235
Table A4.1. Summary of genomic variants and samples filtration steps 260
Table A4.2. Environmental predictors used in Genotype by environment association studies 260
Table A4.3. Summary of sample sizes, predictors and models used in Genotype by Environment association studies 261
Table A4.4. Summary sample sizes and numbered of retained SNPs used for Genome Wide Association studies 262
Table A4.5. Summary of SNPs and genomic windows putatively involved in local adaptation 262
Table A4.6. Top five candidate genes or genomic windows of local adaptation identified using RDA 263
Table A4.7. Top candidate SNPs hits identified in GWAS 264

Glossary

Glossary of terms related to organizations

Term	Definition
CITES	Convention on International Trade in Endangered Species of Wild Fauna and Flora
COPERNICUS	European Union's Earth observation program
GBRMPA	Great Barrier Reef Marine Park Authority
IPCC	Intergovernmental Panel on Climate Change
NASA	National Aeronautics and Space Administration, USA
NOAA	National Oceanic and Atmospheric Administration, USA
RRAP	Reef Restoration and Adaptation Program, Australia

Glossary of terms related to geography and oceanography

Term	Definition
CB	Chesterfield-Bellona atolls, part of New Caledonia EEZ and located within the Coral Sea
EAC	East Equatorial Current
GBR	Great Barrier Reef
LAT	Lowest Astronomical Tide
NC	New Caledonia
NCJ	North Caledonia Jet
SCJ	South Caledonia Jet
SEC	South Equatorial Current
STCC	Subtropical Countercurrent

Glossary of terms related to climate and climate products

Term	Definition
AR	Annual Range in SST
CoralTemp	Historic global satellite SST dataset from NOAA Coral Reef Watch
DHW	Degree heating weeks, a measure of accumulated heat stress integrating duration and intensity of thermal stress
ERA5	Re-analysis of atmospheric models, COPERNICUS
eReefs	Environmental monitoring and modelling platform designed by AIMS, CSIRO and the Bureau of Meteorology, Queensland
GlobColour	Satellite-based Ocean colour product, ESA
MHW	Marine Heat Waves
MMM	Maximum Monthly Mean of SST, a climatology corresponding to the average temperatures during the warmest month of the year for the 1985–1993 baseline period
MODIS	Moderate-resolution Imaging Spectroradiometer, NASA

SST	Sea Surface Temperature, typically acquired from satellite remote-sensing

Glossary of terms related to phenotypic traits

Term	Definition
Chl	Chlorophyll
Coral Watch Health Chart	A standardised colour reference tool used to assess coral bleaching by comparing visual pigmentation to a calibrated colour scale
ED50	Effective dose 50, the treatment corresponding to a 50% decline in a trait relative to baseline levels. Refers to absolute temperatures in the present thesis.
F_v/F_m	Maximum quantum efficiency of Photosystem II (PSII). Refers to the photosynthetic efficiency of coral-associated Symbiodiniaceae in the present thesis.
iPAM	Imaging Pulse-Amplitude Modulated fluorometer, an instrument to measure photosynthetic activity in plants or algae
NDVI	Normalised difference vegetation index, a proxy for chlorophyll content based on red and infrared reflectance measurements of a sample.
RedInt	Intensity of red channel from RGB images, a proxy for chlorophyll content in a sample.
Seasim-in-a-box	An automated experimental system to conduct acute heat stress phenotyping, similar to CBASS

Glossary of terms related to genetics

Term	Definition
DNA	Deoxyribonucleic acid
D_{xy}	Absolute genetic divergence, the average number of nucleotide differences between all pairs of sequences from two populations
h^2	Narrow-sense heritability of a trait, the proportion of phenotypic variance explained by additive genetic variance
HWE	Hardy-Weinberg Equilibrium, a theoretical expectation of genotype frequencies in an infinitely large and randomly-mating population in the absence of evolutionary forces
F_{st}	Fixation index, a measure of genetic differentiation among populations estimated from allelic frequencies
GEAs	Genotype-by-environment association study, a statistical method aiming at detecting genetic variants with shifts in allelic frequencies along environmental gradients.
GWAS	Genome Wide Association study, a statistical method aiming at detecting genetic variants (generally SNPs) affecting a phenotypic trait
IbD	Isolation-by-Distance theory
ITS2	Internal transcribed spacer 2, a non-coding nuclear ribosomal region used for the taxonomic identification of Symbiodiniaceae at the genus or species level
k-mer	A short genomic sequence of length k nucleotides
LD	Linkage Disequilibrium, statistical association between two genetic markers arising from the non-random inheritance across generations
MAF	Minor Allele Frequency, the frequency of the less common allele at a specific locus in a group of individuals

N_e	Effective population size, the size of an idealized Wright-Fisher population losing genetic variation due to drift at the same rate as the focal population
PRS	Polygenic Risk Score, a compound metric summarizing an individual's genetic risk for a trait or disease, computed from the combined effects of numerous genetic variants across the genome
$psbA^{ncr}$	non-coding region of the psbA gene in Symbiodiniaceae chloroplast used to distinguish closely related symbiont strains or populations
π	Nucleotide diversity, the average number of nucleotide differences per site between two random DNA sequences in a group of individuals
RE	Regulatory Element, DNA sequence controlling the timing, location and levels of gene expression
SNP	Single Nucleotide Polymorphism, a single nucleotide substitution at a specific position in the genome.
SV	Structural Variant, a genetic alteration typically larger than 50 base pairs. Includes deletions, insertions, inversions, duplications and translocations of genomic sequences
VCF	Variant Call Format, a standardised file format used to store genetic variation data
WGS	Whole genome sequencing

Glossary of terms related to statistical approaches

Term	Definition
dbMEMs	distance-based Moran's Eigenvector Maps
FDR	False Discovery Rate
FWER	Family Wise Error
RDA	Redundancy Analysis
RF	Random Forest
RR	Ridge Regression
VIF	Variance Inflation Factor
WZA	Weighted-Z Analysis, a method to enhance the detection of loci involved in local adaptation or a trait by integrating information from SNPs in LD

Chapter 1. Introduction



1.1) Coral reefs in the face of climate warming

1.1.1 Impacts of climate warming and marine heatwaves on coral reefs

The anthropogenic release of greenhouse gases (GHG) in the atmosphere has caused global temperatures to rise by more than 1.1 °C above pre-industrial levels over the last decade (2011–2020 and 2015–2024 vs 1850–1900; Forster et al., 2025; Lee et al., 2023). In the ocean, the average 0.88 °C rise (Lee et al., 2023) masks contrasting spatial and temporal disturbances in the form of marine heat waves (MHW). These extreme events, generally defined as sea surface temperatures (SST) above the 99th percentile of pre-industrial climatology, are estimated to have increased by 34% in frequency and 17% in duration between 1925 and 2016 (Oliver et al., 2018). By the end of the century, climate warming is predicted to span from 1.4 °C (under an unlikely very low GHG emissions scenario) to 4.4 °C (under a very high GHG emissions scenario; Lee et al., 2023). As a consequence, MHW are expected to occur 20 to 40 times more often by 2100 (Frölicher et al., 2018).

This is particularly concerning for coral reef ecosystems as the Intergovernmental Panel on Climate Change (IPCC) predicts a 99% loss of corals by 2100 under a warming of 2 °C primarily due to coral bleaching and associated mortality (Lee et al., 2023). This poses a major threat not only to 25–32% of known marine species that depend on hard corals for shelter and food (Fisher et al., 2015; McAllister, 1995) but also to adjacent ecosystems (e.g. seagrasses and mangroves) that interact with coral reefs through nutrient and biological exchanges, erosion and disease control (Stoeckl et al., 2011). In addition to their intrinsic biological value, coral reefs provide many ecosystem services to humans including coastal protection, food supply and fisheries income, support for tourism, source of pharmaceutical compounds and cultural values (Burke et al., 2011; Harrison & Booth, 2007; Stoeckl et al., 2011; Woodhead et al., 2019). These services have been valued at 36k–2,1M $/ha/year (De Groot et al., 2012), stressing the critical importance of stronger governance to protect coral reef ecosystems (Morrison et al., 2020).

1.1.2 Mechanisms of coral bleaching

Exposure to various environmental stressors can impair the finely-tuned relationship between coral hosts and their symbionts and cause a loss of host cells, symbiont cells or photosynthetic pigments known as coral bleaching (Figure 1.1; Hoegh-Guldberg, 1999). These triggers include physical factors (e.g., temperature, light, salinity) and biogeochemical conditions (e.g., disease, pollutants, hypoxia, nitrogen enrichment; van Woesik et al., 2022). However, at a global and

contemporary scale, thermal anomalies during MHW are by far the main cause of coral bleaching (Baker et al., 2008; Donner et al., 2005; Hughes, 2018; Hughes et al., 2017; Hughes et al., 2021).

Multiple triggers imply that various molecular pathways and outcomes can lead to the visual bleaching of coral colonies (Oakley & Davy, 2018; Rädecker et al., 2021; Roberty & Plumier, 2022; Weis, 2008). Although the exact physiological and molecular cascade is context-specific, heat stress has been linked to the generation of reactive species (ROS/RNS) by the host and/or the symbionts, the disruption of nutrient cycling, in particular ammonium and carbon availability and the perturbation of calcium homeostasis. Heat stress itself has been attributed to at least six different outcomes: host cell apoptosis, host cell necrosis, host cell detachment, symbiont exocytosis, symbiophagy and symbiolysosomal digestion (Helgoe et al., 2024).

Given that most coral hosts rely on symbiont photosynthates, the breakdown of the symbiotic association often leads to starvation and eventually death when this physiological state persists (Hoegh-Guldberg et al., 2007). Even when symbionts repopulate the coral host following subsequent water cooling, sublethal effects of bleaching may persist over longer periods (e.g., impairment in reproduction or growth; Anthony et al., 2009; Leinbach et al., 2021).

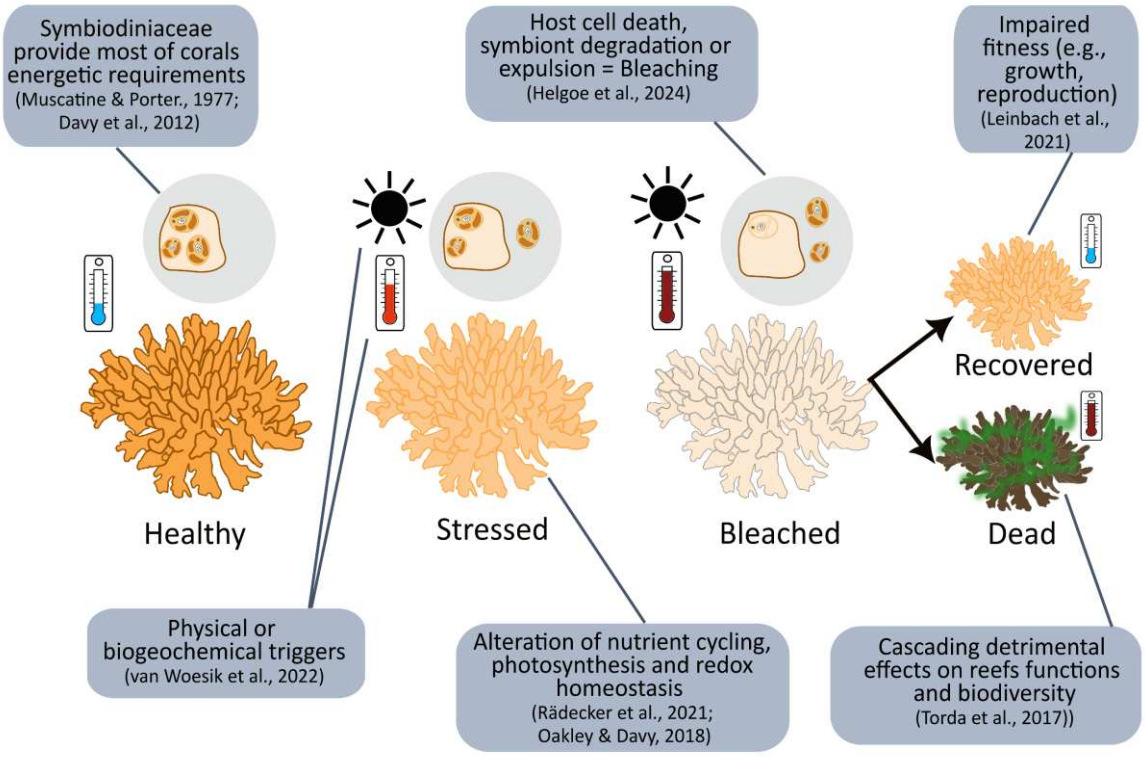


Figure 1.1. Simplified mechanisms of coral bleaching cascade The coral-dinoflagellate symbiosis can be disrupted by multiple stressors, leading to visual paling and transition to prolonged physiological impairment or death of the holobiont.

Box 1. The coral holobiont

Taxonomy: The order Scleractinia or 'hard corals' (phylum Cnidaria, class Anthozoa, subclass Hexacorallia) includes >1,300 different species (Cairns, 1999) and possibly many more cryptic species yet to be discovered (Bongaerts et al., 2021).

Anatomy and growth: Scleractinian corals mostly form colonies encompassing thousands of clones called polyps. These entities have a relatively simple anatomy which consists of a gastrodermal cavity surrounded by two layers of cells (endoderm and ectoderm) and topped by a set of prehensile tentacles. The polyps are embedded in a calcium carbonate lodge named corallite and the growth of the colony is supported by the collective biocalcification of aragonite crystals (Barnes, 1970). Scleractinian corals are thus main contributors to reef accretion through the building of their calcium carbonate skeletons (Kleypas et al., 2001).

Morphology: A large diversity of coral morphologies exists across species including massive, sub-massive, plating, tabular, branching, corymbose, digitate, encrusting or solitary. In addition, morphological plasticity in some species results in profoundly different morphologies across environments from conspecific individuals (Todd, 2008). Together with other benthic species, such as coralline algae, sponges, giant clams, and soft corals, this diversity of morphology provides distinct ecological functions such as habitat structure and food for a wide variety of marine taxa (Darling et al., 2017; Reaka-Kudla, 1997).

Life history traits: Coral species are generally grouped in distinct life history strategies (Darling et al., 2012) including (1) competitive species (e.g., from *Acropora*, *Pocillopora*, *Montipora* genera) often fast growing branching or plating species occurring at shallow depths but more sensitive to perturbations, (2) weedy species that can opportunistically colonize recently disturbed habitats (e.g., from *Stylophora*, *Seriatopora, Agaricia* genera), (3) stress-tolerant corals generally slow-growing with advantageous traits under perturbations (e.g., some species from *Porites*, *Favites, Diploastrea* genera) and (4) generalist corals showing overlapping traits with the aforementioned categories (e.g., some species from *Pachyseris, Pavona, Montipora* genera).

Reproduction: Scleractinian corals have a biphasic life cycle consisting of a dominant sessile benthic phase reaching sexual maturation after 3–8 years and producing offspring in a motile larval phase either via broadcast spawning of gametes (~85% of species) or the release of brooded larvae (~15% of species; Randall et al., 2020). Spawning generally happens at most once a year per colony during synchronized events (Harrison et al., 1984).

Nutrition: Scleractinian corals are mixotrophic organisms. They assimilate photosynthetic products from dinoflagellate symbionts filling up to 90% of their energy requirements (autotrophy; Davy et al., 2012; Muscatine & Porter, 1977). Some species feed on prey ranging from pico-plankton to meso-plankton, particulate and dissolved organic matter and inorganic matter (heterotrophy; Houlbrèque & Ferrier-Pagès, 2009).

Holobiont: The coral 'holobiont' is the emerging entity that results from diverse and co-existing organisms (Thompson et al., 2015; Yoshioka et al., 2021) including the coral animal, endosymbiotic dinoflagellates (family Symbiodiniaceae; LaJeunesse et al., 2018; Muscatine & Porter, 1977; Stat et al., 2006), endolithic algae, bacteria, archaea, fungi, protists and viruses (van Oppen et al., 2017). Symbiodiniaceae live in specialized cells called symbiosomes in the ectoderm layer and can be inherited from maternal colony (vertical transmission) or up taken from the water column (horizontal transmission; Quigley et al., 2019b). Microbes are found across the polyp tissue, surface, mucus layer, gastric cavity and skeleton (Bourne et al., 2016; Rohwer et al., 2002). They are involved in sulfur and phosphorus cycling and provide antimicrobials and nutrient to the host and its symbionts (Bourne et al., 2016; Robbins et al., 2019).

1.1.3 Mass coral bleaching patterns across time and space

Since the end of the 20th century, major MHW event have been linked to the concurrent bleaching of multiple reefs, species and individuals, a phenomenon coined ‘mass bleaching’. Increasingly frequent mass bleaching events have been observed over the past 4 decades (Hughes, 2018; Hughes et al., 2021) and are predicted to have impacted > 70% of the world’s coral reefs (Virgen-Urcelay & Donner, 2023). Four global mass bleaching events have been recorded to date, with the latest occurring in 2023–2024 (Reimer et al., 2024).

MHW lasting for several weeks or months are generally accompanied by widespread coral mortality. For instance, 60% of reefs on the GBR were severely bleached in 2016, resulting in a 30% loss of hard coral cover across the reef system, that was as high as 80% on some reefs (Hughes et al., 2017; Hughes et al., 2018). As an extreme example, Kiritimati Island endured a year-long MHW in 2015–2016 leading to a dramatical loss of 89% hard coral cover (Baum et al., 2023). It is estimated to take 5–15 years for a reef to return to its original pre-bleaching state, depending on the severity of bleaching, water quality management, protection status, and interactions with other reef species (Baker et al., 2008; Connell et al., 2004; Vessaz et al., 2022). Sometimes recovery may even be impossible, and populations have less time to recover as return times between bleaching events decrease. This can lead to local extinctions (Riegl et al., 2018) and shifts towards algae-dominated biotopes with reduced biomass and diversity (Torda et al., 2017). Bleaching-associated mortality is even more concerning given that coral reefs are exposed to numerous other threats including pollution, ocean acidification, habitat destruction, increased frequency of storms and overfishing (Halpern et al., 2008).

Overall, coral bleaching is considered to be the major driver of an estimated 50% decline in global coral cover since 1950 (Eddy et al., 2021; Souter et al., 2021). However, past MHW had varying impacts in space and time because of the interactions between bleaching history, local environmental, and biological factors (McClanahan et al., 2020; Muir et al., 2021). For instance, recent bleaching events can harden the response of coral communities (i.e., less bleaching under the same heat stress exposure), while those that are naïve to thermal stress may be more susceptible to bleaching (Hughes et al., 2021). Large uncertainties remain on how much and where coral reefs will decline in the future (Klein et al., 2024). This is primarily due to the wide taxonomic and spatial variation in heat tolerance (see section 1.2) and a limited understanding of the evolutionary potential of coral hosts and their dinoflagellate symbionts.

1.2) Heat tolerance variation in scleractinian corals

1.2.1 Ecological and evolutionary implications of variation across biological scales

Coral reef communities can be composed from a few to hundreds of different species, living next to each other on the reef. These species display different thermal optima, breadth and upper thresholds, which are conditioned by their morphology and baseline metabolism (e.g., tissue thickness and mass transfer rates; Loya et al., 2001; Muir et al., 2021; Raja et al., 2021). As a result, exposure to MHWs can greatly affect the composition of coral assemblages (Hughes et al., 2018), generally favouring the survival of massive and sub-massive genera (e.g., *Porites*, *Platygyra*, *Favites*, *Goniastrea*) over fast-growing, branching genera (e.g., *Acropora, Montipora, Pocillopora*; Baum et al., 2023). Reefs hosting a large diversity of species and morphotypes may thus maintain higher coral cover but can still suffer a loss of functional diversity if there is little functional redundancy between species (McWilliam et al., 2018).

Variation in thermal tolerance traits also exists within species and can buffer against this loss of genetic and functional diversity (McWilliam et al., 2022). In reefs where there is high-intraspecific variations, physiological plasticity may allow certain individuals to cope with recurrent MHW, and natural selection of tolerant phenotypes can lead to genetic adaptation across generations (Figure 1.2a; Somero, 2010). Conversely, low intraspecific variation may be underpinned by low adaptive genetic diversity and lead to local extinctions (Figure 1.2b; Álvarez-Noriega et al., 2023; Hughes et al., 2018; Riegl et al., 2018). Adaptation to climate warming also depends on variation in heat tolerance at the meta-population scale as novel tolerant phenotypes may emerge from recombination of standing genetic variation between populations (Howells et al., 2021). Additionally, locally adapted populations from warmer environments may also enable 'evolutionary rescue' of cooler populations through migration of heat adapted larvae (Matz et al., 2018). Conversely, when thermal tolerance breadth is conserved across populations, there may be less potential for recombination of adaptive genetic variation and the emergence of heat tolerance phenotypes.

Coral bleaching temperature thresholds have increased globally at the rate of 0.5 °C per decade since 1980 (Shlesinger & van Woesik, 2023; Sully et al., 2019). Underlying causes remain unknown but likely include shifts in community assemblages to more tolerant taxa, acclimatization of individuals and/or adaptation of populations (Coles et al., 2018; Hughes et al., 2018). The rate of increase in thermal tolerance and the upper limit it might reach are likely

to vary among reefs depending on taxonomic composition, phenotypic and genetic variation, rates of warming, and other environmental change (e.g., acidification and water quality). For instance, Lachs et al. (2023a) found an increase in heat tolerance of only 0.1 °C per decade across the Palau archipelago which is considerably slower than the global average. Therefore, documenting phenotypic differences along thermal gradients is key to predict adaptive potential (Bennett et al., 2019), identify temporary climate refugia (Lachs et al., 2023b) or anticipate extinctions (Sinervo et al., 2010) and thus adjust conservation and restoration efforts accordingly (Anthony et al., 2020; Bowden-Kerby, 2022).

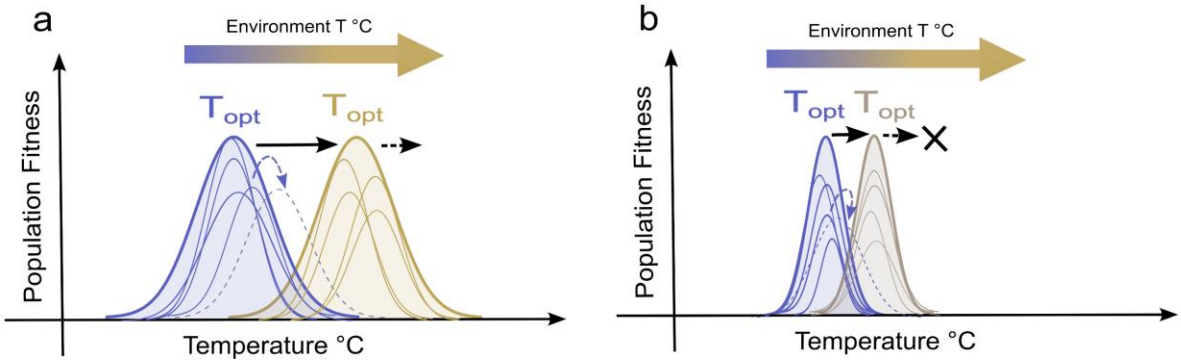


Figure 1.2. Conceptual representation of the adjustment of thermal optima (Topt) of coral populations (thick coloured lines) and individuals (thin coloured lines) to rising seawater temperatures through acclimatization (blue arrow) and adaptation (black arrow) in the case of large (a) and limited (b) phenotypic variation in thermal tolerance traits. In the first case (a), phenotypic plasticity of individuals within their lifespan, along with selection of tolerant phenotypes and the recombination of the underlying genotypes may enable the population to persist under climate warming. In the second case (b), the population's narrow thermal breadth may prevent the survival of a sufficient pool of individuals and lead to local extinction.

1.2.2 Measuring and monitoring corals' heat tolerance traits

Numerous methods are available to monitor and quantify the response of coral reefs under abnormally high temperatures. All have advantages and limitations which make them suitable to study variation in heat tolerance across different biological, spatial and temporal scales. A first low-cost approach consists of predicting coral bleaching risk from SST satellite remote sensing (Liu et al., 2003) using indicators such as Degree Heating Weeks (DHW)—corresponding to cumulative thermal anomalies above a local climatology over a rolling window of 12 weeks. However, multiple other environmental and biological factors contribute to bleaching risk (Ainsworth et al., 2021; Brown et al., 2022), therefore bleaching must be confirmed from *in-situ* observations. Aerial surveys can be conducted across large spatial scales (e.g., Hughes et al., 2017), yet are limited by the depth and taxonomic resolution at which

thermal stress response can be assessed (but see Drury et al., 2022b for promising development of airbone spectral monitoring). Therefore, measuring bleaching variation at a finer taxonomic resolution requires underwater surveys, which generally quantify visible pigmentation as proxy for symbiont cell and/or pigment retention (e.g., through colour reference cards; Siebeck et al., 2006). However, it is technically challenging and resource-intensive to conduct *in-situ* bleaching surveys across large spatial areas and during the short periods of natural MHWs. In addition, heat stress magnitude, duration and the timing of monitoring can bias ecological conclusions (e.g., if some species bleach sooner but survive longer; Claar & Baum, 2019).

Consequently, controlled *ex-situ* experiments have been widely used to characterise variation in thermal tolerance among species (Cornwell et al., 2021; Evensen et al., 2022; Marzonie et al., 2022; Shaw et al., 2016; Voolstra et al., 2021b), populations (Klepac & Barshis, 2022; Marhoefer et al., 2021; Thomas et al., 2018; Voolstra et al., 2020), and individuals (Humanes et al., 2022; Kavousi et al., 2020; Walker et al., 2022b). Many physiological measurements have been proposed to quantify the response of coral colonies to thermal stress (reviewed in McLachlan et al., 2020) with processing time and cost per sample that may vary by a factor of >10 (Nielsen et al., 2022). Among the most frequently measured traits are the photochemical efficiency of symbionts (F_v/F_m), a proxy of bleaching onset (Jones et al., 2000; Schoepf et al., 2015) and visual changes in pigmentation (i.e., estimates of symbiont density and/or chlorophyll content). Despite their conceptual similarity, the large variety of experimental setups, physiological measurements and durations of heat stress (i.e., acute <7 days, moderate 7-30 days, and long-term: >30 days) limits comparisons between studies (Grottoli et al., 2021). The number of individuals that can be evaluated in long-term experiments may also be limited depending on technical and financial resources.

Acute heat stress assays are a relatively new proposed method to quantify thermal stress responses in a standardised, high-throughput and cost-effective manner (Alderdice et al., 2022; Barshis et al., 2013; Cornwell et al., 2021; Cunning et al., 2021; Evensen et al., 2021; Evensen et al., 2022; Klepac et al., 2024; Marzonie et al., 2022; Morikawa & Palumbi, 2019; Naugle et al., 2024; Nielsen et al., 2022; Voolstra et al., 2020; Voolstra et al., 2021b). These assays are generally used to compute individual thermal thresholds as the effective dose 50 of F_v/F_m or pigmentation proxies (ED50; the temperature leading to a 50% decline in a trait, Table 1.1). Acute heat stress assays have been shown to yield consistent results across weeks (Walker et al., 2022a), seasons (Cunning et al., 2024; Cunning et al., 2021), and in comparison to longer-term heat stress (Evensen et al., 2021; Voolstra et al., 2020). However, whether acute stress

response can predict long-term responses and natural bleaching remains a contentious debate (Humanes et al., 2024; Klepac et al., 2024).

Table 1.1. Comparison of thermal thresholds derived from acute heat stress assays across species of the *Acropora* genus. Mean Absolute (ED50) and relative (ED50-MMM) thresholds are reported together with experimental conditions and time of measurement. Ranges of variation among colonies are indicated in brackets. Numeric values that were not directly available in the publication text or supplementary data were manually extracted from the figures using WebPlotDigitizer v4.6 (Rohatgi, 2014).

Species	Region	Season	Local MMM (°C)	*Fv/Fm* ED50 (°C)	Relative ED50 (°C) to local MMM	Water flow turnover (h)	Irradiance (µmol photons m^{-2} s^{-1})	ΔT	DHW at the time of collection
Acropora cervicornis[1]	Florida (USA)	August (Winter) - October (Summer) 2020	29.2–30.3 *	35.9 [35.0–37.6]	NA*	2.2	550	1	0
Acropora hemprichii[2]	Red Sea	August 2018 (Summer)	27.0–31.6	37.2 [36.3–38.1]	7.7 [6.6–10.4]	5	600	1	0
Acropora cf *humilis*[3]	Coral sea	February-March 2020 (Summer)	27.4–29.0	35.3 [34.6–35.7] **	7.0 [6.4–8.3] **	1.2	600	11	5.5–10.0
Acropora tersa[4]	Great Barrier Reef	February-March 2021/2022 (Summer)	27.1–28.8	36.40 [34.6–38.1]	8.0 [5.5–9.7]	1.2	300	2	0–3.90
Acropora spathulata[5]	Great Barrier Reef	February-March 2023 (Summer)	27.1–28.8	37.3 [34.9–39.4]	9.1 [7.1–10.9]	1.2	300	2	0.32–4.67
Acropora hyacinthus[6]	Great Barrier Reef	February 2021 (Summer)	29 °C	37.26 [37.0–37.5]	8.26 [8–8.5]	1.7	350	0	NA

***:** Colonies were held in nurseries and originated from many distinct reefs therefore computation of relative thresholds was not possible. **: ED50 were estimated at the reef level in this study. ΔT: Time between PAM measurement and end of temperature ramp-down (h). 1 Cunning et al. (2021), 2 Evensen et al. (2021), 3 Marzonie et al. (2022), 4 Naugle et al. (2024), 5 This study, 6 Alderdice et al. (2024).

1.2.3 Intraspecific variation in coral heat tolerance

Intraspecific variation in coral heat tolerance exists both among reefs (Evensen et al., 2022; Marzonie et al., 2022; Woolsey et al., 2015), and within reefs (Cunning et al., 2016; Drury et al., 2022a; Drury et al., 2022b; Humanes et al., 2022; Jin et al., 2016; Marhoefer et al., 2021; McWilliam et al., 2022; Sampayo et al., 2008).

Many biological factors interact with environmental conditions across ontogeny to shape individual corals responses to heat stress (Table 1.2). These factors occur on a continuum between rapid, transitory processes with weak inheritance (i.e., acclimatory) and rapid, more rigid processes with high inheritance (i.e., adaptation; Putnam, 2021). The heritability of traits

thus depends on the processes underpinning their variation, as well as the life stage in which they are measured (Bairos-Novak et al., 2021). For instance, maternal effects may play a predominant role during the larval and juvenile stages (Quigley et al., 2016), while symbiont communities may have a stronger influence on heat stress responses during the juvenile to adult stages (Strader & Quigley, 2022). Due to their versatile lifestyle, and the varying modes of transmission of Symbiodiniaceae and other microbes, symbiont taxa may undergo acclimatory and adaptive mechanisms separately or alongside the host (i.e., coevolution; Johnston et al., 2022; Pollock et al., 2018). Genetic adaptation of the host (and its symbionts) is relatively slow compared to acclimatization, as it occurs through the selection of heat-adapted phenotypes across generations (Somero, 2010), but produces long-lasting changes in heat tolerance that can benefit multiple life stages (Drury et al., 2022a) .

Table 1.2. Overview of main underlying genetic and non-genetic drivers of intraspecific heat tolerance variation in reef-building corals.

Type of factor	Factor	Biological scale and inheritance	Acclimatory-Adaptive continuum	Examples
External environment	MHW magnitude and duration	Interacts across life stages with acclimatory and adaptive mechanisms from the individual to multi-generation level		Berkelmans (2009); Hughes et al. (2018)
	Thermal history, in particular thermal variability			Guest et al. (2012); Hughes et al. (2019); Krueger et al. (2017); Schoepf et al. (2021); Thompson and van Woesik (2009)
	Hydrodynamic regime			Fabricius (2006); Nakamura et al. (2005); Page et al. (2021)
	Irradiance			Gonzalez-Espinosa and Donner (2021); Lesser and Farrell (2004)
	Nutrient level and balance			Burkepile et al. (2020); Wiedenmann et al. (2013)
	Zooplankton availability			Meunier et al. (2022)
	Oxygen content			Alderdice et al. (2022)
Non-genetic	Associated microbes	Individual ↓ Parental	Acclimatory ↓ Adaptive	Bourne et al. (2016); van Oppen and Blackall (2019)
	Heterotrophic plasticity			Grottoli et al. (2006); Houlbrèque and Ferrier-Pagès (2009)
	Transcriptional, translational or post-translational plasticity			DeCarlo et al. (2019); Hackerott et al. (2021)
	Epigenetics			Liew et al. (2020); Smith et al. (2022)
	Maternal effects (mitochondrial)			Dixon et al. (2015)
	Gametes macromolecules and metabolites			Torda et al. (2017)
Symbionts	Changes in dinoflagellates and/or microbiome	Individual ↓ Multi-generation		Baker et al. (2004); Bourne et al. (2008)
	Symbiont transmission			Kitchen et al. (2020)
	Associated dinoflagellates (co-evolution)			Berkelmans and van Oppen (2006); Howells et al. (2012); Raja et al. (2021); Sampayo et al. (2008)
Genetic	Symbiont genetic adaptation			Beltran et al. (2021); Logan et al. (2021)
	Host genetic adaptation			Bairos-Novak et al. (2021); Barshis et al. (2013); Dixon et al. (2015); Howells et al. (2021); Jin et al. (2016); Kirk et al. (2018); Rose et al. (2018); Rose et al. (2021)

1.3) Genetic determinants of heat tolerance

1.3.1 Insights from other study systems

Given its ecological and evolutionary significance (Angilletta Jr et al., 2006), heat tolerance has long been a focus of research, initially in domesticated plant and animal populations where early studies demonstrated a heritable component in cattle (Seath, 1947) and crops (Hall, 1992). Subsequent work revealed both positive and negative correlations with other traits such as longevity and productivity, indicating complex trade-offs affecting fitness outcomes (Lithgow et al., 1995; Ravagnolo & Misztal, 2000). Using quantitative traits analysis, co-segregation analysis and genetic stock analysis, individual mutations or genomic regions with large effects on heat tolerance (Quantitative trait loci; QTL) were progressively documented in crops such as cereals (Maestri et al., 2002) and in model species including nematodes (Lithgow et al., 1995), *Drosophila* (Morgan & Mackay, 2006) and *Arabidopsis* (Queitsch et al., 2000). The continuous variation of heat tolerance and its response to selection indicate a polygenic architecture, which was confirmed by QTL mapping studies identifying multiple associated genomic regions (Hancock et al., 1992; Morgan & Mackay, 2006; Zhang & Zhang, 2009). Overall, these studies established heat tolerance as a complex trait with convergent underlying processes across the tree of life despite a flexible genetic basis. For instance, heat shock proteins are highly conserved across eukaryotes, with some consistently upregulated under heat stress (Krebs & Bettencourt, 1999). Other processes including antioxidant responses, maintenance of membrane integrity, and proteostasis are also involved in heat stress response in a wide range of organisms (Maestri et al., 2002; Pamplona & Costantini, 2011).

1.3.2 The effect of host genotype

Over the past two decades, insights into the coral host genetic basis of heat tolerance have been gained from the application and development of quantitative genetic and genomic approaches. Several studies have demonstrated the heritability of heat tolerance through the breeding of individuals from distinct thermal environments or with distinct bleaching phenotypes (e.g., Drury et al., 2022a; Kirk et al., 2018). While heritability estimates vary across life stages and traits, they are high for bleaching and survival under heat stress ($h^2 = 0.53–0.94$; Howells et al., 2022b).

As in most organisms, heat tolerance in corals appears to have a polygenic basis (i.e., many genomic loci of small effect sizes; Bairos-Novak et al., 2021; Dixon et al., 2015; Kirk et al.,

2018; Rose et al., 2018; Rose et al., 2021; Smith et al., 2022). However in some rare cases, remarkably strong association with heat tolerant phenotypes have been detected (QTLs; Jin et al., 2016). The genomic variants undergoing selection by thermal stress can occur in coding or non-coding regions and can be of different types: single nucleotide polymorphisms (SNPs; Adam et al., 2022; Bay & Palumbi, 2014; Drury & Lirman, 2021; Elder et al., 2022; Howells et al., 2021; Kirk et al., 2018; Lundgren et al., 2013), insertions and deletions (e.g., see Anderson et al., 2003 in drosophila), structural variants (e.g., see Yan et al., 2023 in the pearl millet) or epigenetic modifications (Liew et al., 2020; Smith et al., 2022). In corals, SNPs and genomic regions have been linked to constitutive frontloading of thermal tolerance genes such as heat shock proteins (Barshis et al., 2013; Thomas et al., 2021), different transcription levels of certain genes under thermal stress (Dixon et al., 2015; Kirk et al., 2018; Rose et al., 2018) and post-translational modifications (Rose et al., 2021). Collectively these studies have highlighted different molecular pathways promoting heat tolerance, including immune system response, inflammatory and antioxidant responses, calcium homeostasis, apoptotic processes, mitochondrial and nitrogen metabolisms and many others.

Despite evidence of the heritable, polygenic nature of heat tolerance in corals, rates and upper limits of genetic adaptation are yet to be determined. Whether adaptation can keep pace with current rates of climate warming will depend on the recombination of standing genetic variation or genetic innovation (i.e., new mutations), as well as the heritability of heat tolerance traits (Elder et al., 2022), covariance between traits (Wright et al., 2019), and possible fitness tradeoffs (Cornwell et al., 2021; Jones & Berkelmans, 2011). These factors also depend on population demographics, levels of gene flow between reefs (Thomas et al., 2017; Tigano & Friesen, 2016) and interactions with environmental gradients. For instance, the fitness advantage arising from a particular genotype may sometimes not translate into a different environment (Drury & Lirman, 2021).

The majority of previous studies on the genetic basis of heat tolerance in corals were performed at a few locations (e.g., Bay & Palumbi, 2014), with small sample sizes (e.g., Dixon et al., 2015), or indirect associations with phenotypic traits (e.g., Selmoni et al., 2021). This has limited evaluation of the distribution of functional genetic variation in space and time which is crucial to predict adaptive potential. Additionally, many previous studies identified genomic regions associated with larval survival but it remains uncertain whether these regions correspond with tolerance in the adult life stage (e.g., Howells et al., 2021; Kirk et al., 2018; Quigley et al., 2020b). Finally, several of these studies used reduced representation sequencing

techniques (e.g., RAD-tag; Devlin-Durante & Baums, 2017; Thomas et al., 2017), which may only capture a small fraction of the genetic variation underlying heat stress responses. As a result, our understanding of the genomic architecture of corals' heat tolerance is still limited (Selmoni et al., 2024a).

1.3.3 The effect of Symbiodiniaceae genetic variation

Symbiodiniaceae is a highly diverse family of dinoflagellates, comprising at least 11 genera among which >40 species formally described and many more yet to be described (Davies et al., 2023; LaJeunesse et al., 2018; Nitschke et al., 2022). Hard coral species are found to associate with 8 of these genera with varying levels of specificity that primarily depends on whether they acquire their symbionts maternally or from the external environment (i.e., coral species with vertical acquisition of symbionts tend to have higher specificity; Thornhill et al., 2014). Most hard coral species can associate with multiple Symbiodiniaceae taxa across their distribution range, and individual colonies may sometimes host several Symbiodiniaceae taxa at a time (Figure 1.3a). The composition of the Symbiodiniaceae communities is mostly driven by the interaction between host identity and environmental conditions (Brener-Raffalli et al., 2018), in particular temperature, light (Cooper et al., 2011; de Souza et al., 2023) and water quality (Matias et al., 2022).

Symbiodiniaceae thermal tolerance varies significantly across genera, species and strains within coral hosts and in culture (Beltran et al., 2021; Buerger et al., 2020; Chan et al., 2023; Levin et al., 2016; Warner & Suggett, 2016). For instance, the *Durusdinium* genus generally shows high thermal tolerance, which has been linked to whole genome duplication (Dougan et al., 2024). As bleaching results from the interaction between host and symbiont physiological damage, the composition of the symbiont community can affect holobiont tolerance to heat stress (Mieog et al., 2009; Sampayo et al., 2008; van Oppen et al., 2009). During heat stress, changes in the relative abundance of taxa (i.e., shuffling, Figure 1.3b) may also occur in favor of more tolerant symbionts (e.g., from the *Durusdinium* genus Berkelmans & van Oppen, 2006; Palacio-Castro et al., 2023; Quigley et al., 2022b). However, shuffling may only be possible for certain species (Stat et al., 2009) and might be temporary depending on the intensity and duration of heat stress exposure (Cunning et al., 2015; Turnham et al., 2025). Since most of the studies relating Symbiodiniaceae community composition to individual bleaching phenotypes were conducted over reduced spatial scales, its contribution to the thermal tolerance of holobionts across their range has rarely been investigated (e.g., Naugle et al., 2024).

Within symbiont species, particular genotypes can be selected by the host micro-environment (Johnston et al., 2022; Reich et al., 2021) or the macro environmental conditions (Bhattacharya et al., 2024), sometimes promoting the adaptation of the holobiont (Howells et al., 2012). Over evolutionary timescale, natural selection of tolerant genotypes may result in genetic adaptation (Figure 1.3c). For instance, inoculation of corals with artificially heat-selected strains of Symbiodiniaceae successfully increased their heat tolerance (Buerger et al., 2020; Chan et al., 2023).

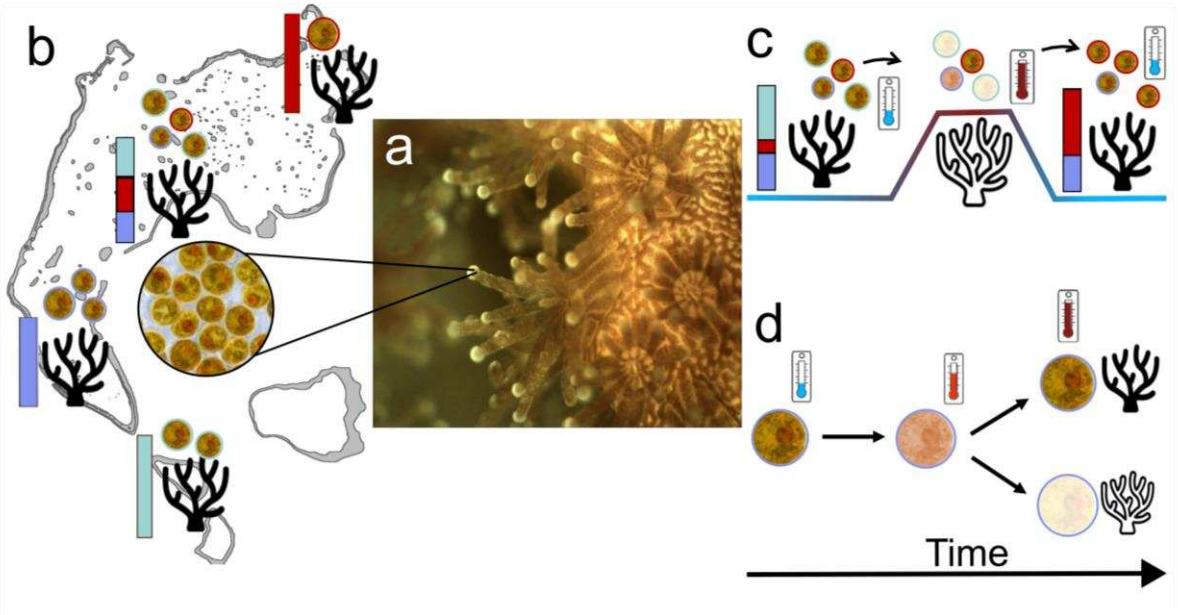


Figure 1.3. The effect of Symbiodiniaceae genetic variation on coral holobionts heat tolerance and thermal adaptation. (a) Coral polyps hosting Symbiodiniaceae cells (©V. Berteaux-Lecellier). (b) Most coral species can host several symbiont taxa across their distribution range, and sometimes a single colony can harbor several symbionts taxa at a time. (c) Corals may undergo changes in their symbiont communities during a period of stress such as marine heatwave and new associations may be transient or last over longer periods. (d) Optimal performing symbionts genotypes under heat stress may be selected during marine heatwaves leading to evolutionary adaptation.

1.4) Identifying genomic markers of heat tolerance

1.4.1 Whole genome sequencing

With the drastic decline in costs of next-generation sequencing technologies over the past decade, genotyping markers across a substantial fraction of individuals genomes is increasingly feasible even in non-model organisms (Lou et al., 2021). Among predominant approaches, reduced representation sequencing (e.g., RAD-seq) and whole genome sequencing (WGS) both allow the identification of genetic polymorphisms but differ greatly in their marker resolution

(Davey et al., 2011). WGS typically yields 0.5 million to millions of SNPS compared to 10–100 thousands for RAD-sequencing (Tam et al., 2019).

Due to its higher marker density, WGS has been claimed to offer a number of advantages over RAD-seq including greater power to detect signatures of selection (Fuentes-Pardo & Ruzzante, 2017). In order to detect adaptive genetic variants, a higher marker density is advantageous because it allows the screening of both neutral and functional polymorphisms. Signals of selection such as reduced nucleotide diversity and linkage disequilibrium (LD) blocks can thus be more readily identified, although the increase in power compared to RAD-seq is likely to vary depending on species and recombination rates (Fuentes-Pardo & Ruzzante, 2017). In addition, whole genome sequencing allows the examination of structural variants (SVs) and mutations in regulatory elements (REs), which are non-coding DNA sequences that control the expression of neighbouring genes (Fuentes-Pardo & Ruzzante, 2017). This provides a better picture of genome-wide genetic variation and a better understanding of its effect on organism fitness as SV and RE can play a strong role in shaping phenotypic diversity (Wittkopp & Kalay, 2012).

The higher versatility and resolution of whole genome sequencing comes however at the price of higher computational and sequencing costs (Tam et al., 2019). In addition, processing pipelines can be more challenging to customize, often involving numerous steps and arbitrary filtering choices, that, if not applied carefully, can significantly impact the results of the analysis (Hemstrom et al., 2024). Nonetheless, new methods and pipelines provide increasingly reliable genotypes (Davies et al., 2016; McKenna et al., 2010) even for medium coverage sequencing. Whole genome sequencing thus provides a great avenue for studying the genomic basis of phenotypic traits and local adaptation but requires careful analytical methods.

1.4.2 Genome wide association studies (GWAS)

Once markers have been genotyped across the genome for a large cohort of individuals, one ‘forward genetic’ approach to identify the basis of phenotypic traits is to conduct GWAS (Tam et al., 2019). This term encapsulates different methods all relying on a common conceptual framework: genomic regions involved in the regulation of a trait are expected to exhibit DNA variations (e.g., mutations, insertions, deletions) that covary to some extent with the trait of interest. In its simplest form, a GWAS consists of running independent linear models for numerous variants across the genome to assess how variation in genotype—such as homozygous reference, heterozygous or homozygous mutant for bi-allelic SNPs—correlates

with changes in a trait. Each test evaluates the alternative hypothesis that a given variant influences the trait, against the null hypothesis that it has no effect.

This approach was primarily invented and used in human medicine—to study the genomic basis of diseases or complex traits (Hirschhorn & Daly, 2005)—and later in agricultural science to improve crops yields (Torkamaneh & Belzile, 2022). With the increasing availability of genomic data, these methods are now gaining considerable traction to study species traits and fitness in the wild (Santure & Garant, 2018). For instance, GWAS has been used to investigate the genomic basis of plant colonization in novel environments (Hamilton et al., 2016), copepod tolerance to changes in salinity (Stern et al., 2022), and polar bears body weight (Malenfant et al., 2018).

Many different methods and tools have been developed to accommodate heterogeneity of studied systems, data availability and research goals when performing GWAS. Some tools rely on a frequentist framework while others use a Bayesian philosophy (Zhou & Stephens, 2014). Other tools rely on genotype likelihoods rather than 'hard called' genotypes to accommodate for uncertainty in genotype calls (Jørsboe & Albrechtsen, 2022). In addition, since most complex traits (including heat tolerance) are highly polygenic, several methods aim to model interactions between genetic variants (i.e., epistasis) through more sophisticated machine learning models (Brieuc et al., 2018; LeBlanc & Pavey, 2023). Other tools allow non monotonic relationships between genotypes and traits (e.g., cases of heterozygous advantage) or handle variant types beyond SNPs (Harris et al., 2024). While all of these advanced approaches offer potentially greater discovery power than a simple linear model, their feasibility depends—among other factors—on the quality of genomic and phenotypic data as well as the cohort sample size, often limiting their application to non-model organisms.

In corals, few studies have applied GWAS so far, primarily due to the difficulty of obtaining both genomic and phenotypic data at sufficient sample sizes. Fuller et al. (2020) conducted a GWAS with natural bleaching associated traits but found no markers with genome-wide significance, possibly due to their low sample size (n<250). A polygenic score (PRS, see section 1.4.5) based on variants effect sizes provided a marginal increase in bleaching prediction accuracy compared to neutral genetic structure, environmental conditions and symbiont's identity. Similarly, Fifer et al. (2024) conducted a GWAS with natural bleaching observations and found no loci with genome wide significance, and variable accuracy of a polygenic score for bleaching resistance and survival across microhabitats. Muller et al. (2025) conducted a GWAS for various phenotypic traits related to growth and photosynthetic efficiency which

resulted in no significant associations. However, their marker density (6,445 SNPs) was limited and some of the traits examined were likely not primarily under host genomic control. Finally, Vollmer et al. (2023) conducted a GWAS on resistance to white band disease, demonstrating that a PRS based on 63 significant SNPs could predict 85% of the variation in disease resistance. The high predictive accuracy of their study, compared to other coral GWAS, may be attributed to the controlled experimental conditions under which phenotypes were measured, the method used to construct the PRS, or to the oligogenic nature of the trait in question.

1.4.3 Gene by environment association studies (GEAs)

GEAs are another promising approach to understand the genomic basis of phenotypic variation in wild populations under the assumption that these populations are locally adapted (Liggins et al., 2020). GEAs are a 'reverse genetics' approach because adaptive phenotypes are not known *a priori*. Instead, this approach seeks statistical associations between allele frequencies and environmental clines to test the hypothesis that allelic variation at a specific locus underlies adaptation to local environments (Lasky et al., 2023). This approach differs from genome scans based on genomic divergence between populations (e.g., F_{st}, D_{xy}) by explicitly examining the correlation between genomic variation and environmental gradients. In theory, with a suitable sampling design that minimizes environmental collinearity, it can identify genomic signals of adaptation to specific environmental factors (Hoban et al., 2016), and thus genomic basis of adaptive phenotypes to these specific environmental conditions (e.g., drought resistance for an association with precipitations).

Similar to GWAS, many statistical methods have been developed to conduct GEAs, including simple linear models, linear mixed models incorporating random effects or controlling for population stratification (Caye et al., 2019) as well as multivariate ordination methods (e.g., redundancy analysis, RDA; Capblancq & Forester, 2021; Capblancq et al., 2018). The latter method which investigates simultaneous changes in allelic frequencies across the genome along multiple environmental clines, has generally proven to exhibit higher performances in terms of power and false discovery rates (Forester et al., 2016; Forester et al., 2018). Other proposed methods under development also seek to accommodate nonlinear associations with the environment (Fitzpatrick & Keller, 2015; Luo et al., 2021) as well as multi-allelic loci (Luo et al., 2021), but are generally computationally limiting.

In corals, several GEAs have been undertaken (Adam et al., 2022; Leiva et al., 2025; Lundgren et al., 2013; Selmoni et al., 2024b; Selmoni et al., 2021; Selmoni et al., 2020a; Thomas et al.,

2017) and have identified candidate genes underlying local adaptation. Some of these studies also predicted maladaptation to future environmental conditions (i.e., genomic offset) based on the contemporary distribution of adaptive variants and future climate projections (Adam et al., 2022). However, candidate markers have rarely been validated for their functional role and effect on fitness, a significant caveat given the high false positive rate of these methods (see section 1.4.4). One exception is the study of Jin et al. (2016) that validated two markers with significant GEA through their additional association with natural bleaching response and antioxidant capacity in *ex-situ* experiments.

1.4.4 Discovery power and controlling for confounding effects

While both GWAS and GEAs are highly valuable to understand the genomic basis of phenotypic traits and environmental adaptation, a number of limitations and caveats need to be considered. In both cases, the power to detect significant associations depends mainly on sample sizes and the genetic architecture of traits, such that causal loci will be easier to detect in oligogenic traits controlled by a few loci of strong effect size and low epistasis (Tam et al., 2019). For GWAS in natural populations, power may also be limited by the accuracy of phenotypic trait measurements, phenotype-by-environment interactions (e.g., acclimatory responses), or other factors affecting the trait (e.g., the microbiome). For GEAs, their power will be affected by environmental autocorrelation (Booker, 2023) as well as the spatial and temporal resolution of available environmental data (Hoban et al., 2016). Furthermore, interactions between demography and genetic architecture can lead to non-monotonic patterns in allelic frequencies of causal variants along environmental clines, making them undetectable by current methods (Lotterhos, 2023).

In addition to discovery power issues, association studies can be also prone to high false positive rates, in particular for GEAs (Rellstab et al., 2015). Indeed, many factors can create patterns of genetic variation that mirror those produced by natural selection, such as demographic history, population structure, isolation by distance (Hoban et al., 2016; Samuk et al., 2017; Tam et al., 2019), and heterogeneous recombination or mutation rates across the genome (Ravinet et al., 2017). Population structure (or the relatedness between individuals) is a primary concern when conducting association studies in wild species because genetic variation resulting from demographic processes and drift will inevitably occur when sampling distant populations with limited gene flow (Rellstab et al., 2015). Methods exist to account for these effects including using latent factors or conditional effects in GEAs (Capblancq & Forester, 2021; Caye et al.,

2019) or kinship matrices and conditional effects in GWAS (Zhao et al., 2012; Zhou & Stephens, 2014). In the context of GEAs, controlling for neutral population structure has been criticized for its tendency to increase false negative rates, as both neutral and adaptive genetic variation are expected to occur primarily along main environmental gradients (Lind & Lotterhos, 2024). The choice of models depends on the context, but the demographic history of populations and confounding factors need to be carefully evaluated before conducting association studies.

1.4.5 Combining methods and markers validation

Because it is inherently difficult to differentiate correlated variants from causal variants in association studies, combining GWAS and GEAs may increase confidence in the functional relevance of candidate markers. When the same genomic regions and/or loci are detected in both approaches, it is more likely that they are effectively involved in local adaptation through the measured trait (Lasky et al., 2023).

For definitive validation, genetic editing tools (e.g., CRISP-Cas9) can be used to create knock-out lines and validate the markers function *in-vitro*. For instance, Luo et al. (2025) validated two GEA candidates in *A. thaliana* lines by demonstrating a genotype-by-environment interaction of mutant lines on fitness. However, this method can be complicated in cases of polygenic traits, or when variants with significant associations are in linkage disequilibrium with an unknown true causal variant.

When the statistical power to detect causal loci is limited or individual validation of candidate markers is difficult, polygenic risk scores (PRS) that incorporate the effect sizes of loci are a suitable approach for assessing genome-wide effects. Although PRS generally assume additive effects, they can also account for non-linear relationships with the phenotype or interactions between loci (Deans et al., 2023). The predictive accuracy of PRS can be assessed using cross-validation, and ideally using independent datasets (Slavov et al., 2024).

1.4.6 Contributions of GWAS and GEAs to heat tolerance genetics

GWAS and GEAs have substantially improved our understanding of the genetic architecture of heat tolerance across diverse biological systems. A major advantage of these methods is that they can be applied to outbred populations, extending their use beyond classical model and cultivated species and enabling the study of trait genetics without controlled crosses (Cortés et

al., 2022; Porcelli et al., 2015). By leveraging higher marker density and increased statistical power, these studies have confirmed that heat tolerance is highly polygenic, involving tens to thousands of loci, and have allowed finer localization of functional genetic variants than was possible with traditional QTL mapping (Longmei et al., 2021; Maulana et al., 2018; Yan et al., 2023; Yu et al., 2021).

GWAS results suggest that a large fraction of variants underpinning heat tolerance lies in non-coding regions such as enhancers or promoters (Ma et al., 2021), consistent with observations for other complex traits (Tak & Farnham, 2015). These approaches have also uncovered or confirmed additional mechanisms contributing to heat tolerance beyond canonical pathways, including signalling pathways and mitochondrial processes (Compton et al., 2023; Hu et al., 2022; Kim et al., 2018). Importantly, GWAS and GEAs have shown that the genetic architecture of many traits—likely including heat tolerance—is context-dependent, varying with life stage and environmental conditions (Huang et al., 2020; Pallares et al., 2023). Finally, GEAs have corroborated the functional relevance of candidate variants affecting heat tolerance by detecting signatures of climate selection in wild populations (Cortés et al., 2022; Ferris et al., 2021; Lasky et al., 2023).

1.4.7 Applications to conservation and restoration

Genomic markers or polygenic scores have the potential to improve the identification of heat tolerant individuals or populations, as well as the design of eco-evolutionary management strategies (Colton et al., 2022; Howells et al., 2022b). For instance, reefs with a high abundance of tolerant genotypes that also a source of larvae to neighbouring reefs can be prioritized for protection from local stressors such as water eutrophication, disease introduction, mass tourism and overfishing (van Woesik et al., 2022). This is expected to maximize local survival and biodiversity, and boost the spread of heat adaptive larvae to neighbouring reefs (Mumby et al., 2021; Quigley et al., 2022a). The spatial mapping of adaptive genetic variation can also be integrated into demographic models to estimate rates of adaptation (Bay et al., 2017; Bozec et al., 2025; Kubicek et al., 2019; Logan et al., 2021; Matz et al., 2020; McManus et al., 2021; McManus et al., 2020) and predict climate genetic vulnerability (Adam et al., 2022), both of which can guide conservation strategies.

Information on the heat tolerance of individuals through biomarkers could be further integrated into approaches aimed at rehabilitating degraded populations using conventional asexual (Boström-Einarsson et al., 2020) and sexual propagation (Sellares Blasco et al., 2021), although

this is likely only feasible for small reef areas with high ecosystemic value (Hughes et al., 2023). They can also be used for novel interventions such as selective breeding (Howells et al., 2021; Humanes et al., 2021; Quigley et al., 2020a) and subsequent seeding of reefs with heat-adapted larvae (dela Cruz & Harrison, 2017). Finally, biomarkers could inform biobanking initiatives (e.g., cryopreservation) to ensure the conservation of adaptive genetic variation in endangered species (Hagedorn et al., 2021; van Oppen et al., 2017).

1.5) Study systems and focal species

1.5.1 New Caledonia and the Great Barrier Reef

The Great Barrier Reef (GBR) and New Caledonian reefs are both UNESCO World Heritage sites located in the Western Pacific, on opposite sides of the Coral Sea (Figure 1.4). The GBR extends along the northeastern coast of Australia over an area of approximately 344,400 km^2, while New Caledonia reefs located on the eastern side of the Coral Sea encompass 4,500 km^2. Both reef systems contain a wide diversity of reef structures (e.g., fringing reefs, single barrier reefs, multiple barrier reefs, atolls with lagoons, raised atolls, and coral banks) and are home to an extensive biodiversity with over 410 species of hard coral on the GBR (Richards & Day, 2018) and over 390 species of hard corals in New Caledonia (Payri et al., 2019).

The dominant oceanographic circulation in the Western Pacific is the westward-flowing South Equatorial Current (SEC). The SEC bifurcates into two branches east of New Caledonia, with the main northern branch contributing to the westward North Caledonia Jet (NCJ), which flows towards the east coast of Australia. The NCJ then splits into the northern New Guinea Coastal Current and the southern East Australia Current (EAC). In turn, branches of the EAC known as the Subtropical Countercurrent (STCC) flow back eastward to New Caledonia (Payri et al., 2019).

While no area is unaffected by climate warming, differences in warming rates and MHW occurrence have led to distinct bleaching histories between the two reef systems. On the GBR, mass bleaching was observed in 1998, 2002, 2006, 2016–2017, 2020 (Hughes et al., 2021), 2022 (McGowan & Theobald, 2023) and 2024 (Cantin et al., 2024), but these events differed greatly in terms of intensity and associated mortality. For instance, the GBR lost 30% of coral cover as a result of the 2016–2017 bleaching (Hughes et al., 2018), but less than 10% in 2020 (Page et al., 2023). In New Caledonia, rare minor bleaching observations were reported in 1983,1996, 1998, 2008 and 2014, but these lacked consistent methods and trained observers

(Payri et al., 2018; Virgen-Urcelay & Donner, 2023). Major bleaching also occurred in 2016, when many reefs experienced bleaching, but 70–80% of colonies monitored at three southern sites recovered and survived (Payri et al., 2018).

Several global meta-analysis and modeling studies have identified New Caledonia reefs and the southern GBR as a temporary refugia from climate warming, due to their high coral cover and low occurrence of bleaching until recently (Shlesinger & van Woesik, 2023), the low projected decrease in coral cover (Sully et al., 2022), and as potential sinks for heat-adapted larvae (Matz et al., 2020). Therefore, understanding the distribution of standing adaptive variation and gene flow within and among these systems could help to re-assess these projections.

1.5.2 Study sites

A total of 29 reefs were sampled across the Coral Sea (Figure 1.4). These reefs were chosen on the GBR to maximise thermal, latitudinal and cross-shore gradients, in order to sample colonies adapted to distinct local environments (Figure 1.5). In addition, sites selection was influenced by known distribution of this coral species and accessibility. In New Caledonia, sites were also chosen to maximize environmental gradients following Selmoni et al. (2020b), with a focus on the western coast of New Caledonia Grande Terre and the Chesterfield-Bellona plateau, as we were primarily interested in the Coral Sea region (Figure 1.6). Overall, study sites encompassed a wide variety of reef structures including reef bommies, upper reef slopes, fringing reefs, lagoons and reef flats.

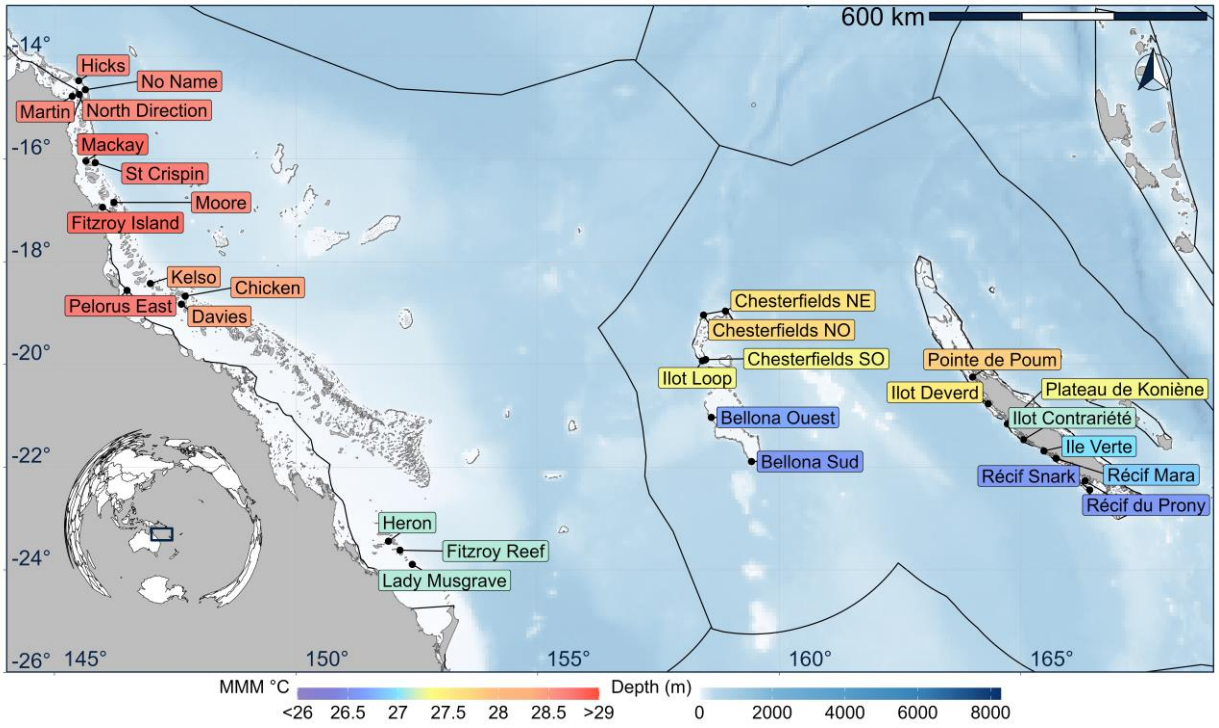


Figure 1.4. Map of the 29 reefs where *Acropora spathulata* colonies were sampled across latitudinal and thermal gradients of the GBR and of New Caledonia. Reefs labels are coloured by their sea-surface temperature Maximum Monthly Mean (MMM, 1985–1990+1993 climatology as defined by NOOA; Liu et al., 2003). Solid lines indicate Exclusive Economic Zone boundaries.

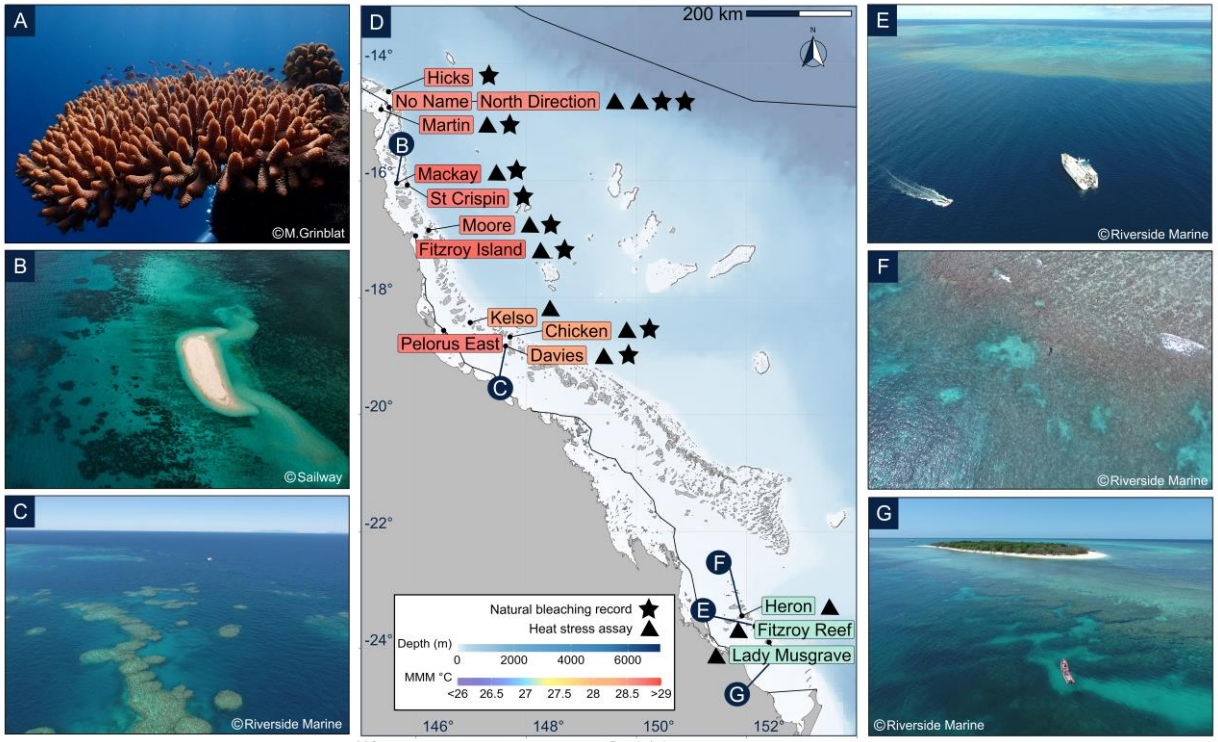


Figure 1.5. Detailed map of the 15 reefs where *Acropora spathulata* colonies were sampled on the GBR. Reefs labels are coloured according to the Maximum Monthly Mean of sea-surface temperatures (MMM, 1985–1990+1993 climatology as defined by NOOA; Liu et al., 2003). Triangle shapes indicate reefs where acute stress assays were performed (Chapter 2), and star shapes indicate reefs where natural bleaching observations were collected in 2024 (Chapter 4). (a) Representative images of the reef-building coral *Acropora spathulata* at Fitzroy Reef, Australia (credit M. Grinblat 2022). (b-g) Fieldwork pictures taken at various reef sites across the GBR (credit Sailway, Riverside Marine).

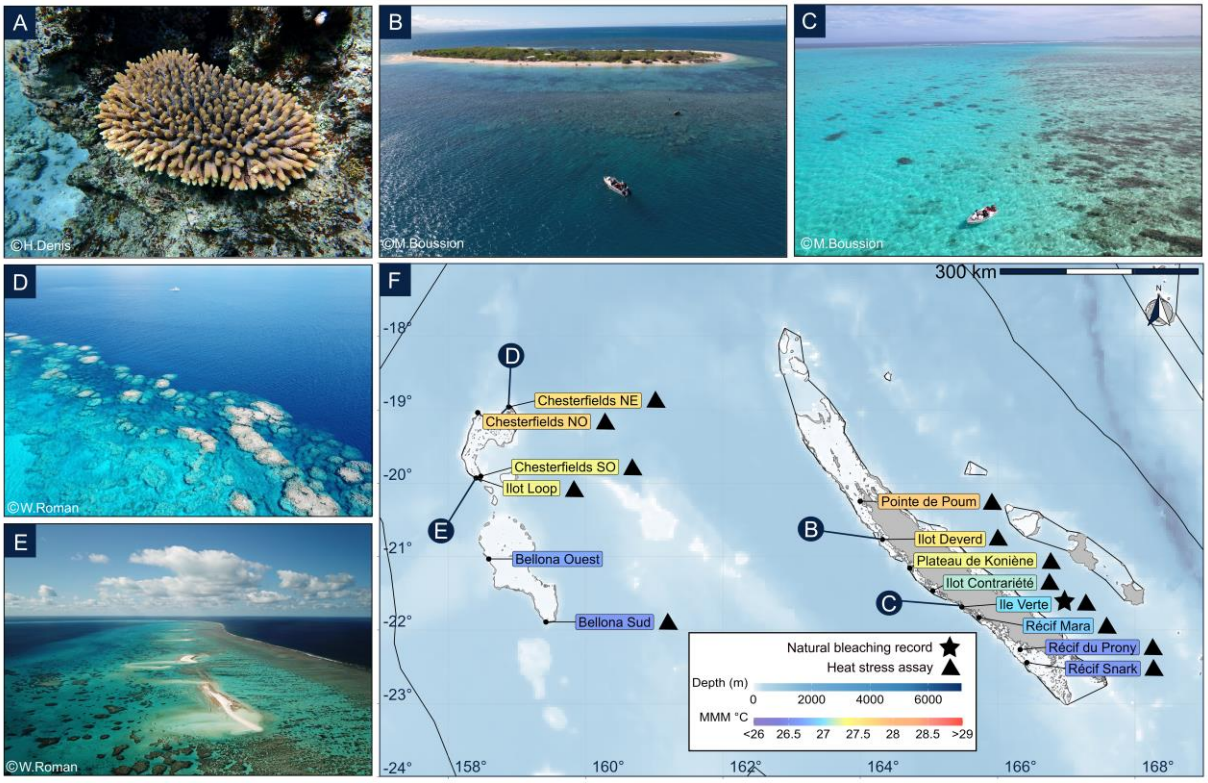


Figure 1.6. Detailed map of the 14 reefs where *Acropora spathulata* colonies were sampled in New Caledonia. Reefs labels are coloured according to the Maximum Monthly Mean of sea-surface temperatures (MMM, 1985–1990+1993 climatology as defined by NOOA; Liu et al., 2003). Triangle shapes indicate reefs where acute stress assays were performed (Chapter 3) and star shape indicate reefs where natural bleaching observations were collected in 2024. (a) Representative images of the reef-building coral *Acropora spathulata* at Ilôt Contrariété, New Caledonia (credit H. Denis 2023). (b-e) Fieldwork pictures taken at various reef sites across NC and CB (credit W. Roman, M. Boussion and H. Denis).

1.5.3 *Acropora spathulata*

Acropora spathulata is a corymbose species of the Acroporidae family found in shallow waters on reef flats, lagoons and upper slopes (Figure 8a; Cooper et al., 2011; Wallace et al., 2012). Colonies can reach over 50cm in diameter (Pisapia et al., 2014) with thick colony branches that provide important structural complexity on the reef and habitat for many species, including fishes and invertebrates (Figure 1.7a). This species is distributed in the Coral Sea region, from the GBR to Papua New Guinea and Fiji (Figure 1.7b). This species is listed on CITES Appendix II.

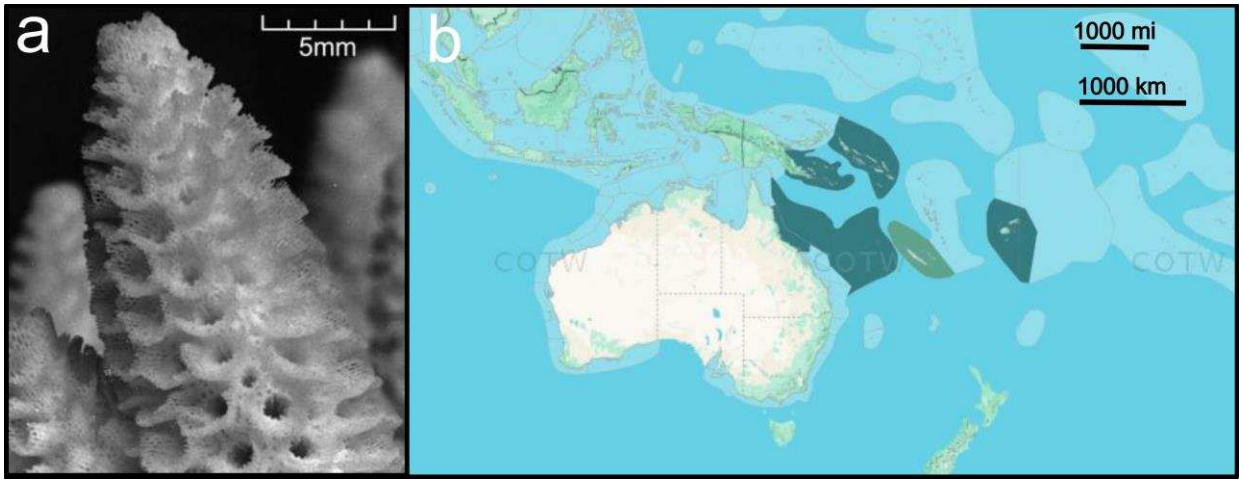


Figure 1.7. Morphology and distribution of *Acropora spathulata*. (a) Detailed picture of *Acropora spathulata* skeleton morphology and radial corallites on the Great Barrier Reef (© Veron archives). (b) *Acropora spathulata* confirmed (dark green) and strongly predicted (light green) distribution in the Coral Sea (© Corals of the World).

A. spathulata is an iteroparous simultaneous hermaphrodite (Baird et al., 2009b) with a broadcast spawning mode. It is known to undergo synchronous spawning events (Baird et al., 2002) at night around 21:00-22:00 on the GBR (van Oppen et al., 2002). Spawning usually occurs a few days after the full moon of October/November at warmer inshore reefs and November/December at cooler mid-shelf and offshore reefs on the GBR (V. Mocellin personal communication), and is expected to occur in November/December in NC. Fecund coral colonies can produce 4–8 oocytes per polyp (Pratchett et al., 2019), which are released along sperm and fertilized in the water column. The resulting larvae have a pelagic larval duration estimated from lipid reserves at ~100 days (Graham et al., 2013), suggesting that they can disperse across large distances. After settling on the reef and undergoing metamorphosis, coral juveniles grow and reach sexual maturity within a few years. Although no estimate of the age at first sexual maturity is available for this species, the closely related species *A. millepora* is known to reach sexual maturity at 3 years, with colonies ranging from 5 to 16 cm in diameter (Baria et al., 2012; Bonilla et al., 2023; Craggs et al., 2020). Its longevity is also unknown, but longevity estimates from somatic mutations indicate that other *Acropora* species can live between 60 and several hundred years old (Irwin et al., 2017).

A. spathulata colonies produce azooxanthellate eggs and newly settled juveniles acquire symbionts horizontally from the environment (van Oppen et al., 2001). The only studies characterizing the symbionts of *A. spathulata* have been conducted in the central GBR, and have found that Symbiodiniaceae communities were dominated by the genus *Cladocopium*,

specifically the ITS2-variants C3k and Cspc (Epstein et al., 2019; van Oppen et al., 2001). However, different Symbiodiniaceae genera have been shown to exert a strong effect on the thermal tolerance of the early life history stages of *A. spathulata* in inoculation experiments (Quigley et al., 2020a). This suggests that symbiont identify may influence the thermal tolerance of individuals in the wild. Further research is needed to evaluate the level of specificity of this symbiosis across *A. spathulata* distribution range and its influence on the holobiont response to heat stress.

Strong differences in the thermal thresholds of *A. spathulata* have been measured between latitudes (>4 °C in larvae survival thresholds; Woolsey et al., 2013) and these differences are partly heritable (Quigley et al., 2020a; Quigley et al., 2020b). In addition, strong intraspecific physiological variation has been reported across small spatial scales, suggesting that natural selection could promote adaptation (Pisapia et al., 2014). However, the causes of this variation are unknown, thus further studies are required to identify the genomic drivers of heat tolerance and quantify adaptive genetic variation.

1.6) Thesis outline and research questions

My objectives in this thesis were to evaluate the resilience and adaptive potential of the corymbose branching coral *Acropora spathulata* to rising sea temperatures in the Western Pacific, and to uncover the genomic basis underlying variation in its heat tolerance across spatial scales. Such knowledge is essential to refine projections of coral futures in warming oceans, and foster the integration of evolutionary adaptation into conservation and restoration frameworks. The specific objectives and research questions for each chapter of this thesis are provided below:

How variable is heat tolerance within a single coral species, and how is its distribution influenced by past and recent environmental conditions?

Chapter 2 describes the variation in acute heat tolerance traits of the common coral *Acropora spathulata* among and within reefs of the GBR. Several phenotypic traits were measured in controlled rapid heat stress experiments and their variation was examined in relation to contemporary and historical environmental conditions. Results demonstrate substantial variation in acute heat tolerance among individuals across spatial scales and reveal the combined influence of short-term environmental memory and long-term local adaptation on

this variation. Moreover, distinct traits reflecting the responses of different holobiont partners modulate the observed patterns of variation, and influence the ranking of individual's tolerance.

Are the variation and distribution of heat tolerance consistent across reef systems?

Chapter 3 measures the variation in acute heat tolerance across other reef systems and environmental gradients in New Caledonia. The extent and distribution of heat tolerance variation were compared with patterns observed on the GBR. Results show a consistent magnitude of variation in acute heat tolerance and further underscore the adaptation of populations to their local environment. The challenges of applying rapid heat stress assays in the context of recurrent marine heatwaves are highlighted.

How do the genetic structure, diversity and connectivity of holobionts shape their resilience potential across the Western Pacific?

Chapter 4 investigates the population genetics of *A. spathulata* hosts and symbionts across the GBR, New Caledonia and Coral Sea atolls. Whole genome sequencing was used to assess the genetic structure, effective population sizes and dispersal capacity of coral hosts. Furthermore, variation in their associated Symbiodiniaceae was characterised, and demographic inferences were used to reconstruct divergence history and gene flow among reef systems. The results identify distinct *Cladocopium* taxa associated with coral hosts across environmental gradients, large effective population sizes, and realized generational dispersal, and provide first insights into pervasive gene flow among these reef systems. Overall, these results suggest substantial resilience and evolutionary rescue potential of these populations under disturbances.

What is the genomic architecture of heat stress responses across thermal regimes, from acute stress to natural marine heatwaves and climates? Have geographically distant populations evolved similar genetic adaptations to heat stress? Can genomes improve predictions of coral bleaching and survival?

Chapter 5 examines genetic variation associated with heat stress responses and local thermal adaptation. Association studies with phenotypes and thermal environments were conducted to reveal candidate markers and regions involved in heat tolerance across populations. In addition, various modelling approaches were employed to assess the utility of polygenic risk scores in predicting bleaching susceptibility and survival outcomes. Results suggest that genetic drivers of heat stress response depend on the type of thermal exposure and are mainly non-parallel across populations. However, key genes across the thermal tolerance landscape, linked to

diverse thermal stress responses or shared among populations, are identified. Finally, candidate loci for local thermal adaptation improve predictions of coral bleaching and survival phenotypes in the wild under marine heatwaves.

How do novel insights into the variation and genetic architecture of heat tolerance and eco-evolutionary processes inform the outlook for these coral populations?

Chapter 6 synthesizes the main findings of my thesis and their implications for the resilience and adaptive potential of *Acropora spathulata* populations in the Western Pacific. The key takeaways for the conservation and restoration of Acroporidae populations in the region are further emphasized. Novelties and caveats of this work are highlighted and discussed to inform the design of future association studies in corals. Finally, I discuss the major remaining gaps and research priorities to better understand the evolutionary adaptation potential of reef-building corals to climate warming.

Chapter 2. Thermal tolerance traits of individual corals are widely distributed across the Great Barrier Reef



Thermal tolerance traits of individual corals are widely distributed across the Great Barrier Reef

Chapter 1 describes the importance of within-species variation in heat tolerance for reef-building corals trajectories under rapid climate warming, and the need for standardised measurements of this variation across individuals, reefs and regions. Within this framework, Chapter 2 uses acute heat stress assays to quantify heat tolerance traits variation across spatial and environmental gradients of the Great Barrier Reef. The chapter examines how different host and symbiont traits influence the ranking of heat tolerance among individuals, and the role of environmental factors in shaping the distribution of these traits. Chapter 2 was published in *Proceedings of the Royal Society B: Biological Sciences* (Denis et al., 2024a):

Denis, H., Bay, L. K., Mocellin, V. J., Naugle, M. S., Lecellier, G., Purcell, S. W., Berteaux-Lecellier, V., & Howells, E. J. (2024a). Thermal tolerance traits of individual corals are widely distributed across the Great Barrier Reef. *Proceedings B*, 291(2030), 20240587.

The results from this chapter were subsequently used in Chapter 5 to perform genome-wide association studies (GWAS) with host genomes.

Thermal tolerance traits of individual corals are widely distributed across the Great Barrier Reef

Hugo Denis[1,2,3], Line K. Bay[4], Véronique J. L. Mocellin[4], Melissa S. Naugle[3], Gaël Lecellier[1,5], Steven W. Purcell[3], Véronique Berteaux-Lecellier[1] and Emily J. Howells[3]

[1] UMR250/9220 ENTROPIE (IRD-CNRS-UR-IFREMER-UNC), Promenade Roger-Laroque, Noumea Cedex, New Caledonia, France

[2] ED 129, Sorbonne Université, 4, Place Jussieu, Paris 75252, France

[3] National Marine Science Centre, Southern Cross University, Coffs Harbour, New South Wales, Australia

[4] Australian Institute of Marine Science, Townsville, Queensland, Australia

5 Institut de Sciences Exactes et Appliquées (ISEA) EA7484, 145, Avenue James Cook, Nouméa BP R4 98 851, New Caledonia

2.1) Abstract

Adaptation of reef-building corals to global warming depends upon standing heritable variation in tolerance traits upon which selection can act. Yet limited knowledge exists on heat-tolerance variation among conspecific individuals separated by metres to hundreds of kilometres. Here, we performed standardised acute heat-stress assays to quantify the thermal tolerance traits of 709 colonies of *Acropora spathulata* from 13 reefs spanning 1060 km (9.5° latitude) of the Great Barrier Reef. Thermal thresholds for photochemical efficiency and chlorophyll retention varied considerably among individual colonies both among reefs (approximately 6 °C) and within reefs (approximately 3 °C). Although tolerance rankings of colonies varied between traits, the most heat-tolerant corals (i.e. top 25% of each trait) were found at virtually all reefs, indicating widespread phenotypic variation. Reef-scale environmental predictors explained 12–62% of trait variation. Corals exposed to high thermal averages and recent thermal stress exhibited the greatest photochemical performance, probably reflecting local adaptation and stress pre-acclimatization, and the lowest chlorophyll retention suggesting stress pre-sensitization. Importantly, heat tolerance relative to local summer temperatures was the greatest on higher latitude reefs suggestive of higher adaptive potential. These results can be used to identify naturally tolerant coral populations and individuals for conservation and restoration applications.

2.2) Introduction

Global warming modifies species' thermal environments (Masson-Delmotte et al., 2022) and directly impacts organism fitness (Angilletta et al., 2003). The persistence of species and the ecosystem services they provide, therefore, depend on their response to rising and extreme temperatures. Yet, considerable intraspecific variation in thermal tolerance exists in marine ecosystems (Bennett et al., 2019) as some species have colonized wide geographical areas spanning large thermal gradients (Reusch, 2014). Individuals can adjust to local temperatures within their lifespan through physiological acclimatization and selection for particular phenotypes within populations can lead to genetic adaptation across generations (Somero, 2010). Documenting phenotypic differences along thermal gradients can thus inform conservation and restoration efforts (Anthony et al., 2020) by improving predictions of species adaptive potential (Bennett et al., 2019), climate refugia (Lachs et al., 2023b) or extinctions (Sinervo et al., 2010).

Reef-building (scleractinian) corals are among the organisms most at risk from global warming as they occupy narrow thermal niches in environments where current summer temperatures often approach and increasingly exceed their upper thermal limits (Hughes et al., 2017). The energetic requirements of corals rely on a finely tuned symbiotic relationship with photosynthetic dinoflagellates (family Symbiodiniaceae; LaJeunesse et al., 2018) that can be severely impaired under heat stress (Hoegh-Guldberg et al., 2007), triggering a loss of symbiont cells and/or their photosynthetic pigments known as coral bleaching (Oakley & Davy, 2018; Roberty & Plumier, 2022). Increasingly frequent mass bleaching events have been observed over the past four decades (Hughes, 2018; Hughes et al., 2021) and are predicted to have impacted >70% of the world's coral reefs (Virgen-Urcelay & Donner, 2023), leading to widespread coral mortality (De'ath et al., 2012; Riegl et al., 2018). Understanding the extent of variation in coral heat tolerance across phylogeny, space and time is, therefore, crucial to predict the future of these ecosystems (Cornwall et al., 2023; Dixon et al., 2022; Matz et al., 2020; Sully et al., 2022).

Intraspecific variation in coral heat tolerance exists at local scales (Cunning et al., 2016; Drury et al., 2022a; Drury et al., 2022b; Jin et al., 2016; Marhoefer et al., 2021; McWilliam et al., 2022; Sampayo et al., 2008) and is an indicator of adaptive capacity and metapopulation persistence probability (Holstein et al., 2022; Howells et al., 2022b). Populations with low intraspecific variation may risk extirpation at local scales (Álvarez-Noriega et al., 2023; Hughes

et al., 2018; Riegl et al., 2018). On the contrary, high intraspecific variation in physiological traits can buffer populations against the loss of genetic and functional diversity (McWilliam et al., 2022). The thermal tolerance traits of individual corals are shaped by the interaction between the environment (i.e. their thermal history (Hughes et al., 2019; Schoepf et al., 2021; Thompson & van Woesik, 2009) but also other factors such as irradiance (Gonzalez-Espinosa & Donner, 2021), hydrodynamic regimes (Page et al., 2019), nutrients (Wiedenmann et al., 2013) and water oxygen content (Alderdice et al., 2022)) and a continuum of biological mechanisms including phenotypic plasticity (DeCarlo et al., 2019; Hackerott et al., 2021), heritable genetic effects (Bairos-Novak et al., 2021; Howells et al., 2021; Jin et al., 2016) and/or differences in symbiont communities (Berkelmans & van Oppen, 2006; Howells et al., 2016; Sampayo et al., 2008; Thomas et al., 2018). Yet, further research is required to understand the relative importance of these drivers for current and future responses to marine heatwaves.

Quantifying intraspecific variation in thermal thresholds during natural marine heatwaves is challenged by differences in heat-stress magnitude and duration over space and time and the technical constraints of surveying large spatial areas during a single heatwave event. Consequently, controlled experiments have been widely used to characterise intraspecific variation in thermal tolerance among reefs (Cornwell et al., 2021; Evensen et al., 2022; Marzonie et al., 2022; Shaw et al., 2016; Voolstra et al., 2021b), habitats (Marhoefer et al., 2021; Thomas et al., 2018; Voolstra et al., 2020) and individuals (Humanes et al., 2022; Kavousi et al., 2020). Recently, acute heat-stress assays (<48 h) have been developed to measure individual thermal thresholds in a standardised, high-throughput and cost-effective manner (Barshis et al., 2013; Cornwell et al., 2021; Cunning et al., 2021; Evensen et al., 2021; Evensen et al., 2022; Klepac et al., 2024; Marzonie et al., 2022; Morikawa & Palumbi, 2019; Voolstra et al., 2020; Voolstra et al., 2021b). Thermal tolerance rankings were shown to yield consistent results across weeks (Walker et al., 2022a), seasons (Cunning et al., 2021) and with long-term heat stress (Evensen et al., 2021; Voolstra et al., 2020) although recent studies suggest that responses to long-term and short-term heat stress might differ at the individual level (Humanes et al., 2024; Klepac et al., 2024). In these experiments, coral heat tolerance has been mostly inferred from photochemical efficiency (F_v/F_m), a common proxy of bleaching onset (Jones et al., 2000). However, the role of symbiont photochemical damage in bleaching initiation has been increasingly questioned (Gardner et al., 2017; Krueger et al., 2015) and can be offset by host protective mechanisms (Baird et al., 2009a; Oakley & Davy, 2018; Roberty & Plumier, 2022) stressing the importance of relating F_v/F_m measurements to subsequent coral bleaching

responses (i.e. the loss of symbiont cells and/or chlorophyll). To date, heat-stress assays have investigated the response from a few colonies at many reefs (e.g. (Marzonie et al., 2022)) or many colonies at a few reefs (e.g. (Humanes et al., 2022)), but have not yet evaluated intraspecific variation across multiple spatial scales.

To address the aforementioned knowledge gaps, we used acute heat-stress assays to measure photochemical efficiency and bleaching traits in 768 colonies of *Acropora spathulata* from 14 reefs spanning 1060 km (approximately 9.5° latitude) of the Great Barrier Reef (GBR, Figure A1.1). *Acropora spathulata* is an abundant corymbose species found on reef flats and upper slopes that builds ecologically important structural complexity on the GBR (Figure A.1.1d; Wallace et al., 2012). We identify reefs where heat-tolerant individuals are most likely to be found and use multiple environmental datasets from satellite observations and numerical models to determine environmental predictors of tolerance traits. The large sample size of this study provides GBR-wide information to inform conventional management via spatial and temporal protection and novel interventions, including seeding heat-tolerant corals onto reefs.

2.3) Methods

2.3.1 Study sites, experimental design and set-up

(i) Study sites and sample collection

We sampled 768 colonies of *A. spathulata* across 14 reefs of the GBR (Figure A1.1). At each reef, 40−60 colonies were sampled on SCUBA from one or two sites (covering 50−4200 m^2) between 28 February and 26 March 2022 (GBRMPA permit G21/45166.1) over a single or two consecutive days. Colonies were sampled from the upper reef slope to reef flat over a total depth range of 5 m across the GBR, and we avoided sampling neighbouring colonies of identical pigmentation to reduce the likelihood of sampling clonemates. For each colony, 12 nubbins (approximately 7 cm) were collected for standardised acute heat-stress experiments and *in situ* metadata was recorded. This included colony-level GPS coordinates linked to *in situ* photographic records (Lukoschek et al., 2016), time-corrected depth (average = 0.51 ± 1.3 m relative to the lowest astronomical tide) and visual pigmentation (Coral Watch Health Chart scores at 0.5 intervals; Siebeck et al., 2006). Colonies showing signs of disease were rarely encountered but intentionally excluded to avoid physiological bias unrelated to temperature effects.

(ii) Acute heat-stress assay design

A portable automated experimental system ('Seasim-in-a-box', National Sea Simulator, Australian Institute of Marine Science; Figure A1.6) was modified from Marzonie et al. (2022) to conduct acute heat-stress assays onboard a research vessel the day following collection (supplementary material and methods). The experimental design consisted of three replicate tanks for each of four temperature treatments of 0 (control), 3, 6 and 9 °C above the local MMM, 1985–1990+1993 climatology as defined by NOAA (Liu et al., 2003) for each reef site. These treatments were designed to elicit increasing levels of thermal stress following Voolstra et al. (2020). Immediately after collection, 12 nubbins from each coral colony were mounted on separate experimental racks with unique identifiers and held overnight at ambient seawater temperature. The following morning, one nubbin from each colony was randomly assigned to each of the 12 tanks (Figure A1.1b). Assays started at 11:00am in the morning and consisted of 3 h ramp-up from ambient temperature (within 1 °C of the MMM) to target temperature, 3 h hold at the target temperature, 2 h ramp-down to MMM and a final approximately 12 h hold at MMM (Figure A1.1c). During the experiments, temperatures in individual tanks were recorded at 1-min intervals using HOBO loggers (Onset) and closely matched their target profiles (meanΔT = 0.36 °C; Table A1.2) with the exception of one site which was removed from further analyses (St Crispin: meanΔT = 1.61 °C).

2.3.2 Phenotypic traits

(i) Photochemical efficiency

The maximum quantum yield of photosystem II (F_v/F_m) of coral photosymbionts (Symbiodiniaceae) was used as an initial rapid, non-invasive measure of heat tolerance. A decline in F_v/F_m reflects early physiological impairment in corals and has been reported to respond consistently between acute and long-term heat exposures (Evensen et al., 2021; Voolstra et al., 2020); but see Klepac et al. (2024) and (Humanes et al., 2024). Measurements were taken 2 h after the end of temperature ramp-down (>1 h dark adaptation) using an Imaging PAM chlorophyll fluorometer (IMAG-K7, Walz Germany) with the following settings: measuring light = 2 (freq = 1), saturation pulse = 7 (int = 30 s), damp = 1, gain = 1. For each fragment, three measurements were extracted from non-overlapping areas and underwent several quality checks and filtration steps (supplementary material and methods). After filtration, a total of 709 colonies and 7847 fragments were retained in further analyses.

(ii) Hyperspectral image-based assessment of chlorophyll content

Non-invasive estimates of chlorophyll content were used as a second metric of heat tolerance. The loss of chlorophyll underpins visual bleaching scores commonly used in acute heat-stress experiments and has been shown to correspond with mortality risk (Walker et al., 2022a). The total chlorophyll content was assessed in fragments from reflectance measurements taken 11 h after the end of the temperature ramp-down using a hyperspectral camera (Resonon, Pika XC2) with the following settings: integration time= 39.2 ms, gain = 0, frame rate = 22 fps. MATLAB software was used to compute the normalised difference vegetation index (NDVI; supplementary material and methods) from reflectance measurements, where NDVI = $(R720 - R670)/(R720 + R670)$ and R_x is the reflectance at x nm. NDVI is a proxy for chlorophyll used in a wide range of organisms including scleractinian corals (Wijgerde et al., 2014) and has been validated in the soft coral *Sarcophyton* cf. *glaucum* (Leal et al., 2015). We repeated this validation in *A. spathulata* using spectrophotometric determination from tissue extractions (Ritchie, 2008) with a strong relationship between NDVI and log-transformed chlorophyll-a ($R^2 = 0.74$; supplementary materials and methods, Figure A1.7).

2.3.3 Phenotypic data analysis

All statistical analyses were conducted using R v. 4.0.4 and figures created using package *ggplot2* and Inkscape v. 1.2. The response of raw F_v/F_m and NDVI measurements to temperature across experiments was first assessed with a linear mixed-effect model using the package *lme4* (Bates et al., 2014) (supplementary material and methods). The model results confirmed that the tank had a minor effect on phenotypic measurements (explained by 1.7% of F_v/F_m random variance σ^2 and 0.8% of NDVI σ^2; Table A1.3). Likewise, the coral fragment size effect was negligible ($B = 1.2 \times 10^{-6}$ for F_v/F_m and $B = 8.5 \times 10^{-6}$ for NDVI; Table A1.3). These factors were thus discarded from further analyses and phenotypic measurements were used to compute metrics of heat tolerance.

(i) ED50 thermal thresholds

For each colony, the decrease in F_v/F_m and NDVI was modelled over temperature treatments using dose–response curves in the R package `drc` (Ritz et al., 2015). Colonies with <2 fragments per treatment after previous quality control filtering (supplementary material and methods) were excluded to ensure robust estimates of individual responses across treatments (excluded colonies: F_v/F_m = 94, NDVI = 4). All models were fitted using the `drm` function

based on the mean hold temperature recorded within each tank for each experiment, with constraints set on parameters (Figure A1.8a). The best model (Weibull type II with three parameters) was chosen as the one with the lowest Akaike's information criterion score for most reef sites using the `mselect` function (6/13 and 11/13 reefs for F_v/F_m and NDVI, respectively; supplementary material). Because using the same model is a prerequisite to compare ED50s, we used this model for all colonies even though some curves showed a better fit to log-logistic or quadratic models. The model equation is

$$f(x; b, d, e) = d(1 - \exp\,(-\exp\big(b(\log(x) - \log(e))\big))$$

where b is the steepness of the curve, d is the upper asymptote (lower asymptote set to 0) and e is the inflexion point. An example of dose–response curves can be found in Figure A1.8. Dose–response curves were filtered to remove individuals that showed poor fit to the data, notably when the decline in phenotypic traits was minor or absent up to +6 °C or +9 °C resulting in ED50s with wide confidence intervals (supplementary material and methods) which may have filtered out some of the most heat-tolerant individuals. After filtration 615 and 675 colony-level ED50 estimates were retained for F_v/F_m and NDVI, respectively.

(ii) Performance retention under thermal stress

Performance retention under extreme heat was computed as

$$Xi_{MMM+9/MMM} = (Xi_{MMM+9}/Xi_{MMM})\,x\;((Tmean_{MMM+9C} - Tmean_{MMM})/9)$$

where Xi is the trait (F_v/F_m or NDVI) averaged across fragments of individual i in the MMM and MMM + 9 treatments, respectively, and $T\text{mean}_{\text{MMM+9 °C}}$ and $T\text{mean}_{\text{MMM}}$ are the average hold temperatures for these treatments. The second term accounts for small differences between target and effective temperatures across tanks and experiments. Performance retention can be computed even for colonies that experienced a minor decline in phenotypic traits under +9 °C, which prevented fitting a dose–response curve. After filtration of colonies with <2 fragments in the MMM and MMM + 9 °C treatments, 675 and 709 colony-level performance retention estimates were calculated for F_v/F_m and NDVI, respectively.

2.3.4 Heat-tolerance variation analysis

The variation in heat tolerance (ED50 and performance retention) was first investigated among sites (*Reef-level variation in coral heat tolerance*; Table A1.4a). The homogeneity of variance between sites was assessed using Levene's test on residuals from group medians (Table A1.4b).

Since variance was unequal across sites, we used one-way Welch's ANOVA to compare site means and Games–Howell *post-hoc* tests with adjusted *p*-values at $\alpha = 0.05$ for pairwise comparisons (Table A1.4c).

The variation in heat-tolerance metrics was then quantified among individuals across and within sites (*Colony-level variation in coral heat tolerance*). Following Cunning et al. (2021) we removed the site effect by computing colony-adjusted ED50 as the grand mean of the total distribution plus residuals from their site of origin and used those adjusted ED50 to assess the range of within-site variation (Figure A1.2).

Finally, we investigated the similarity of colony thermal tolerance rankings between F_v/F_m and NDVI traits using Spearman's rank correlation as the assumption of normality was violated (*Response to acute heat stress differs between traits*). For both ED50 and performance retention, we computed both GBR-wide and site-level correlations (Figure 2.2c,d; Table A1.5).

(i) Environmental data acquisition and analysis

To examine environmental conditions experienced by *A. spathulata* across the GBR, we retrieved 10 environmental variables characterised by 24 predictors computed from *in situ* observations, numerical models and satellite observations (supplementary material and methods, Table A1.6). In addition to environmental variables at the reef level, we included colony-level depth obtained from dive computers and adjusted to the tide at the time of collection (standardised to the lowest astronomical tide; Figure A1.9). We also included pigmentation prior to collection to account for heat stress experienced in the weeks preceding the experiment (0.47−4.67 DHW; Figure A1.4). PCA was performed on environmental predictors for the 709 colonies to visualize the distribution of sites and colonies along environmental gradients (Figure A1.3).

(ii) Phenotype by environment analysis

The influence of environmental predictors on heat-tolerance traits (ED50 and performance retention in F_v/F_m and NDVI) was evaluated using RF ensemble learning and RR on a set of 12 low to moderately correlated predictors (pairwise absolute Pearson correlation = 0.01−0.69; Figure A1.5 and Table A1.7). Because any association of heat-tolerance traits with MMM and DHW at the time of collection may reflect different mechanisms (e.g. adaptation versus acclimatization), both were retained in the dataset despite their strong correlation ($R = 0.78$).

RF models were built using the *cforest* function from the *party* R package (Hothorn et al., 2015). For each of the four heat-tolerance metrics, separate RFs were grown to 1000 trees (ntree) with five environmental predictors tried at each split (mtry). Predictor importance and model accuracy were assessed through repeated 10-fold stratified (across sites) cross-validation (70/30 split; supplementary material and methods). The importance of each predictor was estimated by computing the marginal increase in out-of-bag sample MSE (Mean Inc MSE) when training the model with the predictors randomly shuffled. RR was performed for each phenotypic trait using the *glmnet* R package (Friedman et al., 2021). The optimal tuning parameter λ of the penalty term was selected using k-fold cross-validation (λ.1se; Figure A1.10 and Figure A1.11). Model accuracy (R^2) and environmental predictor coefficients were estimated using bootstrap resampling (repeated 100-fold stratified cross-validation, Figure A1.12).

2.4) Results

Acute heat-stress assays were performed using standardised temperature treatments to elicit increasing levels of heat stress of 0 °C (control), 3, 6 and 9 °C above the local maximum monthly mean (MMM) (Figure A1.1b). Following exposure of replicate fragments of *A. spathulata* colonies to each treatment, two phenotypic traits were measured: the maximum photochemical efficiency of photosystem II (F_v/F_m) and the hyperspectral imagery estimate of chlorophyll content (normalised difference vegetation index; NDVI; Figure A1.1c). As experimental treatments did not reach target temperatures at St Crispin Reef, this site was removed from further analyses resulting in a total number of 709 colonies. The decline of each colony trait was modelled over temperature treatments using dose–response curves and was used to calculate two colony-level metrics of heat tolerance: the temperature that resulted in a 50% decline in response (i.e., the median effective dose, or ED50) which represents an absolute thermal threshold, and the performance under extreme heat (+9 °C), representing how coral traits decline relative to their local reef MMM.

The majority of *A. spathulata* colonies on the GBR showed a minimal decline in photochemical efficiency (F_v/F_m) and chlorophyll content (NDVI) at +3 °C (average ≤5.5%) and +6 °C (average ≤7%) above their local MMM. However, under the more extreme temperature of +9 °C, these traits declined by 2−80% (F_v/F_m) and 10−98% (NDVI), driving differences in thermal threshold (ED50) and performance retention metrics among reefs and individuals (Figure 2.1).

2.4.1 Reef-level variation in coral heat tolerance

The GBR-wide medians of colony thermal thresholds were 37.1 ± 0.9 °C for F_v/F_m ED50 (median ± s.d.) and 36.2 ± 0.7 °C for NDVI ED50, with reef accounting for 34 and 25% of their respective total variation (ANOVA ω2 effect sizes; Table A1.4b). Mean reef-level F_v/F_m ED50s differed by 1.8 °C and generally decreased with latitude (Figure 2.1a). For example, F_v/F_m ED50 thresholds in the southern GBR (Heron Island and Fitzroy Reef; 36.5−36.6 °C) were 0.8 °C lower than all reefs in the central and northern GBR (36.8−38.3 °C; p.adj < 0.0001; post-hoc Games Howell test; Table A1.4c). However, several reefs had higher (Kelso Reef, Pelorus Island, No Name Reef) or lower (Fitzroy Island, North Direction Island) ED50s than nearby reefs at similar latitudes (p.adj < 0.05). Conversely, NDVI ED50 thresholds were less variable among reefs (by 1.3 °C) and were lower at Martin Reef in the northern GBR than all other reefs (p.adj < 0.01; Figure 2.1c).

GBR-wide performance retention (performance under +9 °C relative to local conditions) was 48 ± 12% for F_v/F_m and 29 ± 19% for NDVI with reef accounting for 44 and 59% of their respective total variation (ω2 effect sizes; 0b). Performance retention was 2−41% (F_v/F_m) and 60−65% (NDVI) higher at southern (higher latitude) reefs than the rest of the GBR (Figure 2.2b,d), thus following an opposite trend to F_v/F_m ED50.

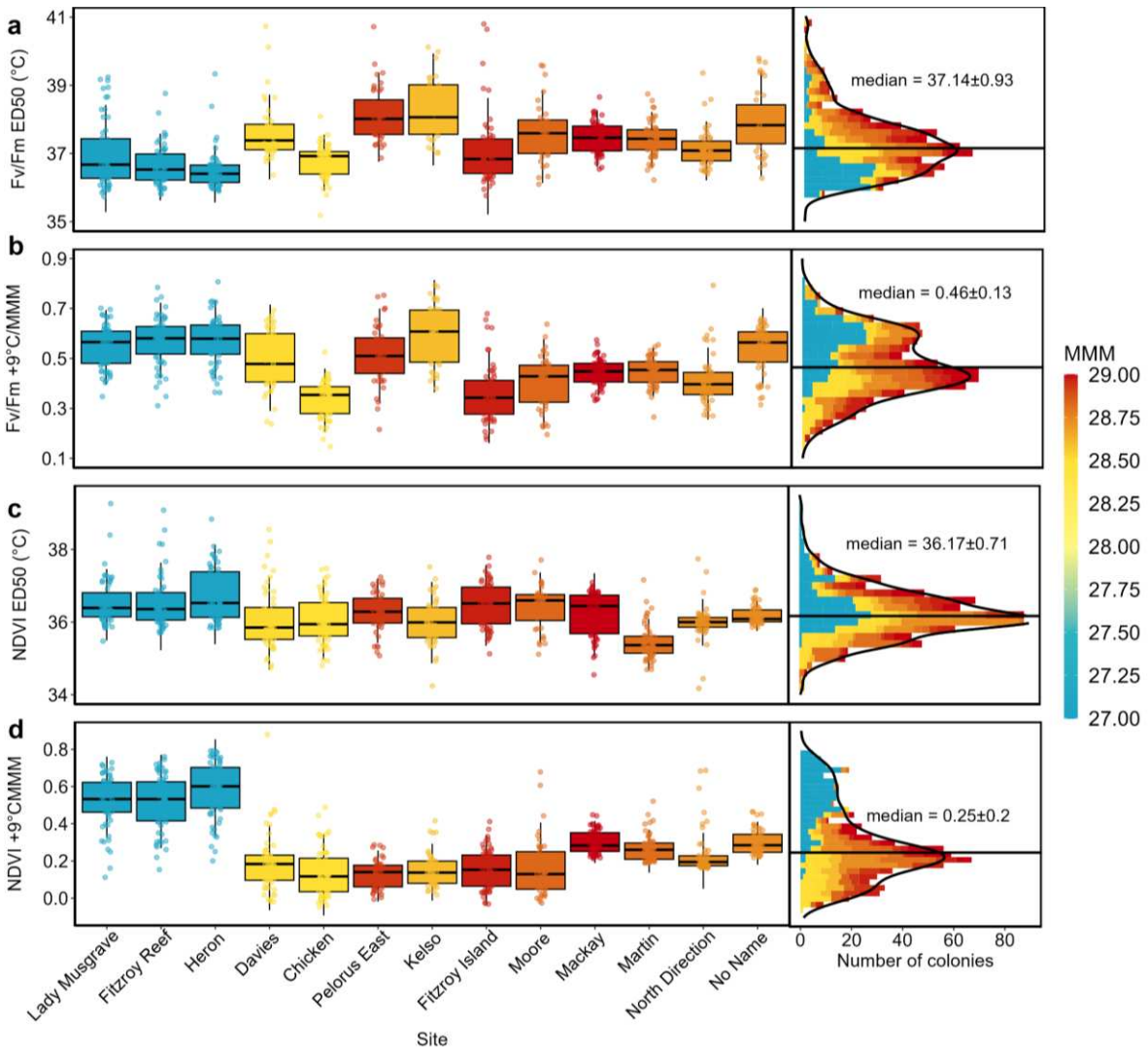


Figure 2.1. Variation in *Acropora spathulata* thermal tolerance among 14 reefs on the Great Barrier Reef (GBR) under acute experimental heat stress. The decline in maximum quantum yield of photosystem II (F_v /F_m) and total chlorophyll content (NDVI) was used to measure ED50 temperatures (a,c) and performance retention under extreme heat (i.e. + 9 °C/MMM; b,d). The left panels display boxplots of the median (solid line) and the first and third quartiles (box) for each reef coloured by their MMM. The right panels show the distribution of values, with the GBR-wide median and standard deviation. Reefs are ordered (left to right) by increasing latitude.

2.4.2 Colony-level variation in coral heat tolerance

At the colony level, thermal thresholds varied by up to 6 °C, approximately three times the reef-level variation (1.8 °C range; Table A1.4a). Within reefs, there was a 3.1 °C and 2.5 °C variation in colony-level ED50s for F_v/F_m and NDVI, respectively (95% range; Figure A1.2). The magnitude of this variation differed among reefs ($p < 0.001$, Levene's test; Table A1.4b) but no specific reef exhibited higher or lower variation for both traits. Colony-level variation in performance retention under +9 °C was also higher than reef-level variation (by 48% for F_v/F_m

and by 17% for NDVI). Although colony-level ED50s were prone to uncertainty (median 95% CI range = 2.51 ± 3.34 °C and 2.99 ± 5.56 °C; supplementary material and methods), congruent patterns between ED50 and performance retention support high variation in acute heat tolerance among and within reefs of the GBR. Importantly, heat-tolerant colonies were widely distributed across the GBR. For example, colonies that were ranked within the top 25% of F_v/F_m ED50 and NDVI ED50 occurred at virtually all reefs (Figure 2.2a,b). However, the most tolerant colonies were generally more abundant at central and northern reefs for F_v/F_m and southern reefs for NDVI. Additionally, several reefs exhibited a high proportion of tolerant individuals for both traits (e.g. Mackay Reef, Moore Reef and Pelorus Island; Figure 2.2).

2.4.3 Response to acute heat stress differs between traits

The ranking of reef- and colony-level responses under heat stress differed between phenotypic traits. Overall, there was no GBR-wide correlation between F_v/F_m and NDVI ED50s (Spearman's-ρ = 0.00, Figure 2.2c), but a moderate positive correlation between their performance retention at +9 °C (ρ = 0.43, Figure 2.2). At the reef level, there was a moderate positive correlation between F_v/F_m ED50 and NDVI ED50 at Chicken and No Name (ρ > 0.3) and a weak positive correlation at Davies, Heron, Mackay, Martin and Moore (ρ = 0.1−0.3, Table A1.5). Similarly, there was a weak to moderate positive correlation between the performance retention of F_v/F_m and NDVI at all reefs (ρ = 0.1−0.3) except at Chicken (ρ = 0.02), North Direction (ρ = 0.84) and Pelorus Island (ρ = −0.22; Table A1.5).

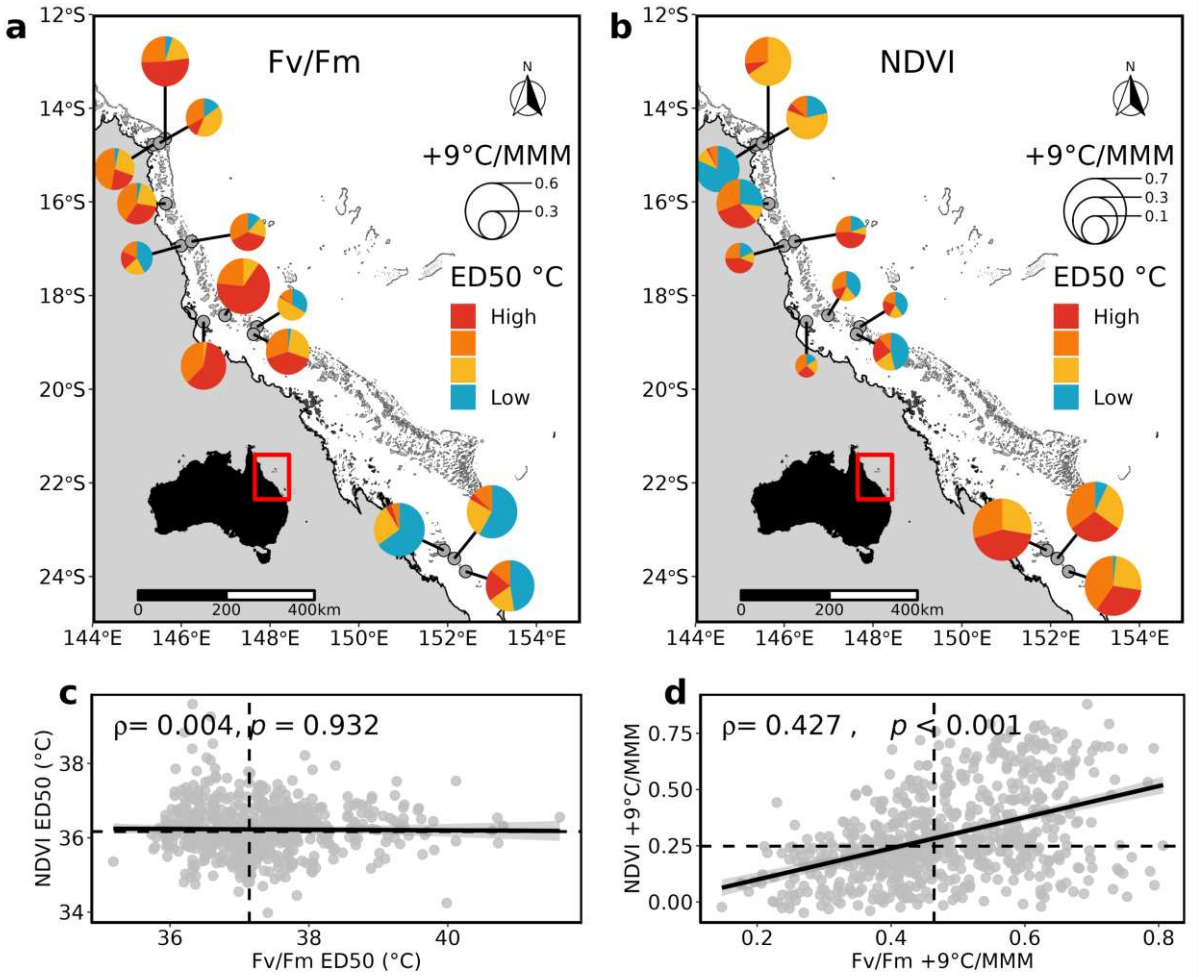


Figure 2.2. Spatial distribution of *Acropora spathulata* acute heat tolerance on the Great Barrier Reef measured by (a) maximum quantum yield of photosystem II (F_v/F_m) and (b) chlorophyll content (NDVI). Pie charts at each reef represent the proportion of individual colony ED50s falling between each quartile of the global distribution (blue: ED50 < Q1, yellow: Q1 < ED50 < Q2, orange: Q2 < ED50 < Q3, red: Q3 < ED50). Pie chart radii are proportional to average retained performance under extreme heat (i.e. +9 °C/MMM), normalised by the global range for plotting purposes. Correlation between (c) F_v/F_m and NDVI ED50s and (d) retained performance under extreme heat (+9 °C/MMM). Each point represents a distinct colony (n = 586 and 675 for (c) and (d), respectively) and Spearman's-ρ and p-values are indicated.

2.4.4 Environmental drivers of acute heat tolerance metrics

To examine environmental conditions experienced by *A. spathulata* across the GBR, we retrieved 10 environmental variables characterised by 24 quantitative predictors computed from in situ loggers, numerical models and satellite observations (Table A1.6). A principal component analysis (PCA) on environmental predictors divided the 709 colonies into three major clusters (Figure A1.3). The first component (46.4% explained variance) separated cooler southern reefs from warmer central and northern (lower-latitude) sites and was mainly driven

by MMM (1.7 °C range) and degree heating weeks (DHW) at the time of collection. The second component (14.7% explained variance) separated northern and central sites along an inshore–offshore gradient that was mainly driven by turbidity, sea surface current velocities and temperature variation (annual range and the rate of change from spring to summer). Within clusters, colonies grouped by reefs as most predictors were retrieved at the site level and were minimally separated by their water depth or pigmentation. Pigmentation scores prior to collection differed between individuals and sites but had no clear association with DHW at the time of collection (Figure A1.4).

Environmental drivers of heat-tolerance traits (ED50 and performance retention in F_v/F_m and NDVI) were evaluated using random forest (RF) ensemble learning and ridge regression (RR) on 12 low to moderately correlated predictors (pairwise absolute Pearson correlation = 0.01−0.69; Figure A1.5). Together, these predictors explained a low to moderate proportion of variation in heat stress responses of *A. spathulata* across the GBR (R^2 = 0.12−0.62). The predictive accuracy of RF and RR was stronger when heat tolerance was expressed for both F_v/F_m and NDVI as performance retention (R^2 = 0.27−0.62) than ED50 thresholds (R^2 = 0.12−0.31). Top environmental predictors slightly differed among traits and metrics but variation in heat tolerance was primarily associated with site-level thermal history (Figure 2.3). MMM (Figure 2.3b) and DHW at the time of collection (Figure 2.3d) were predominant metrics associated with response to acute heat stress (i.e. top RF predictors for three of the four heat-tolerance metrics) while being strongly correlated to each other (R = 0.78). The direction of associations differed between traits with MMM and DHW at the time of collection being positively associated with F_v/F_m ED50 (β = 0.06−0.07), but negatively with performance retention in F_v/F_m and NDVI and NDVI ED50 (β = −0.03 to −0.06). Secondary thermal history associations occurred between the annual range in temperature and both performance retention metrics (F_v/F_m β = −0.03, NDVI β = −0.04; Figure 2.3c), and between the frequency of DHW > 4 and both ED50 thresholds (F_v/F_m ED50 β = 0.04, NDVI ED50 β = −0.06; Figure 2.3e). Particularly, the frequency of DHW > 4 in the year before collection showed a strong negative association with NDVI ED50 (β =−0.060, top predictor in RF), but no significant association with any other trait metric.

To a lesser extent, the heat tolerance of *A. spathulata* was associated with water flow, shading and depth. F_v/F_m tolerance metrics were generally higher at reefs with high sea surface current velocity (F_v/F_m ED50: β = 0.042, +9/MMM: β = 0.037) and lower at sites with positive cloud anomalies in the 30 days prior to collection (F_v/F_m ED50: β = −0.017, +9/MMM: β = −0.031;

Figure 2.3a). Turbidity showed little to no relationship with heat-tolerance metrics. At the colony level, increasing water depth was positively related to F_v/F_m metrics (F_v/F_m ED50: β = 0.042, +9/MMM: β = 0.004) but negatively related to NDVI metrics (NDVI ED50: β = −0.028, +9/MMM: β = −0.015). In addition, colonies with higher levels of pigmentation at the time of collection tended to have higher NDVI ED50 thresholds (β = 0.028), but there was no relationship with other tolerance metrics.

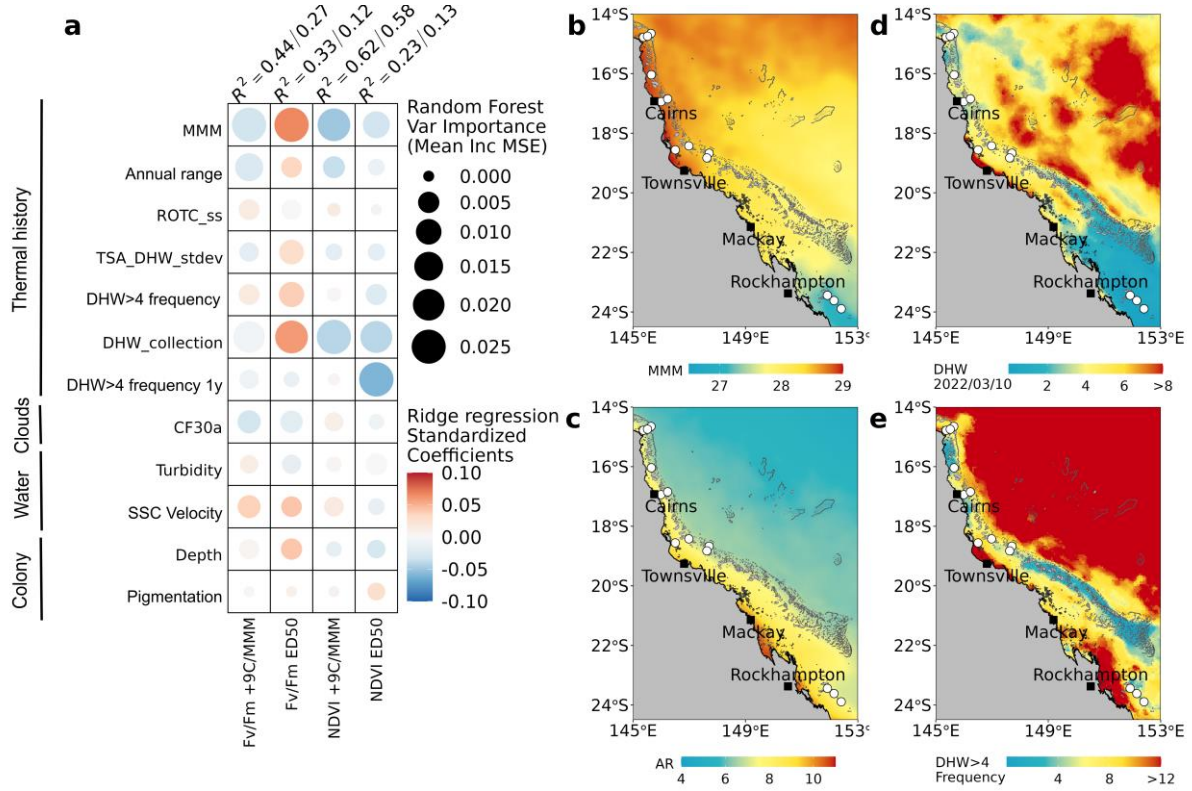


Figure 2.3. Environmental drivers of acute heat tolerance of *Acropora spathulata* on the Great Barrier Reef. Heat tolerance was measured as the maximum quantum yield of photosystem II (F_v/F_m) and chlorophyll content (NDVI) expressed as ED50 temperature thresholds and performance retention under extreme heat (+9 °C). Relationships between environmental predictors (defined in Table A1.6) and heat-tolerance metrics were assessed using ridge regression and random forest models. (a) Heatmap of associations evaluated with random forest variable importance (10-fold stratified cross-validation, circle size) and ridge regression standardised coefficients (multiple bootstrap resampling n = 100, circle colour). The variance explained by each model (random forest/ridge R^2) is shown above each tolerance trait metric. MMM = maximum monthly mean (1985–1990+1993 climatology), ROTC_ss = rate of temperature change in spring/summer, TSA_DHW_s.d. = standard deviation of degree heating weeks (DHW), DHW_collection = DHW at the day of collection, DHW > 4 frequency 1 y = frequency of DHW > 4 in the year prior to collection, CF30a = cloud fraction anomaly, the difference between the average cloud fraction for 30 days prior to collection and the long-term average cloud fraction for that location (2002−2022), SSC Velocity = average sea surface currents velocity. (b–e) Thermal history maps of (b) maximum monthly mean temperature as defined by NOAA (Liu et al., 2003), (c) annual temperature range (2014−2022), (d) peak degree

heating weeks during sampling and (e) the annual frequency of degree heating weeks above four since 1985. White dots indicate reef sites sampled in this study.

2.5) Discussion

The large geographic scope of this study (13 reefs across 9.5° latitude) and sample size (n = 709) revealed extensive intraspecific variation in the heat tolerance of reef-building corals across the GBR. This resulted in more than 6 °C variation in colony thermal thresholds (Figure 2.1; Table A1.4a) where tolerant colonies—based on multiple traits and metrics—were widely distributed among and within reefs. Environmental predictors of heat-tolerance variation support adaptation and/or acclimatization of populations to local conditions while unexplained differences among colonies may be due to host and/or symbiont adaptive genetic variation within reefs.

2.5.1 Acute heat-tolerance metrics linked to historical and recent environmental conditions

All heat-tolerance metrics were most strongly related to thermal history supporting adaptation and/or acclimatization of corals to their local thermal regimes (Figure 2.3a) (Howells et al., 2013; Hughes et al., 2019; Sully et al., 2019; Thompson & van Woesik, 2009). Heat-tolerance metrics first varied along a latitudinal gradient, reflecting differences in average temperatures. For instance, F_v/F_m ED50 thresholds increased at reefs exposed to higher summer temperatures (MMM, Figure 2.3b), which corroborates ecological experiments that found a 4 °C difference in *A. spathulata* larvae survival thresholds between Lizard Island (14.7 °S) and One Tree Island (23.5 °S); i.e. the same latitudinal range as our study (Woolsey et al., 2013). Tolerance metrics also varied by shelf position, with higher F_v/F_m ED50 thresholds at reefs subjected to large annual thermal variation (AR, Figure 2.3c), and by exposure to marine heatwaves (frequency of DHW > 4 and standard deviation of DHW, Figure 2.3e). F_v/F_m ED50 also increased with the accumulated heat stress (DHW) at the time of sampling (Figure 2.3d), supporting that acclimatization of the holobiont to moderate heat stress (0−4 °C week−1), possibly through upregulation of photoprotective mechanisms, can increase the heat-tolerance trait F_v/F_m ED50 as reported by Cunning et al. (2021). However, F_v/F_m ED50 was lower at reefs where accumulated heat stress was the highest (Chicken and Davies; approx. 4.6 °C week−1) suggesting that higher levels of prior heat exposure may be detrimental (Hackerott et al., 2021). As such, we observed weaker unexpected negative associations between NDVI ED50 and

thermal history metrics, notably with the frequency of DHW > 4 in the 12 months prior to sampling. This is similar to F_v/F_m ED50 findings of Marzonie et al. (2022) in the Coral Sea, suggesting that some reef populations may be impacted over long time periods after heat exposure. Differences in the association with thermal history among traits could thus occur from a decoupling between host and symbiont baseline conditions and/or stress responses (discussed below; Baird et al., 2009a; Gardner et al., 2017; Krueger et al., 2015). Nevertheless, several reefs in our study (No Name, North Direction, Mackay) exhibited a high proportion of tolerant individuals for both F_v/F_m and NDVI ED50, showing that some colonies and populations may perform better under heat stress across multiple traits (Lachs et al., 2023c). These populations will be more likely to play a key role in the resilience of the GBR in a warming climate, and thus their mapping in space and time could provide valuable information for spatial planning of Australia's marine parks into the future.

The heat-tolerance metrics of *A. spathulata* measured here were further associated with predictors that influence water movement, light and within-reef temperature (Figure 2.3a). Strong water movement can delay photochemical damage under thermal stress through coral surface cooling, increases in respiration and metabolic transfers and removal of toxins (Nakamura et al., 2005; Page et al., 2019), and the positive association between surface current velocity and F_v/F_m metrics suggests a carryover of these effects to our experiments. Solar irradiance is also a factor known to mediate bleaching responses under high seawater temperatures (Lesser & Farrell, 2004) and F_v/F_m ED50 thresholds decreased at reefs exposed to low irradiance in the weeks preceding collection (i.e. high cloud cover). This may indicate that symbionts acclimated to lower light levels (Anthony & Hoegh-Guldberg, 2003) experienced greater photodamage under the irradiance of the experimental system (Roberty et al., 2015). These results demonstrate that empirically derived thermal tolerance metrics are not only shaped by long-term adaptation but also acclimatization to recent conditions. Overall, the proportion of variation explained by reef-level environmental predictors was low to moderate (R^2 = 12–62%), highlighting the extent of heat-tolerance variation at local scales.

2.5.2 Standing within-reef variation in heat tolerance supports adaptive potential to climate change

There was greater variation in the acute heat tolerance of *A. spathulata* colonies within reefs than among reef-level averages (ED50 3.1 versus 1.8 °C and 2.5 versus 1.6 °C for F_v/F_m and NDVI, respectively; Table A1.4a), despite most colonies being sampled from a narrow depth

range at a single site less than 600 m^2. Importantly, we found that heat-tolerant corals (defined as the top 25 percentile from the GBR ED50 distributions) occurred at nearly every reef, including the cooler southern GBR. These results align with previous results on *A. cervicornis* in the Florida Keys (Cunning et al., 2021), *A. hyacinthus* in Palau (Cornwell et al., 2021) and *A. hyacinthus* in the GBR (Naugle et al., 2024). Within-reef variation remained mostly unexplained by colony-level predictors (depth and pigmentation) and could be elucidated by incorporating genomic data not yet available here. Individual differences in heat tolerance may be underpinned by genomic variation within the host (Drury et al., 2022a; Jin et al., 2016), symbionts (Berkelmans & van Oppen, 2006; Palacio-Castro et al., 2023) and/or their interactions (Kavousi et al., 2020). For example, incorporating the proportion of *Durusdinium* cells and host polygenic scores based on putative heat-adaptive loci increased the predictive accuracy of *A. millepora* bleaching models on the GBR by approximately 22% (Fuller et al., 2020). In addition, deciphering the independent role of environmental drivers requires a better characterization across microhabitats (Ainsworth et al., 2021) and depth (Wyatt et al., 2023), as well as optimization of sampling strategies across environmental gradients to reduce the collinearity of predictors (Selmoni et al., 2020b). The large standing variation in thermal tolerance at the reef scale reported in this study has important implications for the conservation of this species on the GBR. It may notably support *A. spathulata* adaptation to climate change through the selection of pre-existing heat-tolerance alleles (Matz et al., 2020). Furthermore, rather than translocating individuals from warmer reefs (e.g., Howells et al., 2013) restoration projects can target local heat-tolerant individuals when their phenotypes are known or by sampling a diversity of genets.

2.5.3 Coral populations from the southern GBR may live further from their upper thermal limit

Acute thermal thresholds (ED50) for *A. spathulata* populations on the GBR were on average 9.5−9.6 °C above their local MMM on southern reefs compared with 7.5−8.8 °C on central and northern reefs (Table A1.4a). This is consistent with higher performance retention under extreme heat on southern reefs and latitudinal differences in the thermal thresholds of *A. spathulata* larvae (Woolsey et al., 2015). Consequently, under comparable levels of acute thermal stress, southern populations might be less susceptible to bleaching than central and northern populations. In line with this expectation, southern GBR reefs have experienced less frequent and intense bleaching events than central and northern reefs over the 1985−2022 period (Emslie et al., 2024) while undergoing similar maximum DHW across the 2016, 2017

and 2020 major bleaching events (Hughes et al., 2021). The lower frequency and magnitude of bleaching events on southern reefs might also allow more time for adaptation to occur through the migration of heat-tolerance-associated alleles from warmer northern reefs (Matz et al., 2020).

Conversely, the low cumulative heat stress experienced by those regions may result in coral assemblages that are naive to high heat stress (Hughes et al., 2021). As such, southern reefs underwent mild but highly prevalent coral bleaching in 2020 (86% of colonies; Page et al. (2023); 48% of colonies; Nolan et al. (2021)) and the probability of severe bleaching was seven times higher than for central and northern reefs under the same cumulative heat stress (DHW) (Hughes et al., 2021). Further investigations are thus required to understand how recurrent warming disturbances and gene flow with northern regions will shape the evolution of these cooler reefs in natural conditions.

2.5.4 Divergent effects of acute heat stress on thermal tolerance traits

Here we found a moderate correlation between F_v/F_m and NDVI performance retention under extreme heat (Figure 2.2d). This supports the use of photochemical apparatus integrity as an early proxy of coral bleaching (Evensen et al., 2021; Jones et al., 2000; Voolstra et al., 2020) and the importance of symbiont tolerance in bleaching response. For instance, some symbiont species or genotypes may produce more photoprotective pigments or antioxidant compounds, alleviating oxidative stress for the host (Oakley & Davy, 2018; Roberty & Plumier, 2022). Conversely, we found no correlation between ED50s of F_v/F_m and NDVI traits (Figure 2.2c). The only two other studies using F_v/F_m and chlorophyll-related ED50 thresholds found congruent reef-level variation between the two traits for some species (e.g. *Pocillopora verrucosa* (Evensen et al., 2022) and *A. hyacinthus* (Naugle et al., 2024) but not others (e.g. Porites lobata (Evensen et al., 2022)). In both studies, visual chlorophyll scores showed higher noise and lower differences in reef ED50s, which align with *A. spathulata* pairwise reef differences in NDVI ED50s (0.39 °C) being almost half that of F_v/F_m ED50 (0.67 °C). This may also be due to differences in the timing of measurement between traits as their decline occurs at different rates (Gardner et al., 2017). In *A. tenuis*, F_v/F_m values were found to be stable for 0−24 h after the end of an acute heat stress, while chlorophyll decreased up to 24 h after the end of the temperature ramp-down (Nielsen et al., 2022). Therefore, delaying the timing of NDVI measurements in our study may have revealed higher divergence in chlorophyll retention between reefs. Finally, algal oxidative stress and photosynthetic damage can be alleviated by

host processes (Baird et al., 2009a; Roberty & Plumier, 2022) and thus occur without a decrease in chlorophyll content or symbiont density (Middlebrook et al., 2012).

Divergent responses between traits highlight the importance of defining heat tolerance and selecting phenotypic traits accordingly. Chlorophyll content may be an appropriate proxy for holobiont bleaching and mortality as its decline during acute heat stress can persist and reflect mortality in the next month (Walker et al., 2022a). However, photochemical efficiency may be a better proxy to detect sublethal effects as corals can experience physiological stress of reduced tissue biomass and symbiont loss long before changes in pigmentation are visually detectable (Gardner et al., 2017). Finally, which phenotypic trait would best predict heat tolerance in natural conditions remains unclear as colony responses can vary between acute and long-term heat stress (Humanes et al., 2024; Klepac et al., 2024). To validate the ecological relevance of acute heat-stress assays, future studies should compare these rankings with natural bleaching observations, while accounting for the difference of heat stress exposure among reefs under natural marine heatwaves. Our results demonstrate that no single trait or metric can fully capture the complexity of the coral holobiont heat-stress response, and highlight the importance of measuring multiple traits whenever achievable, including relevant host traits (e.g. antioxidant capacity).

2.6) Conclusion

Using standardised acute heat-stress assays, we found that heat-tolerant corals were widely distributed across the GBR, including cooler, southern reefs. This suggests potential for adaptive responses to climate change, if heat-tolerance traits have a heritable basis (Bairos-Novak et al., 2021; Howells et al., 2022b). Rankings of coral heat tolerance can guide human interventions and their interpretation and application may depend on the specific traits and metrics measured. Corals with high absolute thermal tolerance can help to decipher heat stress protective mechanisms (Cleves et al., 2020b; Drury et al., 2022a) and be used as material for assisted gene flow through translocation (Morikawa & Palumbi, 2019; Quigley et al., 2019a) and selective breeding (Howells et al., 2021). On the contrary, corals with high thermal tolerance relative to local conditions may be better targets for local propagation and breeding, decreasing the risk of carrying pathogens and phenotype-environment mismatches (Sellares Blasco et al., 2021). Nonetheless, natural adaptive processes and human interventions must be

accompanied by reduced anthropogenic emissions through ambitious national and international commitments to secure the persistence of species and populations across the entire GBR.

2.7) Acknowledgments

We thank the Traditional Owners of the Great Barrier Reef for their free prior and informed consent to enter and undertake coral sampling in their Sea Country. We pay our respect to their elders, past, present and future. We thank Andrea Severati, Steven Green and Justin Hochen from the Australian Institute of Marine Science for their technical support and for building the acute heat-stress experimental system. We also thank Samantha Goyen, Riverside Marine Cruise crew members and numerous AIMS staff and volunteers for their support while collecting and experimenting at sea. We are thankful to Eric Lawrey and Eduardo Klein for their support with environmental data collection as well as Jonathan Kok and Eric Hochberg for developing tools and pipelines for hyperspectral imaging data extraction. This work was supported by the Reef Restoration and Adaptation Program funded by the partnership between the Australian Government's Reef Trust and the Great Barrier Reef Foundation.

Chapter 3. Intraspecific variation in heat tolerance of *Acropora spathulata* in New Caledonia



Intraspecific variation in heat tolerance of *Acropora spathulata* in New Caledonia

Chapter 2 quantified the intraspecific variation in acute heat tolerance traits of *Acropora spathulata* across spatial scales of the Great Barrier Reef. In Chapter 3, we extended these investigations to distinct reef systems, sampling *Acropora spathulata* populations from New Caledonia's main island ('Grande Terre") and from remote Chesterfields-Bellona plateau atolls in the Coral Sea. These reef systems are also exposed to fluctuations in thermal conditions across latitudinal and cross-shore gradients, providing the opportunity to test whether these selective pressures have shaped comparable variation and distribution in heat tolerance traits. Results from this chapter were subsequently used to perform a genome wide association study with host genomes in Chapter 5.

Hugo Denis[1,2,3], Ombeline Sue[1], Gaël Lecellier[1,4], Magali Boussion[1], Clarisse Marjorel[1], Emily J Howells[3] and Véronique Berteaux-Lecellier[5]

[1] UMR250 ENTROPIE (IRD-CNRS-UR-IFREMER-UNC), Promenade Roger-Laroque, Noumea Cedex, New Caledonia, France

[2] ED 129, Sorbonne Université, 4, Place Jussieu, Paris 75252, France

[3] National Marine Science Centre, Southern Cross University, Coffs Harbour, New South Wales, Australia

[4] Institut de Sciences Exactes et Appliquées (ISEA) EA7484, 145, Avenue James Cook, Nouméa BP R4 98 851, New Caledonia

[5] EMR9001 SANTECO-UMR250 ENTROPIE (CNRS- IRD- UNC - UR), Promenade Roger-Laroque, Noumea Cedex, New Caledonia, France

3.1) Methods

This chapter employs methodologies similar to those outlined in Chapter 2. with slight adjustments to the experimental protocols and the methods used to measure heat tolerance traits. Methods are succinctly described and differences in experimental protocols are highlighted (see Table A2.1).

3.1.1 Study sites, experimental design and set-up

(i) Study sites and sample collection

We sampled 303 colonies of *A. spathulata* across 14 reefs of the western coast of New Caledonia (NC) and atolls of the Chesterfield-Bellona (CB) plateau located in New Caledonia Marine Park (n = 4–25 per reef, Table A2.2) between 26 June 2023 and 28 September 2023 (Coral Reef Marine Park permit 2023-1503/GNC, South Province permit 4508-2022/ARR/DDDT and North Province permit 609011). Colonies were sampled from reef flats and upper reef slopes over a total depth range of 7m. As for GBR colonies, 12 nubbins were used for standardised acute heat-stress experiments and in situ metadata was recorded, including time-corrected depth, in situ photographic records and coral watch health chart scores at 0.5 intervals. Unlike on the GBR, GPS coordinates from colonies were only retrieved at the reef level.

(ii) Acute heat-stress assay design

Acute heat stress assays were performed using aquarium systems that I designed and built with the help of the "Noumea Aquarium des Lagons" staff. The portable experimental system consisted of replicate 30-L PVC tanks supplied with 0.5 $L.min^{-1}$ unfiltered seawater (corresponding to a 22x daily turnover) directly pumped from the ocean using a 1260 2400L/H pump (EHEIM GmbH & Co.KG). The temperature of experimental tanks was controlled through upstream homogenization tanks heated using Eliwell EWDR983 controllers connected to thermal probes and heating resistors (HT300, Tetra and Pro Temp s300, JBL and PVLC 4500W resistors) that filled experimental tanks with heated seawater using Hydor Seltz L pumps. Experimental tanks were equipped with white/blue LED lighting (Maxspect RSX 200) to supply ~ 250 µmol photons. $m^{-2}.s^{-1}$ with a diurnal light regime timed to *in-situ* conditions (11:13). Current pumps (WP100, Tetra) maintained a 5–20 $cm.s^{-1}$ flow rate within tanks and temperatures were recorded at 5 min interval with Hobo loggers (Onset, US).

Due to logistical and technical reasons, slightly different protocols were used at CB and NC reef sites. At CB sites, fieldwork was carried out during an onboard mission on the Marine National vessel d' *Entrecasteaux* with the portable experimental system set up on the vessel (Figure A2.1a). Upon collection, replicate fragments were transported to the vessel, where they were mounted on experimental racks (C3D) labeled with unique identifiers and immediately subjected to acute heat stress assays (starting between 1:00 and 3:00 pm). At NC sites, fieldwork was conducted on the smaller IRD vessel *Archamia* from the shore and the experimental system was set up at the Noumea Aquarium des Lagons (Figure A2.1b). Upon collection, replicate fragments were transported to the aquarium in a cooler filled with sea water. Water was exchanged multiple times during the transport in order to avoid introducing additional stress and hypoxia. Upon arrival at the aquarium, fragments were mounted on racks and held overnight in ambient seawater conditions. In this case, assays started the following day at 11:00am, consistent with the GBR experiments.

Similar temperature treatments of 0, 3, 6 and 9 °C above the local MMM were used to elicit increasing levels of heat stress (3 replicate tanks per treatment). Experimental temperature profiles were consistent with those outlines in 2.3.1 and closely matched target temperatures (meanΔT = 0.26 °C; Table A2.1).

3.1.2 Measure of bleaching intensity

Due to the lack of the experimental tools to measure the same phenotypic traits as on the GBR (Imaging PAM or hyperspectral camera), we used the intensity of the red channel from conventional RGB images as a proxy for chlorophyll content. This proxy has been developed and validated in independent studies (Winters et al., 2009). Photographs were taken of individual coral fragments 11h after the end of the temperature ramp-down using a Canon EOS700D camera with EF-S 18–200mm f3.5/5.6 IS lens on a black background including a grey colour scale for exposure correction. Fragments were immediately frozen after taking the photographs. Photographs exposure and colour was corrected in two steps using a custom MATLAB script modified from Winters et al. (2009). First, exposure was standardised along vertical and horizontal directions within images using the homogenous black background as a reference. Second, exposure was standardised across images using the grey reference scale and following the 'Post hoc' methods described in Winters et al. (2009). Pixels corresponding to the coral fragments were masked using a custom ImageJ script and the median red channel intensity of each fragment was extracted from standardised images.

We also validated the accuracy of this proxy with conventional quantification of chlorophyll content through spectrophotometric measurements. For this purpose, coral tissues from a subset of 60 nubbins from 5 colonies were separated from the skeleton using the air pick method (Ferrier-Pagès et al., 2011). Symbiodiniaceae cells were released in 0.1µm filtered seawater through manual homogenization with a potter tissue grinder. Three 10mL replicates of the tissue homogenate were centrifuged (6000 g, 10min) and the supernatant removed. The pellet containing pigments was extracted in 99% acetone (24 h, 4 °C). The total concentration of chlorophyll a (Chla), chlorophyll c2 (Chlc2) and total chlorophyll were calculated from absorbance measurements taken with a spectrophotometer (UV-Visible Evolution 201, THERMO, 2014) according to Jeffrey and Humphrey (1975). Chlorophyll content was normalised to seawater volume and nubbins' surface area estimated with the paraffin method which is considered to match the accuracy of computer tomography (CT) for the Acropora genus (Naumann et al., 2009). Overall, we observed a strong inverse correlation between the median red intensity channel and chlorophyll a content (R = -0.92, $p < 0.001$; Figure A2.2). For clarity, red channel intensity was expressed as the invert value 255-median$_{Red}$.

3.1.3 Phenotypic data analysis

Data analyses were performed as described in 2.3.3 and 2.3.4 to obtain chlorophyll (Red Intensity) ED50 and performance retention metrics.

3.1.4 Environmental predictors of acute tolerance

A multiple linear regression model was applied to evaluate the influence of environmental conditions on acute heat tolerance (ED50), using the same environmental predictors described in 2.3.4. To avoid multicollinearity, variables with Pearson's R >0.7 or VIF>10 were excluded prior to model construction. A stepwise selection procedure was performed to retain only the variables that contributed significantly to the model. The model fit was assessed using Aikake Information Criterion (AIC, relative to a null model) and the proportion of variance explained (R^2).

3.2) Results

Using acute heat-stress assays, replicate fragments from coral colonies were exposed to increasing levels of heat stress to assess differences in heat tolerance between individuals. The

decline of chlorophyll content (Red Intensity) over temperature was modelled using dose-response curves and used to compute the median effective dose ED50 and performance retention under extreme heat (+9 °C). Preliminary visualization of the data revealed very low chlorophyll content in CB samples (high $median_{Red}$), including in the control treatment, being 75% lower on average than in NC samples. The decline in chlorophyll content over temperature treatments was absent or too small to compute accurate ED50 values (Figure A2.3). In addition, there was no correlation between Red Intensity and spectrophotometric measurements of chlorophyll concentration within CB reef sites (Spearman's correlation; R_{CB4} = -0.344, p_{CB4} = 0.404; R_{CB6} = -0.25, $p_{CB\ 6}$= 0.589) unlike NC reef sites (Spearman's correlation; R_{NC1} = 0.95, p_{NC1} < 4e-4; R_{NC5} = 0.83, p_{NC5} = 0.01; R_{NC8} = 0.72, p_{NC5} < 0.05). This means that the Red Intensity method exhibits limited accuracy in the low chlorophyll concentration range. Therefore, only NC site-specific results are presented below.

3.2.1 Reef-level variation in coral heat tolerance

The New Caledonia-wide median of colonies ED50 was 36.38 ± 0.83 °C (median ± sd) and 0.56 ± 0.16 °C for colonies performance retention under extreme heat (Figure 3.1). A Levene's test indicated that variance was not significantly different among reefs (p_{ED50} = 0.07 and $p_{+9C/MMM}$ = 0.185) and thus a classic analysis of variance (ANOVA) was used to assess differences in reefs means. The reef of origin had a significant effect on both ED50 (F = 6.66, df = 7, p < 0.001) and performance retention (F = 0.20, df = 7, p < 0.001) and explained 21% and 25% of variance respectively (ANOVA ω^2 effect sizes). Median reef-level ED50 varied by up to 1.35 °C between the most and least tolerant reef, and by 0.54 °C on average for pairwise comparisons. Median reef-level ED50 generally increased with latitude; being 0.4−3.8% higher in the four North Province reefs compared to the four South Province reefs. Ilot Contrariete reef had the highest median ED50, being significantly higher than six of the seven other reefs (ANOVA p < 0.01). In addition, the performance retention was also the highest at Ilot Contrariete. The smallest retention was measured at the lowest-latitude reef, Pointe de Poum (Figure 3.1).

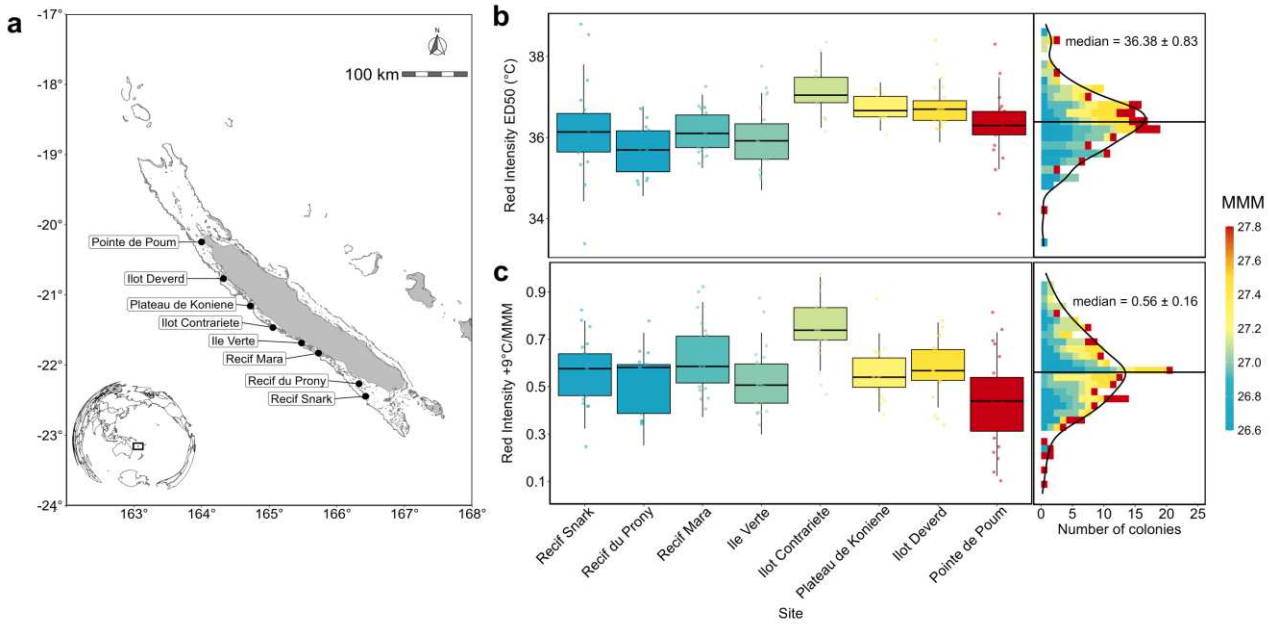


Figure 3.1. Variation in *Acropora spathulata* thermal tolerance among 8 reefs on the western coast of New Caledonia under acute experimental heat stress. (a) Map of the 8 reefs where *A. spathulata* colonies were sampled. The decline in total chlorophyll content (Red intensity) was used to measure ED50 temperatures (b) and performance retention under extreme heat (i.e. + 9 °C/MMM; c). The left panels display boxplots of the median (solid line) and the first and third quartiles (box) for each reef coloured by their MMM. The right panels show the distribution of values, with the NC-wide median and standard deviation. Reefs are ordered (left to right) by increasing latitude.

3.2.2 Colony-level variation in coral heat tolerance

Responses of *A. spathulata* colonies to acute heat stress varied considerably among reefs, by as high as 5.41 °C (33.4−38.8 °C), approximately 4 times the reef-level variation (1.35 °C). As this wide range was due to a few individuals, a more conservative range estimate is 3.41 °C (2.5%−97.5% range). A significant amount of this variation occurred within reefs, as removing site effects still resulted in a 3 °C range in individual thresholds (or a conservative 2.06 °C for 2.5−97.5% range; Figure 3.1). In general, the higher ED50 thresholds were found at warmer, low latitude reefs (Figure 3.2). However individual colonies ED50 falling in the top 25% of the global distribution were found at virtually all reefs (except for the southern reef, Recif du Prony), indicating widespread geographic distribution of heat tolerance traits. Interestingly some of the least tolerant individuals (bottom 25% of the distribution) were found at the warmest reef Pointe de Poum.

3.2.3 Environmental predictors of acute heat tolerance

Following a stepwise selection procedure, only reef-level MMM was retained as a significant predictor of acute heat tolerance ($t = 2.63$, $p < 0.01$, linear model). The model explained a small fraction of the variance in ED50 (Adjusted-$R^2 = 0.045$), reflecting the high variability in acute heat tolerance among colonies within reefs.

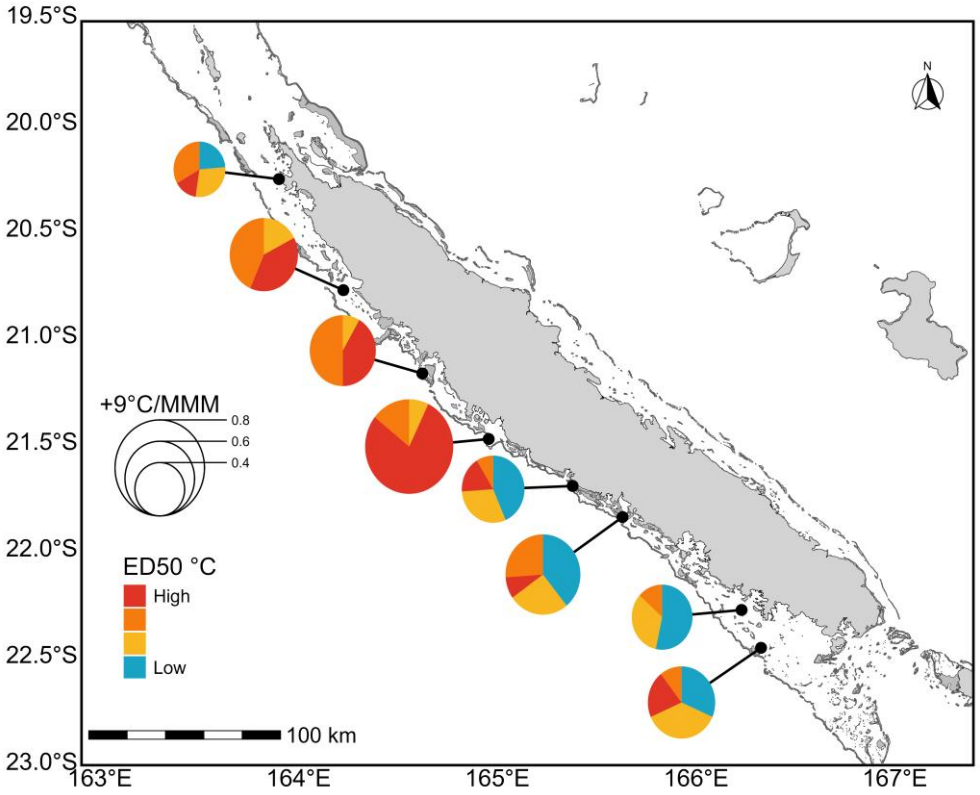


Figure 3.2. Spatial distribution of *Acropora spathulata* acute heat tolerance on the western coast of New Caledonia measured through chlorophyll retention under heat stress. Pie charts at each reef represent the proportion of individual colony ED50s falling between each quartile of the global distribution (blue: ED50 < Q1, yellow: Q1 < ED50 < Q2, orange: Q2 < ED50 < Q3, red: Q3 < ED50). Pie chart radii are proportional to average retained performance under extreme heat (i.e. +9 °C/MMM), normalised by the global range for plotting purposes.

3.3) Discussion

3.3.1 High intraspecific variation in heat tolerance is consistent across reef systems

Acute heat stress assays in New Caledonia (NC) highlighted a large intraspecific variation in acute heat tolerance among reef-building corals, both among and within reefs. The range of

variation identified in this region aligns with our previous results on the GBR, with 3.4 °C and 3.6 °C range in individual ED50 estimates among reefs for NC and the GBR respectively (conservative 2.5−97.5% range; Figure 3.3a). A substantial fraction of this variation occurred within reefs, with 2.1 °C and 2.2 °C ranges in individual ED50 estimates for NC and the GBR respectively after removing reefs effects (Figure 3.3b). A Levene's test on colonies ED50 found that the variation in heat tolerance was not significantly different between reefs in NC at a α=0.05 level but yielded a small *p*-value (p = 0.07) reflecting the average 40% higher interquartile range in the four southern sites compared to the four northern sites. Although additional tests will be needed to confirm this trend, the reduction in thermal breadth at these locations could reflect the effect of past marine heatwaves at these locations that may have filtered out the least tolerant individuals (Bennett et al., 2019). In Australia the association of ED50 values with ongoing degree heating weeks at the time of collection prevented formally testing this hypothesis.

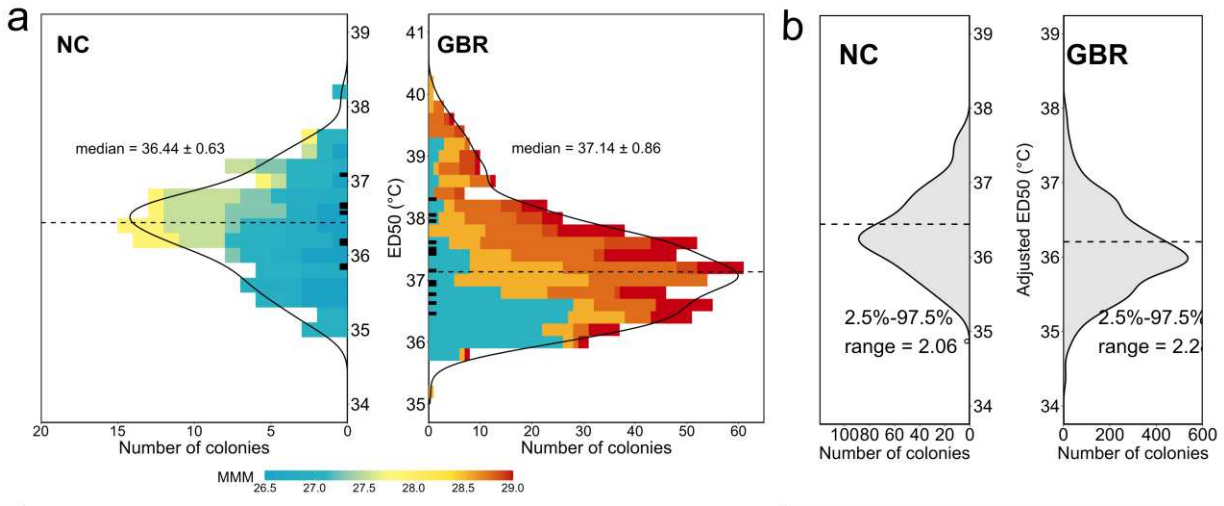


Figure 3.3. Comparison of variation in *Acropora spathulata* acute heat tolerance between western New Caledonia reefs (NC) and the Great Barrier Reef (GBR). ED50 were computed using proxies of chlorophyll content (Red Intensity and NDVI respectively). (a) The distribution of individuals absolute ED50 (°C) are shown and coloured by the MMM of their reef of origin. Median and standard deviation in ED50 is shown for both reef systems. Note that the y-axes differ between figures to enable visualize comparison of variation among reef systems. (b) Distribution of adjusted ED50 (°C), removing sites effect to visualize the within-reef variation in heat tolerance. 2.5%−97.5% ranges are shown.

3.3.2 Congruent patterns of heat tolerance distribution across regions

Consistent with results on the GBR, we found that coral colonies exhibiting the highest absolute heat tolerance were primarily found at warmer, low-latitude reefs of the western New Caledonia Grande Terre. However, in both cases, a fraction of the most heat tolerant individuals (top 25% of global distribution) were found at nearly all reef sites (Figure 2.2 and Figure 3.2). Due to their sessile lifestyle, adaptation of coral populations to their local thermal regimes is expected (Smith et al., 2022; van Oppen et al., 2018). However, our results show that a minority of highly tolerant individuals are also present in cooler environments. The occurrence of heat tolerant individuals at high-latitude reefs could be the result of dispersal of heat adapted larvae from low-latitude reefs (Matz et al., 2018) or genetic recombination within these populations producing tolerant phenotypes. Despite being exposed to cooler temperatures on average, these reefs are not exempt from exposure to marine heatwaves (Hughes et al., 2021) which may favor the maintenance of adaptive genetic variation in these regions.

We also found a consistent decrease in heat tolerance relative to local conditions at low-latitude reefs in both regions (Figure 3.4). On average ED50 were 9 °C−9.6° above their MMM in the South Province compared to 8.5 °C−9.4 °C in the North Province (with the exception of Ilot Contrariete reef, which was 10 °C above the MMM). This difference is relatively modest compared to the difference between southern and central/northern reefs on the GBR (7.5−8.8 °C vs 9.5−9.6 °C), possibly due to the smaller latitudinal range sampled in New Caledonia (2.5° vs 9.5° of latitude). Yet, these results suggest that populations at low-latitude reefs may live closer to their upper thermal limits and be at greater risk under global warming. This phenomenon has already been reported to cause extinction of populations at the low-latitude boundaries of other species distributions (Thomas et al., 2006).

Among New Caledonia reefs, the population of the Ilot Contrariete reef was distinct, exhibiting on average 0.8 °C higher ED50 and 20% higher performance retention under extreme heat compared to other reefs. Environmental conditions such as satellite- and model-derived chlorophyll a, cloud cover, turbidity levels and colonies depth were comparable to other reefs. Further investigations into the distribution of adaptive genetic variation may provide further insights into the higher heat tolerance observed at this reef.

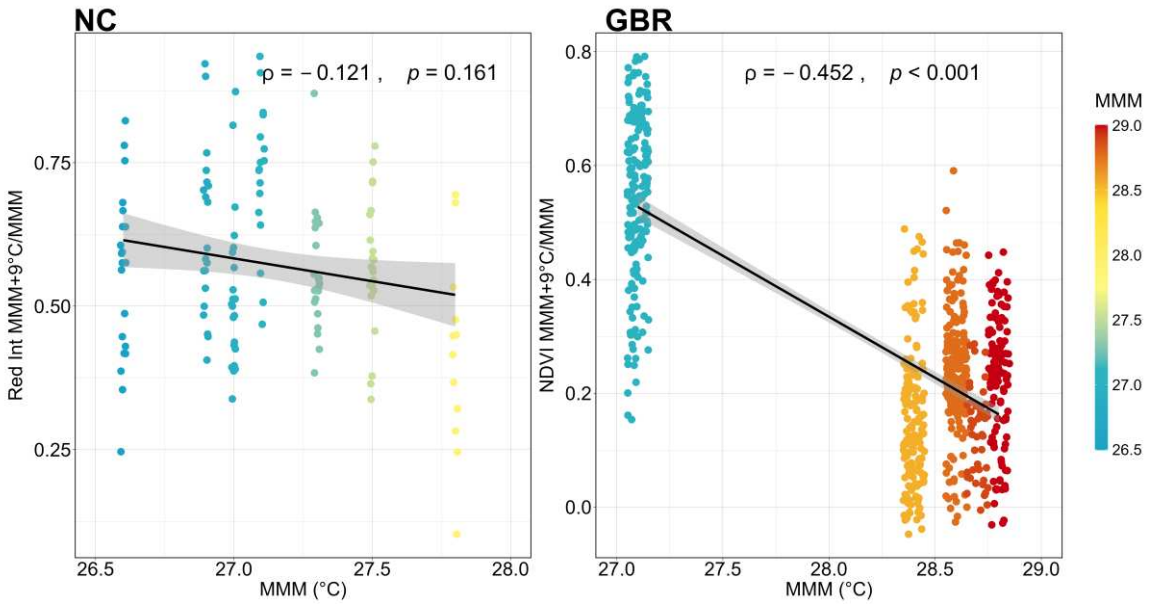


Figure 3.4. Consistent decline in relative acute heat tolerance at lower-latitude reefs in New Caledonia and on the Great Barrier Reef. Chlorophyll retention under extreme heat (NDVI MMM+9 °C/MMM and Red Intensity MMM+9 °C/MMM) correlation with reefs MMM. Spearman's ρ and p-value are shown for both reef systems.

3.3.3 Limits of standardised acute heat stress and chlorophyll proxies at Chesterfield-Bellona reefs

The independent validation of the red intensity measurement as a proxy for chlorophyll content showed that despite an overall strong correlation, this proxy was unable to resolve differences in chlorophyll content in the lower range of values measured at CB reefs. This prevented the analysis of site-level or colony-level estimates of heat tolerance at these reefs.

Several factors could explain the lower chlorophyll concentrations of coral fragments at CB sites. First, most individuals were sampled in shallow environments from inner barrier reefs that are exposed to high light intensity, a factor known to promote a decline in symbiont load and chlorophyll concentrations (Kuguru et al., 2010). This hypothesis is also corroborated by atmospheric model reanalyses (ERA5) showing that these reefs are on average exposed to higher UV radiation than in NC, due to their offshore and lower-latitude geographic position. Another possible explanation is a residual effect from recent exposure to marine heatwaves that may have caused a decrease in symbiont densities. Satellites observations of sea surface temperatures (CoralTemp) indicated a residual 1.8 Degree Heating Weeks (DHW) at the CB sites in June 2023, when sampling was conducted. This residual accumulated heat stress originated from a marine heatwave that peaked at >3 DHW in the preceding month, potentially contributing to mild bleaching (Middlebrook et al., 2010). Finally, due to logistical constraints

acute heat stress assays were performed directly upon collection at the different CB reef sites, unlike GBR and NC reefs where they occurred after one night of acclimation. The absence of acclimation period may have thus further increased the stress for coral fragments and the low baseline chlorophyll concentrations in all treatments.

These results show the logistical challenges of performing standardised acute heat stress assays in a context where bleaching events are increasingly frequent (Virgen-Urcelay & Donner, 2023). Because heat tolerance traits measured in acute heat stress assays can be partly driven by acclimatization to recent conditions (as shown in Chapter 2), they must be conducted under 'normal conditions' to be comparable between reefs. When the latter is not feasible, studies should seek to adjust temperature profiles—by conducting a test batch—to elicit levels of heat stress that can discriminate phenotypic responses among colonies. This test batch can also allow the temperature profiles to be adjusted based on species sensitivity to best capture the temperature range over which the decline in phenotypic traits occurs. In addition, any study seeking to compare heat tolerance between distinct reefs or regions should report and account for the potential influence of recent environmental conditions.

3.3.4 Impacts of chlorophyll proxies on heat tolerance estimates

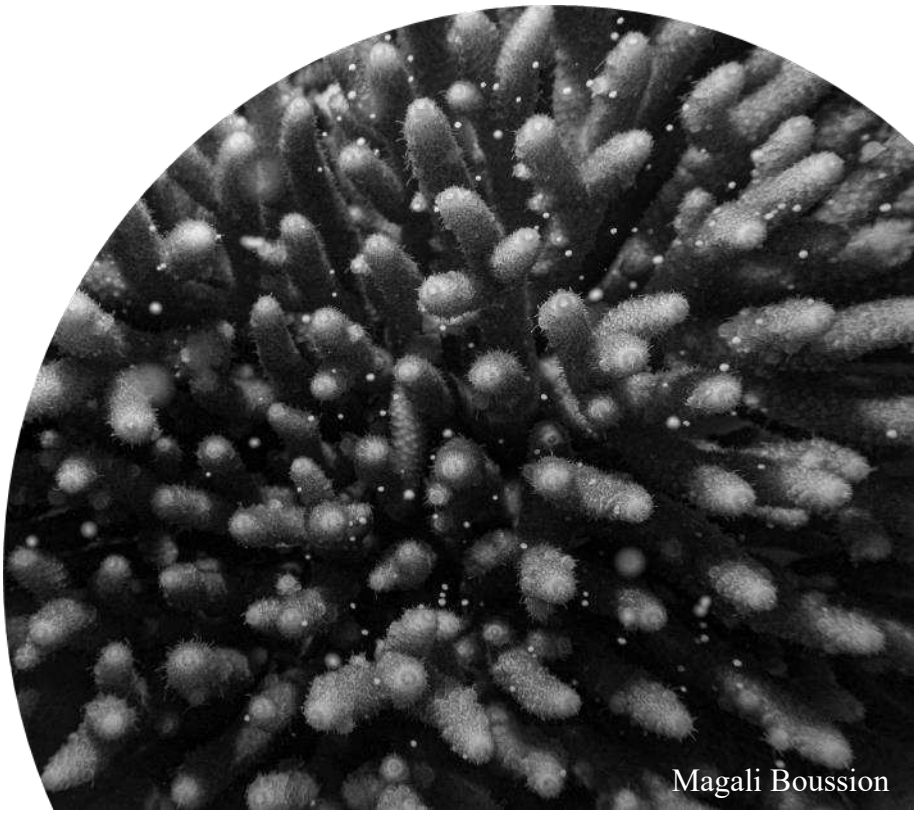
As shown in Chapter 2, heat-tolerance threshold estimates depend on the trait being assessed. Similar limitations likely occur when the same trait is quantified using different proxies, such as NDVI in the GBR and red-channel intensity in NC. Although both proxies were strongly correlated with conventional spectrophotometric measurements of chlorophyll content, NDVI exhibited a log-linear relationship (Figure A1.7), whereas the red-channel intensity displayed a linear relationship (Figure A2.2; Winters et al., 2009). These differences can affect proxy performances across chlorophyll levels: NDVI's log-linear relationship amplifies small changes at low concentrations but saturates at high concentrations (Huete et al., 1997). In contrast, the red-channel intensity was less sensitive at low concentrations but maintains linearity at high concentrations. This linear relationship was confirmed by a recent study, which identified red-channel intensity as the most accurate proxy for chlorophyll content across three coral species and 19 RGB-based indices (Ferrara et al., 2024), being also less costly to implement than hyperspectral imaging. Overall, these findings highlight the value of assessing coral chlorophyll ranges beforehand to guide the choice of the most suitable image-based proxy, as this will affect the accuracy of heat tolerance estimates such as ED50s. They also underscore the importance

of generating calibration curves specific to each dataset, as factors such as taxonomic identity and experimental conditions can influence these relationships.

3.4) Conclusion

We used standardised acute heat-stress assays to investigate standing intraspecific variation in acute heat tolerance traits among 183 colonies from 8 reefs in New Caledonia. We observed consistent ranges of variation in acute heat tolerance traits among colonies from New Caledonia and our previous results in Australia. Heat tolerance traits were also widely distributed across New Caledonia's reefs, including in regions with cooler temperatures. In both reef systems, the level of heat stress that coral colonies could tolerate generally aligned with average temperatures and the magnitude of typical thermal stress in their environment, indicative of local adaptation. However, our results reveal certain populations and reefs diverge from these general trends, possibly due to more complex evolutionary histories or interactions with other biotic or abiotic factors yet to be elucidated. Finally, our results show that a large fraction of heat tolerance variation occurs among individuals within reefs and remains largely unexplained by the macro-environment. This reinforces the need to better understand adaptive genetic variation underpinning heat tolerance traits, in order to guide proposed conservation and restoration approaches.

Chapter 4. Contrasting population structures of reef-building corals and their algal symbionts inform adaptive potential across the Western Pacific



Contrasting population structures of reef-building corals and their algal symbionts inform adaptive potential across the Western Pacific

Chapter 2 and 3 quantified the variation in acute heat tolerance among *Acropora spathulata* colonies across reefs and reef systems, demonstrating the contributions of both short-term environmental memory and long-term local adaptation in shaping the distribution of heat tolerance traits. However, considerable variation occurred within reefs and could not be explained by macro-scale environmental factors, highlighting the need to better understand the roles of host and symbiont factors. The role of gene flow in shaping this distribution, and its implications for the dispersal potential of tolerance traits, also remains unknown. Chapter 4 uses hologenome data to investigate the genetic structure, diversity, and connectivity of *Acropora spathulata* hosts and their associated Symbiodiniaceae across the Western Pacific. The chapter provides insights into the consequences of these eco-evolutionary interactions for the demographic resilience and evolutionary potential of these populations. Chapter 4 is under review in *Current Biology* (Denis et al., 2025).

Denis, H., Prata, K. E., Ishida, H., Popovic, I., Mocellin, V. J. L., Boussion, M., Byrne, I., Purcell, S. W., Bay, L. K., Lecellier, G., Chan, C. X., Riginos, C., Howells, E. J., & Berteaux-Lecellier, V. (2025). Long-distance gene flow and contrasting population structures of reef-building corals and their algal symbionts inform adaptive potential across the Western Pacific. *BioRxiv*. https://doi.org/https://doi.org/10.1101/2025.10.14.682263.

The results from Chapter 4 allow to control for the effects of demographic history, gene flow and symbionts communities in the association studies in Chapter 5.

Contrasting population structures of reef-building corals and their algal symbionts inform adaptive potential across the Western Pacific

Hugo Denis[1,2,3], Katharine Prata[4,5], Hisatake Ishida[6], Iva Popovic[4,5], Véronique J.L. Mocellin[4], Ilha Byrne[5], Magali Boussion[1], Clarisse Marjorel[1], Steven Purcell[3], Gaël Lecellier[1,7], Line K. Bay[4], Cynthia Riginos[4,5], Cheong Xin Chan[6], Emily J. Howells[3], Véronique Berteaux-Lecellier[1]

1 EMR 9001 SantEco - UMR 250 ENTROPIE (CNRS-IRD-UR-IFREMER-UNC), Promenade Roger-Laroque, Noumea cedex, New Caledonia, France.

2 ED 129, SU Sorbonne Université, 4, Place Jussieu, 75252 Paris, France

3 National Marine Science Centre, Faculty of Science and Engineering, Southern Cross University, Coffs Harbour, NSW, Australia

4 Australian Institute of Marine Science, Townsville, QLD, Australia

5 School of the Environment, The University of Queensland, St Lucia, QLD, Australia

6 Australian Centre for Ecogenomics, School of Chemistry and Molecular Biosciences, The University of Queensland, Brisbane, QLD, Australia

7 Institut de Sciences Exactes et Appliquées (ISEA) EA7484, 145, Avenue James Cook – BP R4 98 851 Nouméa, New Caledonia

4.1) Abstract

The genetic diversity and connectivity of reef-building coral populations are key to their survival in warming oceans. Yet, our understanding of corals' demographic resilience and adaptive potential is complicated by cryptic species diversity, wide geographic distributions, and complex coral-algal symbioses. To address these challenges, we investigated genetic connectivity and diversity of the broadcast-spawning coral *Acropora spathulata* and its associated Symbiodiniaceae across 29 reefs spanning the Great Barrier Reef, the Coral Sea and New Caledonia, using whole-genome sequencing of 1,088 colonies. We identified four genetically distinct coral populations that diverged between 0.27 and 0.65 million years ago, likely due to geographic isolation across thousands of kilometres. These populations maintained asymmetrical gene flow along major ocean currents despite demographic isolation, and sustained large local effective population sizes (~2,900), supported by a high dispersal range of ~100 km per generation. In contrast, their Symbiodiniaceae partners varied over finer spatial scales, with five distinct *Cladocopium* taxa distributed along latitudinal and cross-shore

gradients, likely driven by local environmental conditions. These results suggest that high dispersal capacity and large local population size promote demographic resilience within reef systems, while environment-specific symbioses and long-distance gene flow across reef-systems support adaptation and evolutionary rescue.

4.2) Introduction

Reef-building corals and their microbial symbionts constitute coral holobionts that are the foundation of biodiverse but threatened coral reef ecosystems (Souter et al., 2021). As tropical corals are declining globally, it is crucial to better understand the evolutionary, spatial and environmental processes that shape their population dynamics and resilience (Edmunds & Riegl, 2020; van Oppen & Gates, 2006). However, the widespread presence of cryptic coral diversity (Grupstra et al., 2024; Riginos et al., 2024), along with vast geographic ranges (Gleason & Hofmann, 2011), challenges our ability to determine the size and connectivity of coral populations. In addition, variability in symbioses between coral hosts and symbiotic microalgae from the family Symbiodiniaceae can affect holobionts' capacity to grow, survive and adapt under changing conditions (Bourne et al., 2016).

Population genomics, which investigates genome-wide molecular variation, can differentiate coral taxa that are indistinguishable based on morphological criteria (Bongaerts et al., 2021), or traditional population genetic markers such as microsatellites (Arrigoni et al., 2020; Meziere et al., 2024). Within coral species, it can provide a holistic view of spatial genetic variation patterns in both hosts and symbionts across their range (Fuentes-Pardo & Ruzzante, 2017). These analyses are essential to uncover the distinct scales at which gene flow, local adaptation and co-evolutionary dynamics influence the adaptive responses of holobionts.

Contemporary gene flow (over tens of generations) is crucial for coral demographic dynamics, particularly for the recovery of locally depleted coral populations following perturbations (Hock et al., 2017; Holbrook et al., 2018). To quantify its spatial extent, isolation-by-distance (IbD) theory provides a useful framework by estimating a generational gene dispersal distance (Rousset, 1997; Wright, 1946). Combining the slope of IbD with estimates of effective density, one can infer the generational mean axial dispersal distance (σ), over which most dispersal events occur, and vast differences in σ depending on reproductive modes and taxa have been described (Gorospe & Karl, 2013; Japaud et al., 2019; Meziere et al., 2025; Prata et al., 2024). To estimate effective density, the local effective population size (N_e) is estimated and divided

by the area the population occupies. Local N_e indicates the loss rate of genetic variation due to genetic drift at the scale where most breeding events occur (Waples, 2024). This standing variation on which natural selection acts, underpins adaptive potential (Fisher, 1930). Jointly estimating σ and N_e thus provides crucial information on the extinction risk of local coral populations (Hernández-Agreda et al., 2024) and the spatial scale of demographic replenishment (Gaines et al., 2010), which are both essential for defining conservation units.

Over longer evolutionary time-scales, occasional long-distance dispersal can affect species range and adaptation to global changes (Clobert, 2012). However, methods based on high-level genetic differentiation cannot disentangle the effect of migration from genetic drift and shared ancestry, or determine direction of gene flow (Lawson et al., 2018; Whitlock & McCauley, 1999). Demographic history inference approaches that model divergence times, variation in migration rates and long-term effective population sizes (Gutenkunst et al., 2009) offer a complimentary strategy to assess gene flow across a coral species range (Meziere et al., 2025). However, despite potential for coral connectivity spanning thousands of kilometres (Davies et al., 2015; Matz et al., 2018), such methods have been primarily applied within national borders (Matz et al., 2018; Meziere et al., 2025; Tsuchiya et al., 2022; Zhang et al., 2022). This limits the development of coordinated regional conservation strategies that incorporate gene flow from different regions to assess evolutionary adaptation potential of corals (Colton et al., 2022).

Importantly, coral evolution and conservation require consideration of their symbiosis with Symbiodiniaceae microalgae (LaJeunesse et al., 2018) that are genetically and physiologically diverse (Nitschke et al., 2022). For instance, the photosynthetic ability of Symbiodiniaceae is known to differ among taxa under heat stress (Levin et al., 2016); some taxa inhabit warmer environments (McRae et al., 2023) or increase in prevalence during thermal stress (LaJeunesse et al., 2009). Most Symbiodiniaceae are facultative symbionts, therefore both macro-environments and host micro-environments will favor certain taxa or genotypes (Bhattacharya et al., 2024; Quigley et al., 2019b; Reich et al., 2021). In turn, some symbiont taxa may facilitate corals' local adaptation to environmental conditions (Howells et al., 2012). Symbiont diversity has been mostly described using phylogenetic markers such as the ribosomal internal transcribed spacer 2 (ITS2; Hume et al., 2019) and the chloroplastic non-coding region of *psbA* gene, i.e., $psbA^{ncr}$ (Moore et al., 2003), or via multilocus genotyping (e.g., Davies et al., 2020; Lewis et al., 2024). Yet, distinguishing intra- from inter-genomic variants remains challenging, and the dependence on few selected marker genes may limit taxonomic resolution (Armstrong et al., 2024). Emerging methods based on genome-wide sequence composition of hologenome

samples (Ishida et al., 2024; Zhang et al., 2022), or the recovery of additional mitochondrial and chloroplast markers from these samples (Armstrong et al., 2024; Cooke et al., 2020; Ishida et al., 2024; Zhang et al., 2022) are uncovering previously hidden phylogenetic and ecological diversity.

Acropora spathulata is a fast-growing, broadcast-spawning and widespread species that inhabits shallow reef environments in the Western Pacific, including the Great Barrier Reef (GBR), the Coral Sea and New Caledonia (NC). Genetic data have revealed new insights into the cryptic diversity of *Acropora* corals on the GBR (Matias et al., 2022; Naugle et al., 2024), their associated Symbiodiniaceae (LaJeunesse et al., 2004; Matias et al., 2022; Naugle et al., 2024; van Oppen et al., 2001) and realized connectivity, dominated by southward migration of coral larvae (Matz et al., 2018; Riginos et al., 2019). However, such information remains scarce in NC with only one genomic study conducted to date on *Acropora* coral hosts (Selmoni et al., 2021), and few on their symbiont communities (Alessi et al., 2024; Camp et al., 2020; Denis et al., 2024b). In addition, despite being one of the most studied coral reef ecosystems (Alvarado-Cerón et al., 2022), GBR's connectivity with nearby Western Pacific islands such as NC remains unknown. Several ocean currents flow westward and eastward between the GBR and NC (Figure A3.1; Cravatte et al., 2015), offering potential for periodical dispersal via stepping-stone migration through Coral Sea atolls, e.g., the Chesterfield-Bellona (CB) plateau. To our knowledge, no study—in corals or other marine organisms—has systematically assessed gene flow in this Western Pacific region, aside from pumice rafting coral larvae from NC to the GBR (Jokiel, 1990), and some genetic admixture between these reef systems and Coral Sea atolls (Lukoschek et al., 2016; Marzonie, 2025; Oury et al., 2020). NC and the Southern GBR are often considered potential climate refugia with projected stability of coral cover (Matz et al., 2020; Sully et al., 2022) due to the mild occurrence of bleaching until recently (Shlesinger & van Woesik, 2023). Understanding whether these systems have or still exchange migrants is therefore important for their regional conservation.

Here, we systematically assess the host and symbiont population structures and gene flow of the coral *Acropora spathulata*, expanding the common research scope of the GBR (Cooke et al., 2020; Matias et al., 2022; Scott et al., 2024; van Oppen et al., 2018; Warner et al., 2015) to the Western Pacific. By integrating existing and innovative genome-scale approaches, we densely sampled, sequenced, and analysed whole-genome sequencing data from 1,088 colonies from 29 reefs across the GBR, the Coral Sea and NC. Our study represents one of the most

geographically comprehensive efforts to concurrently investigate coral host and symbiont diversity as well as contemporary and long-term connectivity.

4.3) Methods

4.3.1 Study sites and sample collection

A. spathulata was sampled from the east coast of Australia to the west coast of New Caledonia and across a 10 ° latitudinal gradient (Table A3.1). Colonies were identified as *A. spathulata* in the field based on their morphological similarity to the nominal species, and prior taxonomic work on the Great Barrier Reef (GBR; Wallace, 1999). The lack of publicly available genomic data from *A. spathulata* topotypes from the Solomon Islands population prevents a genomic-based verification of their taxonomic status as populations of the same species or currently synonymized species. The first batch of samples consisted of 831 colonies collected across 15 reefs of the GBR (n = 40–60 per reef; Figure 4.1) between 28 February and 26 March 2022 (GBRMPA permit G21/45166.1) as described by Denis et al. (2024a). The second batch comprised 323 colonies collected across 14 reefs of the western coast of New Caledonia (NC) and atolls of the Chesterfield-Bellona (CB) plateau located in the Coral Sea (n = 4–25 per reef) between 26 June and 28 September 2023 (New Caledonia Natural Park of the Coral Sea permit 2023-1503/GNC, South Province permit 4508- 2022/ARR/DDDT and North Province permit 609011). At each reef, small fragments (< 1 cm^3) were collected on SCUBA from coral colonies originating from one or two sites (covering 50–4200 m^2) and immediately stored in 80–100% ethanol for DNA extraction. Depending on reef sites' geomorphologies, colonies were collected from upper reef slopes, fringing reefs, inner barrier reefs or reef flats at an average depth of 0.6 m (−0.7 m to 5.6 m relative to the lowest astronomical tide). Geographic coordinates were recorded for each colony by carrying a GPS in tow on a surface float (except at NC and CB reefs), and whole colony photographs and macrophotographs were taken of each colony using an Olympus TG-6. The occurrence of clones was minimized by avoiding sampling neighbouring colonies of similar pigmentation.

4.3.2 DNA extraction and sequencing

Coral fragments from 1,154 colonies were used for DNA extraction and 1,144 high quality DNA samples were used for library preparation and whole genome sequencing (Table A3.2). While extraction and sequencing of the GBR and New Caledonia samples were conducted at

different facilities, similar extraction and library preparation kits and sequencing platforms were used in order to minimize batch effects. In addition, a subset of 23 technical replicates pairs from the GBR was extracted and sequenced alongside both batches to control for such effects (Supplementary Material and Methods). In both cases, total DNA was extracted from coral tissue slurry (tissue and skeleton) using then DNeasy Blood and Tissue Kit (Qiagen, Hilden, Germany) following manufacturer's instruction, including an RNAse digestion step for GBR samples (30 min at room temperature). For GBR samples, sequencing libraries were prepared using the Lotus DNA Library Prep Kit for NGS (10 ng of input DNA, 8 PCR cycles) and sequenced on the Illumina NovaSeq 6000 platform (200 cycles; 150 bp paired end reads; targeting 10X coverage; Azenta Life Sciences, CSIRO). For New Caledonia samples, the libraries were prepared using the Truseq Nano DNA kit (200 ng of input DNA, 8 PCR cycles) and sequenced on the Illumina NovaSeq X platform (300 cycles; 150 bp paired end reads; targeting 10X coverage; Macrogen, Korea).

4.3.3 Genomic data pre-variant processing and filtering

The bioinformatic pipeline used to process, filter and analyse the genomic data is outlined in Figure A3.2. The dataset consisted of the 1,144 sequenced individuals with technical replicates (n = 25; Supplementary Material and Methods) and *Acropora millepora* samples used as outgroups (n = 13). Pre-variant filtering steps are summarized in Table A3.2. Adapter removal and read quality trimming was conducted using `Trimmomatic` v0.39 (Bolger et al., 2014) with a 4 bp sliding window, a minimum phred score quality of 20, and a minimum read length of 50 bp. Leading and trailing low quality bases were removed (LEADING:3, TRAILING:3) and adapter sequences were removed using the Illuminaclip option in 'palindrome mode' (2:30:10:4). Sample quality was confirmed using `FastQC` v0.12.1 (http://www.bioinformatics.bbsrc.ac.uk/projects/fastqc) and `MultiQC` v1.21 (Ewels et al., 2016). Filtered reads were then aligned to the *Acropora millepora* reference genome v3 assembly (unpublished upgrade from GCA_013753865.1_Amil_v2.1; see Supplementary Material and Methods for a justification of the reference genome choice) using the `Burrow-Wheeler Aligner` v0.7.17 (Li & Durbin, 2010) and the MEM algorithm at default settings. SAM files were converted to indexed and sorted BAM files using `Samtools` v1.20 (Danecek et al., 2021) and PCR duplicates were marked and removed using `Picard` v3.1.1 (VALIDATION_STRINGENCY=LENIENT; http://broadinstitute.github.io/picard/). After filtering of samples that failed sequencing and samples with unexpectedly low percentage of

mapped reads (< 80%; possibly indicative of mis-identified taxa) or number of mapped reads (< 10M), 1,132 BAM files were retained. To provide an initial evaluation of population structure across the study system and pinpoint potential clones and taxa misidentification, this dataset was analysed alongside outgroup samples using a genotype likelihood framework in *ANGSD* v0.940 (Korneliussen et al., 2014; see Supplementary Material and Methods for results). Four samples from the GBR belonging to *A. millepora* and 23 samples from a distinct unknown genetic cluster from NC were removed from further analyses.

4.3.4 SNPs calling, clone identification and filtering

Indexed, duplicate-free BAM files were used to call variants and genotypes from a total of 1,105 remaining samples using *GATK* v4.5.0.0 'Germline short variant discovery best practice' workflow (Van der Auwera & O'Connor, 2020). Variant calling was first performed per sample, focusing only on reads mapping to the 14 reference chromosomes, using the *HaplotypeCaller* tool that performs de novo assembly of haplotypes in active regions. Individual 'gvcf' files were then consolidated per chromosome using *GenomicDBimport* and used for joint genotyping using *GenotypeGVCFs* tool. *GatherVCFs* and *SelectVariants* tools were used to combine chromosome files in a single variant call format (VCF) file and separate SNPs from INDELs and monomorphic sites. The SNPs VCF file was preliminarily filtered using *GATK* VariantFiltration tool following *GATK* stringent filtering best practices (QD > 2, FS < 50, MQ > 40, MQRankSum > -12.5, ReadPosRankSum > -8, SOR < 3, GQ > 20) and 17 individuals with high missingness (> 85%) were discarded. Previously identified putative clonal colonies were confirmed and filtered to retain only one colony with the lowest missingness per clonal group (Supplementary Material and Methods, Table A3.3).

4.3.5 Host population genomics analyses

To confirm the absence of strong batch effects that could confound population structure, a subset of 23 pairs of technical replicates was sequenced along both GBR and NC samples (supplementary material and methods; Figure A3.3). After exclusion of natural clones and technical replicates, a final set of 999 individuals was used for host population genetic analyses. A first dataset of unlinked SNPs was created to investigate population structure and phylogenetic relationship between populations of the Coral Sea, retaining only bi-allelic SNPs

with a minimum mean locus depth of 5 and a maximum of 15, a minor allele frequency (MAF) > 0.05 and a locus missingness < 20% with `vcftools` v0.1.17 (Danecek et al., 2011). In addition, SNPs in linkage disequilibrium with a pairwise $r^2 > 0.2$ were removed using `plink` v1.90b7.2 (Purcell et al., 2007; "Dataset 1", Table A3.4) because we were interested in identifying neutral population structure patterns that occur throughout the genome. To identify genetically distinct groups of individuals, we performed a principal component analysis (PCA) with the `glPca` function from R package `adegenet` v2.1.10 (Jombart, 2008). We then estimated individual ancestry proportion using ADMIXTURE v1.3.0 (Alexander & Lange, 2011). The optimal number of ancestral populations (K=4) was determined using the cross-validation method implemented in ADMIXTURE. To complement these analyses, we estimated individual ancestry proportion using sparse Non-negative Matrix Factorization (sNMF) with the R package *LEA* v3.14.0 (Frichot et al., 2014). The optimal number of ancestral populations was estimated using the minimum average cross-entropy value over five repetitions with α = 100. To investigate potential fine-scale genetic structure, we repeated the ADMIXTURE analysis within each major population using K = 2. Following Hemstrom et al. (2024) best practices, these analyses were also conducted using variable stringency MAF (MAF > 0.01 and MAF > 0.05) and missingness thresholds (5%, 10%, 20% and 50%).

Finally, we used a subset of individuals with the highest ancestral assignment in `ADMIXTURE` (200 colonies, 50 colonies per population) and built an individual-based Maximum Likelihood phylogenetic tree using RAxML (Stamatakis, 2014). To build the tree, the VCF file was converted to the Phylip format using `vcf2phylip.py` script (https://github.com/edgardomortiz/vcf2phylip) and `raxmlHPC-PTHREADS` was run with a GTRGAMMA model and 100 bootstrap replicates.

4.3.6 Population statistics

A second dataset of linked SNPs was used to compute population genetic differentiation and diversity estimates retaining SNPs with a minimum mean locus depth of 5 and a maximum of 50, a minimum allele count (MAC) of 1, a p-value of deviation from HWE test >0.0001 and < 20% missingness ("Dataset 2", Table A3.4) following recommendations of Hemstrom et al. (2024). To generate unbiased estimates of population genomic statistics despite missing data, the SNP dataset was concatenated to include invariant sites, filtered with the same depth and missingness thresholds per above, and used to compute statistics with `pixy` v1.2.10 (Korunes

& Samuk, 2021). Following Sopniewski and Catullo (2024), 10 replicates of 5 randomly selected individuals per population were used to compute the fixation index (F_{st}) using the Weir and Cockerham method (Weir & Cockerham, 1984). Because F_{st} estimates can be affected by within population diversity, we also computed absolute divergence (D_{xy}) for each replicate, to get more-independent estimates of population differentiation. Finally, we computed nucleotide diversity (π) within each population. We reported the median F_{st}, D_{xy} and π estimates across replicates.

4.3.7 Demographic modeling

To investigate the evolutionary history and connectivity of these populations, a subset of Dataset 2 comprising 120 colonies (30 colonies per population, showing >95% admixture cluster assignment) was used to conduct demographic modeling analyses in *∂a∂i* v2.3.3 (Gutenkunst et al., 2009). This dataset was further filtered to retain SNPs with a minimum allele count (MAC) of 3 to minimize the effect of sequencing errors. SNPs showing a deviation from HWE (p-value < 0.0001) were also removed as we observed an excess in heterozygosity creating a peak in the SFS at 0.5 haplotype frequency, potentially due to gene duplication, paralogous loci or balancing selection. Finally, a second round of filtration to ensure <20% missingness within each population was performed using vcf_minrep_filter.py script (https://github.com/pimbongaerts/radseq, "Dataset 3", Table A3.4). VCF files were created for each population pair (n = 6) and analysed using a custom workflow to estimate effective population sizes, divergence time and migration rates between populations (https://github.com/kepra3/kp_dadi).

We computed joint-allelic frequency spectrums (JAFS) for each pair using the subsample method to account for missing data, and masking singletons and doubletons to minimize the effect of sequencing errors or somatic mutations. We initially tested three scenarios: divergence in isolation, divergence with asymmetrical migration and ancestral asymmetrical migration. We optimized the models' parameters to best fit the observed JAFS (Figure A3.4). To avoid getting stuck in local optima, optimization was performed by exploring the parameter space in three stages: first with three-fold, then two-fold, and finally one-fold perturbations of the starting parameters, based on the previously optimized peak values (>100 runs per stage). The final set of parameters was chosen when appearing several times with 1-fold perturbation from different initial values. To get confidence intervals for these parameters, 100 bootstraps were created for each pair by resampling genomic contigs. Optimization runs (n = 50) were performed for each

bootstrap and model, using 1-fold perturbations starting from previously optimized parameters. For each bootstrap replicate, delta-AIC values were computed between models, and the mean delta-AIC across replicates was used to identify the best-fitting model for each population pair (Figure A3.5). Optimized parameters from the best-fitting model (divergence with asymmetrical migration) were used to calculate 95% credible intervals, after excluding bootstrap replicates within the lowest 10% likelihood quantile.

Finally, we converted parameter values obtained in *∂a∂i* (θ, ν_{1dadi}, ν_{2dadi}, M_{12dadi}, M_{12dadi} and T_{dadi}) into physical units: divergence time in years, effective population sizes in number of individuals and gene flow between taxa in number of migrants per generation. To do so we first calculated the effective sequence length for each pair as:

$$L = \frac{SNP_{dadi}}{SNP_{detected}} \times N_{sites}$$

where SNP_{dadi} is the number of SNPs used to construct the JAFS from the specific pair, $SNP_{detected}$ is the number of SNPs originally detected before filtration, and N_{sites} is the number of sites obtained from GATK pipeline (including SNPs, INDELs and monomorphic sites). Next, we computed the ancestral population size (N_{ref}) and the effective population sizes ν_1 and ν_2 in number of individuals, the divergence time (T) in years, migration rates in fraction of migrant individuals at each generation (m_{12} ; from Population 2 to Population 1 and m_{21}; from Population 1 to Population 2) and rates of gene flow in number of individuals per generation (M_{12} and M_{21}), using the following formulas:

$$N_{ref} = \frac{\theta}{4 \times \mu \times L}$$

$$T = 2 \times T_{gen} \times N_{ref} \times T_{dadi}$$

$$\nu_1 = \nu_{1dadi} \times N_{ref}$$

$$\nu_2 = \nu_{2dadi} \times N_{ref}$$

$$m_{12} = \frac{M_{12dadi}}{2 \times N_{ref}}$$

$$m_{21} = \frac{M_{21dadi}}{2 \times N_{ref}}$$

$$M_{12} = m_{12} \times \nu_1$$

$$M_{21} = m_{21} \times \nu_2$$

We used a mutation rate μ of 1.2×10^{-8} mutations per base per generation, previously estimated for *Acropora* corals (Zhang et al., 2022) and a generation time T_{gen} of 5 years following the assumptions of Matz et al. (2018) on generation times of *A. millepora*.

4.3.8 Isolation by distance analysis and estimating N_e

To estimate realized dispersal and effective population sizes, Dataset 2 was further filtered to retain SNPs with <10% missing data and physically pruned to remove SNPs separated by < 20kb, retaining one SNP selected at random ("Dataset 4"). This was done because both isolation by distance (IbD) analyses and N_e estimation methods require no physical linkage (Waples, 2024).

Using this dataset, we estimated σ that represents ecologically relevant gene flow averaged across the last 10–15 generations, following Prata et al. (2024) with modifications. Multiple IbD regressions were performed in `spagedi` v1.5 (Hardy & Vekemans, 2002) using the empirical estimate of Rousset's individual genetic distance (â; Rousset, 1999) and the geographic distance between individuals. Geographic distances were calculated using the Haversine formula, which estimates great-circle distances between latitude-longitude pairs. Regression analysis conducted within each of the four populations (corresponding to geographic regions; Figure 4.1) revealed no significant IbD. Because we were interested in a general dispersal estimate across the species range and the F_{st} estimates amongst populations were low, we used the global dataset for conducting the IbD analysis. Different regressions were performed to estimate the slope β for a range of spatial scales that roughly evenly partitioned the dataset (maximum distance of 50 m to 2,300 km). We queried multiple spatial scales in order to select *a posteriori* the appropriate regression distance spanning minimum σ and maximum 10–50 σ following Hardy and Vekemans (1999). The dimensionality of the habitat was determined for each regression by the width to area ratio, using a 1D analysis for a ratio <0.1 and a 2D analysis and the $\log_{10}$ of geographic distance for a ratio >0.1 (Rousset, 1997). Similarly, for multiple spatial scales, the population density (D_e) was estimated by dividing the effective population size by the habitat area (A) for 2D or length (L) for 1D regressions (see below). Confidence intervals for β were estimated using a jackknifing procedure across individuals and the slope was deemed significant when the confidence intervals did not span 0. All β and D_e estimates were then combined to estimate σ at each spatial scale using the following

isolation-by-distance model equation (Rousset, 1997; Wright, 1946). In the case of the 2D regression, the corresponding equation is:

$$\sigma = \sqrt[2]{\frac{1}{\beta 4\pi D_e}}$$

The linkage disequilibrium method was used to estimate the effective population size (N_e) at the neighbourhood extent (radius of 2σ), which N_e represents the effective number of individuals that can easily mate in a continuously distributed population (N_b; Neel et al., 2013). Neighbourhood N_e was estimated using `LDNe` v2.1 (Waples & Do, 2008) with a minimum allele frequency filter (Pcrit) based on the number of samples (S) following authors recommendations (Pcrit = 0.01 if S > 100, Pcrit = 0.02 if S > 35, and 1/2S < Pcrit < 1/S if S < 25; Waples & Do, 2010). Confidence intervals were obtained for N_e using the jackknifing procedure.

Finally, we filtered our β, σ and N_e estimates to ensure that the spatial scales at which the IbD regression was performed matched a σ value ranging from σ to 10–50σ following Hardy and Vekemans (1999). We also removed any instance where N_e was not estimated at the neighbourhood area, A or L equating to $4\pi\sigma^2$ for two dimensional habitat (or $2\sqrt{\pi}\sigma^2$ for one dimension), because this is the ideal spatial scale to estimate N_e (Neel et al., 2013). Upper and lower confidence intervals for filtered estimates were then used to obtain distributions of β and N_e through resampling (n = 100). A gamma distribution was used for N_e and a log-normal distribution for β. These distributions were then combined to create a joint σ distribution and propagate the error from each separate analysis.

4.3.9 Symbiodiniaceae community analyses

We used genomic reads from 1,088 *A. spathulata* holobionts to characterise symbiont community composition and diversity across our study area, adopting the approach by Ishida et al. (2024), available at https://github.com/hisatakeishida/Symb-SHIN. Genomic reads not mapping to the host reference genome (i.e. non-coral reads) were first re-aligned to several reference genomes of Symbiodiniaceae using the `Burrow-Wheeler Aligner` v0.7.17(Li & Durbin, 2010) and the MEM algorithm (`bwa-mem`) at default setting, with one reference per genus (*Symbiodinium microadriaticum* CCMP2467 (Nand et al., 2021), *Breviolum minutum* Mf1.05b (Shoguchi et al., 2013), *Cladocopium proliferum* SCF055-01 (Chen et al., 2022),

Durusdinium trenchii CCMP2556 (Dougan et al., 2024), *Effrenium voratum* RCC1521 (Shah et al., 2024) and *Fugacium kawagutii* CCMP2468 (Li et al., 2020)).

For the first-pass analysis of the symbiont community composition, we retrieved and classified ITS2 sequences present in the samples using `graftM` (Boyd et al., 2018). All ITS2 sequence variants were classified as belonging to genus *Cladocopium*. To improve intra-specific taxonomic resolution we also analysed *psbA*^{ncr} sequences among the samples. We retrieved *psbA*^{ncr} sequences by mapping reads to a custom *psbA*^{ncr} reference database using `bwa-mem`. We then followed Armstrong et al. (2023) to retain only reads that aligned in full length (100% cover) at >90% identity, and used number of uniquely mapped reads as proxy for abundance.

To capture genetic diversity of symbionts directly using whole-genome sequencing data not restricted to selected marker genes, we adopted a *k*-mer-based alignment-free approach, following earlier studies (Ishida et al., 2024; Zhang et al., 2022). The *k*-mers in each sample were first enumerated using `jellyfish` v1.1.12 (https://github.com/gmarcais/Jellyfish) at k = 21 yielding a 21-mer profile following previous studies (González-Pech et al., 2021). Pairwise distance between samples was computed from these profiles using `d2ssect` (https://github.com/bakeronit/d2ssect), based on D_2^S metric (Reinert et al., 2009). Samples containing similar symbiont compositions are expected to share similar *k*-mer profiles (i.e., short D_2^S -derived distance). The D_2^S-derived distance matrix was used to perform an unconstrained principal coordinate analysis (PCoA; Borcard & Legendre, 2002) using the cmdscale function in R, and was used to infer a neighbour-joining tree using R package `ape` v5.8.1 (Paradis & Schliep, 2019).

To validate the aforementioned methods using a conventional amplicon-based approach, a subset of 36 DNA samples distributed across host populations (Figure A3.6) were used for ITS2 marker amplification (Herculase II Fusion DNA Polymerase Nextera XT Index V2 Kit) and Illumina sequencing at Macrogen (Seoul, Korea) using forward primer SYM_VAR_5.8S 5'-GAATTGCAGAACTCCGTGAACC-3' and reverse primer SYM_VAR_REV 5'-CGGGTT CWCTTGTYTGACTTCATGC-3′ (Hume et al., 2018). ITS2 sequence data were submitted to the SymPortal analytical framework (https://symportal.org; Hume et al., 2019) and ITS2 sequence variants and type profiles output by the pipeline were used to visualize the results. For this subset of 36 individuals, `graftM` results were checked for consistency with SymPortal results using a relative abundance barplot of ITS2 sequence variants. Using the same set of samples, we also compared the hierarchical clustering of Unifrac distances based on ITS2

'defining intragenomic variants' with that based on D_2^S distances, which showed great consistency (Figure A3.7) and thus we named each of the D_2^S clusters according to its corresponding major ITS2 sequence. Both dendrograms were aligned to build a tanglegram with R package *dendextend* and the stepside method (Galili et al., 2015).

4.3.10 Host and symbiont co-clustering analysis

To visualize how Symbiodiniaceae communities varied across host populations, we performed a hierarchical clustering of samples using the pairwise distance matrix derived from the D_2^S metric (above) using all samples (n = 878) for which > 50 M bp of reads mapped to the reference Symbiodiniaceae genomes. This dendrogram was pruned to build a tanglegram with the host phylogenetic tree obtained in *RAxML* using *dendextend*.

4.3.11 Distance based redundancy analysis

We first investigated the influence of geography and environmental conditions on the global host population structure of *A. spathulata* across the Western Pacific (n = 999). For this purpose, we retrieved spatial predictors (reef distance to the coast, colony-level depth), and environmental predictors from several satellite products and models with a focus on variables known to be primary drivers of coral holobiont community composition (temperature, light and turbidity; Supplementary Material and Methods, Table A3.5). We modeled spatial relationships among colonies using distance-based Moran's Eigenvector Maps (dbMEMs), which capture multi-scale spatial relationships using principal coordinate analyses (Borcard & Legendre, 2002). As individual colony-level GPS coordinates were not recorded at NC and CB reefs, randomly jittered coordinates within 300 m around the reef coordinate (recorded using a GPS during sampling; corresponding to the approximate size of the sampling area) were assigned to each colony at these reefs. The neighbour matrix for each colony was computed from spatial coordinates using Haversine distance in R package *geosphere* (Hijmans et al., 2017) and used to compute dbMEMs eigenvectors using R package *adespatial* (Dray et al., 2018). The first four eigenvectors associated with positive eigenvalues were kept in further analyses based on a screeplot of cumulative variance explained (>95%). All predictors were standardised by subtracting the mean and dividing by the standard deviation to ensure comparable units.

We performed a redundancy analysis (RDA; Legendre & Anderson, 1999) using R package *vegan* (Oksanen et al., 2013). RDA is an unsupervised, constrained method (i.e., it makes no

prior assumptions about the number of clusters) designed to identify axes that maximize the variance explained by a set of predictors. The first RDA model was built using the first 10 principal components of the PCA on host SNPs as a dependent matrix, and all environmental variables as predictors. Collinear predictors were removed successively, starting with the variables with the highest variance inflation factor (VIF), recomputing the model VIF and repeating this procedure until all predictors had a VIF < 10. Model significance was tested using an analysis of variance (ANOVA) and individual axes significance was tested using an ANOVA-like permutation test in package `vegan` with 500 permutations per axis. Forward selection was used to select predictors that were statistically significant. We used the framework developed by Capblancq and Forester (2021) to assess the relative influence of geography and environment on host structure. We built a global RDA model using (1) environmental variables previously identified as significant using forward selection and (2) the first four dbMEM eigenvectors as predictors. Separate partial RDA models were built setting either environmental variables or spatial eigenvectors as conditional variables (i.e., 'partialled out'). Model significance was tested using an ANOVA, and models were compared based on inertia, total variance explained, and proportion of constrained variance explained.

We used a similar approach to investigate the influence of geography, environmental factors and host population structure on the differentiation of *A. spathulata* symbiont communities which are horizontally acquired (van Oppen et al., 2001). Our preliminary analysis showed that ordinations based on *k*-mer-derived D_2^S distance were influenced by the number of symbionts reads in each sample. Consequently, all samples were downsampled at random to 50 M bp using `BBMap` v35.85 (`reformat.sh` script) and only samples above this threshold were retained (90% of samples, n = 878). As a small effect on the ordination remained, we included this variable as a conditional variable in all of our models. The first 10 principal coordinates from the PCoA on the *k*-mer-derived D_2^S distance matrix (above) were used as dependent variables in RDA models. As the PCoA did not yield negative eigenvalues indicating the distance matrix was nearly Euclidean, we did not perform negative eigenvalues correction as routinely applied in dbRDA. The first RDA model was built using all environmental variables and significant predictors were selected following the same procedure as above. A second global RDA model was built using (1) environmental variables previously identified as significant using forward selection, (2) the first four dbMEM eigenvectors and (3) the first three host PCs as predictors (representing the major axes of population structure; Figure A3.8). The marginal effect of each category of predictor was then assessed through separate pRDA models, using the two other

categories as conditional variables. All statistical analysis were conducted using *R* v4.0.4 and figures created using package *ggplot2* (Wickham, 2011).

4.4) Results

4.4.1 Genomic data processing and filtering

We recovered 339,720 single nucleotide polymorphisms (SNPs) from 1,088 individual coral colonies of *Acropora spathulata* using a stringent filtering approach (see Methods). This dataset had a mean locus-level sequencing depth of 13.7 ± 1.2 (mean ± sd). Following removal of related individuals and linked SNPs, Dataset 1 used for population structure analyses comprised 999 individuals and 27,175 SNPs. Dataset 2 used to compute genetic differentiation and diversity metrics consisted of ~2.2 M loci (SNPs and monomorphic sites). Dataset 3 used for demographic modeling consisted of 37,841–61,902 SNPs per population pair and Dataset 4 used for IbD analyses and N_e estimates consisted of 2,011 SNPs after pruning for physical linkage.

4.4.2 Coral host population structure

A. spathulata colonies across the Western Pacific were separated into four genetically differentiated groups, hereinafter referred to as populations (Figure 4.1). A PCA revealed geographically distinct populations separated on PC1 and PC2 (1.5% and 0.7% explained variance respectively; Figure 4.1a), corresponding to the Central to Northern GBR (i.e., from Davies to Hicks reefs), the Southern GBR, the Chesterfields-Bellona atolls (CB) in the Coral Sea and the western New Caledonia's main island (NC). PC3 (0.5% explained variance, Figure 4.1a) separated the CB group from the three other groups. Similarly, ADMIXTURE and sNMF analyses found a concordant optimal number of $K = 4$ ancestral populations (Figure A3.9, Figure A3.10). The separation of individuals by their ancestry proportion was consistent with PCA results but revealed small levels of admixture between all populations (Figure 4.1b). In particular, 4 of 137 and 19 of 137 colonies found in the Southern GBR had a >0.5 and >0.25 assignment to the ancestral population of the Central/Northern GBR respectively. Additional ADMIXTURE analyses conducted within each major population revealed no evidence of finer-scale population structure among reefs.

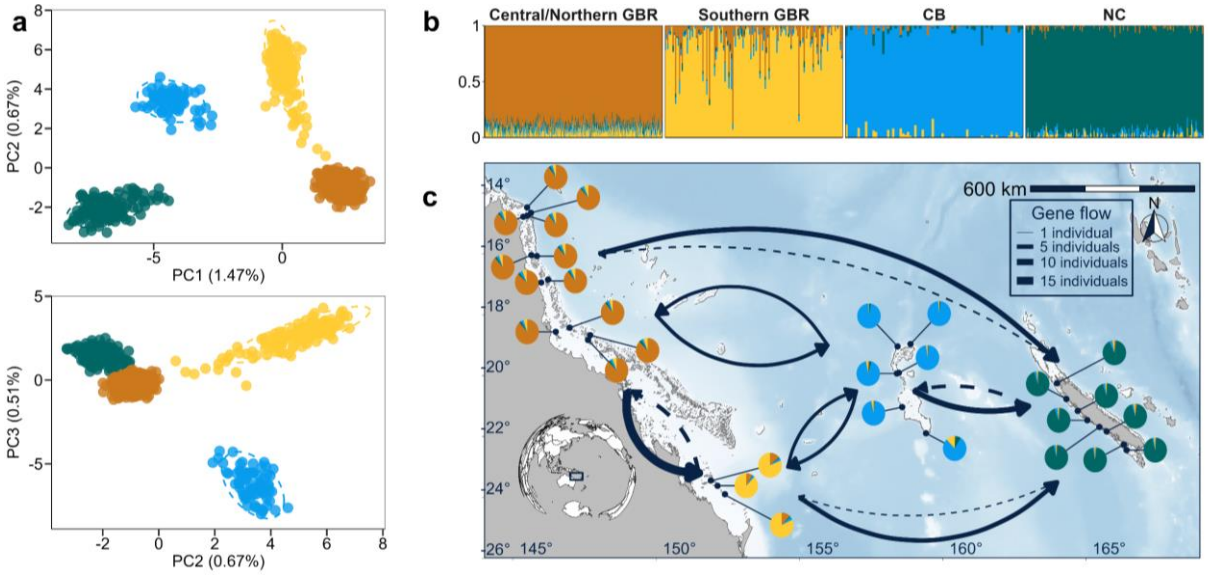


Figure 4.1. Population genomic structure and connectivity of *Acropora spathulata* across reefs from the Great Barrier Reef (GBR), Chesterfields-Bellona atolls (CB) and New Caledonia (NC). (a) Principal component analysis based on 27,175 SNPs showing four genetically and geographically distinct populations across the Western Pacific. PC1, PC2 and PC3 are shown with the proportion of variance explained by each component indicated in percentages. (b) Ancestry proportions from each individual using ADMIXTURE analysis with the optimal number of ancestral populations found using cross-validation (K=4). (c) Map showing ancestry proportion at sampling sites, averaged across colonies (n = 4–60). Arrows indicate average gene flow between populations since their divergence inferred from demographic modeling in dadi. Solid lines are shown in both directions when confidence intervals overlap.

4.4.3 Population divergence and genetic diversity

Genetic divergence, estimated using the fixation index, was low between all of the four populations (F_{st} < 0.030; Table 4.1) and was the lowest between the two GBR populations (F_{st} = 0.014). Pairwise D_{xy} ranged from 0.010 to 0.011 and was the lowest between the NC and CB populations. This corresponds to an average 1% nucleotide difference per bp between populations (Table 4.1). Nucleotide diversity (π) was the highest in the NC population (π = 0.0106) followed by the Central/Northern GBR (π =0.0103) and the Southern GBR populations (π = 0.0100). The CB population appears to have the lowest nucleotide diversity (π = 0.0097).

4.4.4 Dispersal and effective population size

No significant IbD occurred within populations. However, the pattern of IbD was revealed when populations were analysed jointly, with the regression of individual Rousset's genetic distance on geographic distance yielding a significant positive slope ($\beta = 0.00064 \pm 3.7 \times 10^{-05}$; median ± sd; Figure 4.2a). The effective population size at the neighbourhood size across this

geographic range was estimated at N_e = 2,954 ± 1,573 effective individuals (median ± sd; Figure 4.2b). Combining these estimates, the average dispersal distance between parents and offspring across generations was 109 ± 33 km (mean axial dispersal distance; σ; median ± sd; Figure 4.2c).

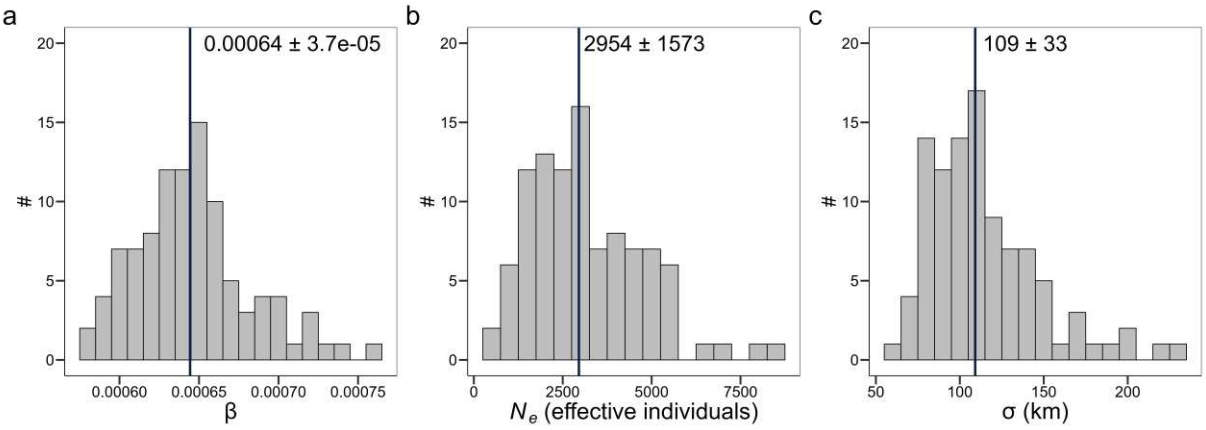


Figure 4.2. Generational dispersal and effective population size in *Acropora spathulata* from the Western Pacific. Isolation by distance at multiple appropriate spatial scales was used to infer the distribution of (a) slope of genetic distance on geographic distance regressions, (b) effective population size at the neighbourhood size and (c) mean axial generational dispersal distance. Vertical lines indicate the median of each distribution with median and standard deviation values indicated next to it.

4.4.5 Demographic modeling of population divergence and gene flow

For all population pairs, observed joint allelic frequency spectra (JAFS) were best explained by demographic models consisting of divergence with asymmetrical gene flow than models with no gene flow or ancestral gene flow (Figure A3.5). This suggests that these populations have diverged across the Western Pacific while exchanging larvae over many generations. Demographic models estimated divergence time between 275 to 651 thousand years ago depending on population pairs (Table 4.1), although these are approximate estimates because germline mutation rates are lacking for this species. Based on these estimates, the two populations from the GBR appear to have diverged most recently (275 [230–319] kya; median [5-95%]). Modelling results suggest that divergence of NC from other populations (323–651 kya) is more ancient than divergence of CB from GBR populations (354–385 kya). However, large overlap in confidence intervals, and possible bias introduced by high migration rates, make it difficult to reconstruct their precise sequential divergence history.

Migration rates and gene flow rates were asymmetrical for most population pairs, and this result was consistent across bootstrap replicates and optimization runs (Table 4.1). On the GBR,

migration rates were on average 5 times higher from the Central/Northern population to the Southern population (2.5×10^{-04}) than vice versa (6.2×10^{-05}), resulting in higher southward gene flow (N_em) in line with predominant oceanographic currents (Figure 4.1c; Figure A3.1). Eastward migration rates from both GBR populations to the CB population (9.3×10^{-05}–1.2×10^{-04}) were higher than the westward rates (5.4×10^{-05}–1.2×10^{-04}). However, differences in long-term effective population sizes (29,000–66,000 effective individuals) resulted in nearly symmetrical gene flow between the GBR and these Coral Sea atolls (6.5–7.1 migrants per generation, Figure 4.1c). Migration rates between the CB and NC populations were broadly symmetrical ($6.5–7.0 \times 10^{-05}$), but the compounding effect of unequal population sizes produced a dominance of eastward gene flow (11.0 [9.8, 12.1] migrants per generation; median [5-95%]). Gene flow was also directed primarily eastward, from both GBR populations toward NC (Figure 4.1c).

Table 4.1. Demographic modeling of *Acropora spathulata* populations divergence across the Western Pacific. For each pair of populations (1: left, 2: right), optimized parameters are presented for the model exhibiting the best fit to the observed joint allelic frequency spectrum (divergence with asymmetrical gene flow) along with genetic differentiation statistics (fixation index F_{st} and absolute divergence D_{xy}). $\boldsymbol{Nref}$, $\boldsymbol{\nu_1}$, $\boldsymbol{\nu_2}$ are the ancestral and current effective population sizes in thousands of individuals. $\boldsymbol{m}$ is the proportion of migrants per generation and $\boldsymbol{M}$ is the number of migrants per generation. $\boldsymbol{T}$ is the estimated divergence time in thousands of years. For each model and parameter, median and 2.5–97.5% confidence intervals based on 100 optimized bootstrap replicates are presented.

Population pair	**Nref**	$\boldsymbol{\nu_1}$	$\boldsymbol{\nu_2}$	$\boldsymbol{T}$	$\boldsymbol{D_{XY}}$
Central/Northern GBR-Southern GBR	7.2 [4.1, 10.6]	63.9 [51.1, 76.3]	32.5 [25.9, 42.3]	276 [231, 320]	0.0102
Central/Northern GBR-NC	9.2 [5.1, 17.6]	82.9 [66.9, 118.9]	25.0 [14.5, 33.6]	323 [218, 379]	0.0107
Central/Northern GBR-CB	4.9 [3.7, 9.9]	61.9 [51.1, 75.8]	29.6 [21.6, 36.6]	354 [292, 373]	0.0102
Southern GBR-NC	6.5 [4.6, 10.9]	82.0 [73.6, 87.9]	32.8 [28.4, 39.5]	436 [378, 461]	0.0107
Southern GBR-CB	7.1 [4.4, 12.3]	65.8 [58.1, 74.5]	34.8 [28.6, 43.9]	395 [334, 431]	0.0100
NC-CB	7.2 [6.6, 9.9]	86.5 [76.4, 96.7]	48.8 [35.2, 56.1]	651 [630, 666]	0.0104
Population pair	**m_{12} (2→1)**	**m21 (1→2)**	**M12 ($N_e m_{12}$)**	**M21 ($N_e m_{21}$)**	$\boldsymbol{F_{st}}$
Central/Northern GBR-South GBR	6.2e-5 [4.6e-5, 8.7e-5]	2.5e-4 [2.0e-4, 3.0e-4]	7.9 [6.6, 9.6]	16.4 [14.7, 18.0]	0.014
Central/Northern GBR-NC	2.1e-5 [9.4e-6, 3.5e-5]	2.0e-4 [1.5e-4, 3.0e-4]	3.6 [2.3, 4.7]	9.9 [8.6, 11.0]	0.025
Central/Northern GBR-CB	5.4e-5 [3.7e-5, 7.2e-5]	1.2e-4 [9.2e-5, 1.7e-4]	6.5 [5.2, 8.0]	7.1 [6.5, 7.8]	0.028
Southern GBR-NC	1.7e-5 [1.3e-5, 2.5e-5]	1.4e-4 [1.2e-4, 1.5e-4]	2.8 [2.2, 3.7]	8.8 [8.2, 9.5]	0.029
Southern GBR-CB	5.1e-5 [3.5e-5, 7.1e-5]	9.3e-5 [5.9e-5, 1.2e-4]	6.8 [5.1, 8.6]	6.3 [5.1, 7.3]	0.026
NC-CB	6.5e-5 [5.2e-5, 7.3e-5]	7.0e-5 [5.6e-5, 1.1e-4]	11.0 [9.8, 12.1]	6.9 [6.2, 7.8]	0.026

4.4.6 Symbiodiniaceae genetic diversity based on molecular markers

We mapped non-coral reads from our 1,088 hologenomes to Symbiodiniaceae reference genomes and recovered a median of 708,000 Symbiodiniaceae reads per sample (range: 63,540 to 24,932,887). All colonies harbored symbionts from the *Cladocopium* genus with

predominant ITS2 sequence variants (recovered from hologenome reads in 950 of 1,088 samples) classified as C50, C3 and *Cladocopium* sp. (Figure A3.11). Hologenome sequencing results were consistent with amplicon sequencing results in a subset of 36 samples, although the latter showed a greater taxonomic resolution, separating profiles dominated by C3k, C3k/C3bo, C50b, and C50c sequences (Figure A3.6). Read mapping against *psbA*^{ncr} sequences revealed classifications of *C. vulgare* (C1) or *C. sodalum* (C3; Figure A3.11). The mapping of reads to *psbA*^{ncr} C1 in samples associated with C50 ITS2 sequences was presumably due to the lack of reference *psbA*^{ncr} sequences of *Cladocopium* C50, limiting the use of this method for finer taxonomic classification. However, our results suggest that the C3 symbionts identified are more closely related to *C. sodalum* than other described C3 species (>80% of mapped sequences; Butler et al., 2023).

4.4.7 Symbiodiniaceae community divergence based on *k*-mer profiles

Alignment-free clustering of symbiont genomic reads revealed five major Symbiodiniaceae genetic clusters across colonies, hereinafter referred to as taxa and named according to their major ITS2 sequence. There was some degree of co-clustering between each of the five main symbiont taxa and the corresponding host populations (Figure 4.3). The host population in the Central/Northern GBR was associated predominantly with *Cladocopium* taxa from C3k and C50c subclades, with a cross-shore partitioning of these communities. Offshore reefs were associated with C3k, while inshore reefs were associated with C50c (Figure 4.4a). At intermediate reefs (e.g., Moore, North Direction, Mackay), some colonies harbored the C50c taxon while others harbored C3k. The host population in the Southern GBR associated with a symbiont taxon of the C50b subclade. A few colonies associated with C3k at Lady Musgrave Island. Corals in Western NC were predominantly associated with a taxon from the C3k/C3bo subclade. The exception was some colonies in most southern reefs, which associated with a distinct symbiont taxon from C50b subclade. Based on ITS2 profiles, *k*-mer profiles clustering and geographic separation, this symbiont taxon is genetically differentiated from the C50b taxa found in the Southern GBR (Figure A3.6 and Figure A3.7). Coral hosts in the CB atolls were also associated with a C3k/C3bo taxon that was indistinguishable from NC C3k/C3bo based on *k*-mer profiles, despite being separated by >400 kilometres.

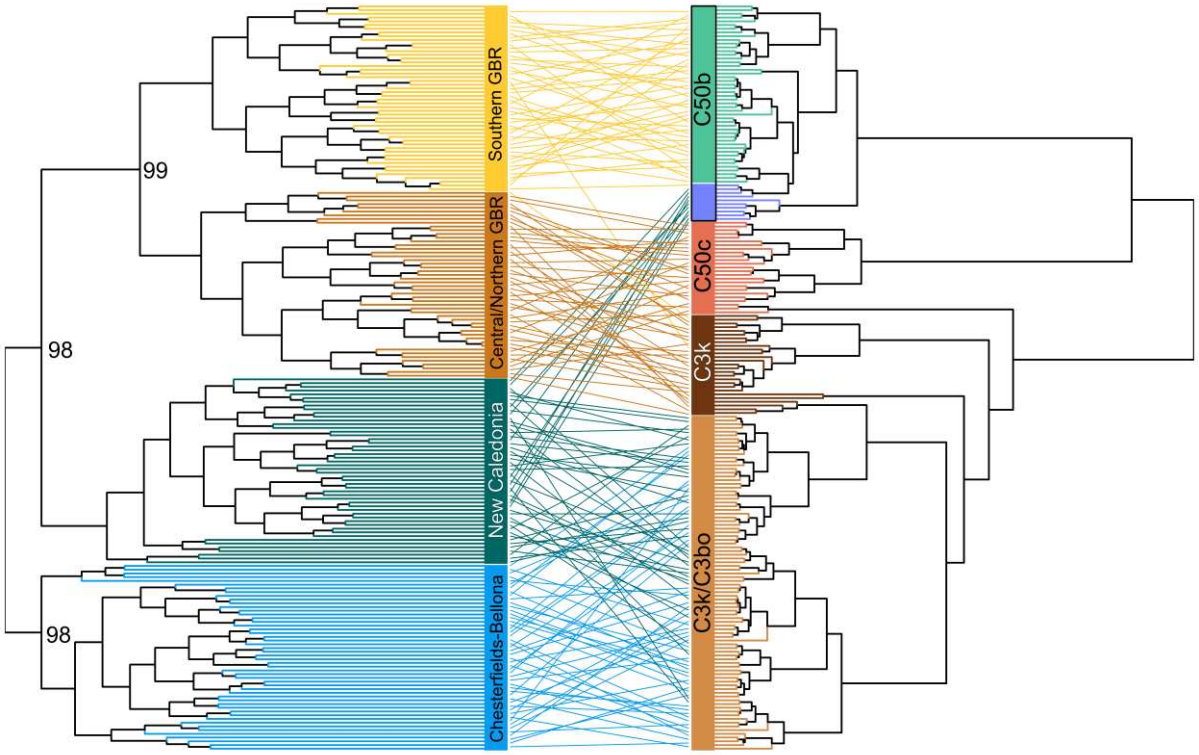


Figure 4.3. Co-clustering of *Acropora spathulata* coral hosts and associated Symbiodiniaceae taxa across the Western Pacific. The host dendrogram (left) is a simplified 200-leaf maximum likelihood tree derived from 27,175 SNPs using RAxML. The node values represent bootstrap support (>90) from 100 bootstrap replicates and branches are coloured based on ADMIXTURE ancestral populations. The symbiont dendrogram (right) is obtained through hierarchical clustering of the $\boldsymbol{D_2^S}$-derived distance matrix based on symbiont *k*-mer profiles and branches are coloured according to majority ITS2 sequences for each sample. Colonies from the southern Great Barrier Reef (GBR) and New Caledonia were associated with Symbiodiniaceae that shared the same dominant ITS2 sequence (C50b; black rectangle) but were distinguishable based on their k-mer profiles.

4.4.8 Drivers of host and symbiont genetic structure

The RDA indicated that environmental variables significantly predicted coral host genetic structure (ANOVA; p-value < 0.01), explaining 64% of the total variance. Maximum Monthly Mean (MMM) sea temperature, the frequency of mild marine heatwaves (DHW > 4), and distance to coast were the strongest reef-level environmental predictors of host population structure (cumulative adjusted R^2 = 0.60). A global RDA including geographic predictors (dbMEMs) on top of significant environmental variables explained 70% of the total variance in host genetic structure. Due to the spatial sampling design, several partial-RDAs indicated that environmental and geographic effects were largely confounded (86% of explained variance, Table 4.2).

Environmental predictors also significantly influenced the community composition of *Cladocopium* symbionts (ANOVA; p-value < 0.01), explaining 37% of the total variance. The MMM, frequency of mild marine heatwaves (DHW > 4) and annual range in sea surface temperature (AR) were retained as significant predictors in the model (p-value = 0.001). The AR separated C3 populations, found in more thermally variable environments at inshore and high latitude reefs, from C50 populations found in offshore and low-latitude reefs (Figure 4.4b). Within the C50 subclade, distinct C50b and C50c populations were separated primarily by the MMM reflecting both temperature variation across latitudinal gradient and cross-shore gradients. Within the C3 subclade, the C3k populations were positively associated with the MMM, while C3k/C3bo populations were found in reefs where MMM was lower on average, but where mild marine heatwaves have been more frequent. Several pRDAs indicated that the environment was the strongest driver of symbiont community composition (6.3% of total explained variance). Geography (1.2%) and host population structure (1%) were less influential, although the effect of these three components was also largely confounded (80% of explained variance, Table 4.2).

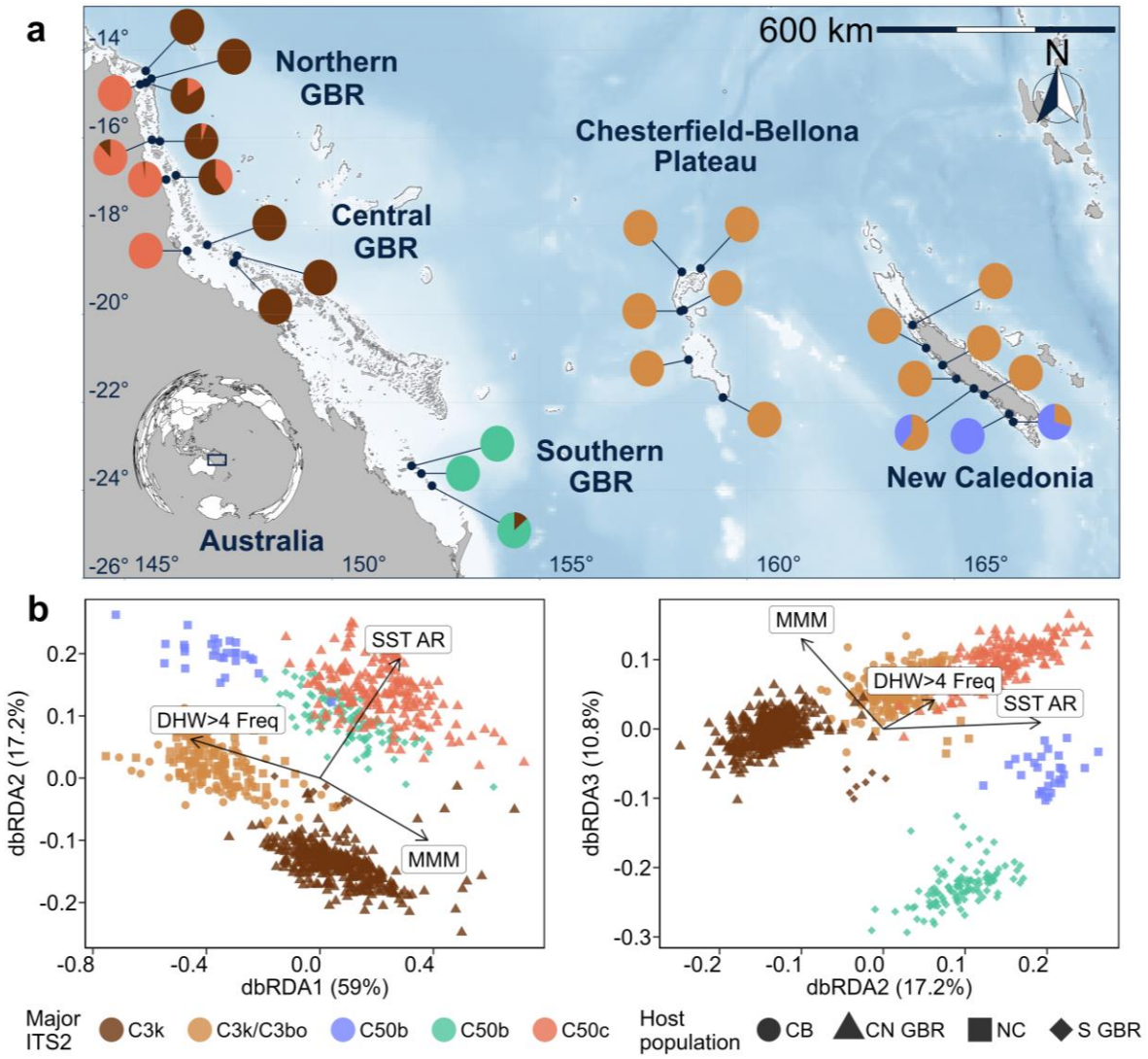


Figure 4.4. Variation in the symbiont (Symbiodiniaceae) communities of *Acropora spathulata* across geographic and environmental gradients in the Western Pacific. (a) Map showing the proportion of colonies harboring each of the symbiont clusters identified using ordination of D2s distance matrix at each sampling site, identified using ordination of $\boldsymbol{D_2^S}$ distance matrix. Symbiont genetic clusters are coloured and labelled based on their major ITS2 type. Symbionts with the same dominant C50b ITS2 sequence are depicted with different colours in the Southern Great Barrier Reef (GBR) and New Caledonia as they were found to be genetically differentiated based on their *k*-mer profiles. (b) Distance-based redundancy analysis (db-RDA) ordination of $\boldsymbol{D_2^S}$ *k*-mer profiles. Each individual is coloured by its major ITS2 sequence and the shape corresponds to each of the host populations (CN GBR = Central/Northern GBR, S GBR = Southern GBR, NC = New Caledonia, CB = Chesterfields-Bellona). Arrows represent significant environmental variables in the model. The first three axes explaining 87% of the constrained variance are shown.

Table 4.2. The influence of geography and environmental conditions on host neutral genetic structure of *Acropora spathulata* and the influence of geography, environmental conditions and host structure on associated Symbiodiniaceae communities. The relative influence of each category of predictors was decomposed using partial redundancy analysis (pRDA). Geography was modeled using distance-based Moran's Eigenvector maps. Environmental variables included factors indicative of temperature, irradiance, and turbidity.

Host model				
Partial RDA models	**Inertia**	**R^2 (Total Variance explained)**	***p*(>*F*)**	**Proportion of constrained variance explained**
Host PC ~ Env + Geography	21.38	0.701	0.001***	1
Host PC ~ Geography | Env	1.898	0.06	0.001***	0.089
Host PC ~ Env | Geography	0.987	0.03	0.001***	0.046
Confounded Env/Geography		0.611		0.865
Total unexplained	9.08	0.29		
Total inertia	30.46	1		
Symbiont model				
Partial RDA models	**Inertia**	**R^2 (Total Variance explained)**	***p*(>*F*)**	**Proportion of constrained variance explained**
Kmer ~ Env + Geography + Host_structure | (Nreads)	0.174	0.40	0.01**	1
Kmer ~ Env | (Nreads + Host_structure + Geography)	0.027	0.063	0.01**	0.15
Kmer ~ Geography | (Nreads +Env + Host structure)	0.005	0.012	0.01**	0.03
Kmer ~ Host_structure | (Nreads +Env + Geography)	0.004	0.01	0.01**	0.02
Confounded Env/Geography/Host structure		0.315		0.8
Total unexplained	0.167	0.6		
Total inertia	0.435	1		

4.5) Discussion

Our results revealed four genetically distinct *A. spathulata* populations in the studied Western Pacific region, which have diverged due to geographic isolation but maintain gene flow through major oceanographic currents. These populations show little genetic structure over distances greater than 500 km, reflecting a generational dispersal distance estimated at ~100 km. In contrast, coral hosts are associated with distinct algal symbionts of five Symbiodiniaceae taxa across shorter latitudinal and cross-shelf gradients. This study presents one of the most extensive datasets for analyzing spatial genetic variation in both corals and their algal symbionts using whole-genome sequences, combining broad geographic coverage and dense local sampling. These results suggest that large local populations and dispersal support resilience of a broadcast-spawning coral, whereas habitat-specific symbionts and long-distance gene flow could enhance its adaptive potential in changing environments.

4.5.1 Regional spatial genetic variation differs among holobiont partners

The spatial scale of genetic variation differed markedly between *A. spathulata* and its associated *Symbiodiniaceae*. This coral species comprised four genetically differentiated populations distributed in distinct regions separated by ~600–2,200 km. However, each population was largely genetically homogeneous based on PCA, ADMIXTURE and isolation-by-distance analyses, despite spanning up to >300 km for NC and CB, and up to >500 km for the Central/Northern GBR. Conversely, Symbiodiniaceae community genetic variation occurred over spatial scales as small as 30 km, and colonies from the same reef sometimes hosted distinct symbiont taxa. These patterns reflect the predominant effect of distinct evolutionary forces acting on holobiont partners.

Patterns of *A. spathulata* genetic variation suggest extensive gene flow promotes genetic homogenization of populations, counteracting the effects of drift and local adaptation (Slatkin, 1987). This was supported by our estimated σ exceeding >100 km. Across the distant Western Pacific populations, reduced gene flow and increasing environmental contrasts (e.g., Δ~3 °C in MMM; Figure A3.1) drive greater genetic differentiation (D_{xy} = 0.0102–0.0107). However, the relative importance of genetic drift and local adaptation in this differentiation could not be disentangled due to spatial confounding between environmental and geographic predictors (Table 4.2). Future studies integrating morphological and genomic data (e.g., Bridge et al., 2024; Rassmussen et al., 2025) across a broader geographic range, including populations from the *A. spathulata* holotype locality in the Solomon Islands, will be necessary to determine whether the lineage described here represents a synonymized species or populations of the same species.

Patterns of Symbiodiniaceae genetic variation suggest that environmental filtering is the predominant driver of *A. spathulata* algal symbioses. Variation in symbiont communities was likely not strongly influenced by dispersal, as it did not follow an IbD pattern. For instance, colonies from Martin and No Name reefs (30 km apart) hosted different taxa, while those from No Name and Chicken reefs hosted the same taxa (500 km apart; Figure 4.4). In addition, the environment had a larger effect on symbioses than host genetic differentiation (although largely confounded; pRDA; Table 4.2), as expected from species that acquire symbionts from their environment after settlement (Davies et al., 2020; van Oppen et al., 2001). Variation in symbioses was particularly pronounced across shelf and latitudinal gradients, similar to other *Acropora* species on the GBR (Cooke et al., 2020; LaJeunesse et al., 2004; Matias et al., 2022).

Notably, *A. spathulata* and *A. tersa* (formerly synonymized with *A. hyacinthus*; Rassmussen et al., 2025) hosted strikingly similar Symbiodiniaceae communities, with identical ITS2 types found across comparable environmental gradients (Naugle et al., 2024). RDA suggest that temperature was the primary driver, although other important factors such as light and turbidity (Cooper et al., 2011) were likely excluded due to multicollinearity. It also remains unclear whether *A. spathulata* associates with specific Symbiodiniaceae because these taxa are locally abundant and/or they form the best performing symbioses (Bhattacharya et al., 2024).

The spatial distribution of Symbiodiniaceae suggests some taxa may be environmental specialists while others may be environmental generalists. Similar to Epstein et al. (2019), we found *A. spathulata* associated with a C3k taxon at cooler offshore Central/Northern GBR reefs, and we also revealed a distinct C50c taxon predominant at warmer turbid inshore Central/Northern reefs. Conversely, C3k/C3bo appears to have a wide distribution as it was indistinguishable based on genome-sequence composition between NC and CB. Taxa from the C50b subclade, found across a 13° longitudinal gradient, might also be widespread in this region but best performing at high-latitudes. Our findings reinforce the idea that niche partitioning can promote ecological diversification of closely related algal symbionts (Hoadley et al., 2021; Sampayo et al., 2007), as the C50c and C50b populations were found in warmer and cooler environments respectively. Importantly, additional genetic diversity within major Symbiodiniaceae taxa may result from local adaptation of symbiont populations and/or genotypes (Howells et al., 2012), potentially explaining the diversity of ITS2 profiles observed within taxa. Such finer-scale genetic variation was not detected by the alignment-free approach and may require tailored methods, including microsatellite analyses (Thornhill et al., 2017) or the retrieval of chloroplast SNPs (Armstrong et al., 2024).

4.5.2 Broadcast spawners maintain long-distance asymmetrical gene flow across the Western Pacific

Demographic models detected substantial historical gene flow between Western Pacific populations separated by thousands of kilometres, that likely started to diverge between 0.275 to 0.651 MYA. While this potential connectivity had been suggested by biophysical models of coral dispersal (Wood et al., 2014), it remained to be empirically tested as these approaches can be biased at coarse spatial resolutions (Saint-Amand et al., 2023). Although some uncertainty remained in the absolute values of gene flow, primary directions of migration rates were

consistent across bootstrap replicates for all population pairs and these models had stronger support than divergence without gene flow.

On the GBR, gene flow was primarily southward, consistent with the predominant EAC direction and other studies on coral broadcast spawners (Matz et al., 2018; Meziere et al., 2025; Riginos et al., 2019). We also observed admixture between the Central/Northern and Southern GBR populations indicating recent southward migration between these regions (Figure 4.1). Conversely, gene flow was largely symmetrical between the GBR and Coral Sea atolls, reflecting the region's complex oceanography, which includes westward currents such as the North Caledonia Jet (NCJ) and the South Caledonia Jet (SCJ; Cravatte et al., 2015), as well as the eastward Sub Tropical Counter Current (STCC; Marchesiello et al., 2010). Demographic models inferred dominant eastward gene flow from the GBR to NC, and from CB to NC, which is unexpected given the prevailing westward NCJ and SCJ in the region (Cravatte et al., 2015). These patterns of realized connectivity may have been influenced by surface circulation associated with the STCC, while the strong NCJ and SCJ reach their maximum intensity in deeper layers (Marchesiello et al., 2010). Observations of plastic debris and Lagrangian dispersal modeling notably suggest that mesoscale currents can generate eastward drift in the region despite the dominance of westward zonal jets (Maes & Blanke, 2015). Because gene flow inferred from demographic models reflects an average across thousands of generations, these estimates could also have been influenced by temporal changes in ocean circulation. Together, these results provide novel insights into a complex realized connectivity across this region and highlight the value of such analyses for informing management in contexts of variable ocean circulation. Beyond uncertainties in the current directionality of gene flow, the models strongly support low but persistent migration between these Western Pacific populations. As such, they should be treated as distinct management units (Hohenlohe et al., 2021) within a broader regional network that also recognizes the importance of their connectivity for evolutionary adaptive potential.

4.5.3 Large breeding population and high dispersal support demographic resilience

The effective population size of *A. spathulata* at the neighbourhood size was relatively high (N_e=2,950) despite drastic coral mortality over last decades (Eddy et al., 2021; Souter et al., 2021). This estimate is particularly important for conservation, as emphasized by the recent Kunming-Montreal Global Biodiversity Framework (Waples, 2024). Although there is no exact

rule of how large N_e should be, our estimate suggests that local breeding populations are sufficiently large to prevent dramatic loss of genetic diversity due to genetic drift (Waples, 2024). In contrast, brooding species with limited dispersal and local recruitment tend to have lower N_e and higher local extinction risk (Hernández-Agreda et al., 2024; Meziere et al., 2025; Prata et al., 2024).

High N_e likely reflects substantial census sizes of this common species densely distributed on reef flats and slopes, combined with a large generation dispersal estimated at ~100 km per generation. This estimate contains some level of uncertainty because IbD theory assumes symmetrical dispersal across a continuous habitat of constant population density, which does not match the typical patchiness of coral reefs. Yet, this value is consistent with a pelagic larval duration estimated from lipid reserves at ~100 days which would allow larvae to be carried across large distances (Graham et al., 2013). Estimates from previous studies using similar methods vary from a few metres in brooding species (Gorospe & Karl, 2013; Hernández-Agreda et al., 2024; Prata et al., 2024) to 1–52 km in broadcast spawning species (Japaud et al., 2019; Meziere et al., 2025). Our estimate also falls at the upper end of broadcast-spawners connectivity predicted by biophysical models (63% of settlement within 100km; Wood et al., 2014) and is comparable to coral trout dispersal on the GBR (Williamson et al., 2016). These findings suggest that *A. spathulata* exhibits one of the highest coral dispersal distances recorded to date. Importantly, we only estimated a global isotropic σ because IbD was not significant within populations, but this estimate could vary among regions. Even if σ is similar across regions, the demographic consequences could differ because the GBR is a fragmented mosaic of numerous discrete reefs while NC and CB contain longer continuous barrier reefs (Andréfouët et al., 2009). Individual reefs are expected to be demographically isolated when separated by more than 2σ (Pinsky et al., 2012) and thus connectivity could differ between these reef systems of contrasting geomorphology.

Large N_e and high dispersal may explain the impressive recovery of *Acropora* communities on many GBR reefs after the 2016–2017 bleaching-related mortality events (Emslie et al., 2024), and will be critical for demographic recovery under increasingly frequent disturbances (Hock et al., 2017). For example, marine heat waves and freshwater floods caused 90–100% mortality of *A. spathulata* colonies at several inshore Northern GBR sites sampled in this study in 2024, while colonies at offshore reefs were relatively unaffected. Larval dispersal from these populations could thus in theory supply larvae to degraded reefs. However, a finer assessment of realized dispersal is needed to evaluate the inbound and outbound connectivity of individual

reefs, as it depends on meso-scale currents and habitat availability. Finally, given the ongoing impacts to these populations from global warming, monitoring possible changes in N_e will be important to track changes in their vulnerability (Howells et al., 2022a).

4.5.4 Habitat-specific symbioses and long-range dispersal affect the evolutionary adaptive potential of *A. spathulata*

A. spathulata formed distinct symbioses with Symbiodiniaceae across distinct thermal conditions, which raises the question of whether a shift to more heat-tolerant symbioses could promote the adaptation of *A. spathulata* to rapid climate warming. *Acropora* corals symbioses with heat tolerant symbionts—notably from the *Durusdinium* genus—have been observed to increase in prevalence during marine heatwaves, but this response appears to be species-specific and has not been yet reported for *A. spathulata* (Quigley et al., 2022b). The absence of *Durusdinium* in colonies sampled outside major marine heatwaves in Epstein et al. (2019) and in our study suggests this association is uncommon in *A. spathulata* under normal conditions. However, we observed variable symbioses among colonies at mid-shelf reefs on the GBR, suggesting that both the C50c and C3k taxa are found in these environments. Under future climate warming, symbioses with C50c typically found in warmer inshore environments may become more prevalent on mid-shelf reefs, especially given that fast growing *Acropora* corals can rapidly shift to better adapted symbionts within 1–2 years (Turnham et al., 2025). Whether this ability varies across regions remains an open question, especially given that the same C3k/C3bo taxon was found in colonies both from NC and CB reefs despite drastically different environments. The absence of other associations may indicate lower potential for adaptation through shifts in symbioses, or on the contrary indicate greater physiological plasticity and resilience to changing conditions of this symbiont taxon. Further sampling around bleaching events is thus needed to assess whether this species can shift symbioses quickly enough to reduce coral mortality over future marine heatwaves.

Another factor that may underlie the evolutionary adaptation of *A. spathulata* is the long-distance gene flow between Western Pacific populations, as it could increase genetic variation or introduce heat-tolerant alleles from warmer to cooler regions (Matz et al., 2020). On the GBR, dominant southward gene flow may allow this process, as observed in other coral taxa (Matz et al., 2018; Meziere et al., 2025; Riginos et al., 2019), particularly given that admixture suggests recent southward migration. Among other populations, the effect of gene flow on adaptive genetic variation may be harder to predict due to more-complex patterns. For example,

the southern GBR showed substantial northeastward gene flow toward CB populations typically found in warmer environments. Nevertheless, occasional long-distance gene flow will benefit populations' adaptive potential by introducing novel genetic variation without swamping adaptive local variants (Fitzpatrick et al., 2020). We only inferred broad-scale patterns of gene flow among the four regions. Sampling a continuum of reefs in these regions and modeling gene flow at a finer resolution among reef groups (e.g., Matz et al., 2018; Meziere et al., 2025), along with construction of high-resolution biophysical models (e.g., Mason et al., 2025), would help building finer networks of reef connectivity (Mumby et al., 2021).

Within regions, high levels of gene flow will constrain evolution by preventing strong local adaptation, for instance along cross-shore gradients. However, it will also facilitate the spread of standing genetic variation, as evidenced by limited differences in genetic diversity between reefs and regions. This gene flow will reduce the risk of inbreeding depression and enable the rapid spread of novel genetic variants across the population range (Slatkin, 1987). Future work investigating the distribution of adaptive genetic variation in this species will help clarify this ambivalent effect.

4.6) Conclusion

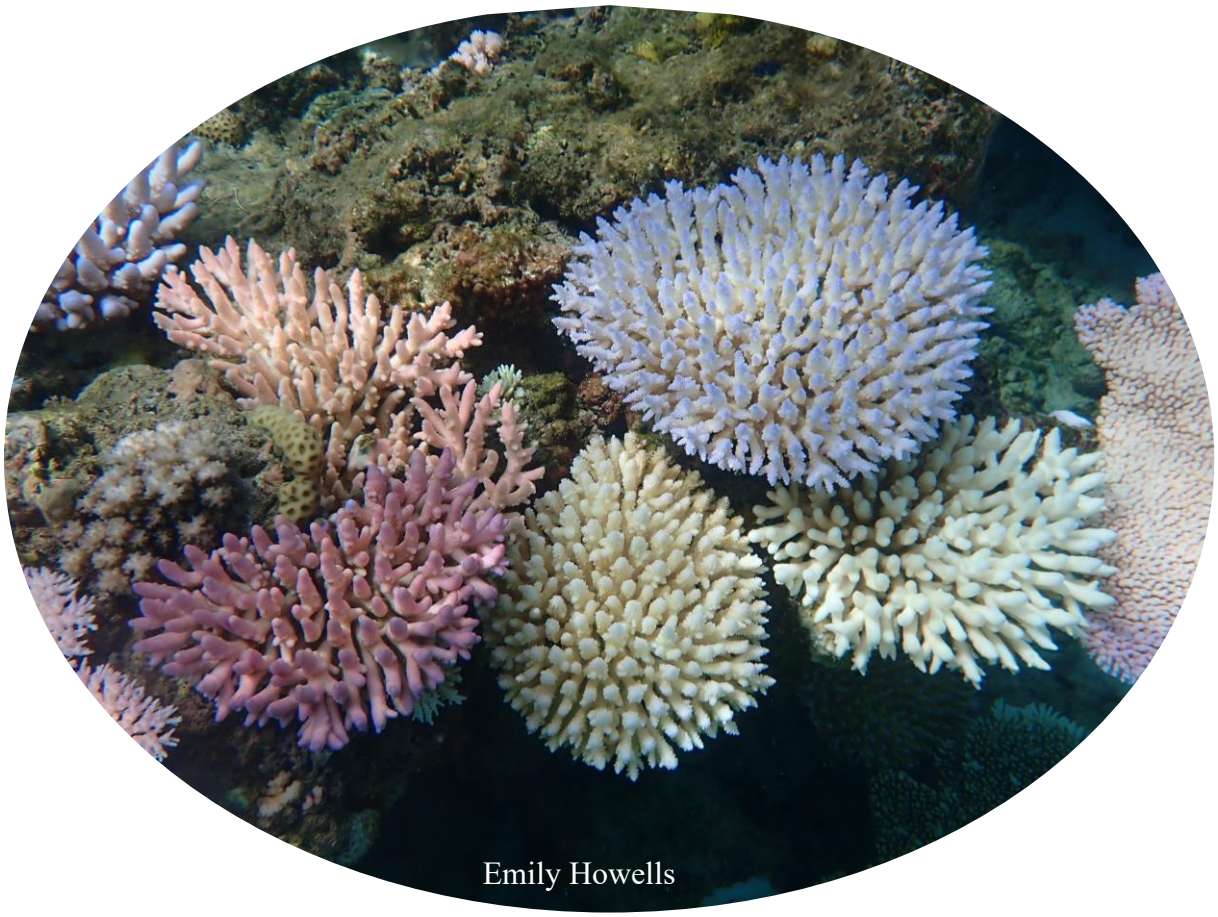
The genetic structure of the Western Pacific coral *A. spathulata* reflects opposing forces of geographic isolation and long-distance dispersal driven by major regional ocean currents. In parallel, variation in associated *Cladocopium* taxa along latitudinal and cross-shore environmental gradients suggests environmental filtering of symbioses. Our results enable the definition of management units across the Western Pacific, and emphasize the importance of considering the connectivity of coral reefs at the regional scale beyond national borders—as maintaining gene flow between distant populations could underlie their evolutionary adaptation (Fitzpatrick et al., 2020). The distinct spatial scales at which evolutionary processes affect coral hosts and their symbionts are also essential to consider for many proposed intervention approaches such as assisted gene flow, selective breeding or symbiont manipulations (van Oppen et al., 2017). Our findings indicate substantial effective population size and exceptional dispersal in *A. spathulata* that may support demographic rescue following disturbances, provided some locations remain unaffected. However, this study only offers a snapshot of the demographic status of *A. spathulata* populations. In light of the recent severe coral mortality

events (Cantin et al., 2024), future reassessment of their vulnerability will be essential for effective conservation.

4.7) Acknowledgements

We thank the Traditional Owners of the Great Barrier Reef and New Caledonia reefs for their free prior and informed consent to undertake coral sampling in their Sea Country. We thank the government of New Caledonia for granting permission to conduct coral sampling within the Natural Park of the Coral Sea, as well as the South Province and North Province. We thank Samantha Goyen, Riverside Marine Cruise crew members and numerous AIMS staff and volunteers for their support while collecting on the GBR. We thank Stéphane Joost and Manon Pribille for their support in the identification and selection of sampling sites in the Coral Sea. We thank the French National Navy, Mahé Dumas, Bertrand Bourgeois, William Roman, Jordi Giraud and Martin Nguyen for their help while collecting in Chesterfield-Bellona atolls and New Caledonia Grande Terre. We thank Samantha Howitt for assisting in the DNA extractions at the University of Queensland and Clarisse Majorel for assisting in the DNA extractions in New Caledonia. We thank Molly Przeworski for providing an upgraded reference genome assembly. We thank Jérôme Lefèvre and Christophe Charbuillet for their support with HPC systems. This research was undertaken with the assistance of resources from the National Computational Infrastructure (NCI Australia), an NCRIS-enabled capability supported by the Australian Government, through Project d85 awarded to C.X.C. Finally, we are thankful to Ryan Gutenkunst for his advice on demographic modeling analyses.

Chapter 5. Genetic basis of coral heat adaptation across thermal exposures from acute stress to climates



Genetic basis of corals heat adaptation across thermal exposures from acute stress to climates

Chapter 4 revealed considerable dispersal of *Acropora spathulata* larvae, resulting in weak genetic structure across large spatial scales, and connectivity across Western Pacific populations separated by thousands of kilometres. Local adaptation of coral holobionts also appears to be partly driven by associations with distinct *Cladocopium* taxa across the species range and environmental gradients. Despite low genetic structure, genetic polymorphisms within specific genes and genomic regions may further support the adaptation of coral hosts to their thermal environment, and contribute to the variation in heat tolerance thresholds among individuals observed in Chapters 2 and 3. Chapter 5 uses association studies to assess the genomic basis of heat adaptation, from acute stress responses to long-term climatic conditions, and investigates potential shared evolutionary signals among distant populations. Finally, the chapter evaluates the utility of genomic markers to improve predictions of coral bleaching and mortality in the wild. Chapter 5 is in preparation for submission to a peer-reviewed journal and was re-formatted for insertion in this thesis.

Genetic basis of corals heat adaptation across thermal exposures from acute stress to climates

5.1) Abstract

Recurrent marine heatwaves caused by climate warming have driven severe declines in coral populations, sparking interest in the genetic basis of heat adaptive traits. Yet, the discovery of causal variants and the assessment of genomic prediction potential for coral heat tolerance remain in their early stages, partly due to limited large-scale genotypic and phenotypic datasets. To address these gaps, we combined genome-wide association analyses of heat tolerance phenotypes and thermal environments from ~1,000 *Acropora spathulata* colonies across four Western Pacific populations, and evaluated the potential for genomic prediction of bleaching and mortality during a marine heatwave. Balanced polymorphisms along thermal gradients indicate largely nonparallel polygenic adaptation across distant populations, with a few overlapping signals highlighting key genes likely involved in heat adaptation such as *TRPA1*, *LIN41*, and *PSTK*. Similarly, variation in the tolerance of corals to an acute heat stress was linked to distinct polymorphisms and genes across populations, yet showed functional convergence in the regulation of apoptosis, proteolysis, calcium and carbohydrate transport and extracellular structures. We found minimal overlap between genomic signals for tolerance to an acute heat stress and a prolonged natural marine heatwave, suggesting that the genetic architecture of heat stress responses varies across thermal exposures. Nevertheless, genetic variants associated with thermal environments substantially improved the predictions of coral bleaching and subsequent mortality in the wild, indicating that genome-environment associations successfully detected adaptive alleles. Overall, our results emphasize the complex and variable genetic basis of heat adaptation of corals across populations and thermal stress regimes, and highlight the value of integrating multiple approaches and taxa to identify genomic markers of broad relevance for coral management under climate warming.

5.2) Introduction

Coral reefs are experiencing a global crisis due to mass bleaching and mortality of reef-building corals caused by intense and frequent marine heatwaves (Souter et al., 2021). The impacts of these events have already led to the functional extinction of certain coral populations (Riegl et al., 2018) and placed some species at risk of global extinction (Manzello et al., 2025; Miller et al., 2022; Thompson et al., 2025). Increase in the upper thermal limits of coral species and populations through natural selection of tolerant individuals will thus be critical for their future persistence (Bozec et al., 2025; Lachs et al., 2024). However, where and how fast this adaptation can occur remains largely unknown due to our limited understanding of the genetic underpinnings of heat adaptive traits in corals (Richards et al., 2023).

There is considerable standing phenotypic variation in heat tolerance traits (e.g., resistance to bleaching and survival) among and within coral populations (van Woesik et al., 2022), and quantitative genetic studies have shown that these traits are partly heritable (Bairos-Novak et al., 2021; Howells et al., 2025; Howells et al., 2022a). This variation occurs across distinct thermal environments (Thomas et al., 2018) as well as among individuals from the same microhabitat (Humanes et al., 2022). Consequently, local selection and interbreeding of tolerant individuals could foster evolutionary adaptation to climate warming (i.e., evolutionary rescue) and the dispersal of heat-adapted offspring may benefit heat-sensitive populations facing demographic collapse (i.e., genetic rescue; Carlson et al., 2014). Many conservation and restoration strategies are under development to preserve and enhance this natural adaptive potential (Bay et al., 2023b; Grottoli et al., 2025; Howe-Kerr & Quigley, 2025; McClanahan et al., 2023). Yet, for these approaches to be effective, it is essential to know the distribution and evolvability of heat-adaptive traits, which depend on their genomic architecture including the number, distribution, and effect sizes of the contributing genes (Richards et al., 2023).

Previous studies show coral heat tolerance traits are polygenic, i.e., controlled by numerous genetic variants each exerting a small effect (Bay & Palumbi, 2014; Dixon et al., 2015; Fuller et al., 2020). The polygenic nature of these traits may benefit corals by enabling rapid adaptation through small allele frequency shifts across many loci (Metheringham et al., 2025; Wu et al., 2025). However, the small effect size of individual loci (i.e., causal variants or variants in linkage with them) complicates the detection of genes and molecular pathways underlying heat adaptation (Fuller et al., 2020). Various methods based on genome-wide molecular information are increasingly used in corals to tackle this issue, including genome-wide association studies

(GWAS) and genotype-by-environment association studies (GEAs; Selmoni et al., 2024a). These approaches test for statistical associations between genotypes and phenotypes (GWAS; Tam et al., 2019), and between allele frequencies and environmental (e.g., thermal) gradients (GEA; Lasky et al., 2023) at thousands to millions of loci across the genome. Although they hold great promise, GWAS and GEA application in corals remains in its infancy, in part due to the lack of reference genomes for many species, and the limited genomic resolution, geographic coverage or sample size of most studies (Selmoni et al., 2024a). In addition, the functional relevance of candidate loci is rarely validated, which restricts their use as biomarkers to identify individuals and populations with elevated tolerance (but see Jin et al., 2016). A systematic application of both approaches could help uncover variants associated with heat-tolerance phenotypes, while simultaneously exhibiting patterns of selection across thermal environments, thereby providing stronger evidence for their functional role in heat adaptation (Lasky et al., 2023; Yeaman, 2022).

Given the limited attainable sample sizes in coral studies, detected markers of heat adaptation are likely biased toward loci with the largest effects, which may account for only a small fraction of the genetic variance underlying heat tolerance (Fifer et al., 2024; Fuller et al., 2020). Genomic prediction—which bypasses the issue of significance thresholds by incorporating effect sizes across all loci—could be a promising alternative to identify corals with greater adaptive potential to future warming (Bay & Guerrero, 2020). In addition, GEA or GWAS candidates can be prioritized in these models to validate their functional relevance (Cheruiyot et al., 2022; Schmidt et al., 2024). Only two genomic prediction studies of heat tolerance in corals have been conducted to date with limited samples sizes (Fifer et al., 2024; Fuller et al., 2020). Further assessment is thus needed to evaluate their potential for advancing conservation and restoration efforts.

The utility of biomarkers and genomic prediction models for inferring heat-tolerance traits and adaptive potential in new individuals depends upon the extent to which the genomic architecture of these traits is conserved across coral species and populations. While several molecular functions and pathways involved in heat-stress response have been identified across multiple studies (Dixon et al., 2020; Selmoni et al., 2024a), the diversity of methods and omics data prevents testing whether they rely on shared genomic variation. The replicability of adaptation across the tree of life is highly variable and depends on many factors including demographic history, pleiotropy, functional redundancy and epistasis (Barghi et al., 2020; Conte et al., 2012; Stern, 2013; Yeaman, 2022). Therefore, testing for repeated selection across populations (i.e.,

convergent evolution) could reveal key genomic regions involved in heat adaptation, and/or clarify the prevalence of parallel adaptation in corals (Selmoni et al., 2024b).

Here, we use a comprehensive dataset from *Acropora spathulata*, a common broadcast-spawning reef-building coral from the Western Pacific, to address key questions regarding the genetic basis of heat tolerance traits and adaptive potential in reef-building corals. *A. spathulata* is a fast-growing species with a shallow depth distribution making it vulnerable to high heat and light exposure during marine heatwaves. We use whole genome sequencing data from ~1,000 individuals at 29 reefs from New Caledonia (NC), the Coral Sea (Chesterfield-Bellona atolls, CB) and the Great Barrier Reef (GBR) to perform GEAs and identify genetic polymorphisms associated with local thermal adaptation. We then conduct GWAS to identify loci and genomic regions associated with acute heat tolerance thresholds from ~750 colonies (including new samples and samples from a previous study; Denis et al., 2024a), and with *in-situ* bleaching and mortality from ~200 colonies during a global marine heatwave. Combining these methods, we investigate the genetic basis of heat adaptation across thermal regimes, from acute stress to long-term climates and assess the potential of genomic prediction to improve the identification of heat tolerant corals. We further leverage our extensive geographic sampling to evaluate the similarity of genetic architectures underlying heat adaptation across distant populations.

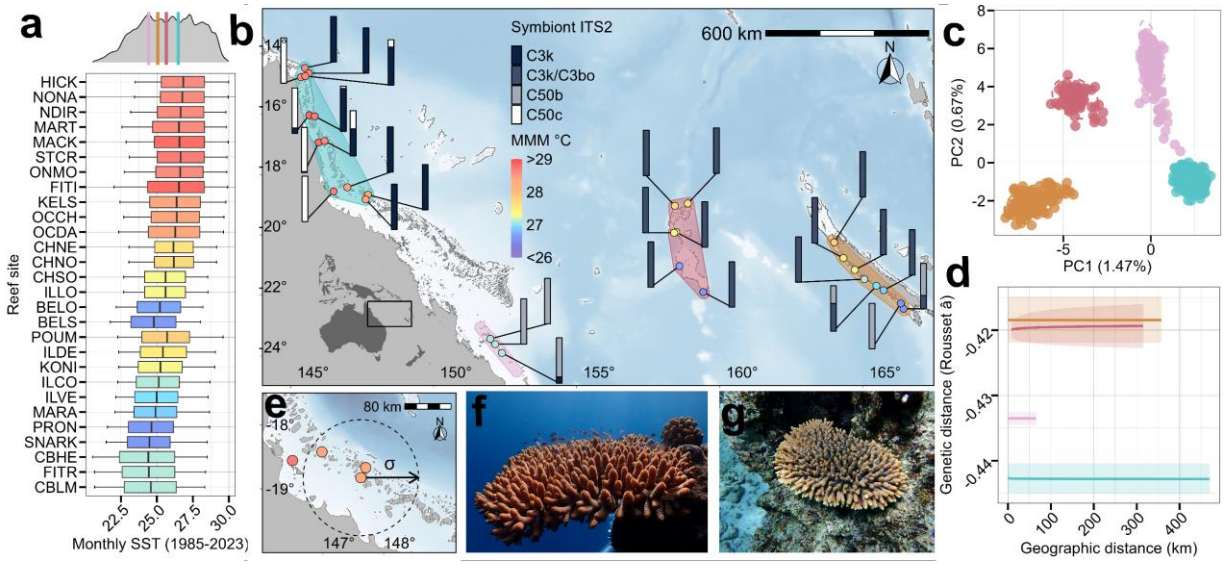


Figure 5.1. Sampling sites, population structure and algal symbioses of the reef-building coral *Acropora spathulata* in the Western Pacific. (a) Distribution of average monthly sea surface temperatures (SST) at sampling sites. Boxplots show the median (solid line), first and third quartiles (box) and 1.5* IQR (whiskers) of SST at each reef coloured by its maximum monthly mean (MMM) and ordered by latitude. Vertical lines on the density plot indicate the mean SST of each population. (b) Map of the study area with dots representing sampling sites, coloured

by their MMM. Vertical bars show the relative abundance of Symbiodiniaceae taxa hosted by *A. spathulata* at each reef, coloured by their dominant ITS2 type. Convex hulls show the distribution of the four populations investigated in this study. (c) Principal component analysis based on genome-wide SNPs showing the four genetically and geographically distinct populations (Denis et al., 2025). PC1 and PC2 are shown with the proportion of variance explained by each component in percentage. (d) Absence of significant isolation by distance within each population shown by the regression of Rousset's genetic distance over geographic distance. The 95% confidence intervals of all regression slopes included 0. (e) Combining all populations, the mean axial generational dispersal distance (σ) was estimated at approximately 100km and is visualized on a map of the central Great Barrier Reef. (f,g) Representative photographs of *A. spathulata* in the Southern GBR and in New Caledonia (credit: M. Grinblat and H. Denis).

5.3) Methods

To better understand the genomic architecture of heat tolerance traits in *A. spathulata*, we conducted genome-wide association studies (GWAS) with heat tolerance traits measured in Chapters 2 and 3, and genotype-by-environment association analyses (GEAs) with thermal predictors retrieved in Chapter 4. We then evaluated the potential of candidate markers to predict coral bleaching and survival during marine heatwaves.

5.3.1 Variant filtering and imputation

(i) Variant filtering

We used the global VCF file generated in Chapter 4 comprising 1,088 individuals and 47,438,630 SNPs for further filtering (Figure 5.1). Our preliminary filtering trials showed that the genotype quality (GQ; `GATK`) filtering threshold had a major impact on the number of retained SNPs (by an order of magnitude). Because there is a tradeoff between marker density (high density required in association studies to detect variants in linkage with causal variants) and accuracy (for genomic prediction), we created a "lenient" dataset (GQ>15; 3.16% expected error rate; Van der Auwera & O'Connor, 2020) and a "stringent" dataset (GQ>20; 1% expected error rate). To maximize the number of retained SNPs, the global SNP VCF file was divided into four VCF files, corresponding to each population identified in Chapter 4. Individual VCF files were then filtered using `vcftools` v0.1.17 (Danecek et al., 2011) to retain bi-allelic SNPs with a minimum mean locus depth of 5 and a maximum of 20 (approximately 4*IQR above the median individual depth), a minimum allele count (MAC) of 1 and a locus missingness < 20%. This resulted in individual VCF files comprising 78–629 individuals with 1,343,192–5,851,159 SNPs for the lenient dataset and 351,887–762,617 for the stringent dataset (Table A4.1). Using

the same filtration steps, we also created global VCF files to conduct association studies at the regional level (i.e., across multiple populations, Table A4.1).

(ii) Variant imputation

Missing genotypes were imputed in each VCF file using *Beagle* v5.5 (gp=true; ap=true; ne=10000; iterations=12; Browning et al., 2018) in "no haplotype panel" mode. This method leverages linkage disequilibrium patterns within the dataset and uses hidden Markov model (HMM) to infer missing genotypes. Haplotypes are first clustered based on the input data. The most likely haplotype path based on known genotypes is then used to fill in missing genotype information at each locus. The accuracy of our imputation method was confirmed using *in-silico* down-sampling of five individuals from each population (R^2 = 0.977 [0.963–0.985], Supplementary Text S1).

(iii) Filtration of rare variants and related individuals

Following imputation, rare variants were removed from the dataset by retaining only SNPs with a minor allele frequency (MAF) > 0.05 and a major genotype frequency < 0.95 using *vcftools* v0.1.17 (Danecek et al., 2011). This was done to remove any spurious variants resulting from sequencing or variant calling errors. Individuals' relatedness was computed using the method of Yang et al. (2010) in *vcftools*. For each group of related individuals (relatedness >0.2; corresponding to 2nd–3rd degree relatives) only one individual was kept. The resulting single population VCF files contained 69–624 individuals with 440,945–2,237,972 SNPs and 130,088–395,274 SNPs for the lenient and stringent datasets respectively (Table A4.1).

(iv) Computation of LD decay

The rate of linkage disequilibrium (LD) decay was estimated separately for each population using *PLINK* v1.90b7.2 (Purcell et al., 2007). Analyses were conducted on imputed and filtered VCF files, retaining only SNPs with a minor allele frequency (MAF) > 0.1. Pairwise LD was calculated as the squared Pearson correlation coefficient (r^2) between alleles, using 10% of loci pairs within 100 kb of each other to reduce computational load. LD decay across genomic distance was visualized by averaging r^2 values within non-overlapping 100 bp distance bins for each population (Figure A4.1).

5.3.2 Genotype by environment association studies

(i) Environmental predictors

We used variables retrieved in Chapter 4 to perform GEAs (Table A4.2). In brief these variables included thermal predictors from the Coral Watch v3.1 sea surface temperature (SST) satellite product (NOAA; 1985–present; 5km) and predictors from variables expected to play a secondary role in coral heat stress response, such as light intensity (cloud fraction and UV radiation; ERA5; Copernicus marine service; 2002–present; 0.25°), seawater turbidity (Kd_{490nm}) and primary productivity (Chlorophyll A; ESA Globcolour; 2002–present; 1/24°). Although other variables (e.g., sea water current velocity) are also expected to influence corals heat stress responses, those were not included in our analysis as global products are generally inaccurate in shallow, inshore environments such as the New Caledonia lagoon.

(ii) Redundancy analysis

We identified candidate genomic markers of local adaptation within each *A. spathulata* population using a redundancy analysis (RDA; Legendre & Anderson, 1999). Among GEA approaches, this multivariate method often shows the highest power and sensitivity in detecting changes in allelic frequencies along environmental clines (Capblancq et al., 2018; Forester et al., 2018). Our previous findings suggested *A. spathulata* populations were mostly demographically isolated (Figure 5.1), therefore we first conducted separate RDA analyses within each population (except for the Southern GBR population that only comprised three reefs of similar conditions; Table A4.3). We did not condition these RDA on population structure, as these populations showed little genetic structure, no significant isolation by distance (IbD; Denis et al., 2025) and their genetic structure was not strongly correlated with environmental clines (Procrustean rotation analyses; r = 0.06–0.24, $p > 0.05$).

For each population, we removed highly collinear predictors by initiating our predictor selection with the maximum monthly mean (MMM; Table A4.2), as our primary focus was adaptation to upper thermal conditions, and sequentially adding other predictors while ensuring that all variance inflation factors (VIF) remained below 10. Due to different number of reefs and collinearity among variables, different sets of predictors were retained for each population (Table A4.3). Therefore, to test for overlapping signals of adaptation to thermal conditions without biasing ordinations by including different predictors, we also built a second single-predictor RDA using only the MMM (Table A4.3). All environmental predictors were mean-centered and scaled and we discarded any reef that had less than 5 individuals ($n = 1$; 26/28 of

retained reefs had >13 individuals). RDAs models were ran using the `rda` function in R package `vegan` v2.6.4 using the lenient datasets to maximize marker resolution (Oksanen et al., 2013). To compare signals of local adaptation within populations to local adaptation at the regional scale of the Western Pacific (i.e., across all populations), we also built a global RDA model. However, due to IbD, this model provided little additional information compared to the intersection of within-population models (supplementary Text S2) and was not considered in later analyses.

In all RDA models, outlier loci exhibiting significant associations with environmental clines were selected using the method described in Capblancq and Forester (2021). We computed the Mahalanobis distance of each locus to the center of the RDA space based on K=2 RDA axes and corrected these distances for the genomic inflation factor (GIF; François et al., 2016) through a division by the median value of a chi-squared distribution of 2 degrees of freedom. These corrected distances were then converted to *p*-values and adjusted for the family wise error (FWER; Bonferroni correction) and false discovery rate (FDR; Benjamini-Hochberg correction). For single-predictor models, loci z-score on the first RDA axis were directly used instead of the Mahalanobis distance. The squared standardised z-scores were then corrected for the GIF using a chi-squared distribution of 1 degree of freedom and corrected for multiple testing as described above.

(iii) Aggregation by windows with WZA

We used the weighted-Z analysis (WZA; Booker et al., 2024) to aggregate significance among SNPs in LD. This approach overcomes noise in individual SNP significance and allows testing for overlapping signals across datasets with distinct SNPs representation. We performed two iterations of WZA, aggregating SNP *p*-values in windows of 20kb with a shift of 10kb between iterations following Rogivue et al. (2025), and adjusted WZA *p*-values to control for FDR (BH correction, α=0.01). A detailed description of the method and justification of distance choice is provided in supplementary Text S3.

5.3.3 Genome-wide association studies (GWAS)

(i) Acute stress assays

We performed GWAS using NDVI ED50 computed in Chapter 2 and Red Int ED50 measured in Chapter 3, which are both proxies for chlorophyll retention under heat stress. We chose chlorophyll content as our heat tolerance trait, as it better correlates with *in-situ* bleaching

responses than other traits commonly measured in acute heat stress assays (e.g., F_v/F_m), and shows greater consistency in the rankings of colonies by heat tolerance over time (Naugle et al., 2025). In addition, we hypothesize this trait is partly under host genetic control in contrary to F_v/F_m which likely reflects Symbiodiniaceae stress response.

(ii) Natural bleaching and mortality on the GBR

A marine heatwave of large intensity occurred over the summer 2023–2024 providing an opportunity to compare the results of GWAS based on acute stress responses and longer, natural heat-stress responses. Colony-level bleaching and mortality were recorded at 12 reefs from the Central/Northern GBR over the course of four surveys, spanning 405 previously genotyped *A. spathulata* colonies (Naugle et al., 2025). Two surveys were conducted during the bleaching event (February and March 2024) when accumulated heat stress ranged from 3.2 to 7.5 Degree Heating Weeks (DHW; Figure A4.2). Two additional surveys were conducted approximately 6 months later, after the conclusion of the marine heatwave (September and November 2024). For each colony, an underwater photograph was taken during the bleaching and mortality surveys, including the coral health chart as a colour reference (Siebeck et al., 2006).

Colony pigmentation was estimated from underwater photographs analysed using a custom workflow in ImageJ including a white balance correction, manual selection of three areas of interest on the coral tissue surface of each colony and computation of their mean intensity grey (MIG; SOP available at https://github.com/melissanaugle/acute_traits). MIG values (27–98 range) were inverted to facilitate interpretation. For a subset of colonies surveyed twice at different time points (n = 26), only the second time point showing the highest bleaching extent was retained in the dataset. In addition, records at Mackay and Fitzroy Island reefs were removed as bleaching and mortality was hypothesized to have been partly caused by freshwater plumes during Cyclone Kirrily (Naugle et al., 2025).

Mortality was estimated *in-situ* or from photographs when *in-situ* data were unavailable, using 5% intervals. To avoid underestimating colony mortality, records collected during the bleaching event (i.e., the first two surveys) were excluded, except for colonies that were already completely dead. We also removed mortality records from Mackay and Fitzroy Island reefs as stated above.

(iii) Phenotypic data filtration & standardization

In the following sections we use Chlorophyll ED50 to refer to both NDVI ED50 and RedInt ED50 as both are proxies for the same trait. We obtained a total of 891 individual Chlorophyll ED50 from acute stress assays (145–530 per population, Table A4.4). Chlorophyll ED50 that were both strong outliers within their population distribution (ED50<q1-1.5*IQ or ED50>q3-1.5*IQ) and associated to large uncertainty (CI>20 °C or CI could not be computed due to a lack of fit of the data) were discarded (n = 32). This filtration aimed to retain most of the observed variation in acute tolerance while removing strong outliers that could skew the GWAS results. Chlorophyll ED50 were then standardised using a rank-based inverse normal transformation, applied separately for each dataset (Table A4.4). The final dataset contained 752 Chlorophyll ED50 (125–501 per population).

For the natural bleaching dataset, MIG values exhibited an approximately bell-shaped distribution with a slight deviation from normality (Shapiro-Wilk test, $W = 0.98455$, $p = 0.017$), thus untransformed MIG values were used in the predictive model. The final dataset consisted of Invert MIG value for 221 colonies from 10 reef sites.

For the natural mortality dataset, most colonies fell into two categories: alive (<5% mortality) or dead (>95% mortality), with relatively few showing partial mortality (n = 34). Given the near-bimodal distribution, these intermediate cases were excluded, and mortality was treated as a binary trait. The final dataset included 113 dead and 105 alive colonies, sampled across 9 reef sites.

(iv) GWAS covariates

We controlled for non-host genetic factors that may affect phenotypes described above. To account for associations with distinct Symbiodiniaceae taxa identified in Chapter 4, we used the principal coordinate analysis (PcoA) performed on a matrix of D_2^s distance based on genome-wide symbiont *k*-mer content. We used the two principal coordinates (PCs) showing the best separation of previously assigned ITS2-types as covariates in our GWAS models (Figure A4.3).

In the GBR dataset, accumulated heat stress at the time of collection (DHW_collection) was also found to be correlated with acute stress responses in Chapter 2, possibly due to phenotypic plasticity (Denis et al., 2024a). To account for this possible non-genetic effect, we tested the effect of DHW_collection on our GWAS results (Figure A4.3). Of note there was no

accumulated heat stress at NC sites during sampling and therefore it was not included in the models. Peak SST reached at each reef was also considered as a covariate in GWAS on *in-situ* mortality given the observed relationship with this trait (Figure A4.4).

(v) GWAS models

GWAS were conducted in *GEMMA* v0.98 (Zhou & Stephens, 2014) using different datasets and traits described above (Table A4.4). We first ran preliminary sensitivity analyses to assess the impact of models, covariates and filtration of genotype datasets (supplementary Text S4). Following these preliminary tests, a linear mixed effect model based on the lenient datasets, including symbionts PCs and accumulated heat stress at the time of sampling as covariates, was used for Chlorophyll ED50 in each population. We also conducted GWAS on *in-situ* bleaching and mortality in the Central/Northern GBR, using linear mixed models with only symbiont PCs as covariates. Finally, we tested whether pooling multiple populations in GWAS models ('All GBR' and 'All populations') could improve power to detect causal variants underlying acute heat stress responses. Given power was not improved, we focused on single-population models (supplementary Text S5).

For each GWAS model, we assessed the significance of individual loci *p*-values in different ways: using a FWER correction controlling for the number of independent tests (SNPs with $r^2<0.1$, $\alpha=0.05$), using a FDR correction ($\alpha=0.05$), and using a permutation-based approach. For the latter approach 100 GWAS models were built on permuted phenotypic values across individuals, and the 5^{th} percentile of the minimum *p*-value for each model was used as our significance threshold. Because no individual loci reached statistical significance, we tested the possibility that no significant hit was found due to lower accuracy of genotype calling by repeating all GWAS analyses using the stringent SNP datasets. No individual loci reached genome-wide significance in that case either. We thus used a threshold of *p*-value $< 1 \times 10^{-5}$ to investigate the most suggestive associations. For each GWAS model, we also applied the WZA procedure described above (see section 5.3.2(iii)) to aggregate individual SNPs *p*-values into WZA *p*-values and windows were deemed significant at an FDR-corrected α level of 0.01.

5.3.4 Functional analyses

Because no official annotation was available for the *Acropora millepora* v3 reference genome at the time of the analyses, we created a custom annotation, combining information from the

A.millepora v2 genome (Fuller et al., 2020) and newly available information from Uniprot/Swissprot (supplementary Text S6).

(i) Functional annotation of candidate markers

First, we investigated genes in the proximity of candidate SNPs identified by GEAs and GWAS respectively. For each dataset, we used our annotation to assign SNPs to intragenomic or intergenomic regions. For intragenomic SNPs, we retrieved the predicted protein function of that gene. For intergenomic SNPs, we retrieved all genes that were located within ± 10kb and their predicted protein function. We chose this distance because it is approximately the minimum linkage disequilibrium threshold (r^2<0.1) across the four *A. spathulata* populations (Figure A4.1). Although it is possible that SNPs were in LD with causal variants beyond this distance in the populations where LD decayed less rapidly (e.g., CB), we use this conservative distance to avoid linking SNPs to unrelated genes in the other populations.

(ii) Expression data of candidate genes

We retrieved gene expression data from the meta-analysis of Dixon et al. (2020) which compiled transcriptomic data from 18 studies of *Acropora* corals under heat stress. We used this dataset to categorize genes of interest within four categories following Selmoni et al. (2024b). Genes were classified as "up-regulated" under heat stress if the meta-analysis adjusted *p*-values were < 0.01 and log-Fold change in expression was positive, "down-regulated" if *p*-values were < 0.01 and log-Fold was negative, "no change" if *p*-values were >0.01 and "no data" if the gene was absent from the meta-analysis.

(iii) GO enrichment analyses

We retrieved Gene Ontology (GO) terms associated to each gene within ±10kb of SNPs represented in our datasets and performed an enrichment analysis of GO terms for each GEA and GWAS model. Enrichment analyses were performed using R package `setRank` v1.1 (Simillion et al., 2017), retaining significantly enriched GO terms with a *p*-value threshold of 0.01 and adjusted *p*-value threshold of 0.05. This approach leverages gene annotations ranked by significance, enabling us to assess enrichment for specific molecular functions in our GWAS models, even when individual loci do not reach genome-wide significance.

5.3.5 Test for repeated signals

(i) Repeated signals across populations

We tested for parallel signals across populations in both GEA, and GWAS with Chlorophyll ED50, at different levels: nucleotides, genes and molecular functions (GO terms). At each level, we tested whether the overlap across two or three populations was greater than expected by chance using a permutation approach to account for structure in our data.

For the nucleotide level we retrieved significant windows using the WZA method after controlling for FDR using different significant thresholds (α = 0.01, 0.05, 0.1) to account for different SNP representation across datasets. We then generated an empirical null distribution by repeating the RDA analyses with random permutations of individuals across reefs followed by WZA aggregation for each population (n = 100). For the GWAS, a similar approach was used with permutations of phenotypes across individuals (n = 100). Numbers of observed overlaps were then compared to these null distributions to compute empirical p-values. We also used Pearson's correlation between individual loci effect sizes from each GWAS to test whether loci effects were correlated across distinct populations.

At the gene level, we retrieved annotations from all coding sequences located ± 10kb from significant SNPs (FDR correction at α = 0.01, 0.05, 0.1) and examined overlaps in their annotated genes (coding sequences mapping to different orthologs were treated as the same gene). For the functional level, we retrieved all significant GO terms from each enrichment analysis. As above, we generated empirical distributions by randomly shuffling observed adjusted p-values across SNPs and repeating the same procedure (n = 100). We report the results for FDR correction at α = 0.01, as similar results were obtained at other thresholds.

(ii) Shared signals between GEA and GWAS

We tested for congruent signals between GEA and GWAS in the Central/Northern GBR and NC populations for which both analyses could be performed. First, we assessed whether SNPs outliers from the GEA (FDR < 0.01) had a significant effect on any phenotypic trait using GWAS-derived effect sizes. A SNP was deemed significant when the 95% confidence interval for its effect size did not span 0. Second, we assessed whether the overlap between significant windows in GWAS and GEAs (WZA, FDR < 0.01) was greater than expected by chance using hypergeometric tests.

5.3.6 Genomic prediction of heat stress responses

We first tested the ability of genomic markers to predict heat stress responses using polygenic risk scores (PRS, supplementary Text S7) and genomic estimated breeding values (GEBV, supplementary Text S8). We then tested the predictive power of climate-associated SNPs identified by our RDA models for *in-situ* bleaching and mortality using a method modified from Hancock et al. (2011). Our approach consisted in first performing repeated RDA analyses in the Central/Northern GBR population with one reef removed at a time (12 model) and retaining 'core' SNPs identified as outliers (FDR<0.01) across >75% of these models. This approach was meant to identify SNPs with broad relevance for heat adaptation, beyond potential location-specific signals inherent to our sampling design. We then performed LD-clumping to reduce redundant information among SNPs, which first consists of removing all SNPs with an $r^2 > 0.5$ within 250kb of the SNP with the minimum *p*-value. The operation is then repeated until all SNPs are clumped with an index SNP representative of that LD group. Each index SNP was linked to its most strongly correlated thermal variable in the RDA, and the z-score–normalised mean of this variable across individuals was used to derive an adaptive score for each genotype. A value of 1 was assigned to the homozygous genotype with the highest z-score (i.e., the genotype most frequently occurring at warmer reefs, or reefs exposed to more frequent marine heatwaves), and 0 to the genotype with the lowest z-score. For the heterozygous genotype, a value of 0.5 was assigned unless the |z-score| difference to one of the homozygous was <0.05, in which case the score of this homozygous was used to account for possible dominance effects. Allele scores were then summed across all SNPs for each individual to obtain an adaptive index value.

The correlation of the adaptive index with *in-situ* bleaching and mortality was assessed using a linear regression and a logistic regression respectively. For mortality, peak SST of the marine heatwave at each reef was included as a covariate in the model (Figure A4.4). We tested whether the adaptive index had predictive power within reefs by repeating the same approach with linear and generalized linear mixed effect models including reef ID as a random effect using R package `lme4` v1.1.35 (Bates et al., 2014). We also tested whether observed correlations with the adaptive index were greater than expected by chance by computing the index from 100 random draws of the same number of SNPs. To control for potential biases introduced by computing the adaptive index from SNPs showing large allelic frequency variation across reefs, we computed the average pairwise fixation index (F_{st}) between reefs at each SNP along the genome, and drew random SNPs from similar F_{st} bins as the core SNPs (Figure A4.5).

Finally, to evaluate the increase in predictive ability offered by the adaptive index compared to environmental and biological predictors, we fitted multivariate regression models of increasing complexity following Fuller et al. (2020). 100 random train/test (80/20) splits of the bleaching and mortality datasets were performed, scoring alleles at core SNPs based on genotypes distributions from the train set, and using the test sets to evaluate the significance of the adaptive index in the model. We assessed whether predictive accuracy—measured as predictive variance for MIG and as AUC for Mortality—significantly improved between models using paired Wilcoxon rank-sum tests. Tested models were:

$$(1)\ Y = \beta_0 peak\ SST + \beta_1 peak\ DHW + \epsilon$$

$$(2)\ Y = \beta_0 peak\ SST + \beta_1 peak\ DHW + \beta_2 MMM + \beta_3 K_d(490) + \beta_4 Depth + \epsilon$$

$$(3)\ Y = \beta_0 peak\ SST + \beta_1 peak\ DHW + \beta_2 MMM + \beta_3 K_d(490) + \beta_4 Depth + \beta_5 SymbPC1 + \beta_6 SymbPC2 + \epsilon$$

$$(4)\ Y = \beta_0 peak\ SST + \beta_1 peak\ DHW + \beta_2 MMM + \beta_3 K_d(490) + \beta_4 Depth + \beta_5 SymbPC1 + \beta_6 SymbPC2 + \beta_7 Adaptive\ Index + \epsilon$$

Where peak SST and peak DHW are the maximum values reached during the marine heatwave prior to the time of the survey, $K_d(490)$ is a proxy for turbidity and Symbionts PCs are the same as the covariates in GWAS models. For bleaching a standard regression was used and for mortality a logistic regression with a logit link was used.

5.4) Results and Discussion

In the Western Pacific, four genetically and geographically separated *A. spathulata* populations were previously identified, spanning 10° of latitude and 20° of longitude, and encompassing a wide range of environmental conditions, notably across shelf positions (Figure 5.1). We performed whole genome sequencing of a total of 1,124 *A. spathulata* colonies from 29 reefs. After filtration of low-quality samples, mis-identified taxa, clones and related individuals, we obtained single nucleotide polymorphisms (SNPs) for 984 unique genotypes. Following imputation, MAF and genotype frequency filtering, we retrieved 130,088–395,274 high quality (GQ>20, ~15X coverage) and 440,945–2,237,972 good quality (GQ>15, ~11X coverage) SNPs respectively per population (Table A4.1).

5.4.1 Shared evolutionary signals amid predominantly non-parallel local thermal adaptation

A. spathulata populations show some degree of local adaptation, particularly to thermal conditions (Denis et al., 2024a; Woolsey et al., 2015). Therefore, we used GEAs with thermal predictors to discover molecular markers (SNPs) putatively involved in heat adaptation (Table A4.2). Separate redundancy analyses (RDA; Capblancq & Forester, 2021; Capblancq et al., 2018) in three populations (Central/Northern GBR, CB and NC, n = 5–12 reefs) showed small overall genetic structure within populations (RDA1=0.16–1.54%, Figure A4.6), in line with our previous PCA, ADMIXTURE and Isolation-by-distance (IbD) analyses (Figure 5.1, Figure A4.7). Yet, we identified balanced polymorphisms significantly correlated with environmental gradients at 632–1008 SNPs (FDR<0.01, Benjamini-Hochberg correction, Figure 5.2a, Table A4.5). These SNPs were distributed in 126–175 unique 20kb genomic windows after applying the WZA method, designed to detect regions with consistent allele frequency shifts across linked SNPs (FDR<0.01; Booker et al., 2024). Across populations, 63–84% of the SNPs most strongly associated with thermal gradients (FWER<0.05, Bonferroni correction, Figure 5.2a) were found in intragenic regions, of which 10–20% were in predicted coding sequences (CDS), 2–7% in 3' untranslated (3' UTR) regions and 71–84% in unannotated mRNA regions. For the intergenic SNPs, 7–17% were predicted to occur in repeated regions. These results are in line with widespread evidence that balanced polymorphisms at specific loci may support local adaptation despite high gene flow (Forester et al., 2016; Hoban et al., 2016; Lasky et al., 2023; Rumberger et al., 2025). A large proportion of SNPs-associated genes were involved in classical heat stress response pathways and have been identified in previous coral studies (Table A4.6). These pathways included immune response (*MADD* ; Helgoe et al., 2024; *WN10A*; Nunn et al., 2025), regulation of oxidative stress by cytochrome P450 proteins (e.g., CP46A, CP3AT; Da-Anoy et al., 2024; Selmoni et al., 2020a), DNA repair (*XRCC1*, *RIF1*; Whitehouse et al., 2001), cell-integrity (hemicentin-2 like protein; Selmoni et al., 2021) and heat shock proteins and chaperones (*DJB12*, DnaJ homologs; Javid et al., 2021; Selmoni et al., 2021)

We then compared the level of parallelism in local thermal adaptation across populations at different levels of biological organization: nucleotide polymorphisms, genes and molecular functions (Gene ontology terms, GO, see methods). Parallelism in nucleotide polymorphisms was tested with the WZA method, as separate dataset filtering produced different SNP representations across populations. Overall, a limited number of genomic windows and functions were detected in several populations and this number was not greater than expected

by chance (empirical p-values > 0.1, Figure 5.2b), suggesting that these populations have mainly adapted to local thermal conditions via distinct evolutionary pathways (Barghi et al., 2020). This result was likely unaffected by the slightly different thermal predictors used in RDA models across populations, as a single-predictor model with reefs MMM produced similar outcomes. Non-parallel adaptation appears to have occurred from shared standing genetic variation (Barrett & Schluter, 2008), as the large majority of significant SNPs in one population had intermediate minor allelic frequencies (MAF) in other populations (0.2–0.5, Figure 5.2c). However, we cannot completely rule out selection acting on novel mutations that have arisen after populations divergence as some of the significant SNPs were not represented in all populations.

The only exception to the patterns of non-parallel adaptation was observed at the genic level, with 8 genes exhibiting significant intragenic or intergenic SNPs within ± 10kb (see methods for distance justification) across the three populations, which is unlikely to occur by chance (empirical *p*-value < 0.0001, Figure 5.2b). These genes were overlooked at the nucleotide level because significant SNPs occurred in genic regions located more than 20kb apart, or putative paralogs (distinct CDS mapping to orthologs from the same gene). Among these genes, three stood out based on their functional annotation or prior evidence for a role in heat adaptation. Significant SNPs were found in several *LIN41* paralogs coding for a E3-ubiquitin protein ligase, previously linked to corals adaptation to distinct thermal environments (Thomas et al., 2022). Other significant SNPs were found within and upstream of one copy of *KI16B* coding for a kinesin protein, previously reported to be down-regulated in corals under heat stress (Poquita-Du et al., 2020). The most striking result was the identification of significant intragenic SNPs in all populations across five putative paralogs of the same gene, *TRPA1*, with some SNPs occurring within the same copy (Figure 5.2d). *TRPA1* encodes for a transmembrane ion channel involved in pain, temperature and irritants sensing across diverse animal species, and was recently identified as one of two key genes driving *A. tenuis* adaptation to extreme mangrove environments, near our NC sampling sites (Leiva et al., 2025). Missense mutations identified in this previous study caused changes in protein structure and heterozygous advantage in the mangrove environment. Given our lower genomic resolution, we could not formally test for an effect on protein structure, but SNPs found in this gene showed strong allelic frequency shifts across environmental clines (e.g., SNP1, Figure 5.2e). More importantly, mortality differed significantly among SNP genotypes during a natural marine heatwave at two Central/Northern GBR reefs (*p*-value < 0.05, logistic regression; Figure 5.2f, Figure A4.2). Although small

sample sizes prevent accurate effect size estimates, the independent identification of this gene in different populations and species, along with its observed fitness effects, makes it a strong candidate for further investigating its role in coral heat adaptation.

Overall, these results point to key genes contributing to corals heat adaptation within a largely non-parallel polygenic architecture across populations. These findings align with foundational work on parallel polygenic adaptation to freshwater habitats in stickleback fishes, where similar phenotypes repeatedly evolved in isolated locations through selection on shared ancestral variation, primarily favouring distinct allelic combinations with occasional reuse of the same alleles or genes (Fang et al., 2020; Hohenlohe & Magalhaes, 2019; Poore et al., 2023; Schluter & Conte, 2009). Non-parallel adaptation is often favoured for polygenic traits with high genotypic redundancy because individual alleles experience weaker selection, allowing different allelic combinations to produce the same phenotype across the seascape (Ravinet et al., 2016; Salmón et al., 2021; Yeaman, 2022). However, gene-level parallel adaptation can occur even within polygenic architecture due to a few large-effect genes (Hohenlohe & Magalhaes, 2019; Orr, 2005), epistasis (Stern et al., 2022) or pleiotropy (Rennison & Peichel, 2022; Whiting et al., 2024). Model organisms such as sticklebacks have begun to uncover factors influencing the likelihood of parallel genetic adaptation, including QTL number and distribution and recombination rates (Rosenblum et al., 2014). The degree of genetic parallelism can also be heterogeneous across a species range due to the demographic history of populations and levels of gene flow (Fang et al., 2020). Importantly, the ability to detect parallel adaptation greatly depends on methods, molecular resolution, and numbers of studied populations (Booker et al., 2023; James et al., 2021). As such, a recent study on six *Acropora* species identified a greater number of overlapping signals of heat adaptation than our study (Selmoni et al., 2024b). It is therefore plausible that having increased the number of reefs and populations would have revealed other signals of parallel adaptation, highlighting the need for more research in corals to assess its prevalence and variation across species' ranges.

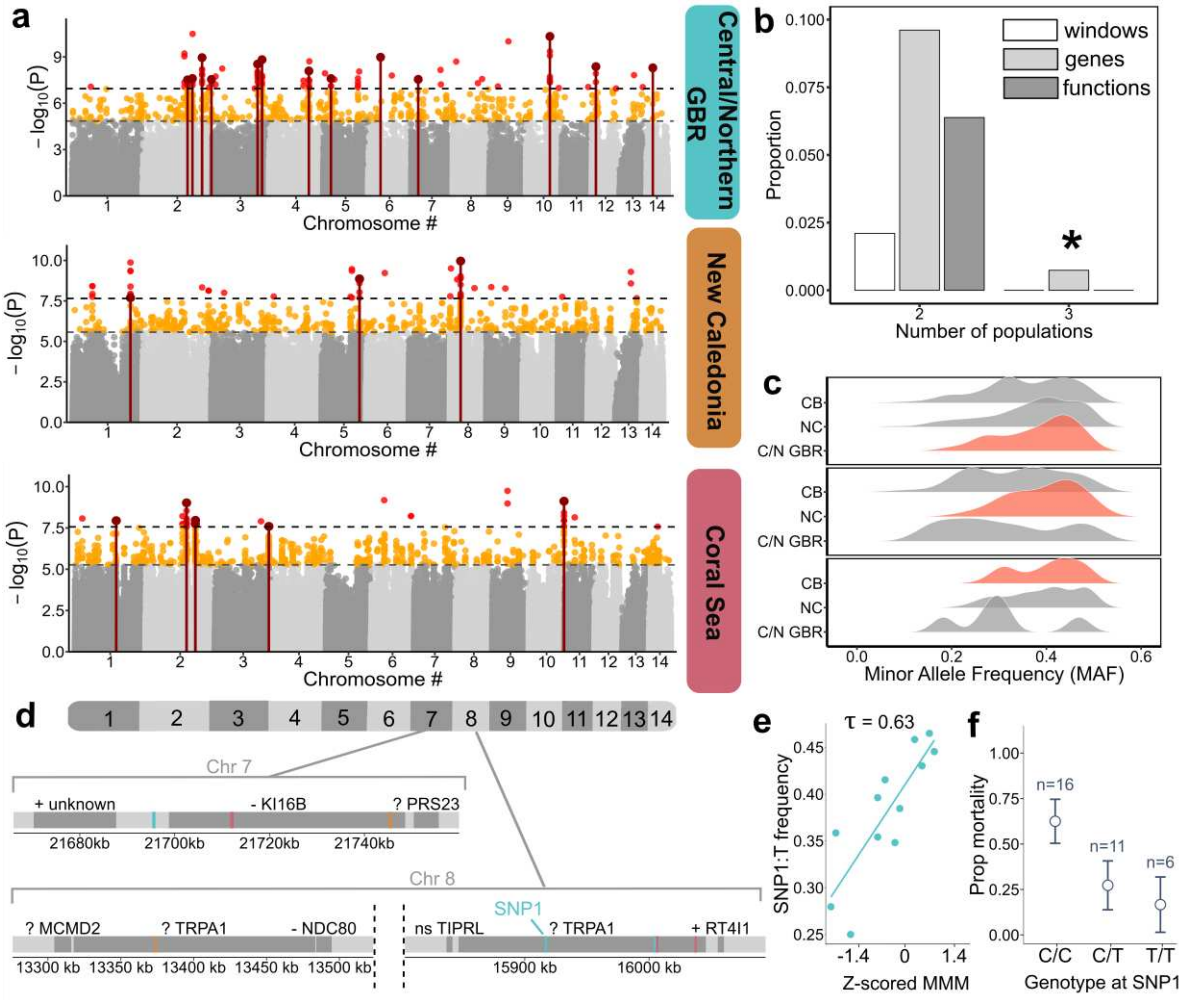


Figure 5.2. Genotype-by-environment association studies reveal shared evolutionary signals amid predominantly non-parallel local thermal adaptation (a) Manhattan plots of *p*-values obtained from testing associations between *Acropora spathulata* allelic frequencies and thermal predictors (Table A4.2) at each SNP using redundancy analysis (RDA) for the Central/Northern Great Barrier Reef (GBR, top), New Caledonia (NC, middle) and Chesterfields-Bellona populations in the Coral Sea (CB, bottom). Significant associations after multiple-tests corrections are shown in yellow (FDR<0.01) and red (FWER< 0.05). Dark red vertical bars indicate 20kb genomic windows found to be significant using the WZA method (FDR<0.1), and containing significant SNPs after FWER correction. (b) Proportion of significant genomic windows, genes and molecular functions (Gene Ontology terms) identified across two or three distinct populations. The asterisk indicates the only hierarchical level for which the number of outliers shared across populations was greater than expected by chance (empirical *p*-value < 0.0001). (c) Distribution of minor allele frequencies (MAF) at candidate SNPs involved in local adaptation (FDR<0.01) across populations. Each facet shows the MAF distribution of the candidate SNPs of that population (red) and the MAF distribution at the same SNPs in the other populations (grey). (d) Chromosome map of two example genes (*KI16B*, *TRPA1*) with shared signals across the three Western Pacific populations. Vertical bars indicate the position of significant SNPs (FDR<0.01), coloured by the population in which they were identified. Symbol next to gene names indicate whether they were found to change in expression during heat stress in a transcriptomic meta-analysis on several *Acropora* species (? = unknown, ns = non significant, + = up-regulated, - = down-regulated; Dixon et al., 2020). Significant SNPs were found in a total of five putative paralogs of the *TRPA1* gene in chromosomes 2,4 and 8.

Only two copies of the *TRPA1* gene are shown for clarity purposes. (e) Correlation between reefs allele frequency change and the maximum monthly mean of sea surface temperatures (MMM, Z-scored) at the SNP1 (chr8:15916947) for the Central/Northern GBR population. (f) Average mortality (mean ± sd) by SNP1 genotype during the 2023–2024 marine heatwave at Kelso and Pelorus reefs in the Central GBR, showing the most contrasted responses among individuals (Figure A4.2).

5.4.2 Functional convergence in acute stress responses despite population-specific polygenic architecture

A limitation of GEAs is that the traits underlying local adaptation are unknown, and false positives can occur due to collinearity among environmental variables or genetic drift (Hoban et al., 2016). Therefore, we conducted GWAS to directly test for associations between coral genotypes and heat tolerance phenotypes derived from standardised acute heat stress assays (<24h; Evensen et al., 2023). Chlorophyll ED50—the temperature at which chlorophyll content drops by 50% compared to ambient summer conditions (i.e., MMM)—was measured in 627 GBR colonies (Denis et al., 2024a) and 125 NC colonies in this study. It was used as the heat tolerance trait in our analyses due to its correlation with *in-situ* bleaching and mortality and temporal consistency of colony rankings (Naugle et al., 2025).

We performed separate GWAS in three populations (the Central/Northern GBR, the Southern GBR and NC, Figure 5.3a). Across all populations, only one SNP reached genome-wide significance after multiple testing correction (FWER at α=0.05, see material and methods, Figure 5.3b). This aligns with previous GWAS in corals (Fifer et al., 2024; Fuller et al., 2020) and occurred despite a sample size twice that of earlier studies in the Central/Northern GBR (n = 501), further underscoring the highly polygenic nature of heat stress responses. As several genomic regions showed visible peaks (Figure 5.3b,c,d), we applied a suggestive threshold of p-value $< 1 \times 10^{-5}$ to identify candidate genes underlying these responses, consistent with methods in previous heat tolerance GWAS in non-model organisms (Longmei et al., 2021; Maulana et al., 2018; Wu et al., 2021; Yu et al., 2021). We emphasize that this threshold is used for hypothesis generation rather than as evidence of definitive associations. Among suggestive associations, SNPs were located in or near genes potentially involved in ROS detoxification pathways, including a peroxidasin-like protein and a glutaredoxin-related protein (*GLRX5,* Table A4.7), and DNA repair (*MSH5*). Suggestive associations were also found with genes encoding sacsin proteins (*SACS*) which are co-chaperones of protein Hsp70. These proteins are up-regulated under experimental heat stress in corals (Mayfield et al., 2018) and increasingly

identified as potentially involved in local heat adaptation (Fuller et al., 2020; Guillaume et al., 2025b; Selmoni et al., 2021).

Consistent with our GEA results, there was low parallelism in genetic polymorphisms associated to acute stress responses; no significant overlap was found between significant genomic windows (empirical *p*-values > 0.1, WZA, Figure 5.3d) and loci effect sizes showed no correlation across populations (Pearson's $R < 0.01$, Figure 5.3e). This result is in line with the low genotypic parallelism in *A. hyacinthus* heat stress responses across microhabitats from the same population (Fifer et al., 2024), and explains why power was not increased in our GWAS with pooled populations ($n = 752$ individuals, no significant SNPs after FDR correction at α=0.05, Text S5). In contrary to the GEAs, no genes were found to be repeatedly associated with acute stress responses across the three populations (empirical *p*-values > 0.1). However, GO-enrichment analyses revealed molecular functions consistently associated with acute stress tolerance across two or three populations (empirical *p*-values < 0.01), including regulation of apoptosis, proteolysis, calcium and carbohydrate transport and extracellular structures (adjusted *p*-value < 0.05, Figure 5.3f). This demonstrates that acute stress tolerance is flexible at the genic level but involves similar molecular and physiological pathways across populations.

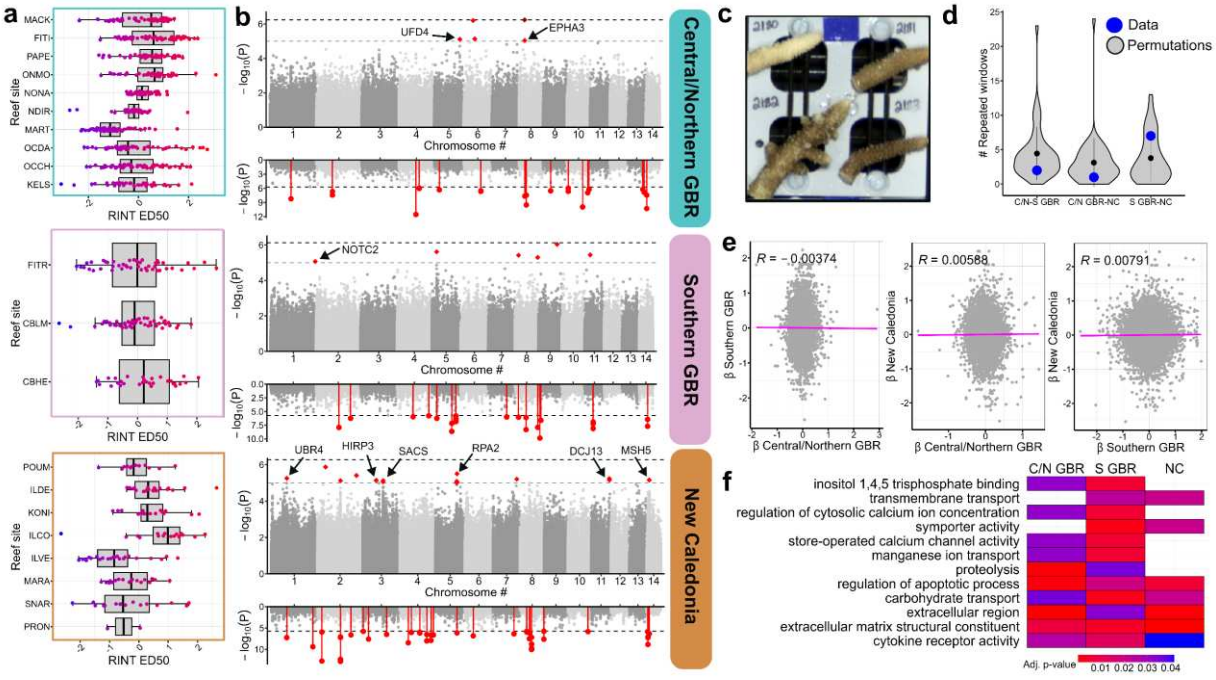


Figure 5.3. Polygenic architecture of acute heat tolerance in *Acropora spathulata* shows functional convergence across populations despite non-parallel genic basis. (a) Distribution of individual acute heat tolerance thresholds used in Genome Wide Association studies are shown for the Central/Northern GBR (top), the Southern GBR (middle) and New Caledonia (bottom). Proxies of chlorophyll content (GBR: NDVI; NC: Red channel intensity) were used to compute

effective dose 50 (ED50), the temperature leading to a 50% decline in chlorophyll content compared to baseline levels. ED50 were standardised separately within each population using Rank-Based Inverse Normal Transformation (RINT). (b) Manhattan plots of *p*-values obtained from testing associations between genotypes and RINT ED50 at each SNP using linear mixed models for the Central/Northern GBR (top), the Southern GBR (middle) and New Caledonia (bottom). For each population, the top Manhattan plot shows individual SNPs *p*-values. The horizontal grey line corresponds to a *p*-value $<1 \times 10^{-5}$ suggesting associations and the horizontal black line corresponds to the genome-wide significance threshold (Bonferroni correction by the number of independent tests). SNPs are coloured in red and dark red if they fall below the suggestive and genome-wide significance thresholds respectively. For intragenic SNPs, orthologous gene names of known protein function are shown. The bottom Manhattan plot shows 20kb windows *p*-values after aggregation using the WZA method. Significant windows (FWER<0.05) are shown in red. (c) Example of different bleaching responses to acute heat stress among coral genotypes. (d) Number of significant windows found in common between each population pairs (WZA, FDR<0.01, blue dot) compared to its null distribution obtained through phenotypes permutations (grey). (e) Pairwise Pearson's correlations between SNPs effect sizes (β) from GWAS across populations pairs. (f) Molecular functions (Gene ontology terms) found to be significantly enriched (adjusted *p*-value <0.05) in most significant SNPs-associated genes across GWAS in two or three populations.

5.4.3 Variability in the genetic basis of heat tolerance across thermal exposures

Heat tolerance traits derived from acute stress assays are likely to be influenced by phenotypic plasticity and environmental memory to recent conditions (Alderdice et al., 2024; Cunning et al., 2024; Denis et al., 2024a; Hackerott et al., 2025), and their heritability remains unknown. Recent work in model organisms such as *Drosophila* also suggests that genetic correlation for heat tolerance declines with increasing differences in temperature exposure (Soto et al., 2025). To test whether adaptive genetic variation linked to acute stress response also affects tolerance to longer heat exposure, we conducted GWAS on field observations of bleaching severity and mortality in ~210 previously tagged and genotyped colonies in the Central/Northern GBR. These phenotypes were recorded during the 2023–2024 global bleaching event (material and methods; Naugle et al., 2025), triggered by maximum SST of 30–30.6 °C across our reef sites (5.8–8.3 DHW, Figure A4.2). This marine heatwave caused the complete mortality of 52% of re-surveyed colonies with variable prevalence across reefs (mortality was < 25% at 5 reefs but > 95% at three reefs, Figure A4.2).

Similar to acute traits, no single loci reached genome-wide significance, and only 4 and 1 SNPs had a *p*-value $<1 \times 10^{-5}$ for bleaching and mortality respectively (Figure A4.8). In addition, there was very little overlap between genetic polymorphisms and genomic windows associated with acute and *in-situ* traits (Figure 5.4a), despite small to moderate correlations of these phenotypes (Figure A4.9). Only two SNPs were found to associate with both acute and longer heat stress

($p < 0.001$, Figure 5.4a). One was located in an unknown gene, and the other in a lactadherin gene homolog possibly involved in the removal of apoptotic cells (Cunning et al., 2018). These results are consistent with the distinct heritability for survival under short-term (1 week) versus long-term (1 month) heat stress observed in corals selective breeding experiments (Humanes et al., 2024). To formally test this, we sought to estimate SNP-heritability h^2 and genetic correlation (Yang & Wang, 2012) between acute and *in-situ* traits. However, estimates were uninformative (confidence intervals spanned 0–1), likely due to our limited number of individuals (Visscher et al., 2014). Nevertheless, our results warrant caution in using acute stress assays to select tolerant individuals, and highlight the need for further research on the heritability of these traits.

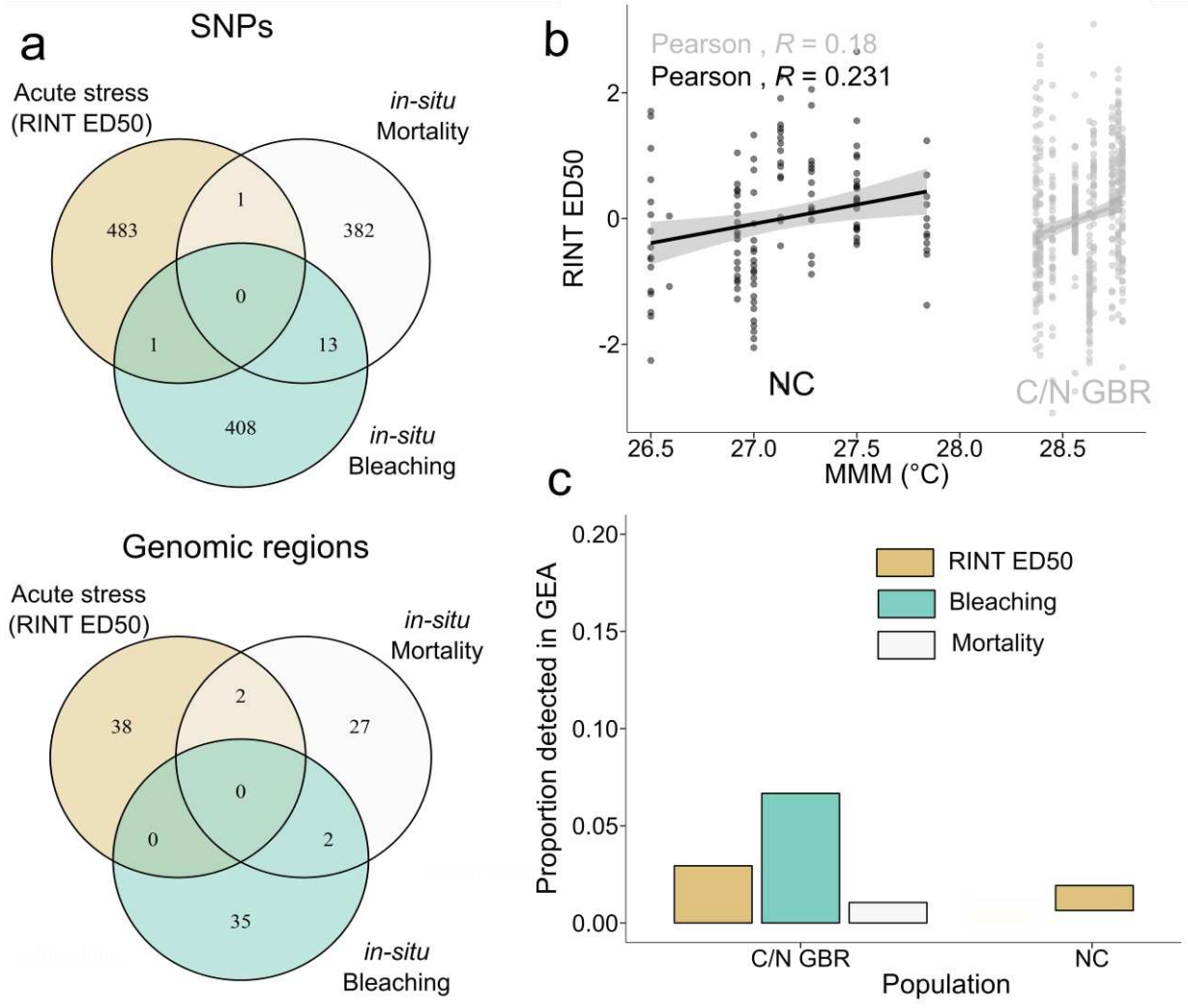


Figure 5.4. Variability in the genetic basis of heat tolerance across thermal regimes. (a) Venn diagram showing the overlap of signals between most significant SNPs ($p < 0.001$) and genomic windows (20kb, WZA, FDR<0.01) in GWAS with acute heat tolerance (measured as rank inverse normalised chlorophyll ED50, n = 501) and in-situ bleaching (mean intensity grey, MIG, n = 210) and mortality (n = 211) during a marine heatwave. Note samples used in these

GWAS partly overlap. (b) Correlation of RINT ED50 with reefs maximum monthly mean (MMM) in New Caledonia (black) and the Central/Northern GBR (grey). (c) Proportion of genomic windows associated with the distinct phenotypic traits (FDR<0.01) showing signals of selection across thermal gradients using redundancy analysis.

5.4.4 Comparison of genomic signatures from associations with phenotypes and environments

Combining GEA and GWAS offers the potential to identify genetic variants more likely to underlie local adaptation through their effects on measured phenotypic traits (Lasky et al., 2023). Indeed, 4.6–11.6% of SNPs significantly associated with thermal gradients (q<0.01, RDA) in the Central/Northern GBR or NC populations had a significant effect size in GWAS on one of the acute or *in-situ* tolerance traits (effect size confidence intervals not spanning 0, 21.4% of SNPs had an effect on at least one trait). The lack of effect for 80% of these SNPs may reflect false positives, a role in other adaptive traits than heat tolerance, or gene-by-environment interactions (Drury & Lirman, 2021) masking their effects in GWAS performed across all reefs (Exposito-Alonso et al., 2019; Lasky et al., 2018; Pallares et al., 2023). In addition to the *KI16B* and *TRPA*1 genes previously highlighted, SNPs with a significant effect were found in diverse genes involved in general pathways of DNA repair (e.g., *ASCC3*, *MSH5*), immune response (collectin-12-like protein; Libro et al., 2013), redox homeostasis (e.g., *CP3AT*) and apoptosis signalling (*MADD*; Helgoe et al., 2024). Interestingly three linked SNPs in a *PSTK* homolog had a significant and concordant effect on both *in-situ* bleaching and mortality. *PSTK* is essential for selenocysteine tRNA phosphorylation, a key step in selenoprotein biosynthesis (Carlson et al., 2004). Selenoproteins play a strong role in homeostasis and oxidative response (Ye et al., 2022) and some were found to be upregulated under thermal stress in *A. palmata* (DeSalvo et al., 2010). In addition one selenium protein candidate was found to be involved in host-symbiont interaction, possibly by mitigating redox stress from symbionts ROS or supplying selenium to the symbionts (Zou, 2011). These three linked SNPs were among the most significantly associated to thermal gradients and showed a significant effect on two heat tolerance traits, making this gene a strong candidate for future functional validation.

Despite the correlation of acute heat tolerance traits with thermal gradients (e.g., MMM, Pearson's R = 0.18–0.23, p-value < 0.01, Figure 5.4c), only a small but significant (1.2–8%, hypergeometric test, p-value < 0.01) percentage of genomic windows associated with heat stress responses in GWAS overlapped with significant windows in the GEA (FDR<0.01, WZA, Figure 5.4d). This suggests that a substantial fraction of the genetic variation associated with standing

heat tolerance traits does not exhibit clinal patterns along thermal environments. Recent modelling work indicates that such patterns could be common for polygenic traits, due to the interactions of pleiotropy with demographic processes and environmental variation (Lotterhos, 2023). These interactions can result in distinct allelic combinations across the seascape to achieve phenotypic optima, generating allele frequency patterns that are undetectable by linear approaches such as RDAs (Lotterhos, 2023). Another plausible explanation is that the high gene flow in *A. spathulata* (Denis et al., 2025) results in the spread of heat adaptive variants across large scales, reducing the magnitude of allelic frequency clines and their detectability by GEAs. Finally, long-term adaptation to environmental conditions and rapid adaptation to both acute and short-term heat stress (i.e., during marine heatwaves) may partly rely on distinct genetic variation (Wu et al., 2025). Overall, these findings highlight the complementarity of GEAs and GWAS, and the need for additional lines of evidence, e.g., using reverse genetics (Cleves et al., 2018; Luo et al., 2025) or common garden experiments (Rellstab & Keller, 2024), to validate certain candidate loci as biomarkers for heat tolerance.

5.4.5 Climate-adaptive loci improve predictions of bleaching and mortality during a marine heatwave

Although a number of candidate loci identified by GEA and/or GWAS exerted a measurable effect on phenotypes, effect sizes were relatively small as expected for polygenic traits, and most loci did not reach genome-wide significance. We used multiple genomic prediction approaches to assess their collective power to predict colony-level variation in acute stress tolerance (Chlorophyll ED50), *in-situ* bleaching (MIG) and mortality. Overall, we found both Polygenic Risk Scores (PRS; Torkamani et al., 2018) and Genomic Estimated Breeding Values (GEBV; McGaugh et al., 2021) did not offer additional power compared to environmental and symbiont information (supplementary Text S7 and Text S8). These results corroborate previous PRS results in corals showing small (Fuller et al., 2020) or no predictive power (Fifer et al., 2024), and highlight the sample size limitation of these approaches in wild species with large effective population sizes (McGaugh et al., 2021).

In contrast to the numerous small-effect loci contributing to standing variation in heat tolerance captured by PRS and GEBV, climate-adaptive alleles that are under migration-selection balance may reflect variants of larger effect (Yeaman, 2022). To evaluate the predictive power of climate-adaptive loci identified by GEAs, we computed an ‘adaptive index’ (modified from Hancock et al., 2011), representing the proportion of alleles harbored by each colony that are

expected to confer a fitness advantage in warmer or more thermally variable environments (see methods). We found that this index had a significant negative correlation with both *in-situ* mortality (odds ratio = 0.83, $p = 9.8 \times 10^{-5}$, logistic regression) and bleaching (Pearson's $R = -0.23$, $t = -3.44$, $p = 6.9 \times 10^{-4}$ linear regression, Figure 5.5b-d) indicating that colonies harboring more 'heat adaptive' alleles were at lower risk of bleaching and mortality. These effects were larger than expected by chance when computing the adaptive index from random SNPs with similar differentiation across reefs (based on the fixation index F_{st}, empirical p-value < 0.01, Figure 5.5b, Figure A4.5) suggesting that GEA successfully detected functional adaptive variation. Using models including reef as a random effect, we found that the adaptive index explained a small but significant fraction of bleaching variation within reefs (β = –0.42, 95% CI: –0.80 to –0.13, mixed effect linear regression). Conversely the index did not exhibit a significant effect on mortality within reefs (β = –0.018, 95% CI: –0.80 to –0.13, mixed effect logistic regression), likely because most of the variation occurred between reefs (Figure A4.2). Finally, we found the index provided a small but significant increase in survival discrimination compared to models based on environmental and symbiont covariates ($p < 0.024$, Wilcoxon rank-sum tests, Figure 5.5e) as well as a significant increase in the variance explained for bleaching ($p < 0.013$, Wilcoxon rank-sum tests, Figure 5.5f). While symbiont principal coordinates explained a substantial fraction of bleaching variation ($p < 0.001$) this effect was likely partially confounded by other reef-level factors (supplementary Text S9). Overall, these results indicate that GEA successfully detected loci with functional relevance for heat adaptation. However, a substantial portion of the variation in heat stress responses remains unexplained, particularly within reefs. This unexplained phenotypic variation may be due to adaptive genetic variation distinct from historical adaptation or not detectable by GEAs, or to other factors not included in our models (e.g., microhabitat conditions, associated microbes; Ainsworth et al., 2021; Bourne et al., 2016). Finally, adaptive alleles may offer limited protective and predictive advantage if the severity of marine heatwaves exceeds the tolerance of even the most heat-adapted genotypes, overwhelming the capacity for evolutionary adaptation (Wu et al., 2025).

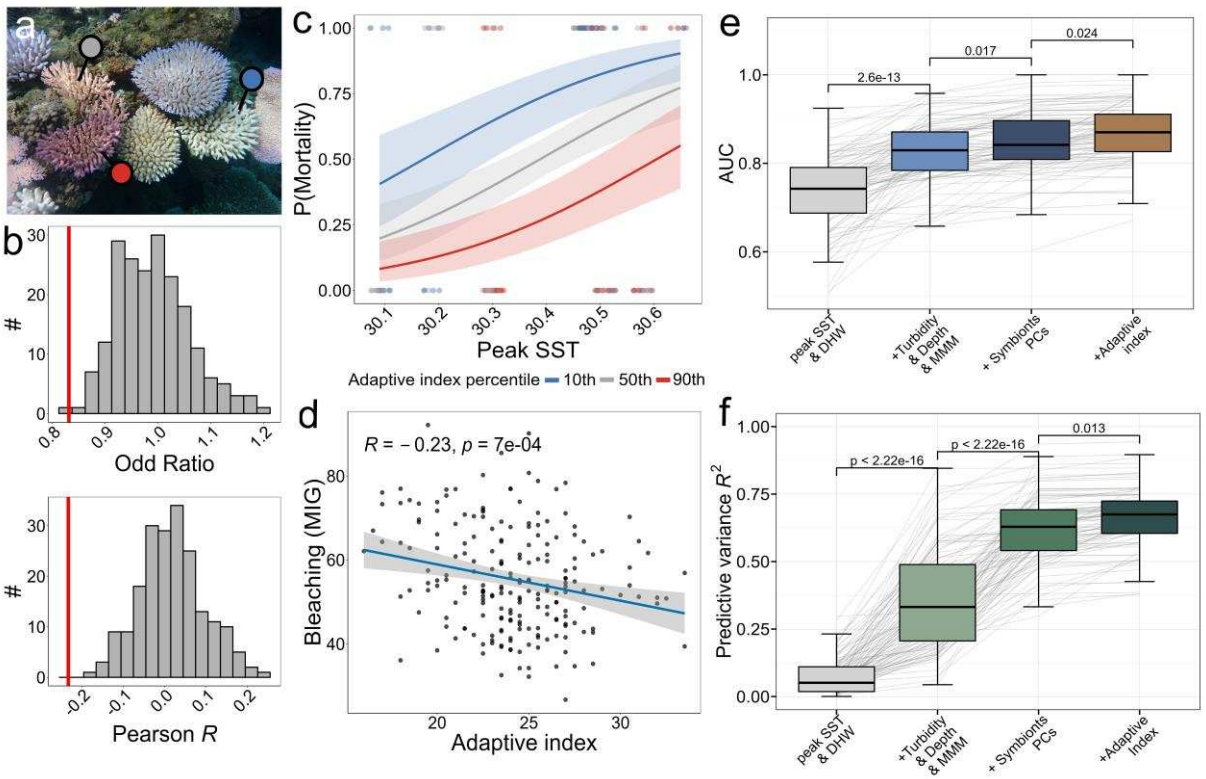


Figure 5.5. Single nucleotide polymorphisms putatively linked to local thermal adaptation improve predictions of *in-situ* bleaching and mortality during the 2023–2024 marine heatwave in the Central/Northern GBR. (a) Heterogeneity of coral bleaching responses among coral colonies at fine spatial scales on the GBR (credit: E.J. Howells). (b) For each coral colony, an adaptive index based on the number of 'heat-adapted' alleles (i.e., found to significantly increase in frequency at reefs with warmer of more variable sea surface temperatures (SST), or at reefs that have been exposed to a greater number of marine heatwaves in the past) was computed and tested for a correlation with bleaching (n = 210) and mortality (n = 211) in the field. The red lines show the observed relationship coefficients with mortality (odd-ratio, top) and bleaching (Pearson's correlation, bottom). Grey histograms show the distribution of these coefficients when the adaptive index is computed from a random set of SNPs with comparable average pairwise fixation index (F_{st}) across reefs. (c) Predicted probability of mortality as a function of thermal stress (peak SST) and colony adaptive index. Points show observed colonies categorized as low (blue), medium (grey) or high (ref) adaptive index based on the distribution quantiles. Lines represent predicted mortality probabilities from a logistic regression model across the observed range of peak SST and adaptive index. (d) Correlation between observed bleaching (MIG) and the adaptive index. Each point is a distinct colony and Pearson's R and p-value are indicated. Bleaching observed at one time point during the marine heatwave showed no significant correlation with peak SST or Degree Heating Weeks (DHW) preceding the observation (Figure A4.4). (e) A multiple logistic regression model was used to evaluate the increase in predictive performance of the adaptive index compared to other predictors, measured as the Area Under the Curve (AUC). Boxplot show the AUC across 100 random train/test splits (80/20%) of the data (median: solid line and first and third quartiles: box) for models of increasing complexity. The significance of accuracy improvement across models was tested using Wilcoxon rank-sum tests and the corresponding p-value is shown. (f) A similar approach was used for bleaching using multiple linear regression models and using the

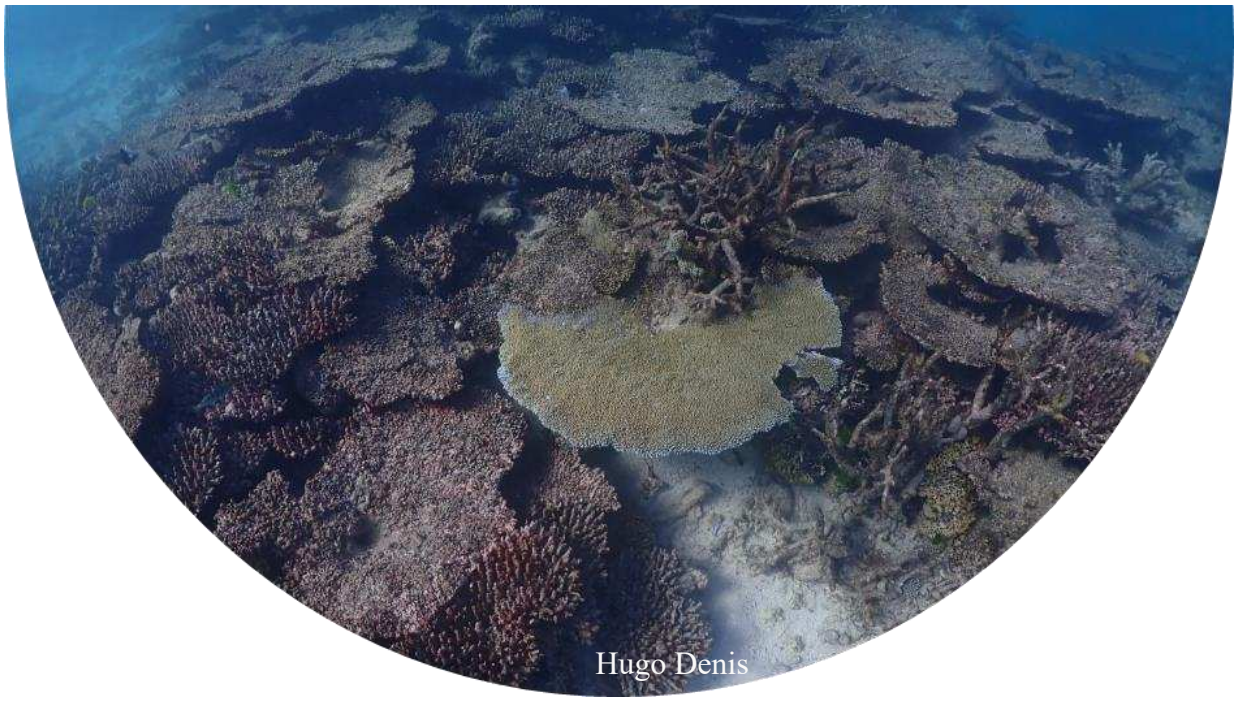
predictive variance *(*R^2*)* for model evaluation. Similar results were obtained for the predictive correlation (*R*).

5.5) Conclusion

Our study provides a comprehensive view of the effect of standing genetic variation on coral heat tolerance traits across spatial scales and thermal exposures. We found that polygenic heat adaptation largely proceeds via non-parallel evolutionary pathways across distinct populations. While this complicates genomic predictions of corals' heat tolerance (Aase et al., 2025), it may confer an adaptive advantage if gene flow recombines the diverse genetic solutions evolved across the seascape (Richards et al., 2023). Nevertheless, we identified several genetic variants, linked to known and novel genes, that contribute to local adaptation through measurable effects on heat tolerance, with some of these genes shared across distant populations. Genes that are repeated targets of selection may be particularly important, as they are also more likely to experience strong temporal selection, which could lead to rapid adaptation to changing environments (Roberts Kingman et al., 2021). To develop biomarkers of broad application for coral conservation, it will be key to better understand the extent of parallel adaptation across coral populations and species, and its importance for variation in heat tolerance traits.

Variability in the polygenic basis of responses between acute and prolonged heat exposure questions the ability of rapid assays to capture heat tolerance variation relevant for evolutionary adaptation. These differences warrant careful evaluation before such assays are applied in management or restoration. Conversely, climate-adaptive loci improved predictions of coral responses to marine heatwaves, suggesting that gene-environment associations can identify genetic variation relevant for coral adaptation in the wild. Due to the large effective population sizes of some *Acropora* species, a substantial fraction of adaptive genetic variation remains undetectable with current methods. As tools and coral genomic datasets continue to expand, our findings can help guide the design of future genomic vulnerability assessments of corals. Beyond heat tolerance, these assessments should consider a broad range of traits relevant to coral persistence to climate warming (Baums et al., 2024) to safeguard adaptive genetic diversity and enhance the robustness of coral communities to environmental fluctuations.

Chapter 6. General discussion



General discussion

Ocean warming has been predicted to pose a threat to the future of coral reefs since the end of the last century (Glynn, 1996; Hoegh-Guldberg, 1999). Over the past decade, within-population variability in heat tolerance traits and their additive genetic basis have gained attention due to their central role in natural selection (Howells et al., 2025; Howells et al., 2022a; Richards et al., 2023) and growing evidence for the critical role of genetic adaptation to prevent extinctions of populations (Bay et al., 2017; Bozec et al., 2025; Lachs et al., 2024; McManus et al., 2021). However, limited empirical data exists on the genomic architectures of heat tolerance traits in corals and their interaction with environmental and evolutionary processes. This knowledge gap creates substantial uncertainty in projections of reef futures, and constrains the integration of evolutionary potential into conservation and restoration strategies (Colton et al., 2022; Hoffmann & Sgrò, 2011; Howe-Kerr & Quigley, 2025).

This thesis aimed to improve understanding of coral adaptive potential in the Western Pacific and the genetic basis and distribution of coral heat tolerance traits, through a focus on the widespread corymbose coral *Acropora spathulata*. To address these questions, I combined empirical individual heat tolerance data from acute stress assays and natural observations, whole genome sequencing and environmental datasets to conduct analyses at the interface of population genetics, quantitative genetics and seascape genomics. The novel insights provided by this thesis are summarized in Figure 6.1 and Table 6.1. The data generated in this thesis has been used to inform selective-breeding experiments (Lamb et al., 2026) and species-distribution models (Guillaume et al., 2025a), and are anticipated to contribute to ongoing efforts to better understand the eco-evolutionary dynamics of corals.

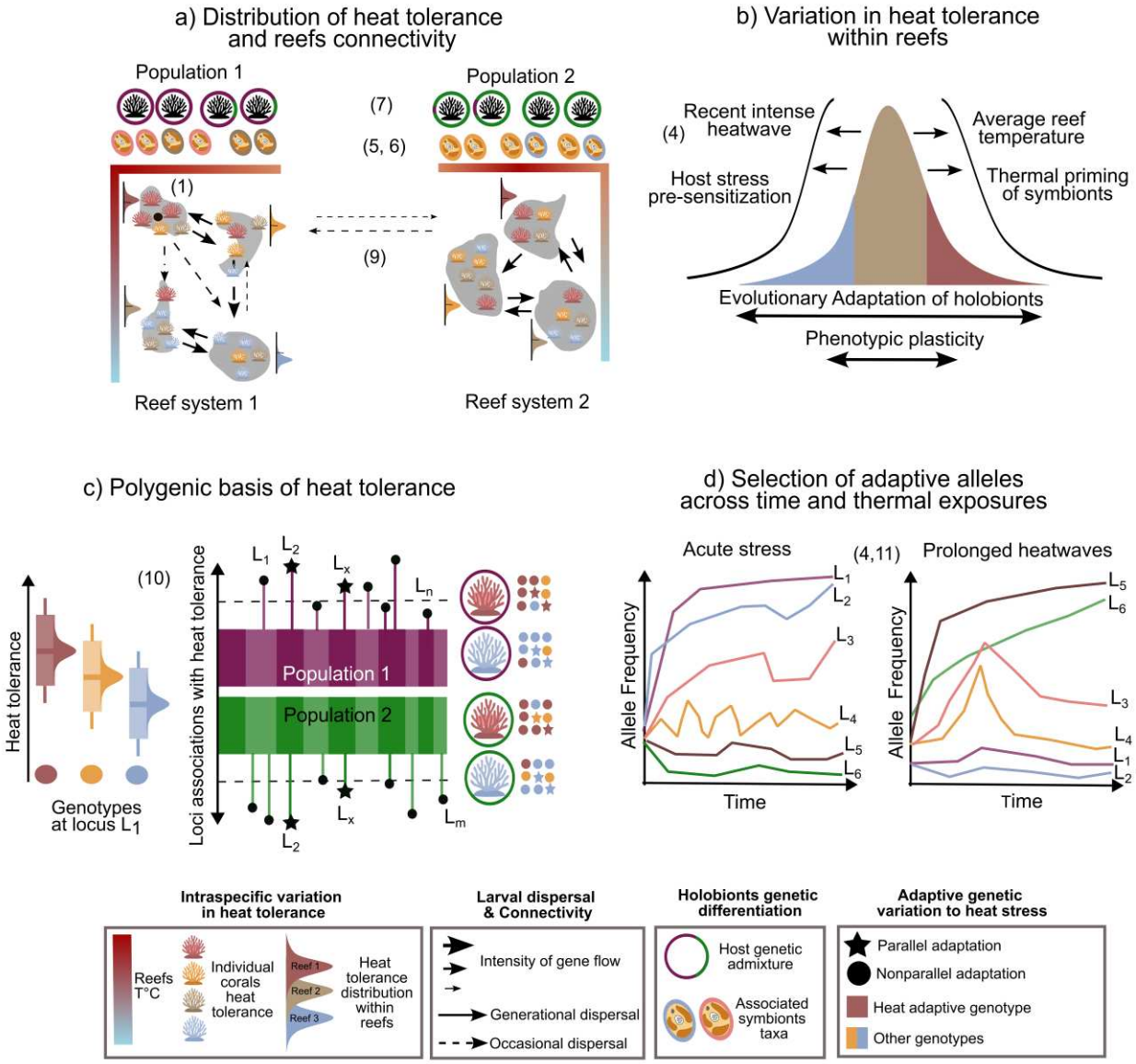


Figure 6.1. Adaptive potential of *Acropora spathulata* to climate warming. A description of main findings from this thesis is provided in Table 6.1, linked to numbers in parenthesis from the figure. (a) Heat tolerance is driven by local adaptation to the thermal condition of reefs, yet heat tolerant genotypes are widely distributed within reef systems due to wide larval dispersal. Distant reef systems experience occasional gene flow. Coral hosts associate with distinct symbiont taxa across environmental gradients. (b) Heat tolerance varies substantially within reefs as a result of evolutionary adaptation and phenotypic plasticity. Both long-term and recent environmental factors can influence the distribution of heat tolerance. (c) Heat tolerance has a largely nonparallel polygenic basis across populations, yet certain genes are repeatedly involved in heat adaptation. Each dot represents a locus significantly associated with heat tolerance (d) Genetic variation underlying heat tolerance varies between acute heat stress and prolonged marine heatwaves. Each line represents a hypothetic trajectory of alleles contributing to heat tolerance phenotypes under repeated selection by acute heat stress (left) or prolonged marine heatwaves (right). Certain alleles may contribute to adaptation only temporarily or within specific locations.

Table 6.1. Summary of the major findings of this thesis, implications for adaptive potential and management and future directions.

#	Findings	Implications for adaptive potential	Implications for management	Limitations	Future directions
1	Acute heat tolerance shows a positive association with reef-average temperatures, suggesting local adaptation, and considerable variability exists among individuals within reefs (Chapters 2 and 3).	Populations have adapted to distinct thermal conditions, and selection may act on existing phenotypic variation. However extreme marine heatwaves can still exceed the upper limits of this variation and cause widespread mortality.	Tolerant individuals can be sourced locally. Preserving both heat-exposed reefs and climate refugia is important to maximize adaptive capacity and resilience.	Acute heat tolerance cannot currently be converted to absolute thermal thresholds in the wild.	Develop models to link tolerance from short- or moderate-term heat stress experiments to longer-term exposure (but see #4).
2	High latitude populations show greater acute heat tolerance relative to local conditions (Chapters 2 and 3).	High latitude populations may have more time to adapt to climate warming, in particular if gene flow from warmer reefs is maintained.	High latitude populations may face lower immediate risk, but maintaining gene flow from lower-latitude populations is crucial.	The impact of lower average temperatures on the rate of increase in heat tolerance at high latitudes is unknown.	Assess temporal changes in heat tolerance.
3	Acute traits (e.g., F_v/F_m and chlorophyll content) capture distinct host and symbiont responses to heat stress and are not always correlated with one another (Chapter 2).	Selective pressures imposed by marine heatwaves may have different evolutionary outcomes among holobiont partners.	Inferences about adaptive potential should consider multiple phenotypic traits.	Most high-throughput phenotyping methods remain prohibitively expensive for many research groups.	Develop low-cost and rapid phenotyping methods encompassing a large range of traits.
4	Acute traits are partly driven by phenotypic plasticity (Chapter 2), and have small to moderate power to predict *in-situ* responses to prolonged thermal stress during natural bleaching (Chapter 5). Genetic variation associated with heat tolerance differs between acute and longer heat stress exposures (Chapter 5).	Acute heat tolerance traits may only be weakly informative of adaptive potential Adaptive genetic variation may vary across the thermal landscape.	Further information on the ecological and evolutionary relevance of acute heat tolerance traits is required before they can be used to guide adaptive management and restoration approaches.	The heritability of acute heat tolerance traits remains unknown.	Use quantitative genetic approaches with related individuals to estimate the heritability of acute stress responses.

#	Findings	Implications for adaptive potential	Implications for management	Limitations	Future directions
5	*A. spathulata* hosts distinct *Cladocopium* symbionts taxa across its distribution, with fine-scale genetic turnover (<30 km) shaped by cross-shore and latitudinal environmental gradients rather than host differentiation (Chapter 4).	Adaptation to warmer conditions may occur via shifts to symbionts typical of warmer reefs, provided these symbionts are present in the local environment.	Translocating adult colonies may cause maladaptation due to habitat-specific symbionts or trigger shifts in symbiont communities. In contrast, aposymbiotic juveniles can acquire locally adapted symbionts after recruitment.	Quantifying the effect of symbionts taxa on holobiont traits is difficult due to confounding host and environmental factors. The effects of marine heatwaves on associated symbiont communities are currently unknown.	Use manipulative experiments to assess the effect of symbionts taxa on adult heat tolerance. Monitor changes in symbiont communities during and after marine heatwaves.
6	Symbionts environmental niche breadths vary widely and do not align with phylogenetic relationships (Chapter 4).	Environmental-generalist' symbionts may buffer holobionts against mild environmental changes but could offer less advantage than specialists under extreme conditions.	Phenotypic diversity in symbionts supports holobiont adaptation and cannot be assumed based solely on phylogenetic relatedness.	Adaptive variation within these *Cladocopium* taxa and its influence on holobiont heat tolerance has yet to be assessed.	Assess symbiont populations differentiation within taxa using microsatellites or hologenome-based methods.
7	Extensive generational dispersal limits detectable host neutral genetic structure at scales >500 km, but local adaptation persists through balanced polymorphisms at specific loci (Chapters 4 and 5).	Large gene flow within populations fosters demographic resilience. Adaptive genetic variation can spread across reefs and accelerate global adaptation.	Assisted gene flow may offer limited benefits within populations; safeguarding natural connectivity and protecting habitat quality is more critical.	The effect of high gene flow on global rates of adaptation is difficult to predict.	Compare demographic trajectories and rates of heat tolerance increase across species varying in dispersal capacity.
8	Local and contemporary effective population size (N_e) of *A. spathulata* is large across its distribution, averaging over 2,000 at the neighbourhood size (Chapter 4).	Deleterious alleles are purged more efficiently, reduced loss of genetic diversity and risk of inbreeding depression due to drift.	Genetic interventions are not an immediate priority for this species.	Possible changes in N_e due to recent mortality are unknown.	Monitor temporal changes in N_e. Obtain population-specific estimates.

#	Findings	Implications for adaptive potential	Implications for management	Limitations	Future directions
9	Across evolutionary timescales, gene flow has been maintained among distant reef systems in the Western Pacific (Chapter 4).	May foster evolutionary adaptation by the introduction of novel genetic variation without swamping locally adaptive variants.	Regional management approaches that integrate conservation units into broader connectivity networks will likely favor the resilience of broadcast-spawner populations.	Gene flow over contemporary scales, and detailed migration patterns among reefs are unknown.	Couple genetic estimates of contemporary gene flow with biophysical modelling at finer spatial scale.
10	Adaptation to thermal conditions, including heat tolerance has a polygenic basis (Chapter 5). Signatures of selection are largely distinct across populations, but a few overlapping signals highlight key genes involved in heat adaptation (Chapter 5).	Polygenic architectures may favor rapid adaptation under moderate environmental shifts but could increase extinction risk under extreme changes. Diverse, alternative genetic solutions may enhance resilience at the metapopulation scale, but rapid adaptation via universally beneficial alleles of large effect is less likely.	Effectiveness of assisted gene flow may be lower than for oligogenic traits as small effect alleles take longer to introgress in the focal population. Nonparallel evolutionary pathways reduce the predictability of adaptation.	The extent of parallel adaptation in corals remains largely unexplored.	Quantify the prevalence of parallel adaptation using multi-populations and species datasets. Assess the fitness effect of genes that repeatedly drive local adaptation.
11	A substantial fraction of genetic variation associated with *A. spathulata* heat tolerance traits is not associated with thermal environments (Chapter 5).	Short-term adaptation to climate warming may partly rely on genetic variation that differs from historical adaptation, and/or is undetectable with linear GEA models.	GEAs and GWAS are complimentary to inform adaptive capacity at distinct spatial and temporal scales.	The relative importance of genetic variation linked to present heat tolerance traits versus long-term climates for future adaptation remains unclear.	Monitor changes in GEAs/GWAS candidates' allelic frequencies over time. Investigate approaches to increase GWAS power.
12	Genomic prediction of coral heat tolerance is hindered by large effective population sizes, but climate-adaptive loci improve predictions of *in-situ* heat stress responses.	Climate-adaptive alleles under a migration-selection balance may play an important role in heat stress responses to marine heatwaves.	Predicting adaptive traits from genomic data is an ongoing challenge. Preserving connectivity and genetic diversity remain priorities.	Accounting for genotype by environment interactions or more robust phenotyping may improve genomic predictions.	Develop models including interactions of genotypes, phenotypes and the environment.

6.1) Can *Acropora spathulata* adapt to climate warming?

6.1.1 Evidence for wide distribution of heat tolerance traits

By using standardised measurements of acute heat tolerance across more than 20 reefs (Chapters 2 and 3), this thesis adds to the growing evidence of widespread variation in the heat tolerance of corals at every ecological scale, from polyps to meta-populations and species (McWilliam et al., 2022; van Woesik et al., 2022; Voolstra et al., 2025). This variation offers a glimmer of hope for the future of corals, as it provides the essential raw material for evolutionary adaptation (Barrett & Schluter, 2008; Gomulkiewicz & Holt, 1995; Hoffmann & Sgrò, 2011). Notably, the broad distribution of the most heat tolerant individuals across nearly all locations (Chapter 2 and 3)—likely facilitated by genetic homogenization from high gene flow (Chapter 4)—indicates that adaptive genetic variation may be widely distributed. This standing adaptive variation could allow populations to adapt more rapidly than if they relied solely on new mutations or the introduction of beneficial alleles from warmer populations (Barrett & Schluter, 2008).

Several sources of uncertainty remain regarding the implications of measured heat tolerance for adaptive potential in *A. spathulata*. Firstly, how much of this variation is genetically determined or the result of phenotypic plasticity is unclear. For example, recent thermal stress boosted the acute tolerance of symbionts (i.e., 'thermal priming'; Hackerott et al., 2021) but negatively affected the overall holobiont acute bleaching response (i.e., stress pre-sensitization, Chapter 2). Environmental memory may thus affect acute heat tolerance thresholds, in line with recent studies showing a decline in thresholds after transplantation to cooler environments (Alderdice et al., 2024; Hackerott et al., 2025). Resolving the contribution of additive genetic variance (V_A) to variation in acute heat tolerance traits is a key area for future research, but would typically require thousands of individuals (Visscher et al., 2014) or pedigree information. Secondly, it remains unknown how acute tolerance translates into survival probability under natural marine heatwaves. For example, longer-term experiments found that within-population variation in heat tolerance could translate to a difference of 10 years of survival under projected warming between the most sensitive and tolerant individuals (Humanes et al., 2022), but such inferences are more challenging for acute stress (see section 6.3.1). Widespread recent bleaching and mortality at several GBR reefs (Cantin et al., 2024; Emslie, 2025) clearly shows how adaptation might be hindered by extreme heatwaves, when they overwhelm even the most tolerant

individuals (Chapter 5). Lastly, even if short-term adaptation occurs through directional selection as observed in the coral *Platygyra daedalea* (Howells., Denis et al., 2025), recurrent marine heatwaves may rapidly deplete adaptive genetic variation and limit adaptation in the long term (Diamond, 2017; Gomulkiewicz & Holt, 1995). This effect could be amplified by the long-lasting consequences of marine heatwaves on coral health, as shown by the negative correlation of acute heat tolerance with the intensity of marine heatwaves in the years preceding the experiment both on the GBR and in New Caledonia (Chapters 2 and 3), as well as in the Coral Sea (Marzonie et al., 2022).

6.1.2 Adaptive variation arising from local adaptation of symbioses and coral hosts

Local adaptation to heterogenous environments can foster both the emergence and maintenance of functional genetic variation (Hoffmann & Sgrò, 2011; Tigano & Friesen, 2016). Despite large variation within reefs, acute heat tolerance was positively correlated with the average sea surface temperatures (MMM) and the past number of strong marine heatwaves (DHW>8, Chapters 2 and 3) of reef sites, indicating that local adaptation partly drives the phenotypic variation in *A. spathulata*. Beyond possible effects of phenotypic plasticity, local adaptation can be explained both by identified genetic polymorphisms in the coral host across thermal gradients (Chapter 5) and variability in *Cladocopium* symbiotic partners (Chapter 4). This multifactorial nature of heat tolerance is corroborated by observations of locally adapted symbioses in other *Acropora* species (Davies et al., 2020; LaJeunesse et al., 2004; Marzonie et al., 2024; Naugle et al., 2024) and balanced host genetic polymorphisms across thermal environments (Bay & Palumbi, 2014; Leiva et al., 2023; Leiva et al., 2025; Lundgren et al., 2013; Selmoni et al., 2021; Selmoni et al., 2020a; Smith et al., 2022; Thomas et al., 2022).

Interestingly, acute traits related to symbionts responses (F_v/F_m) were more variable across reefs than traits related to the host-symbiont bleaching interaction (NDVI, Chapter 2). These patterns may reflect a stronger local adaptation of symbionts owing to limited dispersal (Howells et al., 2012), while high larval dispersal limits local adaptation of coral hosts by repeatedly introducing genotypes from diverse environments (Chapter 4, see section 6.1.3). However, disentangling the roles of symbiosis, host adaptation, and plasticity in shaping heat tolerance remains a challenge due to spatial confounding, and requires tailored sampling strategies, common garden experiments and/or manipulative experiments. Nevertheless, the functional variation arising from local adaptation of holobiont partners will likely have positive effects on

A. spathulata persistence, by providing the necessary toolkit to adapt to future environmental changes (Hoffmann & Sgrò, 2011; Tigano & Friesen, 2016).

6.1.3 The effects of large-scale dispersal on adaptive capacity

An important finding of this thesis is the high realized dispersal of *A. spathulata*, resulting in high gene flow within reef systems, and low but sustained gene flow across geographically distant reef systems (Chapter 4). This life history trait can enhance demographic recovery following disturbances such as marine heatwaves, cyclones or crown-of-thorns starfish outbreaks, as coral larvae can disperse from distant reefs that have escaped these local perturbations (Hock et al., 2017). High dispersal may partly explain the ecological resilience of some reef systems such as the GBR or Palau, with *Acropora* coral cover rebounding within a few years after widespread mortality events (Emslie et al., 2024; Gouezo et al., 2019). However, this dispersal strategy can result in more variable recruitment across years compared to low-dispersive species relying on local settlement (Harper et al., 2023), potentially increasing the risk of local extinction through demographic stochasticity (Gomulkiewicz & Holt, 1995).

High gene flow also has important implications for the evolutionary adaptation of *A. spathulata* populations. First, it limits the loss of genetic variation caused by drift by increasing population sizes (N_e>2,000), lowering inbreeding depression risk and preserving functional variation that could support future climate adaptation (Chapter 4; Hoffmann & Sgrò, 2011). Second, gene flow balances local adaptation (Lenormand, 2002), reducing the risk that populations become unable to adapt to future changes due to environmental specialization (Chapter 5; Tigano & Friesen, 2016). In contrast, past selection for stress tolerance traits in some marginal environments under reduced gene flow has depleted genetic diversity and created fitness tradeoffs in corals that may constrain colonization of new habitats and adaptation to future changes (Scucchia et al., 2023). Occasional long-distance dispersal between the GBR, the Coral Sea and New Caledonia may further enhance genetic diversity by introducing novel alleles, or distinct combinations of adaptive alleles supporting heat tolerance, without swamping locally adapted genotypes (Chapters 4 and 5). Third, adaptation can proceed more rapidly via the spread of climate-adaptive alleles pre-selected in specific regions of the species range (Matz et al., 2020; Tigano & Friesen, 2016). The redistribution of heat adaptive alleles could particularly benefit southern populations, as ocean currents predominantly flow southward on the GBR and in New Caledonia (Marchesiello et al., 2010) and match observed connectivity patterns on the GBR (Chapter 4; Matz et al., 2018; Meziere et al., 2025; Riginos et al., 2019). High gene flow

could however limit adaptation at environmental margins, such as inshore reefs or the lower-latitude edge of *A. spathulata* distribution by introducing maladapted alleles and creating a dispersal load (Hoffmann & Sgrò, 2011; Lenormand, 2002).

6.1.4 Molecular mechanisms of heat tolerance

Chlorophyll retention, which was used as the main proxy for heat tolerance in this thesis, depends on many lower-level phenotypes of holobiont partners (e.g., preservation of photosynthetic apparatus integrity in the algal symbionts and redox homeostasis in the coral host; Barghi et al., 2020). This diversity of lower-level phenotypes likely explains why previous studies investigating genetic differentiation among coral hosts with distinct heat tolerance, or living in contrasting thermal environments point to a wide variety of molecular functions and pathways (Black et al., 2025a; Selmoni et al., 2024a).

Reponses to stress, whether artificial or natural, are initiated by cell-surface receptors that activate molecular signalling cascades. In *A. spathulata*, local adaptation and heat stress responses were linked to genetic variation in genes associated with signalling pathways such as MAPK (Chapter 5), which is the main cascade linking host cell receptors to bleaching (Helgoe et al., 2024). In addition, several heat-associated loci were linked to cyclin dependent kinases, previously suggested to contribute to heat adaptation in corals from the Persian/Arabian Gulf (Smith et al., 2022).

These signalling pathways can trigger numerous molecular cascades and outcomes (e.g., apoptosis, autophagy, symbiont exocytosis; Helgoe et al., 2024). This thesis shows that although the genic drivers of acute heat tolerance differ among geographically distant coral populations, there is a convergence in functions associated to differentiated genes pointing to apoptosis, proteolysis, calcium transport regulation and extracellular organization (Chapter 5). Such functions are well known to be involved in the unfolded protein response (UPR; Helgoe et al., 2024) induced by high heat exposure in corals. This response involves the ubiquitin-mediated tagging of misfolded proteins, and this pathway was largely represented among genes involved in acute stress response and *in-situ* mortality (GWAS) as well as those linked to local thermal adaptation (GEAs; see also Thomas et al., 2017). The UPR leads to the upregulation of heat shock chaperones to assist the refolding or elimination of misfolded proteins (Helgoe et al., 2024), and multiple genes coding for chaperones were identified in GWAS with acute tolerance (e.g., sacsins, DnaJ homologs, Chapter 5). High heat conditions can also enhance calcium transfer from the endoplasmic reticulum to mitochondria, inducing apoptosis through

mitochondrial fragmentation (Helgoe et al., 2024) and both processes were enriched among genes associated to acute tolerance (Chapter 5). These results suggest that, even with limited power, GWAS successfully identified genetic variation underlying acute stress responses.

Our results indicate that distinct genetic variation underlies acute stress responses and *in-situ* responses to marine heatwaves or long-term thermal conditions (Chapter 5). Yet, all of these responses were associated with genes involved in oxidative stress regulation, immune response and DNA repair. This supports the central role of mechanisms mitigating reactive oxygen species generated by the photoinhibition of symbiont photosystem II, or by the coral host itself, in the adaptation to both acute and chronic heat exposures (Roberty & Plumier, 2022; Weis, 2008).

Importantly, approaches like GWAS and GEAs generate long lists of candidate genes that are difficult to fully explore and tend to produce a bias towards genes of known functions. Around 20% of coding sequences most strongly associated with *A. spathulata* heat adaptation also lacked annotations, representing potentially novel genes awaiting characterization (Cleves et al., 2020a). By linking genetic variants to thermal environments and quantifying their effect on heat tolerance, this thesis highlights novel genes—such as *TRPA1* likely involved in temperature sensing (see also Leiva et al., 2025), and *PSTK* possibly involved in selenoprotein synthesis—that are strong candidates for further characterization of their role in corals heat adaptation.

6.1.5 Impacts of heat tolerance genomic architecture on the likelihood of climate adaptation

The expected polygenic nature of corals' heat tolerance (Fifer et al., 2024; Fuller et al., 2020) was supported in *A. spathulata* as GWAS did not identify loci of major effects (Chapter 5). In addition, GEAs identified loci putatively involved in local thermal adaptation with a widespread distribution along the genome (Chapter 5). This somewhat contradicts theoretical expectations that spatially-varying selection under high gene flow should favor concentrated genomic architectures, i.e., small genomic regions of sharp differentiation ('islands of differentiation'; Tigano & Friesen, 2016; Yeaman, 2022; Yeaman & Whitlock, 2011), with some empirical support in corals (Thomas et al., 2022). The realization of this prediction however appears to vary across species (Renaut et al., 2013; Shi et al., 2023). More 'diffuse' genetic architectures are notably expected under temporally variable selective pressures—as is the case for highly variable marine heatwaves (Chapter 1)—because no single allele remains consistently favoured (Yeaman, 2022). In addition, marine heatwaves have likely affected most studied reefs at least

once in the past (Chapter 2), fostering global adaptation to climate warming and 'diffuse' genomic architectures due to reduced tension between migration and selection (Yeaman, 2022). In other words, genotypes best adapted to high temperatures may be occasionally favoured even in the cooler environments, which could explain their broad distribution (Chapter 2). Finally, under high gene flow, genotypes that display the highest phenotypic plasticity tend to be favoured because they can adapt to variable environments within a single generation, thereby reducing divergent natural selection (Crispo, 2008). Overall, the combination of variable selection across space and time, extensive gene flow, and phenotypic plasticity likely explains the lack of large-effect loci identified by GWAS in *A. spathulata* (Chapter 5), and suggests some of the loci identified by association studies may only play a transitory role in adaptation to climate warming.

Understanding factors favouring certain genomic architectures also has implications for the probability of future climate adaptation. Modeling work suggests that polygenic architectures allow evolutionary rescue under moderate environmental shifts, which can prevent extinction (Kardos & Luikart, 2021). However, under extreme environmental changes, polygenic traits are expected to elevate extinction risk, whereas monogenic architectures may occasionally avert it (Bellagio & Exposito-Alonso, 2025). Eco-evolutionary simulations of corals under IPCC warming scenarios consistently show that extinction is delayed in monogenic architectures compared to polygenic ones under severe warming (RCP6.0 and RCP8.5; Bay et al., 2017). In contrast, empirical evidence in ash trees demonstrates that rapid polygenic adaptation within a single generation can prevent extinction from high mortality caused by a fungal disease (Metheringham et al., 2025), although this does not rule out eventual extinction in the long run. Predicting whether the observed genetic architecture of heat adaptation in *A. spathulata* will allow evolutionary rescue is highly complex, as it not only depends on the selection of standing genetic variation within reefs, but also potential tradeoffs with other traits and gene flow among reefs (Carlson et al., 2014; Hoffmann & Sgrò, 2011). This will be further complicated in the presence of gene flow recombining distinct genomic architectures of heat tolerance across populations (Chapter 5). Future modeling studies are thus needed to estimate the critical rates of environmental change for Acroporidae populations. Such models could use insights from this thesis and other empirical studies to parametrize the number and distribution of adaptive alleles and model their propagation across spatially explicit populations using realistic dispersal kernels (Hoffmann & Sgrò, 2011).

6.2) Implications for conservation and restoration

The importance of integrating evolutionary adaptation into the conservation and management of wild species is increasingly recognized (Aitken et al., 2024; Flanagan et al., 2018; Hohenlohe et al., 2021; Theissinger et al., 2023), notably for coral reefs species that are at the frontline of climate warming (Bay et al., 2023a; Colton et al., 2022). This thesis provides information relevant to the conservation of *A. spathulata* (Table 6.1) and other Western Pacific acroporids that are vulnerable to disturbances (Darling et al., 2012; Loya et al., 2001). For highly dispersive acroporids such as *A. spathulata*, conservation would likely be most effective with networks of marine protected areas (MPAs; Mumby et al., 2021) that maintain suitable habitat spaced at intermediate distances (10s of kilometres, Chapter 4). Coordinating networks regionally, beyond national borders, will further favor resilience by maintaining connectivity among populations that may have adapted to past thermal stress through distinct genetic solutions (Chapters 4 and 5). In addition, MPA designs that span reefs with contrasted thermal exposure will maximize adaptive potential, by maintaining genetic variation arising from local adaptation of coral hosts and symbionts (Chapters 2–5; Anthony et al., 2020; Forrest et al., 2024). However, conventional management approaches cannot avert the effect of marine heatwaves as corals in MPAs still experience severe bleaching and mortality (Chapter 5; Graham et al., 2020; Johnson et al., 2022) and the acute heat tolerance traits measured in this thesis were independent of reef zoning (Chapters 2 and 3). A large effective population size suggests *A. spathulata* faces a lower short-term risk of local extinction (Chapter 4) than other taxa relying on localized replenishment and that are sometimes inbred (e.g., Hernández-Agreda et al., 2024; Meziere et al., 2025; Prata et al., 2024), but this finding should be interpreted with caution in light of recent mortality events (Chapter 5; Cantin et al., 2024; Emslie, 2025).

Given the limitations of MPAs and the pace of climate warming, assisted evolution strategies such as symbiont manipulation, assisted gene flow, selective breeding and larval reseeding are increasingly being tested for the adaptive management of coral populations (Suggett & van Oppen, 2022; van Oppen et al., 2015; Voolstra et al., 2021a). This thesis also provides insights into the opportunities and limitations of these approaches. Although *A. spathulata* juveniles can acquire diverse symbionts (Quigley et al., 2020a), non-*Cladocopium* taxa will not likely persist into adulthood based on their absence across the 1,088 corals sampled in this study (Chapter 4; see also Epstein et al., 2019). Inoculation with heat-evolved *Cladocopium* taxa (Buerger et al., 2020) or naturally adapted to warm environments may have higher success, but whether these

associations would persist and provide long-term benefits outside marine heatwaves remains unknown (Turnham et al., 2025).

Assisted gene flow via translocation of adult colonies is unlikely to yield substantial short-term benefits within populations (<500 km), due to potential symbiont maladaptation (Chapter 4; Howells et al., 2013), natural genetic homogenization from high dispersal (Chapter 4), and slow introgression of adaptive alleles with small effects (Chapter 5; Bellagio & Exposito-Alonso, 2025). Conversely, selective breeding may be conducted using naturally occurring tolerant individuals within each reef (Chapters 2 and 3). However, *a priori* identification of tolerant individuals based on genotype is an ongoing challenge, as candidate adaptive loci often explain only a small fraction of phenotypic variation and may vary with the duration and magnitude of thermal stress (Chapter 5). Genomic predictions based on the combined effects of adaptive alleles may improve the identification of populations with elevated heat tolerance beyond environmental and symbiont information, but are limited by large coral effective population sizes (Chapter 5). Phenotypic selection based on the responses of colonies to natural marine heatwaves remains the most reliable approach until genomic predictions can achieve higher accuracy (Chapter 5; Baums et al., 2024).

Finally, larval reseeding from neighbouring reefs may aid locally depleted populations (Chapter 5), but combining high-resolution biophysical models and post-disturbance recruitment monitoring can determine whether this intervention is necessary or natural recovery from allo-recruitment is sufficient. Overall, the long-term success of these interventions will depend on the ability to address local factors contributing to mortality and reducing global emissions (Bozec et al., 2025; Reimer et al., 2024).

6.3) Challenges in characterizing the genetic architecture of corals heat adaptation.

6.3.1 Measuring ecologically and evolutionary informative phenotypes

Acute heat tolerance traits only moderately predicted bleaching and mortality during a natural marine heatwave in *A. spathulata* (Chapter 5) and other *Acropora* species on the GBR (Naugle., Denis et al., 2025, submitted). Heat tolerance depends both on the intensity and duration of thermal stress, therefore differences between acute and long-term responses may be explained by different underlying physiological mechanisms. Some taxonomic groups (e.g., insects) exhibit a trade-off between the maximum temperature that species can endure, and the rate at

which this threshold declines with exposure time (Rezende et al., 2014). Such tradeoffs are largely undocumented for corals but could exist: for example *A. tersa* had substantially lower acute ED50 than *A. spathulata* (Denis et al., 2024a; Naugle et al., 2024) yet exhibited higher survival during a natural marine heatwave (Naugle et al., 2025). Beyond ecological interpretations, these differences could also alter the outlook for corals evolution if the molecular basis (Chapter 5) and heritability (Humanes et al., 2024) of heat tolerance differs across thermal exposures. For example, Soto et al. (2025) found that genetic correlation for heat tolerance in *Drosophila* decreases as temperature conditions diverge. This implies that selecting individuals for acute tolerance may not necessarily lead to increased tolerance under milder but prolonged thermal stress.

There is therefore a great and urgent need to better unify the heat tolerance of corals measured across distinct stressful conditions (affecting short term survival), and with heat tolerance measured under permissive conditions (affecting completion of life cycle). Thermal-death time (TDT) curves, increasingly applied in ectotherms, allow to model changes in the maximum heat tolerance of organisms with exposure time (Ørsted et al., 2022; Rezende et al., 2014). Although technically demanding, this framework would offer multiple advantages provided it can accurately model coral heat tolerance: (1) tolerance estimates from distinct experiments can be reconciled and converted to a common estimate, including under variable temperature regimes (e.g., the maximum temperature tolerable for a 1 week exposure), (2) such estimates can be more directly compared to heat stress experienced by corals in their natural environments and (3) once TDT models have been established, survival predictions can be extrapolated for any temperature or exposure time (Ørsted et al., 2022; Rezende et al., 2020). This approach would also allow formally testing for possible tradeoffs between acute and long-term tolerance across individuals. Not only this framework can be applied to future studies, but may also be used to reanalyse some of the existing datasets (Grottoli et al., 2021; McLachlan et al., 2020).

In addition to the type of thermal exposure, another key consideration for future coral GWAS is the level of phenotype analysed (see section 6.1.4). Conducting GWAS with lower-level phenotypes (e.g. antioxidant production) could improve variant detection, but host-centric traits should be prioritized to identify host adaptive genetic variation. For example, using the maximum photosynthetic efficiency F_v/F_m (e.g., Muller et al., 2025) is unlikely to succeed as it primarily reflects symbiont responses (Chapter 2; Naugle et al., 2025), unless coevolution among holobiont partners is involved. Emerging tools like hyperspectral imaging (used in this thesis for NDVI) may soon enable non-invasive underwater measurements of host-centric traits

such as fluorescent proteins (Teague et al., 2019). Repeating these measurements (or visual bleaching) during marine heatwaves would allow dose response curves to be measured without bias from observation timing (Claar & Baum, 2019), while minimizing impacts of phenotyping on wild populations. Finally, to study the heritability and genetic basis of traits requiring invasive measurements, the coral research community could adopt the plant science model of germplasm collections, where intensive measurements are restricted to a core subset of individuals capturing most of the genetic variation within a population (Halpin-McCormick et al., 2024).

6.3.2 Future horizons in coral association studies

Inspired by pioneering work in plant science (Lasky et al., 2023), a key novelty of this thesis is the joint application of GEAs and GWAS in corals to increase confidence in candidate heat adaptive loci compared to using a single method (reviewed in Selmoni et al., 2024a). Indeed, several SNPs associated with thermal predictors exhibited a significant effect on heat tolerance traits (Chapter 5), but these effects were relatively small. This contrasts with previous studies that identified loci of substantial effect in humans (Pritchard et al., 2010) or corals (e.g., Jin et al., 2016; Kirk et al., 2018), even within polygenic architectures. Such differences may arise from gene-by-environment interactions or gene-environment correlations (Abdellaoui et al., 2023; Drury & Lirman, 2021). These effects can bias the quantification of loci effects when heat tolerance is assessed across distinct environments (Marigorta & Gibson, 2014), unlike studies testing GEA candidates under common environmental conditions (Hancock et al., 2011; Luo et al., 2025). These interactions may be common: in *Drosophila*, a third of lifespan-associated genetic variation showed environment-dependent effects (Pallares et al., 2023). Likewise, in *A. thaliana* most loci associated with drought resistance in distinct locations showed conditional neutrality (i.e., no effect in other locations) or antagonist pleiotropy (i.e., opposite effects across locations; Exposito-Alonso et al., 2019). Future work could test this hypothesis using approaches such as reaction norms (Carvalho Filho et al., 2024; Lasky et al., 2018) or environment-stratified GWAS (Zhang et al., 2024b).

The integration of GWAS and GEAs also indicates that most SNPs associated with heat tolerance do not show clinal allele frequency patterns across thermal environments. This aligns with the rapid allelic turnover expected in polygenic traits with high genotypic redundancy (see 6.1.5; see also Yeaman, 2022). Whether adaptive loci identified by GEAs or GWAS are most relevant for long-term adaptation remains a hotly debated topic (Barghi et al., 2020; Lotterhos,

2023; Yeaman, 2022), especially as rapid adaptation to climate warming versus long-term adaptation may involve partly distinct genetic basis (Wu et al., 2025). In addition to key loci highlighted by both approaches, a promising direction for coral adaptation research is the integration of association studies with temporal monitoring. Although evolve-and-resequence experiments (Schlötterer et al., 2015) would be technically challenging due to coral's long generation times, other strategies such as the sequencing of successive coral generations across bleaching events (Fifer et al., 2024) or comparison of historical and contemporary DNA samples (Turbek et al., 2023) could help validate the importance of specific genes for long term climate adaptation.

The ability of association studies to detect genetic variation underlying heat tolerance will likely improve with larger cohorts, but several strategies could also enhance power and specificity without increasing sample sizes. Although GWAS are limited by power (false negatives, Chapter 5), some adaptive traits may share positive genetic covariance (Wright et al., 2019). Future studies could therefore apply multivariate GWAS to detect pleiotropic loci of ecological significance by leveraging correlations across traits (Yang & Wang, 2012). In GEAs, the main limitation is the low specificity, with false positives often arising from genetic drift or collinear environmental factors (Chapter 5; Lotterhos, 2023). When available, high-resolution environmental data from numerical models and drone imagery will facilitate disentangling genetic variation driven by local adaptation to temperature from that influenced by other factors (Dauphin et al., 2023).

While this work has focused on the detection of adaptive genetic variation using single nucleotide polymorphisms (SNPs), other types of genetic variants such as indels, repeated elements or structural variants may also significantly influence phenotypes. Structural variants are notably strong drivers of ecotype differentiations in sunflowers (Todesco et al., 2020), insects (Gompert et al., 2025) and more generally evolutionary processes across many species (Schneller et al., 2025; Wellenreuther & Bernatchez, 2018). Although these types of variants have begun to be identified in reef-building corals (Thomas et al., 2022; Zhang et al., 2024a), their potential effect on phenotypic traits remain largely unknown. A key future research direction is to identify these variants in corals and test their associations with the environment and phenotypic traits, to uncover potential roles in fitness and adaptation (Harris et al., 2024).

6.3.3 The ongoing challenge of candidate loci validation and genomic prediction

The pace of candidate loci functional validation has not kept up with their rapid discovery through association studies (Abdellaoui et al., 2023; Gallagher & Chen-Plotkin, 2018; Lasky et al., 2023; Uffelmann et al., 2021). This is especially true for corals where genetic resources and tools are in early stages of development (Selmoni et al., 2024a). While the joint application of GEAs and GWAS supports the role of certain loci in heat adaptation, each approach tends to identify distinct signals that cannot always be mutually confirmed (Chapter 5). Alternative strategies are thus needed to confirm these associations and establish a mechanistic role of genes and variants in the traits. CRISPR/Cas9 is a promising method for confirming associations (Cleves et al., 2018; Cleves et al., 2020b; Selmoni et al., 2024a) but remains technically challenging and limited to larval stages. A range of complementary methods could thus be applied in corals including candidate loci colocalization with gene or protein expression and methylation patterns, or testing their associations with transcript levels (Albert & Sauvage, 2022; Cano-Gamez & Trynka, 2020). Methods to predict SNP effects on coding sequences and protein structures can also provide an additional line of evidence for a functional role without additional data (Cano-Gamez & Trynka, 2020; Tam et al., 2019; Torkamaneh & Belzile, 2022). Their application was limited in this work by the lack of a fully curated genome annotation and the likely insufficient marker density in some populations to capture causal variants.

The long time needed to validate individual loci will limit their use to inform the conservation of rapidly declining coral populations, thus genome-wide prediction approaches are an attractive alternative method to predict and validate coral heat tolerance (Bay & Guerrero, 2020; McGaugh et al., 2021). Results from this thesis suggest GEA can identify some important alleles for heat adaptation that collectively improve predictions of coral responses during marine heatwaves. However, GEA cannot identify the entire genomic basis of heat adaptation (see also Lotterhos, 2023), and the accuracy of genomic predictions based on SNP-phenotype associations (e.g., genomic estimated breeding values or polygenic risk scores) remains limited for highly dispersive coral species with large effective population sizes (Chapter 5). These limitations reflect the high variability of SNP effect size estimates from small sample sizes, and their potential sensitivity to environmental interactions (see section 6.3.2). Follow-up analyses are needed to test whether predictive accuracy could be improved by functional prioritization of variants, or by accounting for gene-by-environment interactions.

Given the difficulty of predicting individual phenotypes relevant for climate adaptation (e.g., heat tolerance), approaches based on the generalization of the genetic-environment relationship are increasingly used to estimate the global risk of maladaptation of populations to future conditions ('genomic offset'; Capblancq et al., 2020; Fitzpatrick & Keller, 2015; Matz & Black, 2025). Interestingly, theoretical work suggests that such approaches may accurately resolve multivariate phenotypes even when the underlying loci do not exhibit clinal allelic frequency patterns (Lotterhos, 2023). Although increasingly applied—including in corals (Adam et al., 2022; Black et al., 2025b)—the validation of these predictions generally relies on common garden experiments that may be logistically difficult to conduct in corals (Lind et al., 2024; Rellstab & Keller, 2024). *In-situ* data such as generated in this thesis could be used to test, for example, whether reefs with higher predicted genomic offset (i.e., predicted to show greater climatic vulnerability) experience bleaching and mortality at lower levels of heat stress relative to their local climatology than other reefs. An important caveat however, is that accuracy of genomic offset methods could be low when local adaptation is limited (Lind & Lotterhos, 2024), in the presence of large phenotypic plasticity, or when future environments exceed conditions currently experienced by populations across their range (Capblancq et al., 2020). Research on coral genetic adaptation to climate change is a rapidly growing but still young field. The results presented here represent an initial step that can help future studies to optimize their sampling strategies and evaluate the interest of genomic predictions based on realistic expectations of attainable accuracy.

6.3.4 The effect of genetic variation within symbiont taxa on coral heat tolerance

This work focused on host genetics and symbioses with distinct *Cladocopium* taxa, but functional genetic variation may also exist among symbiont populations within a single taxon (e.g., between populations of the C3k/C3bo taxon found in both NC and CB, Chapter 4). Substantial phenotypic diversity exists within symbiont taxa (Beltran et al., 2021; Takahashi et al., 2009; Xiao et al., 2022) and can influence holobiont traits (Hoadley et al., 2021; Howells et al., 2012), suggesting it may also contribute to *A. spathulata* heat tolerance and local adaptation. Following Reich et al. (2021), SNPs were recovered by mapping symbiont reads to *Cladocopium proliferum* coding sequences (C1; Chen et al., 2022). However, this approach was unable to resolve genetic differentiation between symbiont taxa (in contrary to the *k*-mer approach, Chapter 4), possibly due to low coverage or poor mapping of C50/C3 reads to the C1 reference genome. Recently, new hologenome approaches leveraging reads mapped to

chloroplast minicircle copies have been proposed (Armstrong et al., 2024), and could yield multilocus genotypes at higher coverage. Testing these approaches on *A. spathulata* hologenomes represents a promising next step for a finer characterization of the genetic diversity of its symbioses. To achieve higher molecular resolution and assess functional genetic differentiation of Symbiodiniaceae harbored by *A. spathulata*, I also explored using single-cell sequencing early in my PhD, but this was challenging without a micromanipulator. Nevertheless, its successful application in several dinoflagellates (Frommlet & Iglesias-Rodríguez, 2008; Ruiz Sebastián & O'ryan, 2001; Takano & Horiguchi, 2006) suggests this method could allow the detection of functional genetic variation in coral symbionts.

6.4) New Caledonia and Australia as a case study to understand differences in coral reefs tolerance and resilience to marine heatwaves

Global meta-analyses report large differences in coral cover and bleaching prevalence between the Great Barrier Reef and New Caledonia over the past two decades (Shlesinger & van Woesik, 2023; Sully et al., 2022). I witnessed these differences firsthand during the 2023–2024 fourth global coral bleaching event (Reimer et al., 2024) through research fieldwork on the GBR and New Caledonia, and citizen-science coral reefs monitoring with NGO Pala Dalik in New Caledonia ('Réseau d'Observation des Récifs Coralliens', RORC). *A. spathulata* populations suffered extreme mortality at several inshore locations from the Central/Northern GBR (Chapter 5). Aerial and underwater surveys also reported high to extreme bleaching (>30% of corals) in the Capricorn Bunker Group (Southern GBR), where several studied reefs are located (Emslie, 2025). This was in sharp contrast with my personal observations in New Caledonia, of no visible bleaching at Mara reef, Prony reef and Snark reef, and medium bleaching at Ile Verte (~15% of colonies paling to bleached), despite the fact that these reefs experienced similar levels of accumulated heat stress (ΔDHW<1) and absolute temperatures (ΔSST<0.2, Figure 6.2). These observations are further supported by the fact that less than 2% of New Caledonia's reefs lost coral cover from 2023 to 2024 (RORC, 2024).

Unlike lower-latitude Central/Northern GBR populations that may live near to their upper thermal limits, Southern GBR and New Caledonia coral populations are generally both predicted to have high adaptive capacity and act as future "bright spots" (Matz et al., 2020). This assumption is however greatly challenged for the Southern GBR by widespread bleaching during the 2020 (Nolan et al., 2021) and 2023–2024 marine heatwaves. This raises the important

question of what makes New Caledonia's reefs seemingly more tolerant to marine heatwaves. While a number of hypotheses have been formulated, none have been formally tested to date using comparative analyses with other reef systems. Given their geographic proximity, connectivity, and similar latitudes, the GBR and New Caledonia's reef systems could serve as a case study for understanding differences in coral tolerance and resilience to marine heatwaves. Addressing this question will require multidisciplinary approaches—including oceanography, geochemistry, ecology, and evolutionary genetics—and is an area I hope to contribute to in the future. The first step to do so will be to expand the bleaching monitoring network in New Caledonia, which is currently restricted to Nouméa surroundings, suggesting that some past bleaching events might have been overlooked. Although RORC observations, conducted across the island range for more than 20 years, would detect large changes in coral cover induced by mass bleaching events, their timing is not suited to reliably capture bleaching onset, prevalence and intensity. The establishment of a bleaching monitoring network has been under discussion for several years, but given New Caledonia's small population, it will require coordinated efforts from traditional owners, NGOS, research institutes and dive shops to be effective. I strongly hope that in the future, these stakeholders can collaborate to uncover what makes New Caledonia's reefs unique and to guide the management of these exceptionally rich and diverse ecosystems.

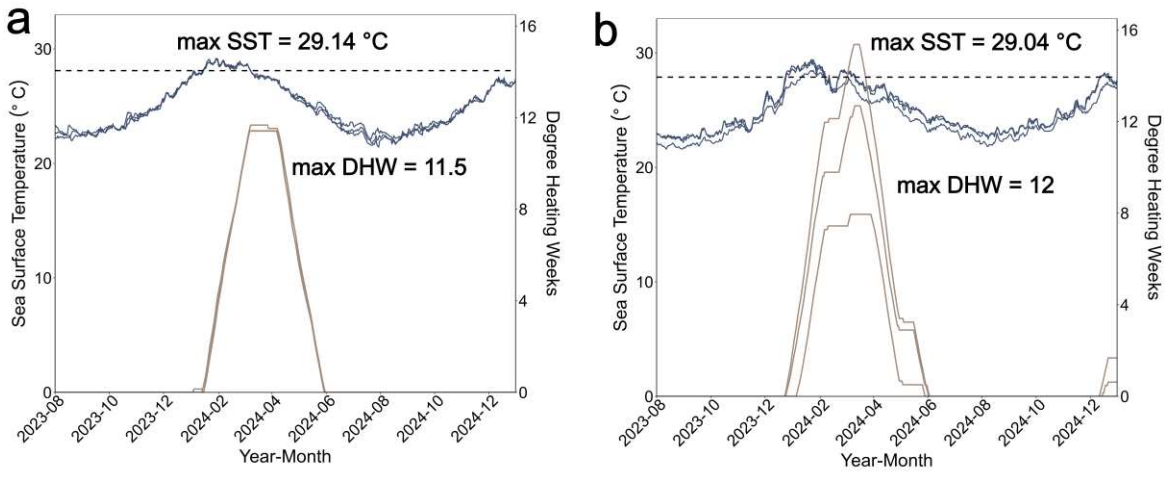


Figure 6.2. Similar accumulated heat stress during the 2023–2024 marine heatwave in the Southern GBR and Southern NC led to drastically different bleaching outcomes. Sea surface temperature (SST, blue) and Degree Heating Weeks (DHW, brown) at (a) Lady Musgrave, Heron Island and Fitzroy Reef in the GBR (b) Prony reef, Mara reef and Ile Verte reef in NC. The horizontal lines indicate the temperature corresponding to 1 °C above the average Maximum Monthly Mean (MMM) across sites. The average maximum SST and DHW reached across sites are indicated for each region.

6.5) Conclusion

Safeguarding coral reefs and the human populations that rely on their ecosystem services from climate warming is an immense challenge. Curbing global emissions remains the most direct and crucial action to limit future coral losses (Bozec et al., 2025; van Hooidonk et al., 2016), yet climate warming will continue for decades even with rapid emissions mitigation. By exploring the environment–phenotype–genotype nexus across ecological scales, this thesis provides timely insights into the adaptive capacity of a key Western Pacific *Acropora* species. Collating these datasets across species provides a foundation for embedding evolutionary processes into policy, conservation, and restoration strategies of coral reef ecosystems. Given the rapid pace of environmental change and decline in these ecosystems, these strategies should progressively integrate validated genomic predictions of adaptive capacity. While heat tolerance is a central focus of coral research and this thesis, climate adaptation depends on more than just the survival of the most tolerant individuals, therefore other key life history traits must be evaluated (e.g., growth rate, fecundity; Baums et al., 2024; Vogt-Vincent et al., 2025). Overall, conservation and restoration strategies should prioritize the preservation of functional, genetic and species diversity, along with reef connectivity, and be ideally coordinated across neighbouring countries (Baker et al., 2025). While such goals may occasionally come at the expense of tradeoffs with heat tolerance, they will likely improve ecosystem robustness to environmental fluctuations and the preservation of their functions in the future (Grumbach & Hamant, 2020).

References

Aase, K., Burnett, H. A., Jensen, H., & Muff, S. (2025). How accurate is genomic prediction across wild populations? *BioRxiv*, 2025.2006. 2016.659953.

Abdellaoui, A., Yengo, L., Verweij, K. J., & Visscher, P. M. (2023). 15 years of GWAS discovery: realizing the promise. *The American Journal of Human Genetics*, *110*(2), 179-194.

Adam, A. A., Thomas, L., Underwood, J., Gilmour, J., & Richards, Z. T. (2022). Population connectivity and genetic offset in the spawning coral *Acropora digitifera* in Western Australia. *Molecular Ecology*, *31*(13), 3533-3547.

Ainsworth, T. D., Leggat, W., Silliman, B. R., Lantz, C. A., Bergman, J. L., Fordyce, A. J., Page, C. E., Renzi, J. J., Morton, J., & Eakin, C. M. (2021). Rebuilding relationships on coral reefs: Coral bleaching knowledge-sharing to aid adaptation planning for reef users: Bleaching emergence on reefs demonstrates the need to consider reef scale and accessibility when preparing for, and responding to, coral bleaching. *BioEssays*, 2100048.

Aitken, S. N., Jordan, R., & Tumas, H. R. (2024). Conserving Evolutionary Potential: Combining Landscape Genomics with Established Methods to Inform Plant Conservation. *Annual Review of Plant Biology*, *75*.

Albert, E., & Sauvage, C. (2022). Identification and validation of candidate genes from genome-wide association studies. In *Genome-Wide Association Studies* (pp. 249-272). Springer.

Alderdice, R., Perna, G., Cárdenas, A., Hume, B. C., Wolf, M., Kühl, M., Pernice, M., Suggett, D. J., & Voolstra, C. R. (2022). Deoxygenation lowers the thermal threshold of coral bleaching. *Scientific Reports*, *12*(1), 1-14.

Alderdice, R., Voolstra, C. R., Lendo, C. I. N., Boote, C., Suggett, D. J., Edmondson, J., Goyen, S., Haydon, T., & Camp, E. F. (2024). Loss of coral thermotolerance following year-long in situ nursery propagation with a consecutively high summer heat-load. *Coral Reefs*, 1-15.

Alessi, C., Lemonnier, H., Camp, E. F., Wabete, N., Payri, C., & Rodolfo Metalpa, R. (2024). Algal symbiont diversity in *Acropora muricata* from the extreme reef of Bouraké associated with resistance to coral bleaching. *PloS One*, *19*(2), e0296902.

Alexander, D. H., & Lange, K. (2011). Enhancements to the ADMIXTURE algorithm for individual ancestry estimation. *BMC Bioinformatics*, *12*, 1-6.

Alvarado-Cerón, V., Muñiz-Castillo, A. I., León-Pech, M. G., Prada, C., & Arias-González, J. E. (2022). A decade of population genetics studies of scleractinian corals: A systematic review. *Marine Environmental Research*, 105781.

Álvarez-Noriega, M., Marrable, I., Noonan, S. H., Barneche, D. R., & Ortiz, J. C. (2023). Highly conserved thermal performance strategies may limit adaptive potential in corals. *Proceedings of the Royal Society B*, *290*(1990), 20221703.

Anderson, A. R., Collinge, J. E., Hoffmann, A. A., Kellett, M., & McKechnie, S. W. (2003). Thermal tolerance trade-offs associated with the right arm of chromosome 3 and marked by the hsr-omega gene in *Drosophila melanogaster*. *Heredity*, *90*(2), 195-202.

Andréfouët, S., Cabioch, G., Flamand, B., & Pelletier, B. (2009). A reappraisal of the diversity of geomorphological and genetic processes of New Caledonian coral reefs: a synthesis from optical remote sensing, coring and acoustic multibeam observations. *Coral Reefs*, *28*, 691-707.

Angilletta Jr, M. J., Bennett, A. F., Guderley, H., Navas, C. A., Seebacher, F., & Wilson, R. S. (2006). Coadaptation: a unifying principle in evolutionary thermal biology. *Physiological and Biochemical Zoology*, *79*(2), 282-294.

Angilletta, M. J., Wilson, R. S., Navas, C. A., & James, R. S. (2003). Tradeoffs and the evolution of thermal reaction norms. *Trends in Ecology & Evolution*, *18*(5), 234-240.

Anthony, K. R., & Hoegh-Guldberg, O. (2003). Kinetics of photoacclimation in corals. *Oecologia*, *134*, 23-31.

Anthony, K. R., Hoogenboom, M. O., Maynard, J. A., Grottoli, A. G., & Middlebrook, R. (2009). Energetics approach to predicting mortality risk from environmental stress: a case study of coral bleaching. *Functional Ecology*, *23*(3), 539-550.

Anthony, K. R. N., Helmstedt, K. J., Bay, L. K., Fidelman, P., Hussey, K. E., Lundgren, P., Mead, D., McLeod, I. M., Mumby, P. J., Newlands, M., Schaffelke, B., Wilson, K. A., & Hardisty, P. E. (2020). Interventions to help coral reefs under global change-A complex decision challenge. *PloS One*, *15*(8), e0236399. https://doi.org/10.1371/journal.pone.0236399

Armstrong, E. J., Lê-Hoang, J., Carradec, Q., Aury, J.-M., Noel, B., Hume, B. C. C., Voolstra, C. R., Poulain, J., Belser, C., Paz-García, D. A., Cruaud, C., Labadie, K., Da Silva, C., Moulin, C., Boissin, E., Bourdin, G., Iwankow, G., Romac, S., Agostini, S., . . . Wincker, P. (2023). Host transcriptomic plasticity and photosymbiotic fidelity underpin *Pocillopora* acclimatization across thermal regimes in the Pacific Ocean. *Nature Communications*, *14*(1), 3056. https://doi.org/10.1038/s41467-023-38610-6

Armstrong, K. C., Lippert, M., Hanson, E., Nestor, V., Cornwell, B., Walker, N. S., Golbuu, Y., & Palumbi, S. R. (2024). Fine-Scale Geographic Variation of *Cladocopium* in *Acropora hyacinthus* Across the Palauan Archipelago. *Ecology and Evolution*, *14*(12), e70650.

Arrigoni, R., Berumen, M. L., Mariappan, K. G., Beck, P. S., Hulver, A. M., Montano, S., Pichon, M., Strona, G., Terraneo, T. I., & Benzoni, F. (2020). Towards a rigorous species delimitation framework for scleractinian corals based on RAD sequencing: the case study of *Leptastrea* from the Indo-Pacific. *Coral Reefs*, *39*, 1001-1025.

Baird, A., Marshall, P., & Wolstenholme, J. (2002). Latitudinal variation in the reproduction of *Acropora* in the Coral Sea. *Proc 9th Int Coral Reef Symp*, *1*, 385-389.

Baird, A. H., Bhagooli, R., Ralph, P. J., & Takahashi, S. (2009a). Coral bleaching: the role of the host. *Trends in Ecology & Evolution*, *24*(1), 16-20.

Baird, A. H., Guest, J. R., & Willis, B. L. (2009b). Systematic and biogeographical patterns in the reproductive biology of scleractinian corals. *Annual Review of Ecology, Evolution, and Systematics*, *40*(1), 551-571.

Bairos-Novak, K. A.-O., Hoogenboom, M. A.-O., van Oppen, M. A.-O., & Connolly, S. A.-O. (2021). Coral adaptation to climate change: Meta-analysis reveals high heritability across multiple traits. *Global Change Biology*, *27*(22), 5694-5710.

Baker, A. C., Baums, I. B., Davies, S. W., Grottoli, A. G., Kenkel, C. D., Kitchen, S. A., Kuffner, I. B., Matz, M. V., Miller, M. W., & Muller, E. M. (2025). Proactive assisted gene flow for Caribbean corals in an era of rapid coral reef decline. *Science*, *389*(6758), 344-347.

Baker, A. C., Glynn, P. W., & Riegl, B. (2008). Climate change and coral reef bleaching: An ecological assessment of long-term impacts, recovery trends and future outlook. *Estuarine, Coastal and Shelf Science*, *80*(4), 435-471.

Baker, A. C., Starger, C. J., McClanahan, T. R., & Glynn, P. W. (2004). Corals' adaptive response to climate change. *Nature*, *430*(7001), 741-741.

Barghi, N., Hermisson, J., & Schlötterer, C. (2020). Polygenic adaptation: a unifying framework to understand positive selection. *Nature Reviews Genetics*, *21*(12), 769-781.

Baria, M. V. B., Villanueva, R. D., & Guest, J. R. (2012). Spawning of three-year-old *Acropora millepora* corals reared from larvae in northwestern Philippines. *Bulletin of Marine Science*, *88*(1), 61-62.

Barneche, D. R., Coleman, G., Fermor, D., Klein, E., Robinson, T., Smith, J., Sheehan, J. L., Dowley, S., Ditton, D., & Gunn, K. (2021). dataaimsr: An R Client for the Australian Institute of Marine Science Data Platform API which provides easy access to AIMS Data Platform. *Journal of Open Source Software*, *6*(62), 3282.

Barnes, D. J. (1970). Coral skeletons: an explanation of their growth and structure. *Science*, *170*(3964), 1305-1308.

Barrett, R. D., & Schluter, D. (2008). Adaptation from standing genetic variation. *Trends in Ecology & Evolution*, *23*(1), 38-44.

Barshis, D. J., Ladner, J. T., Oliver, T. A., Seneca, F. O., Traylor-Knowles, N., & Palumbi, S. R. (2013). Genomic basis for coral resilience to climate change. *Proceedings of the National Academy of Sciences*, *110*(4), 1387-1392.

Bates, D., Mächler, M., Bolker, B., & Walker, S. (2014). Fitting linear mixed-effects models using lme4. *arXiv preprint arXiv:1406.5823*.

Baum, J. K., Claar, D. C., Tietjen, K. L., Magel, J. M., Maucieri, D. G., Cobb, K. M., & McDevitt-Irwin, J. M. (2023). Transformation of coral communities subjected to an unprecedented heatwave is modulated by local disturbance. *Science Advances*, *9*(14), eabq5615.

Baums, I. B., Baker, A., Davies, S. W., Grottoli, A., Kenkel, C. D., Kitchen, S. A., Kuffner, I. B., Matz, M. V., Miller, M. W., & Parkinson, J. E. (2024). Managing expectations for breeding "super corals". *OSFPreprints*. https://doi.org/https://doi.org/10.31219/osf.io/vu45p

Bay, L. K., Gilmour, J., Muir, B., & Hardisty, P. E. (2023a). Management approaches to conserve Australia's marine ecosystem under climate change. *Science*, *381*(6658), 631-636.

Bay, L. K., Ortiz, J. C., Humanes, A., Riginos, C., Baums, I. B., Aranda, M., Peixoto, R., Niehaus, A. C., Le Port, A., & van Oppen, M. (2023b). CORDAP R&D Technology Roadmap for Understanding the Natural Adaptation and Assisted Evolution of Corals to Climate Change. *CORDAP*, 44 pp.

Bay, R. A., & Guerrero, L. (2020). Can genomes predict coral bleaching? *Science*, *369*(6501), 249-250.

Bay, R. A., & Palumbi, S. R. (2014). Multilocus adaptation associated with heat resistance in reef-building corals. *Current Biology*, *24*(24), 2952-2956.

Bay, R. A., Rose, N. H., Logan, C. A., & Palumbi, S. R. (2017). Genomic models predict successful coral adaptation if future ocean warming rates are reduced. *Science Advances*, *3*(11), e1701413.

Bellagio, T., & Exposito-Alonso, M. (2025). Polygenic and monogenic adaptation drive evolutionary rescue at different magnitudes of environmental change. *BioRxiv*, 2025.2006. 2013.659553.

Beltran, V., Puill-Stephan, E., Howells, E., Flores-Moya, A., Doblin, M., Núñez-Lara, E., Escamilla, V., Lopez, T., & van Oppen, M. (2021). Physiological diversity among sympatric, conspecific endosymbionts of coral (*Cladocopium* C1^{acro}) from the Great Barrier Reef. *Coral Reefs*, 1-13.

Bennett, S., Duarte, C. M., Marbà, N., & Wernberg, T. (2019). Integrating within-species variation in thermal physiology into climate change ecology. *Philosophical Transactions of the Royal Society B*, *374*(1778), 20180550.

Berkelmans, R. (2009). Bleaching and mortality thresholds: how much is too much? *Coral bleaching*, 103-119.

Berkelmans, R., & van Oppen, M. J. (2006). The role of zooxanthellae in the thermal tolerance of corals: a 'nugget of hope'for coral reefs in an era of climate change. *Proceedings of the Royal Society B: Biological Sciences*, *273*(1599), 2305-2312.

Bhattacharya, D., Stephens, T. G., Chille, E. E., Benites, L. F., & Chan, C. X. (2024). Facultative lifestyle drives diversity of coral algal symbionts. *Trends in Ecology & Evolution*, *39*(3), 239-247.

Black, K. L., Bay, L. K., & Matz, M. V. (2025a). A Genetic Variant of Delta-9 Desaturase Is Associated With Latitudinal Adaptation in a Coral from the Great Barrier Reef. *Molecular Ecology*, *34*(3), e17634.

Black, K. L., Rippe, J. P., & Matz, M. V. (2025b). Environmental drivers of genetic adaptation in two corals from the Florida Keys. *BioRxiv*, 2025.2003. 2003.641296.

Bolger, A. M., Lohse, M., & Usadel, B. (2014). Trimmomatic: a flexible trimmer for Illumina sequence data. *Bioinformatics*, *30*(15), 2114-2120.

Bongaerts, P., Cooke, I. R., Ying, H., Wels, D., den Haan, S., Hernandez-Agreda, A., Brunner, C. A., Dove, S., Englebert, N., & Eyal, G. (2021). Morphological stasis masks ecologically divergent coral species on tropical reefs. *Current Biology*, *31*(11), 2286-2298. e2288.

Bonilla, K., Guest, J., & Baria-Rodriguez, M. (2023). Contrasting reproductive strategies between stress-tolerant and competitive coral taxa. *Coral Reefs*, *42*(3), 717-728.

Booker, T. R. (2023). Spatial autocorrelation of the environment influences the patterns and genetics of local adaptation. *BioRxiv*, 2023.2005. 2029.542754.

Booker, T. R., Yeaman, S., Whiting, J. R., & Whitlock, M. C. (2024). The WZA: A window-based method for characterizing genotype–environment associations. *Molecular Ecology Resources*, *24*(2), e13768.

Booker, T. R., Yeaman, S., & Whitlock, M. C. (2023). Using genome scans to identify genes used repeatedly for adaptation. *Evolution*, *77*(3), 801-811.

Borcard, D., & Legendre, P. (2002). All-scale spatial analysis of ecological data by means of principal coordinates of neighbour matrices. *Ecological modelling*, *153*(1-2), 51-68.

Boström-Einarsson, L., Babcock, R. C., Bayraktarov, E., Ceccarelli, D., Cook, N., Ferse, S. C., Hancock, B., Harrison, P., Hein, M., & Shaver, E. (2020). Coral restoration–A systematic review of current methods, successes, failures and future directions. *PloS One*, *15*(1), e0226631.

Bourne, D., Iida, Y., Uthicke, S., & Smith-Keune, C. (2008). Changes in coral-associated microbial communities during a bleaching event. *ISME J*, *2*(4), 350-363. https://doi.org/10.1038/ismej.2007.112

Bourne, D. G., Morrow, K. M., & Webster, N. S. (2016). Insights into the coral microbiome: underpinning the health and resilience of reef ecosystems. *Annual Review of Microbiology*, *70*, 317-340.

Bowden-Kerby, A. (2022). Coral-Focused Climate Change Adaptation and Restoration Based on Accelerating Natural Processes: Launching the "Reefs of Hope" Paradigm. *Oceans*, *4*(1), 13-26.

Boyd, J. A., Woodcroft, B. J., & Tyson, G. W. (2018). GraftM: a tool for scalable, phylogenetically informed classification of genes within metagenomes. *Nucleic Acids Research*, *46*(10), e59-e59.

Bozec, Y.-M., Adam, A., Nava, B. A., Cresswell, A. K., Haller-Bull, V., Iwanaga, T., Lachs, L., Matthews, S. A., McWhorter, J. K., & Anthony, K. R. (2025). A rapidly closing window for coral persistence under global warming. *BioRxiv*, 2025.2001. 2023.634487.

Breiman, L., Cutler, A., Liaw, A., Wiener, M., & Liaw, M. A. (2018). Package 'randomforest'. *University of California, Berkeley: Berkeley, CA, USA*, *81*, 1-29.

Brener-Raffalli, K., Clerissi, C., Vidal-Dupiol, J., Adjeroud, M., Bonhomme, F., Pratlong, M., Aurelle, D., Mitta, G., & Toulza, E. (2018). Thermal regime and host clade, rather than geography, drive *Symbiodinium* and bacterial assemblages in the scleractinian coral *Pocillopora damicornis* sensu lato. *Microbiome*, *6*(1), 1-13.

Bridge, T. C., Cowman, P. F., Quattrini, A. M., Bonito, V. E., Sinniger, F., Harii, S., Head, C. E., Hung, J. Y., Halafihi, T., & Rongo, T. (2024). *A tenuis* relationship: traditional taxonomy obscures systematics and biogeography of the 'Acropora tenuis'(Scleractinia: Acroporidae) species complex. *Zoological Journal of the Linnean Society*, *202*(1), zlad062.

Brieuc, M. S., Waters, C. D., Drinan, D. P., & Naish, K. A. (2018). A practical introduction to Random Forest for genetic association studies in ecology and evolution. *Molecular Ecology Resources*, *18*(4), 755-766.

Brown, K. T., Eyal, G., Dove, S. G., & Barott, K. L. (2022). Fine-scale heterogeneity reveals disproportionate thermal stress and coral mortality in thermally variable reef habitats during a marine heatwave. *Coral Reefs*, *42*(1), 1-12.

Browning, B. L., Zhou, Y., & Browning, S. R. (2018). A one-penny imputed genome from next-generation reference panels. *The American Journal of Human Genetics*, *103*(3), 338-348.

Buerger, P., Alvarez-Roa, C., Coppin, C., Pearce, S., Chakravarti, L., Oakeshott, J., Edwards, O., & van Oppen, M. (2020). Heat-evolved microalgal symbionts increase coral bleaching tolerance. *Science Advances*, *6*(20), eaba2498.

Burke, L., Reytar, K., Spalding, M., & Perry, A. (2011). *Reefs at risk revisited*. World Resources Institute.

Burkepile, D. E., Shantz, A. A., Adam, T. C., Munsterman, K. S., Speare, K. E., Ladd, M. C., Rice, M. M., Ezzat, L., McIlroy, S., & Wong, J. C. (2020). Nitrogen identity drives differential impacts of nutrients on coral bleaching and mortality. *Ecosystems*, *23*(4), 798-811.

Butler, C. C., Turnham, K. E., Lewis, A. M., Nitschke, M. R., Warner, M. E., Kemp, D. W., Hoegh-Guldberg, O., Fitt, W. K., van Oppen, M. J., & LaJeunesse, T. C. (2023). Formal recognition of host-generalist species of dinoflagellate (*Cladocopium*, Symbiodiniaceae) mutualistic with Indo-Pacific reef corals. *Journal of phycology*.

Cairns, S. D. (1999). Species richness of recent Scleractinia.

Camp, E. F., Suggett, D. J., Pogoreutz, C., Nitschke, M. R., Houlbreque, F., Hume, B. C., Gardner, S. G., Zampighi, M., Rodolfo-Metalpa, R., & Voolstra, C. R. (2020). Corals exhibit distinct patterns of microbial reorganisation to thrive in an extreme inshore environment. *Coral Reefs*, *39*(3), 701-716.

Cano-Gamez, E., & Trynka, G. (2020). From GWAS to function: using functional genomics to identify the mechanisms underlying complex diseases. *Frontiers in Genetics*, *11*, 424.

Cantin, N., James, N., & Stella, J. (2024). Aerial surveys of the 2024 mass coral bleaching event on the Great Barrier Reef. *Australian Institute of Marine Science, Townsville*, 2024-2004.

Capblancq, T., Fitzpatrick, M. C., Bay, R. A., Exposito-Alonso, M., & Keller, S. R. (2020). Genomic prediction of (mal) adaptation across current and future climatic landscapes. *Annual Review of Ecology, Evolution, and Systematics*, *51*(1), 245-269.

Capblancq, T., & Forester, B. R. (2021). Redundancy analysis: A Swiss Army Knife for landscape genomics. *Methods in Ecology and Evolution*, *12*(12), 2298-2309.

Capblancq, T., Luu, K., Blum, M. G., & Bazin, E. (2018). Evaluation of redundancy analysis to identify signatures of local adaptation. *Molecular Ecology Resources*, *18*(6), 1223-1233.

Carlson, B. A., Xu, X.-M., Kryukov, G. V., Rao, M., Berry, M. J., Gladyshev, V. N., & Hatfield, D. L. (2004). Identification and characterization of phosphoseryl-tRNA [Ser] Sec kinase. *Proceedings of the National Academy of Sciences*, *101*(35), 12848-12853.

Carlson, S. M., Cunningham, C. J., & Westley, P. A. (2014). Evolutionary rescue in a changing world. *Trends in Ecology & Evolution*, *29*(9), 521-530.

Carvalho Filho, I., Arikawa, L. M., Mota, L. F., Campos, G. S., Fonseca, L. F., Fernandes Júnior, G. A., Schenkel, F. S., Lourenco, D., Silva, D. A., & Teixeira, C. S. (2024). Genome-wide association study considering genotype-by-environment interaction for productive and reproductive traits using whole-genome sequencing in Nellore cattle. *BMC Genomics*, *25*(1), 623.

Caye, K., Jumentier, B., Lepeule, J., & François, O. (2019). LFMM 2: fast and accurate inference of gene-environment associations in genome-wide studies. *Molecular Biology and Evolution*, *36*(4), 852-860.

Chan, W. Y., Meyers, L., Rudd, D., Topa, S. H., & van Oppen, M. J. (2023). Heat-evolved algal symbionts enhance bleaching tolerance of adult corals without trade-off against growth. *Global Change Biology*, *29*(24), 6945-6968.

Chen, Y., Shah, S., Dougan, K. E., van Oppen, M. J., Bhattacharya, D., & Chan, C. X. (2022). Improved *Cladocopium goreaui* genome assembly reveals features of a facultative coral symbiont and the complex evolutionary history of dinoflagellate genes. *Microorganisms*, *10*(8), 1662.

Cheruiyot, E. K., Haile-Mariam, M., Cocks, B. G., MacLeod, I. M., Mrode, R., & Pryce, J. E. (2022). Functionally prioritised whole-genome sequence variants improve the accuracy of genomic prediction for heat tolerance. *Genetics Selection Evolution*, *54*(1), 17.

Claar, D. C., & Baum, J. K. (2019). Timing matters: survey timing during extended heat stress can influence perceptions of coral susceptibility to bleaching. *Coral Reefs*, *38*(4), 559-565.

Cleves, P. A., Shumaker, A., Lee, J., Putnam, H. M., & Bhattacharya, D. (2020a). Unknown to known: Advancing knowledge of coral gene function. *Trends in genetics*, *36*(2), 93-104.

Cleves, P. A., Strader, M. E., Bay, L. K., Pringle, J. R., & Matz, M. V. (2018). CRISPR/Cas9-mediated genome editing in a reef-building coral. *Proc Natl Acad Sci U S A*, *115*(20), 5235-5240. https://doi.org/10.1073/pnas.1722151115

Cleves, P. A., Tinoco, A. I., Bradford, J., Perrin, D., Bay, L. K., & Pringle, J. R. (2020b). Reduced thermal tolerance in a coral carrying CRISPR-induced mutations in the gene for a heat-shock transcription factor. *Proceedings of the National Academy of Sciences*, *117*(46), 28899-28905.

Clobert, J. (2012). *Dispersal ecology and evolution*. Oxford University Press.

Coles, S. L., Bahr, K. D., Ku'ulei, S. R., May, S. L., McGowan, A. E., Tsang, A., Bumgarner, J., & Han, J. H. (2018). Evidence of acclimatization or adaptation in Hawaiian corals to higher ocean temperatures. *PeerJ*, *6*, e5347.

Colton, M. A., McManus, L. C., Schindler, D. E., Mumby, P. J., Palumbi, S. R., Webster, M. M., Essington, T. E., Fox, H. E., Forrest, D. L., & Schill, S. R. (2022). Coral conservation in a warming world must harness evolutionary adaptation. *Nature Ecology & Evolution*, *6*(10), 1405-1407.

Compton, S., Stackpole, C., Dixit, A., Sekhwal, M. K., Kolb, T., & De la Torre, A. R. (2023). Differences in heat tolerance, water use efficiency and growth among Douglas-fir families and varieties evidenced by GWAS and common garden studies. *AoB Plants*, *15*(2), plad008.

Connell, J. H., Hughes, T. P., Wallace, C. C., Tanner, J. E., Harms, K. E., & Kerr, A. M. (2004). A long-term study of competition and diversity of corals. *Ecological Monographs*, *74*(2), 179-210.

Conte, G. L., Arnegard, M. E., Peichel, C. L., & Schluter, D. (2012). The probability of genetic parallelism and convergence in natural populations. *Proceedings of the Royal Society B: Biological Sciences*, *279*(1749), 5039-5047.

Cooke, I., Ying, H., Forêt, S., Bongaerts, P., Strugnell, J. M., Simakov, O., Zhang, J., Field, M. A., Rodriguez-Lanetty, M., & Bell, S. C. (2020). Genomic signatures in the coral holobiont reveal host adaptations driven by Holocene climate change and reef specific symbionts. *Science Advances*, *6*(48), eabc6318.

Cooper, T. F., Berkelmans, R., Ulstrup, K. E., Weeks, S., Radford, B., Jones, A. M., Doyle, J., Canto, M., O'Leary, R. A., & van Oppen, M. J. (2011). Environmental factors controlling the distribution of Symbiodinium harboured by the coral *Acropora millepora* on the Great Barrier Reef. *PloS One*, *6*(10), e25536.

Cornwall, C. E., Comeau, S., Donner, S. D., Perry, C., Dunne, J., van Hooidonk, R., Ryan, S., & Logan, C. A. (2023). Coral adaptive capacity insufficient to halt global transition of coral reefs into net erosion under climate change. *Global Change Biology*, *29*(11), 3010-3018.

Cornwell, B., Armstrong, K., Walker, N. S., Lippert, M., Nestor, V., Golbuu, Y., & Palumbi, S. R. (2021). Widespread variation in heat tolerance and symbiont load are associated with growth tradeoffs in the coral *Acropora hyacinthus* in Palau. *eLife*, *10*, e64790.

Cortés, A. J., López-Hernández, F., & Blair, M. W. (2022). Genome–environment associations, an innovative tool for studying heritable evolutionary adaptation in orphan crops and wild relatives. *Frontiers in Genetics*, *13*, 910386.

Craggs, J., Guest, J., Davis, M., & Sweet, M. (2020). Completing the life cycle of a broadcast spawning coral in a closed mesocosm. *Invertebrate Reproduction & Development*, *64*(3), 244-247.

Cravatte, S., Kestenare, E., Eldin, G., Ganachaud, A., Lefèvre, J., Marin, F., Menkes, C., & Aucan, J. (2015). Regional circulation around New Caledonia from two decades of observations. *Journal of Marine Systems*, *148*, 249-271.

Crispo, E. (2008). Modifying effects of phenotypic plasticity on interactions among natural selection, adaptation and gene flow. *Journal of Evolutionary Biology*, *21*(6), 1460-1469.

CSIRO. (2020a). *eReefs GBR 1 hydrodynamic model version 2. Data set accessed 2022-07-13 at https://extraction.ereefs.aims.gov.au/*.

CSIRO. (2020b). *eReefs GBR 4 hydrodynamic model version 2. Data set accessed 2022-04-22 at https://extraction.ereefs.aims.gov.au/*.

Cunning, R., Bay, R., Gillette, P., Baker, A., & Traylor-Knowles, N. (2018). Comparative analysis of the *Pocillopora damicornis* genome highlights role of immune system in coral evolution. *Scientific Reports*, *8*(1), 16134.

Cunning, R., Matsuda, S. B., Bartels, E., D'Alessandro, M., Detmer, A. R., Harnay, P., Levy, J., Lirman, D., Moeller, H. V., & Muller, E. M. (2024). On the use of rapid acute heat tolerance assays to resolve ecologically relevant differences among corals. *Coral Reefs*, *43*(6), 1793-1801.

Cunning, R., Parker, K. E., Johnson-Sapp, K., Karp, R. F., Wen, A. D., Williamson, O. M., Bartels, E., D'Alessandro, M., Gilliam, D. S., & Hanson, G. (2021). Census of heat tolerance among Florida's threatened staghorn corals finds resilient individuals throughout existing nursery populations. *Proceedings of the Royal Society B*, *288*(1961), 20211613.

Cunning, R., Ritson-Williams, R., & Gates, R. D. (2016). Patterns of bleaching and recovery of *Montipora capitata* in Kāne ʻohe Bay, Hawai ʻi, USA. *Marine Ecology Progress Series*, *551*, 131-139.

Cunning, R., Silverstein, R. N., & Baker, A. C. (2015). Investigating the causes and consequences of symbiont shuffling in a multi-partner reef coral symbiosis under environmental change. *Proceedings of the Royal Society B: Biological Sciences*, *282*(1809), 20141725.

Da-Anoy, J., Posadas, N., & Conaco, C. (2024). Interspecies differences in the transcriptome response of corals to acute heat stress. *PeerJ*, *12*, e18627.

Danecek, P., Auton, A., Abecasis, G., Albers, C. A., Banks, E., DePristo, M. A., Handsaker, R. E., Lunter, G., Marth, G. T., & Sherry, S. T. (2011). The variant call format and VCFtools. *Bioinformatics*, *27*(15), 2156-2158.

Danecek, P., Bonfield, J. K., Liddle, J., Marshall, J., Ohan, V., Pollard, M. O., Whitwham, A., Keane, T., McCarthy, S. A., & Davies, R. M. (2021). Twelve years of SAMtools and BCFtools. *GigaScience*, *10*(2), giab008.

Darling, E. S., Alvarez-Filip, L., Oliver, T. A., McClanahan, T. R., & Côté, I. M. (2012). Evaluating life-history strategies of reef corals from species traits. *Ecology letters*, *15*(12), 1378-1386.

Darling, E. S., Graham, N. A., Januchowski-Hartley, F. A., Nash, K. L., Pratchett, M. S., & Wilson, S. K. (2017). Relationships between structural complexity, coral traits, and reef fish assemblages. *Coral Reefs*, *36*, 561-575.

Dauphin, B., Rellstab, C., Wüest, R. O., Karger, D. N., Holderegger, R., Gugerli, F., & Manel, S. (2023). Re-thinking the environment in landscape genomics. *Trends in Ecology & Evolution*, *38*(3), 261-274.

Davey, J. W., Hohenlohe, P. A., Etter, P. D., Boone, J. Q., Catchen, J. M., & Blaxter, M. L. (2011). Genome-wide genetic marker discovery and genotyping using next-generation sequencing. *Nature Reviews Genetics*, *12*(7), 499-510.

Davies, R. W., Flint, J., Myers, S., & Mott, R. (2016). Rapid genotype imputation from sequence without reference panels. *Nature Genetics*, *48*(8), 965-969.

Davies, S., Gamache, M. H., Howe-Kerr, L. I., Kriefall, N. G., Baker, A. C., Banaszak, A. T., Bay, L. K., Bellantuono, A. J., Bhattacharya, D., & Chan, C. X. (2023). Building Consensus around the Assessment and Interpretation of Symbiodiniaceae Diversity. *PeerJ*, *11*, e15023.

Davies, S., Treml, E., Kenkel, C., & Matz, M. (2015). Exploring the role of Micronesian islands in the maintenance of coral genetic diversity in the Pacific Ocean. *Molecular Ecology*, *24*(1), 70-82.

Davies, S. W., Moreland, K. N., Wham, D. C., Kanke, M. R., & Matz, M. V. (2020). *Cladocopium* community divergence in two *Acropora* coral hosts across multiple spatial scales. *Molecular Ecology*, *29*(23), 4559-4572.

Davy, S. K., Allemand, D., & Weis, V. M. (2012). Cell biology of cnidarian-dinoflagellate symbiosis. *Microbiology and Molecular Biology Reviews*, *76*(2), 229-261.

De Groot, R., Brander, L., van Der Ploeg, S., Costanza, R., Bernard, F., Braat, L., Christie, M., Crossman, N., Ghermandi, A., & Hein, L. (2012). Global estimates of the value of ecosystems and their services in monetary units. *Ecosystem services*, *1*(1), 50-61.

de Souza, M. R., Caruso, C., Ruiz-Jones, L., Drury, C., Gates, R. D., & Toonen, R. J. (2023). Importance of depth and temperature variability as drivers of coral symbiont composition despite a mass bleaching event. *Scientific Reports*, *13*(1), 8957.

De'ath, G., Fabricius, K. E., Sweatman, H., & Puotinen, M. (2012). The 27–year decline of coral cover on the Great Barrier Reef and its causes. *Proceedings of the National Academy of Sciences*, *109*(44), 17995-17999.

Deans, P. M., Seah, C., Johnson, J., Gonzalez, J. G., Townsley, K., Cao, E., Schrode, N., Stahl, E., O'Reilly, P., & Huckins, L. M. (2023). Non-additive effects of schizophrenia risk genes reflect convergent downstream function. *medRxiv*.

DeCarlo, T. M., Harrison, H. B., Gajdzik, L., Alaguarda, D., Rodolfo-Metalpa, R., D'Olivo, J., Liu, G., Patalwala, D., & McCulloch, M. T. (2019). Acclimatization of massive reef-building corals to consecutive heatwaves. *Proceedings of the Royal Society B*, *286*(1898), 20190235.

dela Cruz, D. W., & Harrison, P. L. (2017). Enhanced larval supply and recruitment can replenish reef corals on degraded reefs. *Scientific Reports*, *7*(1), 1-13.

Denis, H., Bay, L. K., Mocellin, V. J., Naugle, M. S., Lecellier, G., Purcell, S. W., Berteaux-Lecellier, V., & Howells, E. J. (2024a). Thermal tolerance traits of individual corals are widely distributed across the Great Barrier Reef. *Proceedings B*, *291*(2030), 20240587.

Denis, H., Prata, K. E., Ishida, H., Popovic, I., Mocellin, V. J. L., Boussion, M., Byrne, I., Purcell, S. W., Bay, L. K., Lecellier, G., Chan, C. X., Riginos, C., Howells, E. J., & Berteaux-Lecellier, V. (2025). Long-distance gene flow and contrasting population structures of reef-building corals and their algal symbionts inform adaptive potential across the Western Pacific. *BioRxiv*. https://doi.org/https://doi.org/10.1101/2025.10.14.682263

Denis, H., Selmoni, O., Gossuin, H., Jauffrais, T., Butler, C. C., Lecellier, G., & Berteaux-Lecellier, V. (2024b). Climate adaptive loci revealed by seascape genomics correlate with phenotypic variation in heat tolerance of the coral *Acropora millepora*. *Scientific Reports*, *14*(1), 22179.

DeSalvo, M. K., Sunagawa, S., Voolstra, C. R., & Medina, M. (2010). Transcriptomic responses to heat stress and bleaching in the elkhorn coral *Acropora palmata*. *Marine Ecology Progress Series*, *402*, 97-113.

Devlin-Durante, M. K., & Baums, I. B. (2017). Genome-wide survey of single-nucleotide polymorphisms reveals fine-scale population structure and signs of selection in the threatened Caribbean elkhorn coral, *Acropora palmata*. *PeerJ*, *5*, e4077.

Diamond, S. E. (2017). Evolutionary potential of upper thermal tolerance: biogeographic patterns and expectations under climate change. *Annals of the New York Academy of Sciences*, *1389*(1), 5-19.

Dixon, A. M., Forster, P. M., Heron, S. F., Stoner, A. M. K., & Beger, M. (2022). Future loss of local-scale thermal refugia in coral reef ecosystems. *PLOS Climate*, *1*(2), e0000004. https://doi.org/10.1371/journal.pclm.0000004

Dixon, G., Abbott, E., & Matz, M. (2020). Meta-analysis of the coral environmental stress response: *Acropora* corals show opposing responses depending on stress intensity. *Molecular Ecology*, *29*(15), 2855-2870.

Dixon, G. B., Davies, S. W., Aglyamova, G. V., Meyer, E., Bay, L. K., & Matz, M. V. (2015). Genomic determinants of coral heat tolerance across latitudes. *Science*, *348*(6242), 1460-1462.

Donner, S. D., Skirving, W. J., Little, C. M., Oppenheimer, M., & Hoegh-Guldberg, O. (2005). Global assessment of coral bleaching and required rates of adaptation under climate change. *Global Change Biology*, *11*(12), 2251-2265.

Dougan, K. E., Bellantuono, A. J., Kahlke, T., Abbriano, R. M., Chen, Y., Shah, S., Granados-Cifuentes, C., van Oppen, M. J., Bhattacharya, D., & Suggett, D. J. (2024). Whole-genome duplication in an algal symbiont bolsters coral heat tolerance. *Science Advances*, *10*(29), eadn2218.

Downie, A. T., Cramp, R. L., & Franklin, C. E. (2023). The interactive impacts of a constant reef stressor, ultraviolet radiation, with environmental stressors on coral physiology. *Science of The Total Environment*, 168066.

Dray, S., Blanchet, G., Borcard, D., Guenard, G., Jombart, T., Larocque, G., Legendre, P., Madi, N., Wagner, H. H., & Dray, M. S. (2018). Package 'adespatial'. *R package*, *2018*, 3-8.

Drury, C., Bean, N. K., Harris, C. I., Hancock, J. R., Huckeba, J., Roach, T. N., Quinn, R. A., & Gates, R. D. (2022a). Intrapopulation adaptive variance supports thermal tolerance in a reef-building coral. *Communications biology*, *5*(1), 1-10.

Drury, C., & Lirman, D. (2021). Genotype by environment interactions in coral bleaching. *Proceedings of the Royal Society B*, *288*(1946), 20210177.

Drury, C., Martin, R. E., Knapp, D. E., Heckler, J., Levy, J., Gates, R. D., & Asner, G. P. (2022b). Ecosystem-scale mapping of coral species and thermal tolerance. *Frontiers in Ecology and the Environment*, *20*(5), 285-291.

Eddy, T. D., Lam, V. W., Reygondeau, G., Cisneros-Montemayor, A. M., Greer, K., Palomares, M. L. D., Bruno, J. F., Ota, Y., & Cheung, W. W. (2021). Global decline in capacity of coral reefs to provide ecosystem services. *One Earth*, *4*(9), 1278-1285.

Edmunds, P. J., & Riegl, B. (2020). Urgent need for coral demography in a world where corals are disappearing. *Marine Ecology Progress Series*, *635*, 233-242.

Elder, H., Weis, V., Montalvo-Proano, J., Mocellin, V. J., Baird, A. H., Meyer, E., & Bay, L. K. (2022). Genetic variation in heat tolerance of the coral *Platygyra daedalea* indicates potential for adaptation to ocean warming. *BioRxiv*, 2020.2010. 2013.337089.

Emslie, M. (2025). *Substantial impacts from 2024 mass coral bleaching and cyclones reduce regional coral cover to near long-term averages* (Great Barrier Reef Annual Summary Report, Issue.

Emslie, M. J., Ceccarelli, D. M., Logan, M., Blandford, M. I., Bray, P., Campili, A., Jonker, M. J., Parker, J. G., Prenzlau, T., & Sinclair-Taylor, T. H. (2024). Changing dynamics of Great Barrier Reef hard coral cover in the Anthropocene. *Coral Reefs*, *43*(3), 747-762.

Endelman, J. B. (2011). Ridge regression and other kernels for genomic selection with R package rrBLUP. *The plant genome*, *4*(3).

Epstein, H. E., Smith, H. A., Cantin, N. E., Mocellin, V. J., Torda, G., & van Oppen, M. J. (2019). Temporal Variation in the Microbiome of *Acropora* Coral Species Does Not Reflect Seasonality. *Frontiers in Microbiology*, *10*, 1775.

Evensen, N. R., Fine, M., Perna, G., Voolstra, C. R., & Barshis, D. J. (2021). Remarkably high and consistent tolerance of a Red Sea coral to acute and chronic thermal stress exposures. *Limnology and Oceanography*, *66*(5), 1718-1729.

Evensen, N. R., Parker, K. E., Oliver, T. A., Palumbi, S. R., Logan, C. A., Ryan, J. S., Klepac, C. N., Perna, G., Warner, M. E., & Voolstra, C. R. (2023). The Coral Bleaching Automated Stress System (CBASS): A low-cost, portable system for standardized empirical assessments of coral thermal limits. *Limnology and Oceanography: Methods*.

Evensen, N. R., Voolstra, C. R., Fine, M., Perna, G., Buitrago-López, C., Cárdenas, A., Banc-Prandi, G., Rowe, K., & Barshis, D. J. (2022). Empirically derived thermal thresholds of four coral species along the Red Sea using a portable and standardized experimental approach. *Coral Reefs*, *41*(2), 239-252.

Ewels, P., Magnusson, M., Lundin, S., & Käller, M. (2016). MultiQC: summarize analysis results for multiple tools and samples in a single report. *Bioinformatics*, *32*(19), 3047-3048.

Exposito-Alonso, M., Burbano, H. A., Bossdorf, O., Nielsen, R., & Weigel, D. (2019). Natural selection on the *Arabidopsis thaliana* genome in present and future climates. *Nature*, *573*(7772), 126-129.

Fabricius, K. E. (2006). Effects of irradiance, flow, and colony pigmentation on the temperature microenvironment around corals: Implications for coral bleaching? *Limnology and Oceanography*, *51*(1), 30-37.

Fang, B., Kemppainen, P., Momigliano, P., Feng, X., & Merilä, J. (2020). On the causes of geographically heterogeneous parallel evolution in sticklebacks. *Nature Ecology & Evolution*, *4*(8), 1105-1115.

Ferrara, E. F., Bauer, L., Puntin, G., Bautz, F., Celayir, S., Do, M.-S., Eck, F., Heider, M., Wissel, P., & Arnold, A. (2024). RGB color indices as proxy for symbiont cell density and chlorophyll content during coral bleaching. *BioRxiv*, 2024.2012. 2020.629333.

Ferrier-Pagès, C., Peirano, A., Abbate, M., Cocito, S., Negri, A., Rottier, C., Riera, P., Rodolfo-Metalpa, R., & Reynaud, S. (2011). Summer autotrophy and winter heterotrophy in the temperate symbiotic coral *Cladocora caespitosa*. *Limnology and Oceanography*, *56*(4), 1429-1438.

Ferris, K. G., Chavez, A. S., Suzuki, T. A., Beckman, E. J., Phifer-Rixey, M., Bi, K., & Nachman, M. W. (2021). The genomics of rapid climatic adaptation and parallel evolution in North American house mice. *PLoS Genetics*, *17*(4), e1009495.

Fifer, J. E., Speare, K., Leinbach, S., Hendricks, S., Davies, S. W., Rose, N., Burkepile, D., Adam, T., Hofmann, G., & Strader, M. (2024). Genomic signatures of coral adaptation and recovery following a mass mortality event. *BioRxiv*, 2024.2009.2023.614560. https://doi.org/10.1101/2024.09.23.614560

Fisher, R., O'Leary, R. A., Low-Choy, S., Mengersen, K., Knowlton, N., Brainard, R. E., & Caley, M. J. (2015). Species richness on coral reefs and the pursuit of convergent global estimates. *Current Biology*, *25*(4), 500-505.

Fisher, R. A. (1930). *The genetical theory of natural selection* [doi:10.5962/bhl.title.27468]. Clarendon Press. https://doi.org/10.5962/bhl.title.27468

Fitzpatrick, M. C., & Keller, S. R. (2015). Ecological genomics meets community-level modelling of biodiversity: Mapping the genomic landscape of current and future environmental adaptation. *Ecology letters*, *18*(1), 1-16.

Fitzpatrick, S. W., Bradburd, G. S., Kremer, C. T., Salerno, P. E., Angeloni, L. M., & Funk, W. C. (2020). Genomic and fitness consequences of genetic rescue in wild populations. *Current Biology*, *30*(3), 517-522. e515.

Flanagan, S. P., Forester, B. R., Latch, E. K., Aitken, S. N., & Hoban, S. (2018). Guidelines for planning genomic assessment and monitoring of locally adaptive variation to inform species conservation. *Evolutionary Applications*, *11*(7), 1035-1052.

Forester, B. R., Jones, M. R., Joost, S., Landguth, E. L., & Lasky, J. R. (2016). Detecting spatial genetic signatures of local adaptation in heterogeneous landscapes. *Molecular Ecology*, *25*(1), 104-120.

Forester, B. R., Lasky, J. R., Wagner, H. H., & Urban, D. L. (2018). Comparing methods for detecting multilocus adaptation with multivariate genotype–environment associations. *Molecular Ecology*, *27*(9), 2215-2233.

Forrest, D. L., McManus, L. C., Tekwa, E. W., Schindler, D. E., Colton, M. A., Webster, M. M., Fox, H. E., Essington, T. E., Palumbi, S. R., & Mumby, P. J. (2024). Marine spatial planning to enhance coral adaptive potential. *BioRxiv*, 2024.2008. 2027.609972.

Forster, P. M., Smith, C., Walsh, T., Lamb, W. F., Lamboll, R., Cassou, C., Hauser, M., Hausfather, Z., Lee, J. Y., Palmer, M. D., von Schuckmann, K., Slangen, A. B. A., Szopa, S., Trewin, B., Yun, J., Gillett, N. P., Jenkins, S., Matthews, H. D., Raghavan, K., . . . Zhai, P. (2025). Indicators of Global Climate Change 2024: annual update of key indicators of the state of the climate system

and human influence. *Earth Syst. Sci. Data*, *17*(6), 2641-2680. https://doi.org/10.5194/essd-17-2641-2025

François, O., Martins, H., Caye, K., & Schoville, S. D. (2016). Controlling false discoveries in genome scans for selection. *Molecular Ecology*, *25*(2), 454-469.

Frichot, E., Mathieu, F., Trouillon, T., Bouchard, G., & François, O. (2014). Fast and efficient estimation of individual ancestry coefficients. *Genetics*, *196*(4), 973-983.

Friedman, J., Hastie, T., Tibshirani, R., Narasimhan, B., Tay, K., Simon, N., & Qian, J. (2021). Package 'glmnet'. *CRAN R Repositary*.

Frölicher, T. L., Fischer, E. M., & Gruber, N. (2018). Marine heatwaves under global warming. *Nature*, *560*(7718), 360-364.

Frommlet, J. C., & Iglesias-Rodríguez, M. D. (2008). MICROSATELLITE GENOTYPING OF SINGLE CELLS OF THE DINOFLAGELLATE SPECIES LINGULODINIUM POLYEDRUM (DINOPHYCEAE): A NOVEL APPROACH FOR MARINE MICROBIAL POPULATION GENETIC STUDIES 1. *Journal of phycology*, *44*(5), 1116-1125.

Fuentes-Pardo, A. P., & Ruzzante, D. E. (2017). Whole-genome sequencing approaches for conservation biology: Advantages, limitations and practical recommendations. *Molecular Ecology*, *26*(20), 5369-5406.

Fuller, Z. L., Mocellin, V. J., Morris, L. A., Cantin, N., Shepherd, J., Sarre, L., Peng, J., Liao, Y., Pickrell, J., & Andolfatto, P. (2020). Population genetics of the coral *Acropora millepora*: Toward genomic prediction of bleaching. *Science*, *369*(6501).

Gaines, S. D., White, C., Carr, M. H., & Palumbi, S. R. (2010). Designing marine reserve networks for both conservation and fisheries management. *Proceedings of the National Academy of Sciences*, *107*(43), 18286-18293. https://www.ncbi.nlm.nih.gov/pmc/articles/PMC2972919/pdf/pnas.200906473.pdf

Galili, T., Simpson, G., Jefferis, G., Gallotta, M., & Renaudie, J. (2015). Package 'dendextend'.

Gallagher, M. D., & Chen-Plotkin, A. S. (2018). The post-GWAS era: from association to function. *The American Journal of Human Genetics*, *102*(5), 717-730.

Gardner, S. G., Raina, J.-B., Nitschke, M. R., Nielsen, D. A., Stat, M., Motti, C. A., Ralph, P. J., & Petrou, K. (2017). A multi-trait systems approach reveals a response cascade to bleaching in corals. *BMC Biology*, *15*(1), 1-14.

Gienapp, P., Calus, M. P., Laine, V. N., & Visser, M. E. (2019). Genomic selection on breeding time in a wild bird population. *Evolution Letters*, *3*(2), 142-151.

Gleason, D. F., & Hofmann, D. K. (2011). Coral larvae: from gametes to recruits. *Journal of Experimental Marine Biology and Ecology*, *408*(1-2), 42-57.

Glynn, P. W. (1996). Coral reef bleaching: facts, hypotheses and implications. *Global Change Biology*, *2*(6), 495-509.

Gompert, Z., Feder, J. L., Parchman, T. L., Planidin, N. P., Whiting, F. J., & Nosil, P. (2025). Adaptation repeatedly uses complex structural genomic variation. *Science*, *388*(6744), eadp3745.

Gomulkiewicz, R., & Holt, R. D. (1995). When does evolution by natural selection prevent extinction? *Evolution*, 201-207.

González-Pech, R. A., Stephens, T. G., Chen, Y., Mohamed, A. R., Cheng, Y., Shah, S., Dougan, K. E., Fortuin, M. D., Lagorce, R., & Burt, D. W. (2021). Comparison of 15 dinoflagellate genomes reveals extensive sequence and structural divergence in family Symbiodiniaceae and genus *Symbiodinium*. *BMC Biology*, *19*, 1-22.

Gonzalez-Espinosa, P. C., & Donner, S. D. (2021). Cloudiness reduces the bleaching response of coral reefs exposed to heat stress. *Global Change Biology*, *27*(15), 3474-3486.

Gorospe, K. D., & Karl, S. A. (2013). Genetic relatedness does not retain spatial pattern across multiple spatial scales: Dispersal and colonization in the coral, *P ocillopora damicornis*. *Molecular Ecology*, *22*(14), 3721-3736.

Gouezo, M., Golbuu, Y., Fabricius, K., Olsudong, D., Mereb, G., Nestor, V., Wolanski, E., Harrison, P., & Doropoulos, C. (2019). Drivers of recovery and reassembly of coral reef communities. *Proceedings of the Royal Society B*, *286*(1897), 20182908.

Graham, E., Baird, A., Connolly, S., Sewell, M., & Willis, B. (2013). Rapid declines in metabolism explain extended coral larval longevity. *Coral Reefs*, *32*, 539-549.

Graham, N. A., Robinson, J. P., Smith, S. E., Govinden, R., Gendron, G., & Wilson, S. K. (2020). Changing role of coral reef marine reserves in a warming climate. *Nature Communications*, *11*(1), 1-8.

Grottoli, A. G., Hulver, A. M., Thurber, R. V., Toonen, R. J., Schmeltzer, E. R., Kuffner, I. B., Barott, K. L., Baums, I. B., Castillo, K. D., & Chapron, L. (2025). Future of coral bleaching research. *Bioscience*, biaf066.

Grottoli, A. G., Rodrigues, L. J., & Palardy, J. E. (2006). Heterotrophic plasticity and resilience in bleached corals. *Nature*, *440*(7088), 1186-1189.

Grottoli, A. G., Toonen, R. J., van Woesik, R., Vega Thurber, R., Warner, M. E., McLachlan, R. H., Price, J. T., Bahr, K. D., Baums, I. B., & Castillo, K. (2021). Increasing comparability among coral bleaching experiments. *Ecological applications*, e2262.

Grumbach, S., & Hamant, O. (2020). How humans may co-exist with Earth? The case for suboptimal systems. *Anthropocene*, *30*, 100245.

Grupstra, C. G., Gómez-Corrales, M., Fifer, J. E., Aichelman, H. E., Meyer-Kaiser, K. S., Prada, C., & Davies, S. W. (2024). Integrating cryptic diversity into coral evolution, symbiosis and conservation. *Nature Ecology & Evolution*, *8*(4), 622-636.

Guest, J. R., Baird, A. H., Maynard, J. A., Muttaqin, E., Edwards, A. J., Campbell, S. J., Yewdall, K., Affendi, Y. A., & Chou, L. M. (2012). Contrasting patterns of coral bleaching susceptibility in 2010 suggest an adaptive response to thermal stress. *PloS One*, *7*(3), e33353.

Guillaume, A. S., Ferrari, R., Selmoni, O., Mocellin, V. J., Denis, H., Naugle, M., Howells, E., Bay, L. K., & Joost, S. (2025a). Harnessing Multiscale Topographic Environmental Variables for Regional Coral Species Distribution Models. *Ecology and Evolution*, *15*(4), e71292.

Guillaume, A. S., Joost, S., Curpen, S., Neelayya, D. D., Harree-Somah, L., Sadasing, O., Saponari, L., Dale, C., Barret, L., & Andrews, N. (2025b). Coral genetic structure in the Western Indian Ocean mirrors ocean circulation and thermal stress. *BioRxiv*, 2025.2006. 2016.659828.

Gutenkunst, R. N., Hernandez, R. D., Williamson, S. H., & Bustamante, C. D. (2009). Inferring the joint demographic history of multiple populations from multidimensional SNP frequency data. *PLoS Genetics*, *5*(10), e1000695.

Hackerott, S., Martell, H. A., & Eirin-Lopez, J. M. (2021). Coral environmental memory: causes, mechanisms, and consequences for future reefs. *Trends in Ecology & Evolution*, *36*(11), 1011-1023.

Hackerott, S., Virdis, F., Wong, J. M., Flood, P. J., Travers, C., & Eirin-Lopez, J. M. (2025). The influence of environmental history on the performance of *Acropora cervicornis* corals across a spatiotemporal gradient. *Science of The Total Environment*, *977*, 179385.

Hagedorn, M., Page, C. A., O'Neil, K. L., Flores, D. M., Tichy, L., Conn, T., Chamberland, V. F., Lager, C., Zuchowicz, N., & Lohr, K. (2021). Assisted gene flow using cryopreserved sperm in critically endangered coral. *Proceedings of the National Academy of Sciences*, *118*(38).

Hall, A. E. (1992). Breeding for heat tolerance. *Plant Breed. Rev*, *10*(2), 129-168.

Halpern, B. S., Walbridge, S., Selkoe, K. A., Kappel, C. V., Micheli, F., D'Agrosa, C., Bruno, J. F., Casey, K. S., Ebert, C., & Fox, H. E. (2008). A global map of human impact on marine ecosystems. *Science*, *319*(5865), 948-952. https://science.sciencemag.org/content/sci/319/5865/948.full.pdf

Halpin-McCormick, A., Campbell, Q., Negrão, S., Morrell, P. L., Hubner, S., Neyhart, J., & Kantar, M. (2024). Back to the Future: Environmental genomic selection to take advantage of polygenic local adaptation. *BioRxiv*, 2024.2010. 2009.617488.

Hamilton, J. A., Okada, M., Korves, T., & Schmitt, J. (2016). The role of climate adaptation in colonization success in *Arabidopsis thaliana*. *Invasion Genetics: The Baker and Stebbins Legacy*, 300-312.

Hancock, A. M., Brachi, B., Faure, N., Horton, M. W., Jarymowycz, L. B., Sperone, F. G., Toomajian, C., Roux, F., & Bergelson, J. (2011). Adaptation to climate across the *Arabidopsis thaliana* genome. *Science*, *334*(6052), 83-86.

Hancock, J., Haghighi, K., Krebs, S., Flore, J., & Draper, A. (1992). Photosynthetic heat stability in highbush blueberries and the possibility of genetic improvement. *HortScience*, *27*(10), 1111-1112.

Hardy, O. J., & Vekemans, X. (1999). Isolation by distance in a continuous population: reconciliation between spatial autocorrelation analysis and population genetics models. *Heredity*, *83*(2), 145-154.

Hardy, O. J., & Vekemans, X. (2002). SPAGeDi: a versatile computer program to analyse spatial genetic structure at the individual or population levels. *Molecular Ecology Notes*, *2*(4), 618-620.

Harper, L. M., Huebner, L. K., Cain, E. D., Ruzicka, R., Gleason, D. F., & Fogarty, N. D. (2023). Multi-year coral recruitment study across the Florida Reef Tract reveals boom-or-bust pattern among broadcast spawners and consistency among brooders. *Marine Ecology Progress Series*, *721*, 39-58.

Harris, L., McDonagh, E. M., Zhang, X., Fawcett, K., Foreman, A., Daneck, P., Sergouniotis, P. I., Parkinson, H., Mazzarotto, F., & Inouye, M. (2024). Genome-wide association testing beyond SNPs. *Nature Reviews Genetics*, 1-15.

Harrison, P. L., Babcock, R. C., Bull, G. D., Oliver, J. K., Wallace, C. C., & Willis, B. L. (1984). Mass spawning in tropical reef corals. *Science*, *223*(4641), 1186-1189.

Harrison, P. L., & Booth, D. J. (2007). Coral reefs: naturally dynamic and increasingly disturbed ecosystems. *Marine ecology*, 316-377.

Helgoe, J., Davy, S. K., Weis, V. M., & Rodriguez-Lanetty, M. (2024). Triggers, cascades, and endpoints: connecting the dots of coral bleaching mechanisms. *Biological Reviews*, *99*(3), 715-752.

Hemstrom, W., Grummer, J. A., Luikart, G., & Christie, M. R. (2024). Next-generation data filtering in the genomics era. *Nature Reviews Genetics*, 1-18.

Hernández-Agreda, A., Huckeba, J., Prata, K. E., Vermeij, M. J., & Bongaerts, P. (2024). Hybridization and inbreeding affect the survival of a critically endangered coral. *Current Biology*, *34*(21), 5120-5129. e5124.

Hijmans, R. J., Williams, E., Vennes, C., & Hijmans, M. R. J. (2017). Package 'geosphere'. *Spherical trigonometry*, *1*(7), 1-45.

Hirschhorn, J. N., & Daly, M. J. (2005). Genome-wide association studies for common diseases and complex traits. *Nature Reviews Genetics*, *6*(2), 95-108.

Hoadley, K. D., Pettay, D. T., Lewis, A., Wham, D., Grasso, C., Smith, R., Kemp, D. W., LaJeunesse, T., & Warner, M. E. (2021). Different functional traits among closely related algal symbionts dictate stress endurance for vital Indo-Pacific reef-building corals. *Global Change Biology*, *27*(20), 5295-5309.

Hoban, S., Kelley, J. L., Lotterhos, K. E., Antolin, M. F., Bradburd, G., Lowry, D. B., Poss, M. L., Reed, L. K., Storfer, A., & Whitlock, M. C. (2016). Finding the genomic basis of local adaptation: pitfalls, practical solutions, and future directions. *The American Naturalist*, *188*(4), 379-397.

Hock, K., Wolff, N. H., Ortiz, J. C., Condie, S. A., Anthony, K. R., Blackwell, P. G., & Mumby, P. J. (2017). Connectivity and systemic resilience of the Great Barrier Reef. *PLoS Biology*, *15*(11), e2003355.

Hoegh-Guldberg, O. (1999). Climate change, coral bleaching and the future of the world's coral reefs. *Marine and Freshwater Research*, *50*(8), 839-866.

Hoegh-Guldberg, O., Mumby, P. J., Hooten, A. J., Steneck, R. S., Greenfield, P., Gomez, E., Harvell, C. D., Sale, P. F., Edwards, A. J., & Caldeira, K. (2007). Coral reefs under rapid climate change and ocean acidification. *Science*, *318*(5857), 1737-1742.

Hoffmann, A. A., & Sgrò, C. M. (2011). Climate change and evolutionary adaptation. *Nature*, *470*(7335), 479-485.

Hohenlohe, P. A., Funk, W. C., & Rajora, O. P. (2021). Population genomics for wildlife conservation and management. *Molecular Ecology*, *30*(1), 62-82.

Hohenlohe, P. A., & Magalhaes, I. S. (2019). The population genomics of parallel adaptation: lessons from threespine stickleback. In *Population genomics: Marine organisms* (pp. 249-276). Springer.

Holbrook, S. J., Adam, T. C., Edmunds, P. J., Schmitt, R. J., Carpenter, R. C., Brooks, A. J., Lenihan, H. S., & Briggs, C. J. (2018). Recruitment drives spatial variation in recovery rates of resilient coral reefs. *Scientific Reports*, *8*(1), 7338.

Holst, F., Bolger, A., Günther, C., Maß, J., Triesch, S., Kindel, F., Kiel, N., Saadat, N., Ebenhöh, O., & Usadel, B. (2023). Helixer–de novo prediction of primary eukaryotic gene models combining deep learning and a hidden Markov model. *BioRxiv*, 2023.2002. 2006.527280.

Holstein, D. M., Smith, T. B., van Hooidonk, R., & Paris, C. B. (2022). Predicting coral metapopulation decline in a changing thermal environment. *Coral Reefs*, *41*(4), 961-972.

Hothorn, T., Hornik, K., Strobl, C., Zeileis, A., & Hothorn, M. T. (2015). Package 'party'. *Package Reference Manual for Party Version 0.9-998*, *16*, 37.

Houlbrèque, F., & Ferrier-Pagès, C. (2009). Heterotrophy in tropical scleractinian corals. *Biological Reviews*, *84*(1), 1-17.

Howe-Kerr, L., & Quigley, K. (2025). Integrating an Eco-Evolutionary Perspective for Coral Reef Resistance Into Global Conservation Planning and Policy. *Conservation Letters*, *18*(3), e13108.

Howells, E., Beltran, V., Larsen, N., Bay, L., Willis, B., & van Oppen, M. (2012). Coral thermal tolerance shaped by local adaptation of photosymbionts. *Nature Climate Change*, *2*(2), 116-120.

Howells, E. J., Abrego, D., Liew, Y. J., Burt, J. A., Meyer, E., & Aranda, M. (2021). Enhancing the heat tolerance of reef-building corals to future warming. *Science Advances*, *7*(34), eabg6070.

Howells, E. J., Abrego, D., Meyer, E., Kirk, N. L., & Burt, J. A. (2016). Host adaptation and unexpected symbiont partners enable reef-building corals to tolerate extreme temperatures. *Global Change Biology*, *22*(8), 2702-2714.

Howells, E. J., Abrego, D., Schmidt-Roach, S., Puill-Stephan, E., Denis, H., Harii, S., Bay, L. K., Burt, J. A., Monro, K., & Aranda, M. (2025). Marine heatwaves select for thermal tolerance in a reef-building coral. *Nature Climate Change*. https://doi.org/10.1038/s41558-025-02381-3

Howells, E. J., Bay, L. K., & Bay, R. A. (2022a). Identifying, Monitoring, and Managing Adaptive Genetic Variation in Reef-Building Corals under Rapid Climate Warming. In M. J. H. van Oppen & M. Aranda Lastra (Eds.), *Coral Reef Conservation and Restoration in the Omics Age* (pp. 55-70). Springer International Publishing. https://doi.org/10.1007/978-3-031-07055-6_4

Howells, E. J., Bay, L. K., & Bay, R. A. (2022b). Identifying, Monitoring, and Managing Adaptive Genetic Variation in Reef-Building Corals under Rapid Climate Warming. *Coral Reef Conservation and Restoration in the Omics Age*, 55-70.

Howells, E. J., Berkelmans, R., van Oppen, M. J., Willis, B. L., & Bay, L. K. (2013). Historical thermal regimes define limits to coral acclimatization. *Ecology*, *94*(5), 1078-1088.

Hu, C., Jiang, J., Li, Y., Song, S., Zou, Y., Jing, C., Zhang, Y., Wang, D., He, Q., & Dang, X. (2022). QTL mapping and identification of candidate genes using a genome-wide association study for heat tolerance at anthesis in rice (*Oryza sativa* L.). *Frontiers in Genetics*, *13*, 983525.

Huang, W., Campbell, T., Carbone, M. A., Jones, W. E., Unselt, D., Anholt, R. R., & Mackay, T. F. (2020). Context-dependent genetic architecture of Drosophila life span. *PLoS Biology*, *18*(3), e3000645.

Huete, A. R., Liu, H., & van Leeuwen, W. J. (1997). The use of vegetation indices in forested regions: issues of linearity and saturation. IGARSS'97. 1997 IEEE international geoscience and remote sensing symposium proceedings. Remote sensing-a scientific vision for sustainable development,

Hughes, T. (2018). Spatial and temporal patterns of mass bleaching of corals in the Anthropocene. *Science*, *10*, 359, 380–383.

Hughes, T. P., Baird, A. H., Morrison, T. H., & Torda, G. (2023). Principles for coral reef restoration in the anthropocene. *One Earth*, 656–665.

Hughes, T. P., Kerry, J. T., Álvarez-Noriega, M., Álvarez-Romero, J. G., Anderson, K. D., Baird, A. H., Babcock, R. C., Beger, M., Bellwood, D. R., & Berkelmans, R. (2017). Global warming and recurrent mass bleaching of corals. *Nature*, *543*(7645), 373-377.

Hughes, T. P., Kerry, J. T., Baird, A. H., Connolly, S. R., Dietzel, A., Eakin, C. M., Heron, S. F., Hoey, A. S., Hoogenboom, M. O., & Liu, G. (2018). Global warming transforms coral reef assemblages. *Nature*, *556*(7702), 492-496.

Hughes, T. P., Kerry, J. T., Connolly, S. R., Álvarez-Romero, J. G., Eakin, C. M., Heron, S. F., Gonzalez, M. A., & Moneghetti, J. (2021). Emergent properties in the responses of tropical corals to recurrent climate extremes. *Current Biology*, *31*(23), 5393-5399. e5393.

Hughes, T. P., Kerry, J. T., Connolly, S. R., Baird, A. H., Eakin, C. M., Heron, S. F., Hoey, A. S., Hoogenboom, M. O., Jacobson, M., & Liu, G. (2019). Ecological memory modifies the cumulative impact of recurrent climate extremes. *Nature Climate Change*, *9*(1), 40-43.

Humanes, A., Beauchamp, E. A., Bythell, J. C., Carl, M. K., Craggs, J. R., Edwards, A. J., Golbuu, Y., Lachs, L., Martinez, H. M., & Palmowski, P. (2021). An Experimental Framework for Selectively Breeding Corals for Assisted Evolution. *Frontiers in Marine Science*, *8*, 626.

Humanes, A., Lachs, L., Beauchamp, E., Bukurou, L., Buzzoni, D., Bythell, J., Craggs, J. R., de la Torre Cerro, R., Edwards, A. J., & Golbuu, Y. (2024). Selective breeding enhances coral heat tolerance to marine heatwaves. *Nature Communications*, *15*(1), 8703.

Humanes, A., Lachs, L., Beauchamp, E. A., Bythell, J. C., Edwards, A. J., Golbuu, Y., Martinez, H. M., Palmowski, P., Treumann, A., & van der Steeg, E. (2022). Within-population variability in coral heat tolerance indicates climate adaptation potential. *Proceedings of the Royal Society B*, *289*(1981), 20220872.

Hume, B. C., Smith, E. G., Ziegler, M., Warrington, H. J., Burt, J. A., LaJeunesse, T. C., Wiedenmann, J., & Voolstra, C. R. (2019). SymPortal: A novel analytical framework and platform for coral algal symbiont next-generation sequencing ITS2 profiling. *Molecular Ecology Resources*, *19*(4), 1063-1080.

Hume, B. C., Ziegler, M., Poulain, J., Pochon, X., Romac, S., Boissin, E., De Vargas, C., Planes, S., Wincker, P., & Voolstra, C. R. (2018). An improved primer set and amplification protocol with increased specificity and sensitivity targeting the *Symbiodinium* ITS2 region. *PeerJ*, *6*, e4816.

Irwin, A., Greer, L., Humston, R., Devlin-Durante, M., Cabe, P., Lescinsky, H., Wirth, K., Allen Curran, H., & Baums, I. B. (2017). Age and intraspecific diversity of resilient *Acropora* communities in Belize. *Coral Reefs*, *36*, 1111-1120.

Ishida, H., Riginos, C., & Chan, C. X. (2024). Contaminant or goldmine? In silico assessment of Symbiodiniaceae community using coral hologenomes. *Frontiers in Protistology*, *2*, 1376877.

James, M. E., Wilkinson, M. J., Bernal, D. M., Liu, H., North, H. L., Engelstädter, J., & Ortiz-Barrientos, D. (2021). Phenotypic and genotypic parallel evolution in parapatric ecotypes of Senecio. *Evolution*, *75*(12), 3115-3131.

Japaud, A., Bouchon, C., Magalon, H., & Fauvelot, C. (2019). Geographic distances and ocean currents influence Caribbean *Acropora palmata* population connectivity in the Lesser Antilles. *Conservation Genetics*, *20*(3), 447-466.

Javid, P., Behzadi, S., Farrokhi, N., Bakhtiarizadeh, M., Alavi, S. M., & Ranjbar, M. S. (2021). Evaluation of Hsp70 gene expression in response to heat shock in a species of stony coral *Acropora downingi* (Wallace, 1999).

Jeffrey, S. t., & Humphrey, G. (1975). New spectrophotometric equations for determining chlorophylls a, b, c1 and c2 in higher plants, algae and natural phytoplankton. *Biochemie und physiologie der pflanzen*, *167*(2), 191-194.

Jin, Y. K., Lundgren, P., Lutz, A., Raina, J.-B., Howells, E. J., Paley, A. S., Willis, B. L., & van Oppen, M. J. (2016). Genetic markers for antioxidant capacity in a reef-building coral. *Science Advances*, *2*(5), e1500842.

Johnson, J. V., Dick, J. T., & Pincheira-Donoso, D. (2022). Marine protected areas do not buffer corals from bleaching under global warming. *BMC ecology and evolution*, *22*(1), 58.

Johnston, E. C., Cunning, R., & Burgess, S. C. (2022). Cophylogeny and specificity between cryptic coral species (*Pocillopora* spp.) at Mo'orea and their symbionts (Symbiodiniaceae). *BioRxiv*.

Jokiel, P. L. (1990). Transport of reef corals into the Great Barrier Reef. *Nature*, *347*(6294), 665-667.

Jombart, T. (2008). adegenet: a R package for the multivariate analysis of genetic markers. *Bioinformatics*, *24*(11), 1403-1405.

Jones, A. M., & Berkelmans, R. (2011). Tradeoffs to thermal acclimation: energetics and reproduction of a reef coral with heat tolerant *Symbiodinium* type-D. *Journal of Marine Biology*, *2011*(1), 185890.

Jones, R. J., Ward, S., Amri, A. Y., & Hoegh-Guldberg, O. (2000). Changes in quantum efficiency of Photosystem II of symbiotic dinoflagellates of corals after heat stress, and of bleached corals sampled after the 1998 Great Barrier Reef mass bleaching event. *Marine and Freshwater Research*, *51*(1), 63-71.

Jørsboe, E., & Albrechtsen, A. (2022). Efficient approaches for large-scale GWAS with genotype uncertainty. *G3*, *12*(1), jkab385.

Kardos, M., & Luikart, G. (2021). The genetic architecture of fitness drives population viability during rapid environmental change. *The American Naturalist*, *197*(5), 511-525.

Kavousi, J., Denis, V., Sharp, V., Reimer, J. D., Nakamura, T., & Parkinson, J. E. (2020). Unique combinations of coral host and algal symbiont genotypes reflect intraspecific variation in heat stress responses among colonies of the reef-building coral, *Montipora digitata*. *Marine Biology*, *167*, 1-15.

Kim, K.-S., Seibert, J. T., Edea, Z., Graves, K. L., Kim, E.-S., Keating, A. F., Baumgard, L. H., Ross, J. W., & Rothschild, M. F. (2018). Characterization of the acute heat stress response in gilts: III. Genome-wide association studies of thermotolerance traits in pigs. *Journal of animal science*, *96*(6), 2074-2085.

Kirk, N. L., Howells, E. J., Abrego, D., Burt, J. A., & Meyer, E. (2018). Genomic and transcriptomic signals of thermal tolerance in heat-tolerant corals (*Platygyra daedalea*) of the Arabian/Persian Gulf. *Molecular Ecology*, *27*(24), 5180-5194.

Kitchen, R. M., Piscetta, M., de Souza, M. R., Lenz, E. A., Schar, D. W., Gates, R. D., & Wall, C. B. (2020). Symbiont transmission and reproductive mode influence responses of three Hawaiian coral larvae to elevated temperature and nutrients. *Coral Reefs*, *39*, 419-431.

Klein, S. G., Roch, C., & Duarte, C. M. (2024). Systematic review of the uncertainty of coral reef futures under climate change. *Nature Communications*, *15*(1), 2224.

Klepac, C. N., & Barshis, D. J. (2022). High-resolution in situ thermal metrics coupled with acute heat stress experiments reveal differential coral bleaching susceptibility. *Coral Reefs*, *41*(4), 1045-1057.

Klepac, C. N., Petrik, C., Karabelas, E., Owens, J., Hall, E. R., & Muller, E. M. (2024). Assessing acute thermal assays as a rapid screening tool for coral restoration. *Scientific Reports*, *14*(1), 1898.

Kleypas, J. A., Buddemeier, R. W., & Gattuso, J.-P. (2001). The future of coral reefs in an age of global change. *International Journal of Earth Sciences*, *90*(2), 426-437.

Korneliussen, T. S., Albrechtsen, A., & Nielsen, R. (2014). ANGSD: analysis of next generation sequencing data. *BMC Bioinformatics*, *15*(1), 1-13.

Korunes, K. L., & Samuk, K. (2021). pixy: Unbiased estimation of nucleotide diversity and divergence in the presence of missing data. *Molecular Ecology Resources*, *21*(4), 1359-1368.

Krebs, R. A., & Bettencourt, B. R. (1999). Evolution of thermotolerance and variation in the heat shock protein, Hsp70. *American Zoologist*, *39*(6), 910-919.

Krueger, T., Hawkins, T. D., Becker, S., Pontasch, S., Dove, S., Hoegh-Guldberg, O., Leggat, W., Fisher, P. L., & Davy, S. K. (2015). Differential coral bleaching—Contrasting the activity and response of enzymatic antioxidants in symbiotic partners under thermal stress. *Comparative Biochemistry and Physiology Part A: Molecular & Integrative Physiology*, *190*, 15-25.

Krueger, T., Horwitz, N., Bodin, J., Giovani, M.-E., Escrig, S., Meibom, A., & Fine, M. (2017). Common reef-building coral in the Northern Red Sea resistant to elevated temperature and acidification. *Royal Society Open Science*, *4*(5), 170038.

Kubicek, A., Breckling, B., Hoegh-Guldberg, O., & Reuter, H. (2019). Climate change drives trait-shifts in coral reef communities. *Scientific Reports*, *9*(1), 3721.

Kuguru, B., Achituv, Y., Gruber, D. F., & Tchernov, D. (2010). Photoacclimation mechanisms of corallimorpharians on coral reefs: photosynthetic parameters of zooxanthellae and host cellular responses to variation in irradiance. *Journal of Experimental Marine Biology and Ecology*, *394*(1-2), 53-62.

Lachs, L., Bozec, Y.-M., Bythell, J. C., Donner, S. D., East, H. K., Edwards, A. J., Golbuu, Y., Gouezo, M., Guest, J. R., & Humanes, A. (2024). Natural selection could determine whether *Acropora* corals persist under expected climate change. *Science*, eadl6480.

Lachs, L., Donner, S. D., Mumby, P. J., Bythell, J. C., Humanes, A., East, H. K., & Guest, J. R. (2023a). Emergent increase in coral thermal tolerance reduces mass bleaching under climate change. *Nature Communications*, *14*(1), 4939.

Lachs, L., Humanes, A., Mumby, P. J., Donner, S. D., Bythell, J. C., Beauchamp, E., Bukurou, L., Buzzoni, D., de la Torre Cerro, R., & East, H. K. (2023b). Unexpectedly high coral heat tolerance at thermal refugia. *BioRxiv*, 2023.2006. 2016.545328.

Lachs, L., Humanes, A., Pygas, D. R., Bythell, J. C., Mumby, P. J., Ferrari, R., Figueira, W. F., Beauchamp, E., East, H. K., & Edwards, A. J. (2023c). No apparent trade-offs associated with heat tolerance in a reef-building coral. *Communications biology*, *6*(1), 400.

LaJeunesse, T., Bhagooli, R., Hidaka, M., DeVantier, L., Done, T., Schmidt, G., Fitt, W., & Hoegh-Guldberg, O. (2004). Closely related Symbiodinium spp. differ in relative dominance in coral reef host communities across environmental, latitudinal and biogeographic gradients. *Marine Ecology Progress Series*, *284*, 147-161.

LaJeunesse, T. C., Parkinson, J. E., Gabrielson, P. W., Jeong, H. J., Reimer, J. D., Voolstra, C. R., & Santos, S. R. (2018). Systematic revision of Symbiodiniaceae highlights the antiquity and diversity of coral endosymbionts. *Current Biology*, *28*(16), 2570-2580. e2576.

LaJeunesse, T. C., Smith, R. T., Finney, J., & Oxenford, H. (2009). Outbreak and persistence of opportunistic symbiotic dinoflagellates during the 2005 Caribbean mass coral 'bleaching' event. *Proceedings of the Royal Society B: Biological Sciences*, *276*(1676), 4139-4148. https://doi.org/doi:10.1098/rspb.2009.1405

Lamb, A. M., Morgans, C. A., McCutchan, G. A., Mocellin, V. J. L., Denis, H., Naugle, M. S., Lemonius, A. J., Edmunds, R. C., Wooster, M. K., Bay, L. K., Howells, E. J., & van Oppen, M. J. H. (2026). A selective breeding design based on parental rapid heat stress thresholds did not produce more heat-tolerant coral larvae. *Ecological Solutions and Evidence*, *7*(1), e70178. https://doi.org/https://doi.org/10.1002/2688-8319.70178

Lasky, J. R., Forester, B. R., & Reimherr, M. (2018). Coherent synthesis of genomic associations with phenotypes and home environments. *Molecular Ecology Resources*, *18*(1), 91-106.

Lasky, J. R., Josephs, E. B., & Morris, G. P. (2023). Genotype–environment associations to reveal the molecular basis of environmental adaptation. *The Plant Cell*, *35*(1), 125-138.

Lawson, D. J., Van Dorp, L., & Falush, D. (2018). A tutorial on how not to over-interpret STRUCTURE and ADMIXTURE bar plots. *Nature Communications*, *9*(1), 3258.

Leal, M. C., Jesus, B., Ezequiel, J., Calado, R., Rocha, R. J. M., Cartaxana, P., & Serôdio, J. (2015). Concurrent imaging of chlorophyll fluorescence, Chlorophyll a content and green fluorescent proteins-like proteins of symbiotic cnidarians. *Marine ecology*, *36*(3), 572-584.

LeBlanc, N. M., & Pavey, S. A. (2023). Comparing mixed models and Random Forest association tests using naturalgwas and a Striped Bass SNP data set. *Molecular Ecology Resources*, *23*(1), 145-158.

Lee, H., Calvin, K., Dasgupta, D., Krinner, G., Mukherji, A., Thorne, P., Trisos, C., Romero, J., Aldunce, P., & Barret, K. (2023). IPCC, 2023: Climate Change 2023: Synthesis Report, Summary for Policymakers. Contribution of Working Groups I, II and III to the Sixth Assessment Report of the Intergovernmental Panel on Climate Change [Core Writing Team, H. Lee and J. Romero (eds.)]. IPCC, Geneva, Switzerland.

Legendre, P., & Anderson, M. J. (1999). Distance-based redundancy analysis: testing multispecies responses in multifactorial ecological experiments. *Ecological Monographs*, *69*(1), 1-24.

Leinbach, S. E., Speare, K. E., Rossin, A. M., Holstein, D. M., & Strader, M. E. (2021). Energetic and reproductive costs of coral recovery in divergent bleaching responses. *Scientific Reports*, *11*(1), 1-10, Article sperm.

Leiva, C., Pérez-Portela, R., & Lemer, S. (2023). Genomic signatures suggesting adaptation to ocean acidification in a coral holobiont from volcanic CO2 seeps. *Communications biology*, *6*(1), 769.

Leiva, C., Torda, G., Zhou, C., Pan, Y., Harris, J., Xiang, X., Tan, S., Tian, W., Hume, B., & Miller, D. J. (2025). Rapid Evolution in Action: Environmental Filtering Supports Coral Adaptation to a Hot, Acidic, and Deoxygenated Extreme Habitat. *Global Change Biology*, *31*(3), e70103.

Lenormand, T. (2002). Gene flow and the limits to natural selection. *Trends in Ecology & Evolution*, *17*(4), 183-189.

Lesser, M. P., & Farrell, J. H. (2004). Exposure to solar radiation increases damage to both host tissues and algal symbionts of corals during thermal stress. *Coral Reefs*, *23*, 367-377.

Levin, R. A., Beltran, V. H., Hill, R., Kjelleberg, S., McDougald, D., Steinberg, P. D., & van Oppen, M. J. (2016). Sex, scavengers, and chaperones: transcriptome secrets of divergent *Symbiodinium* thermal tolerances. *Molecular Biology and Evolution*, *33*(9), 2201-2215.

Lewis, A. M., Butler, C. C., Turnham, K. E., Wham, D. F., Hoadley, K. D., Smith, R. T., Kemp, D. W., Warner, M. E., & LaJeunesse, T. C. (2024). The diversity, distribution, and temporal stability of coral 'zooxanthellae'on a pacific reef: from the scale of individual colonies to across the host community. *Coral Reefs*, *43*(4), 841-856.

Li, H., & Durbin, R. (2010). Fast and accurate long-read alignment with Burrows–Wheeler transform. *Bioinformatics*, *26*(5), 589-595.

Li, T., Yu, L., Song, B., Song, Y., Li, L., Lin, X., & Lin, S. (2020). Genome improvement and core gene set refinement of *Fugacium kawagutii*. *Microorganisms*, *8*(1), 102.

Libro, S., Kaluziak, S. T., & Vollmer, S. V. (2013). RNA-seq profiles of immune related genes in the staghorn coral *Acropora cervicornis* infected with white band disease. *PloS One*, *8*(11), e81821.

Liew, Y. J., Howells, E. J., Wang, X., Michell, C. T., Burt, J. A., Idaghdour, Y., & Aranda, M. (2020). Intergenerational epigenetic inheritance in reef-building corals. *Nature Climate Change*, *10*(3), 254-259.

Liggins, L., Treml, E. A., & Riginos, C. (2020). Seascape genomics: contextualizing adaptive and neutral genomic variation in the ocean environment. *Population genomics: Marine organisms*, 171-218.

Lind, B. M., Candido-Ribeiro, R., Singh, P., Lu, M., Obreht Vidakovic, D., Booker, T. R., Whitlock, M. C., Yeaman, S., Isabel, N., & Aitken, S. N. (2024). How useful is genomic data for predicting maladaptation to future climate? *Global Change Biology*, *30*(4), e17227.

Lind, B. M., & Lotterhos, K. E. (2024). The accuracy of predicting maladaptation to new environments with genomic data. *Molecular Ecology Resources*, e14008.

Lithgow, G. J., White, T. M., Melov, S., & Johnson, T. E. (1995). Thermotolerance and extended life-span conferred by single-gene mutations and induced by thermal stress. *Proceedings of the National Academy of Sciences*, *92*(16), 7540-7544.

Liu, G., Strong, A. E., & Skirving, W. (2003). Remote sensing of sea surface temperatures during 2002 Barrier Reef coral bleaching. *Eos, Transactions American Geophysical Union*, *84*(15), 137-141.

Logan, C. A., Dunne, J. P., Ryan, J. S., Baskett, M. L., & Donner, S. D. (2021). Quantifying global potential for coral evolutionary response to climate change. *Nature Climate Change*, 1-6.

Longmei, N., Gill, G. K., Zaidi, P. H., Kumar, R., Nair, S. K., Hindu, V., Vinayan, M. T., & Vikal, Y. (2021). Genome wide association mapping for heat tolerance in sub-tropical maize. *BMC Genomics*, *22*(1), 154.

Lotterhos, K. E. (2023). The paradox of adaptive trait clines with nonclinal patterns in the underlying genes. *Proceedings of the National Academy of Sciences*, *120*(12), e2220313120.

Lou, R. N., Jacobs, A., Wilder, A. P., & Therkildsen, N. O. (2021). A beginner's guide to low-coverage whole genome sequencing for population genomics. *Molecular Ecology*, *30*(23), 5966-5993.

Loya, Y., Sakai, K., Yamazato, K., Nakano, Y., Sambali, H., & Van Woesik, R. (2001). Coral bleaching: the winners and the losers. *Ecology letters*, *4*(2), 122-131.

Lukoschek, V., Riginos, C., & van Oppen, M. J. (2016). Congruent patterns of connectivity can inform management for broadcast spawning corals on the Great Barrier Reef. *Molecular Ecology*, *25*(13), 3065-3080.

Lundgren, P., Vera, J. C., Peplow, L., Manel, S., & van Oppen, M. J. (2013). Genotype–environment correlations in corals from the Great Barrier Reef. *BMC Genetics*, *14*(1), 1-16.

Luo, L., Tang, Z. z., Schoville, S. D., & Zhu, J. (2021). A comprehensive analysis comparing linear and generalized linear models in detecting adaptive SNPs. *Molecular Ecology Resources*, *21*(3), 733-744.

Luo, Y., Lorts, C. M., Lawrence-Paul, E., & Lasky, J. R. (2025). Experimental validation of genome-environment associations in *Arabidopsis*. *BioRxiv*, 2025.2001. 2008.631904.

Ma, Y., Min, L., Wang, J., Li, Y., Wu, Y., Hu, Q., Ding, Y., Wang, M., Liang, Y., & Gong, Z. (2021). A combination of genome-wide and transcriptome-wide association studies reveals genetic elements leading to male sterility during high temperature stress in cotton. *New Phytologist*, *231*(1), 165-181.

Maes, C., & Blanke, B. (2015). Tracking the origins of plastic debris across the Coral Sea: A case study from the Ouvéa Island, New Caledonia. *Marine Pollution Bulletin*, *97*(1-2), 160-168.

Maestri, E., Klueva, N., Perrotta, C., Gulli, M., Nguyen, H. T., & Marmiroli, N. (2002). Molecular genetics of heat tolerance and heat shock proteins in cereals. *Plant molecular biology*, *48*(5), 667-681.

Malenfant, R. M., Davis, C. S., Richardson, E. S., Lunn, N. J., & Coltman, D. W. (2018). Heritability of body size in the polar bears of Western Hudson Bay. *Molecular Ecology Resources*, *18*(4), 854-866.

Manzello, D. P., Cunning, R., Karp, R. F., Baker, A. C., Bartels, E., Bonhag, R., Borreil, A., Bourque, A., Brown, K. T., & Bruckner, A. W. (2025). Heat-driven functional extinction of Caribbean *Acropora* corals from Florida's Coral Reef. *Science*, *390*(6771), 361-366.

Marchesiello, P., Lefèvre, J., Vega, A., Couvelard, X., & Menkes, C. (2010). Coastal upwelling, circulation and heat balance around New Caledonia's barrier reef. *Marine Pollution Bulletin*, *61*(7-12), 432-448.

Marhoefer, S. R., Zenger, K. R., Strugnell, J. M., Logan, M., van Oppen, M. J., Kenkel, C. D., & Bay, L. K. (2021). Signatures of adaptation and acclimatization to reef flat and slope habitats in the coral *Pocillopora damicornis*. *Frontiers in Marine Science*, *8*, 704709.

Marigorta, U. M., & Gibson, G. (2014). A simulation study of gene-by-environment interactions in GWAS implies ample hidden effects. *Frontiers in Genetics*, *5*, 225.

Marzonie, M. R. (2025). *Diversity and Distributions*.

Marzonie, M. R., Bay, L. K., Bourne, D. G., Hoey, A. S., Matthews, S., Nielsen, J. J., & Harrison, H. B. (2022). The effects of marine heatwaves on acute heat tolerance in corals. *Global Change Biology*, *29*(2), 404-416.

Marzonie, M. R., Nitschke, M. R., Bay, L. K., Bourne, D. G., & Harrison, H. B. (2024). Symbiodiniaceae diversity varies by host and environment across thermally distinct reefs. *Molecular Ecology*, *33*(9), e17342.

Mason, R., Langlais, C., Uribe-Palomino, J., Tonks, M., Coman, F., Choukroun, S., Porobic, J., & Doropoulos, C. (2025). Reef-scale variation in larval supply and settlement: validating dispersal predictions with observations of coral larvae. *Authorea Preprints*.

Masson-Delmotte, V., Zhai, P., Pörtner, H.-O., Roberts, D., Skea, J., & Shukla, P. R. (2022). *Global Warming of 1.5° C: IPCC Special Report on Impacts of Global Warming of 1.5° C above Pre-industrial Levels in Context of Strengthening Response to Climate Change, Sustainable Development, and Efforts to Eradicate Poverty*. Cambridge University Press.

Matias, A. M. A., Popovic, I., Thia, J. A., Cooke, I. R., Torda, G., Lukoschek, V., Bay, L. K., Kim, S. W., & Riginos, C. (2022). Cryptic diversity and spatial genetic variation in the coral *Acropora tenuis* and its endosymbionts across the Great Barrier Reef. *Evolutionary Applications*, *16*(2), 293-310.

Matorin, D. N., Antal, T. K., Ostrowska, M. a., Rubin, A. B., Ficek, D., & Majchrowski, R. (2004). Chlorophyll fluorimetry as a method for studying light absorption by photosynthetic pigments in marine algae. *Oceanologia*, *46*(4).

Matz, M. V., & Black, K. L. (2025). RDAforest: identifying environmental drivers of polygenic adaptation. *Molecular Ecology Resources*, e70002.

Matz, M. V., Treml, E. A., Aglyamova, G. V., & Bay, L. K. (2018). Potential and limits for rapid genetic adaptation to warming in a Great Barrier Reef coral. *PLoS Genetics*, *14*(4), e1007220.

Matz, M. V., Treml, E. A., & Haller, B. C. (2020). Estimating the potential for coral adaptation to global warming across the Indo-West Pacific. *Global Change Biology*, *26*(6), 3473-3481.

Maulana, F., Ayalew, H., Anderson, J. D., Kumssa, T. T., Huang, W., & Ma, X.-F. (2018). Genome-wide association mapping of seedling heat tolerance in winter wheat. *Frontiers in plant science*, *9*, 1272.

Mayfield, A. B., Chen, Y.-J., Lu, C.-Y., & Chen, C.-S. (2018). The proteomic response of the reef coral *Pocillopora acuta* to experimentally elevated temperatures. *PloS One*, *13*(1), e0192001.

McAllister, D. E. (1995). Status of the world ocean and its biodiversity.

McClanahan, T., Darling, E., Beger, M., Fox, H., Grantham, H., Jupiter, S., Logan, C. A., Mcleod, E., McManus, L., & Oddenyo, R. (2023). Diversification of refugia types needed to secure the future of coral reefs subject to climate change. *Conservation Biology*.

McClanahan, T. R., Darling, E. S., Maina, J. M., Muthiga, N. A., 'agata, S. D., Jupiter, S. D., Arthur, R., Wilson, S. K., Mangubhai, S., & Nand, Y. (2019). Temperature patterns and mechanisms influencing coral bleaching during the 2016 El Niño. *Nature Climate Change*, *9*(11), 845-851.

McClanahan, T. R., Maina, J. M., Darling, E. S., Guillaume, M. M. M., Muthiga, N. A., D'agata, S., Leblond, J., Arthur, R., Jupiter, S. D., Wilson, S. K., Mangubhai, S., Ussi, A. M., Humphries, A. T., Patankar, V., Shedrawi, G., Julius, P., Ndagala, J., & Grimsditch, G. (2020). Large geographic variability in the resistance of corals to thermal stress. *Global Ecology and Biogeography*, *29*(12), 2229-2247. https://doi.org/10.1111/geb.13191

McGaugh, S. E., Lorenz, A. J., & Flagel, L. E. (2021). The utility of genomic prediction models in evolutionary genetics. *Proceedings of the Royal Society B*, *288*(1956), 20210693.

McGowan, H., & Theobald, A. (2023). Atypical weather patterns cause coral bleaching on the Great Barrier Reef, Australia during the 2021–2022 La Niña. *Scientific Reports*, *13*(1), 6397.

McKenna, A., Hanna, M., Banks, E., Sivachenko, A., Cibulskis, K., Kernytsky, A., Garimella, K., Altshuler, D., Gabriel, S., & Daly, M. (2010). The Genome Analysis Toolkit: a MapReduce framework for analyzing next-generation DNA sequencing data. *Genome Research*, *20*(9), 1297-1303.

McLachlan, R. H., Price, J. T., Solomon, S. L., & Grottoli, A. G. (2020). Thirty years of coral heat-stress experiments: A review of methods. *Coral Reefs*, *39*, 885-902.

McManus, L. C., Forrest, D. L., Tekwa, E. W., Schindler, D. E., Colton, M. A., Webster, M. M., Essington, T. E., Palumbi, S. R., Mumby, P. J., & Pinsky, M. L. (2021). Evolution and connectivity influence the persistence and recovery of coral reefs under climate change in the Caribbean, Southwest Pacific, and Coral Triangle. *Global Change Biology*, *27*(18), 4307-4321.

McManus, L. C., Vasconcelos, V. V., Levin, S. A., Thompson, D. M., Kleypas, J. A., Castruccio, F. S., Curchitser, E. N., & Watson, J. R. (2020). Extreme temperature events will drive coral decline in the Coral Triangle. *Global Change Biology*, *26*(4), 2120-2133.

McRae, C. J., Keshavmurthy, S., Chen, H.-K., Ye, Z.-M., Meng, P.-J., Rosset, S. L., Huang, W.-B., Chen, C. A., Fan, T.-Y., & Côté, I. M. (2023). Baseline dynamics of Symbiodiniaceae genera and photochemical efficiency in corals from reefs with different thermal histories. *PeerJ*, *11*, e15421.

McWilliam, M., Hoogenboom, M. O., Baird, A. H., Kuo, C.-Y., Madin, J. S., & Hughes, T. P. (2018). Biogeographical disparity in the functional diversity and redundancy of corals. *Proceedings of the National Academy of Sciences*, *115*(12), 3084-3089.

McWilliam, M., Madin, J. S., Chase, T. J., Hoogenboom, M. O., & Bridge, T. C. (2022). Intraspecific variation reshapes coral assemblages under elevated temperature and acidity. *Ecology letters*, *25*(11), 2513-2524.

Meng, C., Basunia, A., Peters, B., Gholami, A. M., Kuster, B., & Culhane, A. C. (2019). MOGSA: integrative single sample gene-set analysis of multiple omics data. *Molecular & Cellular Proteomics*, *18*(8), S153-S168.

Metheringham, C. L., Plumb, W. J., Flynn, W. R., Stocks, J. J., Kelly, L. J., Nemesio Gorriz, M., Grieve, S. W., Moat, J., Lines, E. R., & Buggs, R. J. (2025). Rapid polygenic adaptation in a wild population of ash trees under a novel fungal epidemic. *Science*, *388*(6754), 1422-1425.

Meunier, V., Bonnet, S., Camps, M., Benavides, M., Dubosc, J., Rodolfo-Metalpa, R., & Houlbrèque, F. (2022). Ingestion of Diazotrophs Makes Corals More Resistant to Heat Stress. *Biomolecules*, *12*(4), 537.

Meziere, Z., Popovic, I., Prata, K., Ryan, I., Pandolfi, J., & Riginos, C. (2024). Exploring coral speciation: Multiple sympatric *Stylophora pistillata* taxa along a divergence continuum on the Great Barrier Reef. *Evolutionary Applications*, *17*(1), e13644.

Meziere, Z., Prata, K., Lechene, M., Ferrari, R., Popovic, I., & Riginos, C. (2025). Connectivity differs by orders of magnitude among co-distributed corals, affecting spatial scales of eco-evolutionary processes. *Science Advances*, *11*(27), eadt2066.

Middlebrook, R., Anthony, K. R., Hoegh-Guldberg, O., & Dove, S. (2010). Heating rate and symbiont productivity are key factors determining thermal stress in the reef-building coral *Acropora formosa*. *Journal of Experimental Biology*, *213*(7), 1026-1034.

Middlebrook, R., Anthony, K. R., Hoegh-Guldberg, O., & Dove, S. (2012). Thermal priming affects symbiont photosynthesis but does not alter bleaching susceptibility in *Acropora millepora*. *Journal of Experimental Marine Biology and Ecology*, *432*, 64-72.

Mieog, J. C., Olsen, J. L., Berkelmans, R., Bleuler-Martinez, S. A., Willis, B. L., & van Oppen, M. J. (2009). The roles and interactions of symbiont, host and environment in defining coral fitness. *PloS One*, *4*(7), e6364.

Miller, M., Crabbe, J., Villamizar, E., Croquer, A., & Banaszak, A. (2022). *Acropora palmata (e.T133006A165672016)*. The IUCN Red List of Threatened Species 2022. Retrieved July 06 from https://www.iucnredlist.org/species/133006/165672016

Moore, R. B., Ferguson, K. M., Loh, W. K., Hoegh-Guldberg, O., & Carter, D. A. (2003). Highly organized structure in the non-coding region of the psbA minicircle from clade C *Symbiodinium*. *International journal of systematic and evolutionary microbiology*, *53*(6), 1725-1734.

Morgan, T., & Mackay, T. (2006). Quantitative trait loci for thermotolerance phenotypes in *Drosophila melanogaster*. *Heredity*, *96*(3), 232-242.

Morikawa, M. K., & Palumbi, S. R. (2019). Using naturally occurring climate resilient corals to construct bleaching-resistant nurseries. *Proceedings of the National Academy of Sciences*, *116*(21), 10586-10591.

Morrison, T. H., Adger, N., Barnett, J., Brown, K., Possingham, H., & Hughes, T. (2020). Advancing coral reef governance into the Anthropocene. *One Earth*, *2*(1), 64-74.

Muir, P. R., Done, T., & Aguirre, D. J. (2021). High regional and intra-generic variation in susceptibility to mass bleaching in Indo-Pacific coral species. *BioRxiv*.

Muller, E. M., Petrik, C., Conn, T., Osborne, C., Villoch, M., Clark, A., Koch, H., O'Neil, K., Engelsma, C., & Baums, I. (2025). Assisted gene flow yields *Acropora palmata* corals with robust physiological performance under warmer water temperatures in a land-based nursery. *BioRxiv*, 2025.2003. 2003.641242.

Mumby, P. J., Mason, R. A., & Hock, K. (2021). Reconnecting reef recovery in a world of coral bleaching. *Limnology and Oceanography: Methods*, *19*(10), 702-713.

Muscatine, L., & Porter, J. W. (1977). Reef corals: mutualistic symbioses adapted to nutrient-poor environments. *Bioscience*, *27*(7), 454-460.

Nakamura, T., Van Woesik, R., & Yamasaki, H. (2005). Photoinhibition of photosynthesis is reduced by water flow in the reef-building coral *Acropora digitifera*. *Marine Ecology Progress Series*, *301*, 109-118.

Nand, A., Zhan, Y., Salazar, O. R., Aranda, M., Voolstra, C. R., & Dekker, J. (2021). Genetic and spatial organization of the unusual chromosomes of the dinoflagellate *Symbiodinium microadriaticum*. *Nature Genetics*, 1-12.

Naugle, M. S., Denis, H., Guillaume, A. S., Mocellin, V. J., Nielsen, J. J., Van Orman, B. G., C, A. K., Bay, L. K., & Howells, E. J. (2025). Rapid heat stress assays predict survivors of coral bleaching. *Manuscript submitted for publication*.

Naugle, M. S., Denis, H., Mocellin, V. J., Laffy, P. W., Popovic, I., Bay, L. K., & Howells, E. J. (2024). Heat tolerance varies considerably within a reef-building coral species on the Great Barrier Reef. *Communications Earth & Environment*, *5*(1), 525.

Naumann, M. S., Niggl, W., Laforsch, C., Glaser, C., & Wild, C. (2009). Coral surface area quantification–evaluation of established techniques by comparison with computer tomography. *Coral Reefs*, *28*(1), 109-117.

Neel, M. C., McKelvey, K., Ryman, N., Lloyd, M. W., Short Bull, R., Allendorf, F. W., Schwartz, M. K., & Waples, R. S. (2013). Estimation of effective population size in continuously distributed populations: there goes the neighborhood. *Heredity*, *111*(3), 189-199.

Nielsen, J., Matthews, G., Frith, K., Harrison, H., Marzonie, M., Slaughter, K., Suggett, D., & Bay, L. (2022). Experimental considerations of acute heat stress assays to quantify coral thermal tolerance. *Scientific Reports*, *12*(1), 16831.

Nitschke, M. R., Rosset, S. L., Oakley, C. A., Gardner, S. G., Camp, E. F., Suggett, D. J., & Davy, S. K. (2022). The diversity and ecology of Symbiodiniaceae: A traits-based review. *Advances in Marine Biology*, *92*, 55-127.

NOAA Coral Reef Watch. (2018, updated daily). *NOAA Coral Reef Watch Version 3.1, Daily Global 5-km Satellite Sea Surface Temperature Product (a.k.a CoralTemp), Jun. 1, 1985-July. 3, 2022. College Park, Maryland, USA: NOAA Coral Reef Watch. Data set accessed 2022-07-04 at* https://coralreefwatch.noaa.gov/product/5km/index_5km_sst.php.

Nolan, M. K., Schmidt-Roach, S., Davis, A. R., Aranda, M., & Howells, E. J. (2021). Widespread bleaching in the One Tree Island lagoon (Southern Great Barrier Reef) during record-breaking temperatures in 2020. *Environmental monitoring and assessment*, *193*(9), 1-8.

Nunn, B. L., Brown, T., Timmins-Schiffman, E., Mudge, M. C., Riffle, M., Axworthy, J. B., Dilworth, J., Kenkel, C. D., Zaneveld, J., & Rodrigues, L. J. (2025). Protein signatures predict coral resilience and survival to thermal bleaching events. *Communications Earth & Environment*, *6*(1), 191.

Oakley, C., & Davy, S. (2018). Cell biology of coral bleaching. In *Coral bleaching* (pp. 189-211). Springer.

Oksanen, J., Blanchet, F. G., Kindt, R., Legendre, P., Minchin, P. R., O'hara, R., Simpson, G. L., Solymos, P., Stevens, M. H. H., & Wagner, H. (2013). Package 'vegan'. *Community Ecology Package, version*, *2*(9), 1-295.

Oliver, E. C., Donat, M. G., Burrows, M. T., Moore, P. J., Smale, D. A., Alexander, L. V., Benthuysen, J. A., Feng, M., Gupta, A. S., & Hobday, A. J. (2018). Longer and more frequent marine heatwaves over the past century. *Nature Communications*, *9*(1), 1-12.

Orr, H. A. (2005). The genetic theory of adaptation: a brief history. *Nature Reviews Genetics*, *6*(2), 119-127.

Ørsted, M., Jørgensen, L. B., & Overgaard, J. (2022). Finding the right thermal limit: a framework to reconcile ecological, physiological and methodological aspects of CTmax in ectotherms. *Journal of Experimental Biology*, *225*(19), jeb244514.

Oury, N., Gélin, P., & Magalon, H. (2020). Cryptic species and genetic connectivity among populations of the coral *Pocillopora damicornis* (Scleractinia) in the tropical southwestern Pacific. *Marine Biology*, *167*(10), 1-15.

Page, C., Leggat, W., Heron, S., Fordyce, A., & Ainsworth, T. (2021). High flow conditions mediate damaging impacts of sub-lethal thermal stress on corals' endosymbiotic algae. *Conservation Physiology*, *9*(1), coab046.

Page, C. A., Giuliano, C., Bay, L. K., & Randall, C. J. (2023). High survival following bleaching underscores the resilience of a frequently disturbed region of the Great Barrier Reef. *Ecosphere*, *14*(2), e4280.

Page, C. E., Leggat, W., Heron, S. F., Choukroun, S. M., Lloyd, J., & Ainsworth, T. D. (2019). Seeking resistance in coral reef ecosystems: the interplay of biophysical factors and bleaching resistance under a changing climate: the interplay of a reef's biophysical factors can mitigate the coral bleaching response. *BioEssays*, *41*(7), 1800226.

Palacio-Castro, A. M., Smith, T. B., Brandtneris, V., Snyder, G. A., van Hooidonk, R., Maté, J. L., Manzello, D., Glynn, P. W., Fong, P., & Baker, A. C. (2023). Increased dominance of heat-tolerant symbionts creates resilient coral reefs in near-term ocean warming. *Proceedings of the National Academy of Sciences*, *120*(8), e2202388120.

Pallares, L. F., Lea, A. J., Han, C., Filippova, E. V., Andolfatto, P., & Ayroles, J. F. (2023). Dietary stress remodels the genetic architecture of lifespan variation in outbred *Drosophila*. *Nature Genetics*, *55*(1), 123-129.

Pamplona, R., & Costantini, D. (2011). Molecular and structural antioxidant defenses against oxidative stress in animals. *American Journal of Physiology-Regulatory, Integrative and Comparative Physiology*, *301*(4), R843-R863.

Paradis, E., & Schliep, K. (2019). ape 5.0: an environment for modern phylogenetics and evolutionary analyses in R. *Bioinformatics*, *35*(3), 526-528.

Payri, C., Benzoni, F., André, L. V., & Houlbrèque, F. (2018). Le blanchissement corallien de 2016. *IRD Editions/Solaris*, 161-166.

Payri, C. E., Allain, V., Aucan, J., David, C., David, V., Dutheil, C., Loubersac, L., Menkes, C., Pelletier, B., & Pestana, G. (2019). New Caledonia. In *World Seas: An Environmental Evaluation* (pp. 593-618). Elsevier.

Pérez, P., & de Los Campos, G. (2014). Genome-wide regression and prediction with the BGLR statistical package. *Genetics*, *198*(2), 483-495.

Pinsky, M. L., Palumbi, S. R., Andréfouët, S., & Purkis, S. J. (2012). Open and closed seascapes: Where does habitat patchiness create populations with high fractions of self-recruitment? *Ecological applications*, *22*(4), 1257-1267.

Pisapia, C., Anderson, K., & Pratchett, M. S. (2014). Intraspecific variation in physiological condition of reef-building corals associated with differential levels of chronic disturbance. *PloS One*, *9*(3), e91529.

Pollock, F. J., McMinds, R., Smith, S., Bourne, D. G., Willis, B. L., Medina, M., Thurber, R. V., & Zaneveld, J. R. (2018). Coral-associated bacteria demonstrate phylosymbiosis and cophylogeny. *Nature Communications*, *9*(1), 1-13.

Poore, H. A., Stuart, Y. E., Rennison, D. J., Roesti, M., Hendry, A. P., Bolnick, D. I., & Peichel, C. L. (2023). Repeated genetic divergence plays a minor role in repeated phenotypic divergence of lake-stream stickleback. *Evolution*, *77*(1), 110-122.

Poquita-Du, R. C., Goh, Y. L., Huang, D., Chou, L. M., & Todd, P. A. (2020). Gene expression and photophysiological changes in *Pocillopora acuta* coral holobiont following heat stress and recovery. *Microorganisms*, *8*(8), 1227.

Porcelli, D., Butlin, R., Gaston, K., Joly, D., & Snook, R. (2015). The environmental genomics of metazoan thermal adaptation. *Heredity*, *114*(5), 502-514.

Prata, K. E., Bongaerts, P., Dwyer, J. M., Ishida, H., Howitt, S. M., Hereward, J. P., Crandall, E. D., & Riginos, C. (2024). Some reef-building corals only disperse metres per generation. *Proceedings B*, *291*(2027), 20231988.

Pratchett, M. S., Hoey, A. S., Tan, C.-H., Kuo, C.-Y., Bauman, A. G., Kumaraswamy, R., & Baird, A. H. (2019). Spatial and temporal variation in fecundity of *Acropora* spp. in the Northern Great Barrier Reef. *Diversity*, *11*(4), 60.

Pritchard, J. K., Pickrell, J. K., & Coop, G. (2010). The genetics of human adaptation: hard sweeps, soft sweeps, and polygenic adaptation. *Current Biology*, *20*(4), R208-R215.

Purcell, S., Neale, B., Todd-Brown, K., Thomas, L., Ferreira, M. A., Bender, D., Maller, J., Sklar, P., De Bakker, P. I., & Daly, M. J. (2007). PLINK: a tool set for whole-genome association and population-based linkage analyses. *The American Journal of Human Genetics*, *81*(3), 559-575.

Putnam, H. M. (2021). Avenues of reef-building coral acclimatization in response to rapid environmental change. *Journal of Experimental Biology*, *224*(Suppl_1), jeb239319.

Queitsch, C., Hong, S.-W., Vierling, E., & Lindquist, S. (2000). Heat shock protein 101 plays a crucial role in thermotolerance in Arabidopsis. *The Plant Cell*, *12*(4), 479-492.

Quigley, K., Randall, C., van Oppen, M., & Bay, L. (2020a). Assessing the role of historical temperature regime and algal symbionts on the heat tolerance of coral juveniles. *Biology open*, *9*(1), bio047316.

Quigley, K. M., Bay, L. K., & van Oppen, M. J. (2019a). The active spread of adaptive variation for reef resilience. *Ecology and Evolution*, *9*(19), 11122-11135.

Quigley, K. M., Bay, L. K., & van Oppen, M. J. (2020b). Genome-wide SNP analysis reveals an increase in adaptive genetic variation through selective breeding of coral. *Molecular Ecology*, *29*(12), 2176-2188.

Quigley, K. M., Hein, M., & Suggett, D. J. (2022a). Translating the 10 golden rules of reforestation for coral reef restoration. *Conservation Biology*, e13890.

Quigley, K. M., Ramsby, B., Laffy, P., Harris, J., Mocellin, V. J., & Bay, L. K. (2022b). Symbioses are restructured by repeated mass coral bleaching. *Science Advances*, *8*(49), eabq8349.

Quigley, K. M., Willis, B. L., & Bay, L. K. (2016). Maternal effects and *Symbiodinium* community composition drive differential patterns in juvenile survival in the coral *Acropora tenuis*. *Royal Society Open Science*, *3*(10), 160471.

Quigley, K. M., Willis, B. L., & Kenkel, C. D. (2019b). Transgenerational inheritance of shuffled symbiont communities in the coral *Montipora digitata*. *Scientific Reports*, *9*(1), 1-11.

Rädecker, N., Pogoreutz, C., Gegner, H. M., Cárdenas, A., Roth, F., Bougoure, J., Guagliardo, P., Wild, C., Pernice, M., & Raina, J.-B. (2021). Heat stress destabilizes symbiotic nutrient cycling in corals. *Proceedings of the National Academy of Sciences*, *118*(5).

Raja, N. B., Lauchstedt, A., Pandolfi, J. M., Kim, S. W., Budd, A. F., & Kiessling, W. (2021). Morphological traits of reef corals predict extinction risk but not conservation status. *Global Ecology and Biogeography*, *30*(8), 1597-1608.

Randall, C. J., Negri, A. P., Quigley, K. M., Foster, T., Ricardo, G. F., Webster, N. S., Bay, L. K., Harrison, P. L., Babcock, R. C., & Heyward, A. J. (2020). Sexual production of corals for reef restoration in the Anthropocene. *Marine Ecology Progress Series*, *635*, 203-232.

Rassmussen, S. H., Cowman, P. F., Baird, A. H., Crosbie, A. J., Quattrini, A. M., Bonito, V., Sinniger, F., Harii, S., Cabaitan, P. C., & Fadli, N. (2025). The tables have turned: taxonomy, systematics and biogeography of the *Acropora hyacinthus* (Scleractinia: Acroporidae) complex. *Invertebrate Systematics*, *39*(8), NULL-NULL.

Ravagnolo, O., & Misztal, I. (2000). Genetic component of heat stress in dairy cattle, parameter estimation. *Journal of Dairy Science*, *83*(9), 2126-2130.

Ravinet, M., Faria, R., Butlin, R., Galindo, J., Bierne, N., Rafajlović, M., Noor, M., Mehlig, B., & Westram, A. (2017). Interpreting the genomic landscape of speciation: a road map for finding barriers to gene flow. *Journal of Evolutionary Biology*, *30*(8), 1450-1477.

Ravinet, M., Westram, A., Johannesson, K., Butlin, R., André, C., & Panova, M. (2016). Shared and nonshared genomic divergence in parallel ecotypes of *Littorina saxatilis* at a local scale. *Molecular Ecology*, *25*(1), 287-305.

Reaka-Kudla, M. L. (1997). The global biodiversity of coral reefs: a comparison with rain forests. *Biodiversity II: Understanding and protecting our biological resources*, *2*, 551.

Reich, H. G., Kitchen, S. A., Stankiewicz, K. H., Devlin-Durante, M., Fogarty, N. D., & Baums, I. B. (2021). Genomic variation of an endosymbiotic dinoflagellate (*Symbiodinium* 'fitti') among closely related coral hosts. *Molecular Ecology*, *30*(14), 3500-3514.

Reimer, J. D., Peixoto, R. S., Davies, S. W., Traylor-Knowles, N., Short, M. L., Cabral-Tena, R. A., Burt, J. A., Pessoa, I., Banaszak, A. T., & Winters, R. S. (2024). The Fourth Global Coral Bleaching Event: Where do we go from here? *Coral Reefs*, 1-5.

Reinert, G., Chew, D., Sun, F., & Waterman, M. S. (2009). Alignment-free sequence comparison (I): statistics and power. *Journal of Computational Biology*, *16*(12), 1615-1634.

Rellstab, C., Gugerli, F., Eckert, A. J., Hancock, A. M., & Holderegger, R. (2015). A practical guide to environmental association analysis in landscape genomics. *Molecular Ecology*, *24*(17), 4348-4370.

Rellstab, C., & Keller, S. R. (2024). Can We Use Genomic Data to Predict Maladaptation to Environmental Change? *Molecular Ecology Resources*, e14059.

Renaut, S., Grassa, C., Yeaman, S., Moyers, B., Lai, Z., Kane, N., Bowers, J., Burke, J., & Rieseberg, L. (2013). Genomic islands of divergence are not affected by geography of speciation in sunflowers. *Nature Communications*, *4*(1), 1827.

Rennison, D. J., & Peichel, C. L. (2022). Pleiotropy facilitates parallel adaptation in sticklebacks. *Molecular Ecology*, *31*(5), 1476-1486.

Reusch, T. B. (2014). Climate change in the oceans: evolutionary versus phenotypically plastic responses of marine animals and plants. *Evolutionary Applications*, *7*(1), 104-122.

Rezende, E. L., Bozinovic, F., Szilágyi, A., & Santos, M. (2020). Predicting temperature mortality and selection in natural *Drosophila* populations. *Science*, *369*(6508), 1242-1245.

Rezende, E. L., Castañeda, L. E., & Santos, M. (2014). Tolerance landscapes in thermal ecology. *Functional Ecology*, *28*(4), 799-809.

Richards, T. J., McGuigan, K., Aguirre, J. D., Humanes, A., Bozec, Y. M., Mumby, P. J., & Riginos, C. (2023). Moving beyond heritability in the search for coral adaptive potential. *Global Change Biology*, *29*(14), 3869-3882.

Richards, Z. T., & Day, J. C. (2018). Biodiversity of the Great Barrier Reef—how adequately is it protected? *PeerJ*, *6*, e4747.

Riegl, B., Johnston, M., Purkis, S., Howells, E., Burt, J., Steiner, S. C., Sheppard, C. R., & Bauman, A. (2018). Population collapse dynamics in *Acropora downingi*, an Arabian/Persian Gulf ecosystem-engineering coral, linked to rising temperature. *Global Change Biology*, *24*(6), 2447-2462.

Riginos, C., Hock, K., Matias, A. M., Mumby, P. J., van Oppen, M. J., & Lukoschek, V. (2019). Asymmetric dispersal is a critical element of concordance between biophysical dispersal models and spatial genetic structure in Great Barrier Reef corals. *Diversity and Distributions*, *25*(11), 1684-1696.

Riginos, C., Popovic, I., Meziere, Z., Garcia, V., Byrne, I., Howitt, S. M., Ishida, H., Bairos-Novak, K., Humanes, A., & Scharfenstein, H. (2024). Cryptic species and hybridisation in corals: challenges and opportunities for conservation and restoration. *Peer Community Journal*, *4*, Article e106.

Ritchie, R. J. (2008). Universal chlorophyll equations for estimating chlorophylls a, b, c, and d and total chlorophylls in natural assemblages of photosynthetic organisms using acetone, methanol, or ethanol solvents. *Photosynthetica*, *46*(1), 115-126.

Ritz, C., Baty, F., Streibig, J. C., & Gerhard, D. (2015). Dose-response analysis using R. *PloS One*, *10*(12), e0146021.

Robbins, S. J., Singleton, C. M., Chan, C. X., Messer, L. F., Geers, A. U., Ying, H., Baker, A., Bell, S. C., Morrow, K. M., & Ragan, M. A. (2019). A genomic view of the reef-building coral *Porites lutea* and its microbial symbionts. *Nature Microbiology*, *4*(12), 2090-2100.

Roberts Kingman, G. A., Vyas, D. N., Jones, F. C., Brady, S. D., Chen, H. I., Reid, K., Milhaven, M., Bertino, T. S., Aguirre, W. E., & Heins, D. C. (2021). Predicting future from past: The genomic basis of recurrent and rapid stickleback evolution. *Science Advances*, *7*(25), eabg5285.

Roberty, S., Fransolet, D., Cardol, P., Plumier, J.-C., & Franck, F. (2015). Imbalance between oxygen photoreduction and antioxidant capacities in *Symbiodinium* cells exposed to combined heat and high light stress. *Coral Reefs*, *34*, 1063-1073.

Roberty, S., & Plumier, J.-C. (2022). Bleaching physiology: who's the 'weakest link'—host vs. symbiont? *Emerging Topics in Life Sciences*, *6*(1), 17-32.

Rogivue, A., Leempoel, K., Guillaume, A. S., Choudhury, R. R., Felber, F., Kasser, M., Joost, S., Parisod, C., & Gugerli, F. (2025). Locally Specific Genome-Wide Signatures of Adaptation to Environmental Variation at High Resolution in an Alpine Plant. *Molecular Ecology*, *34*(4), e17646.

Rohatgi, A. (2014). WebPlotDigitizer user manual version 3.4. *URL http://arohatgi. info/WebPlotDigitizer/app*, 1-18.

Rohwer, F., Seguritan, V., Azam, F., & Knowlton, N. (2002). Diversity and distribution of coral-associated bacteria. *Marine Ecology Progress Series*, *243*, 1-10.

RORC. (2024). *Résultats 2024 du Réseau d'Observation des Récifs Coralliens*. ANCB. Retrieved 01/05/2025 from https://www.ancb.nc/resultats-2024-du-reseau-dobservation-des-recifs-coralliens-rorc

Rose, N. H., Bay, R. A., Morikawa, M. K., & Palumbi, S. R. (2018). Polygenic evolution drives species divergence and climate adaptation in corals. *Evolution*, *72*(1), 82-94.

Rose, N. H., Bay, R. A., Morikawa, M. K., Thomas, L., Sheets, E. A., & Palumbi, S. R. (2021). Genomic analysis of distinct bleaching tolerances among cryptic coral species. *Proceedings of the Royal Society B*, *288*(1960), 20210678.

Rosenblum, E. B., Parent, C. E., & Brandt, E. E. (2014). The molecular basis of phenotypic convergence. *Annual Review of Ecology, Evolution, and Systematics*, *45*(1), 203-226.

Rousset. (1999). Genetic differentiation between individuals. *Journal of Evolutionary Biology*, *13*(1), 58-62.

Rousset, F. (1997). Genetic differentiation and estimation of gene flow from F-statistics under isolation by distance. *Genetics*, *145*(4), 1219-1228.

Ruiz Sebastián, C., & O'ryan, C. (2001). Single-cell sequencing of dinoflagellate (Dinophyceae) nuclear ribosomal genes. *Molecular Ecology Notes*, *1*(4), 329-331.

Rumberger, C., Armstrong, M., Kim, M., Ponce, R., Melendez, J., DeBiasse, M., Caplins, S., & Bay, R. (2025). Selection Over Small and Large Spatial Scales in the Face of High Gene Flow. *Molecular Ecology*, *34*(6), e17700.

Saint-Amand, A., Lambrechts, J., & Hanert, E. (2023). Biophysical models resolution affects coral connectivity estimates. *Scientific Reports*, *13*(1), 9414.

Salmón, P., Jacobs, A., Ahrén, D., Biard, C., Dingemanse, N. J., Dominoni, D. M., Helm, B., Lundberg, M., Senar, J. C., & Sprau, P. (2021). Continent-wide genomic signatures of adaptation to urbanisation in a songbird across Europe. *Nature Communications*, *12*(1), 2983.

Sampayo, E., Ridgway, T., Bongaerts, P., & Hoegh-Guldberg, O. (2008). Bleaching susceptibility and mortality of corals are determined by fine-scale differences in symbiont type. *Proceedings of the National Academy of Sciences*, *105*(30), 10444-10449.

Sampayo, E. M., Franceschinis, L., Hoegh-Guldberg, O., & Dove, S. (2007). Niche partitioning of closely related symbiotic dinoflagellates. *Molecular Ecology*, *16*(17), 3721-3733.

Samuk, K., Owens, G. L., Delmore, K. E., Miller, S. E., Rennison, D. J., & Schluter, D. (2017). Gene flow and selection interact to promote adaptive divergence in regions of low recombination. *Molecular Ecology*, *26*(17), 4378-4390.

Santure, A. W., & Garant, D. (2018). Wild GWAS—association mapping in natural populations. *Molecular Ecology Resources*, *18*(4), 729-738.

Savtchenko, A., Ouzounov, D., Ahmad, S., Acker, J., Leptoukh, G., Koziana, J., & Nickless, D. (2004). Terra and Aqua MODIS products available from NASA GES DAAC. *Advances in Space Research*, *34*(4), 710-714.

Schlötterer, C., Kofler, R., Versace, E., Tobler, R., & Franssen, S. (2015). Combining experimental evolution with next-generation sequencing: a powerful tool to study adaptation from standing genetic variation. *Heredity*, *114*(5), 431-440.

Schluter, D., & Conte, G. L. (2009). Genetics and ecological speciation. *Proceedings of the National Academy of Sciences*, *106*(supplement_1), 9955-9962.

Schmidt, T. L., Thia, J. A., & Hoffmann, A. A. (2024). How can genomics help or hinder wildlife conservation? *Annual Review of Animal Biosciences*, *12*(1), 45-68.

Schneller, N. M., Strugnell, J. M., Field, M. A., Johannesson, K., & Cooke, I. (2025). Putting Structural Variants Into Practice: The Role of Chromosomal Inversions in the Management of Marine Environments. *Molecular Ecology*, e17776.

Schoepf, V., Sanderson, H., & Larcombe, E. (2021). Coral heat tolerance under variable temperatures: Effects of different variability regimes and past environmental history vs. current exposure. *Limnology and Oceanography*, *67*(2), 404-418.

Schoepf, V., Stat, M., Falter, J. L., & McCulloch, M. T. (2015). Limits to the thermal tolerance of corals adapted to a highly fluctuating, naturally extreme temperature environment. *Scientific Reports*, *5*(1), 1-14.

Scott, C. B., Schott, R., & Matz, M. V. (2024). Cryptic genetic structure of the coral host is the primary driver of holobiont assembly in massive *Porites*. *BioRxiv*, 2024.2001. 2009.574877.

Scucchia, F., Zaslansky, P., Boote, C., Doheny, A., Mass, T., & Camp, E. F. (2023). The role and risks of selective adaptation in extreme coral habitats. *Nature Communications*, *14*(1), 4475.

Seath, D. (1947). Heritability of heat tolerance in dairy cattle. *Journal of Dairy Science*, *30*(3), 137-144.

Sellares Blasco, R. I., Villalpando, M. F., Guendulain-Garcia, S. D., & Cróquer, A. (2021). Assisted coral reproduction in the Dominican Republic: a successful story to replicate in the Caribbean. *Frontiers in Marine Science*, *8*, 927.

Selmoni, O., Bay, L. K., Exposito-Alonso, M., & Cleves, P. A. (2024a). Finding genes and pathways that underlie coral adaptation. *Trends in genetics*, *40*(3), 213-227.

Selmoni, O., Cleves, P. A., & Exposito-Alonso, M. (2024b). Global coral genomic vulnerability explains recent reef losses. *BioRxiv*, 2024.2003. 2025.586253.

Selmoni, O., Lecellier, G., Magalon, H., Vigliola, L., Oury, N., Benzoni, F., Peignon, C., Joost, S., & Berteaux-Lecellier, V. (2021). Seascape genomics reveals candidate molecular targets of heat stress adaptation in three coral species. *Molecular Ecology*, *30*(8), 1892-1906.

Selmoni, O., Rochat, E., Lecellier, G., Berteaux-Lecellier, V., & Joost, S. (2020a). Seascape genomics as a new tool to empower coral reef conservation strategies: An example on north-western Pacific *Acropora digitifera*. *Evolutionary Applications*, *13*(8), 1923-1938.

Selmoni, O., Vajana, E., Guillaume, A., Rochat, E., & Joost, S. (2020b). Sampling strategy optimization to increase statistical power in landscape genomics: A simulation-based approach. *Molecular Ecology Resources*, *20*(1), 154-169.

Shah, S., Dougan, K. E., Chen, Y., Lo, R., Laird, G., Fortuin, M. D., Rai, S. K., Murigneux, V., Bellantuono, A. J., & Rodriguez-Lanetty, M. (2024). Massive genome reduction predates the divergence of Symbiodiniaceae dinoflagellates. *The ISME Journal*, *18*(1), wrae059.

Shaw, E. C., Carpenter, R. C., Lantz, C. A., & Edmunds, P. J. (2016). Intraspecific variability in the response to ocean warming and acidification in the scleractinian coral *Acropora pulchra*. *Marine Biology*, *163*, 1-11.

Shi, Y., Bouska, K. L., McKinney, G. J., Dokai, W., Bartels, A., McPhee, M. V., & Larson, W. A. (2023). Gene flow influences the genomic architecture of local adaptation in six riverine fish species. *Molecular Ecology*, *32*(7), 1549-1566.

Shlesinger, T., & van Woesik, R. (2023). Oceanic differences in coral-bleaching responses to marine heatwaves. *Science of The Total Environment*, 162113.

Shoguchi, E., Shinzato, C., Kawashima, T., Gyoja, F., Mungpakdee, S., Koyanagi, R., Takeuchi, T., Hisata, K., Tanaka, M., & Fujiwara, M. (2013). Draft assembly of the *Symbiodinium minutum* nuclear genome reveals dinoflagellate gene structure. *Current Biology*, *23*(15), 1399-1408.

Siebeck, U., Marshall, N., Klüter, A., & Hoegh-Guldberg, O. (2006). Monitoring coral bleaching using a colour reference card. *Coral Reefs*, *25*, 453-460.

Simillion, C., Liechti, R., Lischer, H. E., Ioannidis, V., & Bruggmann, R. (2017). Avoiding the pitfalls of gene set enrichment analysis with SetRank. *BMC Bioinformatics*, *18*(1), 151.

Sinervo, B., Mendez-De-La-Cruz, F., Miles, D. B., Heulin, B., Bastiaans, E., Villagrán-Santa Cruz, M., Lara-Resendiz, R., Martínez-Méndez, N., Calderón-Espinosa, M. L., & Meza-Lázaro, R. N. (2010). Erosion of lizard diversity by climate change and altered thermal niches. *Science*, *328*(5980), 894-899.

Slatkin, M. (1987). Gene flow and the geographic structure of natural populations. *Science*, *236*(4803), 787-792.

Slavov, G. T., Macaya-Sanz, D., DiFazio, S. P., & Howe, G. T. (2024). Population structure limits inferences from genomic prediction and genome-wide association studies in a forest tree. *BioRxiv*, 2024.2010. 2011.617670.

Smith, E. G., Hazzouri, K. M., Choi, J. Y., Delaney, P., Al-Kharafi, M., Howells, E. J., Aranda, M., & Burt, J. A. (2022). Signatures of selection underpinning rapid coral adaptation to the world warmest reefs. *Science Advances*, *8*(2), eabl7287. https://doi.org/doi:10.1126/sciadv.abl7287

Somero, G. (2010). The physiology of climate change: how potentials for acclimatization and genetic adaptation will determine 'winners' and 'losers'. *Journal of Experimental Biology*, *213*(6), 912-920.

Sopniewski, J., & Catullo, R. A. (2024). Estimates of heterozygosity from single nucleotide polymorphism markers are context-dependent and often wrong. *Molecular Ecology Resources*, *24*(4), e13947.

Soto, J., Pinilla, F., Olguín, P., & Castañeda, L. E. (2025). Genetic Architecture of the Thermal Tolerance Landscape in *Drosophila melanogaster*. *Molecular Ecology*, *34*(7), e17697.

Souter, D., Planes, S., Wicquart, J., Logan, M., Obura, D., & Staub, F. (2021). Status of coral reefs of the world: 2020. In: Global Coral Reef Monitoring Network (GCRMN) and International Coral Reef Initiative (ICRI).

Stamatakis, A. (2014). RAxML version 8: a tool for phylogenetic analysis and post-analysis of large phylogenies. *Bioinformatics*, *30*(9), 1312-1313.

Stat, M., Carter, D., & Hoegh-Guldberg, O. (2006). The evolutionary history of *Symbiodinium* and scleractinian hosts—symbiosis, diversity, and the effect of climate change. *Perspectives in Plant Ecology, Evolution and Systematics*, *8*(1), 23-43.

Stat, M., Loh, W., LaJeunesse, T., Hoegh-Guldberg, O., & Carter, D. (2009). Stability of coral–endosymbiont associations during and after a thermal stress event in the southern Great Barrier Reef. *Coral Reefs*, *28*, 709-713.

Stern, D. B., Anderson, N. W., Diaz, J. A., & Lee, C. E. (2022). Genome-wide signatures of synergistic epistasis during parallel adaptation in a Baltic Sea copepod. *Nature Communications*, *13*(1), 4024.

Stern, D. L. (2013). The genetic causes of convergent evolution. *Nature Reviews Genetics*, *14*(11), 751-764.

Stoeckl, N., Hicks, C. C., Mills, M., Fabricius, K., Esparon, M., Kroon, F., Kaur, K., & Costanza, R. (2011). The economic value of ecosystem services in the Great Barrier Reef: our state of knowledge. *Annals of the New York Academy of Sciences*, *1219*(1), 113-133.

Strader, M. A.-O., & Quigley, K. A.-O. (2022). The role of gene expression and symbiosis in reef-building coral acquired heat tolerance. (2041-1723 (Electronic)).

Strobl, C., Boulesteix, A.-L., Zeileis, A., & Hothorn, T. (2007). Bias in random forest variable importance measures: Illustrations, sources and a solution. *BMC Bioinformatics*, *8*(1), 1-21.

Suggett, D. J., & van Oppen, M. J. (2022). Horizon scan of rapidly advancing coral restoration approaches for 21st century reef management. *Emerging Topics in Life Sciences*.

Sully, S., Burkepile, D. E., Donovan, M., Hodgson, G., & van Woesik, R. (2019). A global analysis of coral bleaching over the past two decades. *Nature Communications*, *10*(1), 1-5.

Sully, S., Hodgson, G., & van Woesik, R. (2022). Present and future bright and dark spots for coral reefs through climate change. *Global Change Biology*, *28*(15), 4509-4522.

Tak, Y. G., & Farnham, P. J. (2015). Making sense of GWAS: using epigenomics and genome engineering to understand the functional relevance of SNPs in non-coding regions of the human genome. *Epigenetics & chromatin*, *8*(1), 57.

Takahashi, S., Whitney, S. M., & Badger, M. R. (2009). Different thermal sensitivity of the repair of photodamaged photosynthetic machinery in cultured *Symbiodinium* species. *Proceedings of the National Academy of Sciences*, *106*(9), 3237-3242.

Takano, Y., & Horiguchi, T. (2006). Acquiring scanning electron microscopical, light microscopical and multiple gene sequence data from a single dinoflagellate cell 1. *Journal of phycology*, *42*(1), 251-256.

Tam, V., Patel, N., Turcotte, M., Bossé, Y., Paré, G., & Meyre, D. (2019). Benefits and limitations of genome-wide association studies. *Nature Reviews Genetics*, *20*(8), 467-484.

Teague, J., Willans, J., Allen, M., Scott, T., & Day, J. (2019). Applied marine hyperspectral imaging; Coral Bleaching from a spectral viewpoint. *Spectrosc. Eur*, *31*, 13-17.

Theissinger, K., Fernandes, C., Formenti, G., Bista, I., Berg, P. R., Bleidorn, C., Bombarely, A., Crottini, A., Gallo, G. R., & Godoy, J. A. (2023). How genomics can help biodiversity conservation. *Trends in genetics*, *39*(7), 545-559.

Thomas, C. D., Franco, A. M., & Hill, J. K. (2006). Range retractions and extinction in the face of climate warming. *Trends in Ecology & Evolution*, *21*(8), 415-416.

Thomas, L., Kennington, W. J., Evans, R. D., Kendrick, G. A., & Stat, M. (2017). Restricted gene flow and local adaptation highlight the vulnerability of high-latitude reefs to rapid environmental change. *Global Change Biology*, *23*(6), 2197-2205.

Thomas, L., Rose, N. H., Bay, R. A., López, E. H., Morikawa, M. K., Ruiz-Jones, L., & Palumbi, S. R. (2018). Mechanisms of thermal tolerance in reef-building corals across a fine-grained environmental mosaic: lessons from Ofu, American Samoa. *Frontiers in Marine Science*, *4*, 434.

Thomas, L., Underwood, J., Rose, N. H., Fuller, Z. L., Dugal, L., Grimaldi, C., Richards, Z. T., Cooke, I. R., Palumbi, S. R., & Gilmour, J. (2021). Mechanisms of ecological divergence with gene flow in a reef-building coral on an isolated atoll in Western Australia. *BioRxiv*.

Thomas, L., Underwood, J. N., Rose, N. H., Fuller, Z. L., Richards, Z. T., Dugal, L., Grimaldi, C. M., Cooke, I. R., Palumbi, S. R., & Gilmour, J. P. (2022). Spatially varying selection between habitats drives physiological shifts and local adaptation in a broadcast spawning coral on a remote atoll in Western Australia. *Science Advances*, *8*(17), eabl9185.

Thompson, A. M., Stathakopoulos, A., Hollister, K. J., Lynch, A. M., Holder, J. C., & Kuffner, I. B. (2025). Acute heat stress and the extirpation of a threatened coral species from a remote, subtropical reef system. *Coral Reefs*, 1-8.

Thompson, D. M., & van Woesik, R. (2009). Corals escape bleaching in regions that recently and historically experienced frequent thermal stress. *Proceedings of the Royal Society B: Biological Sciences*, *276*(1669), 2893-2901.

Thompson, J. R., Rivera, H. E., Closek, C. J., & Medina, M. (2015). Microbes in the coral holobiont: partners through evolution, development, and ecological interactions. *Frontiers in cellular and infection microbiology*, *4*, 176. https://www.ncbi.nlm.nih.gov/pmc/articles/PMC4286716/pdf/fcimb-04-00176.pdf

Thornhill, D. J., Howells, E., Wham, D., Steury, T., & Santos, S. (2017). Population genetics of reef coral endosymbionts (*Symbiodinium*, Dinophyceae). *Molecular Ecology*, *26*(10), 2640-2659.

Thornhill, D. J., Lewis, A. M., Wham, D. C., & LaJeunesse, T. C. (2014). Host-specialist lineages dominate the adaptive radiation of reef coral endosymbionts. *Evolution*, *68*(2), 352-367.

Tigano, A., & Friesen, V. L. (2016). Genomics of local adaptation with gene flow. *Molecular Ecology*, *25*(10), 2144-2164.

Todd, P. A. (2008). Morphological plasticity in scleractinian corals. *Biological Reviews*, *83*(3), 315-337.

Todesco, M., Owens, G. L., Bercovich, N., Légaré, J.-S., Soudi, S., Burge, D. O., Huang, K., Ostevik, K. L., Drummond, E. B., & Imerovski, I. (2020). Massive haplotypes underlie ecotypic differentiation in sunflowers. *Nature*, *584*(7822), 602-607.

Torda, G., Donelson, J. M., Aranda, M., Barshis, D. J., Bay, L., Berumen, M. L., Bourne, D. G., Cantin, N., Foret, S., & Matz, M. (2017). Rapid adaptive responses to climate change in corals. *Nature Climate Change*, *7*(9), 627-636.

Torkamaneh, D., & Belzile, F. (2022). *Genome-Wide Association Studies*. Methods in Molecular Biology.

Torkamani, A., Wineinger, N. E., & Topol, E. J. (2018). The personal and clinical utility of polygenic risk scores. *Nature Reviews Genetics*, *19*(9), 581-590.

Tsuchiya, K., Zayasu, Y., Nakajima, Y., Arakaki, N., Suzuki, G., Satoh, N., & Shinzato, C. (2022). Genomic analysis of a reef-building coral, *Acropora digitifera*, reveals complex population structure and a migration network in the Nansei Islands, Japan. *Molecular Ecology*, *31*(20), 5270-5284.

Turbek, S. P., Bossu, C., Rayne, C., Gruppi, C., Kus, B. E., Whitfield, M., Smith, T. B., Paxton, E. H., Bay, R. A., & Ruegg, K. C. (2023). Historical DNA reveals climate adaptation in an endangered songbird. *Nature Climate Change*, *13*(7), 735-741.

Turnham, K. E., Lewis, A. M., Kemp, D. W., Warner, M. E., Wham, D. F., Smith, R. T., Hoadley, K., Colin, P. L., Golbuu, Y., & LaJeunesse, T. C. (2025). Limited persistence of the heat-tolerant zooxanthella, *Durusdinium trenchii*, in corals transplanted to a barrier reef where it is rare among natal colonies. *Coral Reefs*, 1-16.

Uffelmann, E., Huang, Q. Q., Munung, N. S., De Vries, J., Okada, Y., Martin, A. R., Martin, H. C., Lappalainen, T., & Posthuma, D. (2021). Genome-wide association studies. *Nature Reviews Methods Primers*, *1*(1), 59.

UNEP-WCMC, W.-C. (2010). WRI, & TNC.(2010). *Global distribution of warm-water coral reefs, compiled from multiple sources including the Millennium Coral Reef Mapping Project. Version*, *1*.

Van der Auwera, G. A., & O'Connor, B. D. (2020). *Genomics in the cloud: using Docker, GATK, and WDL in Terra*. O'Reilly Media.

van Hooidonk, R., Maynard, J., Tamelander, J., Gove, J., Ahmadia, G., Raymundo, L., Williams, G., Heron, S. F., & Planes, S. (2016). Local-scale projections of coral reef futures and implications of the Paris Agreement. *Scientific Reports*, *6*(1), 1-8.

van Oppen, M. J., Baker, A. C., Coffroth, M. A., & Willis, B. L. (2009). Bleaching resistance and the role of algal endosymbionts. In *Coral bleaching* (pp. 83-102). Springer.

van Oppen, M. J., & Blackall, L. L. (2019). Coral microbiome dynamics, functions and design in a changing world. *Nature Reviews Microbiology*, *17*(9), 557-567.

van Oppen, M. J., Bongaerts, P., Frade, P., Peplow, L. M., Boyd, S. E., Nim, H. T., & Bay, L. K. (2018). Adaptation to reef habitats through selection on the coral animal and its associated microbiome. *Molecular Ecology*, *27*(14), 2956-2971.

van Oppen, M. J., & Gates, R. D. (2006). Conservation genetics and the resilience of reef-building corals. *Molecular Ecology*, *15*(13), 3863-3883.

van Oppen, M. J., Gates, R. D., Blackall, L. L., Cantin, N., Chakravarti, L. J., Chan, W. Y., Cormick, C., Crean, A., Damjanovic, K., & Epstein, H. (2017). Shifting paradigms in restoration of the world's coral reefs. *Global Change Biology*, *23*(9), 3437-3448.

van Oppen, M. J., Oliver, J. K., Putnam, H. M., & Gates, R. D. (2015). Building coral reef resilience through assisted evolution. *Proceedings of the National Academy of Sciences*, *112*(8), 2307-2313.

van Oppen, M. J., Palstra, F. P., Piquet, A. M.-T., & Miller, D. J. (2001). Patterns of coral–dinoflagellate associations in *Acropora*: significance of local availability and physiology of *Symbiodinium* strains and host–symbiont selectivity. *Proceedings of the Royal Society of London. Series B: Biological Sciences*, *268*(1478), 1759-1767.

van Oppen, M. J., Willis, B. L., Van Rheede, T., & Miller, D. J. (2002). Spawning times, reproductive compatibilities and genetic structuring in the *Acropora aspera* group: evidence for natural hybridization and semi-permeable species boundaries in corals. *Molecular Ecology*, *11*(8), 1363-1376.

van Woesik, R., Shlesinger, T., Grottoli, A. G., Toonen, R. J., Vega Thurber, R., Warner, M. E., Marie Hulver, A., Chapron, L., McLachlan, R. H., & Albright, R. (2022). Coral-bleaching responses to climate change across biological scales. *Global Change Biology*, *28*(14), 4229-4250.

Vessaz, F., Marsh, C. J., Bijoux, J., Gendron, G., & Mason-Parker, C. (2022). Recovery trajectories of oceanic reef ecosystems following multiple mass coral bleaching events. *Marine Biology*, *169*(2), 1-14.

Virgen-Urcelay, A., & Donner, S. D. (2023). Increase in the extent of mass coral bleaching over the past half-century, based on an updated global database. *PloS One*, *18*(2), e0281719.

Visscher, P. M., Hemani, G., Vinkhuyzen, A. A., Chen, G.-B., Lee, S. H., Wray, N. R., Goddard, M. E., & Yang, J. (2014). Statistical power to detect genetic (co) variance of complex traits using SNP data in unrelated samples. *PLoS Genetics*, *10*(4), e1004269.

Vogt-Vincent, N. S., Rocha de Souza, M. S., Feloy, K., Toonen, R. J., & McManus, L. C. (2025). Growth rate and adaptive capacity, not just thermal tolerance, are critical for long-term coral persistence under climate change. *BioRxiv*, 2025.2009. 2024.678233.

Vollmer, S. V., Selwyn, J. D., Despard, B. A., & Roesel, C. L. (2023). Genomic signatures of disease resistance in endangered staghorn corals. *Science*, *381*(6665), 1451-1454. https://doi.org/doi:10.1126/science.adi3601

Voolstra, C. R., Buitrago-López, C., Perna, G., Cárdenas, A., Hume, B. C., Rädecker, N., & Barshis, D. J. (2020). Standardized short-term acute heat stress assays resolve historical differences in coral thermotolerance across microhabitat reef sites. *Global Change Biology*, *26*(8), 4328-4343.

Voolstra, C. R., Schlotheuber, M., Camp, E. F., Nitschke, M. R., Szereday, S., & Bejarano, S. (2025). Spatially restricted coral bleaching as an ecological manifestation of within-colony heterogeneity. *Communications biology*, *8*(1), 740. https://doi.org/10.1038/s42003-025-08150-4

Voolstra, C. R., Suggett, D. J., Peixoto, R. S., Parkinson, J. E., Quigley, K. M., Silveira, C. B., Sweet, M., Muller, E. M., Barshis, D. J., Bourne, D. G., & Aranda, M. (2021a). Extending the natural adaptive capacity of coral holobionts. *Nature Reviews Earth & Environment*. https://doi.org/10.1038/s43017-021-00214-3

Voolstra, C. R., Valenzuela, J. J., Turkarslan, S., Cárdenas, A., Hume, B. C., Perna, G., Buitrago-López, C., Rowe, K., Orellana, M. V., & Baliga, N. S. (2021b). Contrasting heat stress response patterns of coral holobionts across the Red Sea suggest distinct mechanisms of thermal tolerance. *Molecular Ecology*, *30*(18), 4466-4480.

Walker, N. S., Cornwell, B. H., Nestor, V., Armstrong, K. C., Golbuu, Y., & Palumbi, S. R. (2022a). Persistence of phenotypic responses to short-term heat stress in the tabletop coral *Acropora hyacinthus*. *PloS One*, *17*(9), e0269206.

Walker, N. S., Nestor, V., Golbuu, Y., & Palumbi, S. R. (2022b). Coral bleaching resistance variation is linked to differential mortality and skeletal growth during recovery. *Evolutionary Applications*, 16(12), 504-517.

Wallace, C. C. (1999). *Staghorn corals of the world: a revision of the coral genus Acropora (Scleractinia; Astrocoeniina; Acroporidae) worldwide, with emphasis on morphology, phylogeny and biogeography*. CSIRO publishing.

Wallace, C. C., Done, B. J., & Muir, P. R. (2012). Revision and catalogue of worldwide staghorn corals *Acropora* and *Isopora* (Scleractinia: Acroporidae) in the Museum of Tropical Queensland. *Memoirs of the Queensland Museum, Nature*, *57*, 1-255.

Wang, S., Zhang, L., Meyer, E., & Matz, M. V. (2009). Construction of a high-resolution genetic linkage map and comparative genome analysis for the reef-building coral *Acropora millepora*. *Genome biology*, *10*(11), R126.

Waples, R. (2024). The idiot's Guide to Effective Population Size. *Authorea Inc*, 1-51.

Waples, R. S., & Do, C. (2008). LDNE: a program for estimating effective population size from data on linkage disequilibrium. *Molecular Ecology Resources*, *8*(4), 753-756.

Waples, R. S., & Do, C. (2010). Linkage disequilibrium estimates of contemporary Ne using highly variable genetic markers: a largely untapped resource for applied conservation and evolution. *Evolutionary Applications*, *3*(3), 244-262.

Warner, M. E., & Suggett, D. J. (2016). The photobiology of *Symbiodinium* spp.: linking physiological diversity to the implications of stress and resilience. In *The Cnidaria, past, present and future* (pp. 489-509). Springer.

Warner, P. A., van Oppen, M. J., & Willis, B. L. (2015). Unexpected cryptic species diversity in the widespread coral *Seriatopora hystrix* masks spatial-genetic patterns of connectivity. *Molecular Ecology*, *24*(12), 2993-3008.

Weir, B. S., & Cockerham, C. C. (1984). Estimating F-statistics for the analysis of population structure. *Evolution*, 1358-1370.

Weis, V. M. (2008). Cellular mechanisms of Cnidarian bleaching: stress causes the collapse of symbiosis. *Journal of Experimental Biology*, *211*(19), 3059-3066.

Wellenreuther, M., & Bernatchez, L. (2018). Eco-evolutionary genomics of chromosomal inversions. *Trends in Ecology & Evolution*, *33*(6), 427-440.

Whitehouse, C. J., Taylor, R. M., Thistlethwaite, A., Zhang, H., Karimi-Busheri, F., Lasko, D. D., Weinfeld, M., & Caldecott, K. W. (2001). XRCC1 stimulates human polynucleotide kinase activity at damaged DNA termini and accelerates DNA single-strand break repair. *Cell*, *104*(1), 107-117.

Whiting, J. R., Booker, T. R., Rougeux, C., Lind, B. M., Singh, P., Lu, M., Huang, K., Whitlock, M. C., Aitken, S. N., & Andrew, R. L. (2024). The genetic architecture of repeated local adaptation to climate in distantly related plants. *Nature Ecology & Evolution*, 1-15.

Whitlock, M. C., & McCauley, D. E. (1999). Indirect measures of gene flow and migration: FST≠ 1/(4Nm+ 1). *Heredity*, *82*(2), 117-125.

Wickham, H. (2011). ggplot2. *Wiley Interdisciplinary Reviews: Computational Statistics*, *3*(2), 180-185.

Wiedenmann, J., D'Angelo, C., Smith, E. G., Hunt, A. N., Legiret, F.-E., Postle, A. D., & Achterberg, E. P. (2013). Nutrient enrichment can increase the susceptibility of reef corals to bleaching. *Nature Climate Change*, *3*(2), 160-164.

Wijgerde, T., van Melis, A., Silva, C. I., Leal, M. C., Vogels, L., Mutter, C., & Osinga, R. (2014). Red light represses the photophysiology of the scleractinian coral *Stylophora pistillata*. *PloS One*, *9*(3), e92781.

Williamson, D. H., Harrison, H. B., Almany, G. R., Berumen, M. L., Bode, M., Bonin, M. C., Choukroun, S., Doherty, P. J., Frisch, A. J., & Saenz-Agudelo, P. (2016). Large-scale, multidirectional larval connectivity among coral reef fish populations in the Great Barrier Reef Marine Park. *Molecular Ecology*, *25*(24), 6039-6054.

Winters, G., Holzman, R., Blekhman, A., Beer, S., & Loya, Y. (2009). Photographic assessment of coral chlorophyll contents: Implications for ecophysiological studies and coral monitoring. *Journal of Experimental Marine Biology and Ecology*, *380*(1-2), 25-35.

Wittkopp, P. J., & Kalay, G. (2012). Cis-regulatory elements: molecular mechanisms and evolutionary processes underlying divergence. *Nature Reviews Genetics*, *13*(1), 59-69.

Wood, S., Paris, C., Ridgwell, A., & Hendy, E. (2014). Modelling dispersal and connectivity of broadcast spawning corals at the global scale. *Global Ecology and Biogeography*, *23*(1), 1-11.

Woodhead, A. J., Hicks, C. C., Norström, A. V., Williams, G. J., & Graham, N. A. (2019). Coral reef ecosystem services in the Anthropocene. *Functional Ecology*, *33*(6), 1023-1034.

Woolsey, E., Keith, S., Byrne, M., Schmidt-Roach, S., & Baird, A. (2015). Latitudinal variation in thermal tolerance thresholds of early life stages of corals. *Coral Reefs*, *34*(2), 471-478.

Woolsey, E. S., Byrne, M., & Baird, A. H. (2013). The effects of temperature on embryonic development and larval survival in two scleractinian corals. *Marine Ecology Progress Series*, *493*, 179-184.

Wright, R. M., Mera, H., Kenkel, C. D., Nayfa, M., Bay, L. K., & Matz, M. V. (2019). Positive genetic associations among fitness traits support evolvability of a reef-building coral under multiple stressors. *Global Change Biology*, *25*(10), 3294-3304.

Wright, S. (1946). Isolation by distance under diverse systems of mating. *Genetics*, *31*(1), 39.

Wu, X., Bellagio, T., Peng, Y., Czech, L., Lin, M., Lang, P., Epstein, R., Abdelaziz, M., Alexander, J., & Caton-Darby, M. (2025). Rapid adaptation and extinction across climates in synchronized outdoor evolution experiments of *Arabidopsis thaliana*. *BioRxiv*, 2025.2005. 2028.654549.

Wu, Y., Zhou, Z., Pan, Y., Zhao, J., Bai, H., Chen, B., Zhang, X., Pu, F., Chen, J., & Xu, P. (2021). GWAS identified candidate variants and genes associated with acute heat tolerance of large yellow croaker. *Aquaculture*, *540*, 736696.

Wyatt, A. S., Leichter, J. J., Washburn, L., Kui, L., Edmunds, P. J., & Burgess, S. C. (2023). Hidden heatwaves and severe coral bleaching linked to mesoscale eddies and thermocline dynamics. *Nature Communications*, *14*(1), 1-17.

Xiao, L., Johansson, S., Rughöft, S., Burki, F., Sandin, M. M., Tenje, M., & Behrendt, L. (2022). Photophysiological response of Symbiodiniaceae single cells to temperature stress. *The ISME Journal*, 1-5.

Xiao, R., & Boehnke, M. (2009). Quantifying and correcting for the winner's curse in genetic association studies. *Genetic Epidemiology: The Official Publication of the International Genetic Epidemiology Society*, *33*(5), 453-462.

Yan, H., Sun, M., Zhang, Z., Jin, Y., Zhang, A., Lin, C., Wu, B., He, M., Xu, B., & Wang, J. (2023). Pangenomic analysis identifies structural variation associated with heat tolerance in pearl millet. *Nature Genetics*, *55*(3), 507-518.

Yang, J., Benyamin, B., McEvoy, B. P., Gordon, S., Henders, A. K., Nyholt, D. R., Madden, P. A., Heath, A. C., Martin, N. G., & Montgomery, G. W. (2010). Common SNPs explain a large proportion of the heritability for human height. *Nature Genetics*, *42*(7), 565-569.

Yang, Q., & Wang, Y. (2012). Methods for analyzing multivariate phenotypes in genetic association studies. *Journal of probability and statistics*, *2012*(1), 652569.

Ye, R., Huang, J., Wang, Z., Chen, Y., & Dong, Y. (2022). The role and mechanism of essential selenoproteins for homeostasis. *Antioxidants*, *11*(5), 973.

Yeaman, S. (2022). Evolution of polygenic traits under global vs local adaptation. *Genetics*, *220*(1), iyab134.

Yeaman, S., & Whitlock, M. C. (2011). The genetic architecture of adaptation under migration–selection balance. *Evolution*, *65*(7), 1897-1911.

Yoshioka, Y., Yamashita, H., Suzuki, G., Zayasu, Y., Tada, I., Kanda, M., Satoh, N., Shoguchi, E., & Shinzato, C. (2021). Whole-Genome Transcriptome Analyses of Native Symbionts Reveal Host Coral Genomic Novelties for Establishing Coral–Algae Symbioses. *Genome biology and evolution*, *13*(1), evaa240.

Yu, F., Peng, W., Tang, B., Zhang, Y., Wang, Y., Gan, Y., Luo, X., You, W., Gwo, J.-C., & Chen, N. (2021). A genome-wide association study of heat tolerance in Pacific abalone based on genome resequencing. *Aquaculture*, *536*, 736436.

Zhang, G.-l., & Zhang, S.-t. (2009). Bulked segregant analysis to detect QTL related to heat tolerance in rice (*Oryza sativa* L.) using SSR markers. *Agricultural sciences in China*, *8*(4), 482-487.

Zhang, J., Richards, Z. T., Adam, A. A., Chan, C. X., Shinzato, C., Gilmour, J., Thomas, L., Strugnell, J. M., Miller, D. J., & Cooke, I. (2022). Evolutionary responses of a reef-building coral to climate change at the end of the last glacial maximum. *Molecular Biology and Evolution*, *39*(10), msac201.

Zhang, J., Schneller, N. M., Field, M. A., Chan, C. X., Miller, D. J., Strugnell, J. M., Riginos, C., Bay, L., & Cooke, I. (2024a). Chromosomal inversions harbour excess mutational load in the coral, *Acropora kenti*, on the Great Barrier Reef. *Molecular Ecology*, *33*(16), e17468.

Zhang, W., Lu, T., Sladek, R., Li, Y., Najafabadi, H., & Dupuis, J. (2024b). SharePro: an accurate and efficient genetic colocalization method accounting for multiple causal signals. *Bioinformatics*, *40*(5), btae295.

Zhao, Y., Chen, F., Zhai, R., Lin, X., Wang, Z., Su, L., & Christiani, D. C. (2012). Correction for population stratification in random forest analysis. *International journal of epidemiology*, *41*(6), 1798-1806.

Zhou, X., & Stephens, M. (2014). Efficient multivariate linear mixed model algorithms for genome-wide association studies. *Nature methods*, *11*(4), 407-409.

Zinke, J., Gilmour, J. P., Fisher, R., Puotinen, M., Maina, J., Darling, E., Stat, M., Richards, Z. T., McClanahan, T. R., & Beger, M. (2018). Gradients of disturbance and environmental conditions shape coral community structure for south-eastern Indian Ocean reefs. *Diversity and Distributions*, *24*(5), 605-620.

Zou, H. (2011). *Characterization of selenium containing proteins in the coral Acropora millepora* James Cook University].

Appendices

Appendix A1. Supplementary data for Chapter 2

Supplementary Material and Methods

(a) Automated experimental system

The portable experimental system ("Seasim-in-a-box", Australian Institute of Marine Science, AIMS) consists of replicate 50-L acrylic tanks outfitted with insulating water jackets and supplied with 0.8 L. min[1] unfiltered seawater directly pumped from the ocean (Iwaki MX400). Each treatment sumps, with recirculating water supply to the insulating water jackets, were brought from ambient to target temperatures by heating elements (Omega 2kW titanium). In parallel, four distinct flow-through seawater were heated by convection via their titanium coil (Wateco 56″ titanium heat exchanger) placed in the sumps, and pumped to the replicate experimental tanks using submersible pumps (Reefe RP2400LV). Tanks were equipped with independent white/blue LED lighting (300 W) to supply ~ 300 µmol photons. $m^{-2}.s^{-1}$ with a diurnal light regime timed to *in-situ* conditions (11:13). Each tank was equipped with circulators (Tunze 6015), independent temperature probes (TC Direct PT-100) and PAR sensors (Skye Quantum PAR – SKL26250) to control temperature and lighting. The monitoring and control of temperature and lighting were achieved by a system Programmable Logic Controller (Siemens Simatic 571500), a Weidmuller UR20 Remote IO Signal Input and Outputs and a Human Machine Interface (HMI TP700 Comfort panel).

(b) Photosynthetic efficiency measurement

For each fragment, F_v/F_m values were extracted from 3 manually-selected non-overlapping areas from fluorescence images in ImagingWin v2.56 software using a custom PYTHON script to semi-automate the extraction. Fluorescence images underwent posterior quality checks and a subset of fragments was removed from the dataset due to technical artifacts. In addition, filtering steps were applied to remove i) F_v/F_m records above 0.81 as they exhibited an unexpected dependency between F_0 and F_v/F_m (Linear regression, $p < 0.001$, R^2=0.336) and were outliers relative to colony replicates, ii) coral fragments with F_v/F_m standard deviation > 0.2 among areas leading to high uncertainty on the mean F_v/F_m.

(c) Validation of chlorophyll measurements from hyperspectral imaging

Hyperspectral images were analysed using AIMS proprietary app in MATLAB software. Briefly, the pipeline consisted of normalizing reflectance within and across images using a colour reference in the image. Each coral fragment was then manually masked as a 2D- polygon and annotated with its unique identifier on RGB images using Image Processing Toolbox. Finally, reflectance measurements were individually extracted and averaged for each wavelength from pixels belonging to each fragment. We assessed the accuracy of hyperspectral imaging to estimate chlorophyll-a content in *A.spathulata* by independently measuring chlorophyll-a on a subset of individuals originating from two sites (Chicken Reef/Pelorus Island) and MMM/MMM+6 °C treatments. To this end, snap-frozen coral fragments at the end of the experiment were freeze-dried and crushed. For each fragment, an aliquot of homogenized powder was placed in 95% ethanol then sonicated in ultrasound bath (275 W, 20 kHz) and centrifuged (10000 g, 5min) to release chlorophyll content into solution. Chlorophyll a was quantified from absorbance measurements taken in a microplate spectrophotometer (Bio-tek Powerwave) using Ritchie. R. J equation (Ritchie, 2008) and standardised to dry weight. Finally, we performed a linear regression of NDVI on untransformed and log transformed chlorophyll-a content with a strong relationship between NDVI and log- transformed chlorophyll-a (R^2 = 0.74; Figure A1.7). To test whether the saturation of NDVI values at high chlorophyll concentrations could bias heat tolerance metrics, we assessed the relationship between NDVI retention under extreme heat (i.e., +9 °C/MMM) and initial fluorescence (F_0), another proxy of chlorophyll content (Matorin et al., 2004). Overall, there was a strong correlation between the two proxies (R = 0.93, Pearson correlation), supporting that this saturation had a minimal effect on NDVI metrics.

(d) Linear mixed effect models

The response of raw F_v/F_m and NDVI measurements to temperature across experiments was first assessed using a linear mixed effect model incorporating fixed effects of site, treatment, fragment size (estimated from pixel numbers in RGB images) and random intercepts for each colony and tank using package *lme4*, including 95% bootstrap confidence intervals for fixed effects (Table A1.3). Tanks were treated as a block factor in the analysis. Scale-location and Q-Q plots were used to confirm that homoscedasticity and normal distribution of the model residuals assumptions were met.

(e) Filtration of dose response curves

For a large proportion of colonies (F_v/F_m: 55%, NDVI: 21%) the decline in phenotypic traits was small or absent up to +6 °C above control temperatures, and less than 50% under +9 °C relative to MMM. This resulted in predicted ED50s outside the range of temperature treatments used in the experiments and wide confidence intervals (> 10 °C). Furthermore, log-logistic models could not be fitted for some of the most tolerant colonies because there was virtually no decline in traits even under +9 °C. In order to retain naturally tolerant individuals without artificially boosting reported variation in heat tolerance, we discarded from further analysis colonies that were both detected as an outlier based on the boxplot visualization method on the total distribution (ED50 < Q1-1.5*IQ or ED50>Q3+1.5*IQ) and had a confidence interval larger than 10 °C as well as colonies for which confidence interval computation failed indicative of lack of fit to the data (F_v/F_m: n = 20, NDVI: n = 40).

(f) Environmental data acquisition

Reef thermal history was characterised using the NOAA Coral Watch v3.1 sea surface temperature (SST) satellite product (1985–present; 5km) (NOAA Coral Reef Watch, 2018, updated daily) for thermal predictors based on historical climatology (MMM, DHW) as it has the largest temporal coverage. For contemporary thermal predictors (e.g., annual average and thermal range, 2014–present) we used the eReefs GBR1 Hydro model (CSIRO, 2020b) as it delivers temperature predictions at a finer spatial resolution (~1 km, hourly) and higher accuracy for the last decade (ME = 0.4–0.9 °C)[5]. Global averages (2010–2019) of environmental variables that may play a secondary role in heat tolerance (e.g., chlorophyll, turbidity, current velocity) were retrieved from eReefs GBR4 model (hourly; 4 km) (CSIRO, 2020a). In addition, we included the average cloud fraction (% of pixel masked by clouds) and cloud fraction anomaly for the 30 days prior to collection (Gonzalez-Espinosa & Donner, 2021) retrieved from NASA-MODIS 1°, monthly database (Savtchenko et al., 2004). Our environmental dataset also included variables measured at the individual colony level. Depths obtained from dive computers were adjusted to tide level at the time of collection (standardised to Lowest Astronomical Tide, Figure A1.9). Predictors derived from eReefs were computed at each colony depth through vertical interpolation from the model z-levels. As the GBR experienced a marine heatwave during the sampling campaign (0.47–4.67 DHW), we included pigmentation levels prior to collection as an explanatory variable to account for heat stress experienced in the weeks preceding the experiment (Figure A1.4).

(g) Validation of satellite and model temperature predictions

Temperature time-series from both sources were compared to *in-situ* records (1–3m depth, 13/14 sites) from *aimsdata* R package (Barneche et al., 2021). Depending on available *in-situ* records, daily time- series spanning between 1–7 years of the 2014–2022 period were aligned against eReefs and Coral Watch predictions to compute Pearson correlation coefficients (Figure A1.13). We also assessed the accuracy of eReefs at different time resolutions (hourly, daily, weekly, Figure A1.14). Overall, there was a good agreement of satellite observations and model predictions to *in-situ* measurements at a daily resolution ($R > 0.92$, 0). However, subtracting low frequency variability (daily and weekly averages) from hourly and daily temperatures resulted in low/moderate to strong daily correlations at some sites ($0.20< R <0.79$, 0) and no correlations ($R < 0.10$) at an hourly resolution except at two sites (Chicken Reef and Martin Reef). Therefore, we excluded temperature metrics based on hourly measurements (e.g. daily thermal range) from our environmental dataset.

(h) Random forest ensemble learning

Low correlated environmental predictors were used in the random forest approach (absolute Pearson's $R < 0.7$, Figure A1.5) as multicollinearity can introduce bias in evaluation of variables importance. When two metrics were highly correlated, the most ecologically relevant one (or conceptually simple) was kept based on literature of environmental drivers of heat tolerance. Random forest models were implemented using the cforest function from *party* R package (Hothorn et al., 2015). This package uses conditional inference trees in which permutation-based significance tests are used to split nodes (instead of information measure maximization), ensuring unbiased variable selection even when variables have different cardinality and scale of measurement (Strobl et al., 2007). Repeated 10-folds stratified (across sites) cross validation (70/30 split) was used to assess mean variables importance and model predictive accuracies. Random forest parameters were set as 1000 for the number of trees per forest (ntree) and 5 for the number of variables tried at each split (mtry) based on sensitivity analysis (Figure A1.15).

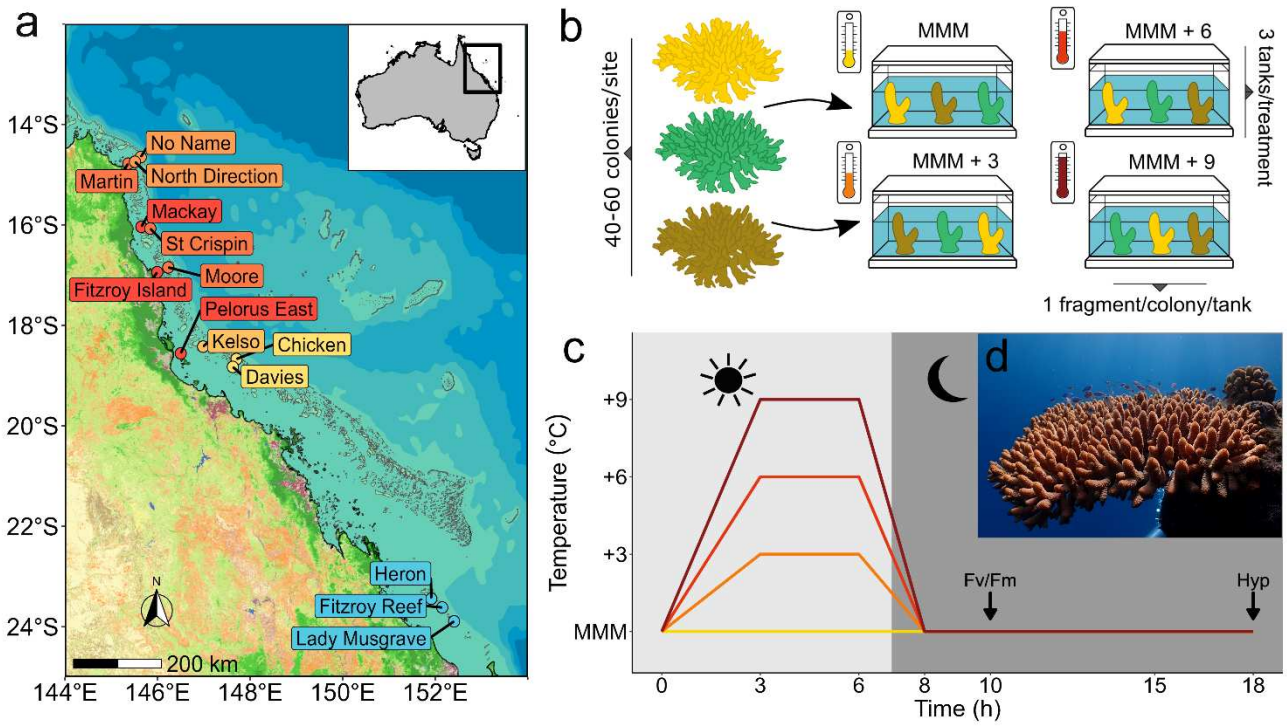


Figure A1.1. Location of sample sites and acute heat stress design to quantify variation in the heat tolerance of the reef-building coral *Acropora spathulata* on the Great Barrier Reef. (a) Map of the 14 reefs sampled across a latitudinal and thermal gradient. Isobaths of 0, 200, 1000 and 2000 m were obtained from the naturalearth 10 m resolution dataset and are represented in shades of blue. Coral reef locations were obtained from the UNEP database (UNEP-WCMC, 2010). Sites labels are coloured according to their maximum monthly mean (MMM) (dark red: > 28.5 °C, blue: < 27.5 °C). (b) A total of 768 coral colonies were measured in standardised acute heat stress experiments. 12 nubbins per colony were randomly divided among 3 tanks for each of 4 temperature treatments relative to the local MMM of each reef. (c) Standardised target temperature profiles to elicit increasing levels of heat stress, following Evensen et al. (2022). Arrows indicate the timing of physiological measurements of the maximum quantum yield of photosystem II (F_v/F_m) and hyperspectral imagery (Hyp). (d) Representative image of *A. spathulata* at Fitzroy Reef (credit: M. Grinblat).

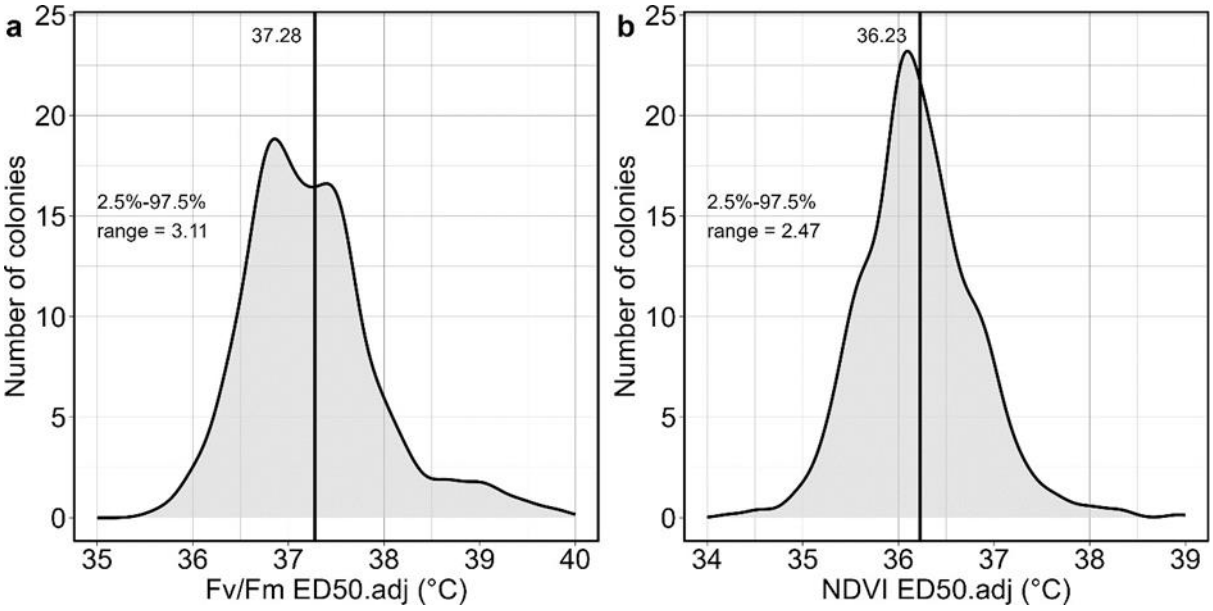


Figure A1.2. Within-site variation in heat tolerance measured on maximum quantum yield (*Fv/Fm*) and chlorophyll a content (NDVI). (a) Adjusted ED50 values from the total population (n = 13 sites) by subtracting site effect from the total variation. Vertical line indicates the mean value of the adjusted distribution and 2.5%–97.5% quartiles range is shown. (b) Same for NDVI.

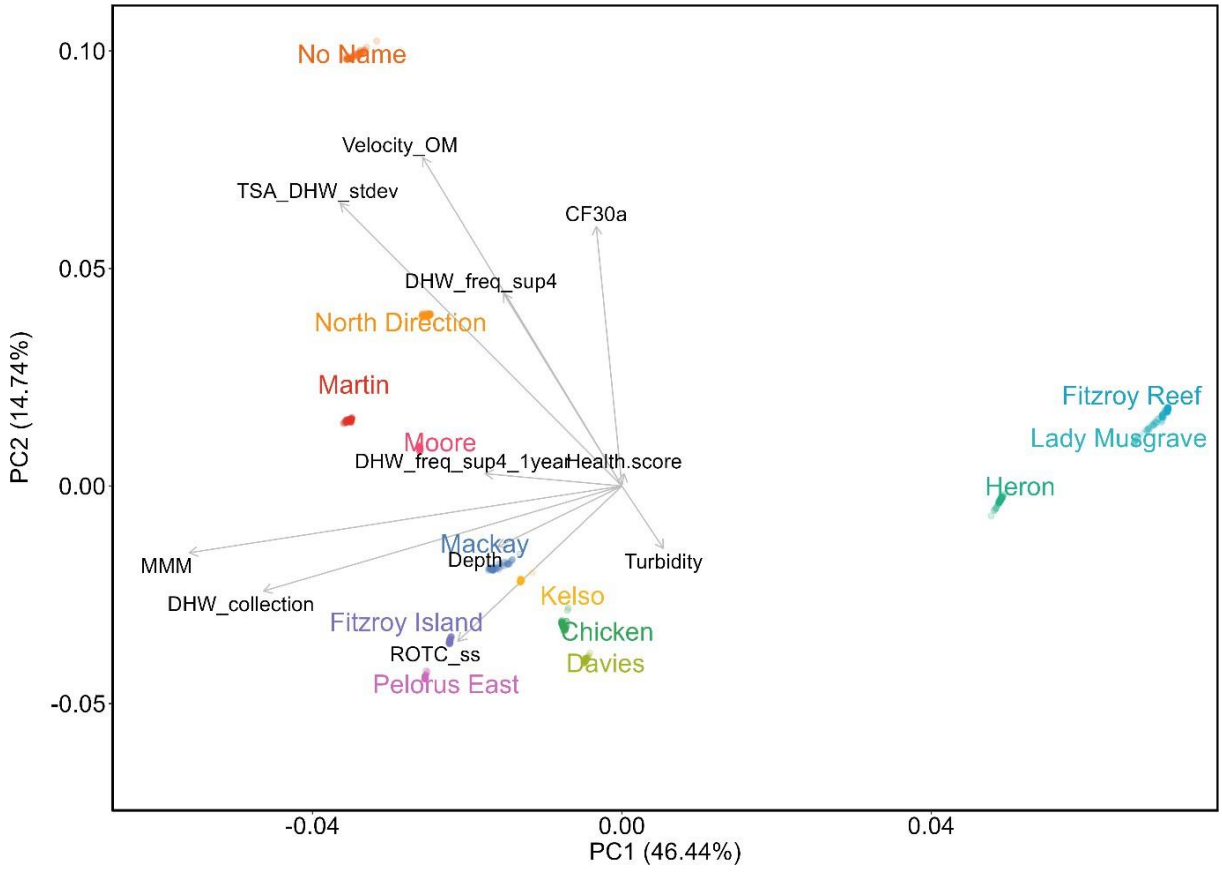


Figure A1.3. Principal component analysis conducted on 24 quantitative environmental predictors of *Acropora spathulata* heat tolerance metrics (n = 768 colonies sampled across the Great Barrier Reef, coloured by their reef of origin). Loadings projected on the first two

components are depicted with arrows for moderately correlated predictors (|R| < 0.7) for visualization purposes. CF30a = Cloud fraction anomaly for 30 days prior collection, DHW_collection = Degree Heating Weeks (DHW) at the day of collection, DHW_freq_sup4 = Frequency of DHW > 4, DHW_freq_sup4_1year = Frequency of DHW > 4 in the year prior collection, MMM = Maximum Monthly Mean (1985–1990+1993 climatology), ROTC_ss = Rate of temperature change in spring/summer, TSA_DHW_stdev = standard deviation of DHW. Numbers in parentheses represent the proportion of variance explained by each principal component.

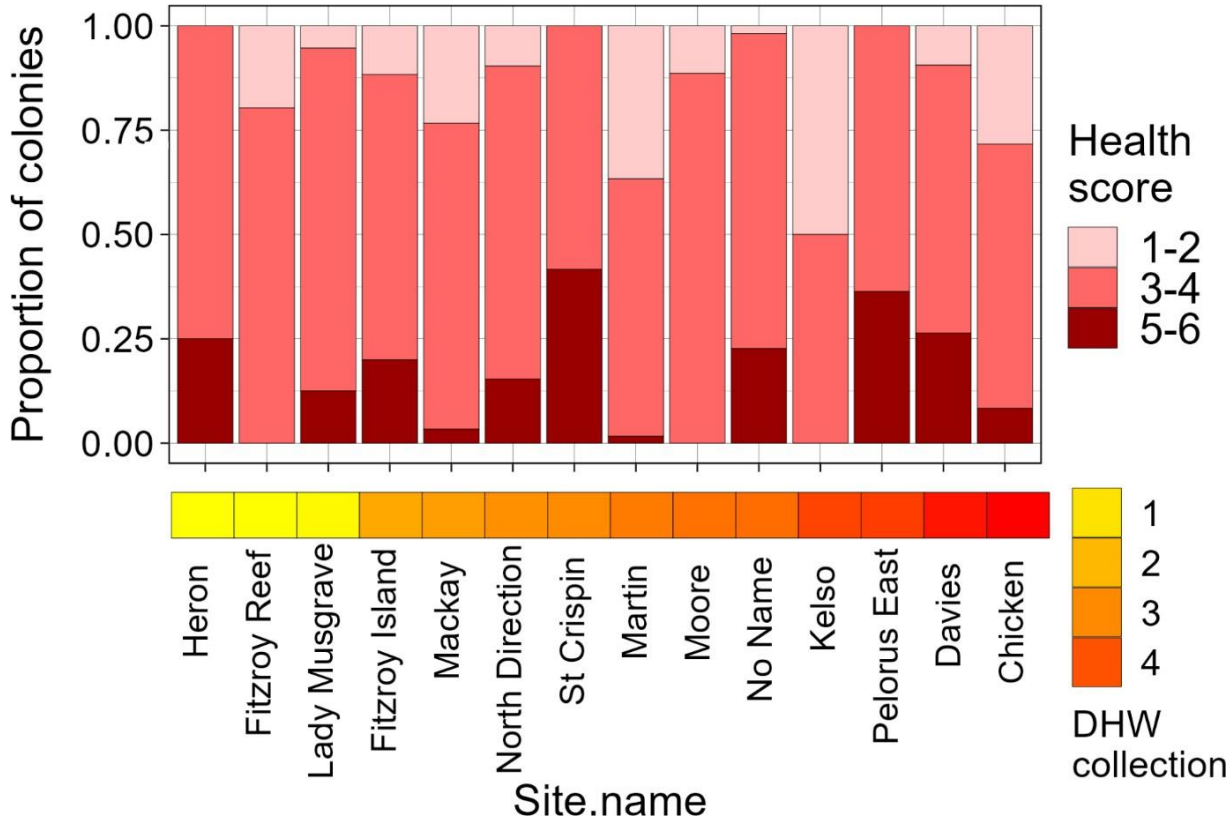


Figure A1.4. Pigmentation of *A.spathulata* colonies prior to collection at the 14 sites where acute heat stress assay was conducted. The stacked bar chart shows the proportion of individual that were assigned a health score from 1=most bleached to 6=least bleached using the Coral Health Chart. Health scores are grouped by 2 given the recording uncertainty. 1d heatmap shows ongoing Degree Heating Weeks (DHW) at the time colonies were collected, computed from NOAA Coral Watch v3.1 satellite product at 5km resolution.

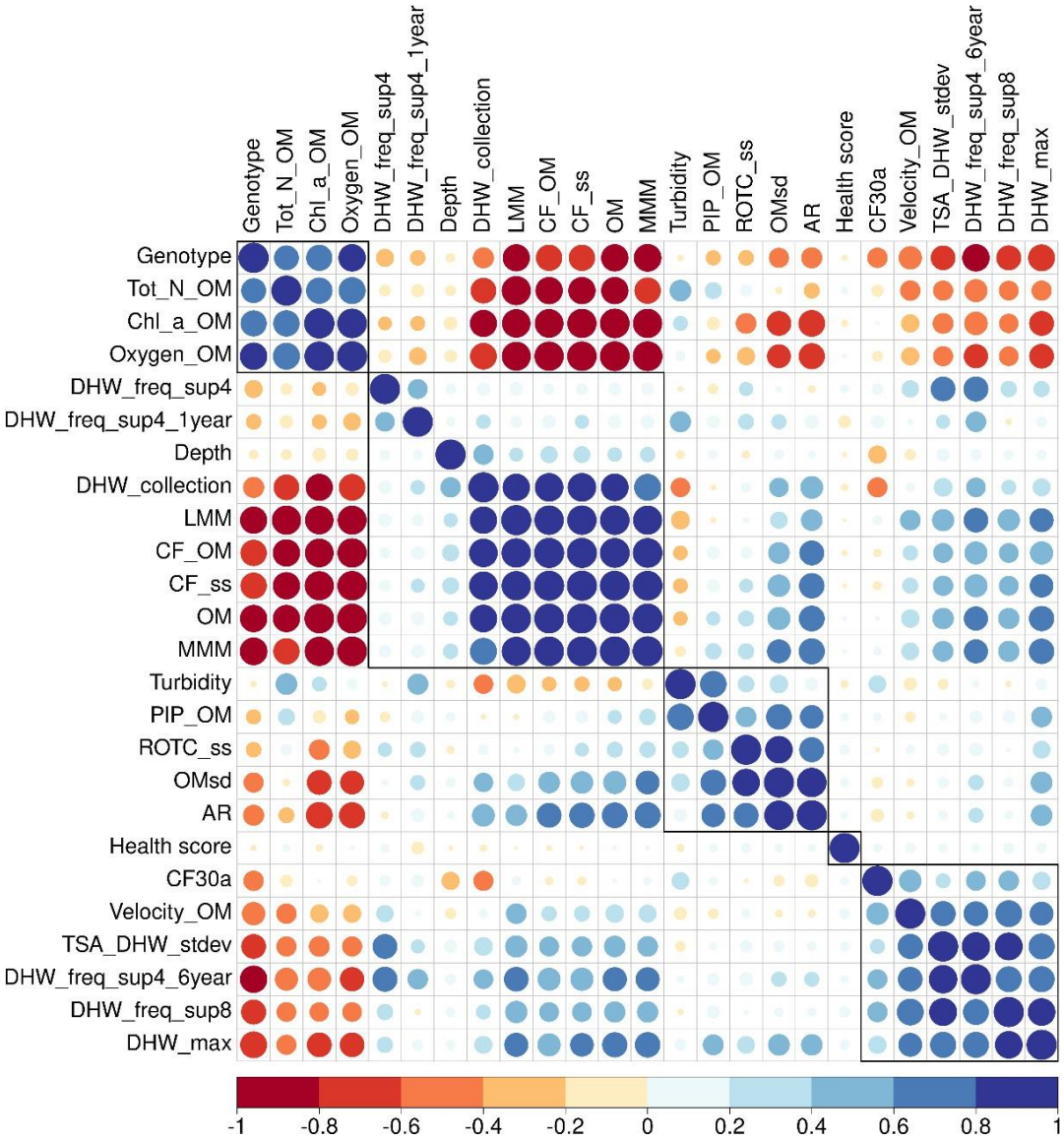


Figure A1.5. Pairwise Pearson's correlation coefficients between the 24 quantitative environmental predictors preliminarily extracted from various sources to assess environmental conditions experienced by *A.spathulata* colonies. Fourteen predictors were discarded from phenotype by environment models as they exhibited high collinearity with other covariates (absolute coefficient >0.7). For each pair of highly collinear variables, the most ecologically relevant one was kept in the model.



Figure A1.6. Picture of the automated acute heat stress system (Seasim-in-a- box, SSIAB) to conduct automated, high-throughput acute heat stress experiments on corals directly in the field. The system is set up on research vessels which enables to conduct large scale phenotyping of coral populations. Southern Great Barrier Reef, March 2022. ©AIMS Credit JoHurford 2022.

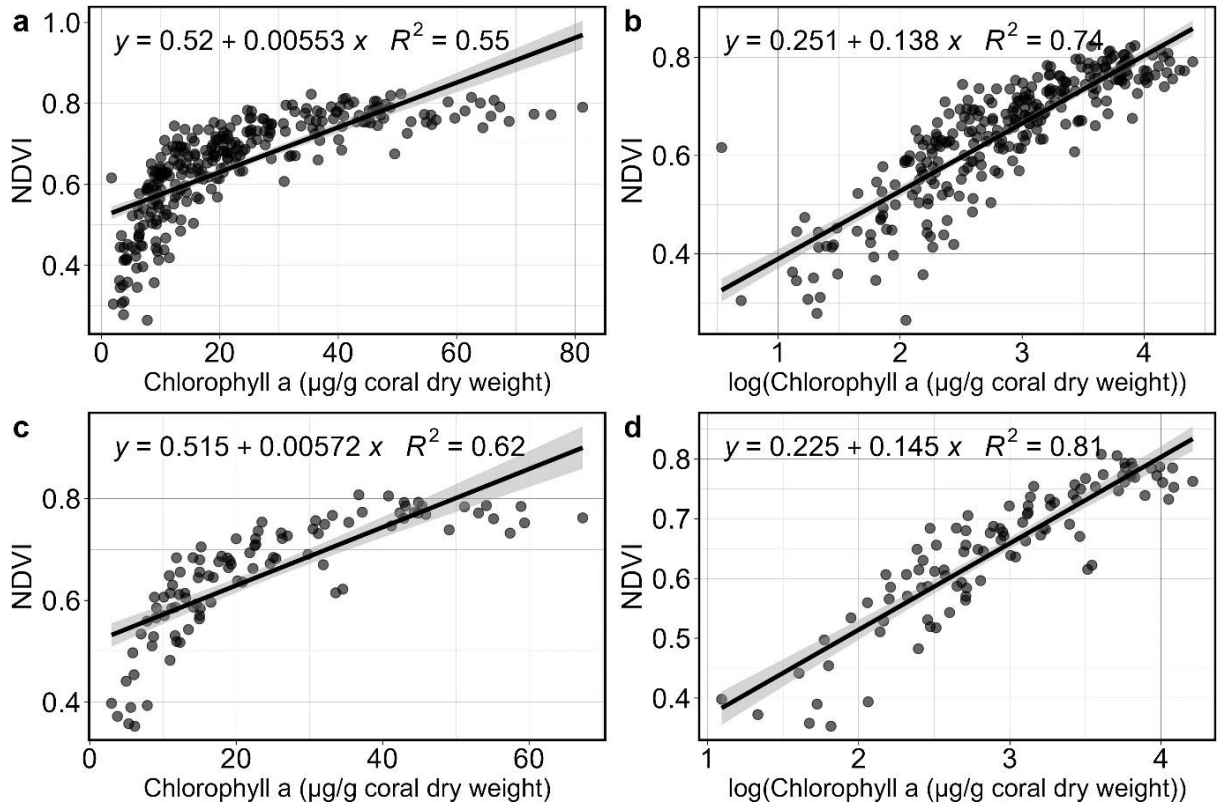


Figure A1.7. Validation of chlorophyll-a quantification using hyperspectral imaging on coral fragments at the end of the heat stress experiment. Correlation between (a) chlorophyll a and (b) log transformed chlorophyll a and the normalised difference vegetation index (NDVI) for a subset of *A.spathulata* samples (n = 285). Each point represents a single coral fragment originating from Chicken Reef or Pelorus Island and MMM or MMM+6 °C. The linear equation and coefficient of determination (R^2) are presented. (c) and (d) panels show the same correlation when values are averaged by colony and treatment (n = 3 fragment/colony/treatment).

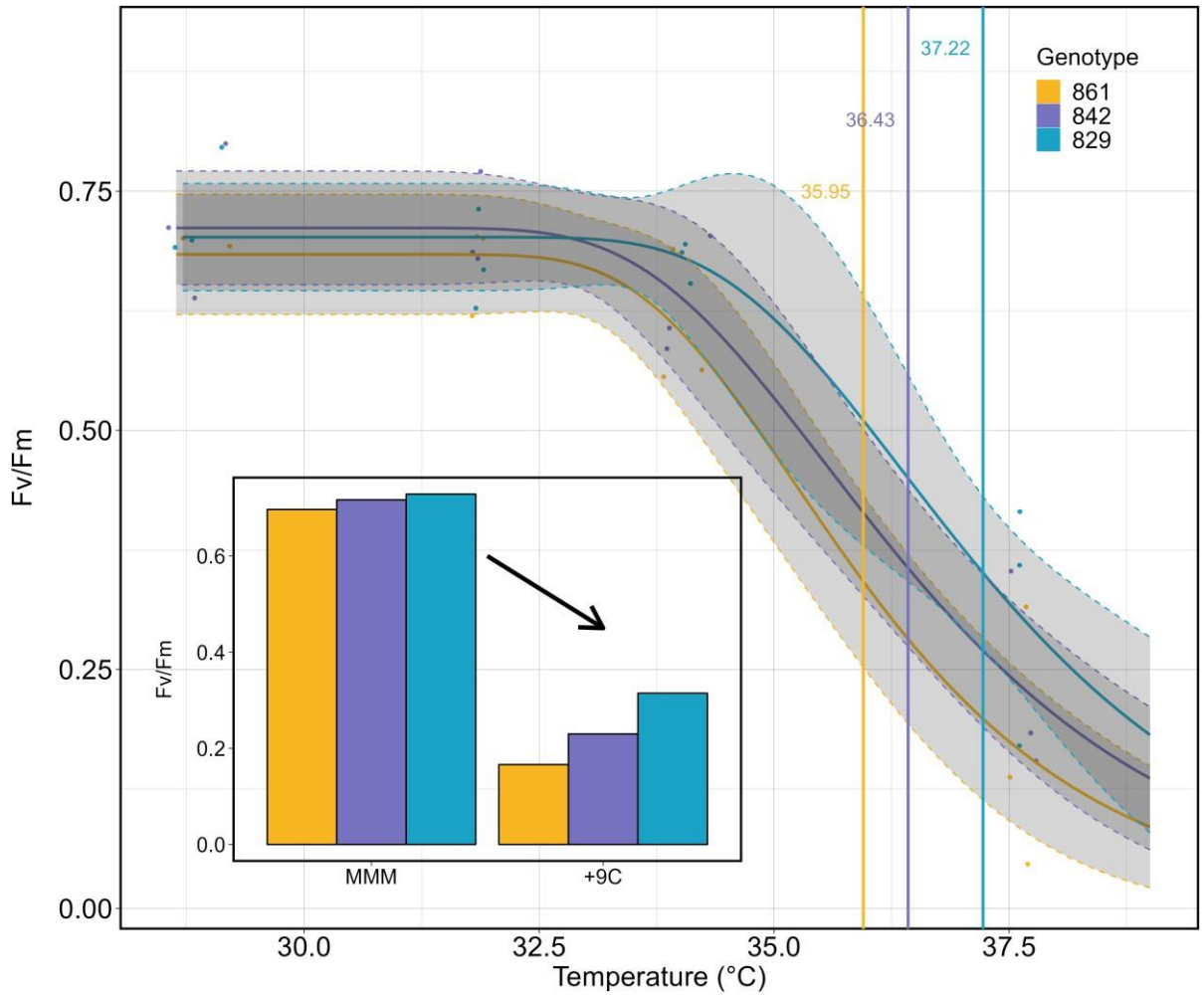


Figure A1.8. Principle of heat tolerance measurements on *Acropora spathulata* across the Great Barrier Reef with the example of maximum photosynthetic efficiency of microalgal symbionts (Fv/Fm). The main panel depicts how individual Fv/Fm measurements from replicate fragments across four temperature treatments are used to compute Effective dose 50 (ED50): the absolute temperature eliciting a 50% drop in Fv/Fm. ED50s are indicated by vertical bars. The inset shows the principle of performance retention under extreme heat as the ratio of Fv/Fm in the +9 °C to the MMM treatment.

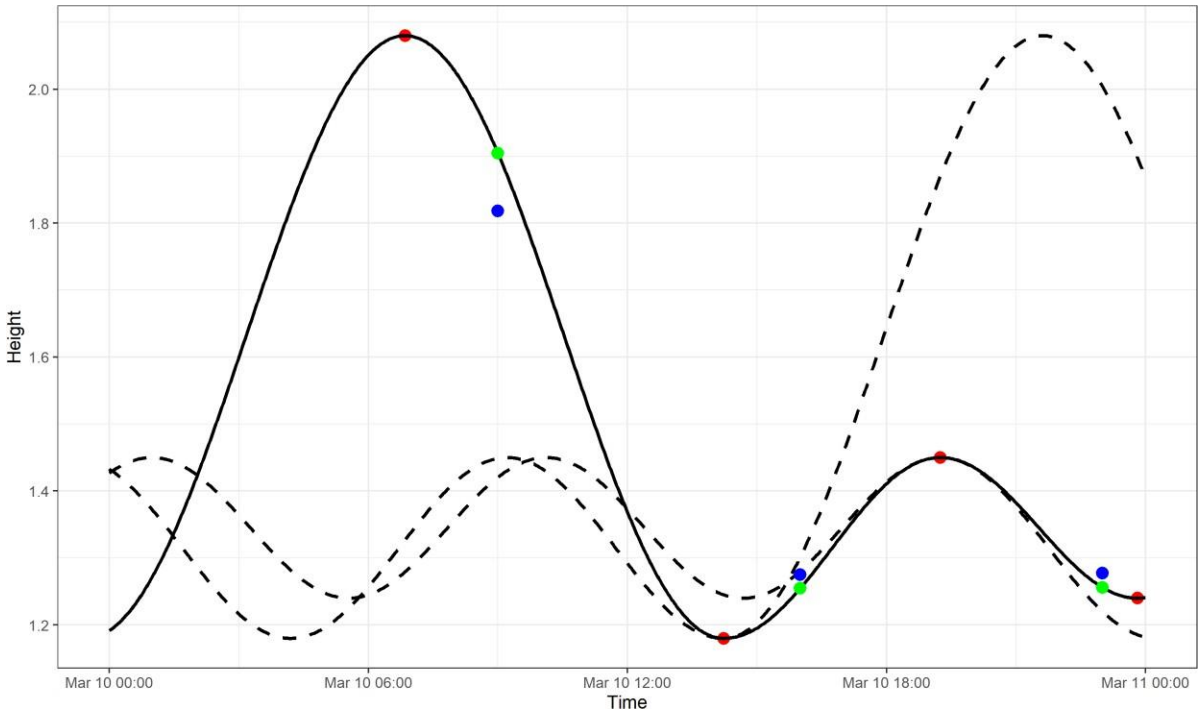


Figure A1.9. Standardization of colonies depth to Lowest Astronomical Tide (LAT). For each individual colony, tide level at the time of collection was estimated from reef- level daily high and low tides (red dots) predicted by the Bureau of Meteorology, Australia and accessed at https://tides.willyweather.com.au/. The solid line displays the modeled tide from the four daily measurements. Green dots show the improvement of tide predictions using a sinusoid function rather than linear interpolation (blue dots). The standardised depth was computed as the colony depth measured from dive computers minus the tide level at time of collection, standardised to LAT. Negative depths indicate colonies above the LAT.

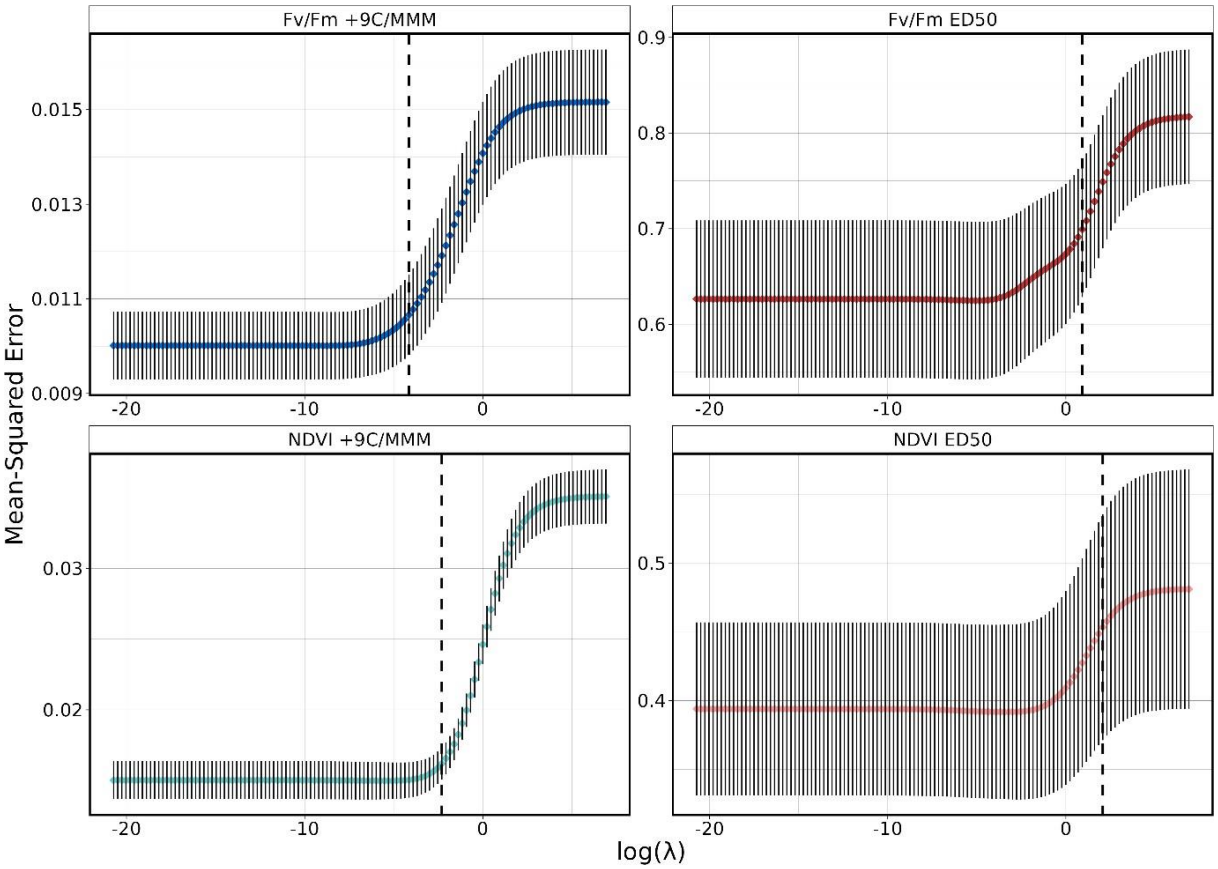


Figure A1.10. Selection of tuning parameter λ of penalization coefficient for phenotypic traits ridge regression on the set of 31 environmental predictors. The optimal λ is chosen separately for each trait through *k*-fold cross-validation. For each λ value, the average mean squared error (coloured dot) and standard deviation (horizontal bars) of ridge regression are computed on the test fold. The vertical dashed line shows the λ.1se parameter retained as the optimal λ, corresponding to the maximum lambda value with MSE within one standard error from min MSE (more regularization than λ.min).

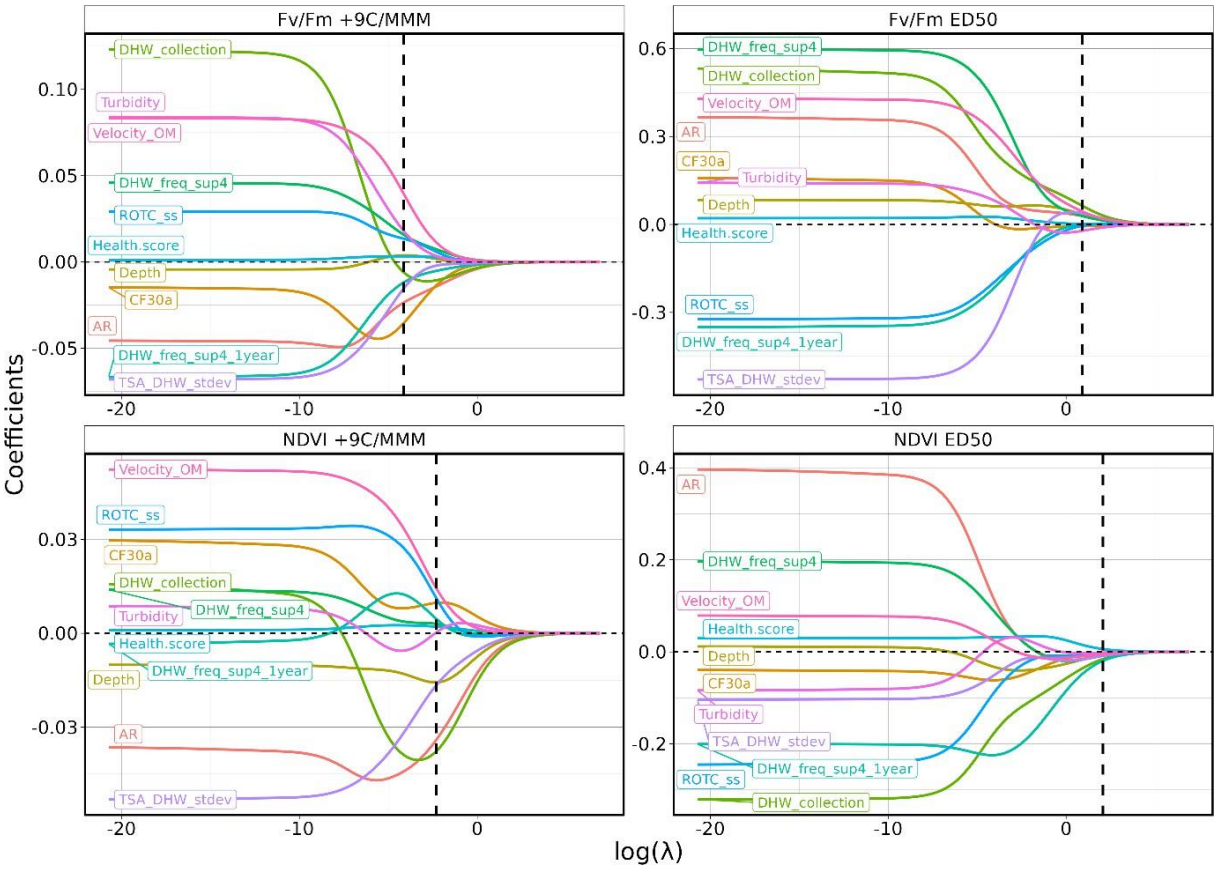


Figure A1.11. Regularization of environmental predictors coefficients across increasing levels of penalization. Each coloured line corresponds the value of a predictor coefficient for different values of tuning parameter λ. Variance in predictor estimates decreases as λ increases and bias increases as λ increases. The vertical dashed line shows the value of λ.1se obtained through cross-validation as providing the best bias-variance trade-off.

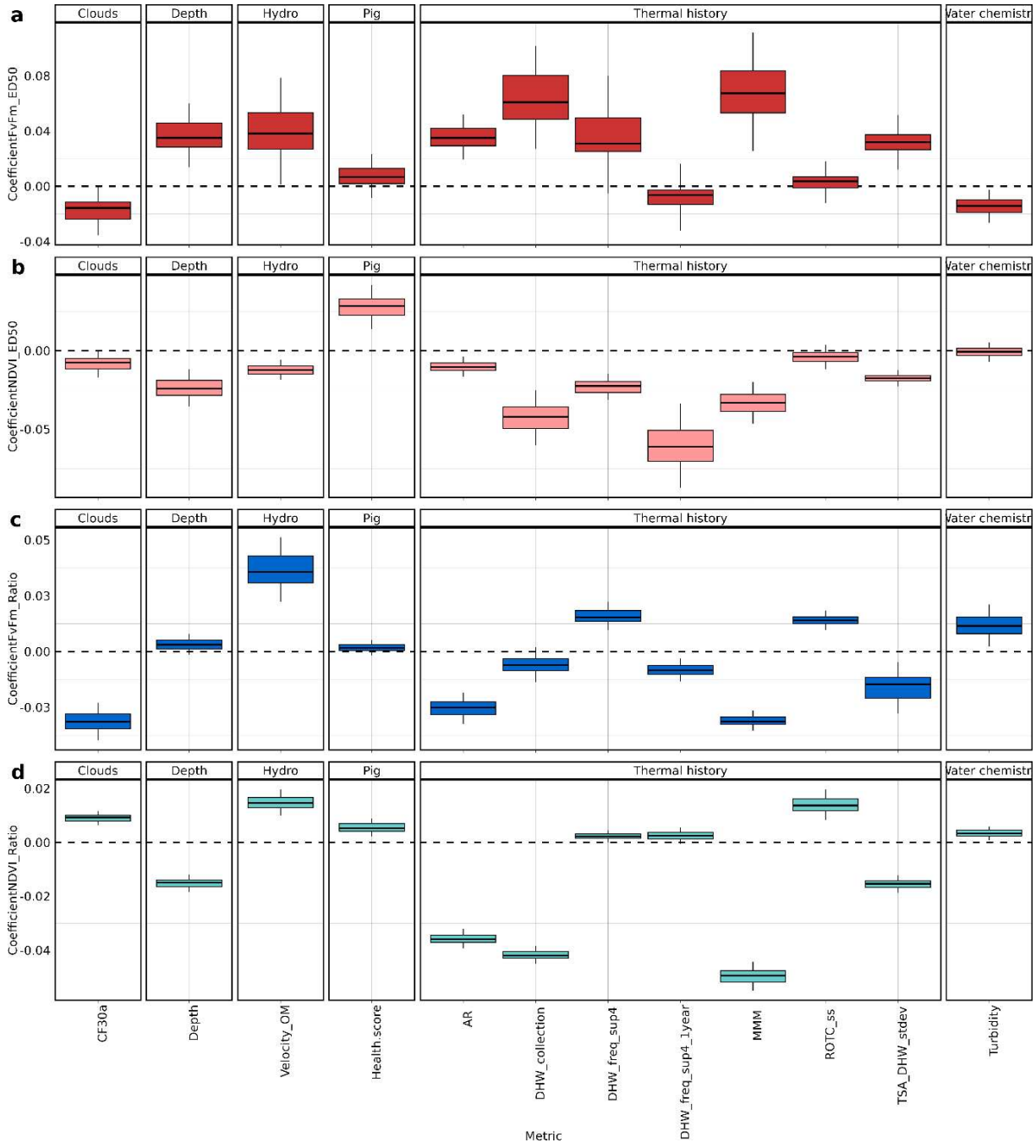


Figure A1.12. Details of ridge regression predictors coefficients for (a) *Fv/Fm* ED50, (b) NDVI ED50, (c) *Fv/Fm* +9 °C/MMM, (d) NDVI +9 °C/MMM. Estimates are grouped by types of environmental predictors and their variance assessed through bootstrap resampling (repeated 100-fold stratified cross validation). Boxplots display first quartile, median and third quartile for each predictor across the 100 folds. Pig=Pigmentation, Hydro=Hydrodynamics.

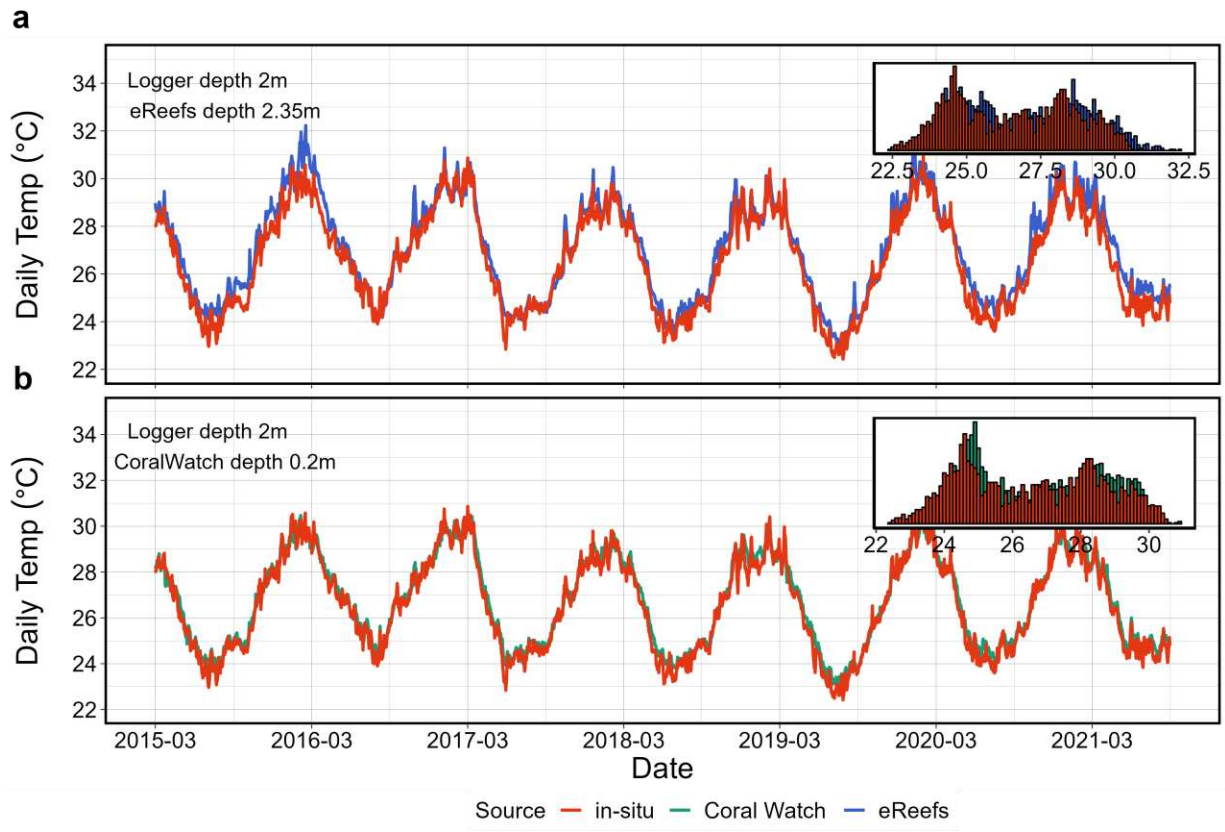


Figure A1.13. Comparison of temperature records from various sources (in-situ loggers, satellite, numerical model) to characterise thermal history of the 14 collection sites. A representative example of temperature time-series is shown at Mackay Reef over the period 2015-2021. (a) Daily *in-situ* logger averages (red) are plotted against eReefs temperatures (blue) extracted from GBR1 Hydro model at 1km resolution. (b) Same against sea surface temperatures from Coral Watch v3.1 (green) at a 5-km resolution. Histograms in the insets show the distribution of daily average temperatures for the various sources.

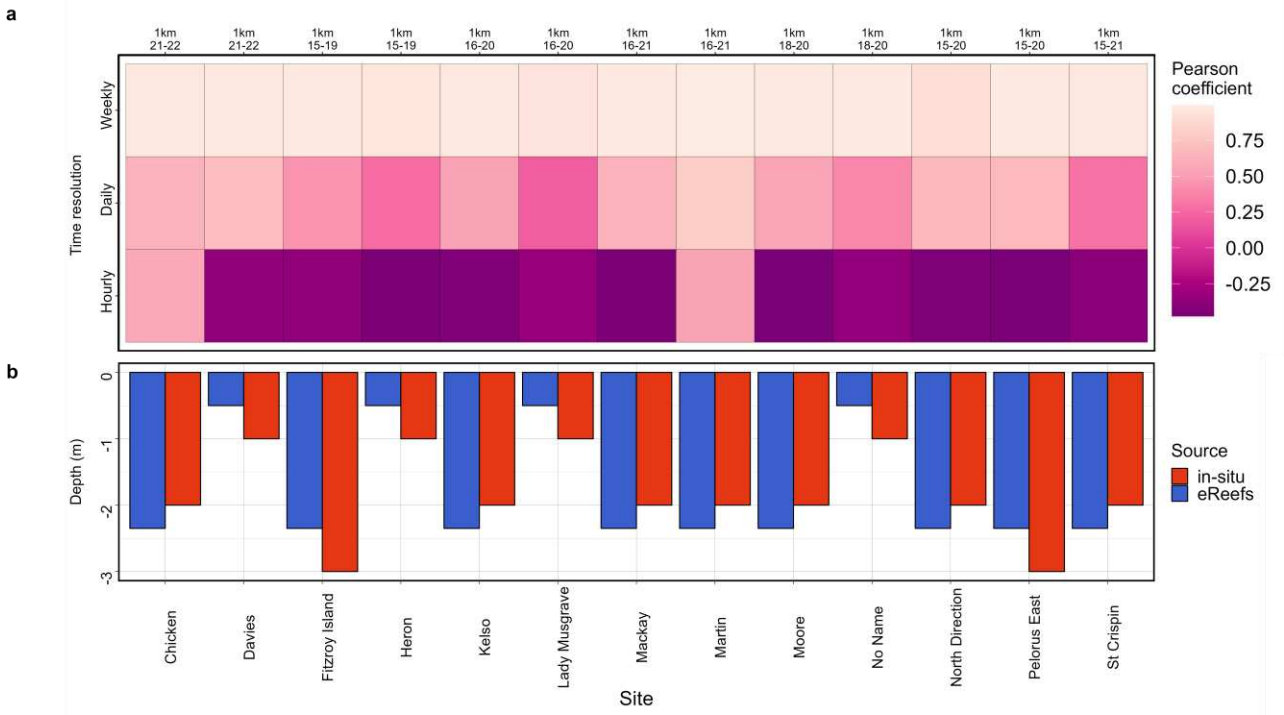


Figure A1.14. Correlation between temperatures recorded by in-situ loggers and predicted by the eReefs model across time resolutions. (a) Heatmap of Pearson's correlation coefficients computed from time-series at hourly, daily and weekly resolutions for the 13 sites were *in-situ* data was available. To compute correlations, daily and hourly temperatures were adjusted to remove low frequency variations by subtracting weekly and daily averages respectively. Above the heatmap is indicated the resolution of the eReefs model and time period used for the comparison. All in-situ loggers had a minimum of one year of data. (b) Depth of temperatures measurements from *in-situ* loggers and predictions from eReefs at each site. For *in-situ* loggers where information was not available, depth was arbitrarily set to 2m.

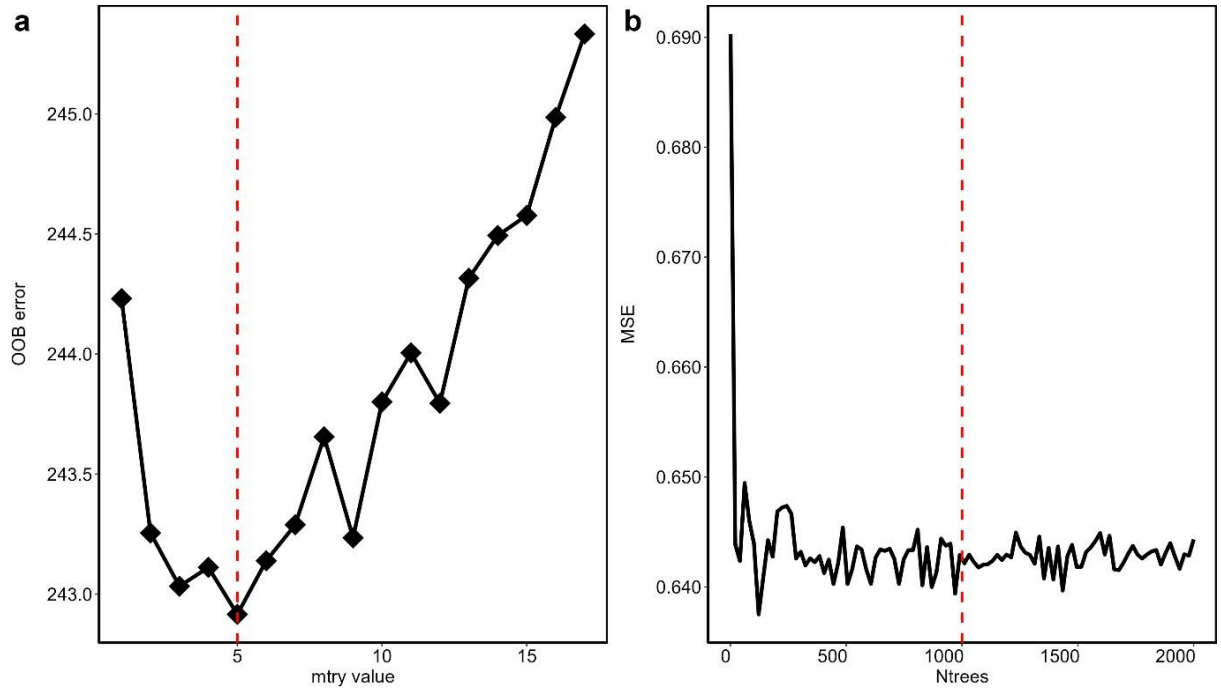


Figure A1.15. Parameter tuning for conditional inference random forest. A representative example of model sensibility to parameters is given for *Fv/Fm* ED50. (a) Variation of out of bag sample average mean squared error (n =10 independent splits) with number of variables randomly tried at each node of the conditional inference tree (*mtry* parameter). The red line indicates the value of *mtry* parameter for which the model has the best predictive accuracy. (b) Variation of test set mean squared error with the number of trees grown for each forest (*ntree* parameter). The red line indicates the value of *ntree* parameter that was used to train the model.

Supplementary Tables

Table A1.1. Summary of sampling conditions and effort

Site name	Lat	Lon	GBRMPA zoning	Distance to coast (km)	Average SST °C	MMM (°C)	Maximum DHW	DHW at the time of collection	N	Average collection depth	Average sampled colony fraction	Number of sites within the reef	Average site area (m2)
Chicken	-18.6706	147.7064	blue	77.065	26.24	28.37	7.2	4.67	60	0.9[-0.4 - 4.6]	9±6.8	2	3600
Davies	-18.827	147.6268	yellow	57.833	26.13	28.38	6.6	4.61	53	1.3[0.1 - 4]	11.9±8.9	1	164
Fitzroy Island	-16.9406	145.9948	yellow	5.782	26.30	28.77	10.71	2.34	60	0.3[-0.5 - 2]	9.9±5.3	2	487
Fitzroy Reef	-23.617	152.15	blue	58.613	24.40	27.09	5.76	0.35	61	-0.6[-0.8 - 0.7]	8.1±3.7	2	4255
Heron	-23.441601	151.912971	green/yellow	64.431	24.33	27.12	7.55	0.32	60	-0.8[-1.3 - 0.8]	14.1±5.5	2	1040
Kelso	-18.424	146.9849	green	47.579	26.21	28.45	7.62	4.21	44	1[0.6 - 5.3]	14.1±5.2	1	487
Lady Musgrave	-23.8929	152.4064	blue	58.827	24.53	27.1	6.15	0.47	56	0.9[-1 - 4.1]	10±6.4	2	1630
Mackay	-16.0384	145.6514	blue	20.37	26.48	28.79	8.81	2.56	60	0.1[-0.9 - 1.9]	14±4.5	1	90
Martin	-14.7801	145.3681	blue	16.686	26.45	28.63	9.54	3.27	60	0.7[0 - 1.4]	12.5±6.4	1	115
Moore	-16.8457	146.2316	green	29.548	26.52	28.65	10.55	3.46	44	0.2[-0.3 - 1.1]	15.3±7	1	615
No Name	-14.6508	145.6383	green	45.102	26.71	28.57	11.28	3.56	53	1.1[-0.2 - 3.5]	10.8±7.9	1	523
North Direction	-14.7434	145.5133	green / scientific research	28.477	26.59	28.56	8.94	2.85	52	0[-0.5 - 0.4]	13.5±3.4	1	160
Pelorus East	-18.5587	146.5023	green / scientific research	16.014	25.60	28.74	9.2	4.27	45	2.1[0.1 - 3.3]	8.5±5.6	1	50
St Crispin	-16.0724	145.8449	blue	40.914	26.57	28.68	8.42	2.96	60	0.2[-0.9 - 3.7]	10.6±8.8	2	491

Temperature metrics were computed from NOAA CoralWatch v3.1 following NOAA guidelines for DHW and MMM computation. MMM = Maximum Monthly Mean; DHW = Degree Heating Weeks. Average SST and maximum DHW indicated for the 1985–2022 period. Distance to coast computed as the Haversine measure of closest distance to the coast. Reef zoning obtained from the Great Marine Park Authority: https://www2.gbrmpa.gov.au/access/zoning/eye-on-the-reef-app. Colony depth standardised to Lowest Astronomical Tide (LAT, [range]), negative values indicate shallow colonies above the site LAT

Table A1.2. Experimental conditions of acute heat stress assays.

	Actual experimental temperatures (3h hold, °C) (±SD)	Target experimental temperatures (3 hours hold, °C)	Flow rate (L.min-1)	Daily turnover	Light Intensity (µmol photons.m^{-2} .s^{-1})	Water Filtration

Site.name	MMM	MMM+3	MMM+6	MMM+9	MMM	MMM+3	MMM+6	MMM+9	0.8	19.2x	300	None
Chicken	28.56±0.07	31.43±0.15	34.23±0.22	37.35±0.24	28.37	31.37	34.37	37.37	0.8	19.2x	300	None
Davies	28.41±0.37	31.36±0.12	32.97±0.57	37.21±0.34	28.38	31.38	34.38	37.38	0.8	19.2x	300	None
Fitzroy Island	28.87±0.08	31.83±0.1	34.02±0.35	37.62±0.39	28.77	31.77	34.77	37.77	0.8	19.2x	300	None
Fitzroy Reef	27.6±0.05	30.11±0.08	33.12±0.1	36.06±0.15	27.09	30.09	33.09	36.09	0.8	19.2x	300	None
Heron	27.54±0.04	30.15±0.08	33.15±0.1	36.02±0.14	27.12	30.12	33.12	36.12	0.8	19.2x	300	None
Kelso	29.11±0.1	31.7±0.1	33.99±0.25	37.52±0.25	28.45	31.45	34.45	37.45	0.8	19.2x	300	None
Lady Musgrave	27.32±0.11	30.1±0.12	33.11±0.14	36.06±0.18	27.1	30.1	33.1	36.1	0.8	19.2x	300	None
Mackay	30.58±0.59	31.79±0.09	33.19±0.42	37.79±0.57	28.79	31.79	34.79	37.79	0.8	19.2x	300	None
Martin	30.6±0.26	31.6±0.15	34.3±0.54	37.42±0.29	28.63	31.63	34.63	37.63	0.8	19.2x	300	None
Moore	28.88±0.17	31.84±0.08	34.08±0.33	37.54±0.2	28.65	31.65	34.65	37.65	0.8	19.2x	300	None
No Name	30.65±0.09	31.61±0.08	34.38±0.19	37.27±0.21	28.57	31.57	34.57	37.57	0.8	19.2x	300	None
North Direction	30.36±0.14	31.59±0.09	34.37±0.22	37.52±0.22	28.56	31.56	34.56	37.56	0.8	19.2x	300	None
Pelorus East	29.11±0.1	31.7±0.1	33.99±0.25	37.52±0.25	28.74	31.74	34.74	37.74	0.8	19.2x	300	None
St Crispin*	29.72±0.57	31.1±0.83	32.42±0.73	35.11±0.6	28.68	31.68	34.68	37.68	0.8	19.2x	300	None

* Experimental treatments failed to match target temperatures

Table A1.3. Linear mixed effect models for phenotypic measurements (F_v/F_m and NDVI).

Fv/Fm						
Linear mixed model fit by maximum likelihood . t-tests use Satterthwaite's method ['lmerModLmerTest']						
Formula: mFvFm ~ Npixel + Site.name + Treatment + (1 | Tank) + (1 | Colony)						
AIC	BIC	logLik	deviance	df.resid		
-15739.9	-15602.6	7889.9	-15779.9	7054,00		
Scaled residuals :						
Min	1Q	Median	3Q	Max		
-5.399	-0.5097	0.0269	0.5388	4.8358		
Random effects:						
Groups	Name	Variance	Std.Dev.			
Colony	(Intercept)	8.373e-04	0.02894			
Tank	(Intercept)	1.137e-04	0.01066			
Residual		5.742e-03	0.07578			
Number of obs: 7074, groups: Genotype, 636; Tank, 16						
Fixed effects:						
	Estimate	Std. Error	df	*t* value	2.5%	97.5%
(Intercept)	5.65e-01	6.74e-03	309	83.907	5.51e-01	5.79e-01
Npixel	1.24e-06	9.09e-07	7041	1.361	-6.15e-07	2.96e-06
Site.nameDavies	1.01e-01	7.37e-03	636	13.777	8.59e-02	1.16e-01
Site.nameFitzroy Island	9.20e-02	6.87e-03	633	13.38	7.87e-02	1.05e-01
Site.nameFitzroy Reef	1.00e-01	6.91e-03	655	14.506	8.65e-02	1.13e-01
Site.nameHeron	9.99e-02	6.96e-03	661	14.357	8.63e-02	1.14e-01
Site.nameKelso	1.38e-01	7.94e-03	645	17.404	1.22e-01	1.54e-01
Site.nameLady Musgrave	1.00e-01	6.91e-03	656	14.521	8.74e-02	1.12e-01
Site.nameMackay	6.81e-02	6.96e-03	662	9.781	5.43e-02	8.14e-02
Site.nameMartin	9.05e-02	7.10e-03	688	12.76	7.52e-02	1.04e-01
Site.nameMoore	9.43e-02	7.94e-03	645	11.872	7.92e-02	1.09e-01
Site.nameNo Name	1.35e-01	7.48e-03	656	18.103	1.20e-01	1.50e-01
Site.nameNorth Direction	1.98e-02	7.07e-03	653	2.793	4.03e-03	3.27e-02
Site.namePelorus East	1.40e-01	7.44e-03	644	18.804	1.25e-01	1.54e-01
Treatment+3C	-7.94e-04	3.25e-03	1808	-0.244	-7.05e-03	5.72e-03
Treatment+6C	-2.22e-02	2.94e-03	3514	-7.546	-2.80e-02	-1.55e-02
Treatment+9C	-3.16e-01	4.67e-03	127	-67.521	-3.25e-01	-3.06e-01

NDVI						
Linear mixed model fit by maximum likelihood . t-tests use Satterthwaite's method ['lmerModLmerTest']						
Formula: MeanNDVI ~ Npixel + Site.name + Treatment + (1 | Tank) + (1 | Colony)						
AIC	BIC	logLik	deviance	df.resid		
-13782.5	-13642	6911.3	-13822.5	8305		
Scaled residuals :						
Min	1Q	Median	3Q	Max		

-5.2063	-0.5523	0.0486	0.5307	3.9681		
Random effects:						
Groups	Name	Variance	Std.Dev.			
Colony	(Intercept)	0.0026993	0.05195			
Tank	(Intercept)	0.0001264	0.01124			
Residual		0.0098070	0.09903			
Number of obs : 8325, groups: Genotype, 709; Tank, 16						
Fixed effects:						
	Estimate	Std. Error	df	t value	2.5%	97.5%
(Intercept)	5.84e-01	9.48e-03	617	61.596	5.64e-01	6.02e-01
Npixel	8.50e-06	1.11e-06	8272	7.646	6.36e-06	1.08e-05
Site.nameDavies	6.35e-02	1.13e-02	724	5.63	4.19e-02	8.54e-02
Site.nameFitzroy Island	1.27e-01	1.09e-02	710	11.721	1.08e-01	1.49e-01
Site.nameFitzroy Reef	1.56e-01	1.09e-02	727	14.353	1.34e-01	1.82e-01
Site.nameHeron	2.04e-01	1.09e-02	731	18.656	1.83e-01	2.26e-01
Site.nameKelso	3.05e-02	1.18e-02	712	2.579	8.03e-03	5.68e-02
Site.nameLady Musgrave	1.92e-01	1.10e-02	727	17.43	1.72e-01	2.13e-01
Site.nameMackay	8.94e-02	1.09e-02	730	8.169	6.72e-02	1.11e-01
Site.nameMartin	8.77e-02	1.10e-02	744	7.943	6.79e-02	1.11e-01
Site.nameMoore	8.87e-02	1.18e-02	710	7.511	6.72e-02	1.13e-01
Site.nameNo Name	7.59e-02	1.13e-02	725	6.732	5.44e-02	9.91e-02
Site.nameNorth Direction	-4.07e-02	1.13e-02	728	-3.585	-6.14e-02	-1.68e-02
Site.namePelorus East	1.11e-01	1.17e-02	713	9.44	8.76e-02	1.35e-01
Treatment+3C	5.83e-04	3.87e-03	1330	0.15	-7.17e-03	8.48e-03
Treatment+6C	-1.85e-02	3.52e-03	2958	-5.263	-2.52e-02	-1.16e-02
Treatment+9C	-4.82e-01	5.36e-03	108	-90.015	-4.92e-01	-4.71e-01

Table A1.4. Summary of within and among reef variation in thermal thresholdsSummary of within and among reef variation in thermal thresholds (ED50, a) and performance retention (MMM+9/MMM) for F_v/F_m and NDVI phenotypic traits. (b) Levene's test results comparing variance and One-way Welch ANOVA comparing means of heat tolerance metrics between sites. (c) Games Howell Post-hoc tests on sites heat tolerance metric means (FWER controlled at level 0.05).This table is available at Supplementary material from "Thermal tolerance traits of individual corals are widely distributed across the Great Barrier Reef" due to its large number of data entries.

Table A1.5. Summary of correlations between Fv/Fm and NDVI thermal thresholds (ED50) and performance retention

Global correlations across all sites			
Correlation	Spearman's ρ	S	p.value
FvFm-NDVI ED50	0,0035	33419322	0.932
FvFm-NDVI MMM+9/MMM	0,4269	29377704	**<0.001**

Correlations within sites				
Correlation	Site.name	Spearman's ρ	S	p.value
FvFm-NDVI ED50	Chicken	0.352	23318	0.006
	Davies	0.289	7028	0.075
	Fitzroy Island	0.256	19506	0.061
	Fitzroy Reef	0.015	18144	0.918
	Heron	0.152	14674	0.308
	Kelso	0.190	3642	0.314
	Lady Musgrave	0.048	22312	0.737
	Mackay	0.286	15782	0.042
	Martin	0.214	19488	0.123
	Moore	0.209	3212	0.276
	No Name	0.395	5980	0.013
	North Direction	0.220	11842	0.146
	Pelorus East	-0.104	10910	0.526
FvFm-NDVI MMM+9/MMM	Chicken	0.020	35288	0.882
	Davies	0.166	18424	0.243
	Fitzroy Island	0.299	19422	0.027
	Fitzroy Reef	0.304	23816	0.020
	Heron	0.246	22052	0.067
	Kelso	0.257	6786	0.119
	Lady Musgrave	0.293	22968	0.026
	Mackay	0.303	21512	0.022
	Martin	0.177	22816	0.196
	Moore	0.226	10254	0.145
	No Name	0.297	14632	0.036
	North Direction	0.659	7106	0.000
	Pelorus East	-0.211	16032	0.175

Table A1.6. Environmental variables retrieved for phenotype by environment analysis.

Variable	Metric	Source	Spatial resolution	Time resolution	Period	Depth(s)	Description
Temperature	LMM	eReefs GBR1_Hydro	1km	daily	2014 - 2022	[0.5.2.35.5. 35.9.13]	Minimum monthly mean
Temperature	OM	eReefs GBR1_Hydro	1km	daily	2014 - 2022	[0.5.2.35.5. 35.9.13]	Overall mean
Temperature	OMsd	eReefs GBR1_Hydro	1km	daily	2014 - 2022	[0.5.2.35.5. 35.9.13]	Overall standard deviation
Temperature	AR	eReefs GBR1_Hydro	1km	daily	2014 - 2022	[0.5.2.35.5. 35.9.13]	Average Annual range

Temperature	ROTC_ss	eReefs GBR1_Hydro	1km	daily	2014 - 2022	[0.5.2.35.5. 35.9.13]	Average Rate of temperature change (spring-summer)
Temperature	MMM	Coralwatch	5km	daily	1985 - 2022	0.2	Maximum monthly mean (adjusted to historical baseline)
Temperature	TSA_DHW_stdev	Coralwatch	5km	daily	1985 - 2022	0.2	Degree Heating weeks standard deviation
Temperature	DHW_freq_sup4	Coralwatch	5km	daily	1985 - 2022	0.2	Average frequency of Degree Heating weeks above 4
Temperature	DHW_freq_sup8	Coralwatch	5km	daily	1985 - 2022	0.2	Average frequency of Degree Heating weeks above 8
Temperature	DHW_max	Coralwatch	5km	daily	1985 - 2022	0.2	Maximum Degree Heating weeks
Temperature	DHW_freq_sup4_1year	Coralwatch	5km	daily	2021 - 2022	0.2	Frequency of Degree Heating weeks above 4 during the year prior to collection
Temperature	DHW_freq_sup4_6year	Coralwatch	5km	daily	2021 - 2022	0.2	Frequency of Degree Heating weeks above 4 since 2016
Temperature	DHW_collection	Coralwatch	5km	daily	1985 - 2022	0.2	Degree Heating weeks at the time of collection (2022 Field Trip)
Depth	Depth	Dive computer	NA	NA	NA	NA	Colonies depth (adjusted to LAT using BOM tides data)
Pigmentation	Health.score	CoralHealth chart	NA	NA	NA	NA	https://coralwatch.org/product/coral-health-chart/
Cloud fraction	CF_OM	NASA-MODIS	1°	monthly	2002 - 2022	NA	Cloud Fraction overall mean (% of pixel covered by clouds)
Cloud fraction	CF_ss	NASA-MODIS	1°	monthly	2002 - 2022	NA	Cloud Fraction summer-spring mean (% of pixel covered by clouds)
Cloud fraction	CF30a	NASA-MODIS	1°	daily	2002 - 2022	NA	Cloud Fraction anomaly for the 30 days prior to collection
Chlorophylle A	Chl_a_OM	eReefs_GBR4_BGC	4km	daily	2010 - 2019	[0.5.1.5.3.5. 5.8.8.12.75]	Chlorophylle A Overall Mean
Vertical attenuation at 490nm	Kd_490_OM	eReefs_GBR4_BGC	4km	daily	2010 - 2019	[0.5.1.5.3.5. 5.8.8.12.75]	Vertical attenuation at 490nm Overall Mean
Dissolved Oxygen	Oxygen_OM	eReefs_GBR4_BGC	4km	daily	2010 - 2019	[0.5.1.5.3.5. 5.8.8.12.75]	Dissolved Oxygen Overall Mean
Particulate Inorganic Phosphorus	PIP_OM	eReefs_GBR4_BGC	4km	daily	2010 - 2019	[0.5.1.5.3.5. 5.8.8.12.75]	Particulate Inorganic Phosphorus Overall Mean
Total Nitrogen	TOTAL_N_OM	eReefs_GBR4_BGC	4km	daily	2010 - 2019	[0.5.1.5.3.5. 5.8.8.12.75]	Total Nitrogen Overall Mean
Sea current velocity	Velocity_OM	eReefs GBR1_Hydro	1km	daily	2014 - 2022	[0.5.2.35.5. 35.9.13]	Total current Overall Mean

Table A1.7. Metrics retained for phenotype x environment analyses.

Metric	**Correlated Metrics (Absolute Pearson coefficient >0.7)**
AR	OMsd
CF30a	
DHW_collection	LMM, OM, MMM, CF_OM, CF_ss, Chl_a_OM, Oxygen_OM, Tot_N_OM
DHW_freq_sup4	
DHW_freq_sup4_1year	
Depth	
Health score	
ROTC_ss	
TSA_DHW_stdev	DHW_freq_sup8, DHW_max, DHW_freq_sup4_6year
Turbidity	PIP_OM
Velocity_OM	

Appendix A2. Supplementary data for chapter 3

Supplementary Figures

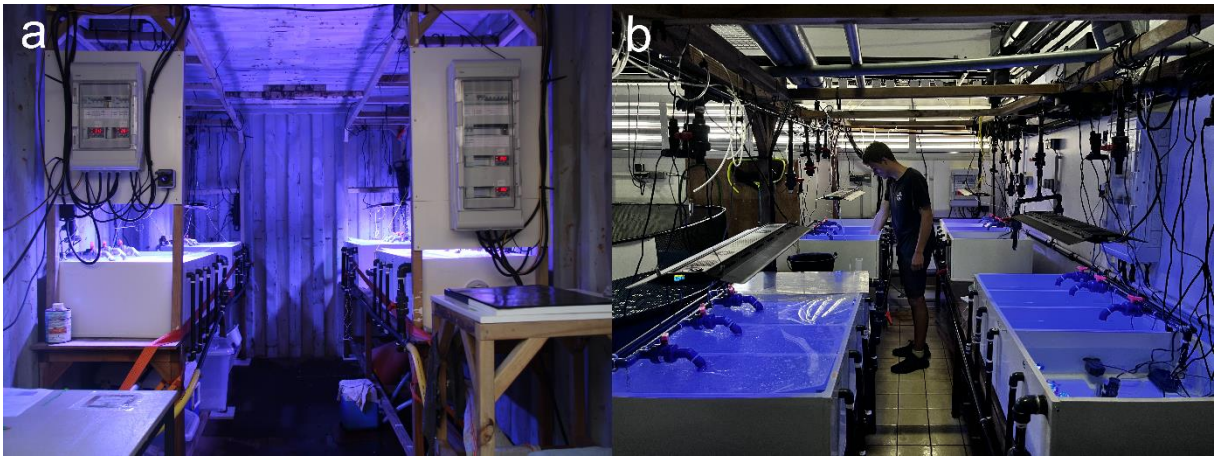


Figure A2.1. Picture of the acute heat stress system to conduct high-throughput acute heat stress experiments on corals (a) onboard of the d'Entrecasteaux vessel and (b) at the Noumea Aquarium des Lagons. Chesterfield's atoll and Noumea, 2023. ©M. Boussion.

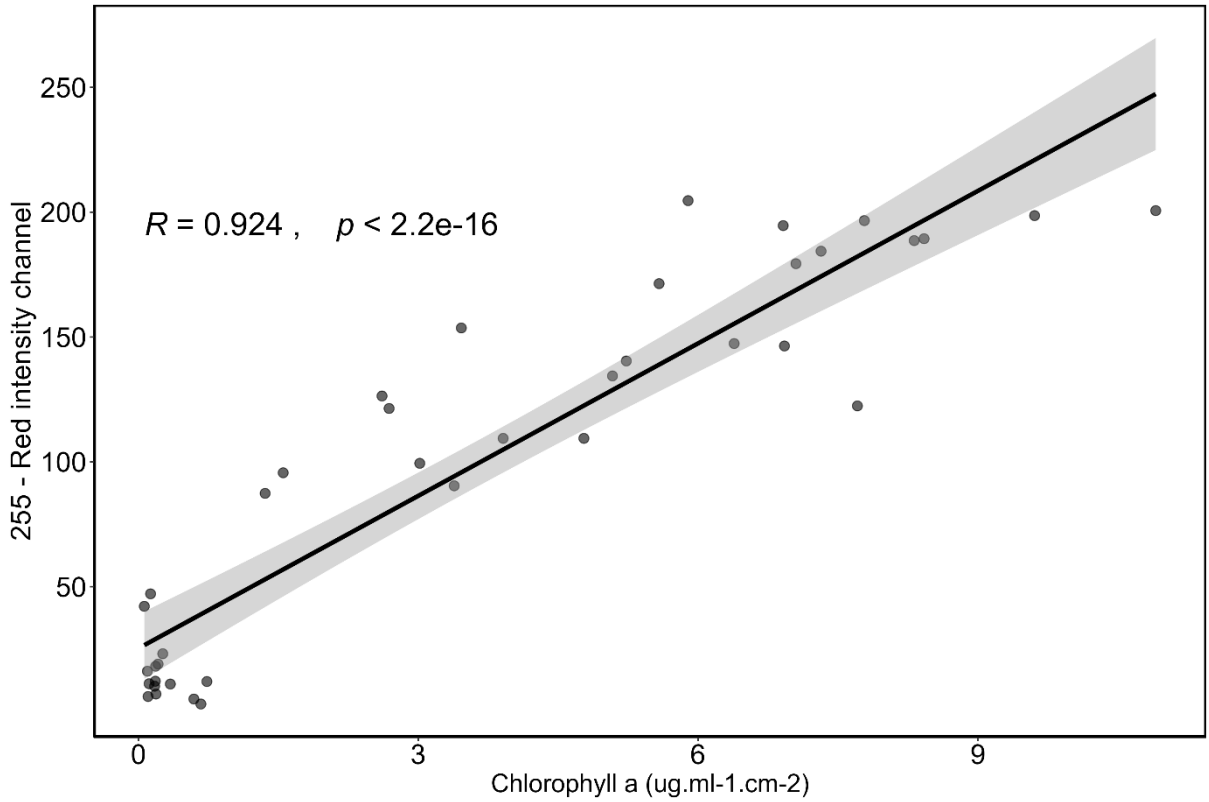


Figure A2.2. Validation of chlorophyll-a quantification using red channel intensity on coral fragments at the end of the heat stress experiment. Correlation between chlorophyll a and the inverted red channel intensity (255-median$_{Red}$) for a subset of *A.spathulata* samples (n = 60). Each point represents a single coral fragment. The Pearson's correlation coefficient R and p value are shown.

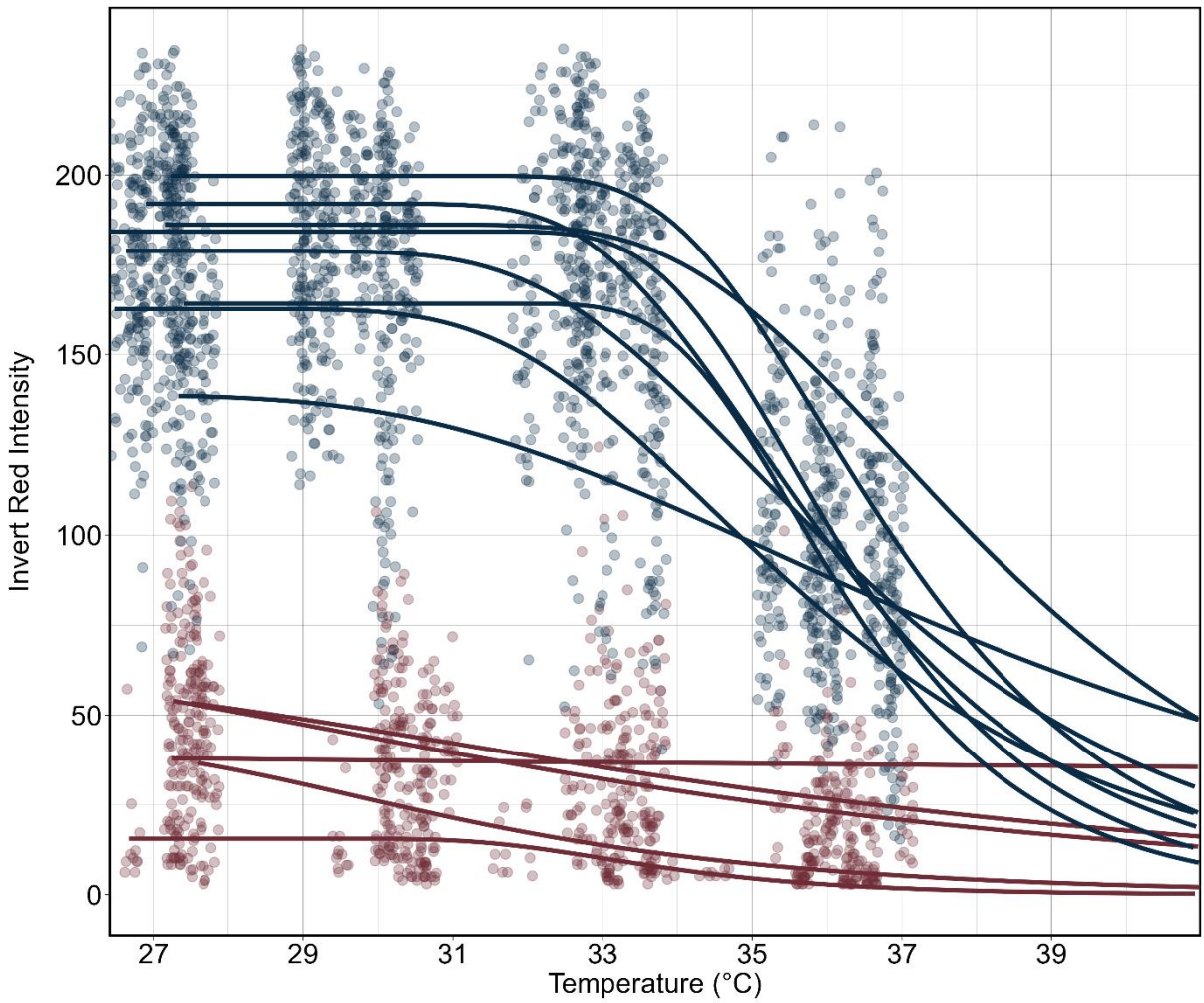


Figure A2.3. Site-level dose response curves for invert red channel intensity at western New Caledonia (blue) and Chesterfields-Bellona (red) sites. Due to lower baseline chlorophyll concentration levels at CB sites, it was not possible to compute ED50 or performance retention metrics at these sites.

Supplementary Tables

Table A2.1. Comparison of experimental conditions, phenotypic data acquisition and analysis between Australia and New Caledonia to characterise intraspecific variation in heat tolerance traits. In New Caledonia, I built a semi-automated experimental system together with the Noumea Aquarium des Lagons staff to ensure experimental conditions as similar as possible to the GBR (i.e., comparable temperature treatments, water flow, light intensity). In New Caledonia experiments, chlorophyll content was estimated from the red-channel intensity of conventional RGB imaging following Winters et al. (2009).

Experimental condition, physiological measurements or analytical steps	Australia	New Caledonia
Target temperature treatments	+0°C (control), +3 °C, +6 °C and +9 °C above MMM	+0°C (control), +3 °C, +6 °C and +9 °C above MMM
mean ΔT = | Target - Actual T°C |	0.36	0.26
Number of replicate tanks / treatments	3	3
Number of nubbins / L (full capacity)	1.2	0.8
Tank seawater daily turnover	19.2x	22x
Light Intensity (µmol photons m^{-2}. s^{-1})	300	250
Light regime (day:night)	11:13	11:13
Water filtration	None	None
F_v/F_m measurements	Whole nubbin, Imaging PAM chlorophyll fluorometer (IMAG-K7, Walz Germany)	Single area, Aquapen-P AP-110P (Photon Systems Instruments)
Chlorophyll content measurements	NDVI, hyperspectral camera (Resonon, Pika XC2)	Red channel intensity, RGB camera (Canon EOS700D with EF-S 18-200mm f/3.5-5.6 IS lens)
Validation of chlorophyll content proxy using spectrophotometric determination from tissue extraction	Yes	Yes
Quantification of thermal tolerance metrics	ED50 (dose response curves) and performance retention (+9 °C/MMM)	ED50 (dose response curves) and performance retention (+9 °C/MMM)

Table A2.2. Summary of sampling effort and sites conditions in New Caledonia.

Site name	Site code	Sampling Date	Lon	Lat	MMM (°C)	Depth mean [range]	N
Bellona Sud	CB1	23/06/2023	159.425853	-21.8905	26.6	-0.2 [-0.5,0]	4
Bellona Ouest	CB2	24/06/2023	158.594	-21.0313	26.7	-0.4 [-0.6-0.3]	23
Ilot Loop	CB3	25/06/2023	158.4083483	-19.9285188	27.3	-0.3 [-0.4-0.1]	24
Chesterfields SO	CB4	26/06/2023	158.478	-19.905	27.3	1.1 [0.4,2.5]	17
Chesterfields NO	CB5	27/06/2023	158.433288	-19.03805	27.7	1.8 [-0.1,4.1]	18
Chesterfields NE	CB6	28/06/2023	158.884708	-18.960638	27.6	2.5 [0.6,5]	22
Recif du Prony	NC1	10/08/2023	166.3273667	-22.26615	26.6	1.1 [-0.2,4.1]	25

Recif Mara	NC2	22/08/2023	165.72805	-21.830483	26.9	3 [0.9,5.6]	24
Recif Snark	NC3	01/09/2023	166.42516	-22.44361	26.6	0.4 [0,1.4]	21
Ile Verte	NC4	06/09/2023	165.47735	-21.68475	27	-0.4 [-0.5-0.1]	25
Ilot Contrariete	NC5	13/09/2023	165.05492	-21.46439	27.1	0.9 [0.4,1.7]	25
Ilot Deverd	NC6	19/09/2023	164.3237	-20.766433	27.5	0.3 [-0.4,1.9]	25
Plateau de Koniene	NC7	20/09/2023	164.7209	-21.157383	27.3	0.2 [-0.2,1.9]	25
Pointe de Poum	NC8	28/09/2023	163.99965	-20.24595	27.8	-0.2 [-0.5,1.3]	25

Appendix A3. Supplementary data for Chapter 4

Supplementary Material and Methods

(a) Testing for batch effects

For logistical and legal reasons, samples collected in Australia and New Caledonia were processed for DNA extraction, library preparation and sequencing at different facilities. While we used similar DNA extraction kits, library preparation kits and sequencing platform to minimize batch effects in our dataset, a subset of 23 GBR samples were extracted and sequenced separately at both facilities to validate the absence of strong batch effects. Following the different data processing steps described in the main manuscript, 17 pairs of samples passed filtering steps and were used to assess the presence of batch effects using 'hard called' variants. First, each pair of replicates were correctly grouped together based on relatedness, irrespective of the batch in which they were sequenced (Figure A3.3a). Second a PCA conducted on SNPs (MAF > 0.01, missingness < 20%) correctly separated GBR samples in the two previously described genomic clusters, rather than by batch (Figure A3.3b). Third, we computed individual autosomal heterozygosity for each batch using 0% missing data. This was done because different factors such as different levels of DNA degradation leading to base transition can alter heterozygosity estimates between batches (Lou & Therkildsen, 2022). A Welch two-sample t-test found no significant differences in heterozygosity between batches. Overall, these results confirm the absence of strong batch effects in our dataset. While slight differences between samples extracted and sequenced separately are to be expected, the genetic patterns described in this study are unlikely to be an artifact of batch effects.

(b) Choice of reference genome

Cleaned reads were initially aligned to *Acropora millepora* v3 reference genome (unpublished upgrade from GCA_013753865.1_Amil_v2.1). This reference was chosen as *A. millepora* is a very close taxa to *A.spathulata*, both phylogenetically and morphologically (Souter et al., 2010) and had a curated chromosome-scale reference genome at the time analyses were performed unlike *A. spathulata*. Since initial analyses were performed, two *A. spathulata* reference genomes have become available on NCBI Genbank (one chromosome scale; GCA_964019555.1 and one contig-scale; GCA_031770025.1). However, alignment of both reference genomes using D-GENIES (Cabanettes & Klopp, 2018) revealed a moderate macrosynteny between the two *A. spathulata* reference genomes and limited microsynteny with less than 5% of the reference genomes showing > 75% identity. For comparison, these levels

of identity or on the same order of magnitude than between two different species: *A. tenuis* with *A.millepora* (Cooke et al., 2020) which suggests that better curation of these references might be needed. In addition, preliminary tests mapping reads from our samples to the contig-scale *A. spathulala* reference (GCA_031770025.1) and *A. millepora v3* showed only a < 0.3% difference in mapping rates between them. The better quality, curation and assembly scale of *A. millepora v3* reference genome thus made it a preferable choice for our analyses.

(c) Host population genetics using genotype likelihoods

To get an initial impression of the population structure across our study system we analysed coral samples genomic data with a genotype likelihood framework in `ANGSD` v0.940 (Korneliussen et al., 2014). The dataset comprised the 1,132 putative *A. spathulata* samples and validated *A.millepora* (*n* = 13) samples used as outgroups, processed using the same pipeline. Polymorphic sites were filtered to retain only those with mapping quality > 30, base quality > 30, coverage ≥ 3 paired-end reads in ≥95% of individuals, and sites mapping to 14 assembled chromosomes. Genotype likelihoods were inferred using `Samtools` model to estimate major and minor alleles frequencies assuming biallelic sites (`-doMaf` = 2) and considered only polymorphic sites with a likelihood ratio test p-value < 0.000001.

A.spathulata is a formally recognized species on the GBR. A first subset of the dataset including 864 GBR individuals was used to pinpoint potential taxon mis-identification. To that end, polymorphic sites with minor allele frequency (MAF) > 0.05 were used to compute a covariance matrix and perform a principal component analysis (PCA) in `PCAngsd` v1.21 (Meisner & Albrechtsen, 2018). Bayesian hierarchical clustering admixture analyses was also performed in `PCAngsd` with the 'admix' option assuming 2–5 ancestral populations. Both analyses revealed two major genomic clusters geographically separated between the central/north and south GBR. In both analyses, 4 samples were also detected as being *A.millepora* colonies that were mis-identified in the field and were discarded in further analyses (Figure A 3.15).

A.spathulata has been less often identified and studied in New Caledonia despite being reported to occur in the Western Lagoon of the main island 'Grande Terre' (Fenner & Muir, 2008). Prior work targeting *A.millepora* has also revealed several genetic clusters that could actually consist of the two species or other related taxa (Selmoni et al., 2021). In the field, colonies most closely matching *A.spathulata* morphology from the Great Barrier Reef were targeted. We further assessed how these colonies related to the GBR *A.spathulata* and *A.millepora* by repeating the same PCA and Ancestry analyses using a dataset of 1,041 colonies from the Central/North and

South GBR, New Caledonia as well as *A.millepora* from the central GBR (Figure A3.16). These analyses suggested that colonies collected in New Caledonia were indeed most closely related to the GBR *A.spathulata* than the GBR *A.millepora*. Colonies sampled in the western coast of New Caledonia (NC) and the Chesterfields-Bellona plateau (CB) formed two genetically distinct groups. In addition, a small subset of 23 samples from the southern west coast of New Caledonia clustered separately from the rest, presumably originating from an undersampled genetically distinct group that may be closer to the GBR *A.millepora*.

(d) Validation of genetic differentiation from *A. millepora* using hard called variants

To confirm genetic differentiation of previously described groups, an even subset of 11 individuals for each of the 6 groups (*GBR A.millepora*, Central/North GBR *A.spathulata*, South GBR *A.spathulata*, NC Cluster 1, NC Cluster 2 and CB) was used for SNPs and variant calling using the same GATK pipeline and filtering steps as described in the main manuscript. The resulting vcf file was used to compute Pairwise F_{st} between each group using the Weir and Cockerham method (Weir & Cockerham, 1984) in `vcftools`, and used to perform a PCA with the `glPca` function from R package `adegenet` v2.1.10 (Jombart, 2008). These analyses confirmed that all sampled taxa in this study were most closely related to the GBR *A.spathulata* (Figure A3.17). The PCA analysis also confirmed the presence of two genetically distinct groups in the western coast of New Caledonia. Due to its low sample size, the under sampled Cluster 2 was discarded from further analyses to focus on the predominant Cluster 1.

(e) Clones and related individuals' identification

Clonemates and related individuals were identified in the dataset using two methods. First, identity-by-state (IBS) matrices were generated in `ANGSD` using the `-doIBS` function from the set of filtered polymorphic sites. Second, relatedness matrices were generated from hard called variants (20% missingness) in `vcftools` using the method of Yang et al. (2010). In both cases, matrices were computed and clonemates identified separately for each of the four genetic groups (NC, CB, South GBR and Central/North GBR). Colonies genetic similarity was compared to the overall background similarity as well as the similarity of technical replicates to infer pairs or groups of clonemates. Both methods were in agreement for all pairs or groups of clones. Using a conservative relatedness threshold of 0.2, there were 11, 17, 3 and 6 groups of clones or related individuals for the Central/North GBR, the South GBR, NC and CB respectively (Figure A3.18). The number of putative clones and highly related individuals was particularly high in the Southern GBR but we could not confirm if this was due to higher

inbreeding rates at these locations or an artifact of the sampling scheme, as colonies were sampled randomly by different groups of divers between locations. All related individuals identified using a conservative threshold were filtered prior to final population structure, demographic and isolation by distance analyses to retain one individual with the lowest missingness per group.

(f) Environmental data acquisition

To assess environmental conditions driving symbiont community composition across coral host populations and our study range, we retrieved environmental data from several satellite products and model reanalysis (Table A3.5). These datasets were preferred to more fine-scale resolution models available in each country for consistency reasons. We focused on variables that are known to affect Symbiodiniaceae communities structuring and can be relatively well estimated in both reef systems. Temperature metrics were computed from the Coral Watch v3.1 sea surface temperature (SST) satellite product (NOAA; 1985–present; 5km). Light intensity metrics (Cloud fraction and UV radiation) were computed from the ERA5 reanalysis (Copernicus marine service; 2002–present; 0.25°). Water turbidity (Kd_{490nm}) and chlorophyll content metrics were computed from ESA Globcolour satellite product (Fanton d'Andon et al., 2009; 2002–present; 1/24°). Finally, we included spatial descriptors in the analysis such as Latitude and the shortest haversine distance to the shore.

Supplementary Figures

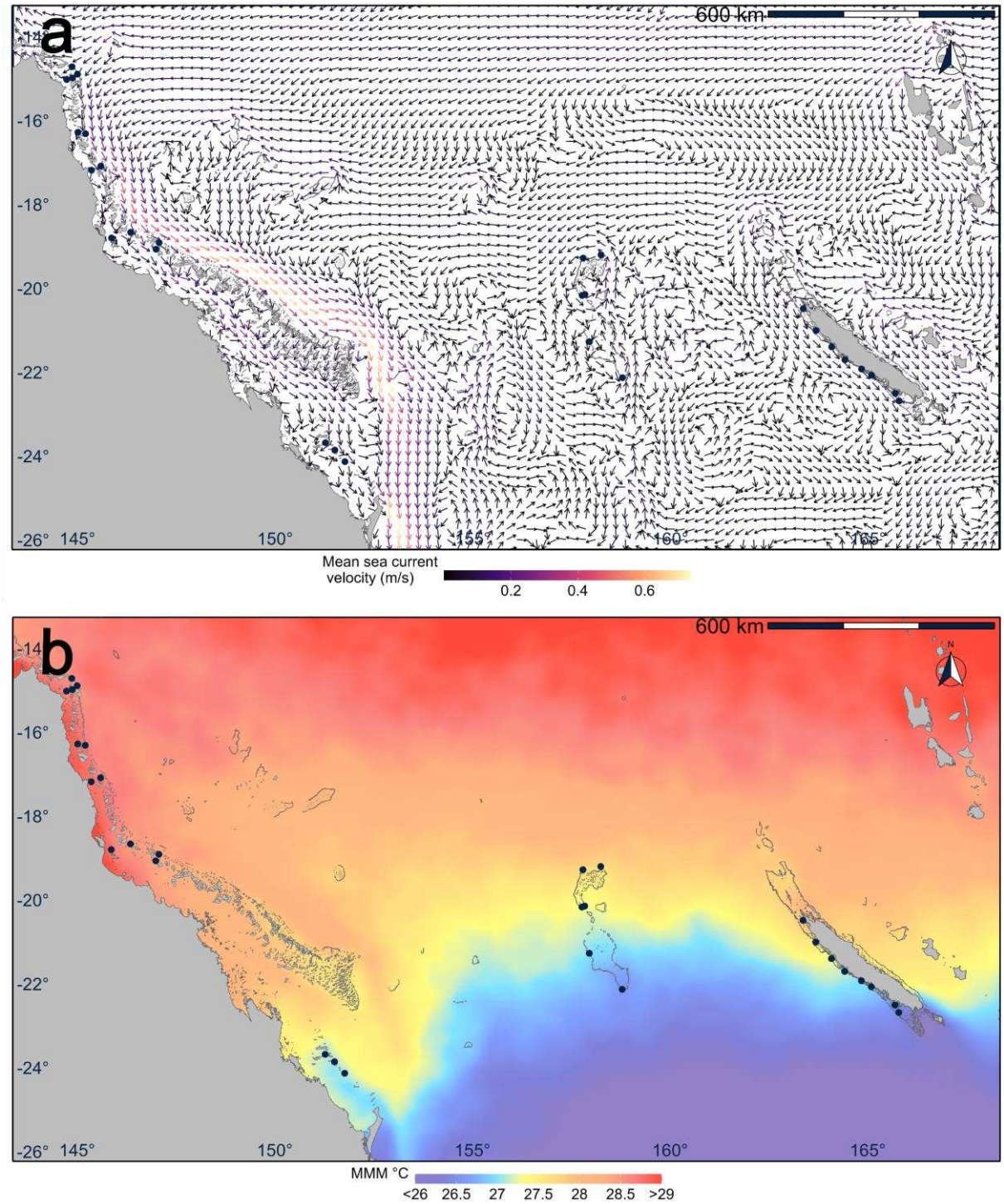


Figure A3.1. Environmental conditions across the Coral Sea. (a) Mean surface sea currents ($m.s^{-2}$) averaged over known spawning months for *A.spathulata* : October, November, December for the period 1993-2021 obtained from Copernicus GLOBAL_MULTIYEAR_PHY_001_030 product. (b) Maximum Monthly Mean (MMM, °C) obtained from NOAA CoralWatch v3.1. Black dots indicate *Acropora spathulata* sampling sites.

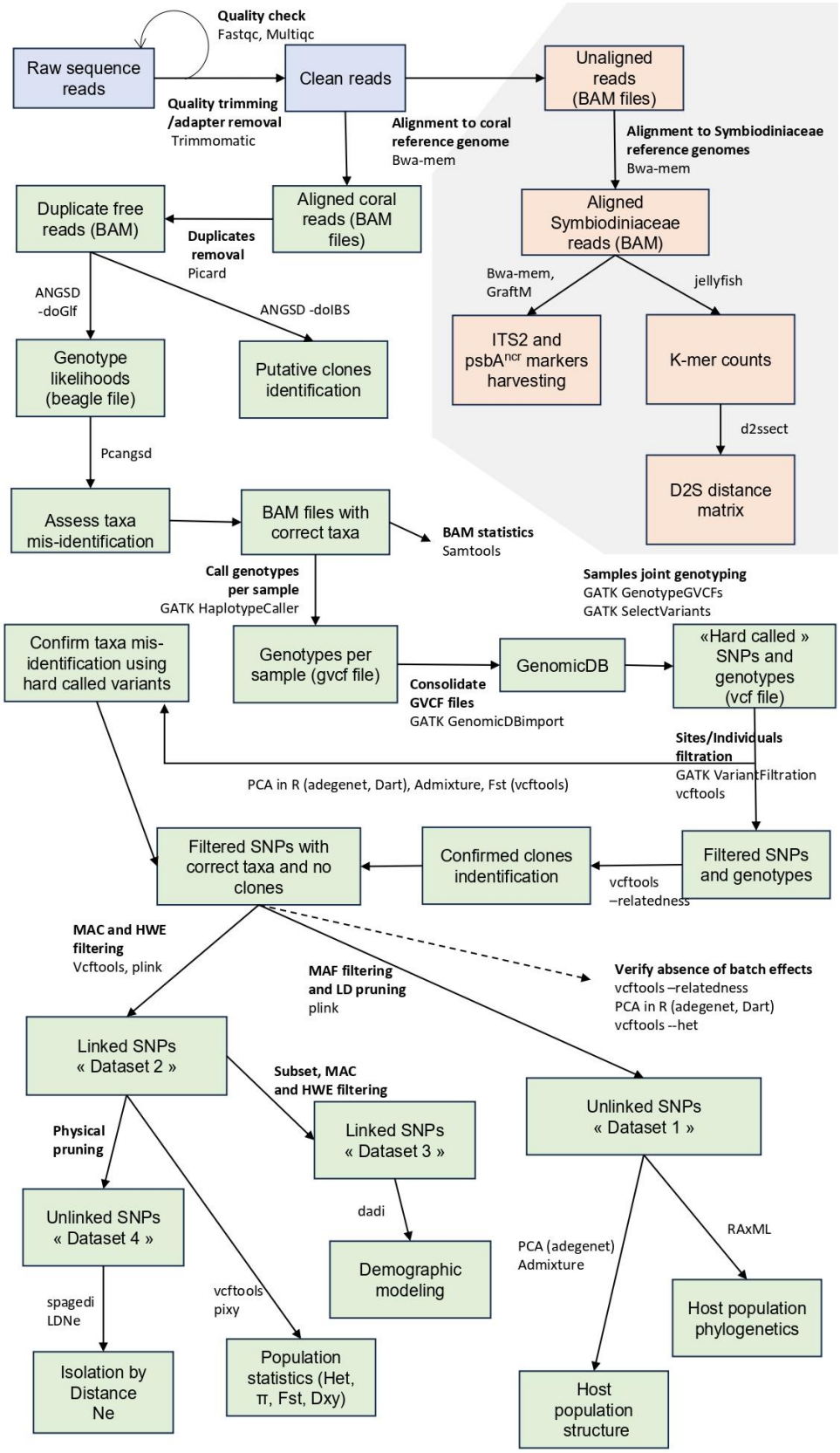


Figure A3.2. Summary of bioinformatic analyses workflow used to assess the population structure of coral hosts and their symbiont communities across the Coral Sea. Green boxes

depict data processing steps for the host and red boxes depict data processing steps for the symbionts.

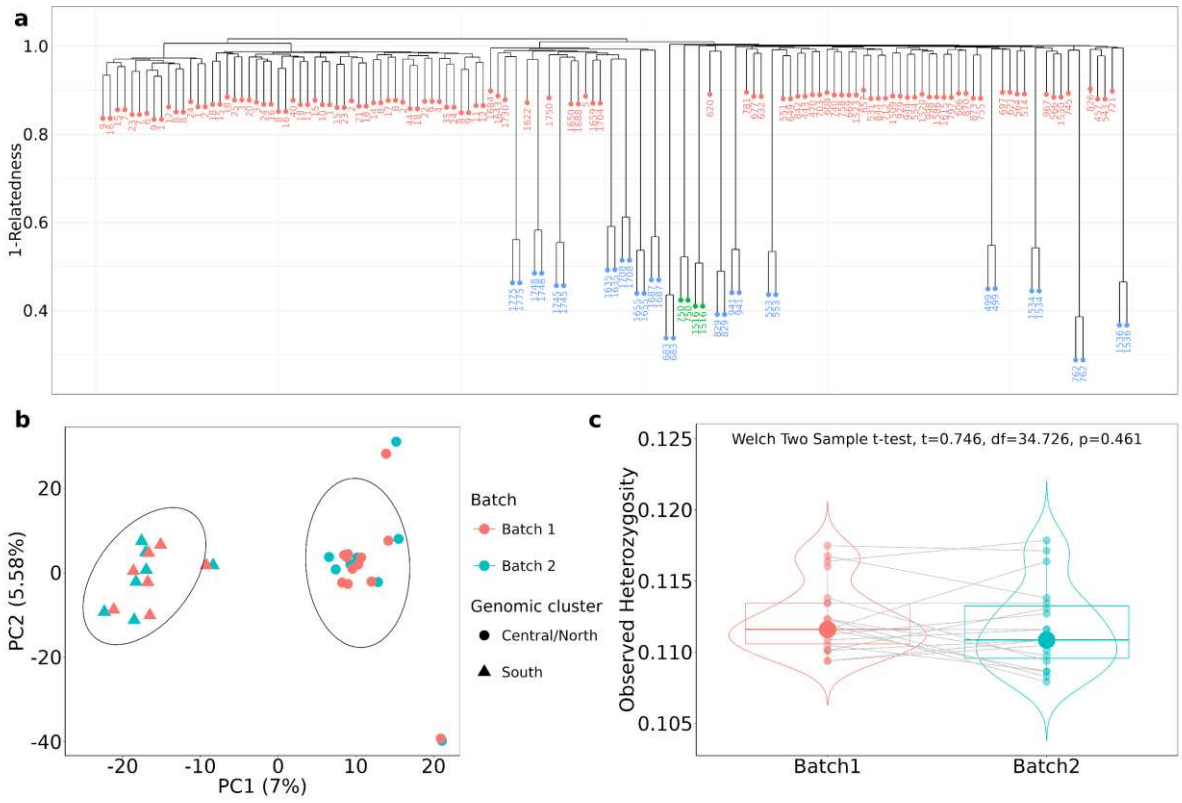


Figure A3.3. Assessment of potential batch effects using technical replicates extracted and sequenced within each batch. (a) Relatedness and (b) Principal component analyses were performed using 130,344 polymorphic sites (20% missingness). (c) Individual autosomal heterozygosity was computed from 2,715 polymorphic and monomorphic sites with 0% missing data, following recommendations of Schmidt et al. (2021).

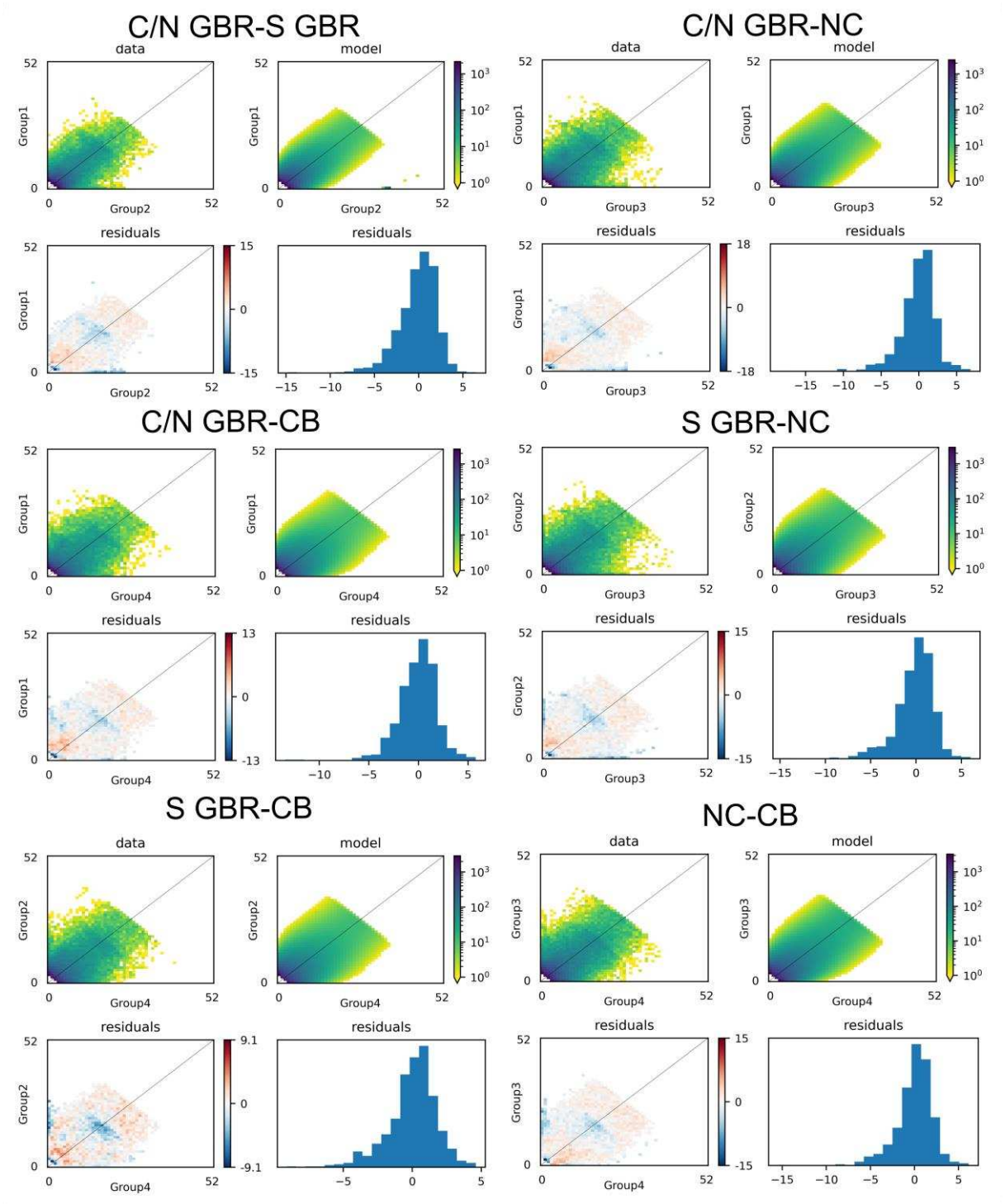


Figure A3.4. Observed and Modeled joint Allelic frequency spectrum (JAFS) for each pair of genomic populations (11 individuals per population) using demographic modeling analyses in Dadi. For each pair of genomic populations panels show observed JAFS (top left), best modeled JAFS (top right), and residuals distribution (bottom plots). Low frequency alleles are masked to account for genotyping errors.

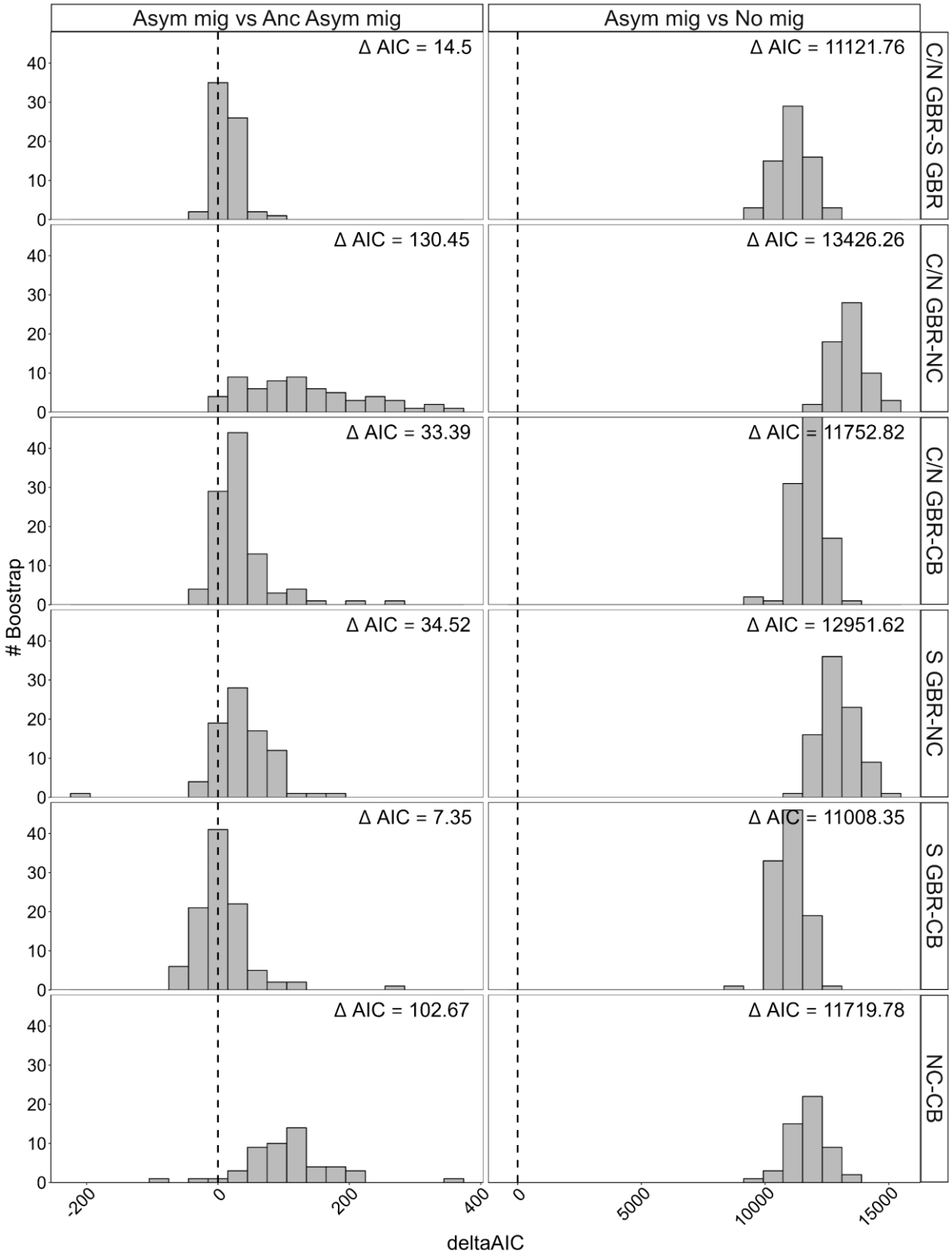


Figure A3.5. Bootstrap analysis of *A. spathulata* populations divergence models. Histograms of delta-AIC values for bootstrap replicates comparing a model of divergence with asymmetrical gene flow to a model of divergence with ancestral gene flow (left, gene flow stopped at some time T in the past) and divergence in the absence of gene flow (right). The

mean delta-AIC across 100 bootstraps is indicated for each population and model comparison. Positive values indicate higher support for a model of divergence with asymmetrical gene flow.

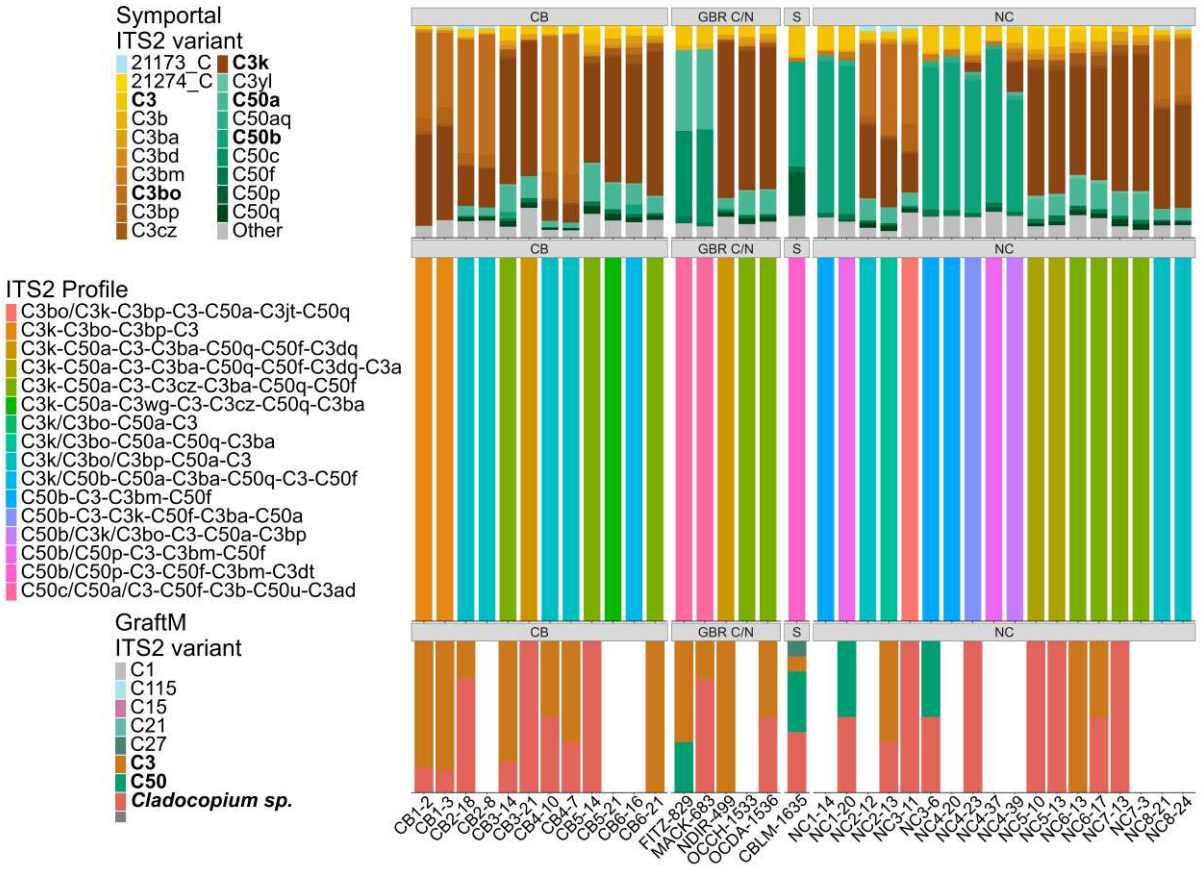


Figure A3.6. Comparison of ITS2 sequence variants recovered using graftM in hologenome data with conventional amplicon sequencing analysed in Symportal. Despite the low number of reads recovered by graftM both identified similar dominant ITS2 subclade in samples as C3 or C50.

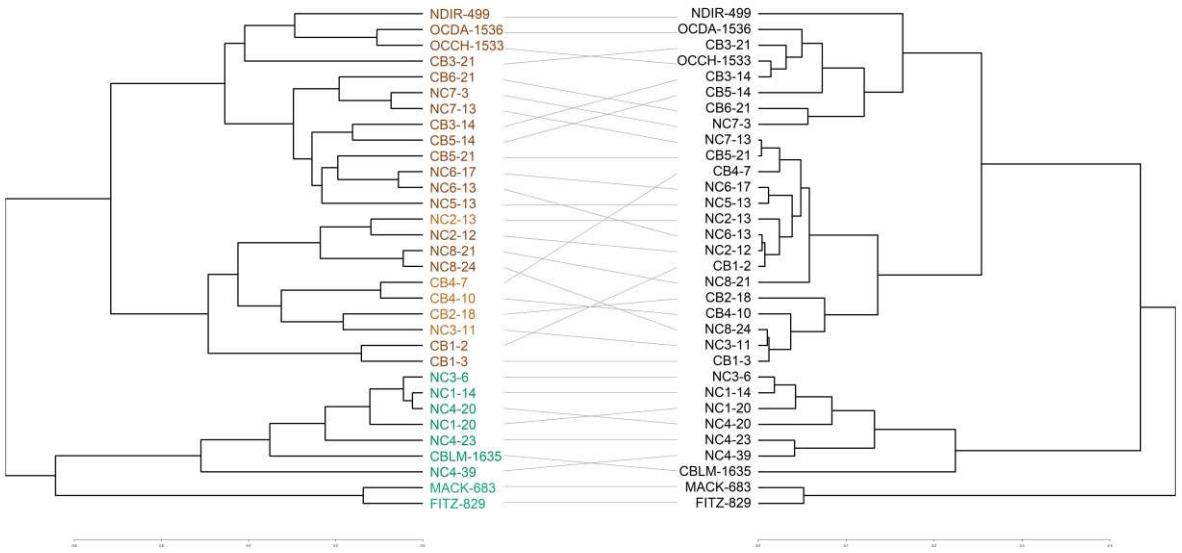


Figure A3.7. Comparison of samples hierarchical clustering using Unifrac distance based on ITS2 'defining intragenomic variants' (DIV, left) and D2S distance based on k-mer profiles (right). Leaves in the left dendrogram are coloured according to the majority ITS2 sequence found in the sample (C3k, C3k/C3bo, C50c or C50b).

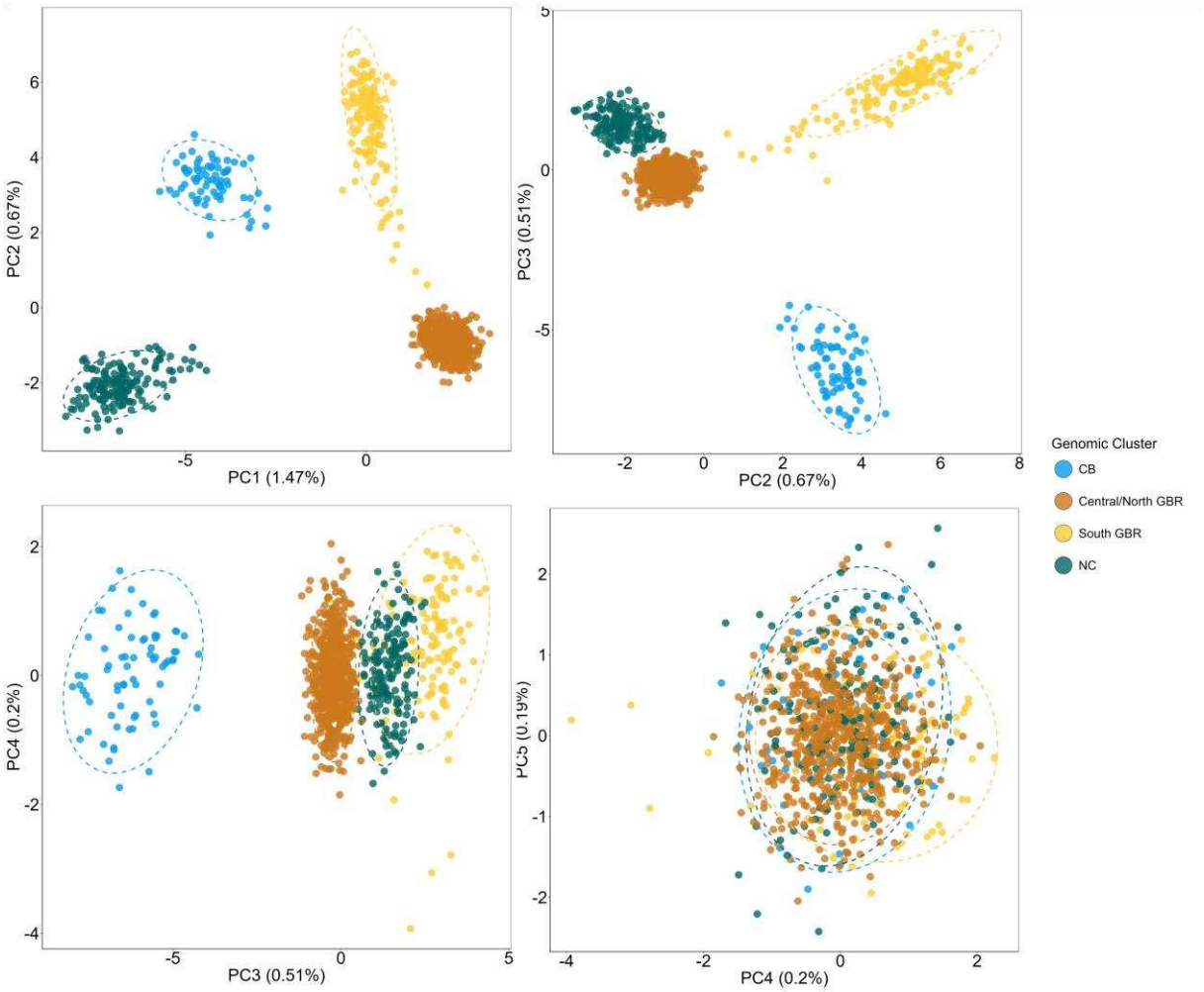


Figure A3.8. Principal component analyses on 27,175 high quality 'hard called' SNPs from 999 colonies collected across the Coral Sea. Each point represents an individual coloured according to its geographic region (CB = Chesterfields-Bellona atolls, NC = New Caledonia, GBR = Great Barrier Reef). The first 5 principal components are shown with number in parenthesis representing the % of total variance explained by that component.

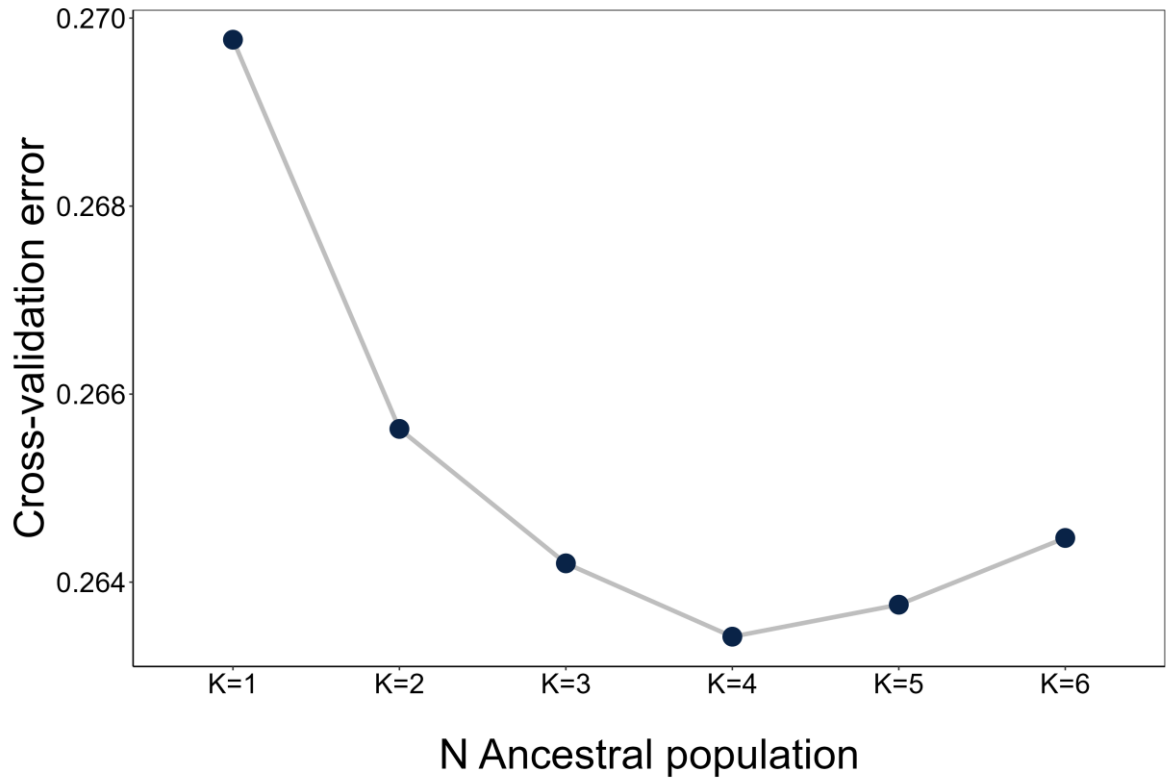


Figure A3.9. ADMIXTURE cross-validation error for different numbers of ancestral population. The optimal choice (K=4) showing the lowest error was used to conduct the final analyses.

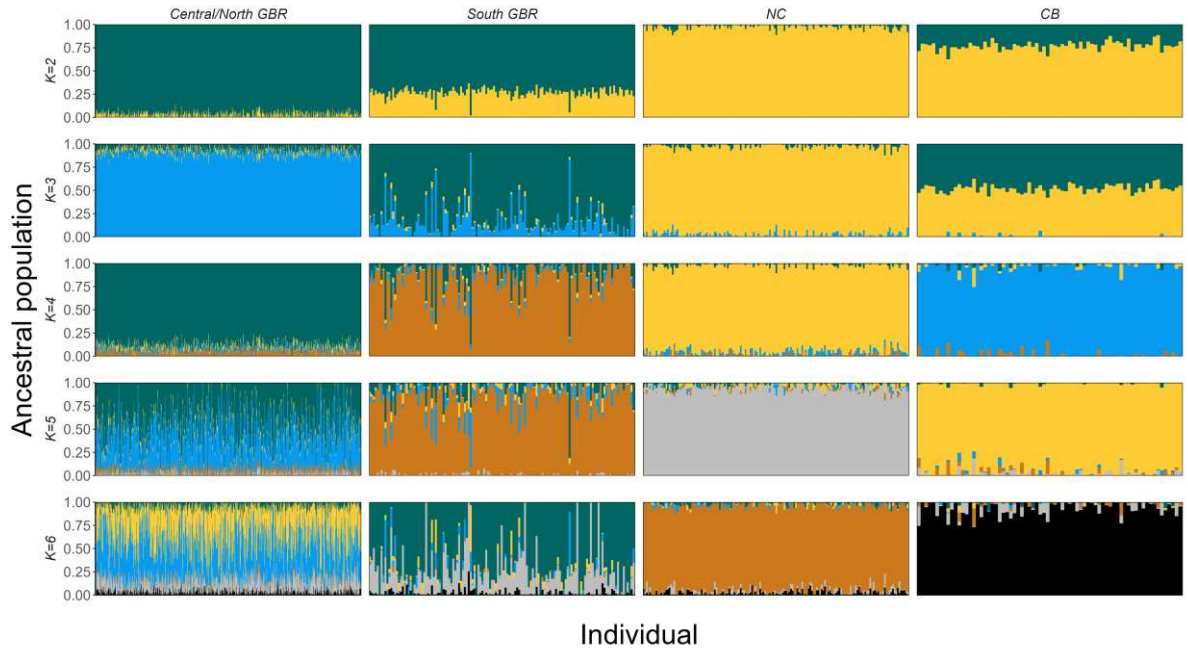


Figure A3.10. Ancestral population proportion for each of 999 colonies across the coral sea using ADMIXTURE analysis on 27,175 'hard called' SNPs and K=2–6 ancestral population.

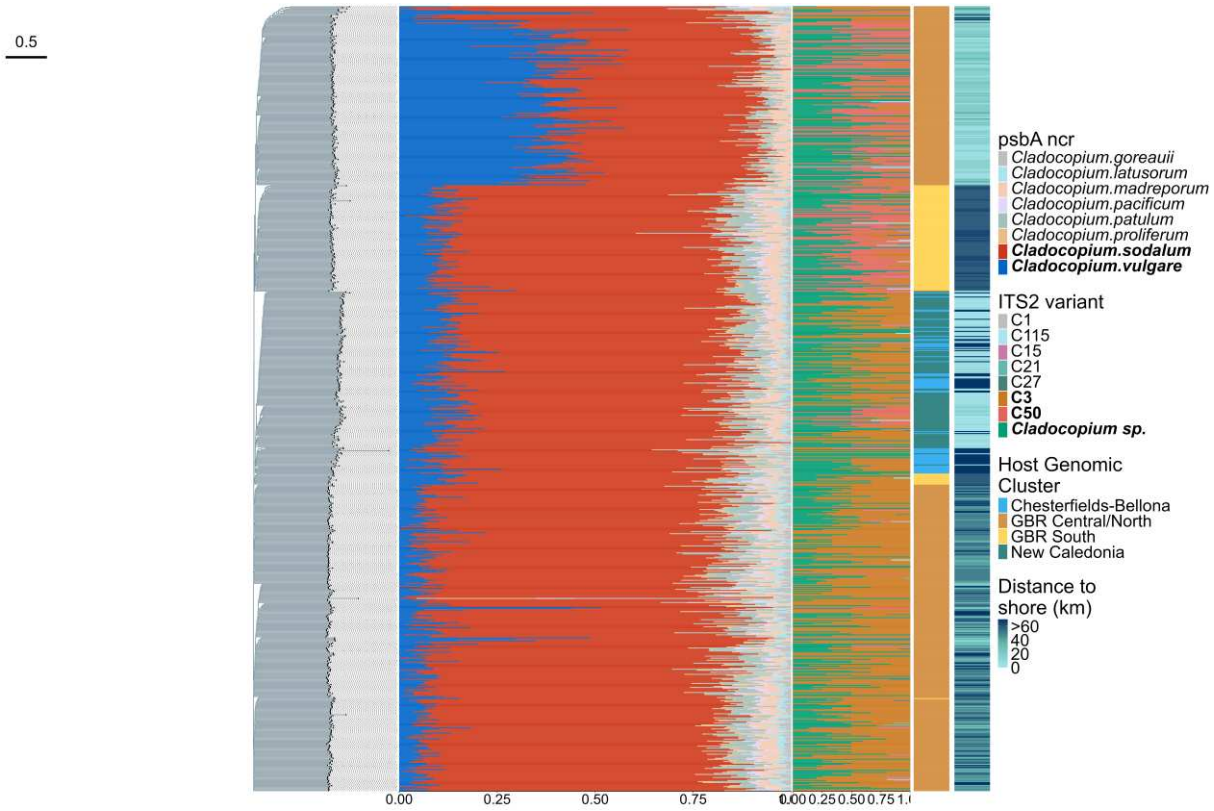


Figure A3.11. Summary of marker-based and alignment-free approaches used to characterise Symbiodiniaceae genetic diversity. A neighbour-joining tree was obtained based on D2S distance computed from k-mer pofiles (left). psbA^{ncr} sequences were aligned to a custom reference database and the relative abundance of uniquely mapping sequences is shown (center). ITS2 sequences were recovered in the samples using graftM and classified using symportal reference database (right). Coloured tiles show assignment to host genomic populations and cross-shore gradients.

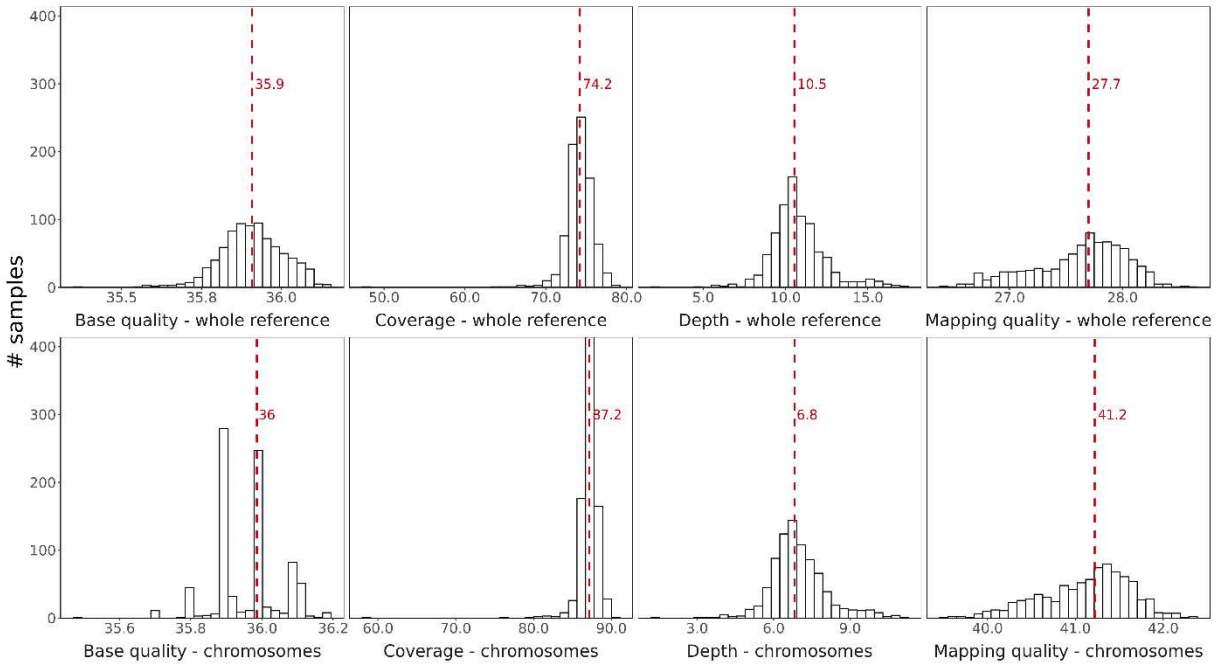


Figure A3.12. Summary of BAM files statistics for GBR samples (Batch1). Statistics are reported for the whole reference (chromosome + contigs) and for chromosomes only. Only reads mapping to the chromosomes were used in further analyses.

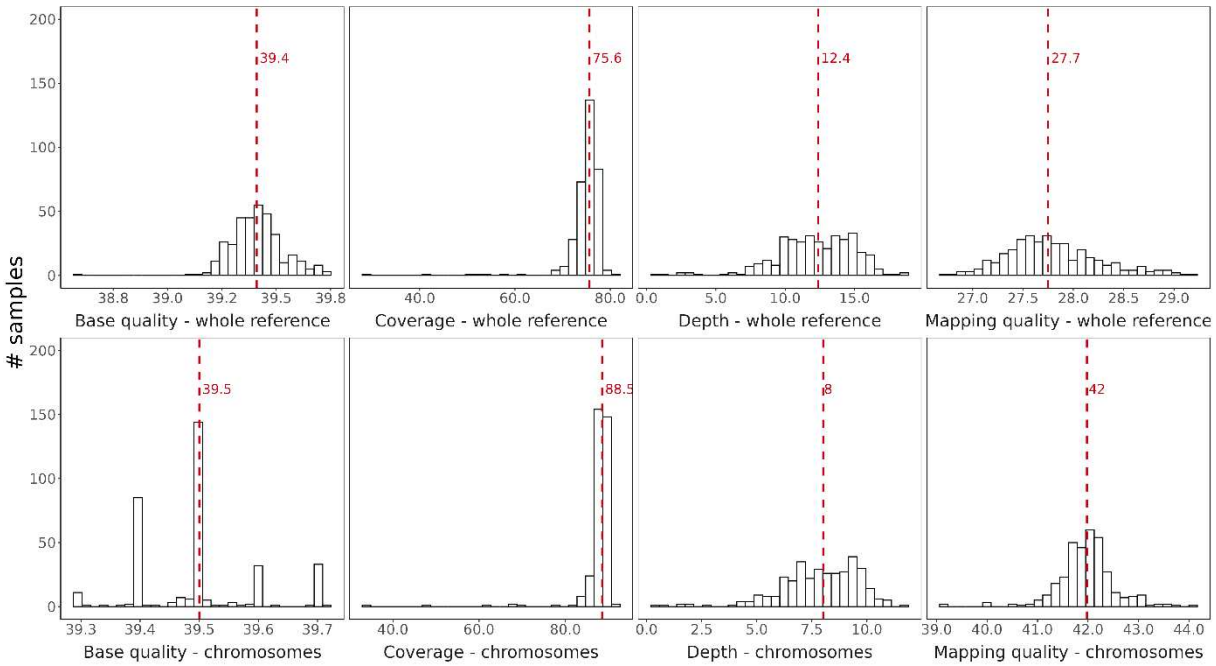


Figure A3.13. Summary of bam files statistics for NC samples (Batch2). Statistics are reported for the whole reference (chromosome + contigs) and for chromosomes only. Only reads mapping to the chromosomes were used in further analyses.

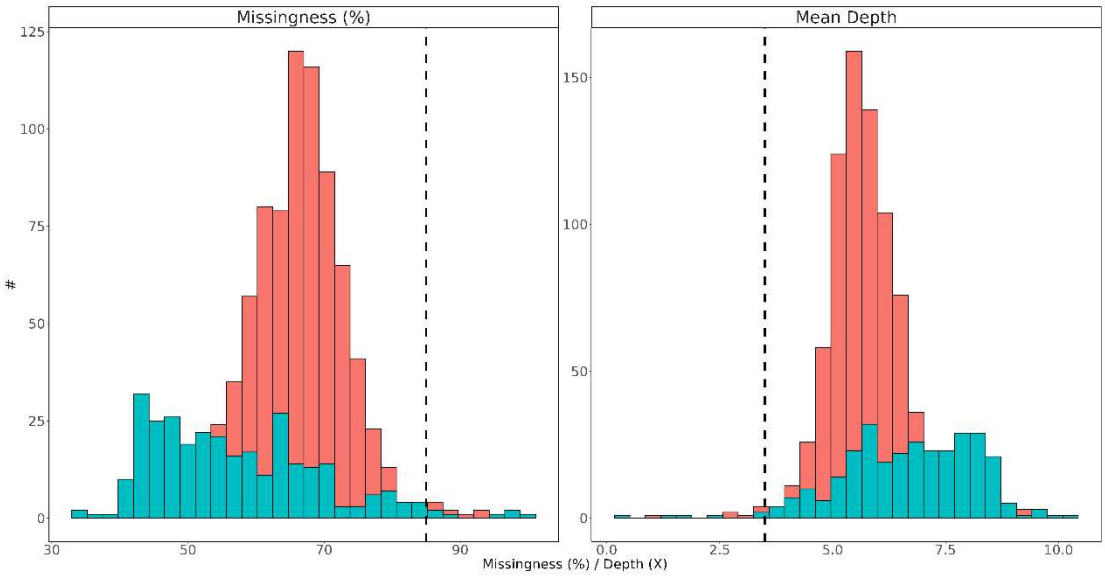


Figure A3.14. Distribution of individual missingness and depth across 1,105 individuals and 47,438,630 SNPs for Batch 1(pink) and Batch 2 (blue). The vertical dashed lines represent the thresholds used to remove individuals with high missingness and/or low average depth resulting in 1,088 high quality individuals (17 individuals removed).

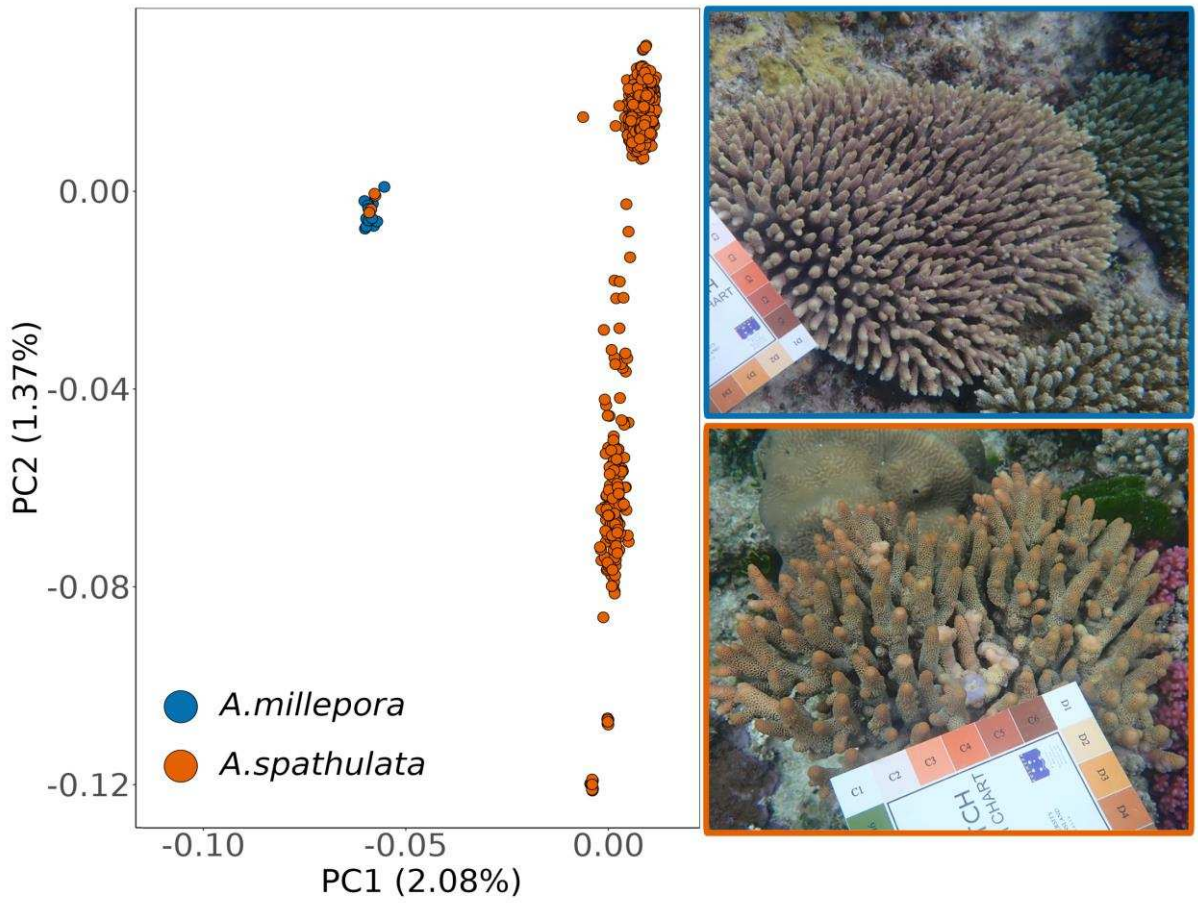


Figure A 3.15. Taxa mis-identification within the GBR dataset. Four samples were identified as *A.millepora* and discarded from following analyses. Pictures on the right show representative examples of *A.millepora* (blue) and *A.spathulata* (orange) colonies at Heron Island.

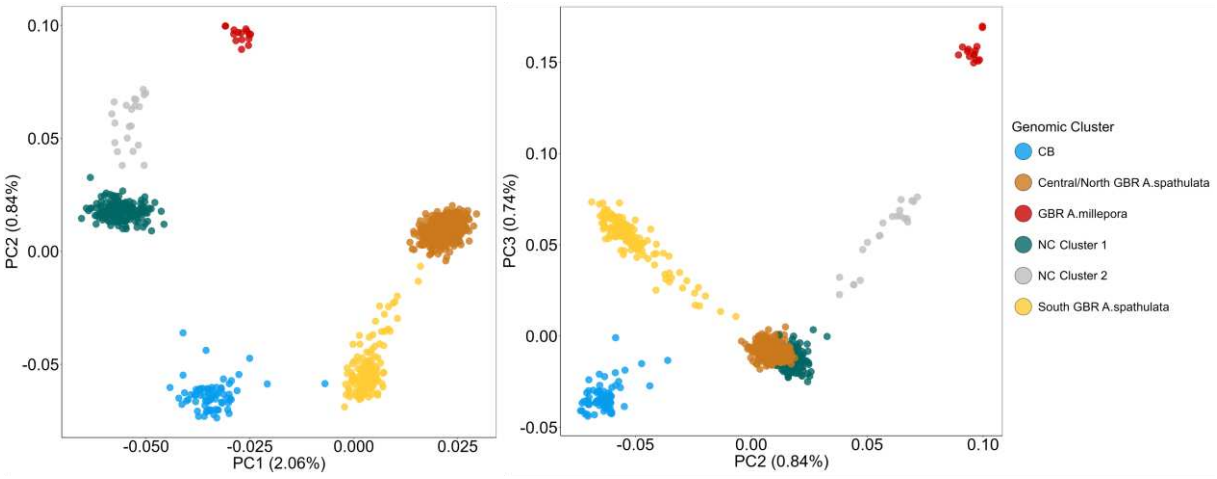


Figure A3.16. Principal component analysis of the global dataset alongside *A.millepora* samples from the Great Barrier Reef using genotype likelihood (1,041 individuals and 1,474,993 polymorphic sites). The putative undersampled Cluster 2 from New Caledonia and *A.millepora* outgroup were discarded from further analyses.

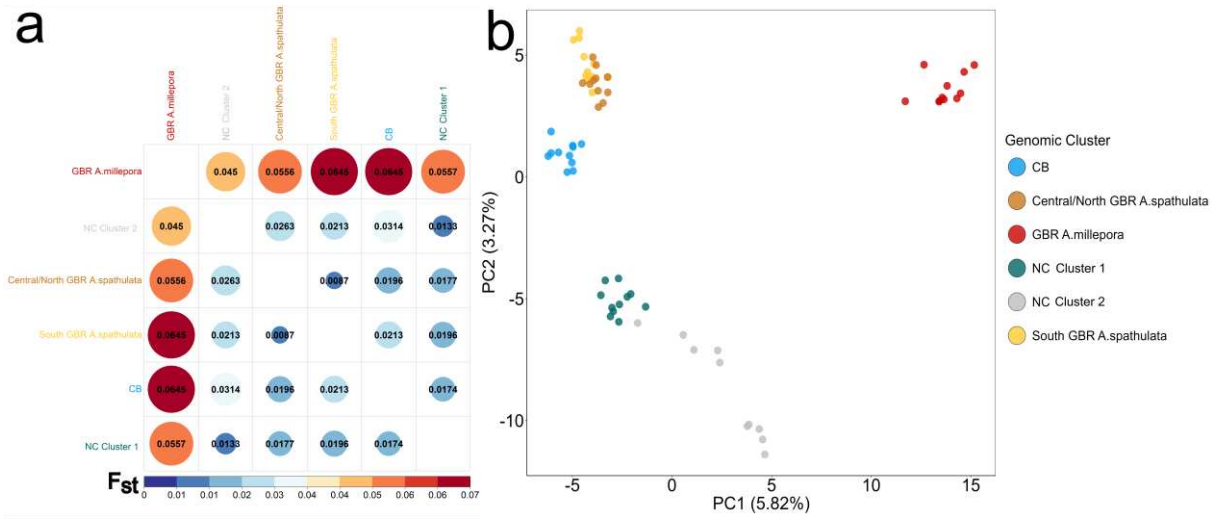


Figure A3.17. Genetic differentiation between groups using hard-called variants Pairwise fixation index (F_{st}) computation (a) and Principal Component Analysis (b) were performed on 7,051 SNPs and a reduced dataset of 66 colonies (11 colonies per group). The putative undersampled Cluster 2 from New Caledonia and *A.millepora* outgroup were discarded from further analyses.

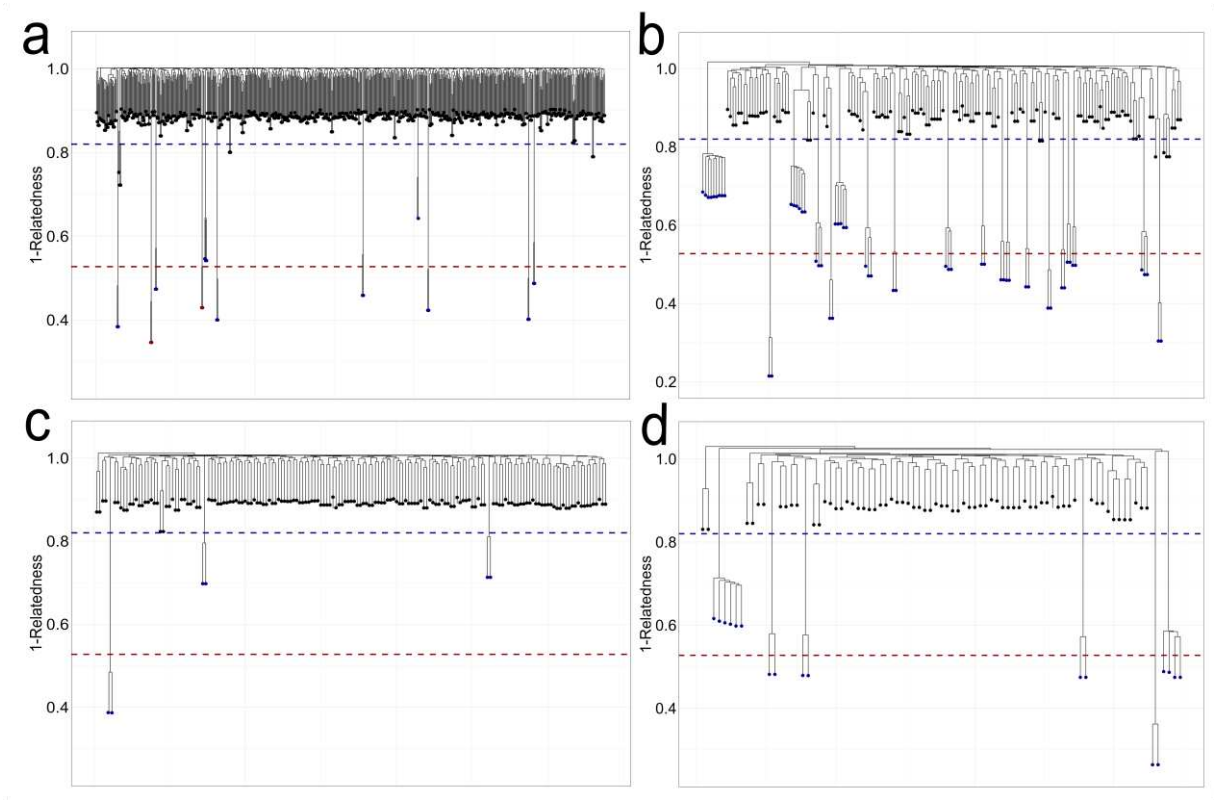


Figure A3.18. Genomic relatedness among individuals for Central/North GBR (a), South GBR (b), NC (c) and CB (d) genomic populations. The red line shows the minimum relatedness among technical replicates and the blue line shows the conservative threshold (r>0.2) used to remove clones and related individuals (blue leaves) from the dataset for further analyses.

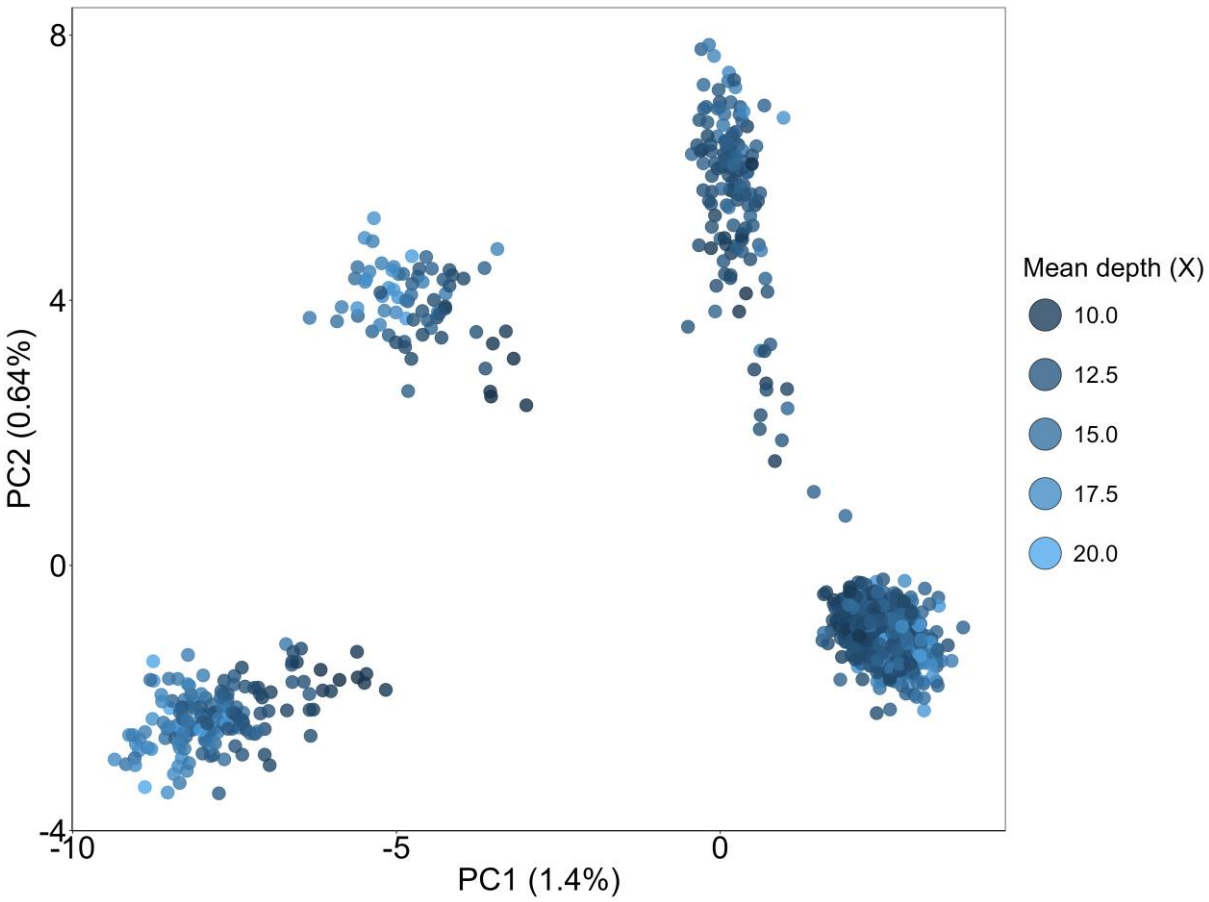


Figure A3.19. Principal Component Analysis on 27,175 high quality 'hard called' SNPs from 999 colonies collected across the Coral Sea. Each point represents an individual and is coloured by its average sequencing depth across all loci to control for potential bias in population structure. The first two principal components explain 1.4% and 0.64% of the total variance respectively.

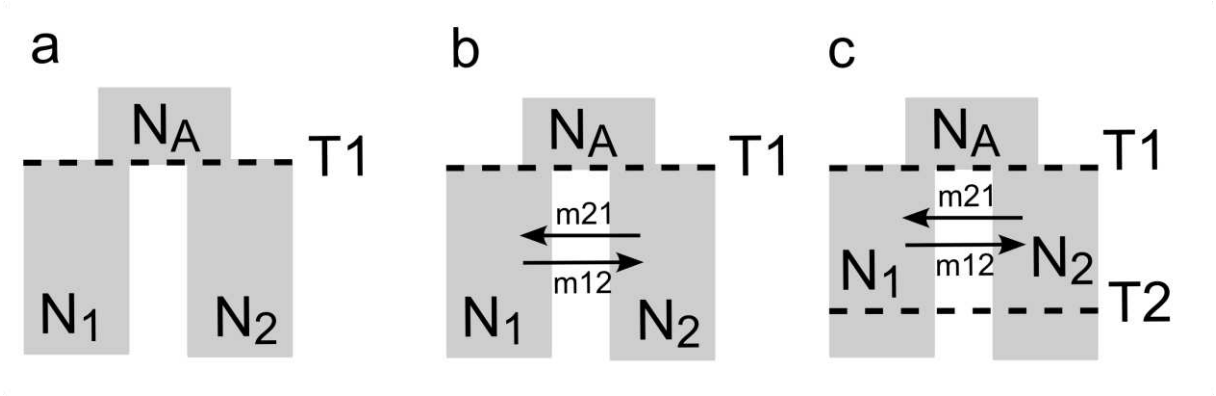


Figure A3.20. Models considered in demographic modeling analyses. (a) divergence in isolation, (b) divergence with asymmetrical homogeneous gene flow, (c) ancestral asymmetrical migration. Preliminary models of no divergence were also tested.

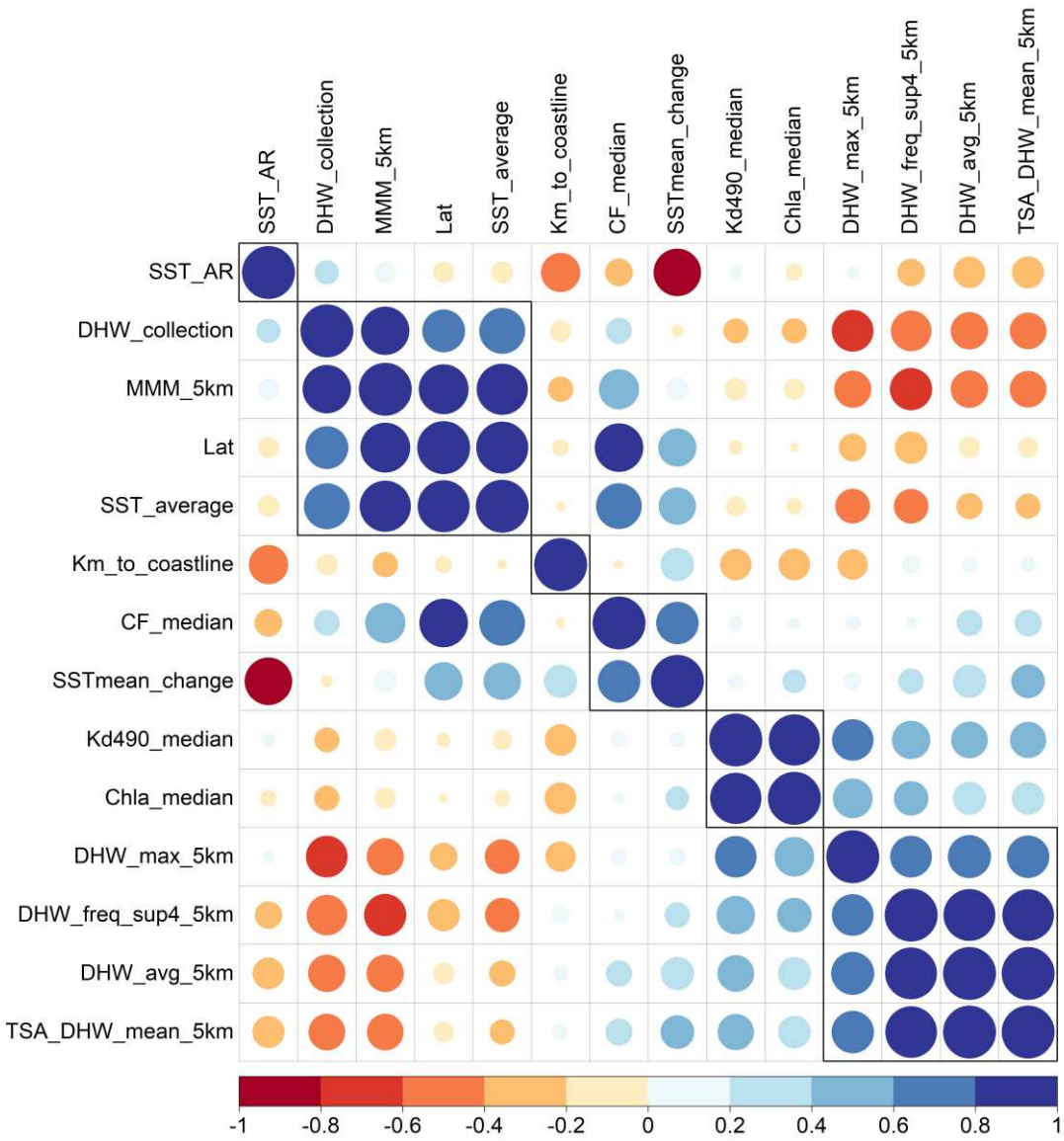


Figure A3.21. Pairwise Pearson's correlation coefficients between the 14 quantitative environmental predictors considered for the redundancy analyses. Only 7 predictors with a variance inflation factor < 10 were used for stepwise forward selection in the final model.

Supplementary Tables

Table A3.1. Summary of sampling effort across coral reef sites in the Western Pacific. Maximum Monthly Mean (MMM) of each reef was computed from the Coral Reef Watch of the National Oceanic and Atmospheric Administration (NOAA Coralwatch v3.1 satellite product). Colonies depth was standardised to the tide at the time of collection and are reported relatively to the Lowest Astronomical Tide (LAT). Negative values indicate shallow colonies above the LAT.

Country	locationID	locationCode	Sampling Date	Lon	Lat	MMM (°C)	Depth mean [range]	N
Australia	Hicks	HICK	28/02/2022	145.502542	-14.475094	28.6	2.2 [0.7,4.7]	61
Australia	North Direction	NDIR	01/03/2022	145.5133	-14.7434	28.6	-0.2 [-0.7,0.1]	52
Australia	Martin	MART	02/03/2022	145.3681	-14.7801	28.6	0.6 [-0.2,1.2]	60
Australia	No Name	NONA	03/03/2022	145.6383	-14.6508	28.6	1.1 [-0.2,3.6]	53
Australia	Mackay	MACK	04/03/2022	145.6514	-16.0384	28.8	-0.2 [-0.9,1.1]	60
Australia	St Crispin	STCR	05/03/2022	145.8449	-16.0724	28.7	0.1 [-0.9,3.5]	60
Australia	Fitzroy Island	FITI	06/03/2022	145.9948	-16.9406	28.8	0.3 [-0.6,2]	60
Australia	Moore	ONMO	07/03/2022	146.2316	-16.8457	28.6	0.2 [-0.3,1.1]	44
Australia	Pelorus	PAPE	08/03/2022	146.5023	-18.5587	28.7	2.1 [0.1,3.3]	45
Australia	Kelso	KELS	09/03/2022	146.9849	-18.424	28.4	0.9 [0.5,5.3]	44
Australia	Chicken	OCCH	10/03/2022	147.7064	-18.6706	28.4	0.9 [-0.4,4.6]	60
Australia	Davies	OCDA	12/03/2022	147.6268	-18.827	28.4	1.2 [0,3.9]	53
Australia	Lady Musgrave	CBLM	24/03/2022	152.4064	-23.8929	27.1	0.9 [-1.1,4.2]	56
Australia	Fitzroy Reef	FITR	25/03/2022	152.15	-23.617	27.1	-0.6 [-0.8,0.7]	61
Australia	Heron	CBHE	26/03/2022	151.912971	-23.441601	27.1	-0.7 [-1.3,1]	60
New Caledonia	Bellona Sud	CB1	23/06/2023	159.425853	-21.8905	26.6	-0.2 [-0.5,0]	4
New Caledonia	Bellona Ouest	CB2	24/06/2023	158.594	-21.0313	26.7	-0.4 [-0.6-0.3]	23
New Caledonia	Ilot Loop	CB3	25/06/2023	158.4083483	-19.9285188	27.3	-0.3 [-0.4-0.1]	24
New Caledonia	Chesterfields SO	CB4	26/06/2023	158.478	-19.905	27.3	1.1 [0.4,2.5]	17
New Caledonia	Chesterfields NO	CB5	27/06/2023	158.433288	-19.03805	27.7	1.8 [-0.1,4.1]	18
New Caledonia	Chesterfields NE	CB6	28/06/2023	158.884708	-18.960638	27.6	2.5 [0.6,5]	22
New Caledonia	Recif du Prony	NC1	10/08/2023	166.3273667	-22.26615	26.6	1.1 [-0.2,4.1]	25
New Caledonia	Recif Mara	NC2	22/08/2023	165.72805	-21.830483	26.9	3 [0.9,5.6]	24
New Caledonia	Recif Snark	NC3	01/09/2023	166.42516	-22.44361	26.6	0.4 [0,1.4]	21
New Caledonia	Ile Verte	NC4	06/09/2023	165.47735	-21.68475	27	-0.4 [-0.5-0.1]	25
New Caledonia	Ilot Contrariete	NC5	13/09/2023	165.05492	-21.46439	27.1	0.9 [0.4,1.7]	25
New Caledonia	Ilot Deverd	NC6	19/09/2023	164.3237	-20.766433	27.5	0.3 [-0.4,1.9]	25
New Caledonia	Plateau de Koniene	NC7	20/09/2023	164.7209	-21.157383	27.3	0.2 [-0.2,1.9]	25

New Caledonia	Pointe de Poum	NC8	28/09/2023	163.99965	-20.24595	27.8	-0.2 [-0.5,1.3]	25

Table A3.2. Pre-variant filtering steps summary. Same filtering parameters were used to process raw sequence reads from GBR (Batch 1) and New Caledonia (Batch 2) samples.

Filtering step	**Statistic**	**Batch 1 (GBR samples)**	**Batch 2 (NC samples)**	**Total**
Samples collection, selection and sequencing	N initial samples collected	831	323	1,154
	N initial samples sequenced	830	314	1,144
	N technical replicates	2	23	25
	N other species samples included as outgroups	36	0	13
Sequence QC	**Total number of samples successfully sequenced**	**845**	**337**	**1,182**
	Total number of reads prior filtering	31.7×10^9	14.2×10^9	45.9×10^9
	Total number of reads after quality filtering	29.8×10^9	12.3×10^9	42.1×10^9
Mapped reads filtering	Number of reads after filtering for PCR and optical duplicates	25.3×10^9	10.5×10^9	35.8×10^9
	Number of reads that mapped	24.3×10^9	97.3×10^8	$34{,}03 \times 10^9$
	Number of reads that primarily mapped	23.1×10^9	92.4×10^8	$32{,}34 \times 10^9$
	Number of reads after filtering improperly paired reads	20.5×10^9	80.7×10^8	$28{,}57 \times 10^9$
	Number of samples after filtering out <80% and <10M reads mapping	**836 (including 13 *A. millepora* samples used as outgroups)**	**309**	**1,145 (including 13 *A. millepora* samples used as outgroups)**
Taxa mis-identification removal	Number of samples identified as distinct from target taxa	4	23	27
	Total number of samples used for SNP and variant calling (after removal of other taxa)	**819**	**286**	**1,105**

Table A3.3. Post-variant filtering steps summary. For each step, the number of retained samples and single nucleotide polymorphisms (SNPs) is reported.

Step	**N samples**	**N SNPs**
Joint genotyping	1,105	92,885,427
GATK VariantFiltration (QD, FS, MQ, SOR, MQRankSum	1,105	47,438,630
Filtration of individuals with high missingness (>85%)	1,088	47,438,630

Preliminary filtration (mac>1, site missingness <20%, bi-allelic SNPs…)	1,088	339,720
Removal of technical replicates and individuals with >0.2 relatedness	999	339,720

Table A3.4. SNPs and genotypes filtering parameters used to conduct the main analyses. Preliminary analyses including variable missingness rates between 5 and 50% showed consistent results with the final threshold used to report the results (20%).

Filtering step	**Population structure (Dataset 1)**	**ML tree (Dataset 1)**	**Population statistics computation (Dataset 2)**	**Demographic modeling (Dataset 3)**	**Isolation by distance/N_e (Dataset 4)**
Min GQ	20	20	20	20	20
Min Genotype coverage	5	5	5	5	5
Max Genotype coverage	15	15	50	15	500
Scope	Study-wide	Study-wide	Between population pairs and within pops	Between population pairs	Within & Across population
Number of samples	999	200 (subset of 50 samples per pop)	20 x 10 (subset of 5 samples per pop x 10 replicates)	120 (subset of 30 samples per pop)	999
Max missing per locus	20%	20%	<20%	<20% within each population	10%
MAF	MAF>0.05	MAF>0.05			
MAC	MAC>1	MAC>1	MAC>1	MAC>3	MAC>3
HWE p-values			p-value>0.0001	p-value>0.0001	
Physical pruning					1 SNP per 20 kb
LD	LD<0.2	LD<0.2			
Number of SNPs	27,175	27,175	~2.2M SNPs + invariant sites	37,841-61,902	2,011

Table A3.5. Environmental predictors considered for Symbiodiniaceae community distance-based redundancy analysis and host structure redundancy analysis. Predictors in bold are those retained after controlling for multicollinearity (VIF<10) and used in forward stepwise selection.

Variable	**Metric**	**Source**	**Spatial resolution**	**Time resolution**	**Period**	**Description**
Temperature	DHW_avg	Coralwatch	5km	daily	1985-2024	Average monthly maximum DHW
	SST_AR	Coralwatch	5km	daily	1985-2024	SST Annual range
	SSTmean_change	Coralwatch	5km	daily	1985-2024	Nonparametric effect size between the distribution of monthly temperature between decade 1985-1995 and 2013-2023
	MMM	Coralwatch	5km	daily	1985-2024	Average temperature of the warmer calendar month (1985-1990+1993 climatology)

	DHW_freq_sup4	Coralwatch	5km	daily	1985-2024	Average number of days above 4 DHW per year
	DHW_max	Coralwatch	5km	daily	1985-2024	Maximum DHW
	SST_average	Coralwatch	5km	daily	1985-2024	Average SST
UV radiation	UVR_median	ERA5	0.25°	hourly	2002-2024	Median UV radiation ($W.m^{-2}$)
Irradiance	**CF_median**	ERA5	0.25°	hourly	2002-2024	Median cloud fraction
Water clarity	**Kd490_median**	Globcolour	1/24°	daily	2002-2024	Median attenuation of irradiance at 490nm, proxy for turbidity
Chlorophyll	Chla_median	Globcolour	1/24°	daily	2002-2024	Median concentration of chlorophyll a = proxy for nutrient load ($mg.\ m^{-3}$)
Spatial	**Km_to_coastline**	GADM 4.1				Shortest haversine distance to the shore
	Lat					Latitude hexadecimal

Appendix A4. Supplementary data for Chapter 5

Supplementary Texts

Text S1. Accuracy of imputation

In order to assess the accuracy of our imputation method, we performed an *in-silico* down-sampling of the five individuals from each population showing the lowest missingness rate (2–5% across loci). These samples were down-sampled to the highest observed missingness rate across individuals (40%) and used for imputation along other individuals from the same population. We then assessed the concordance between imputed genotypes and genotypes originally outputted by $GATK$ (i.e., considered as 'true' genotype) at the specific sites that were down-sampled. This was done separately for all genotypes and non-reference genotypes (i.e., 0/1 and 1/1) only. Accuracy was measured in each sample as

$$Accuracy = \frac{Nsites_{imputed=GATK}}{Nsites_{imputed}}$$

Where $Nsites_{imputed=GATK}$ is the number of sites where imputed genotype and genotype obtained from $GATK$ were concordant and $Nsites_{imputed}$ is the number down-sampled sites for a specific sample. Overall, we found an average $R^2 > 0.96$ for all populations and genotypes (Figure A4.10) and $R^2 > 0.87$ when only non-reference genotypes (i.e., rarer) were considered. Accuracy varied by population, presumably due to differences in LD decay relatively to genetic diversity (Figure A4.1). However, these differences were greatly reduced after filtration of rare variants (MAF>0.05) with a $R^2 = 0.977$ [0.963–0.985] for all genotypes (mean [range across populations]) and $R^2 = 0.970$ [0.953–0.981] for non-reference genotypes respectively. Although small imputation error levels persisted, the accuracy obtained here without a haplotype panel is relatively high, especially compared the alternative approach of setting all missing genotypes as the modal genotype, as commonly done in many association studies.

Text S2. Global RDA models

To compare signals of local adaptation within populations to local adaptation at the regional scale of the Western Pacific (i.e., across all populations), we also built a global RDA model including the four populations. In this case, IbD was significant and environmental predictors were strongly correlated to host genetic population structure (Procrustean rotation analysis; Sum of Squares = 0.43, $r = 0.75$, $p<0.001$; Figure A4.11). Therefore, not accounting for population structure would lead to a large number of false positive signals at neutral loci due

their demographic history (Hoban et al., 2016). We corrected for IbD and population structure using two methods: a partial-RDA (pRDA) conditioned on geographic coordinates (Lon,Lat) and a pRDA conditioned on the first three PCs of a PCA based on unlinked SNPs (r^2<0.2). The pRDA conditioned on geographic coordinates produced a very high number of significant outlier SNPs (914 candidate SNPs, see below for outliers' selection), of which 0/65 intersected with the pRDA conditioned on host PCs. Likewise, only two genomic windows were found in common between the two pRDA. This suggests that this correction was likely insufficient to correct for IbD and neutral variation due to demographic history (Figure A4.12a). As using a pRDA conditioned on host PCs is likely redundant with the intersection of single population models, we focused our present investigations on overlapping signals across single population models. Further investigations are needed to assess potential additional information brought by the global pRDA conditioned on hots PCs (Figure A4.12b).

Text S3. WZA method

Detecting genomic regions under selection using SNPs presents some inherent bias due to non-homogenous missingness across the genome, because power at each locus is partly a function of linkage disequilibrium (LD; r^2) between the tested SNP and the causal variant. Individual SNP significance may also be noisy due to genotyping errors or other artifacts. When different SNPs are represented across datasets this also complicates testing for overlapping signals of selection (Booker et al., 2024). To partly overcome these limitations, we applied the weighted-Z Analysis (WZA; Booker et al., 2024) to each RDA and GWAS results. This method leverages LD among SNPs to increase the statistical power of genome scans or association studies by aggregating individual SNPs significance into windows scores.

Briefly, the different steps of the method are 1) transforming loci p-values (from the RDA or GWAS) into empirical *p*-values using a rank-transformation, 2) converting empirical *p*-values into z-scores from a standard normal distribution, 3) selecting a window size L (in bp), 4) Computing window Z_w score using the equation below and 5) Converting back Z_w scores to WZA *p*-values, 6) Correcting Z_w scores for uneven SNP density along the genome. Z_w scores are computed from SNPs $i = 1 \ldots n$ within each window w using:

$$Z_w = \frac{\sum_{i=1}^{n} p_i q_i z_i}{\sqrt{\sum_{i=1}^{n} (p_i q_i)^2}}$$

Where p_i and q_i are the major and minor alleles frequencies at locus i and z_i its corresponding z-score. Following authors recommendations, we chose a window size larger than the expected rate of LD decay. Across all *A. spathulata* populations, LD declined sharply within 5kb and pairwise r^2 was below 0.1 for all populations at 20kb (Figure A4.1). Therefore, we performed two iterations of WZA, aggregating SNP *p*-values in windows of 20kb with a shift of 10kb between iterations following Rogivue et al. (2025). Finally, WZA *p*-values were adjusted to control for FDR (BH correction, α=0.01). We also ran preliminary analyses using varying window sizes of 10–50kb and the main signals matched those reported here.

Text S4. GWAS models sensitivity

We ran separate GWAS for each of the three population (Central/Northern GBR; Southern GBR; New Caledonia). For each dataset we ran a simple linear model (equation 1; lm), a linear mixed model controlling for relatedness as a random effect (equation 2; lmm) and a linear mixed model including fixed covariates effects (symbionts and accumulated heat stress at the time of sampling; equation 3; lmm_covar).

$$(1)\ \boldsymbol{y} = \mathbf{x}\beta + \boldsymbol{\varepsilon}, \boldsymbol{\varepsilon} \sim \mathrm{MV}N_n(0, \lambda\tau^{-1}I_n)$$

$$(2)\ \boldsymbol{y} = \mathbf{x}\beta + \mathbf{u} + \boldsymbol{\varepsilon}, \mathbf{u} \sim \mathrm{MV}N_n(0, \lambda\tau^{-1}\boldsymbol{K}), \boldsymbol{\varepsilon} \sim \mathrm{MV}N_n(0, \lambda\tau^{-1}\boldsymbol{I}_n)$$

$$(3)\ \boldsymbol{y} = \boldsymbol{W}\alpha + \mathbf{x}\beta + \mathbf{u} + \boldsymbol{\varepsilon}, \mathbf{u} \sim \mathrm{MV}N_n(0, \lambda\tau^{-1}\boldsymbol{K}), \boldsymbol{\varepsilon} \sim \mathrm{MV}N_n(0, \lambda\tau^{-1}\boldsymbol{I}_n)$$

where $\boldsymbol{y}$ is a phenotype vector for n individuals; $\mathbf{x}$ is an n-vector of SNPs and β additive effect size for each SNP. $\boldsymbol{W}$ is an $n\ x\ c$ matrix of covariates including a column of 1s (intercept), α is the c-vector of the corresponding coefficients including the intercept. $\mathbf{u}$ is an n-vector of random effects, $\boldsymbol{\varepsilon}$ is an n-vector of errors, τ −1 is the variance of the residual errors and λ the ratio between the two variance components. $\boldsymbol{K}$ is a $n\ x\ n$ relatedness matrix and $\boldsymbol{I}_n$ a $n\ x\ n$ identity matrix. MVNndenotes the n-dimensional multivariate normal distribution. GEMMA tests the alternative hypothesis $H1$: $\beta \neq 0$ against the null hypothesis $H0$: $\beta = 0$ for each SNP using a Wald's test.

We assessed results consistency across models by computed Spearman's correlations between individual SNPs -log10(p-values) (Figure A4.13) and by producing Q-Q plots to assess inflation in *p*-values distributions. As expected, controlling for samples relatedness had little effect on within-population GWAS results because related individuals were previously removed (Spearman's $\rho_{\text{lm-lmm}} > 0.99$). Controlling for associated symbionts and accumulated heat stress at the time of the experiment also had a small (Spearman's $\rho_{\text{lmm-lmm_covar}} = 0.92–0.96$) effect.

Given these results, we used lmm_covar models for each population and trait as a conservative method to identify candidate genomic regions underlying heat stress responses.

We also conducted GWAS using bleaching (MIG) and mortality traits measured under natural marine heatwave in the Central/Northern GBR. In this case, only symbiont communities were included as covariates. Given the relationship of *in-situ* mortality and the peak SST reached at each reef during the marine heatwave, we also tested a model including this factor as a covariate which produced consistent results (Spearman's $\rho = 0.91$, no other loci reached a p-value $< 1 \times 10^{-5}$).

For survival, the same models were used as for continuous variables, as justified in *GEMMA* manual with dead colonies encoded as 2 and alive colonies encoded as 1. As a sanity check, a GWAS was also conducted in *PLINK* v1.90b7.2 using a logistic regression on this binary trait which produced highly similar results (Pearson's $R = 0.998$ between *GEMMA* β and *PLINK* Odd-ratio).

Text S5. Global GWAS models

Given virtually no single-loci reaching genome-wide significance in any of the GWAS models, we tested whether pooling multiple populations in a single GWAS on Chlorophyll ED50 could improve statistical power. We built too separate models: one including the two GBR populations ('All GBR', Table A4.4) and one with all populations ('All populations'). As expected, controlling for population structure in these models had a large effect (Spearman's $\rho_{lm\text{-}lmm}$ = 0.56–0.71, Figure A4.13) and was essential to avoid inflation in models p-values (λ>1.7 in linear models).

As outlined in Chapters 2 and 3, heat tolerance phenotypes were measured using different proxies, slight deviations in acute heat stress systems and during different seasons on the GBR and in New Caledonia. While this is not a problem for within-population GWAS models, this could introduce a bias in these global models and therefore the population of origin was encoded as a dummy variable (Spearman's $\rho_{lmm\text{-}lmm_covar} = 0.89–0.93$). We found that pooling populations did not increase statistical power (no loci reached genome-wide significance either) and therefore we focused on single-population model results in the main text.

Text S6. Annotation of the v3 reference genome

We used *Helixer* (Holst et al., 2023) to perform *de-novo* annotation of the v3 genome using deep learning and a Hidden Markov models, and retrieved CDS were mapped to the v2 genome

to recover gene annotations. In addition we performed a second iteration of annotation using the online a version of *MOGSA* (https://mosga.mathematik.uni-marburg.de/), which compiles multi-omic data (Meng et al., 2019) and re-annotated CDS using the updated Uniprot/swissprot database. GeneMark tool was used to predict ORFs, Red to predict repeated sequences, tRNAscan for tRNA and Barrnap for rRNA. The two annotations were then compiled into a single dataset that was used to identify genes in genomic regions of interest.

Text S7. Genomic prediction based on polygenic risk scores

Text S7.1 Method

We sought to assess the combined ability of genomic markers to predict heat stress responses using polygenic risk scores (PRS) based on GWAS loci effect-sizes from linear mixed models following Fuller et al. (2020). To reduce redundant information shared by closely related SNPs due to LD, we first performed LD-clumping on GWAS results using *plink*. This process consists of clumping all loci with an r^2>0.5 within 250kb of the locus with the minimum p-value. The operation is then repeated until all loci are clumped with an index SNP representative of that LD group. Then additive PRS were computed from effect sizes in *plink*, using increasing number of index SNPs (n = 10,50,100,500,1000,2000,3000, all index SNPs). For all GWAS, we used cross-validation to assess the accuracy of PRS by performing 100 random 80/20 train-test splits. The GWAS and LD clumping procedures were performed on the train set for each split and PRS computed for the test set. The PRS was used to predict test phenotypes using standard regression and we computed the correlation accuracy (Pearson's R) and the proportion of variance explained (R^2) for Chl ED50 and MIG. For mortality, a logistic regression was used and accuracy was measured as the area under the curve (AUC). Finally, to evaluate the contribution of polygenic risk scores (PRS) alongside environmental and biological predictors, we fitted multivariate regression models of increasing complexity on the test sets following Fuller et al. (2020) as described in the main text, but with the PRS instead of the Adaptive Index.

To test whether including interaction between genetic variants (i.e., epistasis) could improve predictive performance, we built random forest prediction models using *randomforest* R package (Breiman et al., 2018). Separate random forests models were built using the top 1,000 SNPs from each GWAS train/test split and 1,000 random SNPs. Random forests were grown to ntree=20,000 and mtry=100 predictors were tried at each split. Accuracy was measured using the test dataset as outlined above.

Text S7.1 Results

Although PRS from 1,000 index SNPs explained most Chlorophyll ED50 variation in the training data ($R^2 > 0.91$), predicted variance in the test sets was very low across populations (average $R^2 = 0.013–0.032$, Figure A4.14a-c), in line with previous coral studies (Fifer et al., 2024; Fuller et al., 2020). Similar results were obtained for the *in-situ* bleaching (average $R^2 < 0.022$) and mortality (average AUC < 0.58, Figure A4.14d-e). In addition, the PRS showed weak predictive correlations, with no differences across pigmentation quantiles (Figure A4.15a) and a negative correlation with mortality (Figure A4.15c), reflecting limited accuracy due to overfitting. This low accuracy was also unlikely to be the result of non-additive interaction among SNPs (i.e., epistasis), as a random forest model trained on 1,000 top GWAS index SNPs did not significantly improve the predicted variance (*p*-value > 0.05, Wilcoxon- rank sum test) and did not perform better than a model based on 1,000 random SNPs (*p*-value > 0.05). This result held true when using both the lenient and string genotype datasets.

To evaluate PRS predictive accuracy alongside other factors, we fitted multiple regression models for *in-situ* bleaching and mortality, including environmental covariates and Symbiodiniaceae composition (Figure A4.15). The magnitude of the marine heatwave (peak SST and DHW, measured at the reef-level) did not explain the variation in bleaching responses at the time of the surveys ($R^2 < 0$, Figure A4.15a, b) and a small fraction of variation in mortality after the conclusion of the marine heatwave (AUC = 0.725, Figure A4.15c, d). Colonies depth and long-term reef-level environmental conditions (Turbidity, MMM) explained substantially higher variation in traits ($R^2 = 0.175$ and AUC=0.824). Likewise, associated Symbiodiniaceae communities provided an increase in accuracy of 44% and 3% for bleaching and mortality respectively ($R^2 = 0.849$, AUC = 0.849), although this increase likely reflected other reef-level differences in addition to Symbiodiniaceae composition (Figure A4.16). The PRS did not significantly improved the variance explained beyond other predictors (*p*-value >0.05, Wilcoxon rank sum test, Figure A4.15b,d), consistent with Fifer et al. (Fifer et al., 2024), who reported variable accuracy and utility across microhabitats.

Text S8. Genomic prediction using ridge and lasso regression

Text S8.1 Methods

Individual SNPs effect sizes are often overestimated in GWAS especially when conducted over small number of individuals, reducing PRS transferability to independent datasets—a phenomenon known as the ‘winner’s curse (Xiao & Boehnke, 2009). Conversely, genomic

prediction methods based on the infinitesimal model estimate all marker effects simultaneously, preventing overfitting and prioritizing accurate prediction over the identification of causal loci (McGaugh et al., 2021). Widely used in agriculture to produce genomic estimated breeding values (GEBV), these methods are increasingly applied to wild populations, but have not yet been applied to corals.

As a second approach, we built genomic prediction models for Chlorophyll ED50 and MIG using Best Linear Unbiased Prediction (BLUP) approaches implemented in R package *rrBLUP* v4.6.3 (Endelman, 2011). These methods are biased on the infinitesimal model and can provide unbiased estimates of effect sizes by assuming all SNPs share a common variance, which shrinks extreme estimates toward the overall average (McGaugh et al., 2021). For both traits we computed Genomic Estimated Breeding Values (GEBV) using ridge-regression BLUP with function *mixed.solve*. Similar to the PRS, we built *rrBLUP* models on 100 random train sets (80% of samples) and assessed the predictive correlation (*R*) on the 100 corresponding test sets (20%).

For mortality, we used the R package *BGLR* v1.1.4 (Pérez & de Los Campos, 2014) to fit ordinal Bayesian ridge regressions. The model was run for 12000 iterations with a burn-in of 2000 iterations and thinning interval of 5 to sample from the posterior distribution of marker effects, producing genomic estimated breeding values (GEBVs) for each individual. Predicted GEBV from the test set were converted into probabilities of mortality using the cumulative normal function *pnorm* and used to compute models AUC as indicated above. We used the same approach as described for the PRS to estimate the increase in predictive accuracy of GEBV relative to other environmental and symbionts predictors.

Text S8.2 Results

For all tested traits, GEBV were positively correlated with observations, indicating reduced overfitting compared to PRS, but the predictive correlation was low with confidence intervals overlapping 0 (Figure A4.17). Compared to other environmental predictors, GEBV did not provide a significant increase in predictive correlation for bleaching and mortality (p-value > 0.1, Wilcoxon rank sum test, Figure A4.15c, f).

Although our genomic predictions were likely underpowered, considering most genomic predictions studies use tens of thousands of samples, some achieved relatively high accuracy with sample sizes comparable to our study (McGaugh et al., 2021). Because genomic prediction

accuracy decreases with increasing effective population size (N_e), these findings support previous evidence of large N_e in *Acropora spathulata* (Denis et al., 2025), and the need for much larger sample sizes for accurate predictions. For example, assuming a bleaching heritability of $h^2 = 0.6$ (Bairos-Novak et al., 2021), $N_e = 1{,}000$, and using the size of *A. millepora* genetic map (Wang et al., 2009), roughly 10,000 individuals would be needed to achieve a predictive correlation of r=0.4, from eq.1 in (McGaugh et al., 2021). In addition, genotype by environment interactions have been previously reported for coral bleaching (Drury & Lirman, 2021), which would imply distinct ranking of GEBV across environments (Gienapp et al., 2019). This could reduce the accuracy of predictions in the present study, which assumes a consistent genetic architecture across all reefs within a population.

Text S9. Predictive power of symbionts PCs

Across our genomic prediction models, symbionts PCs explained a large fraction of bleaching variation ($p < 0.001$, Figure 5.5, Figure A4.15) and a significant fraction of mortality variability ($p < 0.05$, Figure 5.5, Figure A4.15). However, symbionts community composition varied mostly across shelf position in the Central/Northern GBR (Figure A4.3), also corresponding to the main axis of variation in bleaching and mortality (Figure A4.2). To test whether symbionts PCs explained variation in heat stress responses beyond differences among sites, we compared the AUC and R^2 of multiple regression models using all environmental predictors + symbionts PCs or all predictors + Reef ID. We found symbiont PCs did not explain a significantly larger variation in in-situ responses than Reef ID (Figure A4.16). In fact, for bleaching, Reef ID explained a significantly larger variation than symbiont PCs (Figure A4.16b). These results indicate that while associated symbionts may affect colonies responses during the marine heatwave, this effect is largely confounded with other reef-level factors (e.g., hydrodynamics, reef topology).

Supplementary Figures

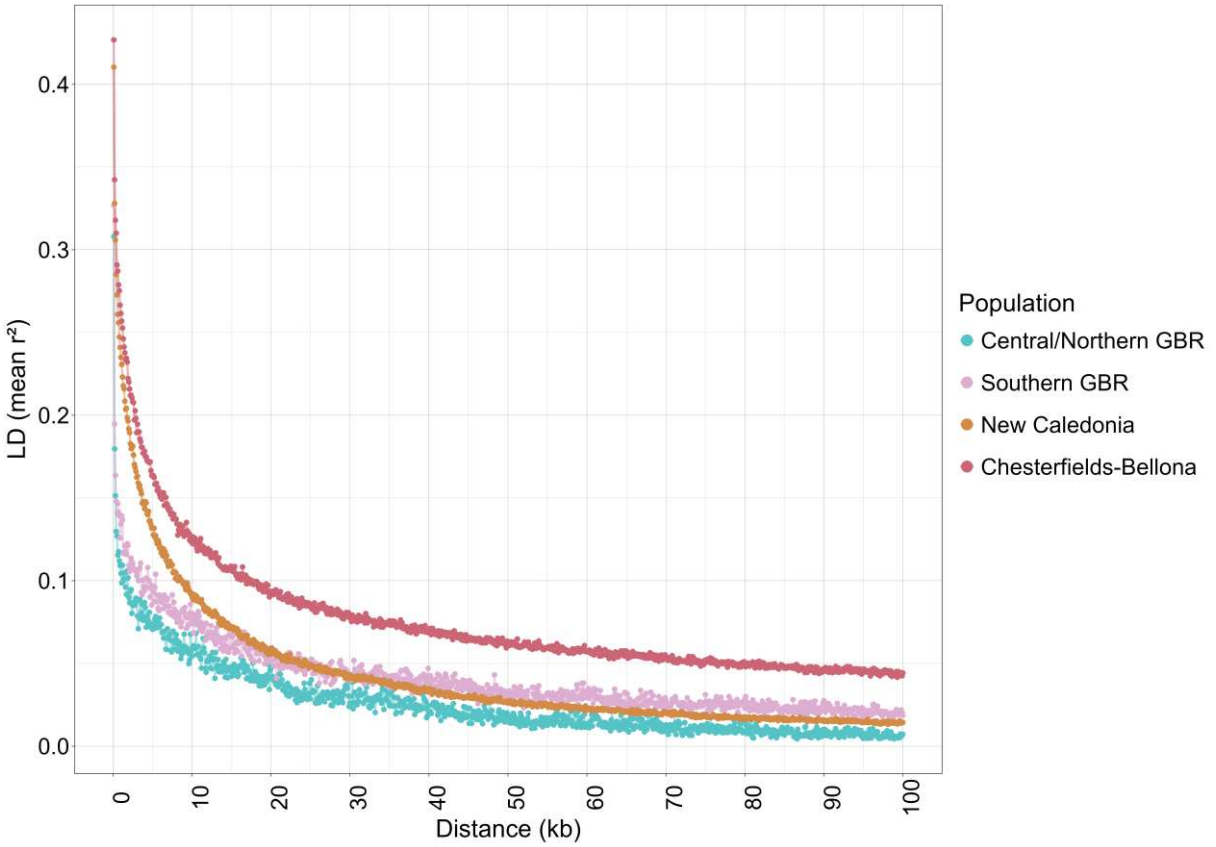


Figure A4.1. Rate of linkage disequilibrium (LD) decay within each *Acropora spathulata* population. Each point represents the average pairwise squared Pearson correlation coefficient (r^2) between alleles, calculated for 10% of all possible SNP pairs within 100 kb. Values were averaged within non-overlapping 100 bp distance windows to visualize the decay of LD with increasing physical distance. Note sample sizes differed among populations ($n_{Central/Northern\ GBR} = 624$, $n_{Southern\ GBR} = 156$, $n_{New\ Caledonia} = 163$, $n_{Chesterfields\text{-}Bellona} = 69$).

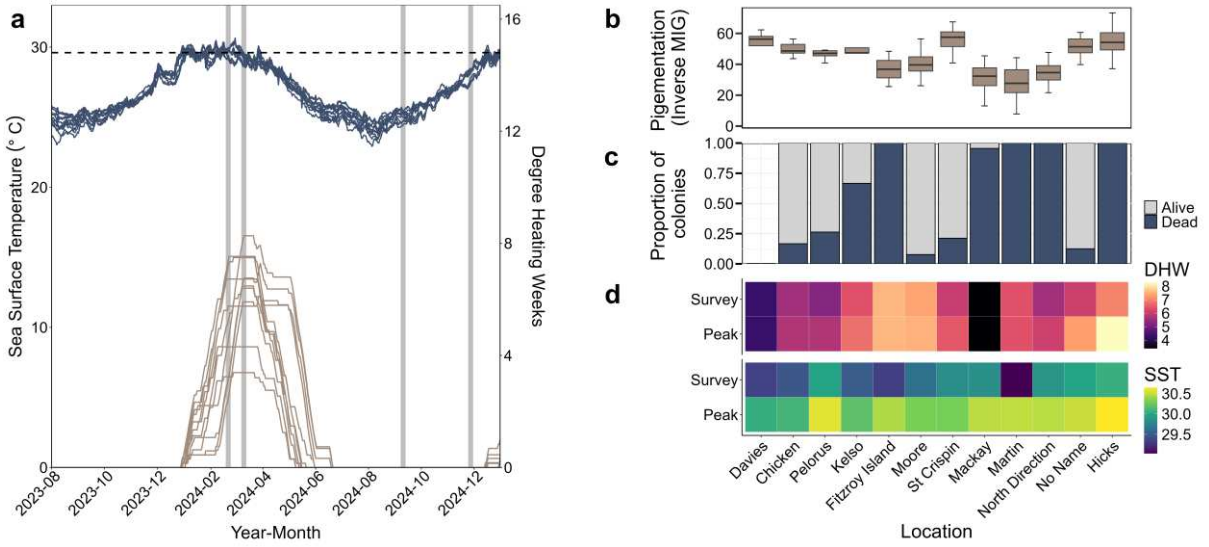


Figure A4.2. Bleaching and Mortality of *Acropora spathulata* during the 2023–2024 marine heatwave (a) Sea surface temperature (SST, blue) and Degree Heating Weeks (DHW, brown) at twelve survey sites on the Central/Northern Great Barrier Reef (NOAA Coral Reef Watch, 2018, updated daily). The horizontal lines indicate the temperature corresponding to 1 °C above the average Maximum Monthly Mean (MMM) across sites. Grey vertical bars mark the timing of surveys conducted during the bleaching event (the first two bars) and after the bleaching event (the last two bars). (b) Pigmentation across surveyed colonies during the bleaching event measured as the inverse mean intensity grey (MIG). Boxplot show the median MIG (solid line) and the first and third quartiles (box) for each reef site. (c) Mortality levels across surveyed colonies 6 months after the bleaching event. Barplot show the proportion of colonies categorized as dead (>95% mortality) or alive (<5% mortality). d) Intensity of heat-stress (SST and DHW) experienced by coral colonies at the different reef sites during the bleaching survey and at the peak of the marine heatwave.

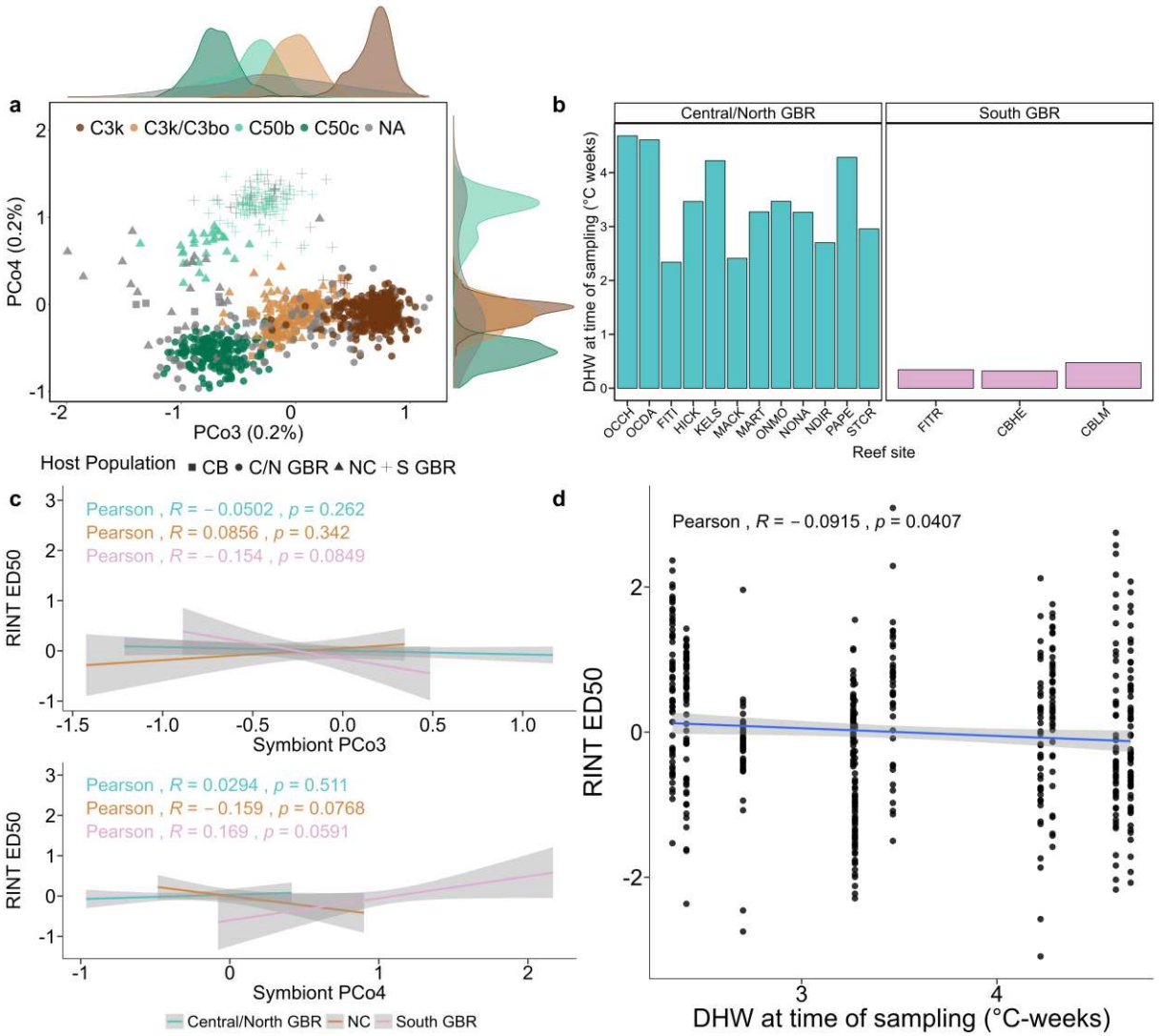


Figure A4.3. Controlling for confounding factors in Genome-Wide-Association studies (GWAS) with acute heat tolerance. (a) Principal coordinate analysis on microalgal symbionts genome-wide kmer-derived D_2^s distance. Each point represents the metagenomic composition of the Symbiodiniaceae community from one colony, coloured by symbiont clusters ITS2-type assigned to clusters using complimentary analyses. Shapes represent the host population of origin. The two principal coordinates best separating Symbiodiniaceae communities (based on ITS2 markers) were used as covariates in linear mixed-effect models, to account for a potential influence of symbioses on heat stress. (b) Accumulated heat stress on reef sites at the time of acute assays phenotyping on the GBR measured as Degree Heating Weeks (DHW). Sites are ordered by latitude. DHW at the time of sampling was used as a covariate in linear mixed-effect models to account for potential non-genetic acclimatory effects. (c) Relationship of rank-inverse normalised (RINT) chlorophyll ED50 with symbiont principal components. (d) Relationship of RINT in the Central/Northern GBR sites with DHW at the time of sampling.

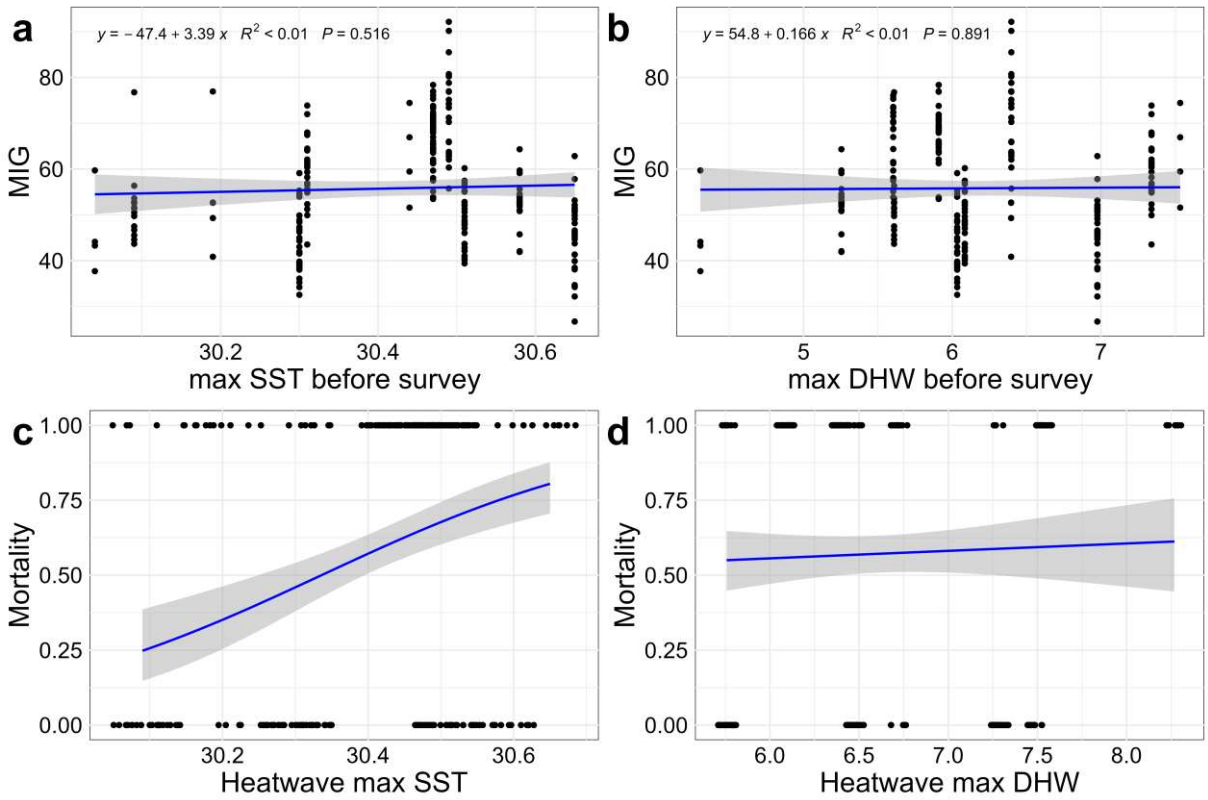


Figure A4.4. Response of *A. spathulata* populations to heat stress during a natural marine heatwave (2023-2024). Individual bleaching extent (MIG) surveyed over the course of the marine heatwave showed no significant correlation with reefs (a) peak sea-surface temperatures (SST) and (b) peak accumulated heat stress (degree heating weeks; DHW) before the survey. Mortality after the conclusion of the marine heatwave was significantly associated with (c) the peak sea-surface temperature reached during the marine heatwave but was not associated with the peak accumulated heat stress measured as DHW.

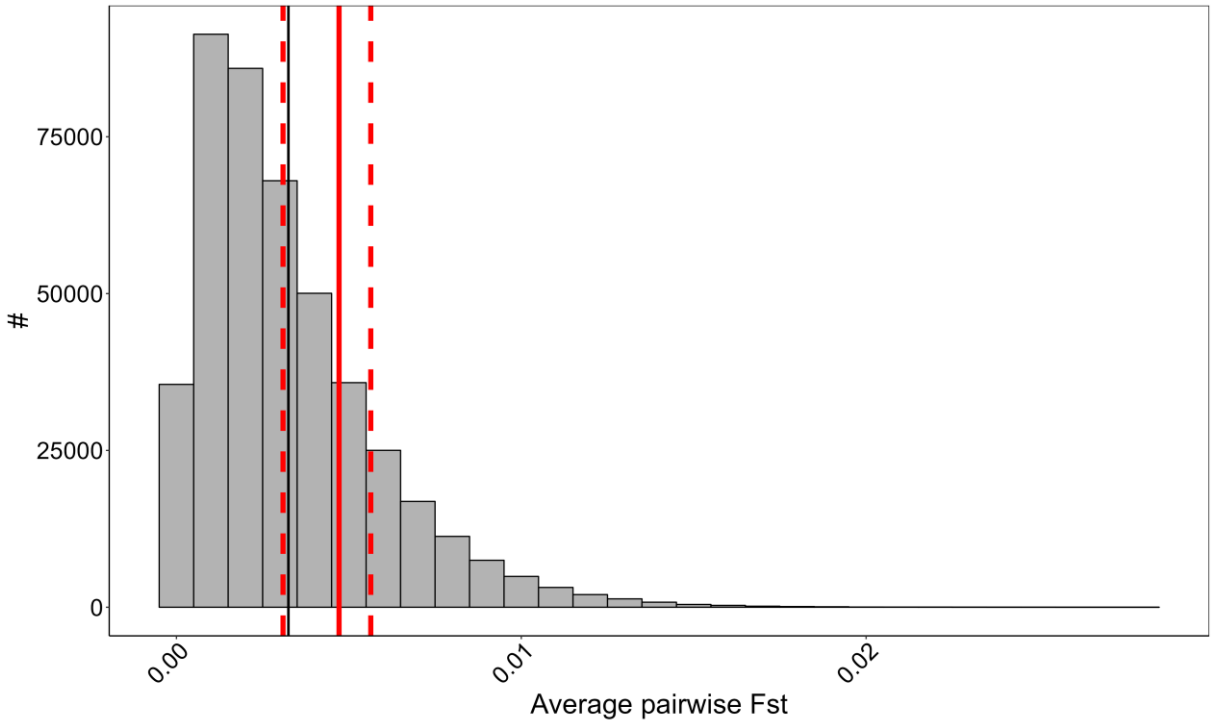


Figure A4.5. Average pairwise F_{st} among reefs along the genome The histogram shows the distribution of F_{st} values across all SNPs positions for the Central/Northern GBR dataset. The vertical line shows the median of the genome-wide distribution. The red solid line indicates the median distribution of F_{st} values for 'core' SNPs used in the computation of the adaptive index and dashed lines the first (Q1) and third quartiles (Q3). Random SNPs were drawn between Q1 and Q3 to confirm the functional relevance of 'core' SNPs.

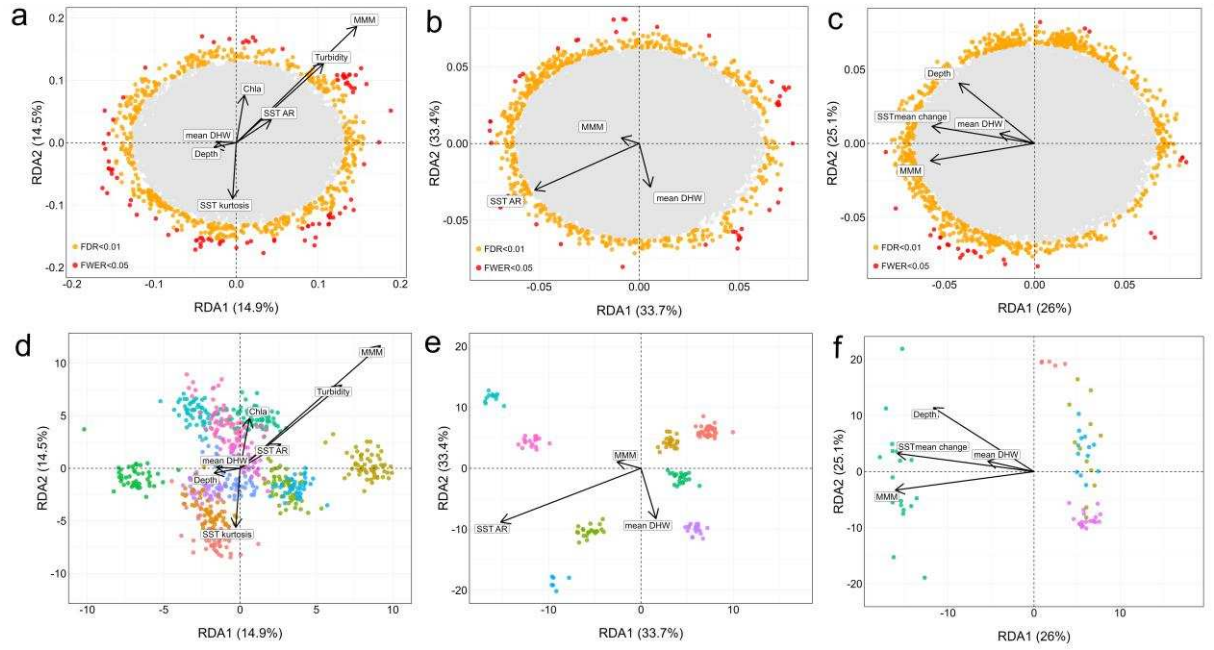


Figure A4.6. Candidate genomic markers of local adaptation identified using Genotype by environment association studies within three *Acropora spathulata* populations. RDA models were used to test for correlation between allelic frequency changes and environmental clines.

Top plots show the distribution of SNPs in RDA space for (a) the Central/Northern GBR, (b) the NC and (c) the CB population. SNPs exhibiting significant correlation with the first two RDA axes are coloured in orange (FDR<0.01, suggestive association) and red (FWER<0.05, strong association). Arrows indicate environmental predictors used to constrain the ordination. MMM: Maximum monthly mean; DHW: Degree Heating Weeks, Turbidity measured as the coefficient of light attenuation Kd_{490nm}; Chla: Chlorophyll a, SST AR: Annual Range in Sea Surface Temperatures. Bottom plots (d,e,f) show the distribution of individuals in RDA space for the corresponding populations. Number in parenthesis indicate the percentage of constrained variation explained by the first and second RDA axes respectively. Note this is different from the percentage of total variation explained by RDA1/RDA2 which were 0.166/0.163% for the Central/Northern GBR, 0.62/0.61% for NC and 1.54/1.49% for CB.

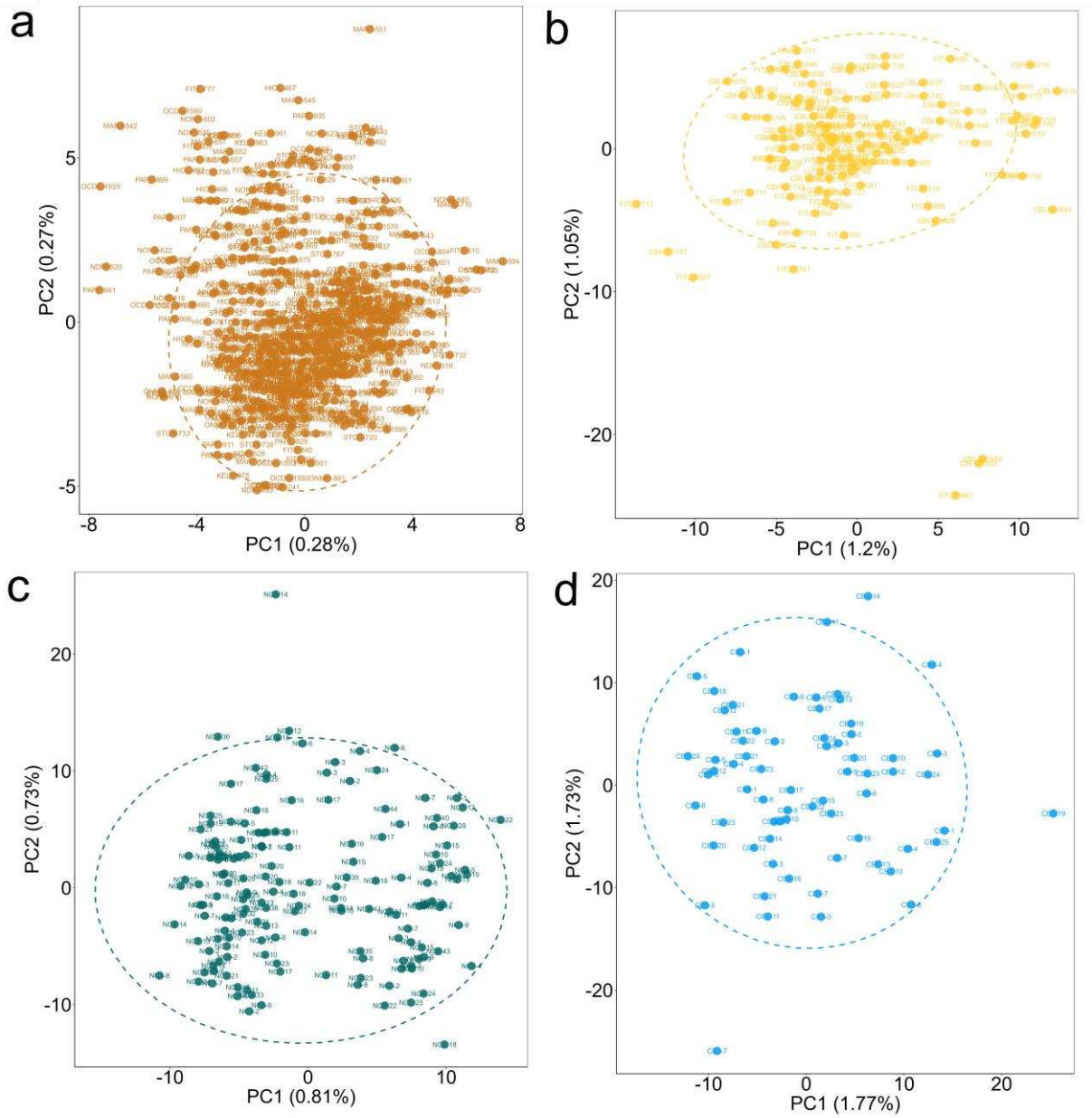


Figure A4.7. Little genetic population structure within *Acropora spathulata* populations Separate principal component analyses (PCA) were conducted within each population on high quality 'hard called' SNPs (stringent dataset), following imputation, MAF>0.05 filtering and LD pruning (r^2<0.2). Each point represents an individual coloured according to its population: (a) Central/Northern GBR, (b) Southern GBR, (c) New Caledonia, (d) Chesterfields-Bellona atolls. For each PCA, the first two PCs are shown with number in parenthesis representing the % of total variance explained by that component. The same PCA were conducted on linked SNPs (no LD pruning) and matched those reported here. Despite the presence of outliers, no visible genetic structure was observed within populations.

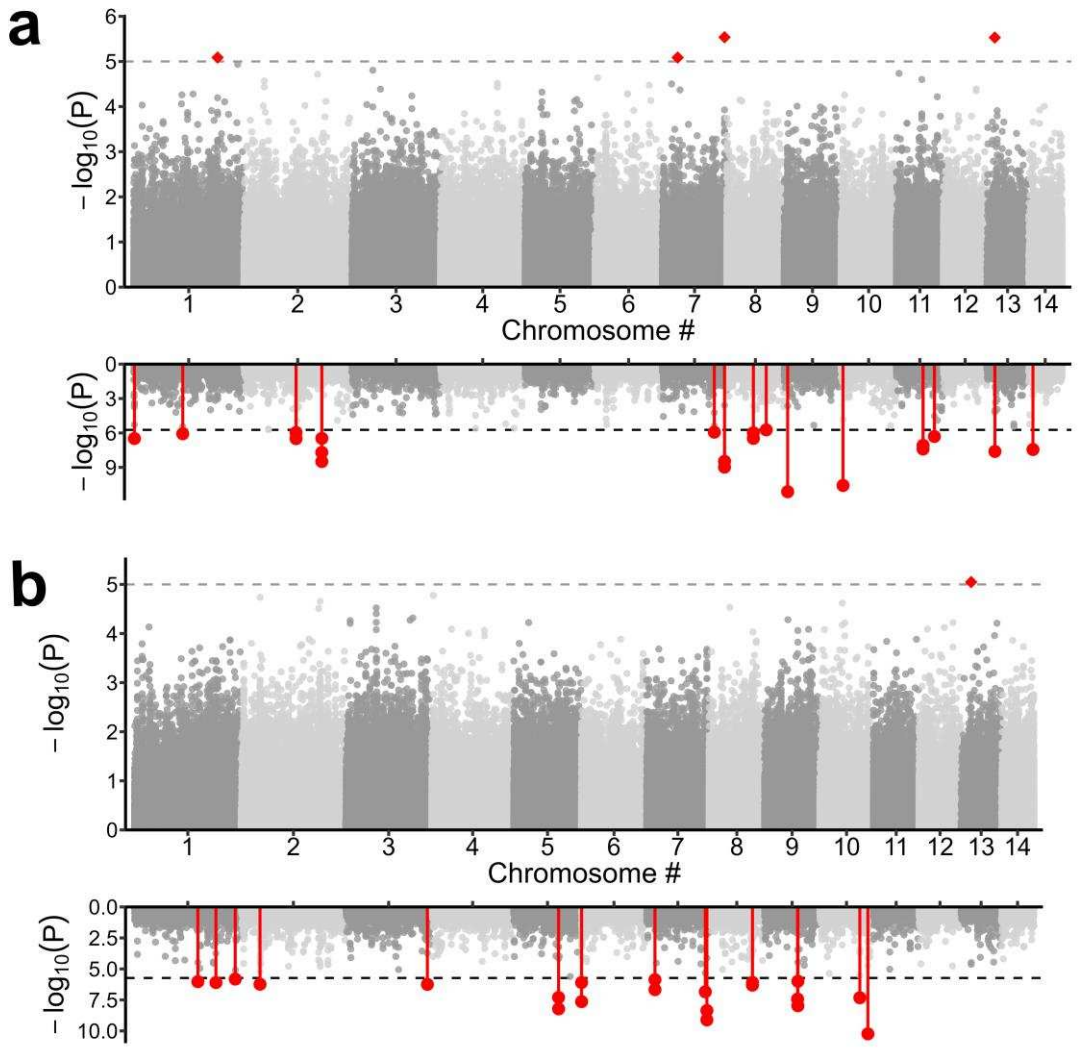


Figure A4.8. GWAS with *in-situ* traits. Manhattan plots of p-values obtained from testing associations between genotypes and (a) *in-situ* bleaching and (b) *in-situ* mortality at each SNP using linear mixed models for the Central/Northern GBR. For each population, the top Manhattan plot show individual SNPs p-values with the horizontal grey line corresponds to a p-value <1e-5 suggesting associations. SNPs are coloured in red if falling below the suggestive threshold. The bottom Manhattan plot shows 20kb windows p-values after aggregation using the WZA method. Significant windows (FWER<0.05) are shown in red.

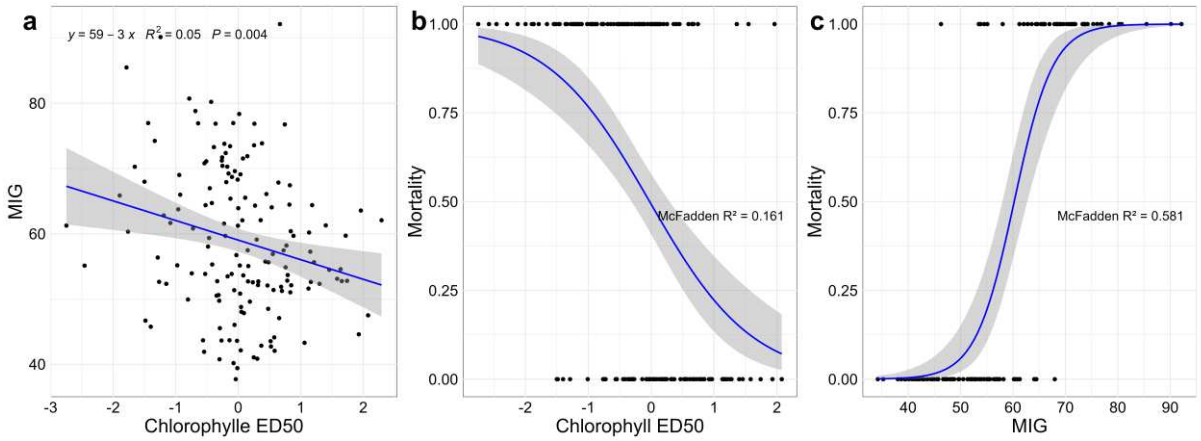


Figure A4.9. Correlation between heat tolerance traits measured in the Central/Northern GBR population. Individual colonies heat tolerance was inferred from Chlorophyll (NDVI) ED50 measured in acute stress assays, Pigmentation retention (MIG) and Mortality during a natural marine heatwave. (a) Correlation between MIG and Chlorophyll ED50 (n = 124 across 8 reefs). Higher MIG indicates higher bleaching. Proportion of variance explained and best linear regression fit are shown. (b) Logistic regression between Mortality scored as binary trait (1: >95% dead; 0: <5% dead) and Chlorophyll ED50 (n = 168 colonies across 7 reefs). Pseudo-R^2 is shown. (c) Same as (b) for the correlation between MIG and Mortality (n = 153 across 8 reefs).

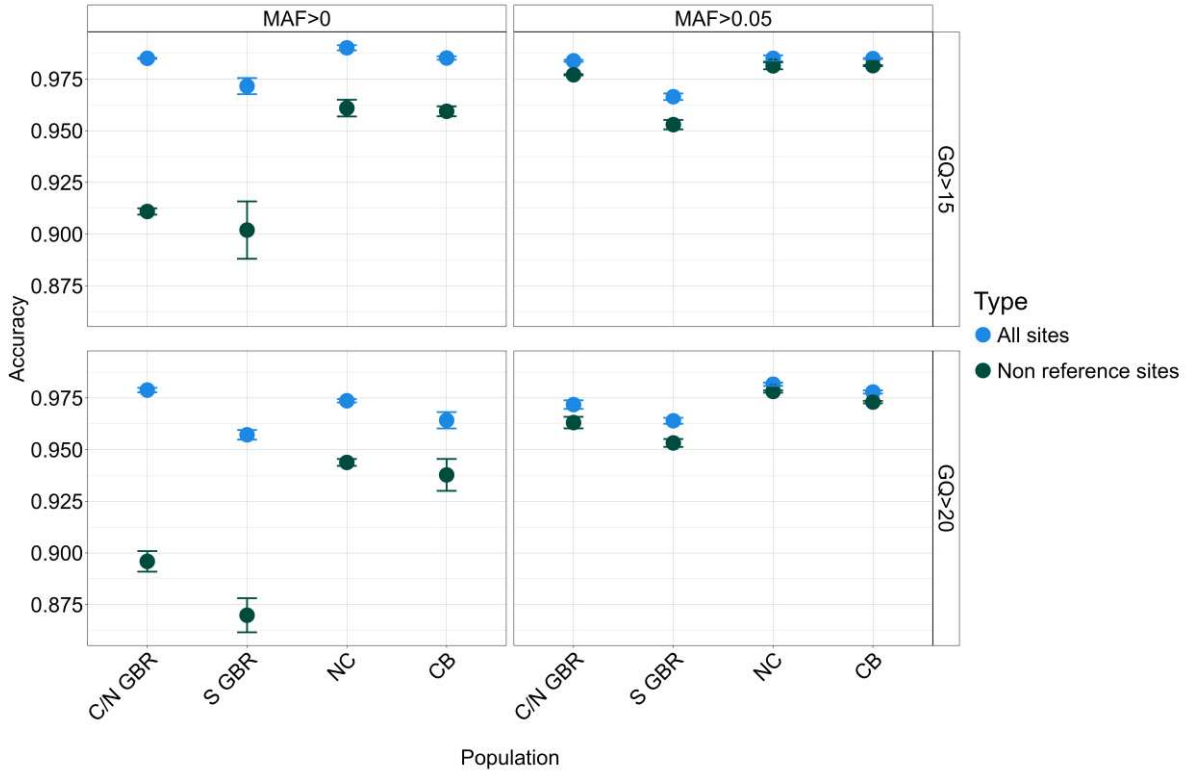


Figure A4.10. Accuracy of missing genotype imputation across *Acropora spathulata* populations. Imputation was performed within each population using the *de-novo* haplotype method in Beagle. Accuracy was assessed by comparing imputed genotypes to observed genotypes in artificially down-sampled individuals, and was calculated as the proportion of concordant genotype calls. The mean and standard deviation in accuracy is presented for

different filtration before (MAF>0) and after removal of rare variants (MAF>0.05) and for different genotype quality filtration. Colours show the type of genotype used for the computation (blue = all genotypes, green = non reference genotypes only).

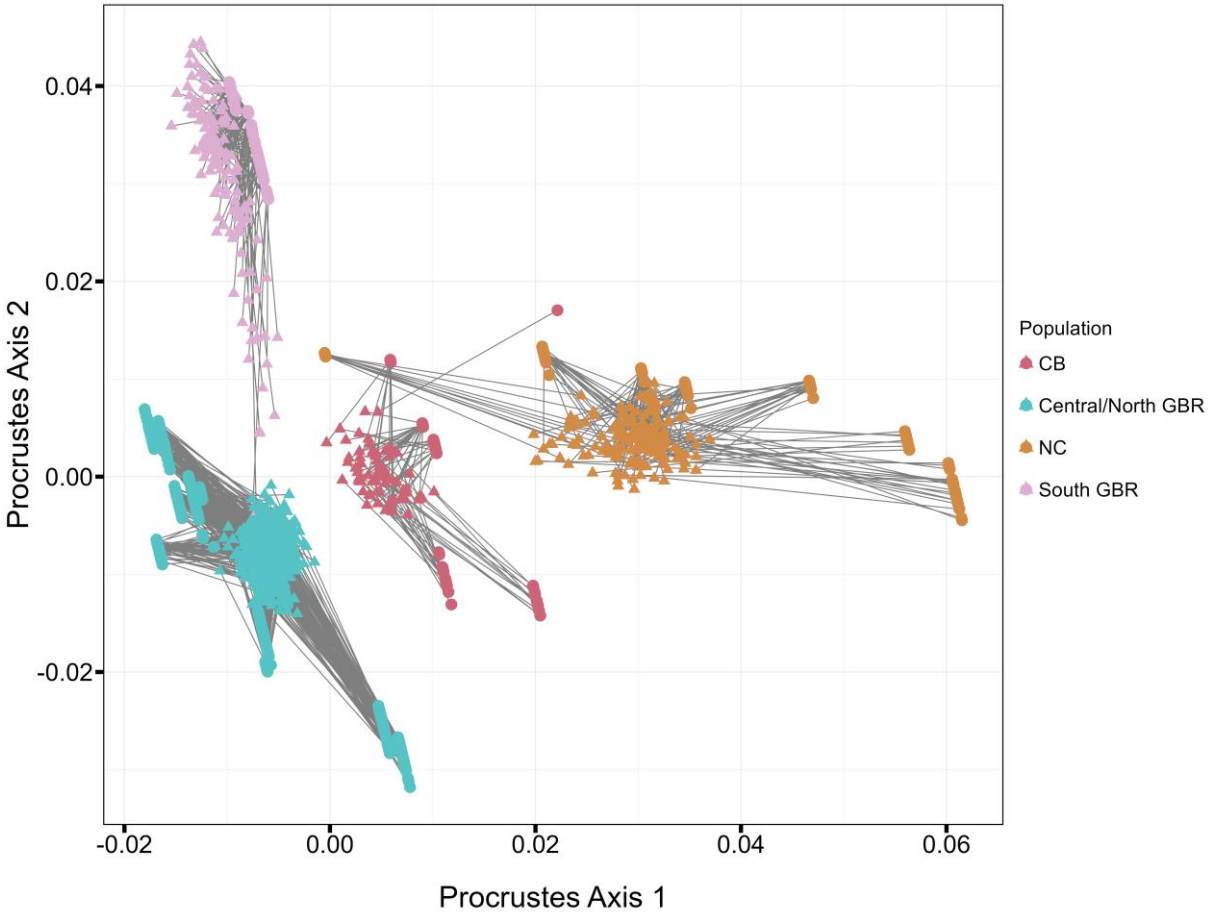


Figure A4.11. Correlation of global population structure and environmental condition of *Acropora spathulata* populations across the Western Pacific. Correlation was assessed using a procrustean rotation analysis. Each point represents a coral colony, with the host genotype (triangle) and its corresponding environment (circle) connected by a segment. Points are coloured according to population.

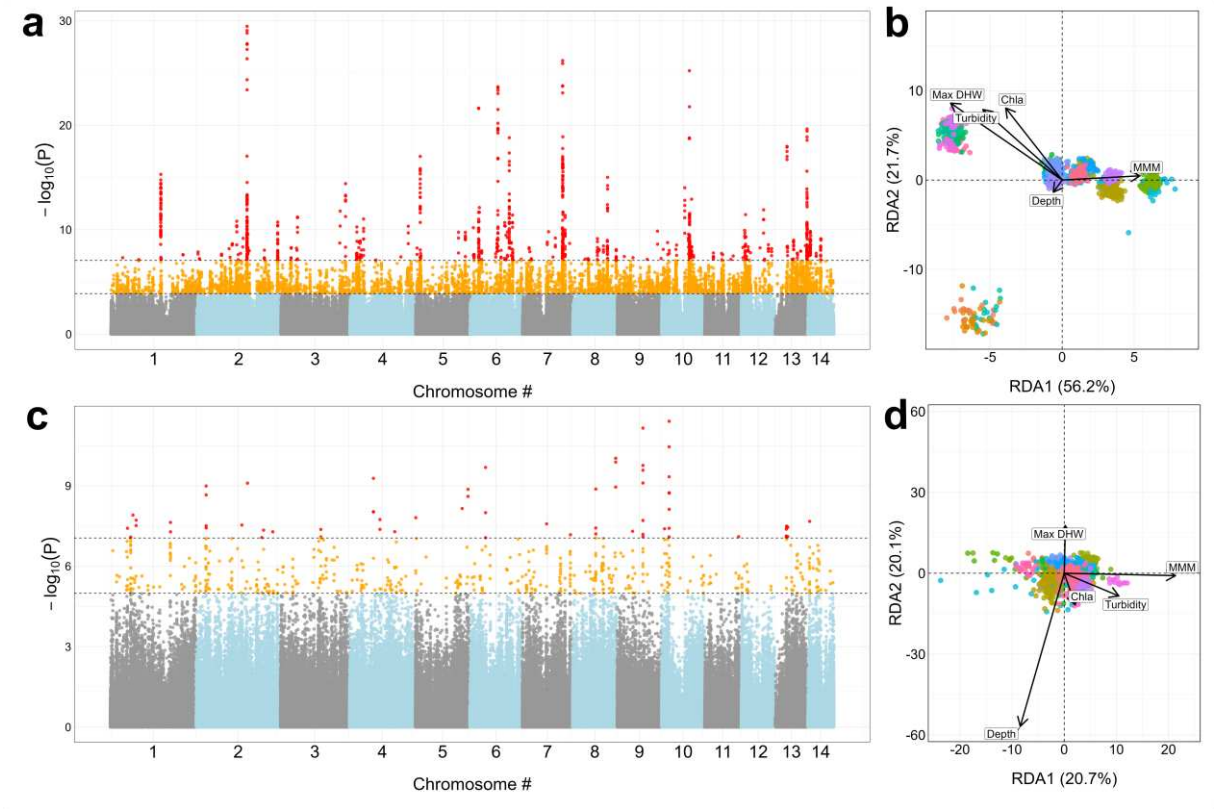


Figure A4.12. Candidate genomic markers of local adaptation at the regional level (i.e., across four Western Pacific populations) identified using Genotype by environment association studies. In (a) and (b) partial RDA models were used to test for correlation between allelic frequency changes and environmental clines, while controlling for the effect of isolation-by-distance (IbD) by conditioning the RDA on individuals' geographic coordinates. In (c) and (d) the same approach was used but the pRDA was conditioned on the first three PCs of the PCA on unlinked SNPs. Manhattan plots in (a) and(b) show the significance of associations between allelic frequencies and environmental variables at each locus (point) across the genome after multiple testing corrections (orange: FDR<0.01, red: FWER<0.05). RDA ordination plots in (b) and (d) show the distribution of individuals in RDA space coloured by their reef of origin. Arrows indicate environmental predictors used to constrain the ordination. MMM: Maximum monthly mean; DHW: Degree Heating Weeks, Turbidity measured as the coefficient of light attenuation Kd_{490nm}; Chla: Chlorophyll a.

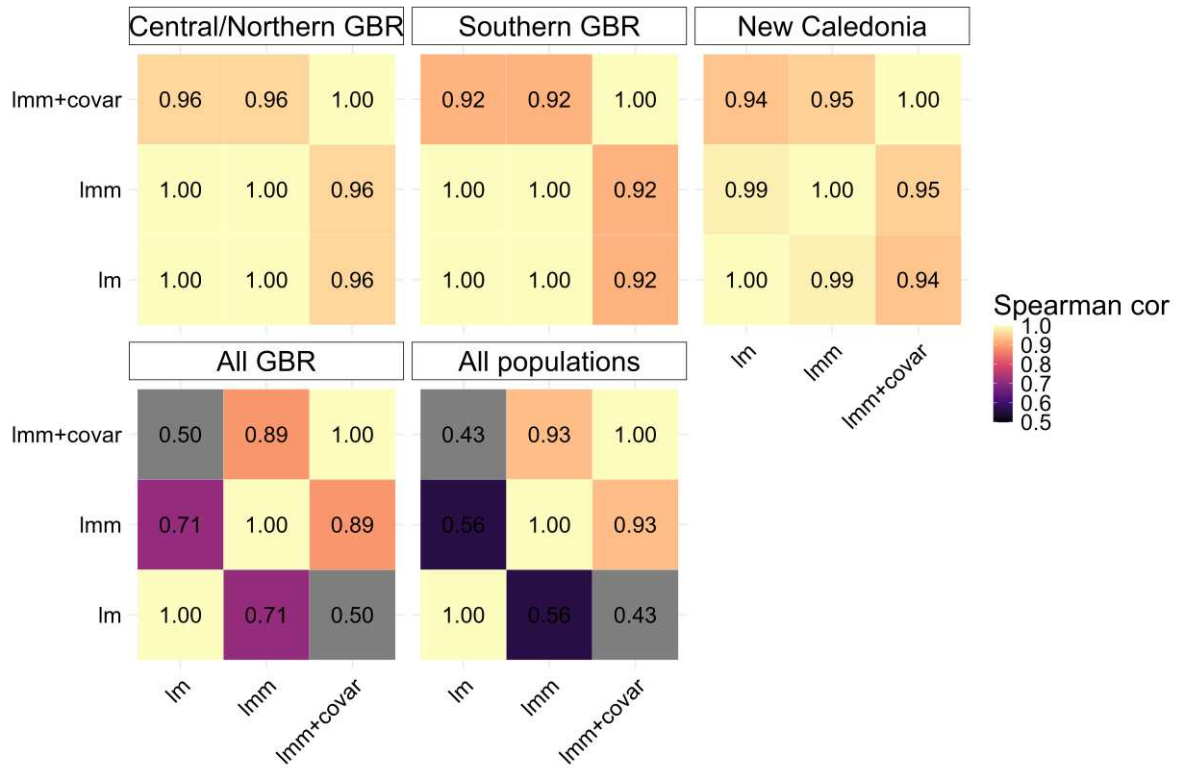


Figure A4.13. Sensitivity analysis of GWAS results to model choice. For each dataset separate GWAS were conducted using linear models (lm), linear mixed models accounting for individuals' relatedness (lmm) and linear mixex models with fixed covariates (lmm+covar). The consistency of GWAS results across models was visualized using Spearman's correlation between -log10(p-values).

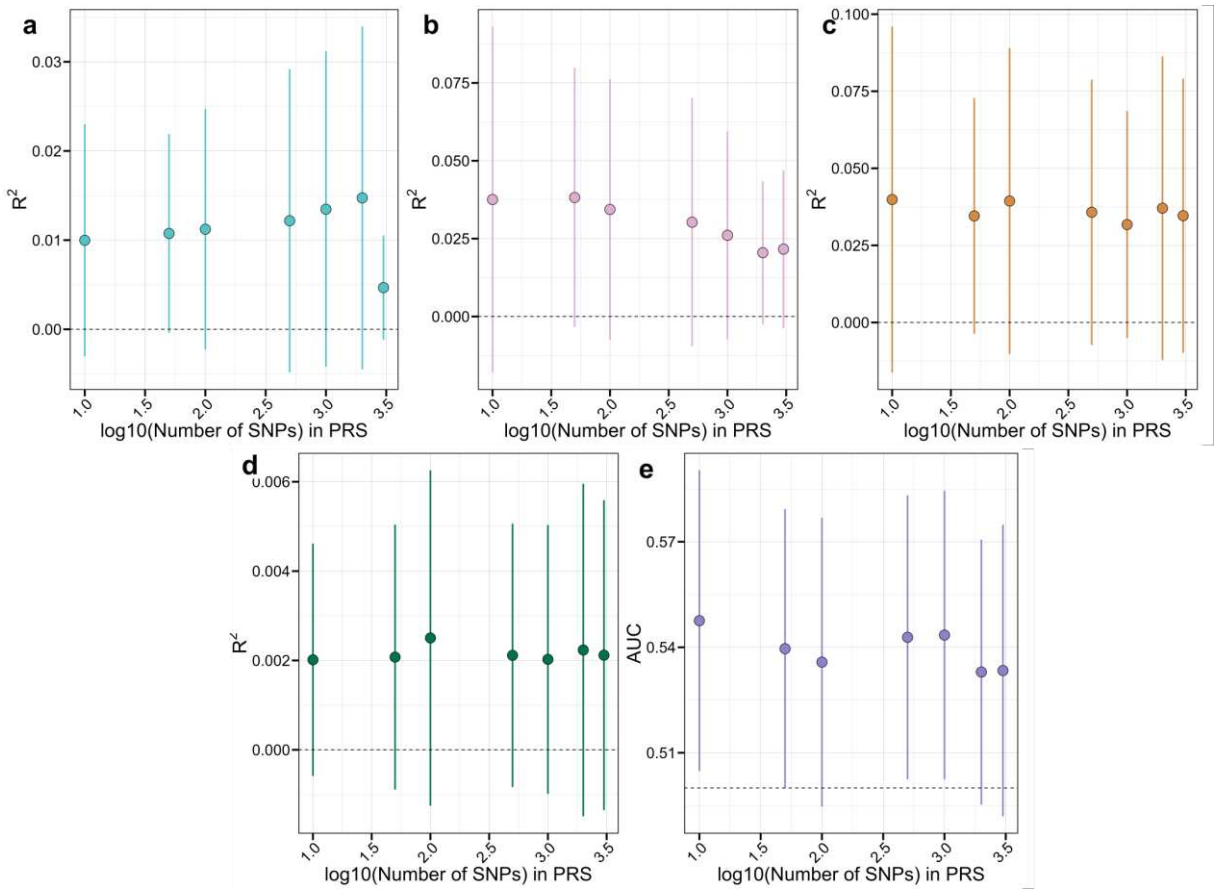


Figure A4.14. Predictive accuracy of heat tolerance traits using polygenic risk scores (PRS) across *Acropora spathulata* populations. Accuracy is shown for predictions of Chlorophyll ED50 in (a) the Central/Northern GBR, (b) the Southern GBR and (c) New Caledonia populations. In addition, accuracy is shown for (d) *in-situ* bleaching (MIG) and (e) mortality in the Central/Northern GBR. The accuracy of PRS was evaluated on 100 random 80/20 train-test splits for each trait and population. Graph show the fraction of variance explained (R^2) as the function of the number of index SNPs (after LD clumping) used in the computation of the PRS. Points show the mean R^2 and vertical bars the standard deviation across 100 test sets. For mortality measured as a binary trait the area under the curve (AUC) as a function of the number of SNPs is shown instead. Note the log10 scale on the x-axis (points correspond to 10,50,100,500,1000,2000 and 3000 index SNPs).

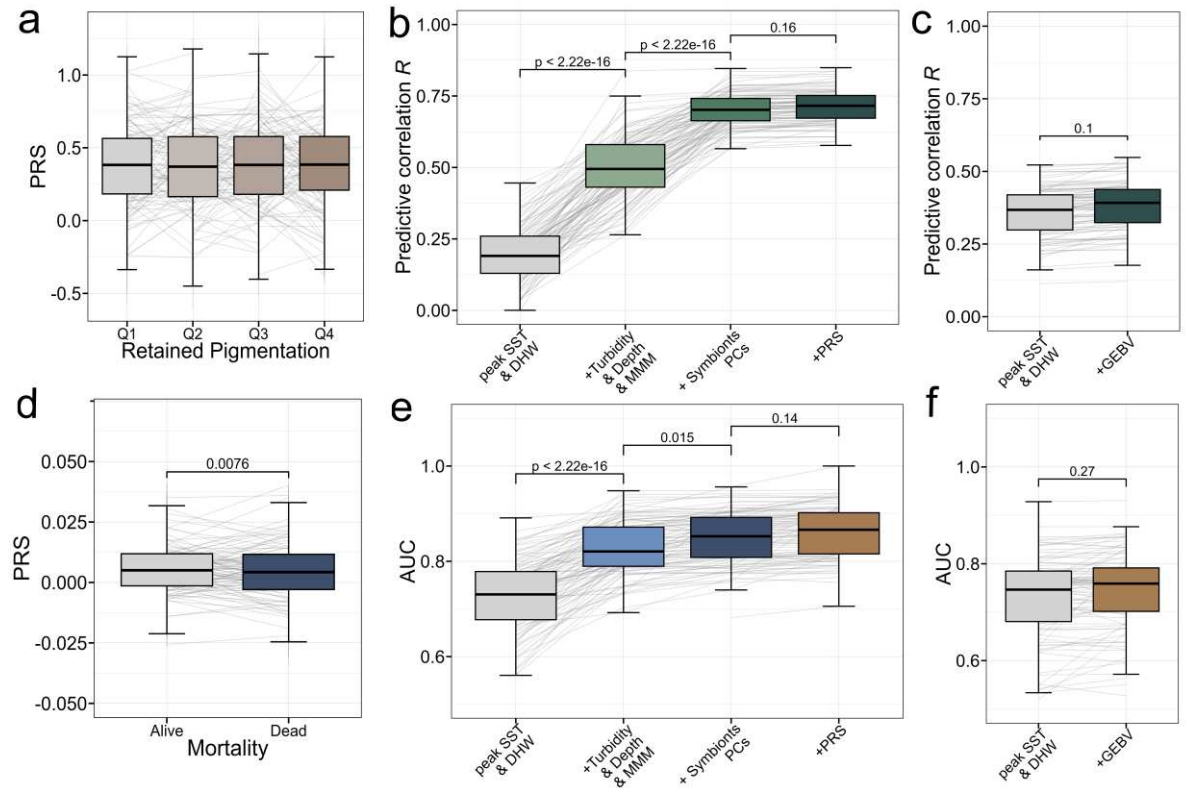


Figure A4.15. Polygenicity, genotypic redundancy and large effective population sizes limit the accuracy of coral bleaching and mortality genomic predictions (a) An additive polygenic risk score (PRS) was computed from the effect sizes of the top 100 SNPs (after LD clumping) showing the stronger associations in a GWAS with retained pigmentation during a natural bleaching event. 100 random train/test split were performed with 80% of coral colonies used in the GWAS and 20% used to assess the accuracy of the PRS. The distribution of the PRS for the 100 test sets across retained pigmentation quantiles is shown. (b) A multiple linear regression model was built to evaluate the accuracy of the PRS along other covariates. Boxplot show the predictive correlation for retained pigmentation for models of increasing complexity. The significance of accuracy improvement across models was tested using Wilcoxon rank-sum tests and the corresponding p-value is shown. (c) The same approach was used to test the increase in predictive accuracy of Genomic Estimated Breeding values (GEBV) using ridge regression. (d,e,f) A similar approach was used to predict coral mortality after the conclusion of the marine heatwave, recorded as a binary trait. A multiple logistic regression model was used to evaluate the accuracy of (e) the PRS along other predictors, measured as the Area Under the Curve (AUC) and (f) the accuracy of GEBV.

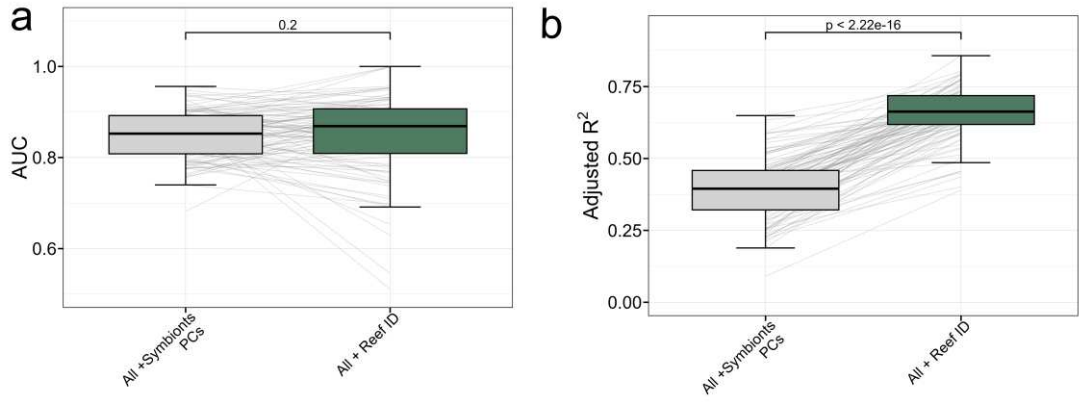


Figure A4.16. Predictive accuracy of symbionts genetic variation Comparison of the increase in predictive accuracy of (a) coral mortality and (b) bleaching from models integrating Symbiodiniaceae communities' composition relative to models treating reef as a fixed effect. Boxplot show the predictive accuracy (AUC and adjusted-R^2) of multiple regression linear models based on all environmental covariates + Symbiodiniaceae principal coordinate components or + reef identity. The p-value from a Wilcoxon rank-sum test comparing predictive accuracies is shown above.

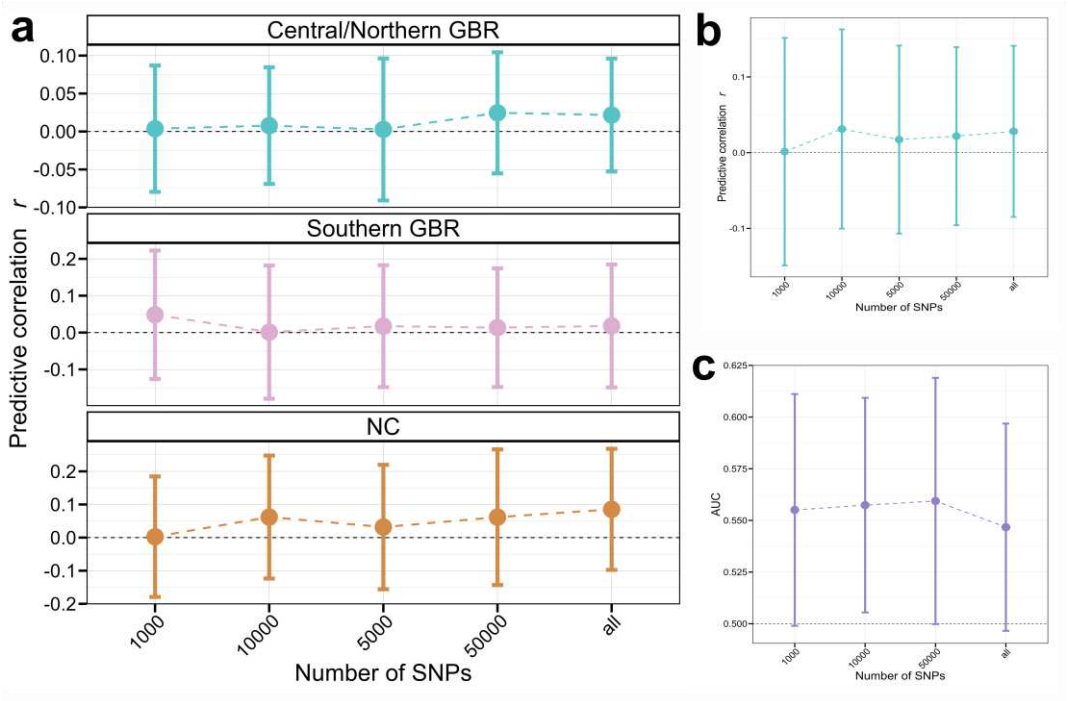


Figure A4.17. Comparison of the predictive accuracy of Genomic estimated breeding values (GEBV) for each tolerance trait and *Acropora spathulata* populations. GEBVs were computed using ridge regression best linear unbiased prediction (rrBLUP) for continuous traits (Chlorophyll ED50, MIG) and bayesian ridge regression for the Mortality treated as binary trait. The predictive correlation with the observed traits across 100 test sets for different number of random SNPs included as random effect in the model are shown for (a) Chloropyll ED50, (b) *in-situ* bleaching (MIG) and (c) *in-situ* mortality.

Supplementary Tables

Table A4.1. Summary of genomic variants and samples filtration steps. For each step and dataset, number of retained samples and single nucleotide polymorphisms (SNPs) are reported along filtration parameters. C/N GBR: Central/Northern GBR population, S GBR: Southern GBR population, NC: New Caledonia Population, CB: Chesterfields-Bellona Coral Sea plateau population. For All_GBR_NC and All_populations datasets, variants were filtered jointly across populations.

Dataset	Scope	n samples	Filtration Step 1	n SNPs	Filtration Step 2	n SNPs	n samples
C/N GBR	Within population	629	Locus missingness < 20%; 5 ≤meanDP≤ 20; MAC≥1; bi-allelic SNPs, GQ≥20	537,203	MAF>0.05; major genotype frequency< 95%; individual relatedness <0.2	130,088	624
S GBR	Within population	156		351,887		141,646	129
NC	Within population	166		762,617		395,274	164
CB	Within population	78		558,713		365,576	69
All_GBR_NC	Across populations	951		611,260		131,867	915
All_populations	Across populations	1028		619,067		133,187	984
C/N GBR	Within population	629	Locus missingness < 20%; 5 ≤meanDP≤ 20; MAC≥1; bi-allelic SNPs, GQ≥15	1,847,007	MAF>0.05; major genotype frequency< 95%; individual relatedness <0.2	440,945	624
S GBR	Within population	156		1,343,192		542,927	129
NC	Within population	166		5,851,159		2,237,972	164
CB	Within population	78		3,266,571		1,828,804	69
All_GBR_NC	Across populations	915		2,419,378		546,477	915
All_populations	Across populations	1028		2,304,951		567,189	984

Table A4.2. Environmental predictors used in Genotype by environment association studies (GEA) performed using redundancy analyses (RDA). MMM: Maximum monthly mean, SST: Sea surface temperatures, DHW: Degree Heating Weeks.

Variable	Metric	Source	Spatial resolution	Time resolution	Period	Description	Rationale and references
Temperature	*MMM*	Coralwatch	5km	daily	1985-2024	Average temperature of the warmer calendar month (1985-1990+1993 climatology)	Upper historical baseline used in routine bleaching alerts (Liu et al., 2003)
	SST_AR	Coralwatch	5km	daily	1985-2024	SST Annual range	Thermal variability can affect heat tolerance (Schoepf et al., 2021)
	SSTmax_99th	Coralwatch	5km	daily	1985-2024	99th percentile of monthly maximum SST	Extreme temperatures select for heat tolerance through bleaching and mortality
	SST_kurtosis	Coralwatch	5km	daily	1985-2024	Kurtosis of SST distribution	Thermal variability can affect coral

							heat tolerance (Zinke et al., 2018)
	SST_skewness	Coralwatch	5km	daily	1985-2024	Skewness of SST distribution	Thermal variability can affect coral heat tolerance (Zinke et al., 2018)
	SSTmean_change	Coralwatch	5km	daily	1985-2024	Nonparametric effect size between the distribution of monthly temperature between decade 1985-1995 and 2013-2023	Selective pressure may be higher at reefs experiencing faster warming (Whiting et al., 2024)
	DHW_avg	Coralwatch	5km	daily	1985-2024	Average monthly maximum DHW	Recurrent marine heatwaves may select for coral heat tolerance (Selmoni et al., 2024b)
	DHW_freq_sup4	Coralwatch	5km	daily	1985-2024	Average number of days above 4 DHW per year	Level 1 alert of Coralwatch (widespread bleaching)
	DHW_freq_sup8	Coralwatch	5km	daily	1985-2024	Average number of days above 8 DHW per year	Level 2 alert of Coralwatch (widespread mortality)
	DHW_max	Coralwatch	5km	daily	1985-2024	Maximum DHW ever experienced	Extreme marine heatwaves induce coral bleaching and mortality (McClanahan et al., 2019)
Irradiance	*UVR_median*	ERA5	0.25°	hourly	2002-2024	Median UV radiation ($W.m^{-2}$)	UV radiation is a compounded stressor with heat (Downie et al., 2023)
	CF_median	ERA5	0.25°	hourly	2002-2024	Median cloud fraction	Irradiance is a compounded stressor with heat (Gonzalez-Espinosa & Donner, 2021)
Seawater turbidity	*Kd490_median*	Globcolour	1/24°	daily	2002-2024	Median attenuation of irradiance at 490nm, proxy for turbidity	Turbidity may alleviate or increase stress during bleaching (Sully et al., 2022; Zinke et al., 2018)
Primary productivity	*Chla_median*	Globcolour	1/24°	daily	2002-2024	Median concentration of chlorophyll a = proxy for nutrient load ($mg.\ m^{-3}$)	Under stress conditions, plankton can supplement heterotrophic energy intake (Meunier et al., 2022)
Depth	*Depth*	Dive computer	Individual-level			Tide-corrected depth (standardised to the lowest astronomical tideà	Irradiance decreases with depth

Table A4.3. Summary of sample sizes, predictors and models used in Genotype by Environment association studies (GEA) in *A. spathulata*. RDA: redundancy analysis, pRDA; partial redundancy analysis. C/N GBR: Central/Northern GBR population, S GBR: Southern GBR population, NC: New Caledonia Population, CB: Chesterfields-Bellona Coral Sea plateau population. In addition to models shown here, a single-predictor model with the maximum

monthly mean was ran for each dataset. PCs indicate principal component from a PCA based on all SNPs. Explanatory variables were retained, controlling for a VIF <10.

Dataset	Scope	N colonies	N reefs	n colonies/reef	Model	Conditional variables	Explanatory variables
C/N GBR	Within population	624	12	39–60	RDA		MMM+DHW_avg+SST_AR+Chl a_median+Kd490_median+SST_kurtosis
NC	Within population	164	8	6–42	RDA		MMM+DHW_avg+SST_AR
CB	Within population	69	5	5–20	RDA		MMM+DHW_avg+SSTmean_change+Depth
All_populations	Across populations	984	25	5–60	pRDA	Lon+Lat	MMM +Kd490_median+Chl a_median+Depth+DHW_max
All_populations	Across populations	984	25	5–60	pRDA	PC1+PC2+PC3	MMM +Kd490_median+Chl a_median+Depth+DHW_max

Table A4.4. Summary sample sizes and numbered of retained SNPs used for Genome Wide Association studies (GWAS) in *A. spathulata*. The number of successfully genotyped and retained individuals after filtration of related individuals are shown. Phenotypes = number of individuals originally phenotyped, GWAS = number of individuals retained after removal of low-quality phenotypes.

Dataset	Scope	Genotypes (r<0.2)	SNPs	Trait	Phenotypes	GWAS	n reefs GWAS
C/N GBR	Within population	624	440,945	Chl ED50	530	501	10
S GBR	Within population	128	542,927	Chl ED50	179	126	3
NC	Within population	163	2,237,972	Chl ED50	145	125	8
All_GBR	Across populations	752	546,477	Chl ED50	709	627	13
All_GBR_NC	Across populations	915	546,477	Chl ED50	891	752	21
C/N GBR	Within population	624	440,945	MIG	221	210	10
C/N GBR	Within population	624	440,945	Mortality	218	211	9

Table A4.5. Summary of SNPs and genomic windows putatively involved in local adaptation identified using GEA. RDA: redundancy analysis, pRDA; partial redundancy analysis. For each model, the number of significant SNPs for different multiple test correction is shown as well as the number of significant 20kb window using WZA method.

Dataset	Model	Variables	#SNPs (FDR<0.01)	#SNPs (FWER<0.05)	#Windows (WZA FDR<0.01)
C/N GBR	RDA	all	632	91	43
NC	RDA	all	602	47	33
CB	RDA	all	1008	33	40
C/N GBR	RDA	MMM	263	39	83
NC	RDA	MMM	236	41	52
CB	RDA	MMM	77	42	84

Table A4.6. Top five candidate genes or genomic windows of local adaptation identified using RDA-based GEAs for each population and model. Environmental predictors used in the RDA model are indicated. The number of associated SNPs (#) in a gene or genomic window is indicated along the position and p-value of the most significant association and the region type (intragenic/intergenic). The WZA column indicate whether these SNPs were also present in a significant window based on the WZA analysis (Yes/No). For intragenic SNP, the protein annotation of the gene is shown. For intergenic SNPs, the number and position of genes located within ± 10kb of its position are shown. Position, function and known differential gene expression (DGE) in Dixon et al. (2020) is shown for each gene (+: up-regulation, -: down-regulation, ns: non-significant, ?: unknown).

SNPs							Genes					
Pop	**Pred**	**Chr**	**#**	**Pos.**	**p**	**WZA**	**Locus ID**	**Start**	**End**	**Distance**	**Annotation**	**DGE**
C/NGBR	MMM	4	4	20852913	3.9e-11	Y	LOC114953173	20851666	20880111	intragenic	MAP kinase-activating death domain protein	?
		3	7	24653370	2.1e-9	Y	LOC114960915	24645068	24679191	intragenic	kinase D-interacting substrate of 220 kDa-like	?
		3			4.7e-11	Y	LOC114976230	12971726	12973215	9373 AFE	-tropomyosin-like	?
							LOC114976859	12974231	12978111	4477 AFE	-60S ribosomal protein L23a-like	ns
								12983216	12983855	628 BFS	-	
		10		12984826			LOC114976847	12985415	12999692	2827 BFS	-	
		1	5	37267108	2.7e-8	Y	LOC114964516	37247704	37271406	intragenic	centrosomal protein of 290 kDa-like	ns
		12	1	2326372	5.5e-8	Y	LOC114966048	2302278	2336804	intragenic	Cilia- and flagella-associated protein 54	?
NC	MMM	2	6	20375887	1.1e-10	Y	LOC114964467	20372648	20389442	intragenic	-	?
		5	12	24213164	2.1e-10	Y		24208684	24213555	intragenic	-	
		7	4	3723765	1.1e-9	Y	LOC122947673			intragenic	collectin-12-like	?
								3720091	3735323			
		14	1	2163722	1.4e-9	Y	LOC114961510	2156121	2177973	intragenic	DNA mismatch repair protein MSH5	-
		5		24198670	1.6e-9	Y	LOC114976903	24190649	24207273	intragenic	Autophagy-related protein 9B	?
CB	MMM	7	1	6983892	9.7e-9	Y	LOC122965249	6982918	6991878	intragenic	-	?
		1	2	1583409	7.8e-11	N	LOC114958833	1570133	1580415	2994 AFE	Disintegrin and metalloproteinase domain-containing protein	?
							LOC114951230	1584139	1596498	730 BFS	xaa-Pro aminopeptidase 3-like	-
		14	3	6736005	1.3e-9	N	LOC114965645	6736270	6736731	265 BFS	transcription factor 21-like	?
							LOC114961535	6741255	6742836	5250 BFS	E3 ubiquitin-protein ligase	?
							LOC122958325	6743959	6752476	7954 BFS	D-inositol 3-phosphate glycosyltransferase	?
		1	2	34742542	2.9e-9	N	LOC114966591	34720286	34737458	5084 AFE	exocyst complex component 5-like TIMELESS-interacting protein-like	?
							LOC114966623	34748513	34754666	5971 BFS		+
		6	1	4522677	6.6e-9	N	LOC114975511	4500577	4534597	intragenic	Myotubularin-related protein 13(SBF2)	?
C/NGBR	MMM+DHW_avg+SST_AR+Chla_median+	10	8	12984826	4.7e-11	Y	LOC114976859	12974231	12978111	6715 AFE	60S ribosomal protein L23a-like	?
								12983216	12983855	971 AFE	-	?
							LOC114976847	12985415	12999692	589 BFS	-	-
		6	1	6772287	1e-9	Y	LOC114976120	6757439	6764148	8139 AFE	centromere-associated protein E- beta-1,4-N-acetylgalactosaminyltransferase troponin I-like	?
							LOC122958271	6767411	6772218	69 AFE		?

	Kd490_median+SST_kurtosis						LOC114973414	6773661	6787185	1374 BFS		ns
		2	7	32074184	1.1e-9	Y	LOC114975875 LOC122953555 LOC114975872	32066557 32075962 32080290	32070429 32076960 32083872	3755 AFE 1778 BFS 6106 BFS	Homeobox protein EMX1 Nucleoporin NDC1(ndc1) Cytochrome P450 3A29(CYP3A29)	ns ? ?
		3	9	24653370	2.9e-9	Y	LOC114960915	24645068	24679191	intragenic	kinase D-interacting substrate of 220 kDa-like	?
		14	1	3644035	5e-9	Y	LOC114966048	3628916	3649034	intragenic	Cyclin-G-associated kinase	?
NC	MMM+DHW_avg+SST_AR	8	9	5831432	1.1e-10	Y	LOC114957554	5830586	5836769	intragenic	-	-
		1	8	31462954	1.1e-10	N	LOC114953833	31404164	31465012	intragenic	-	?
		8	1	583981	1.3e-10	N	LOC114955331	579583	585571	intragenic	hemicentin-2-like	?
		5	3	16506436	3.1e-10	N	LOC114960675	16488971	16513178	intragenic	Telomere-associated protein RIF1	?
		13	2	8481127	3.5e-10	N	LOC114954002	8468071	8483086	intragenic	DNA repair protein XRCC1	?
CB	MMM+DHW_avg+SSTmean_change+Depth	10	9	19023372	7.5e-10	Y	LOC114976283	19010935	19022134	1238 AFE	helicase domino-like	?
		2	8	22157084	9.5e-10	Y	LOC114963825	22161108	22164019	4024 BFS	D-glutamate cyclase,	-
		2	1	26933688	1.1e-8	Y	LOC122956892	22086360	22154622	2462 AFE	protein Daple-like	?
		2	1	26869122	1.7e-8	Y	LOC114976296	19034295	19037700	9102 BFS	coronin-6-like	ns
		9	2	8233091	1.8e-10	N	LOC122950944 LOC122962896	26934390 26942925	26935051 26944691	702 BFS 9237 BFS	- -	? ?

Table A4.7. Top candidate SNPs hits identified in GWAS with acute and long-term heat stress responses using. For each *A. spathulata* population and phenotypic trait, the number of suggestive associations (#, p-value<1e-5) is indicated and details from these associations are shown. For intragenic SNPs, the location and annotated protein function of the corresponding gene is shown, along known differential gene expression (DGE) from Dixon et al. (2020) (+: up-regulation, -: down-regulation, ns: non-significant, ?:unknown). For intergenic SNPs, the location and annotation of genes located ± 10kb from its position are shown, along the relative SNP position (AFE: After end, BFD: before start).

SNPs						**Genes**					
Pop	**Trait**	**#**	**Chr**	**Pos.**	**p**	**Locus ID**	**Start**	**End**	**Distance**	**Annotation**	**DGE**
C/N GBR	Chl ED50	5	8	4648396	5.8e-7	LOC122960238	4647412	4647886	510 AFE	-	?
			6	7748131	6.3e-7	LOC122956367	7748553	7748553	422 BFS	-	?
			6	9200420	7,3e-6	LOC122950807 LOC114975989 LOC114966975	9183242 9192686 9209422	9192157 9196166 9220510	8263 AFE 4254 AFE 9002 BFS	- Serine threonine-protein phosphatase 6 regulatory ankyrin repeat subunit C-like	? + -
			5	21049835	7,7e-6	LOC122961273	21045898	21052050	intragenic	E3 ubiquitin-protein ligase Ufd4-like	?
			8	4718223	9,1e-6	LOC114967570	4711132	4732044	intragenic	ephrin type-B receptor 1-like	ns
S GBR	Chl ED50	6	9	15714720	9.2e-7	LOC114975449	15714319	15718881	intragenic	-	?
			5	4084186	2.4e-6	LOC114959188 LOC122960799	4061647 4093646	4082701 4096735	1485 AFE 9460 BFS	gastrula zinc finger protein xLCGF3.1-like gastrula zinc finger protein XlCGF7.1-like	? ?
			11	4680211	3.6e-6	LOC114968071 -	4670346 4687475	4676440 4687758	3771 AFE 7264 BFS	hemicentin-1-like -	ns ?
			8	3110973	3.8e-6	LOC114949133 -	3098529 3109330	3103541 3109973	7432 AFE 1000 AFE	peroxidasin-like -	- ?

			8	19219331	5e-6	LOC114962771	37492197	37513682	intragenic	inhibitor of Bruton tyrosine kinase-like	?
			1	37510170	8.5e-6	LOC114975449	15714319	15718881	intragenic	neurogenic locus notch homolog protein 1-like	?
NC	Chl ED50	15			1.4e-6	LOC122949835	6714972	6715451	2989 AFE	-	?
			2	6718440		LOC114966570	6726439	6728154	7999 BFS	homeobox protein engrailed-2-like	?
			5	17800164	3.2e-6	LOC114971022	17796713	17817147	0 NA	DNA-directed RNA polymerase III	?
					3.9e-6	LOC114975883	32188688	32218068	5168 AFE	-	?
			2	32223236		LOC114953127	32219627	32220448	2788 AFE	Protein ABHD14B	?
			1	12859479	5.6e-6	LOC114947134	12850535	12912591	0 NA	E3 ubiquitin-protein ligase UBR4-like	+
			11	14955153	5.8e-6	LOC114961708	14921552	14965425	0 NA	DnaJ homolog subfamily C member 13	?
				19604276	6.2e-6	LOC114953604	19592844	19598592	5684 AFE	Putative sphingolipid delta(4)-desaturase	+
						LOC114966288	19600118	19601384	2892 AFE	iron-sulfur cluster assembly 2 homolog	?
						LOC114966351	19606496	19609115	2220 BFS	C4-monooxygenase(ttm-5)	?
			7			LOC114966333	19613227	19619239	8951 BFS	Kanadaptin-like	?
			14	2167593	6.9e-6	LOC114976903	2156121	2177973	intragenic	DNA mismatch repair protein MSH5	-
				11173668	7.2e-6	LOC114976789	11152006	11167096	6572 AFE	pleiotropic regulator 1-like	-
			3			LOC114976805	11179386	11185482	5718 BFS	C2 domain-containing protein	-
			3	16910558	7.4e-6	LOC114969951	16900613	16918172	intragenic	sacsin-like	-
				19061977	7.5e-6	LOC114963953	19028345	19054217	7760 AFE	DNA-directed RNA polymerase II	?
			2			LOC114964543	19069371	19090798	7394 BFS	RING finger protein 37-like	?
				17535991	8.2e-6	LOC114971875	17529755	17534220	1771 AFE	prefoldin subunit 5-like	?
			5			LOC114971628	17537411	17552940	1420 BFS	kinesin-like protein KIF28P	?
				16762418	8.6e-6	LOC114947476	16745722	16754814	7604 AFE	3-hydroxyanthranilate 3,4-dioxygenase-	?
			3			LOC114969951	16764477	16784805	2059 BFS	sacsin-like	-
C/N GBR	MIG	4	7	21548687	2.9e-6	LOC114957871	21534940	21542911	5776 AFE	replication stress response regulator SDE2-like	-
						LOC122947785	21545165	21547262	1425 AFE	-	?
						LOC114957853	21555206	21557063	6519 BFS	-	?
			13	2741730	3.0e-6	LOC122951125	2741063	2742404	intragenic	-	?
			1	29053522	8.2e-6	LOC114968444	29016838	29062423	intragenic	integrator complex subunit 3-like	?
			7	5319458	8.2e-6	LOC114963640	5299816	5321119	intragenic	Xanthine dehydrogenase/oxidase	?
C/N GBR	Mortality	1	13	3602380	9.0e-6	LOC122961566	3598351	3598864	3516 AFE	-	?
						LOC122962169	3601495	3601978	402 AFE	ATP-dependent DNA helicase RecQ-like	?

Appendix A5. Statement of co-authorship

The following people and institutions contributed to the publication of work undertaken as part of this thesis:

Hugo Denis	-Santé des Ecosystèmes tropicaux (SantEco) EMR9001, CNRS, IRD, Univ. de Nouvelle-Calédonie, Univ. la Reunion, UMR 250 ENTROPIE, Noumea 98800, New Caledonia, France. -ED 129, SU Sorbonne Université, 4, Place Jussieu, 75252 Paris, France -National Marine Science Centre, Faculty of Science and Engineering, Southern Cross University, Coffs Harbour, NSW, Australia
Annie S. Guillaume	-Australian Institute of Marine Science, Townsville, QLD, Australia
Clarisse Majorel	-UMR250 ENTROPIE (IRD-CNRS-UR-IFREMER-UNC), Promenade Roger-Laroque, Noumea Cedex, New Caledonia, France
Cynthia Riginos	-Australian Institute of Marine Science, Townsville, QLD, Australia -School of the Environment, University of Queensland, Brisbane, QLD 4072, Australia
Cheong Xin Chan	-Australian Centre for Ecogenomics, School of Chemistry and Molecular Biosciences, The University of Queensland, Brisbane, QLD 4072, Australia
Emily J. Howells	-National Marine Science Centre, Faculty of Science and Engineering, Southern Cross University, Coffs Harbour, NSW, Australia -Lizard Island Research Station, Australian Museum, Sydney, NSW 2010, Australia
Gaël Lecellier	-Institut de Sciences Exactes et Appliquées (ISEA) EA7484, 145, Avenue James Cook – BP R4 98 851 Nouméa, New Caledonia
Hisatake Ishida	-Australian Centre for Ecogenomics, School of Chemistry and Molecular Biosciences, The University of Queensland, Brisbane, QLD 4072, Australia
Ilha Byrne	-School of the Environment, University of Queensland, Brisbane, QLD 4072, Australia
Iva Popovic	-Australian Institute of Marine Science, Townsville, QLD, Australia -School of the Environment, University of Queensland, Brisbane, QLD 4072, Australia
Katharine E. Prata	-Australian Institute of Marine Science, Townsville, QLD, Australia -School of the Environment, University of Queensland, Brisbane, QLD 4072, Australia
Line K. Bay	-Australian Institute of Marine Science, Townsville, QLD, Australia
Magali Boussion	-UMR250 ENTROPIE (IRD-CNRS-UR-IFREMER-UNC), Promenade Roger-Laroque, Noumea Cedex, New Caledonia, France
Melissa S. Naugle	-National Marine Science Centre, Faculty of Science and Engineering, Southern Cross University, Coffs Harbour, NSW, Australia
Ombeline Sue	-UMR250 ENTROPIE (IRD-CNRS-UR-IFREMER-UNC), Promenade Roger-Laroque, Noumea Cedex, New Caledonia, France
Steven W. Purcell	-National Marine Science Centre, Faculty of Science and Engineering, Southern Cross University, Coffs Harbour, NSW, Australia
Véronique Berteaux-Lecellier	Santé des Ecosystèmes tropicaux (SantEco) EMR9001, CNRS, IRD, Univ. de Nouvelle-Calédonie, Univ. la Reunion, UMR 250 ENTROPIE, Noumea 98800, New Caledonia, France.
Véronique J.L. Mocellin	-Australian Institute of Marine Science, Townsville, QLD, Australia

Article 1 (Located in Chapter 2)

Denis, H., et al. (2024). Thermal tolerance traits of individual corals are widely distributed across the Great Barrier Reef. *Proceedings B* 291(2030): 20240587.

Candidate contribution: data curation, formal analysis, investigation, methodology, software, visualization, writing—original draft, writing— review and editing. Candidate contributed approximately 60% to the planning, execution and preparation of the work for the paper.

Line K. Bay: conceptualization, funding acquisition, investigation, methodology, project administration, supervision, writing— review and editing

Véronique J.L. Mocellin: data curation, methodology, resources, writing—review and editing

Melissa S. Naugle: data curation, investigation, writing—review and editing

Gaël Lecellier: supervision, writing—review and editing

Steven W. Purcell.: supervision, writing—review and editing

Véronique Berteaux-Lecellier.: supervision, writing—review and editing

E J. Howells: conceptualization, formal analysis, funding acquisition, investigation, methodology, project administration, supervision, writing—review and editing.

Chapter 3

Candidate contribution: project administration, data curation, formal analysis, investigation, methodology, visualization, writing—original draft, writing— review and editing. Candidate contributed approximately 70% to the planning, execution and preparation of the work for the paper.

Clarisse Majorel: investigation.

Gaël Lecellier: investigation, methodology, supervision, writing—review and editing

Magali Boussion: investigation.

Ombeline Sue: data curation, methodology.

Véronique Berteaux-Lecellier: investigation, methodology, supervision, project administration, writing—review and editing

E J. Howells: supervision, writing—review and editing.

Article 2 (Located in Chapter 4)

Denis, H., et al. (2024). Long-distance gene flow and contrasted population structures of reef-building corals and their algal symbionts across the Western Pacific. [In review in *Current Biology*]. https://doi.org/10.1101/2025.10.14.682263.

Candidate contribution: data curation, formal analysis, investigation, methodology, software, visualization, writing—original draft, writing— review and editing. Candidate contributed approximately 60% to the planning, execution and preparation of the work for the paper.

Katharine E. Prata: formal analysis, investigation, methodology, writing— review and editing

Hisatake Ishida: methodology, software, writing— review and editing

Iva Popovic: methodology, supervision, writing— review and editing

Véronique J.L. Mocellin: investigation, resources, writing—review and editing

Magali Boussion: investigation, writing—review and editing

Ilha Byrne: investigation, writing—review and editing

Steven W. Purcell: supervision, writing—review and editing,

Line K. Bay: conceptualization, funding acquisition, project administration, supervision, writing— review and editing

Gaël Lecellier: investigation, supervision, writing—review and editing

Cheong Xin Chan: supervision, resources, methodology, writing—review and editing

Cynthia Riginos: supervision, writing—review and editing

Emily J. Howells: conceptualization, funding acquisition, project administration, supervision, writing— review and editing

Véronique Berteaux Lecellier: conceptualization, funding acquisition, project administration, supervision, writing— review and editing

Article 3 (Located in Chapter 5)

Candidate contribution: data curation, formal analysis, investigation, methodology, software, visualization, writing—original draft, writing— review and editing. Candidate contributed approximately 75% to the planning, execution and preparation of the work for the paper.

Gaël Lecellier: investigation, methodology, resources, supervision, writing— review and editing.

Line K. Bay: conceptualization, funding acquisition, project administration.

Véronique J.L. Mocellin: investigation, ressources.

Steven W. Purcell: writing— review and editing.

Annie S. Guillaume: data curation, software.

Melissa S. Naugle: investigation.

Cyntia Riginos: supervision, methodology.

Emily J. Howells: investigation, conceptualization, funding acquisition, project administration, supervision, writing— review and editing.

Véronique Berteaux Lecellier: investigation, conceptualization, funding acquisition, project administration, supervision, writing— review and editing

We the undersigned agree with the above stated "proportion of work undertaken" for each of the above published (or submitted) peer-reviewed manuscripts contributing to this thesis:

Candidate 

Gaël Lecellier 

Melissa S. Naugle 

Annie S. Guillaume 

Hisatake Ishida 

Steven W. Purcell 

Clarisse Majorel 

Ilha Byrne 

Véronique Berteaux-Lecellier 

Cynthia Riginos 

Iva Popovic 

Véronique J.L. Mocellin 

Cheong X. Chan 

Katharine E. Prata 

Emily J. Howells 

Magali Boussion 

Line K. Bay 

Ombeline Sue 

Appendix A6. Scientific presentations during candidature

Denis, H., et al. Identification de marqueurs génétiques de la thermotolérance du corail *Acropora spathulata* de Nouvelle Calédonie et d'Australie par des études d'associations pangénomiques. Workshop ADNe, Nouméa, New Caledonia, November 2023. (Oral presentation)

Denis, H., et al. Thermal tolerance traits of individual corals are widely distributed across the Coral Sea. RISE postgraduate conference, Lismore, Australia, October 2024. (Oral presentation)

Denis, H., et al. Using hologenome sequencing to assess the effect of symbiont genetic variation on the heat tolerance of corals across the Coral Sea. Asian Pacific Congress of Protistology, Brisbane, Australia, November 2024.

Denis, H., Naugle. M. Phenotypes and Genotypes on the GBR. RRAP symposium (online). May, 2025

Denis, H., et al. Identifying genetic drivers of coral adaptation to global warming. International Congress for Conservation Biology, Brisbane, Australia, June 2025.